ELECTRO-HYDRODYNAMIC SPOT-SPRAY APPLICATION OF FOOD-GRADE OIL & EMULSIFIER BLENDS AS A RELEASE AGENT IN BAKING

By

ROBERT JOSEPH MACKEY

Bachelor of Science in Mechanical Engineering
Oklahoma State University
Stillwater, Oklahoma
2013

Master of Science in Engineering & Technology
Management
Oklahoma State University
Stillwater, Oklahoma
2015

Submitted to the Faculty of the
Graduate College of the
Oklahoma State University
in partial fulfillment of
the requirements for
the Degree of
DOCTOR OF PHILOSOPHY
May 2018

ELECTRO-HYDRODYNAMIC SPOT-SPRAY APPLICATION OF FOOD-GRADE OIL & EMULSIFIER BLENDS AS A RELEASE AGENT IN BAKING

Dissertation Approved:

Timothy Bowser, Ph.D.
Dissertation Adviser

Paul Weckler, Ph.D.

Ning Wang, Ph.D.

Terry Collins, Ph.D.

ACKNOWLEDGEMENTS

Choosing who to thank in these situations is usually easy as it's a process that requires a lot of guidance and assistance. Choosing what to say is much harder. While there are countless people who helped me get to this point, I wanted to take the time to recognize four very special people:

Fred Springer is the President and CEO for the Burford Corporation in Maysville, Oklahoma. He was also my boss. When I approached Fred about the prospect of continuing my education to earn a Doctorate, Fred was not only supportive, he was genuinely happy for me. He lent his support in every way imaginable to include having Burford support my research (both with time and financial assistance). Fred is the kind of leader that I hope to be someday. He is compassionate and, yet, demanding. He loves people and, yet, expects the best of those around him. Fred, thank you for what you've done for me. I consider you a true friend and mentor.

Lucas Beckner is a Controls Engineer and colleague whose help was vital in working through the research for this project. Lucas helped build the (many) test fixtures, helped design the controls for the project, got oily with me when we stated testing, and jumped in to help any time I needed it. His brand of sarcasm kept me focused on the right things and smiling the whole way. Lucas is the kind of friend who shows up to help move furniture. He's the kind of guy you want to keep in your life. Lucas, thank you for all that you've done. I really do appreciate it!

DEDICATIONS

For my Papa, **Ralph Clouse**, who raied me. He taught me to love people, the value of hard work, and that I could do anything if I set my mind to it.

I love you and I miss you every day.

For **Angee,** who loves me.

27 years and six beautiful children later, you're still my best friend (and editor).

Name: ROBERT JOSEPH MACKEY

Date of Degree: MAY 2018

Title of Study: ELECTRO-HYDRODYNAMIC SPOT-SPRAY APPLICATION OF
FOOD-GRADE OIL & EMULSIFIER BLENDS AS A RELEASE
AGENT IN BAKING

Major Field: BIOSYSTEMS & AGRICULTURAL ENGINEERING

ABSTRACT:

In industrial baking, vegetable oil is used as a release agent for bread depanning. The conventional process of applying oil uses pressure and shear to atomize the oil. This works but generates over-spray and, thus, creates a sanitation problem and a potential food safety risk. The objective of this research project is to determine if the four major commercially available vegetable oils (Palm oil, Soybean Oil, Rapeseed oil, Sunflower Oil) can be made, by the introduction of an emulsifier/surfactant, to carry an electrical charge greater than the Rayleigh point so that they can be electro-hydrodynamically (EHD) atomized. Coulombic attraction pulls the atomized liquid to the target without the problem of over-spray. To accomplish this, each base oil was blended with a surfactant (Lecithin, Polysorbate, Propylene Glycol) at concentrations of 5% and 10%. The solution was sprayed through a capillary tube (19ga, 22ga) in a spot spray mode onto oil sensitive paper at 25kV and 50kV at varying temperatures and pressures. An ANOVA of the DOE structured experiment was performed to analyze the inputs (concentration, voltage, temperature, and pressure) relative to the outputs (droplet count, droplet size, coverage area, and sample weight) to determine the performance of the experiment at different interaction points.

Twenty-four separate experiments involving 865 individual tests provided the data to determine EHD viability for each oil and emulsifier blend. The criteria of average droplet count >200/in^2, average droplet size <1mm^2, average coverage area between 15%-60%, and average sample weight <0.2g was used as a minimum target for success. Every experimental group tested with a 22ga capillary tube met or exceeded the target. Tests using the 19ga capillary produced generally poor results. From this, it was determined that energy density relative to mass flow was a determining factor in successful EHD atomization. Energy density relative to mass flow, at the given input 2.5 and 5 Joules followed the exponential regression of respectively $E_d=6\dot{m}^{(-1.004)}\cdot 10^2$ and $E_d=6\dot{m}^{(-1.004)}\cdot 10^4$ respectively. Based on the success of all four base oils with all three emulsifiers, it is reasonable to assume that other oils/emulsifiers might follow the same energy density curve.

TABLE OF CONTENTS

Chapter Page

LIST OF TABLES

LIST OF FIGURES

CHAPTER I

1. INTRODUCTION

"If we're going to develop something new for the Baking Industry, we either must solve a problem that no one else can, find a way to bring new products to market, or find a way to save our customers some money!" declared Mr. Fred Springer, President and Chief Executive Officer for the Burford Corporation. The seed for this research was planted with that statement. Unlike a lot of traditional research projects, this project was funded by the Burford Corporation who employed the author, Mr. Robert Mackey, as their Director of Engineering (and a non-traditional student). The research is an attempt by Mr. Mackey to add, academically, to the body of knowledge and by the Burford Corporation to bring new technology to market. This declaration is made in the spirit of transparency. Some statements regarding the Baking Industry are based on Mr. Mackey's extensive experience (23 years) in the field as a Director of Engineering, Design Engineer, Plant Engineer, Plant Manager, and Project Engineer within the Baking Industry.

While Mr. Springer's declaration is a guidepost for all project development within the Burford Corporation, what made this project, in particular, ripe for the academic plucking is the fact that it likely will solve a problem for the industry in a novel way and it involves science that has yet to be examined in the academic world. In the course of this research, some intellectual property was developed Mr. Mackey and patent protection was filed (Patent

Pending Application Number 2512US00 Dated 8-2-2017) with the Patent Assignment given to the Burford Corporation. As to the scientific principles explored in this research, it is the both Burford Corp. and the author's intent that it provides meaningful assistance to the Baking Industry at large.

The research, like much of the product development at Burford, stemmed from customer feedback. Burford, like it's competitors, manufactures equipment for applying oil to bread pans. Due to the run rates of industrial bakeries, Burford, like it's competitors, uses high pressure or hydraulic atomization of the release agents applied. The technology, in general, works well, but produces overspray. This is a problem for the bakeries as this oil tends to deposit itself in undesirable locations (on the floor, on the equipment, in the overhead spaces) and produces a sanitation nightmare and the potential for product contamination. Bakeries combat this with mist collection systems, but they are not 100% effective and bakeries generally don't like them. The feedback, from Burford's customers, was to build a better mousetrap.

The use of Electro-hydrodynamic (EHD) spraying as a method to coat industrial bread pans holds a lot of appeal. The Coulombic effect of charging liquid particles inside an electric field and having them self-attract to the bread pan (collector) could potentially mitigate the overspray problem. However, several challenges must be overcome for this to be a viable solution. First, vegetable oil (Palm, Soybean, Rapeseed, or Sunflower), is not electrically conductive. Second, EHD research has been limited to mass flow rates that are insufficiently low for the run rates of industrial bakeries. Finally, technology has not been developed to spot spray in concert with EHD atomization. However, based on an exhaustive review of the literature, there is a scientific basis for further research. Some work has been done with EHD spraying of soybean oil. By building on this research, and the research of others, it is hopeful that a new and novel approach to pan oiling can be discovered.

1.1. GENERAL DESCRIPTION

The application of vegetable oil as a release agent in baking allows for the successful removal of bread products post baking. Without such aid, the irregularities in the surfaces of both the bread and the pan creates friction that cannot be overcome by traditional depanning devices. Traditionally, this surface interaction is overcome by applying a thin layer of release agent to act as a barrier between the bread and the pan. Conventional oil applicators use one of several methods to atomize the oil for coating the pan prior depositing the wet dough into the pan. These methods include hydraulic or pressure atomization, air assisted atomization, and mechanical atomization. These methods have been used for roughly a hundred years in industrial baking and provide sufficient performance in their application.

A problem exists with conventional application methods. Conventional oil applicators produce a significant amount of overspray. Overspray, in bakeries, end up depositing in undesirable areas such as along conveyors, in overhead areas, and on the floor. Oil on the floor creates an unsafe condition for employees who work in the area. Oil attracts other airborne particulates onto the equipment creates a sanitation issue that must be cleaned with special cleaners. Oil above a product zone creates a risk of contamination as it is prone to drip back onto the product. Bakeries have tried to combat this problem for years with covers and mist collectors. While these solutions provide some remedy, the problem has never been completely solved.

Stokes law tells us that aerosol particles behave according the physics. In Stokes equation (Stk), the dimensionless number is driven by the density of particles, the diameter of particles, the exit velocity of the nozzle, the viscosity of the air the fluid is sprayed into, and the jet diameter of the fluid leaving the nozzle. If we examine the product of Stokes number (Stk) and π/2, we get an impaction efficiency that is the reciprocal of our estimated overspray (as a percentage). Particles with a diameter greater than 6.5 x 10^{-5}meters have nearly a hundred percent chance of impacting the target and particles with a diameter of 2 x 10^{-6} meters have a 99.9 percent chance of becoming overspray (Jayjock, 2012). The percentage of overspray in actual application depends on a number of different factors including viscosity, temperature, type of applicator and geometric conditions of each type, and desired pattern geometry. The best of systems are only 98% efficient. This creates a significant problem for bakers.

The use of electro-hydrodynamic (EHD) spraying has been shown to mitigate the problem of over-spraying of aqueous solutions. With regard to the food industry, some progress has been made in the study of electro-hydrodynamic spraying of soybean oil with a 5-10% soy lecithin additive in a continuous spray application (Aykas & Barringer, 2012). That technology is in its infancy with the very few applications where continuous spray would provide adequate relief, such as Band Ovens, are starting to emerge. However, research thus far has been limited and has not addressed the need for spot-spraying at a greater than static pressure environment. Moreover, research has been limited to soybean oil and lecithin and has not yet examined other the other major commercially available vegetable oils (Palm, Sunflower, Rapeseed). While lecithin is a known surfactant, no other emulsifiers have been examined with vegetable oil to determine EHD performance.

If there were a way to electro-hydrodynamically spot-spray vegetable oil into pan cavities, then the problems regarding human safety, sanitation, and food safety that plague bakers regarding the existing methods could be mitigated. Research into this topic could determine if each of the four major commercially available vegetable oils could be electrically atomized, if atomization by this means is possible, could it be accomplished at the temperatures and pressures required to meet the needs of the baking industry? If these conditions are met, could the release agent be sprayed into pan cavities using a spot-sprayed method?

Answering these questions could provide significant relief to industrial bakers and advance EHD technology into new markets and applications.

1.2. CONCEPTUAL FRAMEWORK

The conceptual framework for this research starts by understanding what success might look like and what components make up such success. Existing research suggests that if EHD spraying technology were developed in use for pan coating that the misting problem associated with pan oiling by conventional means might be overcome. However, in order to do this, it becomes necessary to EHD spray at volumetric flow rates higher than what is currently used in other applications. This creates the first problem that must be overcome. Second, if EHD Spraying is successful in pan oiling, it must be done as a spot-spraying application. Currently, EHD is only employed as a continuous spray application. Finally, if EHD spraying is to be successful in pan oiling, it must overcome the high surface tension of vegetable oils and must be universally effective using vegetable oils of varying types.

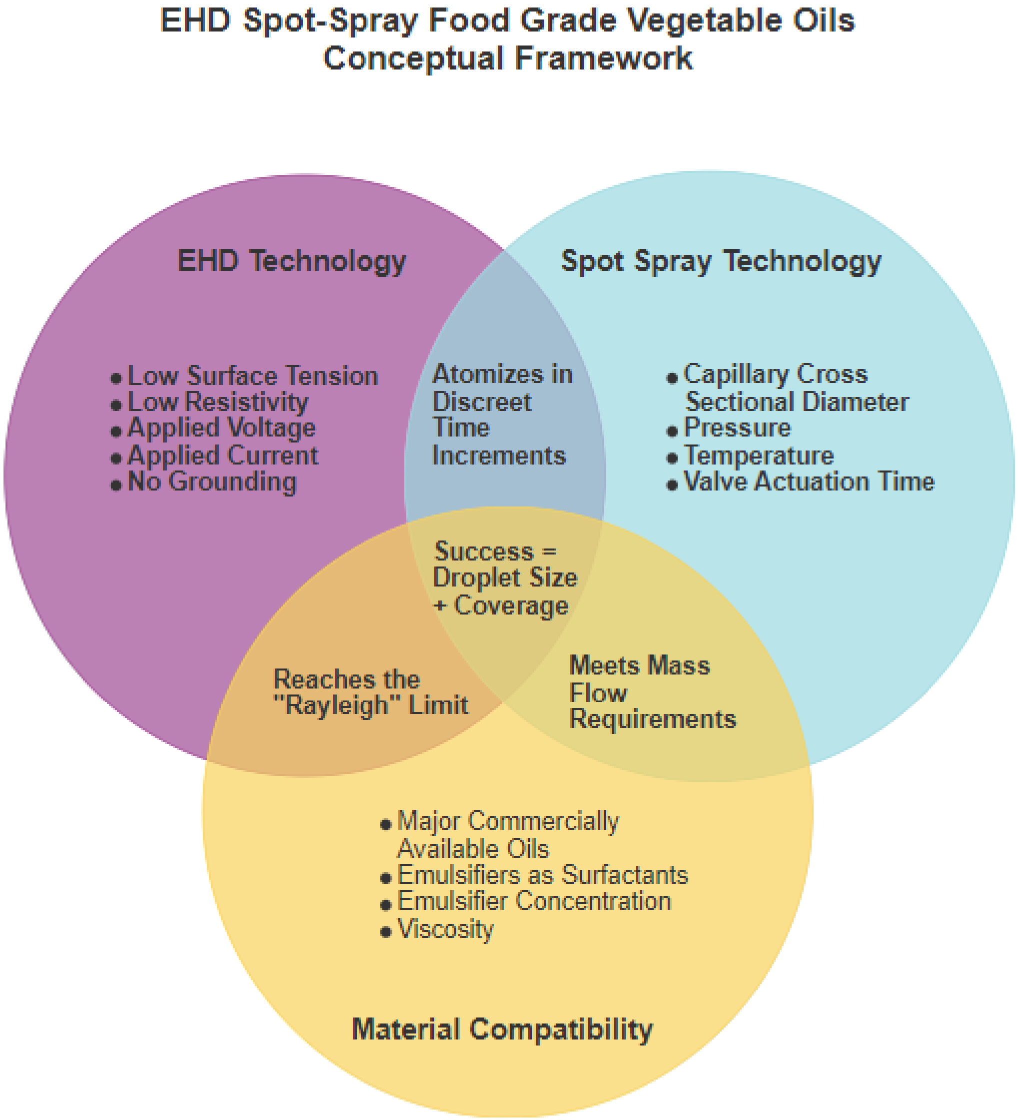

Figure 1: EHD Venn Diagram - Conceptual Framework

In light of the challenges and gaps in current research, what does success look like? Success, assuming EHD technology could be used to spot spray vegetable oil, is providing adequate coverage for the release agent to work in the baking environment. This means that droplet size needs to be sufficiently small with a close enough pattern density as to provide complete coverage of the bakery pan cavity with as thin as film as possible. We know from Stokes Law that droplet size from a jet is somewhat heterogeneous within a range. Success, from the lens of pan oiling would be a range of droplets that are as small as possible but impact closely enough together to provide a consistent thin layer between the dough and the bread pan.

From the Literature Review (see Chapter II), a series of dependent and independent variables were identified as necessary for a successful outcome of the experiment. For the purposes of this experiment, an independent variable is any variable in which the direct manipulation results in a change in output. A dependent variable is any variable in which directly influences the output but is not directly manipulated by the parameters of the experiment. For example, a change in temperature may directly change the viscosity of a fluid and this change may directly result in a change in droplet size. For the purpose of this experiment, both the change in temperature and viscosity change the output, but the experiment only directly alters temperature. Temperature is the independent variable and viscosity is the dependent variable.

1.2.1. Independent Variables

- **Vegetable Oil** – Oil type is an independent categorical variable. In order for the research to translate into a viable universal technology, an examination of the major commercially available vegetable oils must be considered. As of 2017, global production of vegetable oil exceeded roughly 196 million metric tons. Of this production, 171 million metric tons were made up of just four commercially available food grade oils (82.2%); palm at 69.42 tons (35.4% of global production), soybean at 56.15 tons (28.6%), rapeseed at 28.35 tons (14.45%), and sunflower at 17.75 tons (9.05%) (US Foreign Agricultural Service, 2018). Of the four major vegetable oils, only soybean oil has been proven capable of electrohydrodyamic atomization with the addition of the surfactant Lecithin (Aykas & Barringer, 2012).

- **Emulsifier** – Emulsifier is an independent categorical variable. Because surfactants have been proven to lower the surface tension of vegetable oil (Wilkerson, 1989) (Abu-Ali & Berringer, 2004 & 2008) (Abu-Ali, 2004) (Aykas & Barringer, 2012) and allow for EHD spraying (in Soybean oil). Based on this, several other non-ionic surfactants have been selected for testing in the experiment (Soybean Lecithin, Sunflower Lecithin, Polysorbate 20, Polysorbate 80, and Propylene Glycol).
- **Concentration** – Concentration is an independent analog variable. For the purpose of this experiment, concentration was measured as a percentage of the base oil by volume. Abu-Ali and Barringer (2008) studied the optimization of EHD spraying of soybean oil at concentrations between 10% and 15% with voltages of 20-40kV. Studies from Aykas & Barringer (2012) indicate that concentrations in the neighborhood of 5% to 10% by volume produced the most favorable results when a charge of around 40kV. Based on this study, this experiment will test at the same concentrations.
- **Temperature** – Temperature is an independent analog variable. The slip melting point of Palm Oil is around 95F. In research by Aykas and Barringer (2012), they studied EHD performance of soybean oil at temperatures between roughly 40F and 117F and found that EHD performance was improved at higher temperatures. For this study, temperatures of 120, 180, and 240 were selected. At 240F, the temperature is at roughly half of the smoke point of each oil. Additionally, at temperatures above 116, a comparison of how heat affects the experiment can be seen for all four oils. Downer, Hall, Escallon, and Chapple (1993) determined that by manipulating the temperature

of soybean oil that they lowered the resistivity of the oil. This is critical in achieving EHD atomization of generally insulative oils.

- **Pressure** – Pressure is an independent analog variable. Pressure at a cross-sectional area of the capillary tube will provide a volumetric flow at a given time. Traditionally EHD spraying is accomplished using syringe pumps operating at very low pressure. This is done so that the Coulombic velocity of the liquid can be measured (Abu-Ali, 2004) (Abu-Ali & Barringer, 2004 &2008). Aykas and Barringer (2012) used a continuous spray apparatus that was able to achieve slightly higher mass-flow rates (9.91 g/minute). To be viable as a pan oiler in the baking industry, each spray valve must be able to output between 15-60 g/minute. For the experiment, two pressure ranges were explored (1psi, 2psi, 4psi for 22ga vs 4psi, 8psi, and 16psi for 19ga).
- **Capillary Cross-sectional Area** – Capillary area is an independent categorical variable. The cross-sectional area of the capillary is the determiner in mass flow. As the experiment is holding time constant (based on the need to cycle at a given rate), the two variables that impact mass/volumetric flow (measured as weight at a fixed spray time), become pressure and cross-sectional area. For this study, two varying capillary sizes are to be examined (19ga and 22ga). The pressure for each capillary size will be determined by the volumetric output at various pressures for a fixed time.
- **Voltage** - Voltage is an independent analog variable. Voltage applied is considered by many researchers as the most important factor in achieving EHD atomization (Bailey, 1974 & 1981 & 1988) (Abu-Ali & Barringer, 2004 & 2008) (Aykas & Barringer, 2012). Voltage is the mechanism by which the charge is carried to the droplets. When a charge

exceeds the Rayleigh limit, EHD atomization occurs (Gaultney et al., 1987) (Wang, 2012) (Abu-Ali & Barringer, 2008).

1.2.2. Dependent Variables

- **Surface Tension** – Surface Tension is a dependent analog variable. It is impacted by temperature, the emulsifier type, and emulsifier concentration. While most impactful variable to EHD spray capability (Aykas & Barringer, 2012), it is required as a pass/fail for EHD spraying. The surfactants blended into the oil work directly to lower the surface tension of the base oil thereby weakening the interfacial forces applied at the surface of the liquid (Wisdom, 2004). Temperature greatly influences surface tension on a liquid and can be modeled by Eötvös rule (Adam, 1941). Moreover, the Rayleigh limit (critical point of the fluid) is directly influenced by the surface tension (Bailey, 1974).
- **Viscosity** – Viscosity is a dependent analog variable. Viscosity is a representation of the ionic mobility of a substance. Research has shown that, in edible oils, as viscosity lowers, electrical conductivity increases (Kumar et al., 2011). Viscosity is directly influenced by temperature and can be seen via Reynold's equation (equation 20).
- **Resistivity** – Resistivity is a dependent analog variable. Resistivity has been cited as the most important factor in EHD atomization (Downer at al., 1993) (Abu-Ali, 2004) (Aykas & Barringer, 2012). Resistivity in food grade oil is influenced by temperature (equation 25) and the content of an emulsifier (Aykas & Barringer, 2012). Electrical conductivity of a fluid is also influenced by viscosity (Adamczewski, 1969).

1.2.3. Outputs

- **Droplet Count** – droplet count, measured as the number of independent droplets per square inch of sprayed surface, gives an indication of how well the oil/emulsifier blend is atomizing. A higher droplet count, and subsequent droplet pattern density, is an indicator that EHD forces are breaking the liquid into smaller and more numerous droplets. For the purpose of this experiment, the droplet count will be measured empirically as the number of droplets in the defined area of the oil sensitive paper target.
- **Droplet Size** – droplet size has been used as a measurable output (Bailey, 1974 & 1981 & 1988) (Jayasingh & Edirisingh, 2002) (Abu-Ali & Barringer, 2004 &2008) (Aykas & Barringer, 2012). For the purpose of this experiment, droplet size will be measured as the area of the droplet on an oil sensitive paper target. It is desirable for the droplet size to be as small as possible while not falling prey to becoming overspray (droplets that do not land in the targeted area).
- **Coverage Area** – Coverage area is the area within the test target area that is covered by the sprayed medium. This can be measured empirically or represented as a percentage of total area. While true success would require trials in a bakery and exceeds the scope of this research, relative success can be measured as a comparison of the data in its entirety.
- **Weight/Mass Flow Rate** – The amount of oil/emulsifier blend that is sprayed per unit of time can be measured as the Mass Flow rate (measured as weight at a fixed spray time). Because time, system pressure, and the cross sectional area of the depositor's

capillary tube are variables to the process, mass flow is an output from the process. From the perspective of the Industrial Bakery lens, successful ‘Mass Flow’ would be any discrete deposit that sprayed greater than 15 grams per minute. For the purpose of the experiment, sprayed liquid was weighed to determine mass flow.

1.3. CRITICAL ANALYSIS AND REVIEW OF LITERATURE

Understanding EHD atomization and determining whether it can be applied to vegetable oils starts with a tour of the physics and it can be explained through the equations that govern the science. Bailey (1974) and Wang et al. (2012) provide a solid understanding of the central equation to EHD atomization with a review of Rayleigh’s limit (see equations 5 & 6). The Rayleigh limit is the point in which a liquid becomes critically unstable and by which any additional charge will cause the liquid stream to break apart. From Rayleigh’s limit equation, we know that applied charge, surface tension, the liquid jet’s or droplet’s diameter, and the permittivity of the gas in which the jet passes through will dictate the critical point for the liquid. Since air constitutes, exclusively, the gaseous medium for this application, the two variables to consider are applied charge and surface tension. In this case, as the surface tension decreases, so does the charge required to reach the critical point.

With respect to atomizing vegetable oil via EHD atomization, scientific opinions differ as to which of the two, charge (voltage) or surface tension, play a more significant role, but the science holds that the surface tension must be in the appropriate range for EHD atomization to occur (Abu-Ali & Barringer, 2004 & 2008) (Aykas & Barringer, 2012). As vegetable oil is generally considered an insulator, this is the first challenge that must be overcome (Martin et al., 2017). In research by Abu-Ali (2004), Abu-Ali and Barringer (2004 & 2008), and Aykas and Barringer (2012), the use of the emulsifier ‘Lecithin’ has enabled soybean to reach the critical point when a charge is applied. It stands to reason that lecithin, or other surface active agents, could be used to lower the surface tension of other vegetable oils. It is also important to examine the other half of Rayleigh’s limit; the applied voltage. More of the available literature than not suggests that voltage is the most important factor in achieving EHD atomization. The study by Aykas and Barringer (2012) has shown that 40kV produced the best EHD atomization as measured by droplet size and pattern density. However, the study incrementally increased voltage and 40kV was the highest voltage applied in the study.

Studies involving EHD spraying and vegetable oil have been limited to soybean oil and lecithin as the surface active agent (surfactant). Sheryl Barringer has teamed up several times to research the subject (Abu-Ali & Barringer, 2004 & 2008) (Aykas & Barringer, 2012). Barringer and Sumonsiri (2015) wrote a white paper outlining the totality of research involving EHD atomization in the food industry. They cited seven different studies where liquid atomization via EHD has been researched. Of the four studies cited using oil, lecithin was the emulsifier in each case. There is a notable gap in the research involving EHD atomization of oils other than soybean and emulsifiers other than lecithin.

Soybean, sunflower, and rapeseed oils all have very similar melting points (1F to 14F range). While Palm oil has a higher melting point (95F), all four oils have similar densities and kinematic viscosities (See Table 2) (Bailey, 2005). The combined production for all four vegetable oils equates to over 87% of global production (US Foreign Agricultural Service, 2018). While there is a gap in the research regarding EHD atomization and palm, rapeseed, and sunflower oils, they constitute the majority of world production and it is reasonable to believe that these oils may perform similarity to that of soybean oil. Any technology that means to be universally viable must consider all four of the major commercially available food grade oils.

Several complex relationships occur in viscous liquids. First, there is a relationship between the use of emulsifiers that lower surface tension and the resistivity of oil/emulsifier blends. As the active energy of the oil's surface decreases, the resistivity of the fluid decreases. As the resistivity decreases, droplet size decreases (Wilkerson & Gaultney, 1989). Moreover, temperature also plays a role in lowering the surface tension of a liquid. At temperature increases, the surface tension of a liquid decreases. This is demonstrated by Eötvös rule (see equation 24) (Adam, 1941). Temperature also directly influences viscosity. As temperature rises, the viscosity of a liquid decreases. The discovery, made by Osborne Reynolds in 1886, can be demonstrated mathematically as an exponential relationship between temperature and dynamic viscosity (see equation 20) (Falkovich, 2018).

Lecithin is produced naturally in soybeans and sunflower plants (Gunstone, 2011). Refined soy and sunflower lecithin are obvious choices as emulsifiers for these oils. Rapeseed and Palm, however, offer no surfactant byproducts. With the negative stigma around Lecithin and GMOs (Soybeans), some countries, such as the United Kingdom, have strict laws regarding the domestic production of GMO oils (Feikert-Ahalt, 2014). A gap in the research exists with respect to emulsifiers other than soy lecithin. This means that alternative emulsifiers will need to be tested to determine their effectiveness as a surfactant in oil/emulsifier blends. Using the Hydrophile - Lipophile Balance (HLB) number of common food grade emulsifiers might be a good starting point for determining other surfactants that may also work with these oils. This means using a non-ionic surfactant and staying within the oil-in-water range of greater than 6 on a scale of 0-20 (Gaonkar et al., 2014). Propylene Glycol should also be considered as it is a weak emulsifier used in the food industry that generally has no HLB number.

Reaching the Rayleigh point is only half the battle with EHD atomization. Once EHD atomization is achieved, the spray pattern will follow one of 10 different spray modes. Cloupeau and Prunet-Foch (1990) and Jaworek & Krupa (1998) have studied the various modes in depth. Because of the desirable droplet size and pattern, the cone-jet mode is the most desirable. In this particular mode, viscosity plays a significant role in maintaining kink varicosities (the condition required to produce the best spray characteristics in cone-jet mode). Jet diameter and droplet size also contribute greatly to maintaining kink varicosities (Cloupeau & Prunet-Foch, 1994). Emulsifier concentration should have some impact on lowering viscosity as surfactants are lower in viscosity than oils. However, since viscosity, resistivity, and surface tension are all greatly influenced by temperature (see equations 20, 24, 25 and table 2), exploring the impact of temperature on the oil/emulsifier blend should be considered.

Mass or Volumetric flow rate in an important factor in determining the viability of EHD spraying as a technology in the baking industry. Traditionally, research regarding EHD spraying has been at low mass flow rates. In the study by Abu-Ali and Barringer (2004), samples were ran at 27.5 g/min and 47.5 g/min at 35kV. In Abu-Ali and Barringer (2008), samples were ran at 15 g/min at 35kV. In Aykas and Barringer (2012), samples were ran at 9.91 g/min at 40kV. The research has shown a trend of actually reducing mass flow rate to achieve progressively better results. In order to meet the demands of industrial bakeries, a mass flow of between 15 g/min and 60 g/min will need to be achieved (measured as weight at a fixed spray time),. To do this means finding the right combination of pressure and cross sectional diameter of the depositor’s capillary tube.

In the above examples, a charged rake and conveyor were used to spray the test samples. The rake provided a continuous waterfall flow and the samples passing under it. In other research, a syringe pump and charged capillary tube was used. This method also involves continuous spraying and moving the target through the path of the spray. The charged rake method, developed by Sheryl Barringer and associates was able to produce EHD spraying at much higher mass flow rates than the syringe pump method used by Bailey and Balachandran (1981), Jaworek and Krupa (1998 &1999), or Hartman et al. (1999 & 2000). None of these systems, however, were able to deposit on intermitted discrete targets or ‘spot-spray’. That is to say that none of the previous testing turned the spray on and off in a cycle.

In industrial bread bakeries, a baking pan consists of clusters of discrete pockets where dough is deposited and then sent through the baking process. It is important that any technology used to deposit release agents into the pans be able to do so on a spot-spray basis. Bakery pans are typically not cleaned between baking cycles and overspray onto the pan can lead to carbonization and a deterioration of the pan glaze (Atchley, 2014). This shortens the life of the pan between glazing cycles and results in the bakeries needing to re-glaze the pans prematurely (increased cost of operation). There is a gap in existing research as it involves EHD spot-spraying. This suggests that technology may need to be developed to meet this need.

1.4. PROBLEM STATEMENT

Conventional methods for the deposition of release agents into pans in a bakery environment result in an overspray condition. Available methods of generating a fine mist for the even application of release agents include; Air Assisted Atomization, Hydraulic or Pressurized Atomization, and Mechanical Atomization. These methods, in the process of generating an atomized spray, produce a fine mist that doesn't land in the intended target area. This spray, within the industry, is known as 'overspray'. While technology, such as mist collectors, have sought to mitigate the problem, it is impossible to create an environment where stray droplets from overspray do not come into contact with unintended surfaces. This raises the potential for the contamination of food goods. In fact, the desirable condition of creating fine droplets for evenly distributed pan coverage furthers the overspray phenomena predicted by Stokes law (Jayjock, 2012).

Because bakery pans are made from highly conductive materials, one possible solution to the overspray problem is the use of Coulombic attraction of charged liquid droplets in an electric field (electrostatic spraying). Electrostatic spraying comes in two general varieties. The first involves charging particles atomized by conventional means post atomization. Given the short distance between spray nozzle and target, this method is generally unfeasible. The second method involves conductively charging the fluid prior to spraying. This less popular method is known as Electro-Hydrodynamic atomization. This method, as a solution to bakery overspray, has some scholarly basis. Successful research involving soybean oil and lecithin has been conducted by Abu-Ali (2004), Abu-Ali and Barringer (2004 & 2008), and Aykas and Barringer (2012).

For any solution to be viable in an industrial baking market, it needs to be able accomplish three things:

1. Vegetable oils being generally recognized as electrical insulators, EHD spraying technology needs to be made compatible with the top four (4) commercially available vegetable oils. Additionally, a wider range of emulsifiers needs to be identified as viable surfactants to aid in lowering the surface tension of the base oil.
2. EHD spraying technology needs to be made capable of discrete intermittent depositing (spot spray) at a mass flow rate (measured as weight at a fixed spray time), and cycle speed fast enough to be competitive with conventional alternatives
3. Droplet size needs to be sufficiently small and pattern droplet density sufficiently close enough together to provide adequate coverage of the release agent for a pan oiling application.

1.5. RESEARCH QUESTIONS AND HYPOTHESIS

1. Can the top four (4) commercially available vegetable oils (Soybean, Rapeseed, Sunflower, and Palm) be made to carry a charge with the addition of food grade surfactants?
    a. Hypothesis 1: All vegetable oils have common enough physical characteristics so that the addition of a surfactant (such as Lecithin) will lower the surface tension and resistivity enough to carry a charge. This assumption is based largely on the research by Aykas and Barringer (2012) where emulsifier

    concentration, applied voltage, and temperature produced varying droplet sizes in soybean oil and lecithin EHD testing.

    b. Hypothesis 2: Palm oil will not perform the same as the other three major vegetable oils. This assumption is based on the fact that Palm oil has a much higher kinematic viscosity at lower temperature than the other oils. Palm oil is the only one of the four vegetable oils that is not liquid at room temperature.

2. Can spot spray technology can be made to work with EHD spraying?

    a. Hypothesis 1: Because syringe pump testing of EHD spraying systems have been done at close to static pressures, initial velocity at the capillary tube discharge face need not be very high to achieve EHD atomization. This assumption is based on the syringe pump fluid train used in EHD research by Bailey and Balachandran (1981), Jaworek and Krupa (1998 &1999), or Hartman et al. (1999 & 2000).

3. What is the relationship between mass flow rate and the energy required to electro-hydrodynamically atomize good grade vegetable oil? Can flow rates greater than 15 g/min successfully EHD atomize?

    a. Hypothesis 1: EHD atomization is a function of surface tension and applied voltage at a given flow rate. This creates an energy density per unit measure that can be manipulated by further lowering the surface tension (adding more surfactant) or increasing the voltage to balance the energy density required for atomization.

   b. Hypothesis 2: EHD atomization can be influenced by the temperature and resistivity of the liquid and raising the temperature will lower the resistivity of the liquid and allow the atomization at higher mass flows.
   c. Hypothesis 3: Increasing sizes of capillary tubes (cross sectional facial surface area) will allow for more mass flow at a lower pressure due to the time the fluid has to charge in the system prior to exiting the capillary.

4. Can emulsifiers other than Lecithin be used as a surfactant in lowering surface tension of the base oil?
   a. Hypothesis 1: All surfactants lower the interfacial energy needed to resist droplet breakup (Rosen & Kunjappu, 2012) and, as such, any food grade emulsifier with an HLB value greater than 6 will work. This is based on the "more is more" approach.
   b. Hypothesis 2: Only surfactants with an HLB value similar to that of Lecithin (HLB 7-8) will work as they are in the 'wetting' range (6-12) of the HLB scale. This is based on the fact that all of the existing research in EHD spraying of vegetable oils has used Lecithin as the emulsifier.
5. What is the relationship between the different input variables (concentration of emulsifier in solution, voltage, temperature, and pressure) and the outputs (droplet count, droplet size, area coverage percentage, and sample weight)??
   a. Will be determined by applying Design of Experiments to the varying factors of the experiment and performing a full factorial ANOVA.

CHAPTER II

2. LITERATURE REVIEW

A review of available literature has shown that there is extensive research regarding electrostatic spraying (in the general sense). Conventional electrostatic spraying, the use of mechanical, hydraulic, and pneumatic atomizers to charge liquids by spraying into an electric field, has been widely documented. Research on Electro-Hydrodynamic (EHD) spraying, atomization of liquid into droplets through electrical atomization alone, is a much narrower field. Research on EHD spraying for food applications is a very narrow field. EHD spraying of low conductivity vegetable oils has been limited almost exclusively to soybean oil with the use of lecithin as an emulsifier. The research that exists has largely been focused on using oil with a water/emulsifier blend to deliver coatings for the food industry. Research concerning the use of EHD technology to deliver food grade oil as a release agent does not exist. Research on ‘spot spraying’ using EHD technology does not exist.

Finding academic works regarding the tertiary support for this research has been easy and information is abundant. This includes research on the properties of oils, emulsifiers, surfactants, and conventional spraying technology. Research into release agents and technology is scarce in academic circles but available in industry trade publications. Some of these trade publications have been cited in this review. This is less for the academic information they provide and more for understanding industry needs.

2.1. ELECTRO-HYDRODYNAMIC (ELECTROSTATIC) ATOMIZATION

The ability to charge particles, solid or liquid, and use electromagnetic attraction (Coulombic force) to move those particles from one location to another continues to be a promising and still emerging technology. From its origins as a scientific curiosity in the in the mid-17th century to its mainstream use in industrial coating by the late 19th century, the field of Electrokinesis offers large opportunity for the manipulation and control of particles and fluids in a wide variety of applications and industries.

In low volume applications such as crop spraying and horticulture or sanitizers for food surfaces, often low pressure dispensing, <20psi, and low pressure air assisting, <0.05psi, are used to atomize fluids. While operating pressures are generally much lower than those of their high volume cousins, one defining characteristic of this method is that the charge is generally introduced conductively in the fluid path flow prior to exiting the nozzle (Lyons, 2010). In Flow-Limited Field-Injection Electrostatic Spraying (FFESS) applications, or Electro-hydrodynamic spraying, the formation of droplets occurs at the opening of the capillary tube and are solely due to the charge applied. The results can produce nanoparticles with very controllable morphologies that can be used for producing a very fine film (Gu, 2009).

The problem at hand presents three challenges. First, the conductivity of oil (an insulator) is too low without an additive to carry a charge and must be raised to the atomizable range (~10^{-9} to 10^{-12} S/m). The second challenge is that, in order to fit the application of a release agent in a bread baking application, the technology must be viable using more than one vegetable oil (palm, rapeseed, sunflower, and soybean). Thus far all research regarding the application has been limited to soybean oil and lecithin. Finally, the application must be able to target and apply a coating to discreet and indexed targets (pan cavities). This means that the technology must spot spray, at least, 60 cavities per minute to be commercially viable for industrial baking.

2.1.1. History of the Technology

If you've ever rubbed a balloon against you head and stuck it to the wall then you've personally experimented with electrostatic attraction (Coulombic force). This 'natural charging' is quite common in nature and is seen extensively with when water sprays are exposed to air such as with waterfalls or oceanic spray. This happens because the earth is charged negatively with respect to the atmosphere. In fact, on a normal day, the earth carries a charge of roughly 130 V/m at its surface (Bailey, 1988).

When N. J. Felici conducted his experiment on the Electrostatic Spraying of Water in 1859, he observed, quite by accident, that blood didn't flow normally from the electrostatically charged human body when cut. It actually sprayed! Because of this, some of the initial experiments in the field were conducted with human blood (Bailey, 1988).

William Thomson, the 1st Baron Kelvin, demonstrated this phenomenon with his Kelvin Water Dropper experiment in 1867 (see Fig 1). Two independent streams of water droplets fall from a common earth grounded reservoir into two metal containers. These containers are each connected to a ring that the water from the opposite supply must pass through. As the water falls, a charge is induced in both streams and on the surface of the metal containers (negative on one and positive on the other).

Charged droplets will start to deflect from the ring as a potential difference builds between the two surfaces. Eventually the potential difference builds to between 10-20 thousand volts. As this voltage starts to build, an appreciable amount of charge is conveyed to each droplet and each droplet experiences an increase in the downward force. Thusly, droplets start to break apart and fall at an increased rate (Bailey, 1988).

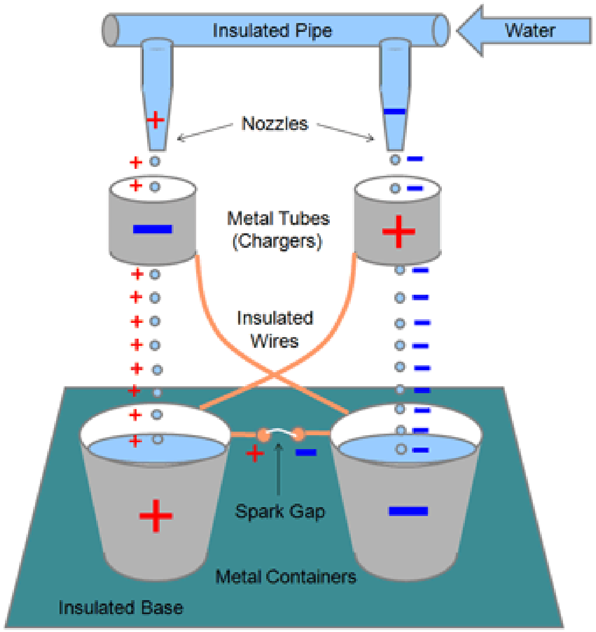

Figure 2: KELVING WATER DROPPER EXPERIMENT

In 1908, a Russian scientist by the name of F.F. Reuss discovered that ionically charged clay particles could be enticed to move. With this discovery, the field of electrokinesis and, subsequently, Electrostrictive hydrodynamics was born (Wall, 2010). The science remained largely academic until the early twentieth century. In 1931, a college dropout named Harold Ransburg discovered that charged fluids could be used in industrial spray applications. Ransburg postulated that, since oppositely charged particles were attracted to one other, particles with the same charge must thusly repel and that this phenomenon could be used with painting applications. He also reasoned that, if a work piece was oppositely charged from that of the spray, the charged paint particles must attract themselves to it. In his experiments, he was able to achieve a better than 90% transfer efficiency. This was largely due to the ‘wrap’ phenomenon in electrostatic spraying. Particles that miss the workpiece are attracted back to it and will change trajectory to satisfy this electrical affinity. His discovery reduced overspray and lowered the cost of materials compared to conventional spray applications (Rupp et al., 1999).

Today, electrostatic spraying and powder coating is using ionic attraction (Coulombic force) in a wide variety of applications to provide better coverage with less waste than by conventional means. Applications range from spraying crops to coating foods to uses in organic mass spectrometry (electrostatic spray ionization).

2.1.2. Electro-Hydrodynamic (EHD) Theory

There exists an important distinction between EHD spraying and conventional electrostatic praying. With conventional electrostatic spraying, such as that used in painting and powder coating applications, a spray is generated by conventional means (via pressure, air, or centrifugal force) and that spray then passes through an electric field thus picking up a positive or negative charge creating an ionic spray. In EHD spraying, the liquid is conductively charged prior to exiting the nozzle (or capillary tube) and the charge (positive or negative) creates a jet cone that is exposed to an electric field that deforms the jet and disrupts flow into droplets. The breakup of the droplets and their movement towards the oppositely charged collector is almost entirely due to the electrical potential conduced and/or induced and no other forces are needed to achieve liquid atomization (Jaworek, 2007).

While different authors often interchange the terms, for the purpose of this paper, ‘Electrospraying’ or ‘EHD Spraying’ will refer to Electro-hydrodynamic spraying and ‘Electrostatic Spraying’ will refer to all forms in the general sense. Conventional Electrostatic spraying (requiring mechanical atomization) such as the types used in paint and powder coating applications will be specifically called out as such as needed.

One advantage of EHD spraying is that it allows for the generation of extremely fine droplets. Droplets produced from EHD spraying can reach as small as one half of the Rayleigh limit. The Rayleigh limit in electrostatic spraying is the magnitude of the electrical charge on the surface of a droplet required to overcome the surface tension. A droplet becomes unstable when it reaches the Rayleigh limit and starts to disintegrate into smaller droplets. This means that the size of a droplet can be controlled to some extent by adjusting the voltage and flow rate applied to the EHD process (Vantzos & Betelu, 2006) (Jayasingh& Edirisingh, 2002).

Atomization occurs by making the surface of a droplet unstable. When this happens, the surface ruptures into filaments that disintegrate into smaller droplets. Atomization occurs because of the mutual repulsion of net charges accumulation on the surface of the droplets. Electrostatic stress expands the surface area against the resisting force of the surface tension. When electrostatic stress exceeds the resisting force of the surface tension the droplet becomes unstable and atomizes. If surface charges continue to

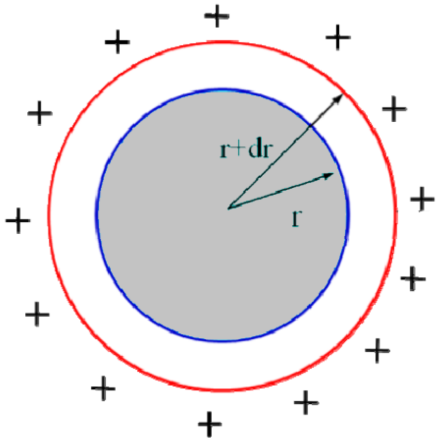

Figure 3: Diagram of a charged liquid droplet

accumulate causing the electrostatic stress to remain greater than the resisting force of the surface tension then the process of atomization will continue to occur (Wang et al., 2012).

According to Wang (2012), if we examine a single droplet we can determine the instability condition required atomization. If a droplet with a radius of 'r' has a surface charge of 'q', the intensity of the electrical field, $E_{i,}$ that it generates can be calculated using the permittivity of vacuum, $\varepsilon_{0,}$ and the distance to any point in space, r_i:

Equation 1: Wang's Instability Equation of a Droplet

$$E_i = \frac{q}{4\pi\varepsilon_0 r_i^2} \tag{1}$$

Integrating equation (1) from negative infinity to 'r' gives us the voltage (electrical potential) for the droplet:

Equation 2: Voltage Requirement for Droplet Instability

$$U = \int_{-\infty}^{r} \frac{q}{4\pi\varepsilon_0 r_i^2} dr_i = \frac{q}{4\pi\varepsilon_0 r} \tag{2}$$

By integrating equation (2) from 0 to the charge, q, we can determine the electrical energy on the surface of the droplet:

Equation 3: Electrical Energy on the Surface of a droplet

$$W = \int_{0}^{q} \frac{q}{4\pi\varepsilon_0 r} dq = \frac{q^2}{8\pi\varepsilon_0 r} \tag{3}$$

The total energy on the droplet is equal to the electrical energy on the droplet and the energy from the surface tension,γ, so that:

Equation 4: Total Energy in a Droplet

$$W_{total} = (\gamma \cdot 8\pi r) - \frac{q^2}{8\pi\varepsilon_0 r} = 0 \tag{4}$$

Finally, the Rayleigh's limit equation is defined by q_{crit} which represents the critical charge, γ which represents surface tension, and where η represents the Rayleigh limit coefficient (Wang et al., 2012):

Equation 5: Rayleigh's Limit Equation using Rayleigh Limit Coefficient

$$q_{crit} = \eta \cdot 8\pi(\varepsilon_0 \gamma r^3)^{1/2} \tag{5}$$

The Rayleigh limit, the governing equation in electro-hydrodynamics, is most commonly presented without the coefficient as (Bailey, 1974):

Equation 6: Rayleigh's Limit Equation Standard Form

$$q_{crit}^2 = 64\pi^2 \varepsilon_0 \gamma r^3 \tag{6}$$

EHD spraying has several advantages over its mechanical spraying counterparts. First, it can achieve a droplet size much smaller than that of conventional mechanical atomizers (down to 1 µm). Charged droplets tend not to agglomerate and will self –disperse heterogeneously in the target space. Because the droplet is formed by exceeding the Rayleigh limit inside an electrical field, the motion and trajectory of the droplets can be easier to control than by conventional mechanical means. This is done by controlling the electric field of the spray. This means that the overspray problem associated with conventional spraying methods can be overcome. Moreover, the efficiency of deposited droplets in the target area is much higher than by conventional means (>95%) (Jaworek, 2007).

With all of the upside to the technology, there are some drawbacks. Drawbacks of all electrostatic spraying systems include a potentially higher investment costs, working with high voltage poses a potential risk if not handled properly, and not every material can carry a charge (the challenge of electrostatically charging oils and other insulators).

The electric field acting on the liquid is a combination of the potential applied to the capillary tube, E_0, the charged droplets, E_k, and the ionic charge due to electrical discharge in gas, E_i (Jaworek & Krupa, 1999):

Equation 7: Electric Field Acting on a Liquid

$$E = E_0 + E_i + \sum_k E_k \tag{7}$$

Determining droplet diameter, D_d, and current, I, associated with EHD spraying, as it relates to the Rayleigh limit (equation 5) is complex and dependent on the spraying mode. As we are most concerned with the Cone-Jet mode, droplet diameter (8) and current (9) can be expressed for this spray mode where ‘q’ is the charge, ‘σ’ represents conductivity, γ is the surface tension, and ε_0 represents permittivity of a vacuum (Hartman et al., 1999):

Equation 8: Doplet Diameter in EHD Srpaying

$$D_d = 3.78\pi^{-2/3} 0.6 q^{1/2} \left(\frac{\rho\varepsilon_0}{\gamma\sigma}\right) \tag{8}$$

Equation 9: Current Required to Reach Rayleigh Limit

$$I = 4.25\left(\frac{q\sigma\gamma}{\ln\left(\left(\frac{q}{q_0}\right)^{1/2}\right)}\right)^{\frac{1}{2}} \tag{9}$$

Moreover, the flow rate for the electrical charge is equal to:

Equation 10: Charge Flow Rate at Rayleigh Limit

$$\dot{q} = \rho\sigma\varepsilon_0^{-1}\gamma^{-1} \tag{10}$$

Given the combination of cross sectional diameter of the spray tube (capillary), energy introduced into the system, the force of gravity, the physical characteristics of the spray media (conductivity, permittivity, surface tension, viscosity, and dielectric constant), and liquid flow rate, it is important to remember that very few materials have actually been scientifically tested. With a relatively narrow conductively window in which EHD atomization is possible (~10^{-9} to 10^{-12} S/m), most materials (specifically liquid blends) would require scientific testing to know the viability and range for each mode (Jaworek & Krupa, 1998).

Droplet diameter in an EHD system can be calculated a number of different ways. Jaworek (2007) was able to work with Hagiwara's equation (11) (for mean droplet size) as a platform to calculate the mean surface diameter of droplets. This is particularly useful in this experiment as Voltage (U) is one of the variables controlled in our experiment. In Hagiwara's equation, D, the diameter is calculated using, C, a material specific constant,β_i, the materials conductivity, and, v_i, the liquid viscosity.

Equation 11: Hagiwara's Equation for Droplet Diameter

$$D = C * \beta_i^{-.03} v_i^{.04} \tag{11}$$

From this, the equation can be expanded to calculate the volume-surface diameter of droplets produced in Cone-jet mode (Ogata et al. 1977):

Equation 12: Volume Surface diameter of Droplets in Cone Jet Mode

$$\frac{d_{vs}}{D_c} = C * C_a^{\frac{2}{3}} T_i^{\frac{.2}{9}} P_0^{-\frac{10}{9}} S_e^{\frac{2}{5}} + C \tag{12}$$

$$\text{for } \frac{\sigma}{v_i} \leq 10, C = 11.4$$

For equation (12), the following dimensionless numbers are used:

$$C_a = \frac{V_j v_i}{\gamma_i} \tag{12a}$$

$$T_i = \frac{\varepsilon_i}{\gamma_i} \frac{\gamma_i}{D_c v_i} \tag{12b}$$

$$P_0 = \frac{U}{\left(D_c \frac{\gamma_i}{\varepsilon_0}\right)^{\frac{1}{2}}} \tag{12c}$$

$$S_e = \frac{h}{D_c} \tag{12d}$$

Where:

D_c = Outer diameter of the capillary tube

D_0 = Inside diameter of the capillary tube

v_i = Viscosity of the liquid

γ_i = Surface Tension

V_j = Velocity of the Jet

ε_i = Liquid's Permittivity

σ_i = Liquid's Conductivity

U = Applied Voltage

h = Distance between Capillary tube and oppositely charged electrode

P_0 = the minimum voltage necessary to accomplish liquid spraying

There are no less than four additional equations that have been presented since Cloupeau and Prunet-Foch's work that address droplet size in the Cone-jet mode. Using the same variable definition presented for equations 9-12, we have droplet diameter, D:

- (Tomita et al., 1986) determining drop size from Weber and Reynolds numbers:

Equation 13: Droplet Size from Weber and Reynolds Number

$$\frac{D}{D_c} = .025\frac{\sigma_i}{\sigma_0}^{0.05}\left(\frac{D_0}{D_c}\right)^{0.025}\left(\frac{\varepsilon_0 E^2 D_0}{\gamma_i}\right)^{-0.88} We^{0.21}Re^{0.25} \tag{13}$$

- (de la Mora & Loscertales, 1994) determining drop size from constant based on permittivity (denoted as α) and flow rate (denoted as $\dot{q}$):

Equation 14: Droplet Size from Permittivity

$$D = \alpha\left(\frac{\dot{q}\varepsilon_0\varepsilon_r}{\sigma_i}\right)^{1/3} \tag{14}$$

- (Hartman et al., 2000) variant on Loscertales using liquid density, ρ_i, and surface tension, σ_i:

Equation 15: Droplet Size from Liquid Density and Surface Tension

$$D = \alpha\left(\frac{q\varepsilon_0\rho_i}{\gamma_i\sigma_i}\right)^{1/6} \tag{15}$$

- (Ganan-Calvo, 1999) determined from scaling laws:

Equation 16: Droplet Size from Scaling Laws

$$D = \alpha \left(\frac{q^3 \varepsilon_0 \rho_i}{\pi^4 \gamma_i \sigma_i}\right)^{1/6} \tag{16}$$

2.1.3. EHD Spray Modes

While electrostatic spraying was first discovered by Bose in 1745, the science remained largely a mystery until John William Strutt, the 3rd Baron Rayleigh, postulated his theorem on the critical point of a charged droplet in 1882 (Rayleigh limit see equation 5 & 6) (Jaworek & Krupa, 1998). His work set the foundation of understanding in electro-hydrodynamics. A little over a hundred years later, French scientist Cloupeau and Prunet-Foch (1990) established a system for classifying the modes of operation for electro-hydrodynamic spray systems. In their work, they called out the variables that impacted the spray mode including:

- The liquid's physical properties (they placed emphasis on electrical conductivity and the surface tension and viscosity of the liquid);
- The flow rate of the fluid;
- The voltage applied to the fluid;
- The geometry of the system (to include the capillary tube's cross-sectional diameter);
- And the "dielectric strength of the ambient medium".

From their work they identified five different modes that in which an EHD spray system would operate (Dripping, Microdripping, Cone-jet, Simple-jet and Ramified-jet, and Spindle). Their work also explored the transitions from one mode to another.

Microdripping mode moves to Cone-jet mode at an applied voltage, Dripping mode goes to spindle mode, Spindle goes to cone jet, and Cone-jet goes to simple jet. Their experiments utilized water and various organic compounds with very controlled physical parameter. They were able to determine the drip rate per unit of applied voltage for the materials tested and, thus, reinforced Rayleigh's limit and the understanding of how the charge on a jet can predictably determine its behavior (droplet rate and shape). By 1998, the original 5 modes had increased to 10. Building on Cloupeau and Prunet-Foch's work and using high speed imaging, Jaworek and Krupa were able to identify all the known modes of operation (see Table 1).

2.1.3.1. Dripping

Dripping mode behaves much the same with or without voltage applied. Liquid will drip from the capillary in a regular and constant pattern. However, when voltage is increased, droplet frequency will increase and droplet size will decrease. This is due to a decrease in the surface tension and an elongation in the meniscus allowing an increased electrostatic pressure to pull on the droplet. In dripping mode, droplets do not have satellites and will drip at a consistent frequency. Droplet diameter will generally be larger than the capillary diameter. Additionally, the electrostatic field will attract the liquid towards the collector (Cloupeau & Prunet-Foch, 1990).

2.1.3.2. Microdripping

Like Dripping mode, Microdripping produces a drop-by-drop emanation from the capillary tube. Unlike Dripping mode, the diameter of the droplets are smaller in diameter than the capillary tube and generally exhibit low flow rates. Production frequencies are commonly 1-2 orders of magnitude higher then Dripping mode. The meniscus is more or less conical shaped having accumulated fluid. This will often result in an intermittent larger droplet. Because of this, the meniscus may exhibit variable lengths from the periphery of the end of the capillary (Cloupeau & Prunet-Foch, 1990).

Often a filament, only a few micrometers in diameter, will attach itself between the droplets and the meniscus. For fluids with a low viscosity, this filament will break free with the droplet and create smaller sister droplets. For liquids with high viscosity, the filament will withdraw back into the meniscus. The diameter of the micro droplets can be quite small ranging from a few micrometers to a few hundred micrometers and the frequency of release can range up to a few thousand per second. The charge carried by micro droplets can approach 50% of the Rayleigh limit (Jaworek & Krupa, 1998).

2.1.3.3. Spindle

In Spindle mode, the meniscus will elongate in the direction of the electric field (towards the collector plate) and a thick jet of liquid will detach along the capillary axis taking the shape of a spindle of fluid. Often the detached spindle will disintegrate into smaller droplets of varying size and will spread out between the capillary and the collector plate. The meniscus elongates as the spindle is formed and contracts once the droplet has pulled away. As voltage increases, the size of the main droplet will increase but the sister droplets will decrease. With a voltage increase, spindle can migrate to multi-spindle mode. The change will start with two jets and expand. The mode may also change to oscillating-jet mode. Droplet size is usually between 100 and 300 μm (Jaworek & Krupa, 1998).

2.1.3.4. Multi-spindle

Multi-spindle mode is associated only with liquids with high viscosity. In Multi-spindle mode, spindles are only generated periodically from points along the circumference of the capillary's periphery end. Only one spindle is generated at a time and will usually detach and disintegrate into pieces. The number of undetached spindles around the capillary at any point in time is dependent on the characteristics of the fluid being sprayed. Droplets will be uniformly distributed around the axis of the capillary. The number of points that will generate a spindle will increase as voltage increases. Droplet size is generally smaller than those generated in Spindle mode (Jaworek & Krupa, 1998).

2.1.3.5. Cone-jet

The Cone-jet mode has received the most attention in academia due to its usefulness. An EHD system spraying in Cone-jet mode produces a cone shaped meniscus and stream symmetric about the capillary axis with a thin jet at its apex. The jet flows along the capillary axis with very little deflection (less than 10 degrees) and produces droplets of a mean diameter of 30 μm. As the jet pulls away from the capillary it generates one of two types of instabilities (Jaworek & Krupa, 1998).

The two types of instabilities in the Cone-jet mode are Varicose and Kink. Varicose instabilities generate waves on the surface of the jet without changing the jet's linear position. The nodes of the wave disintegrate in to equal droplets which flow close to the axis of the capillary. With Varicose instabilities the average droplet size decreases and the droplet production frequency increases as flow rate decreases and/or conductivity of the liquid increases (Cloupeau & Prunet-Foch, 1990). With varicose instabilities droplet diameter, D_d, is a function of the jet diameter, D_j, and a constant, k, which is a function of viscosity (Cloupeau & Prunet-Foch, 1994).

Equation 17: Droplet Size in a Varicose Instability as a Function of Jet Diameter

$$\frac{D_d}{D_j} = \left(\frac{3k}{2}\right)^{1/3} \tag{17}$$

Kink instabilities result with the entire jet moving irregular off the axis of the capillary. This happens with a high amplitude that breaks the stream into fine droplets. This is due to both electrical and inertial forces on the jet. With Kink instabilities the droplets leave the capillary with a charge that exceeds the Rayleigh limit. At higher voltages, the jet breaks up into fine droplets of vastly different sizes. Kink instabilities often occur at higher flow rates (Cloupeau & Prunet-Foch, 1990).

For liquids with high conductivities, the cone and jet formation remain close to the axis of the capillary and the jet formation occurs at the apex of the meniscus. For liquids with low conductivities, the geometry of the capillary outlet is similar to that of an open cone. That is to say that in the former case a convergent jet is created and in the ladder case a Taylor cone is formed (Jaworek & Krupa, 1998).

It is important to note that Cloupeau & Prunet-Foch give honorable mention to multi-jet and multi-spindle modes but classify them as a variant of the Cone-jet mode. Jaworek & Krupa, however, classify them as independent modes and dedicate more energy into understanding how they work.

2.1.3.6. Oscillating-jet

While the cone and jet in the Cone-jet mode sprays in line with the capillary axis, in the Oscillating-jet mode, the cone and jet oscillate between the capillary axis and the plane tangent to it. The cone will elongate into a thin take with fine droplets breaking away from it. The plane of oscillation is stable, but the cone may move to any point in the tangential plane and may even rotate about the capillary axis. It may also spontaneously change orientation within that plane (Jaworek & Krupa, 1998).

2.1.3.7. Precession

Precession mode is similar to oscillating-jet mode in that the cone forms in the tangential plane to the capillary axis. The cone, however, does not oscillate between planes. It forms a small liquid jet at the apex of the cone (generally smaller than 100 μm). The cone will continually rotate about the capillary axis, but as it draws out thinner and thinner, the jet, itself, will rotate spirally. The spray is fairly uniform, due to kink instabilities, and droplet sizes average between 25 and 60 µm. As voltage increases, the rate that the cone rotates also increases. In tests of distilled water as the medium, the cone rotated between 200 and 300 revolutions per second. The cone and jet act much like the Cone-jet mode with the addition of the rotation around the tangential plane (Jaworek & Krupa, 1998).

2.1.3.8. Multi-jet

In liquids with a low surface tension, it is possible to achieve multi-jet mode. In this mode, the meniscus withdraws and becomes flat to the surface of the face of the capillary tube. Fine cones appear around the circumference of the capillary tube. From these fine jets, a very fine spray is generated. The diameter of these jets can be measured in tenths of a micrometer. Droplets are formed due to kink instabilities. The streams form uniformly around the axis of the capillary and the number of streams (2 to 8) increases as voltage increases. Droplet sizes are extremely small and measure less than a few micrometers in diameter (Jaworek & Krupa, 1998).

2.1.3.9. Ramified-meniscus

In Ramified-Meniscus mode, short irregular jets spread out different lengths and in random directions. Droplet sizes are large and irregular as they tend to be fragments of the jets pulled from the capillary tube (on the order of the diameter of the capillary). Essentially, Ramified-meniscus consists of jets of differing form that emit in different directions. This differs from the ramified jet in that the jets at the face of the capillary tube are unpredictable. This phenomenon general occurs in liquids with a low viscosity. The nature of liquids with low viscosity is such that the liquid can change shape quickly to follow inconsistencies in the electric field (Jaworek & Krupa, 1999).

2.1.3.10. Ramified-jet

In the Ramified-jet mode, liquid flow is higher than most other EHD modes with liquid flow rates on the order of magnitude of a few hundred mm^3/s. In the ramified jet mode, one or more jets will form from at the capillary tube and several secondary jets are generated along the primary jet. The production of droplet size ranges from 100 μm to over 2 mm (Grace & Marijnissen, 1994). Ramified jets rarely appear due to the fact that when voltage increases, the multi-jet mode appears before the electric field on a single jet reaches a high enough value (Cloupeau & Prunet-Foch, 1994).

Table 1: ELECTRO-HYDRODYNAMIC SPRAY MODES

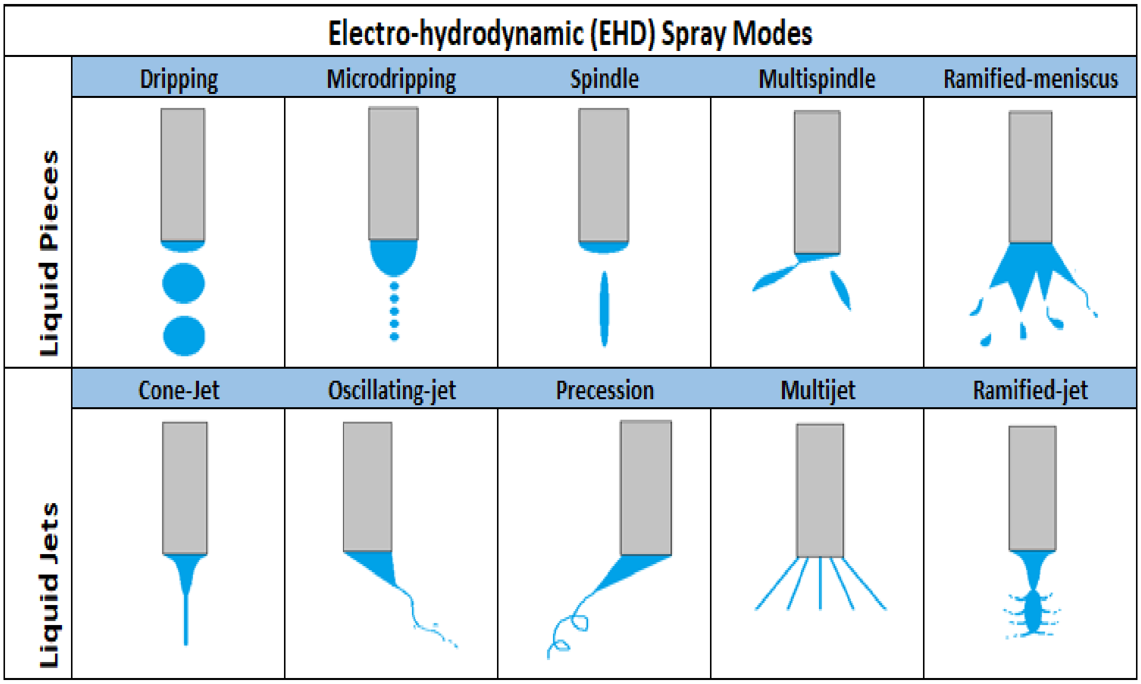

Jaworek & Krupa (1998) point out that only a few of the known modes are useful for practical applications. This is to say that not every mode produces a stable and spatially regular spray. Modes that are stable enough for coating applications include:

- Precession Mode
- Cone-Jet Mode
- Multi-jet Mode
- Multi-spindle Mode
- Microdripping mode

2.1.4. Established Research on the use of EHD and Food Grade Oil

In order for electrostatic spraying technology to be practical in the Baking (food) industry, it must be made to be useful for the application of food grade coating and release agents. While the use of electrostatic spraying or powder coating for food applications is still in its infancy, some progress has been made. According to the annual review of Food Science and Technology, research on powder coating applications includes applying salts, sugars, and starches to popcorn, powdered flavors on candy and chocolate, salt and other powders on potato chips and pork rinds, antimicrobial agents on meats and cheeses, coatings on French fries, and calcium on diced tomatoes (Barringer & Sumonsiri, 2015).

Research on liquid electrostatic coating applications has not been extensive. However, the research that exists includes applying oil and emulsified additives on crackers, applying soybean oil on cheese, milk chocolate, and crackers, applying cocoa butter and other confectionary coatings on glass slides, applying malic, tartaric and lactic acid on spinach, lettuce, and cantaloupe cubes, applying soybean oil on oil-sensitive paper, and applying alginate and chitosan on fresh cut melons (Barringer & Sumonsiri, 2015).

Abu-Ali and Barringer’s (2003) experiments with emulsifiers determined that, while the conductivity of pure oil is to low to electrospray without the addition of a surfactant, adding an emulsifier in the 3-20% range sufficiently lowered the surface tension of the selected food grade oil and emulsifier blend so that the EHD spraying was possible with reproducability. In their experiment, they tested soybean oil, butter, peanut oil, sunflower oil, corn oil, and extra virgin olive oil. In their experiment, the emulsifier (lecithin) was blended with water (5g lecithin in 1ml of distilled de-ionized water). The oil/water blend was mixed at varying concentrations up to 50% and EHD sprayed on various foods including: saltine crackers, graham crackers, club crackers, and glass slides. Water soluble additives were added to the emulsion to determine their effect on EHD spraying performance. Their results showed that reproducibility increased and droplet size decreased as the water concentration of the emulsification increased. Moreover, conductivity increased as water concentration increased (25 kV spraying voltage) producing a better atomization.

Abu-Ali and Barringer (2008) next experimented with soybean oil and emulsified it with lecithin to determine the EHD performance characteristics at varying concentrations of emulsifier and varying flow rates. In their experiment, they tested with voltage (20kV - 40kV), emulsifier concentrations (10 15%), and flow rate (28 - 88 g/s). They targeted 1cm cubes of Colby jack cheese, 5 x 1 cm of chocolate rectangles, and 2.5 x 2.5 cm club crackers. In contrast to Wilkerson and Gaultney's (1989) research which stated that conductivity had the greatest impact on droplet size and charge mass ratio, Abu-Ali and Barringer found that voltage had the highest impact on droplet size and reproducibility. They found that as voltage increased that reproducibility also increased until around 35kV at which point reproducibility started to decrease again. As the charge to mass ratio increases, drop size decreases. This also agrees with Wilkerson and Gaultney. Abu-Ali and Barringer found that conductivity came in second behind voltage as the most impactful to droplet size and reproducibility.

Aykas and Barringer (2012) further experimented with soybean oil and lecithin determining the impact of temperature, voltage, and lecithin concentration on droplet concentration in an EHD spraying system. In their experiment, they sprayed soybean oil and lecithin in concentration of 0-15% lecithin on oil sensitive paper at temperatures ranging from 39 to 116 degrees Fahrenheit with voltages ranging between 0 and 40kV. They found that increasing temperature decreased surface tension, viscosity, and resistivity while also decreasing droplet size. They reaffirmed that voltage had the greatest impact on droplet size followed by lecithin concentration. Droplet size decreased by increasing either voltage or lecithin content.

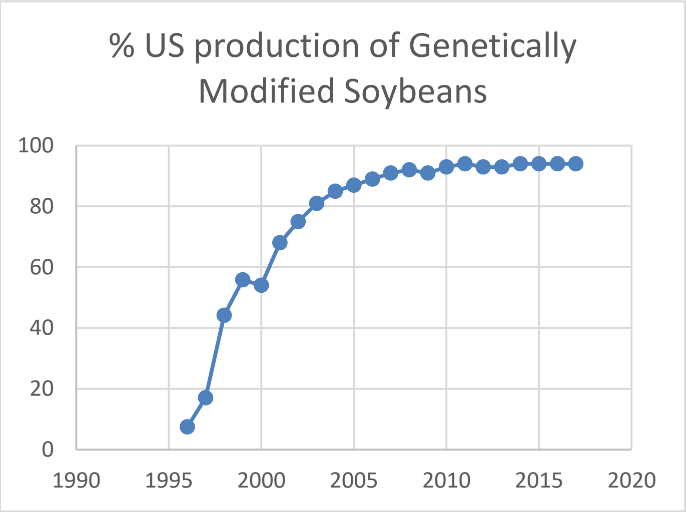

Figure 4: US Department of Agriculture statistics on genetically modified soybean production as a percentage of total production

The research regarding the electro-hydrodynamic spraying of food grade oil has progressively been honed down to soybean oil and lecithin. Early research by Abu-Ali and Barringer included several food grade oils, but the most favorable combination from that research involved soybean oil and lecithin. Subsequent research has grabbed onto this combination and refined the results of earlier work. There exists a gap in the research involving other oils and emulsifiers or surfactants for use in the food industry.

The lack of research involving product other than soybean oil and soy lecithin is problematic as soybean oil is a highly genetically modified organism and, while the particular GMO has been proven to be much healthier than its unmodified cousin, 96% of

US soybean production comes from genetically modified seed stock and consumer fear over GMO’s have created concern in the marketplace (US Foreign Agricultural Service, 2018). Additionally, soy allergies are on the rise, and while it is possible to remove allergen from the oil, soy lecithin cannot be made to be allergen free (Darwin, 2003). Another problem with soybean oil is that, while it is widely available in the US, other areas of world rely on different food grade oils such as palm or rapeseed. In the UK, for instance, while some GMO products are imported, they have restrictive laws on the domestic production of such products (Feikert-Ahalt, 2014).

Because of the different commercially available oil supplies regionally and health concerns regarding GMO’s and allergens, different oils are used for baking depending on the region and the product. As such, it is important to understand the characteristics of different oils and emulsifiers for any universal technology that is developed. Currently, there exists a gap in the research regarding EHD spraying and commercially available oils other than soybean oil and any other emulsifier/surfactant other than soy lecithin.

2.2. SPOT SPRAY

Pan oiling in industrial baking often requires a precise high speed intermittent application of a thin layer of oil commonly known as ‘spot spaying’. Spot spraying allows for oiling individual cavities without over-spray on the areas of the pan that are not in contact with baking products. Conversely, over application can lead to wasted release agent, product on the floor or undesirable areas of the equipment (unsafe environment), carbonization of unused release agent on the pan, and finished product out of specification

(Darwin, 2003). Preventing excess oil on industrial bakery pans reduces the costs of maintenance associated with the pan and can extend the life of the pan (Atchley, 2004).

Currently, spot spray application of food grade oils is performed by mechanical atomization. Hydraulic pressure atomization (airless) and low pressure air assisted atomization (air spray) are the two most widely used methods of apply release agents to industrial baking pans. Both methods are effective but rely on shear forces and air resistance to atomize the product. Hydraulic pressure atomization is preferred where high speed application is required and low pressure air assisted atomization is used with lower speed applications. An example of hydraulic pressure atomization is the cleaning wand at a car wash. If you've ever noticed how water tends to mist and drift in every direction (including on the person washing the car), then you have a good idea of how hydraulic pressure atomization works in bakery pan oiling. While the mist produced is lower than that of a car wash, the problems associated with it causes problems with the bakery such as cross contamination, sanitary issues, slick floors, and capital required for mist collectors.

Currently, there is no available research involving high speed 'spot spray' applications using electro-hydrodynamic spraying. Research regarding EHD spraying has been done at static or very low pressure and generally with very low volumetric flow rates. An opportunity exists in this gap to research and develop solutions to the problems generated by conventional spray applications using EHD spraying technology.

2.3. ATTRIBUTES AFFECTING LIQUID ELECTROSTATIC SPRAY

Electro-hydrodynamics (EHD), often referred to as electro-fluid-dynamics (EFD) or electrokinetics, is the study of the kinematic behavior of electrically charged fluids. Specifically, it is concerned with the motion of ionized particles and their behaviors when introduced to an electric field (Castellanos, 1998). Electrostatic spraying imparts electrical forces to a liquid stream and increases the surface energy to the critical point or Rayleigh Limit (equation 4). At this point, the liquid flow becomes unstable and breaks down into small atomized droplets (Baily, 1974). This ionic mist exhibits two behaviors useful to coating applications. First, because the charged droplets share a common electrical polarity, their natural tendency to repel each other prevents agglomeration of droplets (Aykas and Barringer, 2012) and, subsequently, provides homogeneous and uniform surface coating. And second, their affinity to an oppositely charged surface controls overspray and reduces waste of the spraying medium.

Several factors play into the droplet formation in an electro spraying application that includes viscosity, temperature, surface tension, applied voltage, and electrical resistivity (or its reciprocal conductivity). Of these, the most important to an EHD spraying application is electrical resistivity (Downer, Hall, Escallon, and Chapple, 1993). Electrical resistivity is greatly impacted by temperature and the relationship is believed to be inversely proportional where resistivity drops as temperature increases (Palaniappan and Sastry, 1991). That is to say that ionic mobility determines the resistivity of a fluid. Higher temperatures increase the kinetic energy of a liquid and, therefore, result in greater ion mobility and lower resistivity.

Unfortunately oil's relatively high viscosity and low smoke point make it a poor choice, on its own, for EHD spraying. This can be overcome by the addition of an non-ionic emulsifier to the oil's base. Emulsifiers, such as Lecithin, lowers the resistivity of the solution to within a range of 10^5 to 10^9 Ωm (Abu-Ali and Barranger, 2005). Lowering the resistivity both improves the electro hydrodynamic properties of the solution and decreases the droplet size in electro spraying. This effect occurs because a lower resistivity allows for a greater charge, and subsequent difference of potential, to be carried on the surface of the fluid (Baily and Balachandran, 1981).

Another factor impacting resistivity of oil is the temperature in which it is sprayed. As the temperature of a solution is increased, its resistivity lowers. This is due to the fact that higher temperature solutions carry more kinetic energy at the molecular level. The surface tension of a liquid oppose the electrical forces that break the liquid into droplets. With most liquids, increasing the temperature will result in a lower surface tension and produce smaller diameter droplets. Emulsifiers work to lower the surface tension of liquids while higher temperatures lower the viscosity. Both are required to bring oil into the sweet spot for electro spraying.

For the proposed experiment, the desired response is an electro resistivity that is within the prescribed band width so that droplet size, coverage, adhesion, and trajectory are suitable for pan oiling. For this experiment, it is important to examine several factors. The first factor to consider is the oil media. Within the industrial baking industry, four commercially available vegetables oils are predominately used as a release agent. These include Palm oil, Rapeseed oil, Soybean oil, and Sunflower oil. Next, it is important to consider the emulsifier used to alter the surface tension. The experiment isn't designed to find every emulsifier that works with the selected media, but to identify one or more that might work across all four commercially available vegetable oils. For this we will consider both soy and sunflower lecithin, Polysorbate 20 &80, and Propylene Glycol.

A large factor in EHD atomization is the amount of electrical energy imparted to the solution. A balance must be reached between the energy from the electrical charge and the energies from kinematic or thermal energy. Too much electrical charge and the fluid atomizes completely passing the desirable cone-jet mode all together. Too little electrical charge and the fluid doesn't make it to the Rayleigh limit. Too much pressure and the mass flow increases thus requiring more electrical charge to maintain the charge density. Too low of a temperature and the viscosity increases and it becomes harder to break the surface tension. Too high of a temperature and the viscosity decreases but mass flow increases (at a given pressure) requiring more charge to stay above the Rayleigh limit.

Each of these input variables constitutes a change in energy state of the solution and acts upon the attributes of that solution. Each solution has attributes that directly affect its ability to EHD atomize. Attributes such as temperature, voltage and charge, viscosity, mass flow, and conductivity or resistivity, all must exist in concert for EHD spraying in the correct mode to be possible. A change in thermal energy, for instance, will certainly impact temperature, viscosity, mass flow rate, surface tension, and conductivity and a change in kinematic energy will effect mass flow rate.

2.3.1. Temperature

The temperature of the charged fluid in an electro-hydrodynamic spray system has a direct effect on the performance of the system. Increases in temperature result in an increase in thermal and kinetic energy of the fluid. This has a direct effect on the density, viscosity, and conductivity (the reciprocal of resistivity). Increasing the temperature of a solution increases the mobility of the ions in the solution. Raising the ionic mobility of charge carriers lowers the resistivity of the solution. (Aykas & Barringer, 2012).

When the temperature of soybean oil, for instance, moves from 120 degree to 240 degrees Fahrenheit, the density drops from 0.9 to 0.859 g/cm^3 and the kinematic viscosity decreases from 23.94 to 6.08 mm^2 s^{-1} (Esteban el al., 2012). Additionally, increasing temperature generally results in a lowering of surface tension. This is due to the fact that cohesive forces decrease with an increase in molecular thermal activity. This can be proven by:

Equation 18: Surface Tension as a Function of Temperature, Molar Mass, and Avogarado's Number

$$\gamma \approx \left(\frac{n}{4}\right)\left(\frac{N_0 \rho}{M}\right)^{\frac{2}{3}} k(T_c - T) \tag{18}$$

where the surface tension, γ, is solved by finding molar mass of a liquid, M, the number of atomic neighbors, *n*, the number of atoms in one, N_0, mole, finding Boltzmann's constant, k, Avogadro's number, N_0, the liquid's density, ρ, the critical temperature, T_c, and the temperature of the fluid, T (Palmer, 1976). The equation involves temperature, density, surface tension and ionic mobility.

2.3.2. Voltage and Charge

Voltage has a direct influence on the charge of a liquid in an EHD spraying system (Jayasingh& Edirisingh, 2002). As the applied voltage increases there is also an increase in the charge mass ratio of the liquid (Gaultney et al., 1987). This is seen in equation (4). Moreover, if you recall, Wang's (2012), equation (2) gave us the minimum voltage required for EHD atomization. In fact, Abu-Ali and Barringer (2008) declared that voltage had the highest impact on reproducibility and a significant impact on lowering mean droplet weight. In their research of soybean oil and emulsifier blends, they noticed that droplet weight decreased as voltage increased to a point (around 30kV) at which point droplet weight began to slightly increase again. This is likely due to the effect of spraying in a different spraying mode.

The charge density is directly proportional to the strength of the electric field and the breakup of liquid droplets during EHD atomization is governed by the Rayleigh limit (see equation 6). Droplet size is regulated by the charge on the droplet (see equation 13, 14, & 15). In fact, we can calculate voltage required at the point where dripping mode stops (remember that dripping mode can occur without voltage applied) and other modes begin. If voltage rises past this point then a stable cone-jet mode will form. In this equation, the voltage, U, is determined by finding the outer radius of the capillary, r, the distance between the end of the capillary and the collector plate, L, the surface tension of the liquid, γ, the Harkin's (1926) correction factor, φ, and the liquids permittivity, ε_0 (Lee at el., 2011):

Equation 19: Voltage Required for Cone-Jet Mode

$$U = \sqrt{\left(\frac{r\gamma\varphi}{2\varepsilon_0}\right)} \ln\frac{4L}{r} \tag{19}$$

2.3.3. Viscosity

Viscosity plays an important role in determining droplet size in electro-hydrodynamic spraying by influencing the mobility of the fluid's ions. The viscosity of liquids and droplets is the property that resists deformation by shear or tensile stress. By increasing the ability of ions to move in a fluid, the ability to carry a charge also increases (Kumar et al., 2011). The amount of charge carried by a surface of a liquid is proportional to the voltage applied and the flow rate of the liquid. As viscosity decreases, droplet size also decreases. Because of this, the number of ions in a liquid is a function of viscosity (Abu-Ali, 2004).

Dynamic viscosity expresses a fluid's ability to resist shear stress in a liquid flow. The exponential model for temperature dependent viscosity was developed by Osborne Reynolds in 1886 (Falkovich, 2018). Dynamic viscosity is useful for measuring viscosity when a force is applied to a fluid. Reynolds equation shows the temperature relationship in dynamic viscosity. The Reynolds equation solves dynamic viscosity, μ, with:

Equation 20: Dynamic Viscosity as a Function of Temperature

$$\mu(T) = \mu_0^{-bT} \tag{20}$$

Where μ_0 and 'b' coefficients and 'T' is temperature.

Kinematic viscosity expresses the relationship between the dynamic viscosity and density of a fluid. Measuring kinematic viscosity is a useful way to determine the fluidity of a substance when the only force acting on it is gravity. The equation for kinematic viscosity, v, is:

Equation 21: Kinematic Viscosity as a Function of Density and Dynamic Viscosity

$$v = \frac{\mu}{\rho} \tag{21}$$

Where ‘ρ’ is the density of the fluid.

2.3.4. Mass flow rate

Mass flow rate (measured as weight at a fixed spray time), impacts electro-hydrodynamic spraying by increasing or reducing the charge to mass ratio. The amount of charge induced on the surface of a liquid is directly proportional to the fluids flow rate. At lower flow rates, more charge is induced on the fluid and droplet size decreases. At higher flow rates, more volume is sprayed in the same amount of time and, thus, droplet size increases (Downer et al., 1993). Mass flow, $\dot{m}$, can be found by dividing the difference in mass, Δm, by the difference in time, Δt:

Equation 22: Mass Flow Rate Equation

$$\dot{m} = \frac{\Delta m}{\Delta t} \tag{22}$$

Because volumetric/mass flow has such an impact on electro-hydrodynamic spray systems, there is very little research involving systems using much more than static pressure. Most EHD research want to measure the kinematic movements of the fluid attributed to ionic attraction (Coulombic force).

2.3.5. Surface Tension

Surface tension, famously known for the water droplet phenomenon, is the elastic tendency of a liquid to assume the minimum surface area. Surface tension is the reason why bubbles are always round and why some insects can walk on water. Imagine that surface tension is an imaginary wall separating a liquid from a gas. The physics of surface tension govern this interaction and is the reason why the meniscus forms at the mouth of the capillary tube. This interaction can be universally represented by the Young-Laplace equation (Wisdom, 2004) where the Laplace pressure (the pressure between the liquid and the gas), Δp, is equal to:

Equation 23: LaPlace Pressure with Respect to Surface Tension

$$\Delta p = \gamma \left(\frac{1}{R_x} + \frac{1}{R_y} \right) \tag{23}$$

where 'γ' represents the surface tension and 'R_x' and 'R_y' represent the radii of curvature.

Surface tension is influenced by several factors including, temperature, oxidation and surfactants. In the operation of an electro-hydrodynamic system, the effect of temperature and surfactants determine the ability of high resistivity liquids to carry a charge. The relationship between temperature and surface tension on a liquid can be modeled by Eötvös rule (Adam, 1941) where the surface tension, γ, can be found from the molar volume, V, the critical temperature of the liquid T_C, the temperature of the liquid, T, and the material specific constant, k:

Equation 24: Temperature and Surface Tension

$$\gamma V^{2/3} = k(T_c - T) \tag{24}$$

We see from the Rayleigh Limit (equations 5 & 6), that the critical charge of a droplet is dependent upon the surface tension of a liquid, the dielectric constant, and the geometry (radius) of the droplet. This explicitly implies that surface tension is also influenced by the charge carried by the droplet. Surface tension forces oppose the coulombic forces that cause liquids to atomize. While surface tension has an impact on EHD performance, it is important to note that it is not as significant as conductivity, viscosity, voltage, or mass flow (Abu-Ali, 2004).

2.3.6. Conductivity and Resistivity

Often cited as the most critical factor in electrostatic atomization, conductivity or resistivity (the reciprocal of conductivity) plays an important role in coating effectiveness (Downer at al., 1993). Electro-hydrodynamic atomization of food grade oils requires that the conductivity range of the substance be in the atomizable range between (~10^{-6} to 10^{-9} µS/cm) micro-seimens per centimeter. This presents a challenge as these liquids gave conductivity ranges at greater than (<10^{-10} µS/cm) micro-seimens per centimeter (Abu-Ali, 2004). In Kykas and Barringer's (2012) tests with soybean oil and lecithin, none of the samples with 0% lecithin (100% soybean oil) achieved atomization.

Like many of the material properties discussed, electrical conductivity depends on a large number of factors including the type and concentration of ions present, the viscosity of the substance (due to ion mobilies), and temperature (Adamczewski, 1969).

Conductivity exhibits an upper limit for stable electrostatic atomization and has the largest impact to droplet size (Abu-Ali, 2004). Because conductivity is a substances ability to carry current, it poses the greatest potential in electrostatic spraying as high conductivities could potentially allow current to flow back up the lines and create an unsafe condition (Wilkerson, 1989).

The temperature dependency of conductivity, σ, can be expressed as a function of Temperature (T):

Equation 25: Temperature Dependency of Conductivity

$$\frac{1}{\sigma}(T) = \frac{1}{\sigma_0}[1 + \alpha(T - T_0)] \tag{25}$$

Where the temperature coefficient of resistivity is expressed as 'α' and comes from measured data (Ward, 1971).

2.4. FOOD GRADE VEGETABLE OILS

Global production of vegetable oil topped a 5 year high at roughly 196 million metric tons in 2017. Of this production, 171 million metric tons were made up of just four commercially available food grade oil types; palm (69.42), soybean (56.15), rapeseed (28.35), and sunflower (17.75) (US Foreign Agricultural Service, 2018). Because these top four vegetable oil types make up over 87% of world production, any conversation regarding the application of vegetable oil by electro-hydrodynamic means must address all four varieties.

All vegetable oils are considered electrical insulators. In fact, due to their dielectric properties, extremely low conductivity, renewable nature of their supply line, and lower environmental impact, vegetable oil is being used as liquid insulation in electrical transformers (Martin et al., 2017). While this bodes well for the transformer industry, it presents a unique challenge for electro-hydrodynamic spraying applications. Research involving the EHD spraying of food grade vegetable oil has been exclusively confined to soybean oil blended with the emulsifier lecithin (surfactant).

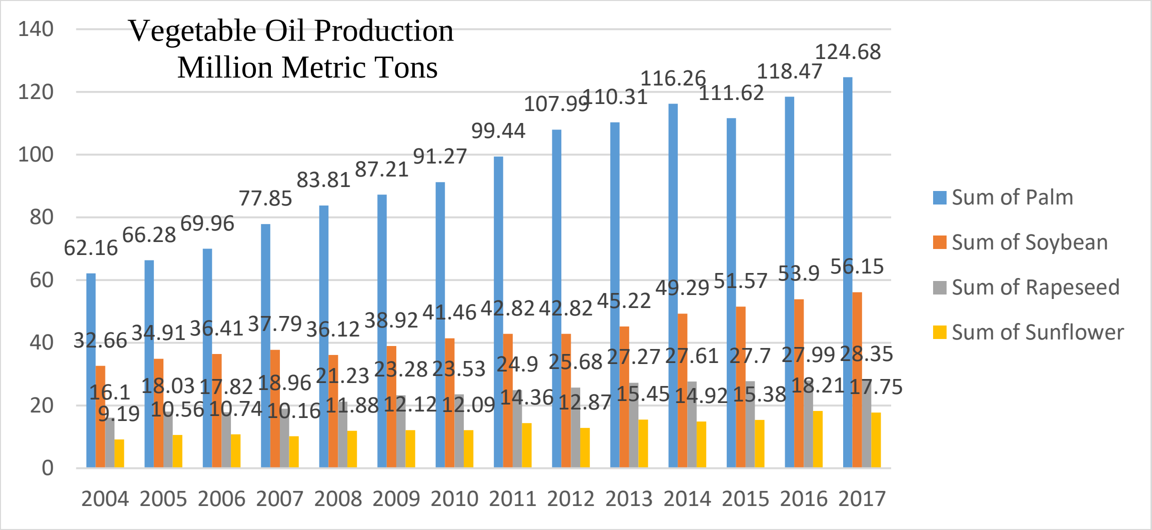

Figure 5: USDA 2018 data on Food Grade Oil Production in Million Metric Tons (US Foreign Agricultural Service, 2018)

Table 2: Properties of Vegetable Oils

	Density (g/cm^3)			**Kinematic Viscostiy (mm^2 s^-1)**		
Temperature (F)	120	180	240	120	180	240
Soybean	0.900	0.8802	0.8593	23.935	10.717	6.0800
Rapeseed	0.897	0.8765	0.8562	25.722	11.107	6.233296
Palm	0.893	0.8708	0.8492	30.095	11.814	6.307732
Sunflower	0.900	0.8786	0.8565	25.513	11.066	6.011072

2.4.1. Palm Oil

Palm oil is a food grade vegetable oil derived from the palm family (Arecaceae). It is produced, primarily, from the orange-red mesocarp of the species Elaeis Guineensis (known as the African Oil Palm). Elaeis Oleifera, the American Oil Palm, and Attalea Maripa, the Maripa Palm, also contribute, to a much lower degree, to global palm oil production. Oil is produced both through a mechanical process that can take the form of highly automated processing plants or more traditional methods. (Obahiagbon, 2012). Worldwide production of food grade Palm Oil has doubled in the last twelve (12) years (US Foreign Agricultural Service, 2018). One reason for this rapid growth is the fact that the plant has an economic life span of 25 to 30 years (Koushki et al., 2015). Unlike other sources of food grade oils such as soybeans, rapeseed, or sunflower, palm oils do not have to be both planted and harvested every year. Globally, Palm oil is the leading source of edible vegetable oil making up over 35% of all global vegetable oil production (US Foreign Agricultural Service, 2018).

Of the four major commercially available vegetable oils, Palm Oil holds the distinction of being the only one not completely solid at room temperature. The melting points for Sunflower (1F or -17C), Soybean (3F or -16C), and Rapeseed (14F or -10C) are far lower than Palm's (95F or 35C) melting point (Bailey, 2005). In general, Palm oil is valued for its flexibility and overall stability. Palm oil has very little polyunsaturated acids and is thus oxidatively stable and its semi-solid nature requires little need for hydrogenation. When mixed with its kernel oil/fractions or other vegetable oils, a wide variety of products can be produced. In regards to food applications, it can be refined into cooking/frying oil, or produced as a margarine, shortening, Vanaspati, or coco butter equivalent (CBE) (Gunestone, 2007).

2.4.1.1. Palm Oil as a Cooking/Frying Oil

Refined Palm oil is highly valued as a frying oil due to its long induction period (The period in which no oxidative or volatile components are generated under defined conditions). Refined Palm oil has an induction period of 51.7 hours at 100 degrees Celsius. In fact, it is so stable that Palm Olein is used as a stabilizer for other products. What this means is that Palm oil has a longer useful life when used as a frying agent in comparison to other commercially available oils. Moreover, the demand of health conscience consumers for oils having low saturated and polyunsaturated acids, high monosaturated acids, and no transfatty acids, has made Palm Olein, especially double-fractionated palm Olein, quite popular.

Palm oil is commonly used in the baking industry as a release agent in baking. Its long induction period means pans can be recycled many times without oxides fouling residual oils left in the pan after bread depanning. It also has excellent release properties making it ideal for pan oiling. Palm oil has a flash point of 250 degrees Celsius, a specific density of 0.88 mg/ml (comparable to SAE 30 engine oil at 0.895 mg/ml) and a low viscosity of 81.30cst at 40C and 5.70cst at 100C (Musa 2010). Moreover, its relatively low viscosity allows the oil to be applied thinly to the pan creating a thin lubrication barrier between the bread dough and the pan. This reduces the ‘frying’ effect of heavily applied oils.

2.4.1.2. Palm Oil as a Margarine/Shortening

Legally, Margarine must contain at least 80% fat. Margarine, as a commercial product, contains fat blended with water and other minor ingredients. The properties of differing margarines are a result of the oils used to make them. In particular, the solid fat content of oils and their fractions at different temperatures determine the crystallization properties of the Margarine. A major benefit to Palm oil over its competitors is the ability to blend Palm oil with Palm olein. This allows for interstrerificaton of ternary blends that achieve hard stock without hydrogenation which produces transfatty acids (Gunstone 2011).

Shortenings (traditionally a term for naturally occurring solid fats such as lard or butter), is now defined as a product that can, "effect the emulsification, lubricity, structure, aeration, flavor, and heat transfer of prepared foods" (Gunstone 2011). Shortenings are composed entirely of oils and fats. The blend of oils, stearin, and olean at different ratios along with aeration of the product produce the finished texture. For example, increasing the oil ratio or volume of aeration will produce a softer shortening.

Shortenings are used in the baking industry largely in the sweet goods segment where laminated doughs and pastries require separation between dough layers. Croissants and puff pastries are prime examples of the use of shortening to create flakey layers in a finished product. In these cases, the goal is to keep the shortening in solid state until baking occurs. While this is far from the only example, it is a good representation of how the solid stock of shortening can produce the 'flakey layer' effect in sweet goods.

2.4.2. Rapeseed Oil (Canola)

Brassica oilseeds have grown in popularity over the past twenty five years. Production of Brassica, known as rapeseed, has grown significantly following the development of low-erucic acid, low glucosinolate Canola oil. High levels of Glucosinolates are believed to impair liver function and high levels of Erucic acid is believed to contribute to fatty acid deposits in the heart, skeletal muscles, and adrenals. It is also been linked to the stunting of grown in young people. Erucic acid in Canola oil has been reduced to less than 2% with many producers developing product with less than 1% Erucic acid. This has led some to believe that Canola oil is the most nutritional edible oil available (Gunstone, 2011).

The term 'Canola Oil' came out of the development of the double zero strain of Rapeseed in the late 1970s and was coined by the Western Canadian Oilseed Crushers in 1978. Today, a double-zero strand of rapeseed known as *Brassis napus* accounts for nearly all rapeseed grown in the US and Canada. This, however, is a genetically modified oilseed. An advantage to the now heavy high-oleic, low linolenic transfatty acid free Canola oil is that genetic modification was achieved through classic breeding and thus is not considered a genetically modified organism.

Canola oil's oxidative stability is affected by the presence on linolenic acid and chlorophyll and its decomposition products. In addition to this there are trace amounts of fatty acids containing more than three double bonds. Canola oil contains 7-11% linolenic acid which places it in the same category as Soybean oil in terms of oxidative stability (Gunstone, 2011).

2.4.2.1. Physical Properties of Rapeseed Oil

Canola oil is composed of 74% oleic acid, 14% linoleic acid and 5% linolenic fatty acid. The relative density of 0.9~ is slightly denser than Soybean or palm but generally in the same range. A flash point of 275-290 also put it in the same class as Soy and Palm oils. The viscosity is slightly higher than that of Soybean oil, but overall performance characteristics are comparable. Reducing the Erucic acid content has dramatically affected the melting characteristics and crystalline structure when hydrogenated. The formation of transfatty acids through this practice, along with the tendency of Rapeseed oil to form a beta-crystalline structure has led to the elimination of this process from food manufacturers. Canola oil, due to its low saturated fatty acid content, is the preferred oil for the liquid oil component of soft tub margarines (Gunstone, 2011).

2.4.2.2. Rapeseed as a Salad Oil/Cooking Oil

The second largest oil by volume in the US, Canola oil considered a ‘natural’ salad oil due to the fact that it remains transparent at refrigeration temperatures and does not require ‘winterization’ or fractionation (Gunstone, 2011). Newer Omega-9 oils account for about 40% of the Canola used domestically and have an oxidative stability of 16 hours (Gorton, 2014).

While oxidative stability isn’t as good as Soy or Palm oil, Canola excels in its low values of pure unsaturated fatty acids (PUFA). Canola has 30% compared to 60% for Soybean oil. This makes it healthy yet only moderately stable. Therefore as an ingredient in food or as a salad oil, it is an excellent nutritional choice, but as a frying agent, it is a poor choice. While this certainly shouldn't discourage residential consumers from using it for frying (oil is not reclaimed and reused in these circumstances), it is often not a good choice for commercial or institutional applications.

2.4.2.3. Canola oil as a margarine/shortening

Fully hydrogenated Canola oil tends to form into a beta-crystalline structure that produces transfatty acids. As such, Canola oil is not used for hard stick margarines. However, it is the oil of choice for the liquid portion of soft tub margarine blends where hydrogenation of the oil is not required. The demand for hard stick margarine is on the decline and the development of multi-blend soft margarines has improved the role of Canola oil in soft margarine blends. Its use as a liquid component in such margarines allows for the lowering of the total PUFA in the finished product.

The same strategy applies to the use of canola in shortenings. Canola, rather than being hydrogenated, is blended with other hard fats such as Tallow, Palm, and fully hydrogenated Soybean or Cottonseed oils to meet target specifications (Gunstone, 2011). Unfortunately for the baking industry, the reliance on beta prime crystalline structure in shortenings is critical for product performance and, therefore, shortenings based totally on Canola oil cannot be used. This is unfortunate as Canola oil has the best fatty acid composition among all commodity oils.

2.4.3. Soybean Oil

Soybean oil constitutes the second largest amount of vegetable oil produced internationally. Domestically, however, it is the largest vegetable oilseed produced. One advantage of Soybeans over Palm is that there exists a strong trade in beans and meal. Palm fruits, on the other hand, have no commercial use. With this, there has been a slight narrowing of the production gap between the two products. Genetic modification through selective breeding, especially in the USA, means that 85-90% of all soybean seeds have been genetically modified. In fact, non-GMO is only available domestically through identity-preserved beans. This has created a problem for sourcing non-GMO lecithin (Gunstone, 2011). The non-GMO fad is in conflict with the transfatty acid free movement as growers have been reducing the plants saturated fats to create higher oleic acid and lower linoleic in the bean (Gorton, 2011).

The composition of Soybeans includes the seed coat or hull, cotyledon, and germ or hypocotyls. Cotylendon constitutes 90.3% of the whole seed, the hull constitutes 7.3 percent, and the hypocotyl makes up the remaining 2.4%. Soybean oil can be extracted by means of mechanical pressing and solvent extraction. However, mechanical extraction is expensive and produces significantly lower yield and account for only 1% of processed soybean oil in the US (Gunstone, 2011). Instead, the solvent, Hexane, is applied to the soybeans to extract the oil from the bean and then the solvent is evaporated off. With strict federal regulation of solvent loss to the atmosphere, the design of extractors, evaporators, and desolventizer-toasters have evolved significantly since the 1970s (Gunstone, 2011).

2.4.3.1. Production of Lecithin as a byproduct of oil production

Soybeans account for the lion's share of lecithin production for the pharmaceutical and food industries. Lecithin has long been used as an emulsifier in food. Its amphiphilic properties lend well to emulsification. While lecithin was out of vogue for some time, recent studies have shown benefits of improved liver function and lowering cholesterol and triglycerides while improving HDL. (Gorton, 2011).

Within the baking industry, lecithin has been used as a wetting and dispersing agent, emulsifier, and antioxidant. Lecithin is also used as a stabilizer for baked products and increase shelf life. While soy lecithin is FDA approved (generally recognized as safe GRAS), it is required to be labeled as an allergen. When used as a release agent that makes contact with cooking surfaces, the product it touches becomes allergen unsafe (Gorton, 2011).

2.4.3.2. Physical Properties of Soybean Oil

The melting point of soybean oil is 0.6C with an induction period of 16 hours. The specific density of Soybean oil is similar to that of Palm oil at .902 mg/ml. The viscosity of Soybean oil is also similar to that of Palm oil at 6.73cP at 100C (vs 5.7cP for Palm oil), and it has a similar flashpoint of 232C.

The advantage of Palm oil over Soybean oil lies in its greater stability. While GM products have made leaps towards breeding in traits that protect against oxidation and the forming of transfatty acids (eliminating the need for hydrogenation), the recent fad towards non-GMO has presented a challenge for producers.

2.4.3.3. Soybean Oil as a Cooking/Frying /Salad Oil

Commodity Soybean oil is comprised of 61% polyunsaturated fatty acids, 25% monosaturated fatty acids, and 15% saturated acid. Soybean oil is a linoleic-type oil and there are concerns about inflammation and its associated diseases such as type II diabetes and cardiovascular disease. However, absorption in humans is believed to be very low (Gunstone 2011).

While it can be consumed either in its natural or refined state, Soybean oil in the United States is generally refined to dull the taste. The level of refinement also provides the distinction between cooking and salad oils. Cooking oils are refined to be used at higher temperatures and thus need improved oxidative and thermal stability. Fully refined Soybean oil can be used directly as salad oils. Other oils such as Sunflower and Corn oils must be dewaxed before they meet this criteria (Gunstone 2011).

As a release agent, Soybean oil performs similar to Palm oil. The advantage of Palm oil lies in its improved stability. Price between both Palm and Soybean oils have remained comparable with Palm coming in slightly under that of Soy. The advantage to growers is that Soy has several byproducts and more than one market to sell into. Soybeans can be sold as oil, bean, or meal. Conversely, Palm oil is the only product from its fruit. Another advantage is that Soybean can be grown domestically and Palm tree cannot. This provides a transportation advantage to soybean oil retailers.

In the baking industry, Palm and Soybean oil are often interchangeable. Performance characteristics are similar and some bakeries will switch between the two based on commodity costs. Soybean oil is often used as an ingredient and label savvy producers will use the oil as a release agent for the pans required to bake bread. In that these pans are often washed between uses, the lower stability of Soybean oil is not a significant issue.

2.4.4. Sunflower Oil

The Sunflower, known to botanist as *Helianthus annuus L.*, is one of the most ancient species originating in North America. There is evidence of cultivation in North America as far as 3000 years before Christ (Gunstone 2011). During the reign of Peter I the Great, Tsar of Russia between 1682 -1725, the sunflower was imported to Russia from the Netherlands and there cultivated into the world's largest provider of Sunflower oil. Today, sunflowers in North America are cultivated from Russian seed stock.

High-linoleic Sunflower oil was considered "regular" until a couple of decades ago when growers started using the process of selective breeding to work in desirable traits into the seed stock. This particular practice is much preferred over the genetic modification techniques used with soybean to those who favor the non-GMO fad. Of the two basic types of sunflower seed, oil type and non-oil type or confectionary and bakery grade, only the oil type seeds produce oil in commercially viable quantities. The weight of 1000 oil type seeds would equate to between 30-80 grams (Gunstone 2011).

Like most vegetable oils, triacylglycerols comprise 98-99% of Sunflower oils composition. Sunflower seeds differ in their fatty acid composition by variety, but for purposes of this article we will explore the mid and high oleic Sunflower oils. In regular Sunflower oil the amount of triacylglycerols having at least four double bonds exceeds 80% by weight (Genstone 2011). Sunflower oil is non-hydrogenated, non-GMO, and low in saturated fats. This has prompted an increase in demand and the USDA reports that sunflower plantings may grow to an unprecedented 1.7 million acres this year (Gelski 2016). Efforts to further reduce Sunflowers already low 7% saturated fat to around 3% are expected to be commercially viable in the next 2-3 years. Sunflower oil is considered a neutral oil and blends well with other oils without changse the taste profile. This will further allow for the blending of oils to achieve an optimal performance and nutritional target. Blends with Canola oil because of its favorable saturated fat content and Sunflowers high stability content make an excellent pairing. The fact that sunflowers are considered clean label, or non-bioengineered, makes the product very popular with food processors (Gelski 2016).

2.4.4.1. Physical Properties of Sunflower Oil

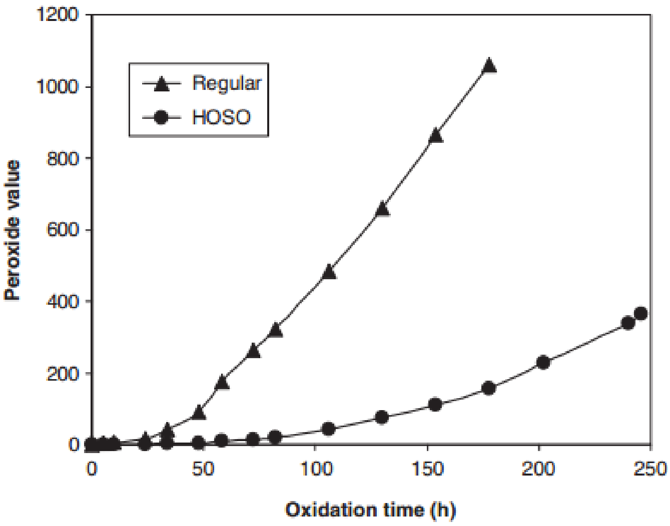

Figure 6: Oxidation Time of Regular vs HOSO Sunflower Oil (Gunstone, 2011)

The relative density of Sunflower oil is 0.9~ and similar to that of all of the four commercial vegetable oils. It has a high flash point at 316C and a viscosity of 31cP at 40C and 8cP at 100C. This is slightly more viscous than the other three commercial vegetable oils discussed in this article. Sunflower oil can be used as a salad oil once refined and remains clear at 0C. However, refined Sunflower oil has the lowest induction period at 6 hours. Regular Sunflower oil has a relatively good oxidative stability as a result of very low linolenic acid. High-oleic Sunflower oil is suitable as a commercial frying agent. High-Oleic Sunflower oils (HOSO) have a greatly improved oxidation time with respect to their ‘regular’ counterparts.

Producers often address the stability issue of regular Sunflower oil with the use of antioxidants. Tert-butyl hydroquinone (TBHQ) is often added to the blend to improve oxidative stability. By adding antioxidants to high-oleic Sunflower oil the inductive index can be improved from 16.5 hours to 49.6 hours (Gunstone 2011). It is also important to note that Sunflower oil is highly susceptible to oxidation by exposure to sunlight and should be stored in the dark or in dark containers when possible. This is improved with the addition of antioxidants but not eliminated.

2.4.4.2. Sunflower Oil as Salad Oil/Cooking Oil

While Sunflower oil comes in several varieties, all are acceptable as a salad oil after refining. Generally, however, high-oleic Sunflower oil is used predominately as frying oil. In countries where Sunflower oil in a mainstay commodity, it is commonly used as a frying oil. Between high-oleic fatty acid and regular Sunflower oil, studies have shown high-oleic Sunflower oil to have a lesser degree of deterioration in both continuous and discontinuous frying. Product fried using high–oleic FA Sunflower oil showed a higher product stability and longer shelf life when stored at 60C. Moreover, oxidative stability of the High-oleic oil was greater than that of its regular counterpart (Gunstone 2011).

Frying using Sunflower oils with a high content of saturated fatty acid such as high-palmitic or high-oleic acid and with a low linoleic acid content showed favorable results and indicated a good performance of this oil as a frying medium. Also, while mid-oleic Sunflower oil is relatively new to the industry, early studies have showed favorable results in the manufacture of fried potato or corn chips. When compared to Canola oil, both showed similar pan frying stability (Gunstone 2011).

Sunflower oil has made headway into the industrial Baking industry as a release agent. It is important to note that Sunflower oils tendency to form beta crystalline structure when exposed to heat must be addressed when using circulating pan oiling system. Some Sunflower oils, especially High-oleic oil, are not as stable as their ‘regular’ cousins. They have a tendency to grain or cloud as crystals form and often fall out of suspension.

2.4.4.3. Sunflower oil as a Margarine/Shortening

Sunflower oil has a tendency to crystallize into the beta form when partially hydrogenated. This will result in a grainy or sandy texture. To reduce this effect, producers often blend sunflower oil with other products such as cottonseed oil to achieve targeted cream texture. Cottonseed oil tends to form into beta prime structures which are favorable for margarines when blended with partially hydrogenated Sunflower oil and unhydrogenated Sunflower oil. The push for zero transfat has challenged producers who are now blending completely hydrogenation oil with interesterification of an unhydrogenated oil. The result meets the transfat requirements but lowers the stability, and consequently the shelf life, of the finished product.

2.5. FOOD GRADE EMULSIFIERS

Emulsifiers have been present in the food we eat for as long as our species has been eating products made with egg yokes (casein) or drinking milk. Mayonnaise is an example of emulsifiers in action. Bread, ice cream, and cake are all examples of food that relies on emulsifiers for texture and stability. Based on their lyophilic (hydrophilic for water) groups, and their polar functionality, there are four categories of food emulsifiers (Hasenhuettl & Hartel, 2009):

- Anionics- have a negatively charged molecule with a positive counterion; and.
- Non-Ionics- contain no charge but produce a dipole; and
- Cationics- have a positively charged molecule with a negative counterion, and
- Amphoteric- have both positive and negative charges on the same molecule.

There are three types of emulsions that are common in food. Oil-in-Water (O/W) are emulsions where droplet of oil are suspended in water. Examples include mayonnaise, creamers, whip toppings, and ice cream. Water in oil (W/O) emulsions contain water droplets suspended in oil and include butter and margarines. Finally, water-in-oil-in-water (W/O/W) which can be seen in yogurts and processed cheese (Kralova & Sjoblom, 2009).

2.5.1. Surfactants

Surfactants are a class of emulsifiers. Most of us know that a detergent lowers the surface tension of water making it ‘wetter’ and that this phenomenon helps to get clothes clean. The answer to the question of ‘why’ involves the complex chemistry of surfactants. The term Surfactant is derived from the contraction “Surface Active Agent” where, since the 1950s, the study of the science of interfacial interactions has grown out of Colloid science. Surfactants, in low concentrations, absorb into the interfaces of liquids, thus, altering them such that the free energy at the interface is lowered. Interfacial free energy is the physical property measured per unit area to determine the tension between a gas and a liquid. This free energy is the minimum amount of work necessary to create the interface.

Interfacial tension, or surface tension, is a measure of the differences of free energy between two phases, most often a liquid and air, at their boundary (Rosen & Kunjappu, 2012). In the most general terms, this can be expressed using the following equation where the minimum Work, W, can be found by examining the relationship between the Surface Tension, γ, and the difference in the interfacial area:

Equation 26: Minimum Work and Surface Tension

$$W_{min} = \gamma \times \Delta_{interfacial\ area} \tag{26}$$

Surfactants are generally organic compounds that contain both lyophobic and lyophilic components. It is akin to having a substance with a head and a tail. The head contains lyophilic, hydrophilic if the solvent is water, properties and is attracted to a solvent and the tail has lyophobic properties that generally repel solvent. In the example of water, surfactants are both water soluble and oil soluble at the same time. A unique phenomena of adsorption and aggregation occurs when forces oppose each other in the same molecule. In our water example, when a surfactant is introduced, the surfactant molecules move towards the surface and orientate themselves so that the hydrophilic heads face the water and their hydrophobic tails face away towards the gas. This example of adsorption results in a lowering of the interfacial tension between the two phases. Aggregation, also referred to as micellisation, occurs within a solution wherein groups of surfactant molecules gather and arrange themselves such that regions within the solution will solubilize and create an emulsion (Farn, 2007).

2.5.1.1. Soybean Lecithin and Sunflower Lecithin

The word, Lecithin ($C_{44}H_{85}NO_9P$), comes from the Greek *lekythos* which means "egg yoke" and is a natural blend of phospholipids. This is fitting as the use of egg whites as an emulsifier goes back centuries. In food, it has applications primarily as an emulsifier and stabilizer, but is used generically as a wetting agent, antioxidant, release agent, or dispersing agent. Lecithin's properties make it an excellent (O/W) emulsifier but it also has the ability to form (W/O) emulsions (Nieuwenhuyzen, 1976). Moreover, Lecithin has a net negative charge and is an anionic surfactant (Xu et al., 2011). It also has a relatively low HLB value of seven to eight (7-8).

Aykas and Barringer (2011) have successfully used Soy lecithin to reduce the surface tension of electrostatically sprayed soybean oil. In their research, they found that resistivity and surface tension lowered as the concentration of lecithin increased (0-15%) and temperature increased (4C to 47C). They also determined that droplet pattern density increased with both temperature and lecithin concentration. Finally, they confirmed that droplet size decreased with an increase of applied voltage.

2.5.1.2. Polysorbate 20 and 80

Polysorbates are a class of emulsifiers used in food, pharmaceuticals, and cosmetics. A sorbitol derivative, they are defined by the number of polyoxyethylene groups in each variant. Polysorbate 20 ($C_{58}H_{114}O_{26}$) and Polysorbate 80 ($C_{64}H_{124}O_{26}$) are nonionic surfactants used as a detergent or as an emulsifier in the food industry. Polysorbate 20 has a HLB rating of 16.7 and Polysorbate 80 has a HLB rating of 15 (Wiley & Sons, 2008). Polysorbate is hydrophillic and provides for excellent oil-in-water (O/W) emulsions.

2.5.1.3. Propylene Glycol

Propylene Glycol ($C_3H_8O_2$) is a synthetic organic emulsifier that is miscible with water. Propylene Glycol is also a weak nonionic surfactant with an HLB rating of zero (0). It is often used as an emulsifier in food products and as an antifreeze in applicaitons where the potential exists for the fluid to come into contact with food. Because of its highly polar nature, surfactant molecules self-assemble in propylene glycol. Propylene glycol is similar to water in that it forms hydrogen bonds and has a high dielectric constant (Garti at el., 2001). The surface tension of the liquid is 36 (mN/m) with an electrical conductivity of 0.1 x 10^{-6} (S/cm). The surface tension of Propylene Glycol is lower than that of water. While heat tends to lower the surface tension of liquids, it does not affect the surface tension of glycols except at the boiling points (Dow Chemical Company, 2003)

2.6. RELEASE AGENTS IN BAKING

Anyone remembering Elmer’s brand school paste as a child might recall that the primary ingredients were water, flour, and sugar (Bratton, 2013). If you were one of the children who actually ate Elmer’s School Paste, don’t worry. It turns out that most of us have been eating it our whole lives. The same ingredients found in any kindergarten classroom are the basis for most bread products. From this, we can draw a couple of conclusions. First, school paste must have certain nutritional value, and second, bread dough is likely sticky!

Anyone who has baked bread at home can attest to the second fact. Interestingly enough, it is this property of bread dough, in part, that has birthed an entire niche within the industrial baking community. Industrial bread pans, lubricating oils, and pan coatings have all worked in competition and concert to address the challenge of sticky dough. To date, there has been no 'magic bullet' solution for this problem. In an environment where there is no single solution, it can be hard to navigate through the sea of varied options. It is here, therefore, that we examine the relationship between the bread pan, pan coating, and pan oiling and derive some insight in what industrial bakers face when choosing equipment to tackle the issue.

As a practical matter, release agents, in their various forms, have been integral to baking since the advent of bread some 30,000 years ago. Flour itself, coarse grain refined by hand crushing grain with rocks, is likely the oldest release agent, thus, used to provide a barrier between bread products and baking medium. With the advent of leavening by the Egyptians in the 3rd century B.C. (used to make sour breads), the need for more dynamic release agents led to the use of oils and grease (Lohman, 2012). With the use of leavening, bread's geometry became dynamic during baking and, thus, pans were invented to capture and form the finished product. While pans provide an excellent encasement mechanism and allow the bread to take on a uniform shape, the use of pans created a problem when removing the finished product from the pan. Generally, this calls for the extrication of the bread from the pan by either pulling on the crown of the loaf or flipping the pan and allowing gravity to remove the loaf. In either application, grease provided a flexible barrier between the bread and the side walls of the pans.

With the mechanization of the baking process, hand greasing pans became impractical and the use of oils became the mainstay release agent for bread pans. Oil can be applied quickly, is easy to automate, and is more affordable than grease. Today, a wide variety of oils such as Palm, Rapeseed, Sunflower, and Soy are used as release agents in industrial baking. Not only do these oils provide excellent release properties for the bread products, they act as a frying agent, thus, providing the color and texture of the bread's crust.

Release agents, such as oils, facilitate the removal of finished product from the baking pan by making the surface of the pan hydrophobic and reducing the van der Waals forces imparted by the dough. They also form an uninterrupted homogeneous film between the surface of the pan and the dough. To do this, they must be able to form a strong adhering bond on the pan's steep walls. The film between the dough and the side wall fills the gaps in the surface of the pan and reduces the static friction between the finished baked product and the pan (Wissensforum Backwaren, 2009). Release agents mitigate both the potential tearing of the surface of the crust and subsequent potential defects caused by pan and dough/bread adhesion. This allows the vacuum depanning system to remove bread from the pan.

Additionally, release agents must stand up to baking temperatures, not react negatively with the dough they come into contact with, not carbonize or form resins, and they must not react with the surface of the pan. Moreover, release agents must not have, "detrimental effect on the taste or the odor of a food product" (Wissensforum Backwaren, 2009). Stability is often a critical concern for oil based release agents as oil residue can remain on the surface of the pan for many baking cycles. Because of this, pan oils are often a unique combination of vegetable oils and/or mineral oil, lecithin, and antioxidants (Lallemand, 2000). Given all of this, they still must be easy to apply and economical.

2.6.1. Dough Adhesion

In order to understand the relationship between bread dough and the pan it is baked in, it is important to have a cursory understanding of dough adhesion and the rheology at play in this relationship. Dough adhesion follows the widely accepted absorption theory. The theory states that materials will adhere because of the interatomic and intermolecular forces established between the atoms and molecules on the surface of the adhesive and substrate. Most commonly, this is a result of secondary chemical bonds known as van der Walls forces (Kinloch, 2010). The peeling energy of dough is the combination of surface energy (G_0) and the cohesive energy (ψ) contributions and can be described as:

Equation 27: Peeling Energy of Dough

$$G_C = G_0 + \psi \tag{27}$$

In this equation, the surface energy represents the type and strength of the bond between the adhesive and the substrate and the cohesive energy represents the energy dissipated in viscoelastic and plastic deformation with the adhesive (Dobraszczyk, 1997).

With bread dough, the cohesive energy represents the dominant force in the equation and is dependent on the viscoelastic properties that make-up of the dough (water to solids ratio). As a result, the adhesive property of dough is highly dependent on imposed rate, temperature, and deformation (Dobraszczyk, 1997). This is to say that much of the adhesive property of bread dough comes from its rheology. When Dobraszczyk (1997) performed peel tests on various flour and water mixtures, it was discovered that it took between 6.4 J/m^2 and 11.4J/m^2 to successfully separate samples from the substrate. It was further discovered that the Storage Modulus for these samples ranged from 12-16kPa. Dobraszczky also determined that the peeling energy increased as the sample thickness increased.

Dobraszczyk (1997) concluded that measurements performed at a range of strains indicated a dynamic and non-Newtonian relationship between low and high strain testing. In materials, the measure of tack is highly influenced by the storage modulus. Maximum tack occurs when an adhesive has a low modulus in the bonding range and a high modulus in the debonding range (Dahlquist, 1959). For bread dough, the adhesive rate is highly dependent on the rate of debonding and on the amount of water added to the solution. This further reinforces the notion that adhesive property of dough is primarily based on the rheological properties of the dough (Dobraszczyk, 1997).

2.6.2. Impact of Geometry on Bread Depanning

Pressure from the leavening process pushes dough into the surface of the bread pan. Needless to say, the geometry of the pan, therefore, imparts resistive forces onto the depanning process. The impact of this is highly dependent on the geometry of the finished bread product and the geometry of the pan. In the case of bun and rolls, for instance, the pan wall is shallow with respect to the height of the overall finished product and the angle of the pan walls is relatively shallow. Thus, interference between the geometry of the bread and the geometry of the pan is relatively minor. As a result, bun and roll pans do not require an additional release agent above and beyond the coating applied to the pan. Flour, rather than oil, is often used in these cases. Moreover, bun and roll dough composition tends to be drier and less sticky than their bread-loaf counterparts.

Other products such as bread, cake, and biscuits tend to have a much higher surface tackiness, softer and wetter dough composition, and steeper draft angles in the side walls of the pans used to process them. In these cases, a release agent is often required regardless of any glazing applied to the pan. Moreover, pans, through normal wear and tear, develop abrasions, scratches, residue buildup, nesting interferences, burning, and damage from handling abuse. This creates an environment ripe for interference fit concerns, and these concerns deepen with every baking cycle. Industrial bakeries typically do not wash baking pans. This means that the surface conditions of the pan tends to deteriorate as the cycle count of the pan increases. In fact, a bakery running silicone glazed pans will often run 600 cycles between reglazing and cleaning (Atchley, 2014). Bakeries, therefore, rely on release agents to combat and extend the life of dirty pans.

2.6.3. Pan Composition

While historically baking pans have been constructed from cast iron, steel, or ceramic materials, contemporary industrial baking pans are made from either aluminum, tin, steel, stainless steel, or aluminized steel. Of these materials, aluminized steel makes up the lion's share of the industrial market. Aluminum pans tend to damage easily but have very good thermal properties. Steel pans are strong but have poor chemical resistance and only moderate thermal properties. Aluminized steel offers the best of both of these materials. In the process of making these pans, carbon steel sheets, typically 12 to 26 gauge, are hot dipped in an aluminum-silicon alloy and stamped into shape (Atlas Steel, 2016). The pans then may or may not be hard coat anodized. Finally, the pans are then finished with either a glaze or a finished coating.

All pans require either a seasoning (the baking in of oil), glazing, or coating to create a smooth barrier between the surface of the pan and the product’s surface. Silicone glazing remains the predominate method for preparing pan surfaces. Older methods such as seasoning are virtually non-existent in modern bakeries, and the application of Fluoropolymers are slowly gaining acceptance. Fluorocarbon based polymers, such as Teflon®, provide better release characteristics, but cost significantly more upfront. Fluoropolymers offer up to 10 times the performance between re-coatings but cost 12 times as much as silicone glazing. Additionally, the lack of locally available Fluoropolymer coating providers means a longer turnaround time for bakeries. Fluoropolymer coating providers tout a reduced need for pan oiling as a release agent, but are reluctant to declare an elimination of pan oiling for all products across the life of the coating. However, the reduced dependency on oil based release agents make the investment relatively cost neutral for consumers.

2.6.4. Silicone-Glazed Pans (Requires Oiling)

US Bakeries tend to prefer silicone glaze over fluorocarbon based polymers or any other coating method. The silicone glaze is a semi-permanent coating that protects pans for 400 to 800 oven cycles before the glazing needs replaced. Bakeries expect, on average, 20 glazing cycles per pan. Pan glazing companies all tout the virtues of their product and offer subtle differences that improve pan life, improve thermal conductivity, or last longer between reglazing. Silicone, however, remains the predominate material. Silicone providers maintain an advantage in that pans can be turned around in a matter of days where Fluorocarbon coating takes two to four weeks (Whitaker, 2011).

Pan Glazing companies also offer other value added services such as ding and dent removal. Because pans must be reglazed more frequently than their Fluorocarbon coated cousins, pan damage is repaired before pans become critically damaged. Pan glazers are also quick to point out that silicone is a food grade product where Fluorocarbon polymers such as polytetrafluorethylene (or Teflon®) are toxic if inhaled (a condition that could occur of pans are over heated) and there is a low risk that Perfluorooctanic Acid could potentially leach into food and present reproductive and fetal development issues (Huang, 2015). They also point out the malleability of silicone and note that pan damage on a PTFE coated pan often leads to critical coating failures.

Figure 7: Bakery Pans Before and After (www.thebakerynetwork.com/clean-and-glaze-bakery-equipment)

2.6.5. Fluorocarbon based Polymer (PTFE) Coated Pans

We've all heard the slogan, "Nothing sticks to Teflon!" From a strictly performance perspective, this appears to be true with Teflon coated baking pans as well.

Many Fluoropolymer coating providers brag that the use of their product negates the need for oil based release agents. In some cases, this is true. However, the same can be said for silicone glazing in the right application. Many bakers who use Fluoropolymer coating still report the need to use oil as a release agent (Whitaker, 2011). However, even if this is true, PTFE still has much to brag about.

Polytetrafluoroethylene, known as PTFE and branded as Teflon by DuPont in 1938, is a synthetic fluorocarbon based polymer. It is a high molecular weight material consisting wholly of carbon and fluorine and, like silicone glazing, is hydrophobic (Britannica, 2009). PTFE is known for its slippery surface, high melting point, and resistance to almost all chemicals. These properties have made it wildly popular as a non-stick coating in cookware. Pan suppliers with Fluoropolymer coating note that reducing the recoating frequency lowers transportation costs associated with reglazing, reduces pan oiling consumption, minimizing carbonization of pan oils, reduces fire risks associated with pan oils, and provides longer pan life due to a less frequent need to strip and recoat pans.

While silicone glazing is the dominant provider of pan coatings to US industrial baking manufacturers, PTFE coatings are making headway. Today, many bakery pan suppliers and silicone glazing suppliers are also offering PTFE coating. These pan suppliers claim their PTFE coatings (and proprietary derivatives) can reach 3000 to 6000 cycles between recoating. Release agents can still be applied to assist these pans and extend the life between cycles.

Of course, there are some concerns with PTFE coatings. Abrasive ingredients such as cornmeal, a baking staple, tends to damage the coating. Another large drawback for coated pans is their need to stack without making contact to the coated surface. In an industrial baking environment, pans are changed often, handled manually, warped by heat, and damaged from handling. Pan styles that currently stick together or have high or narrow cavities will not work with non-stick coatings. Uneven or partially unsupported pan stacks could potentially damage the non-stick coating. If this happens early in the pan's life then any saving associated with the coating is lost (Orion, 2014). Conventional continuous vacuum depanners often drag the product over the lip of the pan and this, too, could result in premature coating failure. Many factories are moving to robotic pick and place depanning to mitigate this issue. Recent concerns with PTFE coatings and Perfluorooctanoic Acid (PFOA) have given pause to the use of these types of coatings. Some studies suggest that PFOA can be released at normal cooking temperatures and much is still unknown about the toxicity of PTFE (Sajid & Llyas, 2017).

Furthermore, unlike PTFE coated cookware used in the average home, industrial bakeries operate with hundreds of pans that must cycle through the baking process without constant visual inspection. Pan failures within this system can potentially go unnoticed for long periods of time. The frequent inspection and repair offered by glazing pans mitigates what could be a long duration of a pan in a failure mode. Moreover, silicone glazing is more robust and forgiving to incidental damage than PTFE coatings whose failures tend to be more catastrophic in nature. Also, because PTFE coatings tend to not play well with some conventional bakery equipment and ingredients, it may require reformulation and significant investment capital to convert existing bakeries from glazing to non-stick coatings.

Silicon glazing, on the other hand, requires a release agent to work with most bread dough, requires reglazing on a frequent basis, and deteriorates at a much faster rate than its non-stick cousin. Bakers must load pans in and out of the bakery and schedule around this absence. Moreover, the pans tend to produce darker crusts as they become increasingly fouled. As pans become dirtier, the amount of release agent must be increased to maintain the depanning ability the process requires. While this is also true with non-stick coatings, the magnitude is much greater with glazed pans.

In the end, bakers are faced with the two very different choices. Some non-stick coating providers claim they can eliminate the use of release agents with their coatings, but this opinion isn’t substantiated by the baking community (especially over the life of the coating). Their claims of lower lifecycle costs might be accurate if the baking community can find ways to mitigate their higher number of failure modes. Directionally, however, it does seem that non-stick coating may one day overtake traditional pan glazing.

CHAPTER III

3. DESIGN OF EXPERIMENT

3.1. DOE MODEL

The use of oil as a release agent in baking is commonplace in the industry. While concerns over trans fatty acids, the impact of genetically modified organisms, and the negative health perception of animal fats has changed the nature and type of oils consumed, the basic purpose remains the same. Essentially, vegetable oils are used to create a low friction barrier between the dough and the pan in which it is baked. Conventionally, when oils is applied to the pan, it is done so by mechanical means. The temperature of the oil is raised to lower the surface tension and viscosity of the lubricant and the product is pumped at high temperature through a small orifice designed to impart shear forces and, subsequently, atomize the oil. This allows for the light homogenous distribution of oil within a pan cavity. Volume too low in an application will result in poor release properties and bread sticking in the pan. Volume too high in an application will result in fouling of the pan and oil acting like a cooking agent and, thus, frying the crust of the bread. However, even when all of the environmental factors are in perfect harmony, modern pan oiling still has an undesirable side effect on the production environment. Atomization of the oil results in undesirable overspray of the area surrounding the pan oiler.

The concept of electro-hydrodynamic (EHD) atomization of liquids is still in its infancy. While applications where water is the base have become commonplace in the electrostatic coatings industry, the use of oils, especially food grade oils, is still fairly uncommon due to their relatively high electro-resistivity. Researchers Didem Aykas and Sheryl Barringer, out of Ohio State University, broached the subject by examining the criteria needed to electrostatically charge soybean oil by use of the emulsifier additive 'lecithin'. Their research, however, did not address the other major commercially available vegetable oils, alternative food grade emulsifiers, or the implications of charging a pressurized liquid and then spot applying. Moreover, their research did not include the discrete cavity application (spot spray) needed to meet the needs of commercial bakeries. In order for their findings to translate into a commercially viable technology, further research and experimentation using alternative base oils, commercial food grade emulsifies, and pressurized atomization is needed.

In Aykas and Barringer's research (2012), experimental testing validated the response of varying levels of temperature, lecithin content, and applied voltage on the droplet size and dispersion pattern during electrostatic spraying of soybean oil. Many industrial bakeries, however, have moved away from the use of lecithin as an emulsifier and often use other commercially available oils as a release agent. To make EHD atomization commercially viable for the baking industry, it is necessary to perform similar experimentation and include additional oils and emulsifiers, and to simulate the environmental conditions found in commercial bakeries. The proposed experiment will examine the droplet count, droplet size, coverage area, and sample weight of each of the identified base oils when presented with the variable inputs of emulsifier concentration, temperature, applied voltage, and pressure. These tests will be performed in groups using two different capillary tube sizes.

3.1.1. Experimental Methods and Materials

For this experiment, an ANOVA with the outlined series of factors at different levels will be imperially tested via a Full Factorial Design of Experiment (DOE) to determine their effect on droplet count, droplet size, film coverage, and weight (a term of mass flow) of the sample. The DOE for the experiment will be structured as follows:

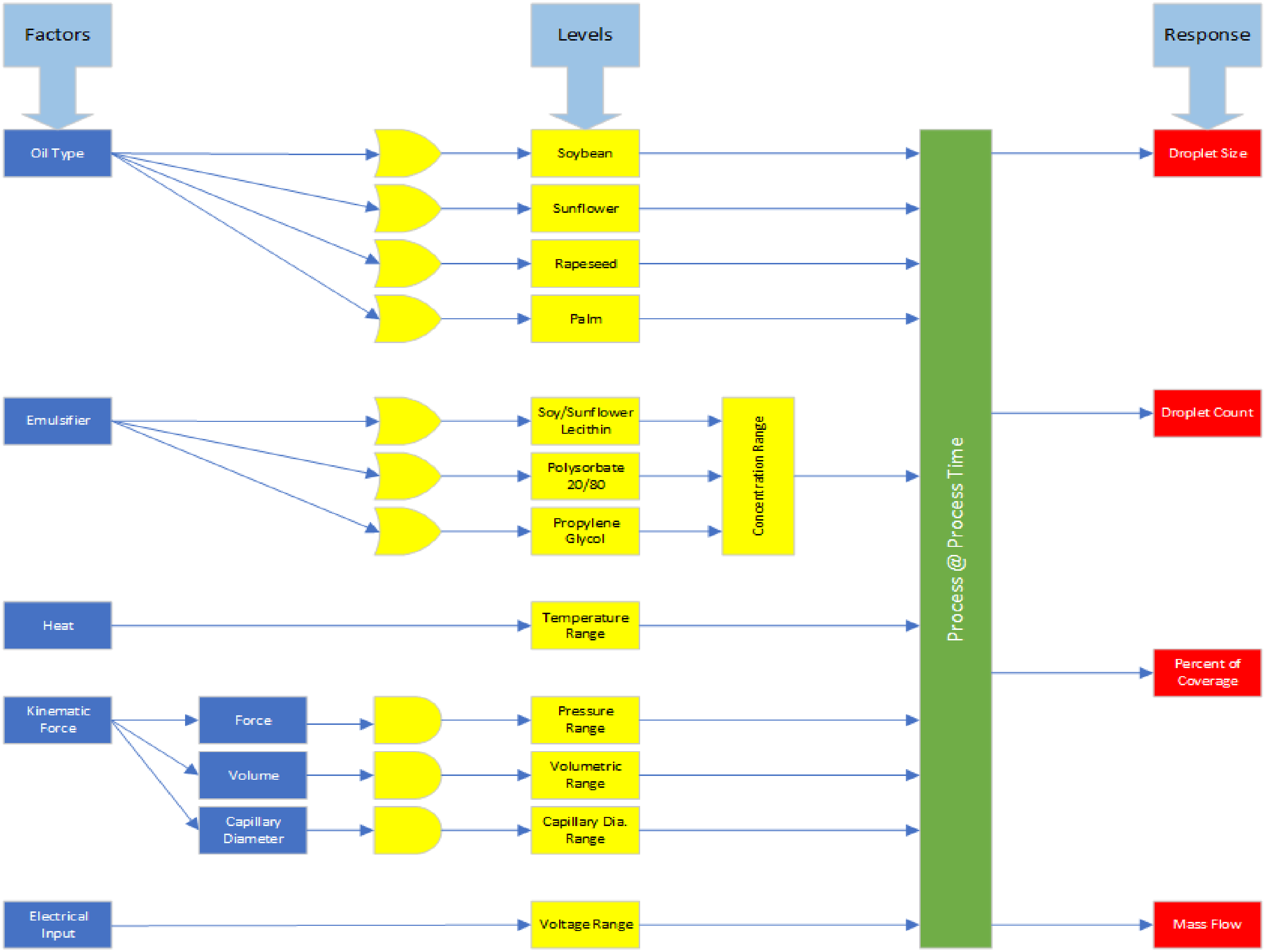

Figure 8: Full Factorial DOE Chart

Factor #1 – Oil Type (4 levels) - The four most commonly used commodity oils in the food industry will be used for the experiment and are listed below:

- Palm Oil
- Rapeseed Oil (Canola)
- Soybean Oil
- Sunflower Oil

Factor #2 – Emulsifier (minimum 3 levels) – A list of commonly used emulsifiers are given below. The three emulsifiers are all surfactants and have varying HLB levels. The level of this factor will be measured as a percentage of concentration and is expected to be a range of 2 measurements.

- Soy or Sunflower lecithin – HLB 7-8
- Polysorbate 20 or 80 – HLB 15-17
- Propylene Glycol – HLB < 1 (Special Case)

Factor #3 – Heat (3 levels) – The oil/emulsifier solution will be heated up in increments of 40 degrees Fahrenheit for 3 measurements up to a range of (52-60%) of the base oil's smoke point. Smoke points for the four oils are as follows:

- Soybean oil – 460F
- Sunflower Oil – 450F
- Rapeseed Oil – 400F

- Palm Oil – 450F

Factor #4 – Pressure (3 levels for pressure, 2 levels for orifice size) – Kinematic force is imparted by forcing a pressurized liquid through a capillary. Flow will be laminar through the capillary and the jet at discharge. Several factors contribute to the mass flow rate including density, viscosity, and temperature. Therefore, the mass flow rate will be impacted by the relationship between the pressure, temperature of the fluid, and the orifice geometry.

Factor #5 – Electrical Input (2 levels) – For the experiment 25k – 50k Voltage will be applied to the media at 5W at 0.1mA. As the spray time is defined at 300ms, 2.5 Joules will be imparted during the 25kV tests and 5 Joules will be imparted during the 50kV tests.

3.1.2. Proposed Experiments

In order to understand the interactions of different oil/emulsifier blends when tested at differing environmental conditions, several separate experiments must be conducted. They include:

1. The viability of different emulsifiers with varying HLB levels when combined with a base oil to induce electro-hydrodynamic atomization (exceed Rayleigh point) and achieve spraying modes (cone-jet) while spot spraying.
2. Impact of temperature on the solutions mass flow rate (measured as weight at a fixed spray time), droplet count, droplet size, and coverage area at varying conditions.

3. Impact of pressure and capillary diameter on the solutions mass flow rate, energy density, droplet count, droplet size, and coverage area at varying conditions.
4. Impact of applied voltage on mass flow, energy density, droplet count, droplet size, and coverage area at varying conditions.

3.1.3. The Viability of Varying Emulsifiers

The full factor ANOVA experiment started with the first two sets of factors (Factor 1 at 4 levels and Factor 2 at 3 levels). The purpose of this experiment was to determine if blending different emulsifiers with each of the of top four major commercially available food grade vegetable oils, in varying concentrations, would produce an electro-hydrodynamic spraying effect. Research conducted by Abu-Ali and Barringer (2005 & 2008) and Aykas and Barringer (2012) have shown that Soybean oil and Lecithin can be sprayed in a low-pressure continuous-spray application and achieve EHD atomization. Their research, however, leaves the questions of, “Does the technology across multiple oils and emulsifiers?” and “Can it be made to work in a high-speed spot-spray application?” unanswered.

For this experiment, each of the four major vegetable oils was blended with three separate emulsifiers in concentration of 5% and 10% by volume. In the Soybean/Lecithin tests, Aykas and Barringer (2012) determined that, with lecithin concentrations greater than 5%, voltage had the greatest impact on droplet size. They observed that at 10% concentration, 40kV, and 47C, the maximum number of droplets/cm^2 was observed. As Barringer has completed the most extensive research on the subject, and making the assumption that other oils might perform similarly, the 5-10% concentration mark was used as the basis for the experiment.

Five different emulsifiers (surfactants) were chosen for the experiment. Each are widely used in the food industry. The first two, Soy and Sunflower Lecithin, were chosen because they had a Hydrophile-Lipophile Balance (HLB) level of 7-8 (middle of the road for W/O emulsions), had success in previous EHD experimentation, and are distilled from two of the four tested vegetable oils. While they have the same chemical formula, having validated both independently allows for the use of either in scenarios where the GMO status of soybean products has negative commercial appeal. Polysorbate 20 & 80 was chosen due to their high usage as an emulsifier in the food industry. Both are nonionic surfactants derived from sorbitan esters. The main characteristic difference is their HLB values. In this case, Polysorbate 20 falls in the 'detergent' range and Polysorbate 80 falls in the 'solubilizing agent' range (Gaonkar et al., 2014). Propylene Glycol is a non-ionic emulsifier that was chosen due to its special nature in the food industry. Propylene Glycol has polar head groups that contain oxygen, nitrogen, and phosphorus as electronegative heteroatoms (Hasenhuettl & Hartel, 2009). While Propylene Glycol is used as an emulsifier in the food industry, it doesn't have a generally recognized HLB number.

For the Soybean oil test, samples were made up with either Soy Lecithin, Propylene Glycol, or Polysorbate 20 in concentration of 5% and 10%. For the Sunflower oil test, samples were made up with either Sunflower Lecithin, Propylene Glycol, or Polysorbate 80 in concentration of 5% and 10% For the Rapeseed (Canola) oil test, samples were made up with either Sunflower Lecithin, Propylene Glycol, or Polysorbate 20 in concentration of 5% and 10%. Finally, for the Palm Oil test, samples were made up with wither Soy Lecithin, Propylene Glycol, or Polysorbate 80 in concentration of 5% and 10%.

The purpose of this experiment was to measure the impact of surfactant on the atomization ability of various oil/emulsifier combinations. Samples of oil and emulsifier solutions at varying concentrations, pressures, cross-sectional capillary diameter, temperature, and applied voltage were tested to determine the impact of adding a surfactant to vegetable oils at different conditions. It was generally believed that adding a surfactant to the base oil would decrease the surface tension of the solution so atomization could occur. It was also generally believed that it was possible to utilize EHD spray technology in a spot-spray application.

As outlined in Chapter IV, each test was conducted by spot spraying a piece of oil sensitive paper for a duration of 300ms. The oil and emulsifier blend was sprayed through a patent pending (USPTO Application # P2512US00) electrically-actuated spray-valve. The sample was then photographed with a 24MP digital camera and data analysis was conduction using Image-J scientific image analysis software.

3.1.4. Impact of Temperature

Testing Factor #3 (three levels), the purpose of this experiment was to measure the impact of temperature on various oil/emulsifier combinations. Samples of oil and emulsifier solutions at varying concentrations, pressures, cross-sectional capillary diameter, and applied voltage were tested to determine the impact of increased temperature at different conditions. Tests were conducted at temperatures of 120F, 180F, and 240F. It was generally believed that increasing the temperature of a solution would lower its kinematic viscosity and density and allow for a greater volumetric flow at constant pressure, capillary cross sectional diameter, and spray time. It was also generally believed that at lower pressures, the impact of temperature on droplet count, droplet size, and percentage of area covered would be favorable with a result of lowering the average droplet size and increasing the percentage of area covered. It was believed that the opposite case would occur for higher temperatures at higher pressures.

As outlined in Chapter IV, each test was conducted by spot spraying a piece of oil sensitive paper for a duration of 300ms. The oil and emulsifier blend was sprayed through a patent pending (USPTO Application # P2512US00) electrically-actuated spray-valve. The sample was then photographed with a 24MP digital camera and data analysis was conduction using Image-J scientific image analysis software.

3.1.5. Impact of Pressure and Capillary Diameter

Testing Factor #4 (3 levels for pressure and 2 levels for cross sectional diameter of the capillary tube), the purpose of this experiment was to measure the impact of pressure on various oil/emulsifier combinations at differing cross-sectional capillary diameters (varying volumetric flow). Samples of oil and emulsifier solutions at varying concentrations, temperatures, and applied voltage were tested to determine the impact of increased pressure and volumetric flow rate at varying conditions. Two different capillary needles were used (gauges 19 & 22) measuring 2" long. Pressures for the 22ga (0.01625" diameter) capillary tests were 1psi, 2psi, and 4psi. Pressures for the 19ga (0.027" diameter) were 4psi, 8psi, and 16psi. It was generally believed that increasing the pressure of a solution would increase volumetric/mass flow rate (measured as weight at a fixed spray time), and result in an increased droplet size and increased percentage of area covered. It was believed that the kinematic forces of increased liquid flow would overcome the ability to maintain successful EHD modes of spray at high mass flow rates (greater than 1 g/s).

As outlined in Chapter IV, each test was conducted by spot spraying a piece of oil sensitive paper for a duration of 300ms. The oil and emulsifier blend was sprayed through a patent pending (USPTO Application # P2512US00) electrically-actuated spray-valve. The sample was then photographed with a 24MP digital camera and data analysis was conduction using Image-J scientific image analysis software.

3.1.6. Impact of Applied Voltage

Testing Factor #5 (two levels), the purpose of this experiment was to measure the impact of voltage on various oil/emulsifier combinations. Samples of oil and emulsifier solutions at varying concentrations, pressures, cross-sectional capillary diameter, and temperature were tested to determine the impact of increased voltage applied to the solution. It was generally believed that increasing the voltage applied would follow Rayleigh’s limit (equation 4) and produce smaller droplets. It was unclear how an increase in voltage would impact the percent of area covered.

As outlined in Chapter IV, each test was conducted by spot spraying a piece of oil sensitive paper for a duration of 300ms. The oil and emulsifier blend was sprayed through a patent pending (USPTO Application # P2512US00) electrically-actuated spray-valve.

The sample was then photographed with a 24MP digital camera and data analysis was conduction using Image-J scientific image analysis software.

3.1.7. Data Analysis

Given the large amount of data generated by the proposed experiment, DOE software was used to help draw conclusions regarding the responses generated. Quantum XL (QXL) software was used to process the data. A series four (4) factor experiments were carried out for concentration, voltage, temperature, and pressure. The experiment was be conducted once for the 19 gauge capillary and once again for the 22 gauge capillary (see table 2). The experiment set was be repeated for each oil and emulsifier combination (4 oils and 3 emulsifiers) for a total of 864 individual runs. From the DOE analysis of Y-hat data, it was possible to determine the relationship between concentration, voltage, temperature, and pressure as they relate to the outputs of mass flow (measured as weight at a fixed spray time), droplet size, droplet count, and coverage area. An analysis of the data is provided in Chapter V.

While the experiment was built on the work of Aykas and Barringer's research (2012), it incorporated the additional complexity of addressing non-continuous, or spot spray, application and several oil/emulsifier blends. Data analysis was reviewed looking at each oil and emulsifier combination as a separate experiment. Four factor ANOVA was conducted to determine the relationship between inputs within each experiment. Additionally, the entire data set was examined to determine patterns across all test runs.

Table 3:DOE Experimental Template

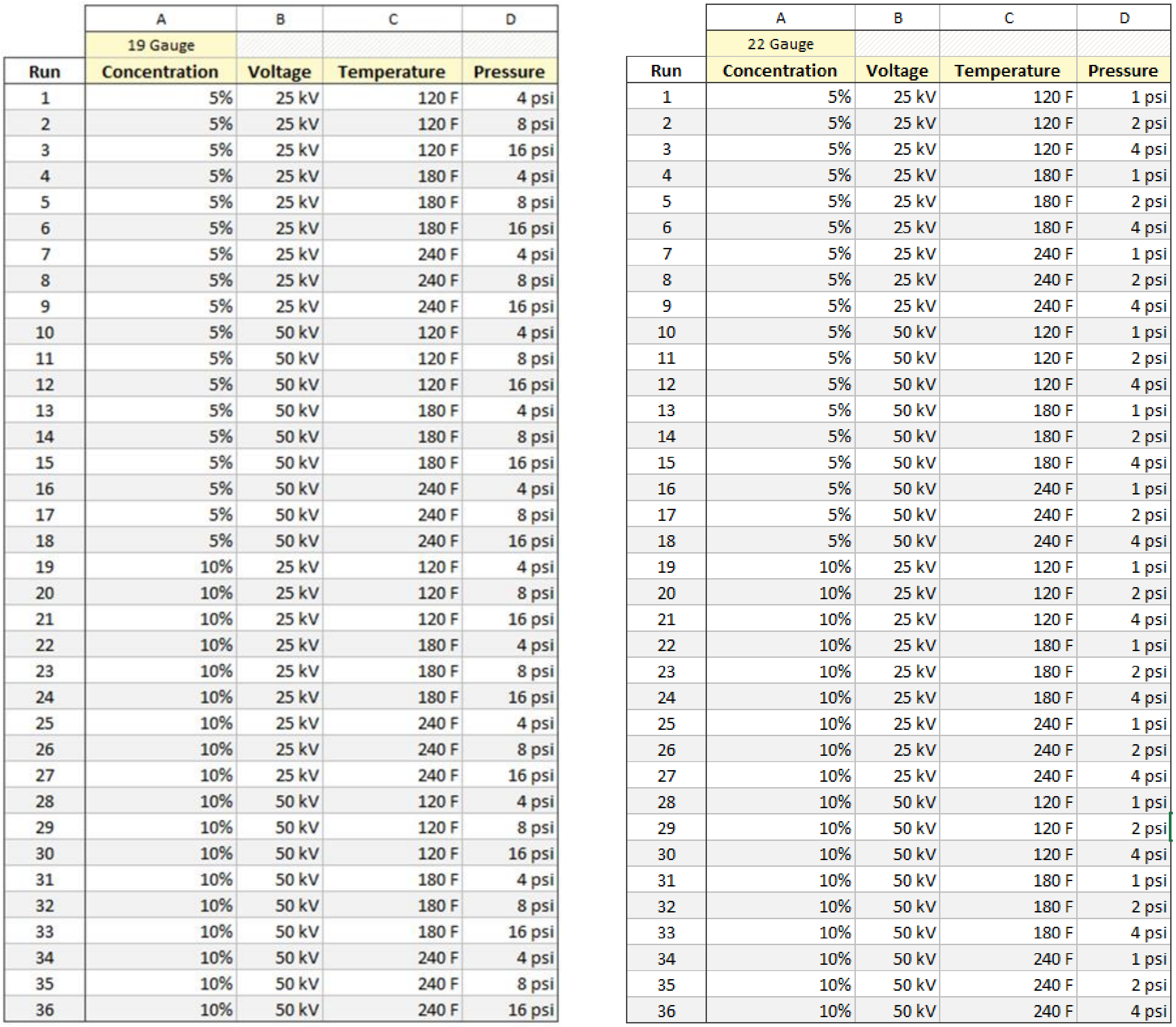

	A	B	C	D
	19 Gauge			
Run	Concentration	Voltage	Temperature	Pressure
1	5%	25 kV	120 F	4 psi
2	5%	25 kV	120 F	8 psi
3	5%	25 kV	120 F	16 psi
4	5%	25 kV	180 F	4 psi
5	5%	25 kV	180 F	8 psi
6	5%	25 kV	180 F	16 psi
7	5%	25 kV	240 F	4 psi
8	5%	25 kV	240 F	8 psi
9	5%	25 kV	240 F	16 psi
10	5%	50 kV	120 F	4 psi
11	5%	50 kV	120 F	8 psi
12	5%	50 kV	120 F	16 psi
13	5%	50 kV	180 F	4 psi
14	5%	50 kV	180 F	8 psi
15	5%	50 kV	180 F	16 psi
16	5%	50 kV	240 F	4 psi
17	5%	50 kV	240 F	8 psi
18	5%	50 kV	240 F	16 psi
19	10%	25 kV	120 F	4 psi
20	10%	25 kV	120 F	8 psi
21	10%	25 kV	120 F	16 psi
22	10%	25 kV	180 F	4 psi
23	10%	25 kV	180 F	8 psi
24	10%	25 kV	180 F	16 psi
25	10%	25 kV	240 F	4 psi
26	10%	25 kV	240 F	8 psi
27	10%	25 kV	240 F	16 psi
28	10%	50 kV	120 F	4 psi
29	10%	50 kV	120 F	8 psi
30	10%	50 kV	120 F	16 psi
31	10%	50 kV	180 F	4 psi
32	10%	50 kV	180 F	8 psi
33	10%	50 kV	180 F	16 psi
34	10%	50 kV	240 F	4 psi
35	10%	50 kV	240 F	8 psi
36	10%	50 kV	240 F	16 psi

	A	B	C	D
	22 Gauge			
Run	Concentration	Voltage	Temperature	Pressure
1	5%	25 kV	120 F	1 psi
2	5%	25 kV	120 F	2 psi
3	5%	25 kV	120 F	4 psi
4	5%	25 kV	180 F	1 psi
5	5%	25 kV	180 F	2 psi
6	5%	25 kV	180 F	4 psi
7	5%	25 kV	240 F	1 psi
8	5%	25 kV	240 F	2 psi
9	5%	25 kV	240 F	4 psi
10	5%	50 kV	120 F	1 psi
11	5%	50 kV	120 F	2 psi
12	5%	50 kV	120 F	4 psi
13	5%	50 kV	180 F	1 psi
14	5%	50 kV	180 F	2 psi
15	5%	50 kV	180 F	4 psi
16	5%	50 kV	240 F	1 psi
17	5%	50 kV	240 F	2 psi
18	5%	50 kV	240 F	4 psi
19	10%	25 kV	120 F	1 psi
20	10%	25 kV	120 F	2 psi
21	10%	25 kV	120 F	4 psi
22	10%	25 kV	180 F	1 psi
23	10%	25 kV	180 F	2 psi
24	10%	25 kV	180 F	4 psi
25	10%	25 kV	240 F	1 psi
26	10%	25 kV	240 F	2 psi
27	10%	25 kV	240 F	4 psi
28	10%	50 kV	120 F	1 psi
29	10%	50 kV	120 F	2 psi
30	10%	50 kV	120 F	4 psi
31	10%	50 kV	180 F	1 psi
32	10%	50 kV	180 F	2 psi
33	10%	50 kV	180 F	4 psi
34	10%	50 kV	240 F	1 psi
35	10%	50 kV	240 F	2 psi
36	10%	50 kV	240 F	4 psi

3.2. DESIGN OF EXPERIMENTAL TEST FIXTURE

3.2.1. Origin of the Experiments Concept

The Burford Hydroplate® Breadpan Oiler Model 7000 debuted in 1996. The 7000 series oiler, while the beneficiary of some upgrades, is still the flagship offering in Burford's pan oiler line and well respected in the industry. There are a couple of reasons

Figure 9: Burford Model 7000 Breadpan Oiler

why Burford's 7000 series oiler is still in production. The first, a matter of opinion, is that Burford is a quality manufacturer of industrial baking equipment. The second, a matter of fact, is that pan spraying technology hasn't advanced much in the last twenty years. The three methods of atomizing oil (air atomized, hydraulically atomized, mechanically atomized) haven't changed much in the last 100 years. In fact, Cook et al. (1925) claimed of their patent (US 1522867 A), "it is the object of the invention to provide bread pan oiling means of the above character wherein the oil is blown by means of air under pressure, in a finely atomized condition into several pans simultaneously."

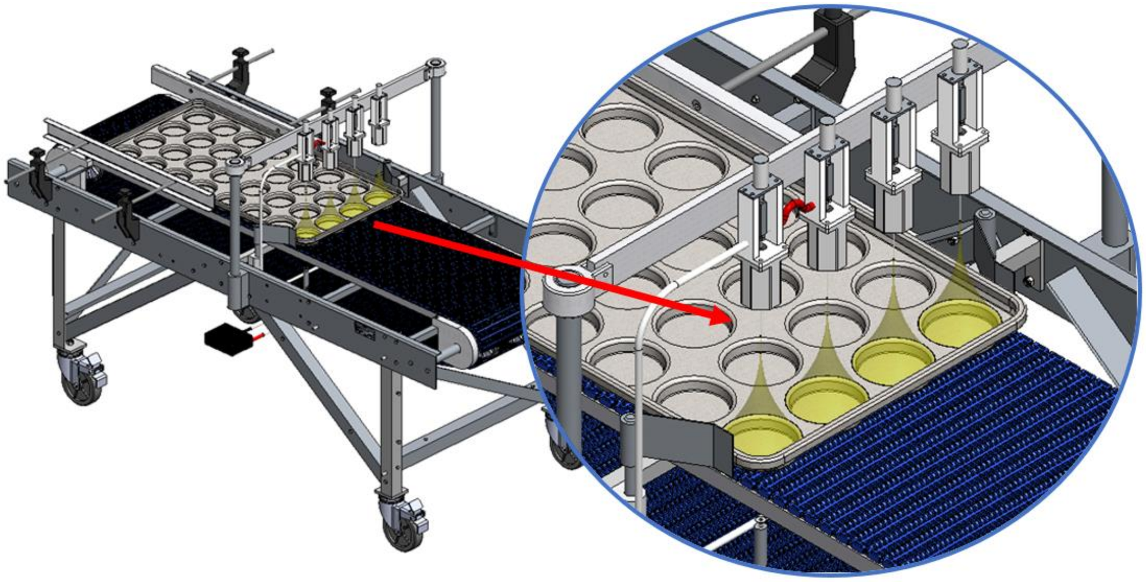

Figure 10: Electrostatic Spraying Machine Concept for Patent Application

Burford Corp. provided funding for the research described in this dissertation. In an interview with Burford's CEO, Mr. Fred Springer, he stated, "For years, bakeries have had to deal with the problem of overspray in pan oiling. Surely, there's a way this problem can be solved." This simple problem statement kicked off the research into advancing pan oiling technology. From this, the concept of using EHD spraying technology in pan oiling was born. It also provided three unique challenges with respect to EHD spraying that had not been addressed in academia before. First, to solve the problem, the application would need to be able to spot-spray the pan cavities. Second, it would have to spray at pressures higher than static pressure. Finally, it would need to address all four major commercially available vegetable oils and more than one emulsifier.

3.2.2. Design of the Test Fixture

The test fixture is designed as a 15" (width) by 15" (length) by 12" (height) enclosure made from Acetal Photopolymer (trade name Delrin by DuPont). The material was chosen for two reasons. First, it is easy to machine, and, second, it has a high dielectric constant (3.5-4 times that of air) and has a high electrical resistivity (1×10^{16} ohm-cm) (DuPont Corporation, n.d.). The uprights and bracing material was machined out of 1.5" Delrin square

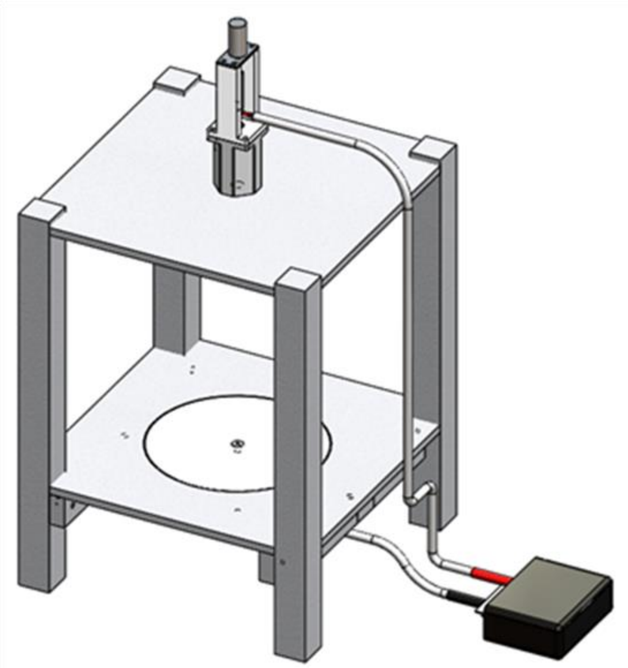

Figure 11: EHD Test Fixture

stock and the top and bottom plates were machined from 0.375” Delrin plate. The dimensions of the enclosure were determined by a couple of factors. First, 12” of clearance was needed between the uprights so that paper from a paper roll could be pulled through the enclosure. Second, a target collector plate of 8” in diameter needed to have enough clearance to determine if an overspray condition was present. The 8” diameter target was determined by using common sizing for bread and sweet goods pans. The height of the enclosure was determined by trial and error.

A collector plate 8” in diameter was made from 0.375” 6061-T651 Aluminum Plate (ASTM B209). Aluminum plate was chosen for two reasons. First, it is also easy to machine and second it has a very low resistivity (2.82 x 10^{-8} Ω/m) (Cutnell and Johnson, 1995). Polycarbonite covers were designed for the enclosure (12” x 15” x 0.25”) and used on three sides during the experiment. Polycarbonate was chosen because it is transparent and has a high resistivity (10^{15} Ω/cm) (Harper, 2003).

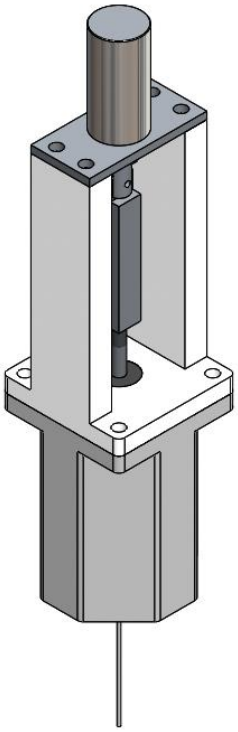

Figure 12: EHD Valve Assembly

Atop of the text fixture sits the electronic spray valve. The valve acts as the electrical charging point for the fluid pathway and as the valve for the spot-spray operation. The charging valve is made from Polytetrafluoroethylene (trade name Teflon). Teflon was chosen because its machinability and its exceptional insulative properties. Teflon has a dielectric constant of 2.1 with respect to air and a short time dielectric strength of 24 kV per millimeter. Teflon is highly electrically resistant with a resistivity of greater than 10^{18} Ω/cm. Teflon also has a Surface Arc-resistance of more than 300 seconds. All of these properties make it an excellent insulator and choice material for applications involving high voltage (DuPont Corporation, n.d.). A charging-rod/valve-stem was designed using Tungsten. Tung son was chosen for its hardness and its ability to carry a charge. The charging cage was designed and made from aluminum. A fast acting actuated 24v actuated but spring returned solenoid valve was chosen due to it actuation speed and ability to carry the appropriate load. The Patent Pending design (Application Number 2512US00 Dated 8-2-2017), discussed in the next section, allows fluid to enter the valve cavity where it is electrically charged as the valve stem lifts and the charged fluid escapes through a capillary tube.

The fluid path was designed to provide heated fluids at relatively low, but consistent pressure. A reservoir tank supplied pre-blended oil and emulsifier to a positive displacement pump. The pump supplied pressurized fluid, through a pressure accumulator, to a high-accuracy low-pressure regulator. The insulated line, from the regulator to the valve assembly, housed an in-line thermal heater. The control system for the apparatus was governed by a programmable logic controller (PLC) (Allen Bradley MicroLogix 1100). A temperature controller using a proportional-integral-derivative (PID) control loop (Watlow Electric Manufacturing Co.) provided steady thermal control to the inline direct current fluid heater.

3.2.3. Design of the High-Speed EHD Spot-Spray Valve

Will Rogers once said that, “Good judgement comes from experience, and a lot of that comes from bad judgement.” Quite literally all of the research in the field of EHD atomization has been done at extremely low pressure using syringe pumps in a continuous application mode. This is done so that the problem of conductivity to ground can be avoided. Traditionally, electrostatic spraying systems, such as those used in paint and powder coating, introduce the charge via an ionizing needle that produces an electric field after the liquid is atomized (typically by air assistance, hydraulic pressure, or mechanical atomization). This solves the grounding problem but is not as efficient as EHD spraying in eliminating the problem of misting. EHD spraying involves charging the liquid prior to exiting the capillary tube. The liquid and the capillary tube generate the electric field. Thus, the liquid must be able to carry a charge and any path to ground in the fluid pathway creates a grounding problem. In a bakery environment, the metal pans touch each other, or have the potential to touch each other, and, therefore, the spray must be positively charged and the collector (pan) must be negatively charged for safety reasons. Additionally, pan oiling requires discreet applications of oil that must occur rather quickly. The average bread line runs between 60 and 80 loaves per minute. This means that release agents must be spot sprayed and such technology does not exist.

The use of several different conventional spray solenoids valves was attempted prior to designing new technology. Each failed for one or two reasons. Either the charge carried through the liquid to the valve and grounded out internal components (most common) or the voltage applied to the fluid caused damage to the solenoid or the power supply. In one attempt, the valve was moved upstream 36 inches and high temp poly holes was used to try to isolate the valve from the applied charge (connected to the capillary tube). Not only did this not work (grounded the power supply), it failed to stop fluid from dripping when the system was not in use. The line would simply empty its contents. It was also hard to hold a consistent temperature with the valve so far from the capillary tube.

The failure of commercially available solenoid valves to perform led to a unique set of criteria in solving the problem. The valve would need to:

1. Be made of materials that were conducive to EHD spraying (50 kV application)
2. Be fast acting enough to be used as a spot-spray valve
3. Be made in such a way to isolate the valve stem from earth ground
4. Have a solenoid far enough removed from the valve body to prevent electrical arcing
5. Have a way to charge the fluid designed into the valve

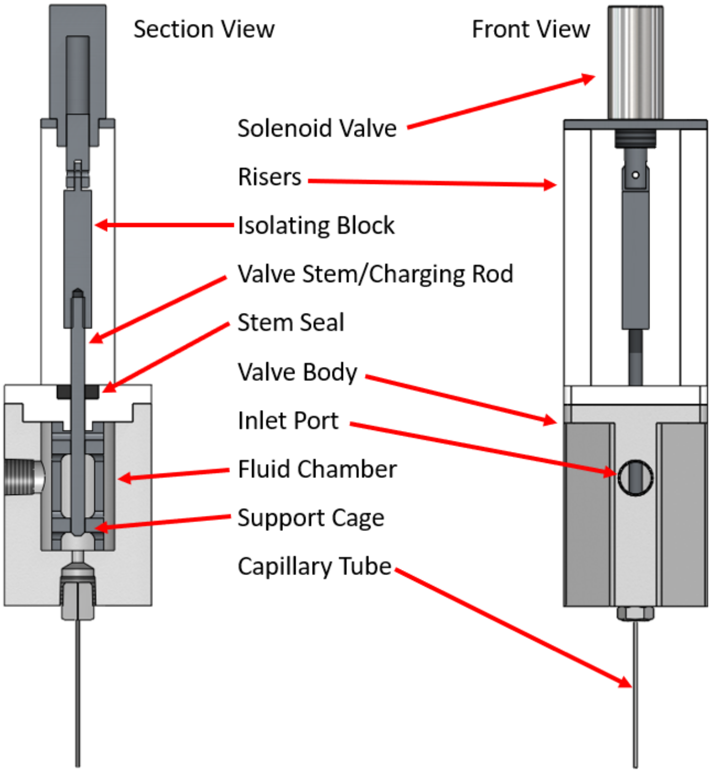

Figure 13: EHD Spot-Spray Valve (Patent Pending: P2512US00)

Because the spray valve is to be used in a food processing environment, all of the materials used needed to be food safe (FDA approved). For the valve body, Teflon was used. Teflon was selected due its high electrically insulative properties (resistivity $>10^{18}$ Ω/cm). Tungsten was used for the charging-rod/valve-stem. Tungsten was selected due to its high tensile strength (100-500 K psi), Hardness (Brinell 2570), high corrosive resistance, and low electrical resistivity (5.5 x 10^{-6} Ω/cm). 316 grade Stainless Steel was chosen for the rod support cage. This was due to its acceptance as a sanitary material and it low electrical resistivity (74 x 10^{-6} Ω/cm) (McLean, 1977). The capillary tubes were purchased buy were also made from 316 Stainless Steel as was all of the hardware.

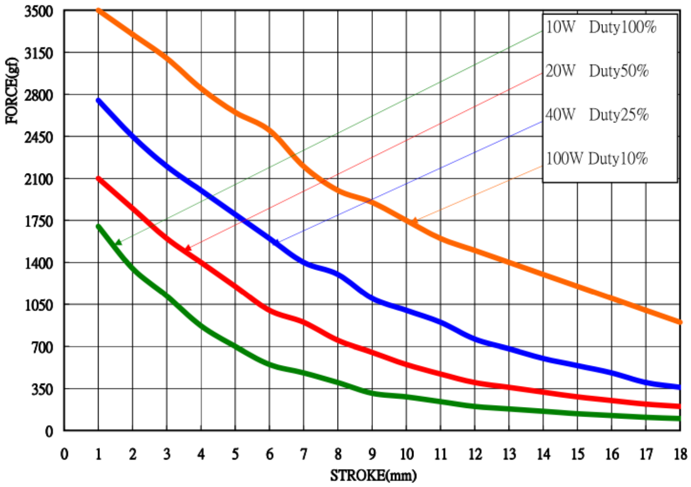

Figure 14: Force-Stroke Chart for Pull Solenoid (Source: Goldsun Electronics Co.,LTD, n.d.)

The solenoid valve chosen for the design was manufactured by Goldsun Electronics Co., LTD (pn SH-T2551L-24V) and was a 24V and 20W pull type solenoid with a spring return and an 18mm stroke. In the design, the stroke was mechanically limited to 1-2 mm at the retracted state. This allowed for the maximum pull strength (approximately 1925 gf or 4.24 lbf at 50% duty cycle). The reaction time for the solenoid at this stroke was 8.5 ms^{-1}. It was estimated that in a production environment that the solenoid would operate between a 50% and 100% duty cycle. This was based on 1-2 valves per cavity, 6 cavities per pan, and 60 pans per minute (60 seconds). For the test runs, a PLC processor controlled the actuation time, 300 ms^{-1} test time plus 17 ms^{-1} actuation time, via the PLC's high-speed counter clocking 20 KHz.

In the design, the valve body is separated from the solenoid by 3.5" risers. A connector block made of Delrin was used to connect the solenoid to the valve stem. This provided electrical isolation between the solenoid and the valve body. While not shown in the EHD spot-spray drawing (Fig 13), the risers are to be covered by 0.25” Delrin to isolate the charging rod from the environment.

The valve body was designed from Delrin and contains a 1” diameter by 2.5” deep fluid cavity. Within the cavity rests the support cage (made from 316 stainless steel). The purpose of the cavity is to allow fluid to collect around the valve stem/charging rod. The support cage is a lattice cage with an opening at top and bottom where a hole with a diameter that is a slip fit to the valve stem/charging rod. The support cage allows fluid to pass through while supporting the alignment of the charging rod. The inlet and outlet of the valve body is tapped 0.25” NPT thread. High temperature silicone hose feeds a 0.25” NPT fitting on the infeed and the capillary tube threads into the discharge. Atop of the discharge threads is geometry that matches the charging rod. When pressure from the solenoid valve is transferred to the valve stem/charging rod, it seats within this geometry and creates a seal. This seal acts as a plug atop of the capillary tube and creates a weak vacuum. The vacuum prevents the liquid in the capillary from dripping out once the valve is closed.

The valve stem/charging rod performs two tasks. First, it acts as a valve stem and plug for the flow of liquids through the system. The solenoid is a pull operated spring return type device that opens the fluid pathway via the solenoid’s pulling force, but closes the valve via a spring return. There is a specific reason for this. The solenoid retracts quickly to start the fluid flow and rests on the back stop geometry within the solenoids housing. This means that the solenoid is only electrified when the system is spraying fluid.

In the opposing configuration, voltage would need to be applied to ensure the solenoid stayed shut. Second, the spring return means that the pressure acting on the seat of the valve body is adjustable by adjusting the spring compression and K factor. The solenoids pull pressure, howeber, is binary. The second function of the valve stem/charging rod is to act as a conductor for the applied voltage. The voltage is applied by attaching the positive terminal of the DC power supply to the charging rod. The charging rod passes through the seal and into the fluid chamber. This transfers the charge to the liquid.

3.2.4. Design of the Fluid Train and Control System

The fluid train for the test fixture is as important to the process as the EHD spray valve. The fluid train ensures that the oil/emulsifier blend reaches the spray valve at the right temperature and pressure. It is important to do this without grounding the fluid pathway. To do this, liquid is drawn up from a supply reservoir through a low-volume high-pressure (ProCon Model 113A070F31BA 250) rotary vane pump. The liquid is pushed into/past a high pressure accumulator and into the inlet of a regulating valve. The duel stage regulator (Matheson Model 3810A) has the ability to deliver constant pressure with a decreasing or inconsistent inlet pressure. Duel stage regulators are used in applications where constant delivery pressure is important (Matheson Tri-Gas, 2014). Fluid leaves the regulator at a pressure between 0.1 psi and 30 psi. From the regulator, the fluid enters an in-line electric heater. The heater raises the temperature of the oil/emulsifier blend from room temperature to 240F. At the discharge of the heater, the fluid enters high-temperature silicone tubing. The tubing carries the fluid to the EHD spraying valve.

The motor for the system was a Baldor 0.5 hp, 1725 rpm, 480V, 3 phase motor on a NEMA 56TC frame. The motor was linked to a ProCon Series 3 rotary vane pump, operating at 15 GPH at 250 psi, via a Lovejoy S-Flex coupling. The coupling is important as it isolates the motor shaft from the input shaft of the vane pump and creates a ground break. The standoff's connecting the motor to the pump were also isolated using 0.25" thick Teflon spacers. Nominal speed for the rotary vane pump is 1725 RPM at 15 GPH.

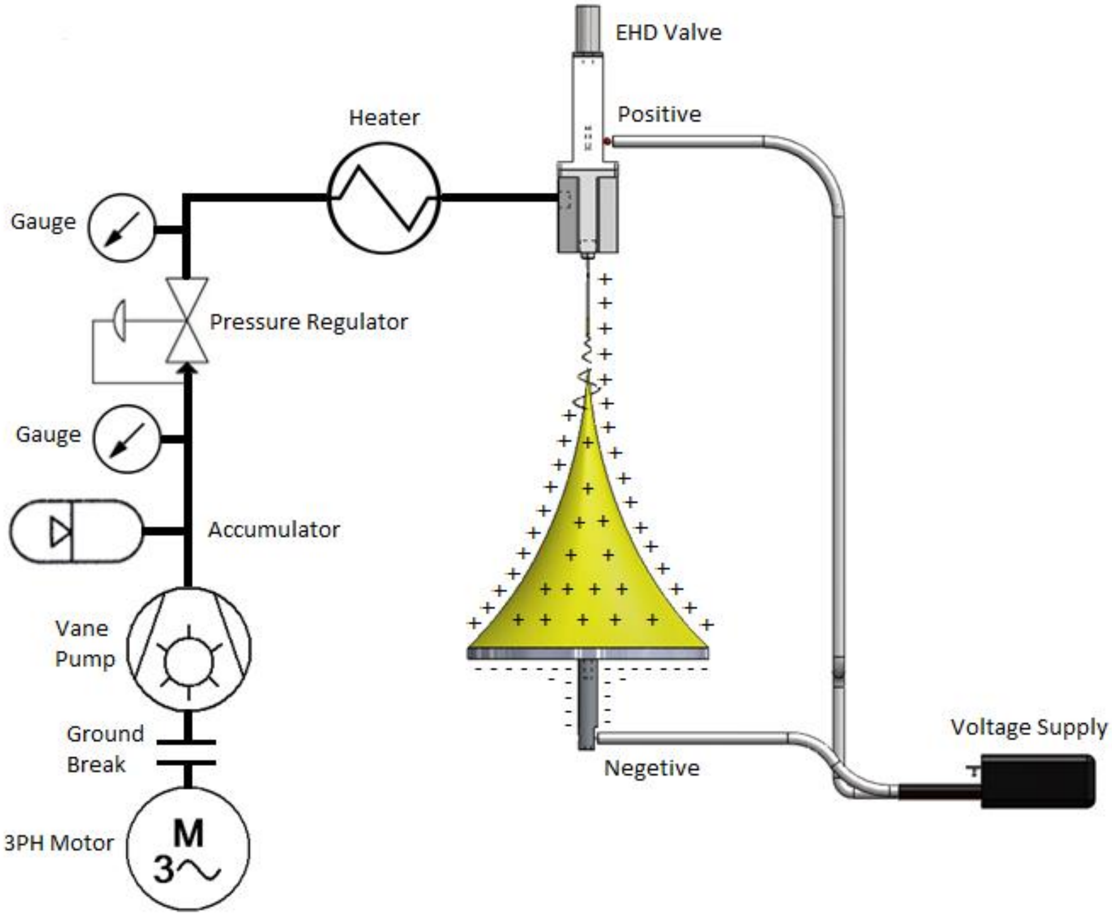

Figure 15: Fluid Train for the EHD Spraying System

The hydraulic pressure accumulator chosen for the system was a Parker-Hannifin 150 Cubic inch, 3K psi, single-port unit with a fluoroelastomer bladder. The accumulator was plumbed in a standard 'T' configuration between the vane pump and the pressure regulator. The pressure regulator chosen was a Matheson Model 3810A dual stage high purity stainless steel regulator. The regulator was designed to take the high pressure discharge from the vane pump and regulate it down to under 30 psi of pressure.

Next, a Watlow 1/8th inch diameter FireRod 240V heater with a design maximum operating temperature of 1400F and a maximum Wattage density of 400 W/in^2 was used to raise the temperature of the oil/emulsifier blend to 240F. High temperature silicone tubing was used to carry the fluid to the EHD valve and the fluid path from the discharge of the regulator to the spray valve was insulated with fiberglass insulation and reflective jacketing. A Watlow EZ-Zone PM Express temperature controller was used to power the heater. It used a PID control loop to maintain the temperatures at the set points via 240V output.

The control center for the unit was a MicroLogix 1100 PLC processor. The PLC handled sequencing for startup, purge operation, outputs to the motor starter, power supply, EHD valve, timing operations, and inputs from the trigger and voltage selector. A 12/24V power supply was wired to an American High Voltage G Series high voltage power supply operating at up to 50kV at 5W and 0.1 mA. A two position switch was wired to the PLC and used to determine whether a 12V or 24V output was supplied from the DC power supply to the high voltage supply. This determined whether 25kV or 50kV was supplied to the EHD valve.

3.2.5. Theory of the EHD Test Fixture

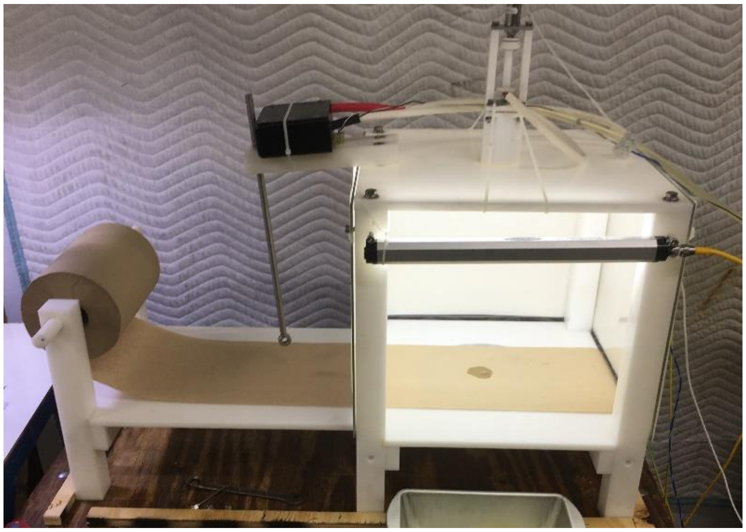

Figure 16: As Built EHD Test Fixture

The test fixture was designed to provide an environment that would minimize influence on the experiment by the outside environment and to provide a safe enclosure where high voltage (25kV and 50kV) could be applied to the oil/emulsifier blends. The enclosure was closed on all four sides by clear Polycarbonite covers. The enclosure was designed so that paper could be pulled through the enclosure and across the collector plate to provide a clean target for each test run. The Polycarbonite would clearly show if mist/overspray landed on their surfaces.

The EHD valve with capillary tube was designed to ensure the liquid flow from the capillary was laminar at all applied pressures. This is in direct contrast to traditional electrostatic spray guns. The purpose of this design was to ensure that any influence exerted on the laminar stream that would cause it to break up into droplets was only from the applied voltage. The charge was applied to the valve stem/charging rod only when the valve stem lifted and only for the duration of the test run (300 ms).

The fluid train was designed to provide the oil/emulsifier blends to the EHD valve at precise temperature and pressure. It also needed to do so without providing a path to earth ground. To accomplish this a rotary vane pump, pressure accumulator, dual stage regulator, and inline heater were used. Heated fluid traveled along an insulated 1 meter high-temperature silicone tubing to the EHD valve.

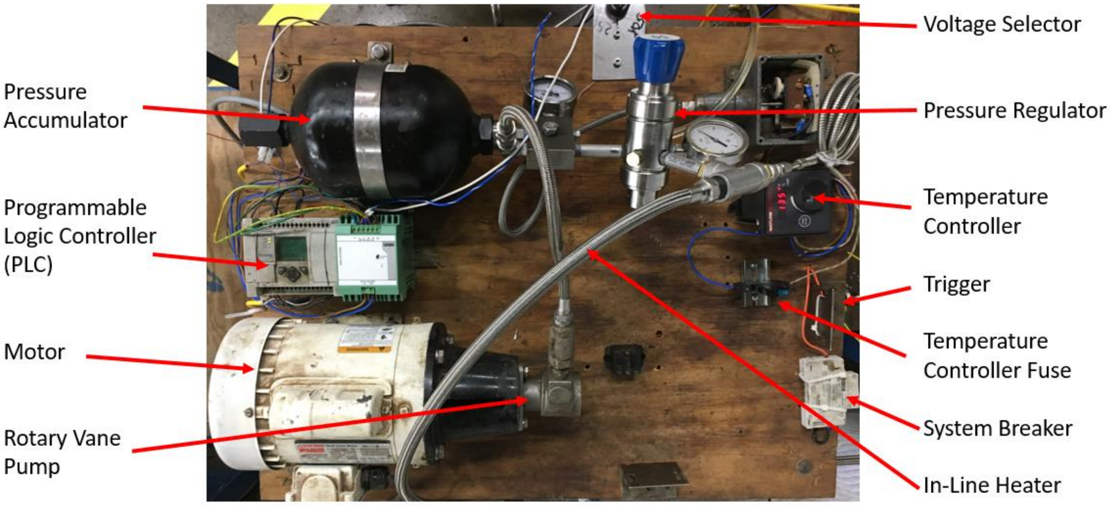

Figure 17: As Built Fluid Train

3.2.6. Photographic Imaging

The design call for images of test sprayed oil sensitive paper to be captured by a Nikon D7200 DSLR high-speed high-resolution camera. The camera is capable of delivering images at 24.2 megapixels, ISO range between 100 and 25600, and a shutter speed of 1/8000 second. This allows for both very high quality and very fast image capturing. The lens for the experiment was a Nikon DX 10-55 mm. Images were taken at the 55mm setting, at a distance of 15.75”, and an ISO setting of 80.

To ensure that every image was captured under the same conditions, an Image Fixture was designed to fix the tripod in a particular position. The fixture also included a fixed location for the oil sensitive test swatches. The location included millimeter incremented rulers for both the X and Y axis. This allowed for the scaling of the images in

Figure 18: As Built Image Fixture

the image processing software. A focus target was affixed to the Image Fixture so that the cameras focus point was always targeting the same location. This ensured that minor movements in the cameras location could be corrected. A Banner LED light (part#: WLAW105X180Q) was used to illuminate the work area. This provided a consistent 6500K wavelength for color temperature and gave 550 lumens of light.

3.2.7. Image Processing Software

The design of the experiment called for the spraying of oil/emulsifier blends onto oil sensitive paper. This allowed for the determination of droplet size and coverage area. High resolution digital images were taken of each test sample. These images were processed using ImageJ image analysis software. ImageJ is a Java based open source application developed by the National Institute of Health (NIH). Developed by programming pioneer Wayne Rasband in 1987, the National Institute of Health first introduced the biological image processing software, “NIH Image”, for Macintosh. By 1997, Rasband developed the first version of ImageJ (Schneider et al., 2012). Recognized extensively by the scientific community, ImageJ is capable of processing multidimensional images. In addition to standard image processing function such as sharpening, edge detection, smoothing, contrast manipulation, and median filtering, the software is capable of measuring distances and angles within and image, determining distinct geometric patterns, and can generate density histograms and line profile plots (Ferreira & Rasband, 2012).

For this experiment, the goal was to determine droplet size and pattern density for each sample. To do this multiple steps requires such as changing the image to an 8 bit image, performing threshold adjustments and then converting the image to a binary image, correcting for noise and contrast discrepancies, performing water-shedding to distinguish individual droplets, and perform data analysis on the sample. This data could then be used to determine performance characteristics of the oil/emulsifier blends and provide statistical data of the same.

CHAPTER IV

4. METHODOLOGY

The experiment used Design of Experiments (DOE) methodology to assess the relationships between each of the factors influencing the outputs of the process (see Figure 8). The experiment was broken into a series of categorical variables to include oil type, emulsifier type, and capillary gauge. For each category, separate experiments were conducted varying temperature, pressure, voltage, and emulsifier concentration.

4.1. OVERVIEW OF THE EXPERIMENT

Given the Test Fixture and parameters from the Design of Experiment (see Chapter III), a series of 864 samples of the four differing oils (Palm, Soybean, Rapeseed, and Sunflower) and five separate emulsifiers (Sunflower Lecithin, Soy Lecithin, Polysorbate 20, Polysorbate 80, and Propylene Glycol) were blended and sprayed through a capillary tube onto oil sensitive paper at high voltage. DOE factors for the experiment included:

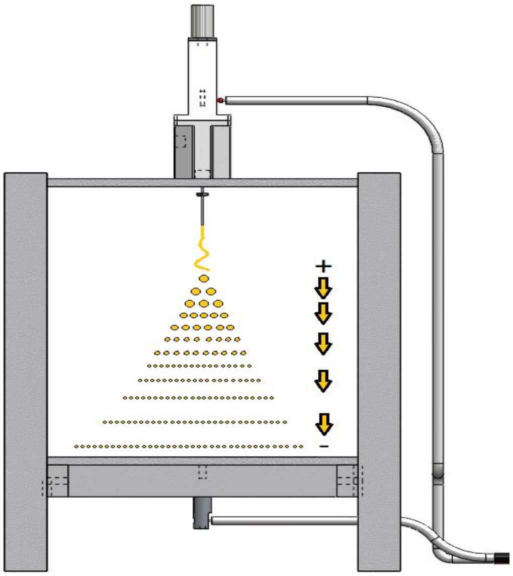

Figure 19: EHD Spray Concept - Varicose to Kink Instabilities

- Four different oil types (Palm, Soybean, Rapeseed, and Sunflower);
- Five Different Emulsifier Types, 3 per oil tested (Soy Lecithin, Sunflower Lecithin, Polysorbate 20, Polysorbate 80, and Propylene Glycol);
- Two different emulsifier concentrations (5% and 10%)
- Two Different High Voltages (25kV and 50kV) and at the null state;
- Two different pressure ranges (1, 2, and 4 psi @ 19ga) and (4, 8, and 16psi @ 22ga);
- Three different Temperatures (120, 180, and 240 F)

Separately, the four base oils were sprayed without the addition of an emulsifier at high voltage as a control. The performance of each of these tests were recorded and analyzed to determine the impact of the DOE factors on droplet size, area covered, and mass flow rate. Additionally, weights were taken at each experimental condition to determine the mass flow rate.

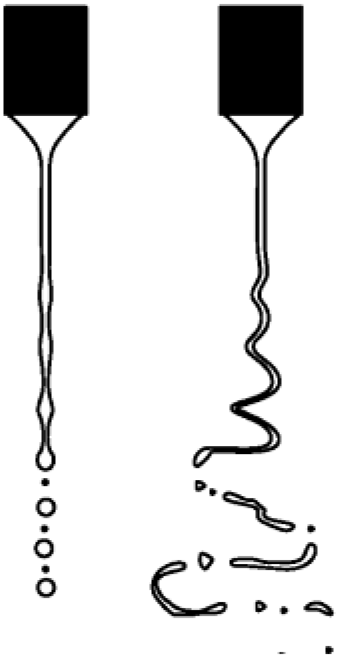

Figure 20: Cone-Jet transformation from Varicose to Kink instabilities (Source: Hartman et al., 2000)

For each test, pressurized fluid (1-16psi) was fed to a custom spray valve with a capillary tube affixed to the bottom. High voltage (25kV – 50kV) was applied to the charging rod in the EHD spraying valve (see Figure 13) and a charge was imparted to the respective oil/emulsifier blend. The fluid exited the nozzle in laminar flow. An electric field was generated between the capillary tube on the EHD spray valve and the collector plate (see Figure 15). The fluid was positively charged and the collector was negatively charged. Once the fluid left the capillary tube, the charge applied, being greater than the Rayleigh

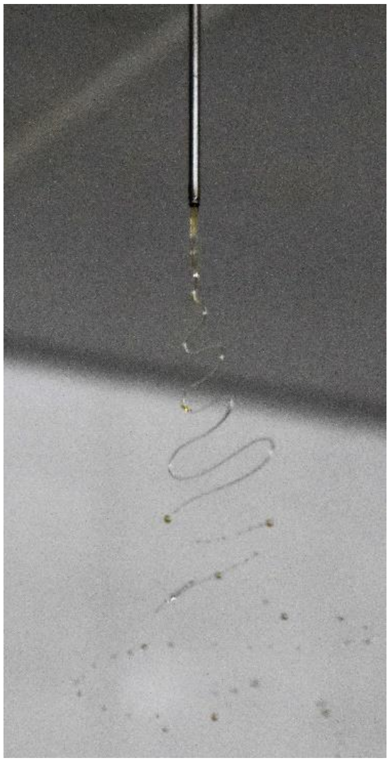

Figure 21: Cone-Jet mode from Experiment (Soybean oil & Lecithin @ 22ga, 16psi, 120F) showing Kink Instabilities

Limit (see Equation 5 & 6), caused the liquid to reach the critical point and the cone-jet to form first a varicose and then a kink instability (see Figures 20 & 21). The instabilities, due to additional charge picked up in the electric field, continue to break heterogeneously into smaller and smaller droplets between the discharge of the capillary tube and the collector plate (see Figures 19 & 20).

The goal of the experiment is to replicate the conditions of a coating application such as what might be expected in an industrial bakery. Electrically charged droplets were sprayed (positive ionically charged liquid), through an electric field, toward towards a collector plate (negatively charged). An oil sensitive paper test swatch was placed in the center of the collector plate and the charged droplets impacted the test swatch. The test swatch was then allowed to sit for 60 seconds to allow for contrast to activate. The test swatch was then photographed at high resolution. This method of sampling for droplet size and coverage density follows that of Jayasinghe and Edirsinghe (2002), Aykas and Barringer (2012), and Barringer and Sumonsiri (2015).

Image analysis software (ImageJ version 1.51s) was then used to process the images into data than could be interpreted into droplet size and coverage density. Pivot tables and DOE statistical software (Quantum XL) for Microsoft Excel was used to analyze the collective data from the image analysis software.

4.2. EXPERIMENT SETUP

The experiment's input factors (Time, Temperature, Pressure, Voltage, Emulsifier Concentration, and Capillary Size) were setup so that the conditions could be repeated across the entire series of experiments. Several mechanical and electrical devices (outlined in Section 3.2) were used to control these input parameters. These include a Programmable Logic Controller (PLC), a Direct Current voltage regulator, a Dual Stage pressure valve, a Thermal Controller, and two switches.

4.2.1. Controls Scheme

Several mechanisms where used to control the input parameters of the experiment as follows:

4.2.1.1. Spray Time

Spray time was controlled by the Programmable Logic Controller (PLC). Using a laptop computer, ladder logic was written to control an electrical output of the MicroLogix 1100 processor. Scan time for the PLC is 240μs (Rockwell Automation, 2011). A fixed spray time of 317ms was used for each experiment. 300ms was established as the spray time and 17ms was determined to be the auction time (open and closed) for the EHD spray valve. A timer was programmed into the PLC and controlled by a push button switch wired into one of the PLC's inputs. When the push button was pressed and released (total engagement less than 1 sec) then the PLC timer would engage and spray for the allotted time.

4.2.1.2. Valve Actuation Time

Valve Actuation time was controlled by the Programmable Logic Controller (PLC) and established through empirical testing. Canola oil, having a kinematic viscosity of 25.72 $mm^2 s^{-1}$ and falling in the mid-range of all of the tested oil, was heated to 120F and sprayed through the EDH spray valve. Without any applied voltage, an oil sensitive test paper was placed under the capillary tube (19ga and 22ga), the timer was set at 5ms, and the valve was actuated. This produced no noticeable oil flow at the capillary. The timer was increased by 1ms and the process repeated until liquid flow was present at the discharge of the capillary. Liquid was visibly noticed, via the oil sensitive paper, at 18ms. From this test, it was determined that the valve actuation time was estimated to be 17ms.

4.2.1.3. Valve Purging

The PLC was programmed, via ladder logic, to treat the input switch differently under two separate conditions. In condition one (1), when the TEST SWITCH is depressed for less than one (1) second, the EHD spray valve is actuated for 317ms with voltage applied to the Charging Rod (see Figure 13). In condition two (2), when the Test Switch is depressed for more than one (1) second, the system goes into purge mode and the valve stays open and voltage is applied until the switched is depressed for a second time. This allows for fluid to pass through the system and ensure that the proper temperature of the oil is carried through to the EHD spray valve.

4.2.1.4. Temperature Control

A Watlow FireRod 240V in-line internal heater was used to heat the oil prior to spraying. The heater operated at 240V produced a maximum heat density of 400 W/in2 at a maximum temperature of 1400F. The heater had an internal temperature probe that connected back to a Watlow EZ-Zone PM Express temperature controller. The temperature controller used the feedback from the temperature probe to control the temperature in the fluid line via a Proportional-Integral-Derivative (PID) loop. This allowed for the temperature to be controlled to within one degree of the set point (+/- 1 deg F) at 240F. The temperature controller and was controlled via a 4-20 mA signal between the PLC controller and the temperature controller. This allowed the temperature controller to be turned on and off with the systems Master Control switch. It also allowed for the temperature set point to be controlled via the PLC.

Figure 22: Watlow EZ Zone Temperature Controller

4.2.1.5. High Voltage Control

High voltage direct current was supplied to the EHD spray valve charging rod via an American High Voltage Series G power supply. The Series G power supply is capable of producing between 0 and 50kV at 0.1mA. The input voltage for the power supply is proportional to the output with input requirements between 0 and 24V. For this experiment, two voltages were supplied to the power supply. The first, 12VDC produced 25kVDC from the power supply. The second, 24VDC produced 50kVDC from the power supply.

The 12/24VDC was supplied from a 120VAC dual output 12/24VDC transformer and controlled by a 12VDC relay. The 12VDC relay was controlled by the PLC from an input selector switch (Voltage Selector Switch) wired into the PLC.

When the High Voltage selector switch was set to either voltage AND the Test Switch was depressed (in either test or purge mode), the PLC activated the output to the High Voltage power supply by means mentioned above and the system became charged. As programmed by ladder logic, this operation occurred 10ms prior to the section of programming that operated the solenoid valve for the EHD spray valve. Moreover, the system was programmed to stay charged 10ms after the solenoid valve for the EHD spray valve was deactivated.

4.2.1.6. Pressure Control

Pressure control for the system was done manually by adjusting the set point of a dual stage pressure regulator (Matheson Model 3810A). Upstream of the dual stage regulator pressure was supplied via a rotary vane pump and stored in a pressure accumulator. While the ProCon Series 3 rotary vane pump was capable of producing 82GPM at 250psi, pressure was regulated with an electronic pressure switch set at 100psig. Upstream pressure was monitored via a mineral oil filled pressure gauge with a range of 0-500 psig with increments at every 10 psig. The downstream pressure was also measured with an oil filled pressure gauge with a range of 0-30 psig with increments at every 0.5 psig.

Downstream system pressure was increased or decreased by turning the dual stage pressure valve. In the case of increasing pressure, the Pressure Regulator's valve was turned clockwise until the downstream static pressure met the requirements of the test. Each test started from low pressure and moved to higher pressure with subsequent tests. When lowering the system pressure, the Pressure Regulator's valve was turned counter-clockwise to lower the pressure and the EHD spray valve's solenoid was actuated to relieve system pressure before the new pressure was recorded.

Figure 23: Matheson Dual State Pressure Regulator with infeed and discharge pressure regulators

Upstream pressure was maintained using a diaphragm type pressure accumulator. This allowed for pressure to be built and maintained upstream greater than the downstream pressure required by the test. As such, the rotary vane pump would cycle as needed to maintain the pressure. The diaphragm pressure accumulator was ported so that up to 125psi of pressure could be maintained on the non-fluid side of the accumulator. The diaphragm's bladder for the accumulator was replaced with each oil/emulsifier sample group.

4.2.2. Blending Oils and Emulsifiers

A two gallon glass container was used as the storage tank for the system. The lid was modified to allow for the input hose for the rotary vane pump to pass through and reach the bottom of the container. The container was emptied and cleaned with dish soap and warm water between sample groups. A two cup glass measuring cup (Catemount Flameware) was used to measure out the oil and emulsifier at room temperature (set to approximately 80F). Twenty (20) cups of each sample group were blended for each series of tests. For the 90/10 percent blend, nine of the (2) cup containers of oil were poured into the 2 gallon glass storage container and one (2) cup container of emulsifier was added. For the 95/5 blend, nine and one half of the (2) cup containers of oil were poured into the 2 gallon glass storage container and one-half of a (2) cup container of emulsifier was added. For each of the measuring cups added, liquid was filled to the proper increment mark and measured by the meniscus of the fluid. Once the (20) cup mixture was poured into the (2) gallon storage tank, the blend was mixed thoroughly with a long metal spoon. This process was repeated for each sample group as the liquid required to charge the accumulator and line was roughly equal to (24) cups of solution.

Figure 24: 2 CUP capacity mixing cup by Catamount Flameware

Observations from the blending process indicated that some foaming occurred after vigorous stirring and some air bubbles remained in suspension for a short time (usually less than 5 minutes), but both seems to settle in just a short amount of time. The blend was mixed thoroughly with a long metal spoon. The emulsifiers stayed in suspension in each case. The dark color of the lecithin (Soy and Sunflower) darkened the mixture, but no other changes were noted.

4.2.2.1. Palm Oil Blending

Palm oil is not completely liquid at room temperature. In order to blend Palm oil with the three emulsifiers chosen for the experiment, the Palm oil was placed in a 1000W microwave, in its original one-gallon plastic container, and heated on high for one (1) minute. The container was removed and slowly shook by hand. This process was repeated several times (approximately 3) before the Palm oil was completely liquid. Once the Palm oil was completely liquid (target of 100F), the respective emulsifier was heated similarly to a temperature of 100F (as measured by a cooking thermometer). The Palm oil was then blended with the respective emulsifier in accordance with the procedure outlined in Section

4.2.2.2. Oil/Emulsifier Storage

The (2) gallon glass storage tank was kept in a modified portable chest cooler. A small portable heater was placed inside the chest and a temperature probe (thermocouple) was placed between the heater and the glass container. The heater (via a 12VDC relay and switch) and thermocouple were wired to the PLC. When the temperature inside the chest cooler fell below 95F, the heater was turned on. When the temperature inside the chest cooler reached 110F, the heater was turned off.

4.2.3. Sample Weights

For each of the 865 test runs and the 4 control tests, a weight was taken at experimental condition. An Ohaus Scout SPX422 balance scale was used for taking weights. The scale had a maximum capacity of 420g and a readability of 0.01g. A collection cup was utilized to weigh each test run. The scale was zeroed out and a tare was performed with an empty sample cup on the scale. Utilizing the collection cup and a fixture to hold the cup so that the discharge of the capillary tube was inside the cup, a series of 10 spray deposits were made into the collection cup at each experiment condition. The collection cup was then weighed and the weight recorded in the results spreadsheet. The weight was then divided by ten to provide an average weight across ten (10) samples.

4.2.4. Restrictions/Limiting Conditions

All materials and methods of construction of the test fixture were compliant with NSF-51 Standards for food equipment. All food materials consumed were Generally Recognized as Safe (GRAS) by the US Food and Drug Administration (FDA).

4.2.4.1. ***Restricting Spray Time*** – Each test run was conducted at a spray time of 317ms. This allowed for a deposit time of 300ms. This was done for two reasons. First, spray times longer than 300ms would make the system effectively too slow for industrial applications. Since the experiment was performed from the lens of an industrial bakery's need to coat bread pans, the spray time needed to be fast enough so that a series of two EHD spray valves could accomplish this task. Second, holding the spray time to 300 ms for each test run allowed the mass flow rates to be more easily defined. The cross-sectional diameter of the capillary tube was defined and the system's fluid pressure was defined for each test. Using a constant spray time allowed for a simple mass/volumetric flow calculation and provided clear contrast in the operating conditions at different pressures and cross sectional diameters.

4.2.4.2. ***High Temperature Silicone Tubing-*** In order to meet the temperature requirement of the heated oil, high temperature silicone tubing was used between the end of the inline heating section and the input to the EHD Spray valve. Silicone is also generally considered an electrically non-conductive material. This tubing had a temperature rating of -150F to 500F, but only had a maximum pressure rating of 30psi. The tests were designed to ensure a safety factor of 2 was employed for both the temperature and pressure of this limitation (max of 240F on temperature and max of 16psi on pressure). Several mistakes in adjusting pressure resulted in rupturing the line during the purge cycle.

4.3. EXPERIMENTAL PROCESS

4.3.1. Sampling Technique

The samples for this experiment fall in to two categories. The first category is the vegetable oil category. The second category is the emulsifier category. Sampling in both of these categories is biased based on:

- Oil category – Samples from this category include Palm, Soybean, Rapeseed, and Sunflower. These samples were chosen because they represent more than 87% of the world's oil production (US Foreign Agricultural Service, 2018) and are very commonly used as release agents in the baking industry.

- Emulsifier Category – Samples from this category were chosen based on the fact that they are commonly used in the baking industry and that they are surfactants with a HBL greater than a 6 on a scale of 0-20. Lecithin was chosen because of the previous research using this material (Aykas and Barringer, 2012 & others).

4.3.2. Procedures

Prior to performing any tests, the Test Coordinator ensured that the area was clean and that latex gloves were worn when handling test specimens. A spreadsheet was used to track each of the test samples. The spreadsheet listed each of the parameters for the individual test. With this established, the following procedures were used in running the test samples:

Step 1: *Review the testing parameters.* A review was conducted for each test sample. This included a review of each of the input variables for the test sample. A Test Swatch (oil sensitive paper) was selected from the supply and numbered to reflect that of the spreadsheet.

Step 2: ***Set Parameters.*** Set parameters to those required by the spread sheet for the particular test sample. This included:

- Setting voltage to the correct voltage by moving the voltage switch to the indicated setting.

- Setting temperature parameter on the Watlow temperature controller to the correct setting and waiting for the temperature to normalize at that temperature
- Setting the pressure to the correct setting by adjusting the dual stage regulator, purging the pressure, and viewing the normalized pressure after the correction. This process often required more than one iteration to get correct.
- Purging the system to ensure that the heated oil/emulsifier blend was at the correct temperature at the EHD spray valve.
- Observe temperature of the purged liquid with the infrared thermometer to ensure that the temperature at the capillary tube matched that of the Watlow temperature controller.

Step 3: *Perform weight testing.* As outlined in Section 4.2.3, a weight test was performed for each test sample. This included using the collection cup and running the sample with the test sample parameters ten (10) times and collecting the oil/emulsifier blend in the collection cup. The collection cup was then weighed and the weights were recorded in the spreadsheet. The weights were divided by ten (10) to get the average weight. The collection cup was then washed and replaced for the next test sample.

Step 4: *Ensure Test Area is Clean.* The test area, including the Polycarbonate covers, were sprayed with glass cleaner and wiped clean to ensure that any overspray observed was from the test sample run. This including pulling clean paper across the collector plate.

Step 5: *Placement of the Test Swatch.* The numbered test swatch (oil sensitive paper) was placed in the center-line of the capillary tube as indicated on the test fixture. The chemically treated side of the oil sensitive paper was set to face the discharge of the capillary tube.

Step 6: *Spray the Test Swatch*. After a quick review of the input parameters (variables) and a validation of the numbered Test Swatch, the Test Button was depressed for less than one (1) second to allow the EHD valve to spray the material onto the Test Swatch.

Step 7: *Removal of Test Swatch and Inspection of Test Fixture*. After the Test Swatch had been sprayed, the Test Swatch was removed by pulling the brown paper back from the test area and lifting the Tech Swatch gently by the edges and placing it on the Image Fixture (Section 3.2.6). An examination of the Text Fixture was conducted to ensure the area remained clean. Any unusual conditions were noted.

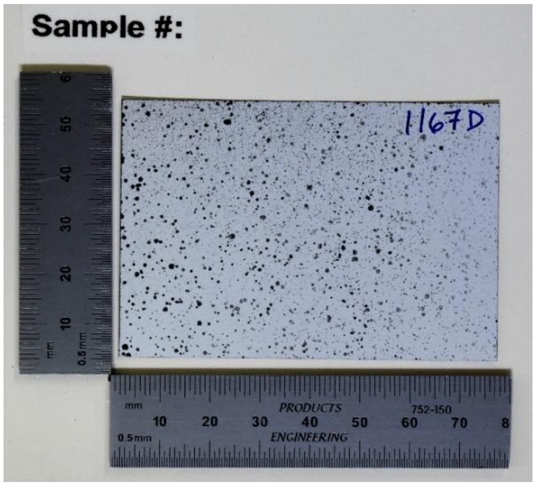

Figure 25: Sample of Raw Test Swatch Image (Before image processing) showing proper paper position.

Step 8: *Resting the Test Swatch*. Once the Test Swatch was sat on the Image Fixture, it was allowed to rest for 60 seconds to allow the chemicals in the oil sensitive paper to react with the oil and create contrast with the background color of the Test Swatch. The Test Swatch was affixed into the proper position in the Image Fixture so that a high-resolution photograph could be taken.

Step 9: *Photographing the Test Swatch.* Once the Test Swatch is located into the correct position on the Image Fixture, using a 24.2 Megapixel camera (Nikon D7200), a series of four (4) images were taken at the 55mm setting, at a distance of 15.75”, and an ISO setting of 80.

Step 10: *Photographic Image Processing*. Once all of the images were collected, Image processing was performed using ImageJ software to determine the outputs of the experiment. Outputs include:

- Number of Droplets per 25.4 mm^2
- Average Droplet Size in mm^2
- Weight of the sprayed liquid in grams.
- Percentage of area covered

4.3.3. Variables

The experiment was set up with three (3) different ordered categories (Oil type, Emulsifier Type, and Capillary Size). The experiment also had four (4) different variables that were tested for each of the categories as outlined in Section 3.1 (DOE) that include voltage applied, temperature of the oil/emulsifier blend, and the system pressure at the time of the sample. The following is a list of categories and variables:

4.3.3.1. Experiment Categories

The following ordered categories established the framework for the individual test samples. Each of the four (4) oil types were tested with three (3) different emulsifiers and (2) different capillary sizes. The categories do not indicate any variable other than the binary presence of the categorical variable. However, within this structure, four (4) different variables were tested including emulsifier concentration, voltage applied, system pressure, and liquid temperature. These variables had different values for the same property. The three categories are:

- *Oil Type* – Palm oil, Soybean Oil, Rapeseed Oil, and Sunflower Oil
- *Emulsifier Type* – Soy Lecithin (used with Soybean Oil and Palm Oil), Sunflower Lecithin (used with Sunflower Oil and Rapeseed oil), Polysorbate 20 (used with Soybean Oil and Rapeseed Oil), Polysorbate 80 (used with Palm Oil and Sunflower Oil), and Propylene Glycol (used with all four oils)
- *Capillary Size* – 19 gauge and 22 gauge

4.3.3.2. Experiment Variables

For each ordered category of experiments, empirical variables at varying values were examined. These variables include Concentration Percentage of Emulsifier, the Voltage applied to the system, the Temperature of the liquid sprayed, and the Pressure at which the liquid was sprayed. Examining these variables indicates how different factors interact with each other in a real-world environment. All of the variables were incrementally increased in linear fashion to determine if a linear change produced a nonlinear response. These variables include:

- Concentration Percentage of Emulsifier – the concentration of emulsifier to base oil was tested at 5% and 10% to determine the impact of higher concentration surfactant on EHD atomization outputs.
- Voltage – the voltage was tested at 25kV and 50kV to determine the impact of higher voltage on EHD atomization outputs.
- Temperature of the Liquid Sprayed – The temperature at which the liquid was sprayed was tested at three different points (120F, 180F, and 240F) to determine the impact of Temperature on EHD atomization outputs.
- Pressure Sprayed – The pressure at which the liquid was sprayed was tested at three different values (1psi, 2psi, and 4psi for the 19ga capillary) and (4psi, 8psi, and 16psi for the 22 ga capillary) to determine the impact of mass flow(measured as weight at a fixed spray time) on EHD atomization outputs.

4.4. IMAGE ANALYSIS

Image analysis software was used to convert the data from the EHD spray tests into meaningful data. Each test sample ran was photographed via a procedure that allowed for repeatability of image capturing. This allowed the images to produce data individually that could be compared to each other to help assess performance of the experiment against the expected results. The data was then subjected to DOE analysis to determine the inter-dynamics of all of the factors of the experiment.

4.4.1. ImageJ Software

ImageJ image analysis software, developed by the National Institute of Health (NIH) is public domain, Java based image processing software (see Section 3.2.7). FIJI (Fiji is Just ImageJ) is the latest version of ImageJ (version 1.51). While ImageJ has broad and in depth image processing capabilities, for the purpose of this experiment, the focus was on the software's Particle Analysis tools. ImageJ was able to take a 24.2MP picture and process it to a binary image where the contrast between the droplets from the test samples and the background of the oil sensitive paper could be analyzed to determine a numerical value for the droplets size (mm^2), concentration (number of droplets per unit measure), area covered by the liquid sprayed (mm^2), and the percentage of area covered.

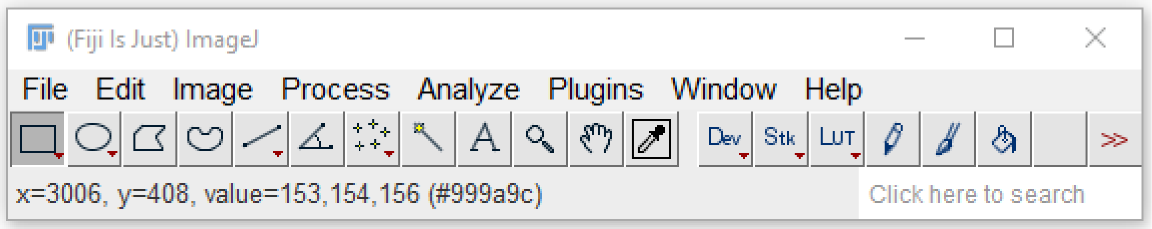

```
x=3006, y=408, value=153,154,156 (#999a9c)
```

Figure 26: Control Panel for ImageJ software (version 1.51)

Several steps were required to process each of the 865 test samples. They include calibrating the image software, cropping the imported image, converting that image to an 8 bit black and white image, adjusting the threshold to convert the image to a binary image, selecting a representative sample area within the image and cropping it, removing outliers (noise reduction) and despeckling the image, filling the holes in the image, manually making corrections to the image, water-shedding the image, performing data analysis on the image, and exporting data from the image to the experiment's Excel spreadsheet.

The following is a step-by-step process for converting the image to useful data:

4.4.1.1. Image to Software Calibration

The first step in converting the digital photographs to meaningful information was to calibrate the software to the same aspect ratio of the image. This was done via the 'Set Scale' feature in ImageJ. The photograph was placed in the Image Fixture (see Figure 18) along the two scales representing the 'X' and 'Y' axis of the image. The 'Measure Line' feature of ImageJ allowed the picture to be measured on two scales photographed and a distance, in pixels, was established between the millimeter line gauge markings. In the case of images used for this experiment, it was determined that 32 pixels existed per linear millimeter. This established 1,024 pixels per square millimeter.

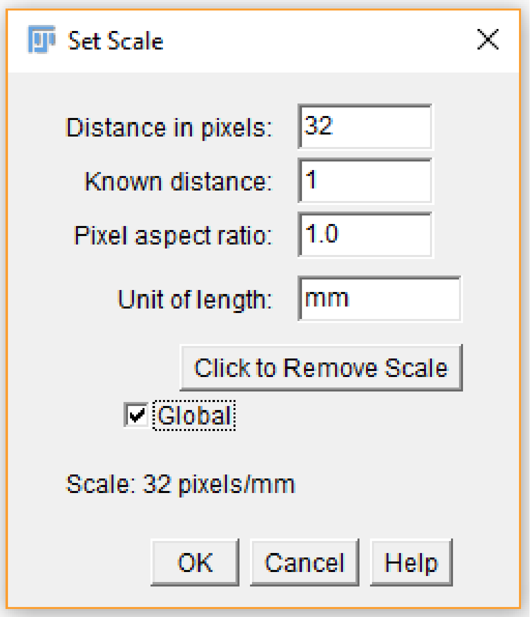

Distance in pixels: 32
Known distance: 1
Pixel aspect ratio: 1.0
Unit of length: mm
☑ Global
Scale: 32 pixels/mm

Figure 27: Set Scale feature in ImageJ allowed for the calibration of the photograph to the software

4.4.1.2. Crop Image

The 'Crop' feature of ImageJ was used to remove unnecessary material from the image. Once the software was calibrated, the stationary rulers on the Image Fixture were no longer needed in the image. This is the first step in converting the image to useful data (8 bit black and white image).

Figure 28: Image Cropping in ImageJ software

4.4.1.3. Set Image to 8 Bit

An 8 bit black and white image, commonly known as Grayscale, is an image that only represents the amount of light it carries. This information is converted by the software into the closest black and white value on a scale from 0% (total black) to 100 % (total white). For 8 Bit imaging, these values are rounded to the nearest bit value.

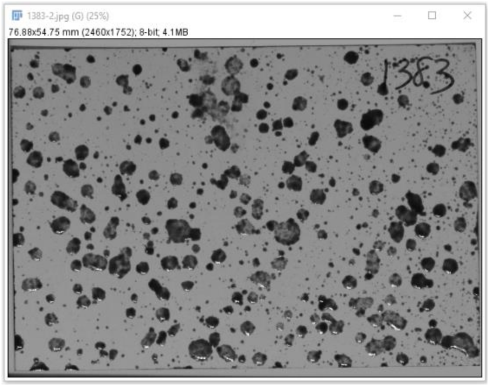

Figure 29: 8 Bit Black and White Image Converted by ImageJ Software

ImageJ software requires that images be converted to 8 bit black and white images before the threshold of the image can examined and the image can be further converted to binary (true black or white) scale.

4.4.1.4. Adjust Threshold to Binary Image

After converting the image to an 8 bit black and white image, the image must be further converted to binary by a process called 'Threshold' adjusting in the ImageJ software. ImageJ uses a method of conversion called 'Clustering' where grey-level pixels from the 8-bit image are clustered into either foreground or background. This process is done manually by adjusting the foreground and background ratios (see Figure 29). If the foreground value is too great, noise will appear in the photograph. If the foreground value is too low, then critical data might be missed. As this is a manual process, it requires the discretion of the individual performing the sampling task. As the process uses discrete values to determine foreground from background, reflections and other imperfection in the image may appear as holes.

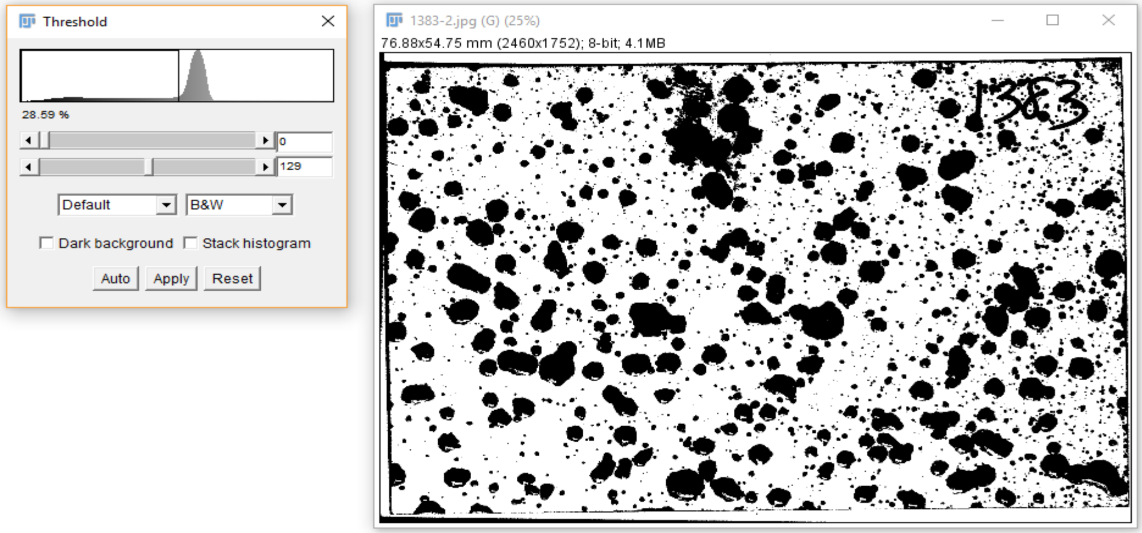

28.59 %

0

129

Default

B&W

☐ Dark background ☐ Stack histogram

76.88x54.75 mm (2460x1752); 8-bit; 4.1MB

Figure 30: Threshold Processing in ImageJ Software

4.4.1.5. Select Representative sample

Once the image has been conveted to a binary image, the next step is to determine a representative sampe within the image for further processing. This is important because the varying images have noise (black

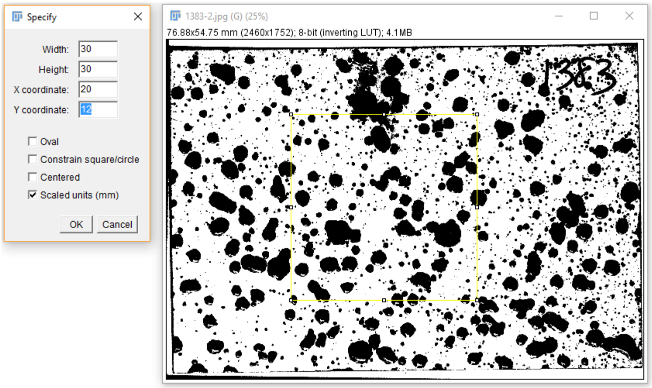

Width: 30

Height: 30

X coordinate: 20

Y coordinate: 12

☐ Oval

☐ Constrain square/circle

☐ Centered

☑ Scaled units (mm)

76.88x54.75 mm (2460x1752); 8-bit (inverting LUT); 4.1MB

Figure 31: ImageJ Crop Specification

edge value) at the edges, imperfections or variations in the sample handing (smudges and other imperfections), and misalignment of the Test Swatch in the Image Fixture at the time of the photograph.

ImageJ ‘Specify’ feature allows for the specific dimensions and locations of an image to be determined and for further actions, in this case cropping, to be performed on the image (see Figure 30). Like the ‘Threshold’ adjustment, the selection of a representative area relies on the judgement of the individual performing the sampling task. If the individual errors in the selection process, the data can be skewed to the heavy or light droplet size or the heavy or light droplet density (area coverage).

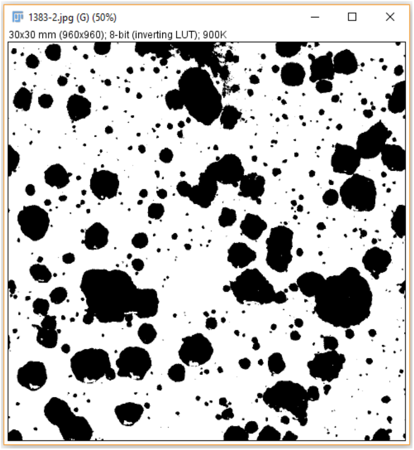
1383-2.jpg (G) (50%)
30x30 mm (960x960); 8-bit (inverting LUT); 900K

Figure 32: Cropped Representative Sample by ImageJ software

4.4.1.6. Remove Outliers and Despeckle

With the ‘Remove Outliers’ feature in ImageJ, noise from the Threshold adjustment can be removed from the image. That is to say that material that is of specified size can be automatically removed from the image. When despeckling the image, areas where black and white are inter-dispersed (checkered) are filled or removed based on the surrounding geometry. This

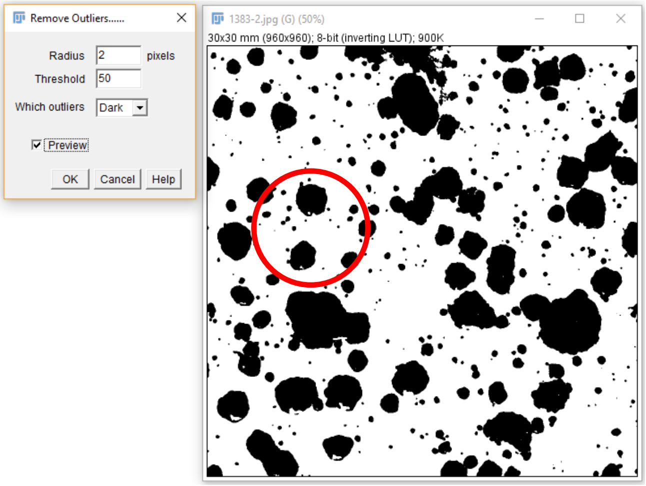
Remove Outliers......
Radius: 2 pixels
Threshold: 50
Which outliers: Dark
☑ Preview

1383-2.jpg (G) (50%)
30x30 mm (960x960); 8-bit (inverting LUT); 900K

Figure 33: Remove Outliers Function of ImageJ

provides for a smoother picture. This action should be performed before the ‘Fill Holes’ function as it will artificially fill in the holes instead of smoothing them.

4.4.1.7. Fill Holes

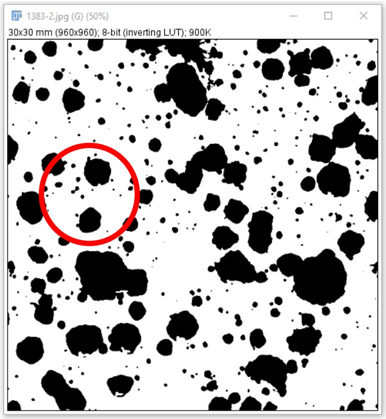

Figure 34: Image after Fill Holes feature has been run in ImageJ

The ‘Fill Holes’ feature in ImageJ fills in areas completely surrounded by foreground material (Black). This is useful for removing reflections and other imperfections from the Thresholding process. Notice the filled holes between Figure 32 and Figure 33. The ‘Fill Holes’ feature, however, does not fill in edge holes. That is to say that a reflection that is not completely enclosed will appear as an indention into the droplet in question. These holes must be manually filled in with the ‘Paint’ tool in ImageJ.

4.4.1.8. Manually Correct Defects

Once the image has been processed as far as it can be utilizing the available correction tools in ImageJ, the task of manually correcting defects must be done manually using the ‘Paint’ feature. The paint feature allow the individual processes sing the sample to manually fill in the reflections on the edge of droplets. As this is a manual process, there is room for some error,

Figure 35: Image after Paint feature has been used to correct edge defects

but it is generally minor as the amount of material added is generally small relative to the overall image.

4.4.2. Watershed

Water-shedding is the automated process of determining if individual droplets can be separated when they are connected in the image. ImageJ analyses the image and inserts a line the width of a single pixel between bodies that it determines should be individual droplets. This feature allows for a more accurate accounting of the total droplets in the image and a more accurate calculation of the average droplet size.

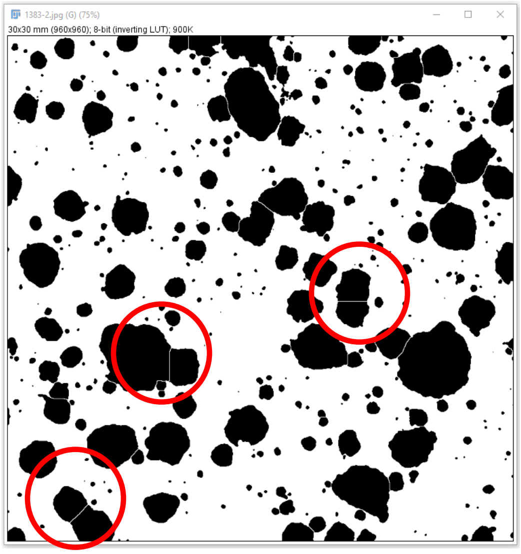

Figure 36: Image after Watershed feature has been run in ImageJ

4.4.3. Analyze Particles

Particle analysis in ImageJ is one of the primary features of the program. The software examines every individual element in the binary image and renders a unique identification number for the element, and determines the area of the element (as defined by the Set Calibration) feature. Then the software compiles a summary of the image analysis wherby it provides a count of the individual elements in the image, the total area covered by the elements (as defined by the calibration), the average size of each element, and the percent of the area covered by the elements.

For the purpose of this experiment, the individual results were not captured. However, the summary results were captured and exported to the experiment's Excel spreadsheet.

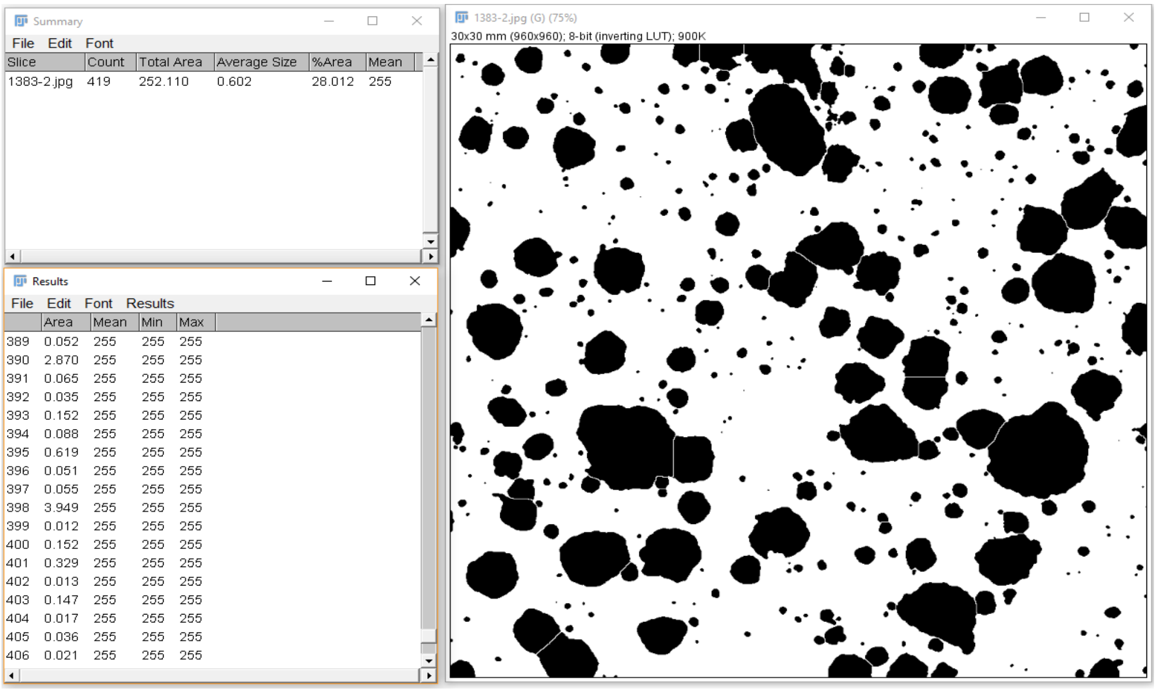

Slice	Count	Total Area	Average Size	%Area	Mean
1383-2.jpg	419	252.110	0.602	28.012	255

	Area	Mean	Min	Max
389	0.052	255	255	255
390	2.870	255	255	255
391	0.065	255	255	255
392	0.035	255	255	255
393	0.152	255	255	255
394	0.088	255	255	255
395	0.619	255	255	255
396	0.051	255	255	255
397	0.055	255	255	255
398	3.949	255	255	255
399	0.012	255	255	255
400	0.152	255	255	255
401	0.329	255	255	255
402	0.013	255	255	255
403	0.147	255	255	255
404	0.017	255	255	255
405	0.036	255	255	255
406	0.021	255	255	255

Figure 37: ImageJ Data Analysis of Processed Image

4.4.4. Information into Excel Spreadsheet

As a final step in the Image Analysis process, the data from the image analysis was copied and pasted into the experiment's Excel spread sheet. This information, along with other information entered into the spreadsheet or derived from information entered into the spreadsheet, became the basis for the Statistical Treatment of the data.

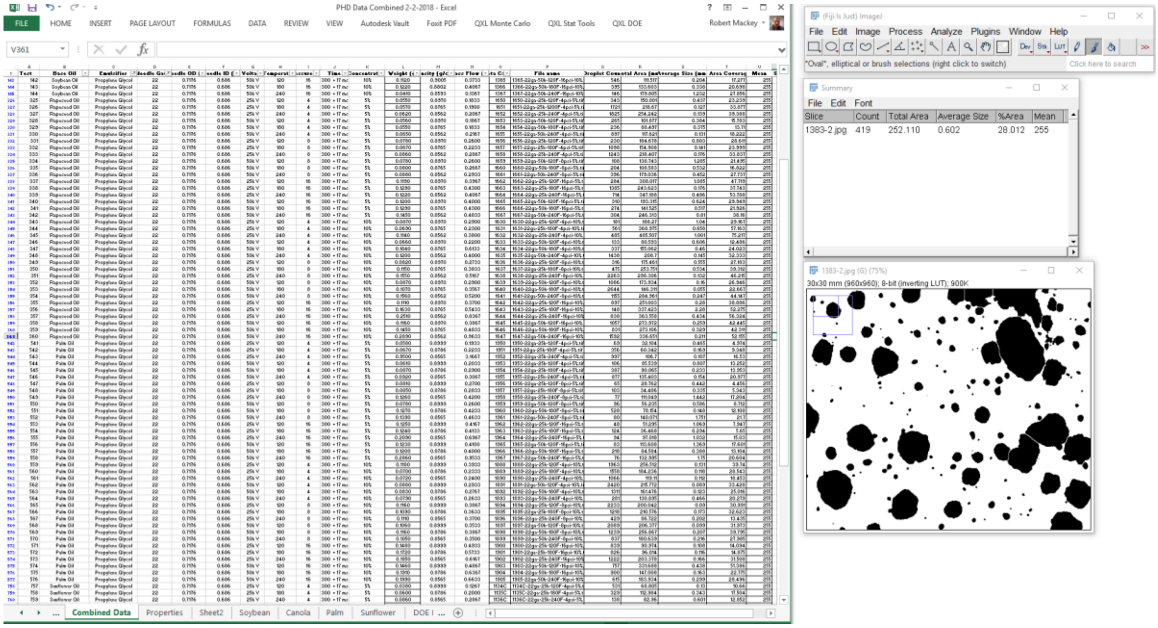

Slice	Count	Total Area	Average Size	%Area	Mean
1383-2.jpg	419	252.110	0.602	28.012	255

Figure 38: Data from ImageJ imported into Excel

4.5. STATISTICAL TREATMENT

Using Quantum XL statistical software, a Design of Experiment Matrix was built using the oil/emulsifier blend's concentration (2 levels), the voltage (2 levels), the temperature (3 levels), and the pressure (3 levels) for each oil type, emulsifier type, and capillary size combinations (24 separate experiments). Each matrix was set up to capture the four outputs of the experiment (droplet count, droplet size, coverage area, and weight). Using a factorial ANOVA model, a statistical ordinary least squares regression was run for each experiment. From this, a projection matrix was generated for each of the four outputs and for each of the 24 different test groups. The data was then plotted into charts as follows:

Interactions Plot – an Interactions plot was generated for level of the experiment as defined by DOE. The chart represents the interaction between the mean of each level and each output (separate graphs) from the experiment. For this chart, y-bar data was used to determine the impact on and interaction between the average values of each dataset within a test series.

Main Effects Plot- The main effects plot displays the statistical mean (y-bar) for each interaction within a category as it effects the output of the test. That is to say that it examines the difference between the mean of each level for one factor of the experiment and compares it against one of the four outputs. As such, the Main Effects Plot matrix consists of 16 different plots for each experimental group (24 groups).

Surface and Contour Plot- This plot uses the predictive matrix to show the interaction between two different factors and an output for each experimental group. For this, y-hat data from two different factors is represented graphically in a 3D pattern and compared against a single output for the experiment. For this experiment, two sets of comparative combinations were plotted against each of the four outputs of the experiment. In the first set, Concentration % (5% and 10%) and Voltage (25kV and 50kV) were plotted against Droplet Count, Droplet Size, Coverage Area, and Sample Weight y-hat values. This represents to two different outside variables of each experiment group. The second set of plots compared Pressure (1 or4psi, 2 or8psi, and 4 or 16psi) against Temperature (120F, 180F, and 240F) against the same four output variables. This represents the physical state of the oil/emulsifier blend.

Energy Density Splatter Chart - To determine the impact of mass flow (g/s) on the energy density (J/m^3) of a test, a plot of each major oil group, by voltage applied (25kV and 50kV) was generated. Because the spray time for each test was the same and because the cross sectional capillary diameter for each test group was the same, changes in mass flow and energy density are directly attributed to changes in material properties. This plot allows us to see the impact of increased mass flow on energy density and how that effects the experiment.

CHAPTER V

5. EXPERIMENTAL FINDINGS

5.1. PALM OIL

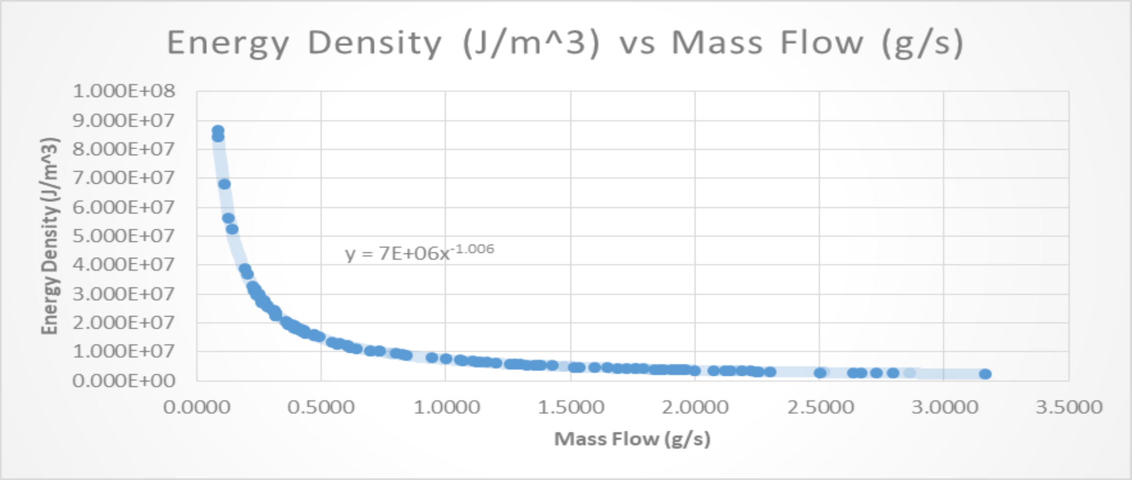

Figure 39: Palm Oil Energy Density vs Mass Flow Chart 25kV

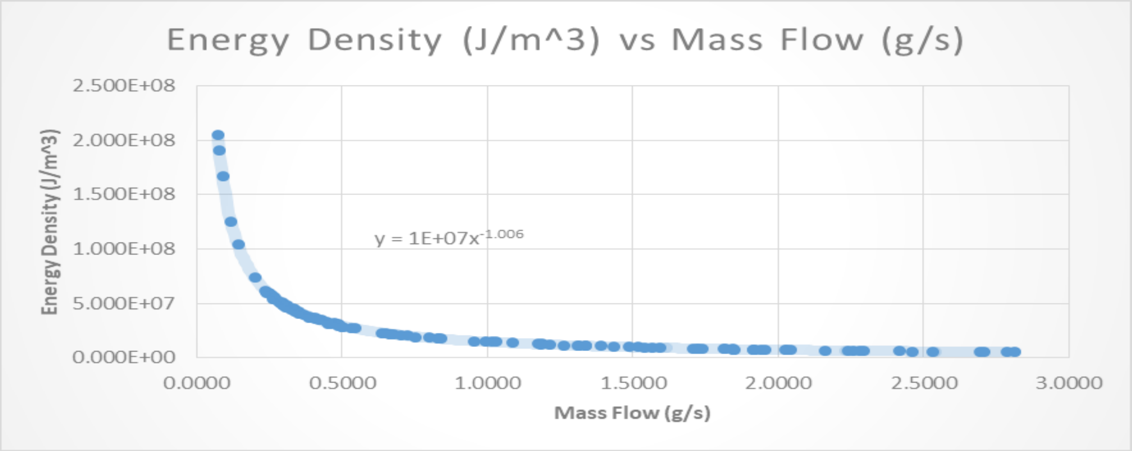

Figure 40: Palm Oil Energy Density vs Mass Flow Chart 50kV

5.1.1. Soy Lecithin with 19 Gauge Capillary

Table 4: Main Effects Plot for Palm Oil & Soy Lecithin @ 19ga Capillary

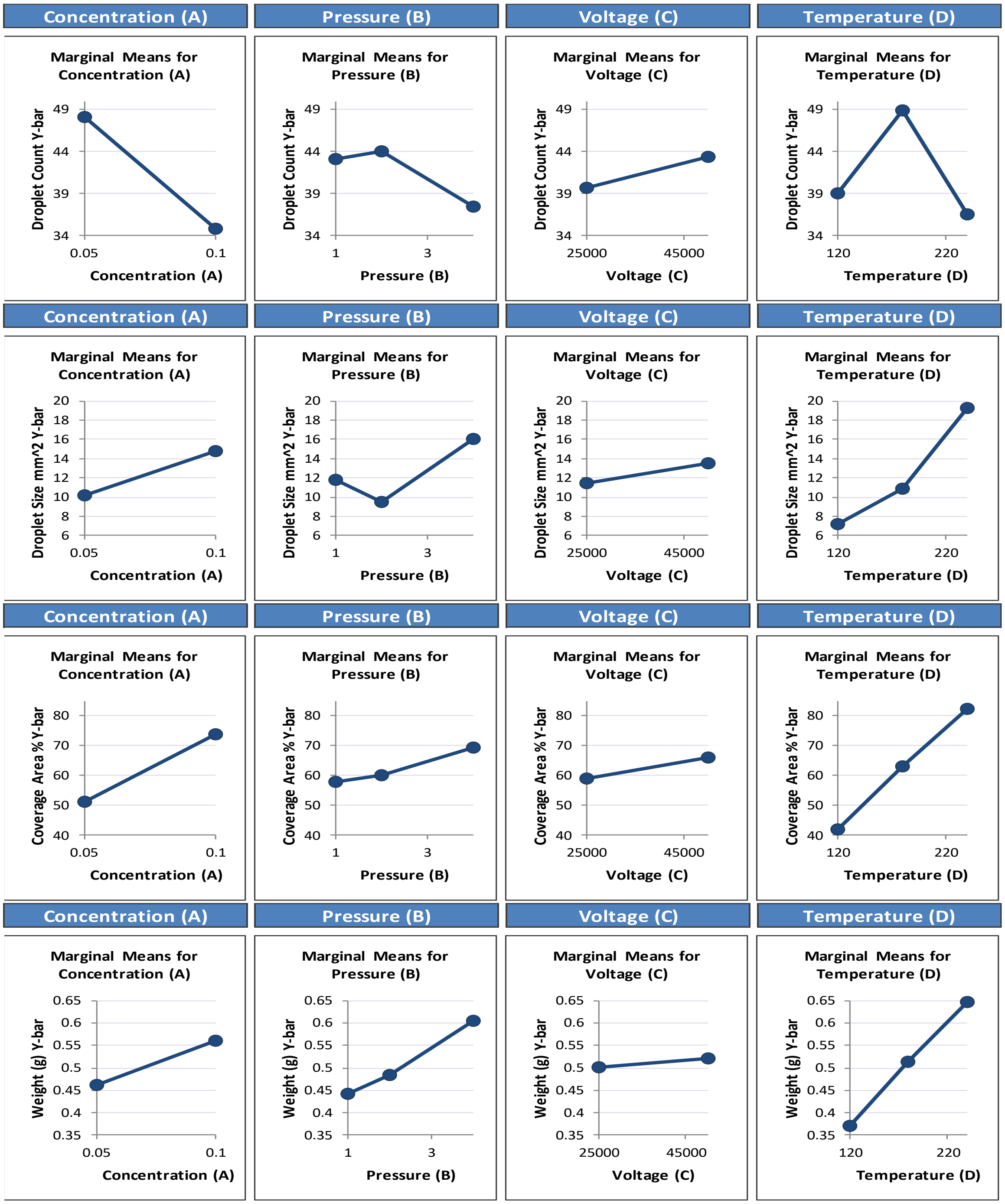

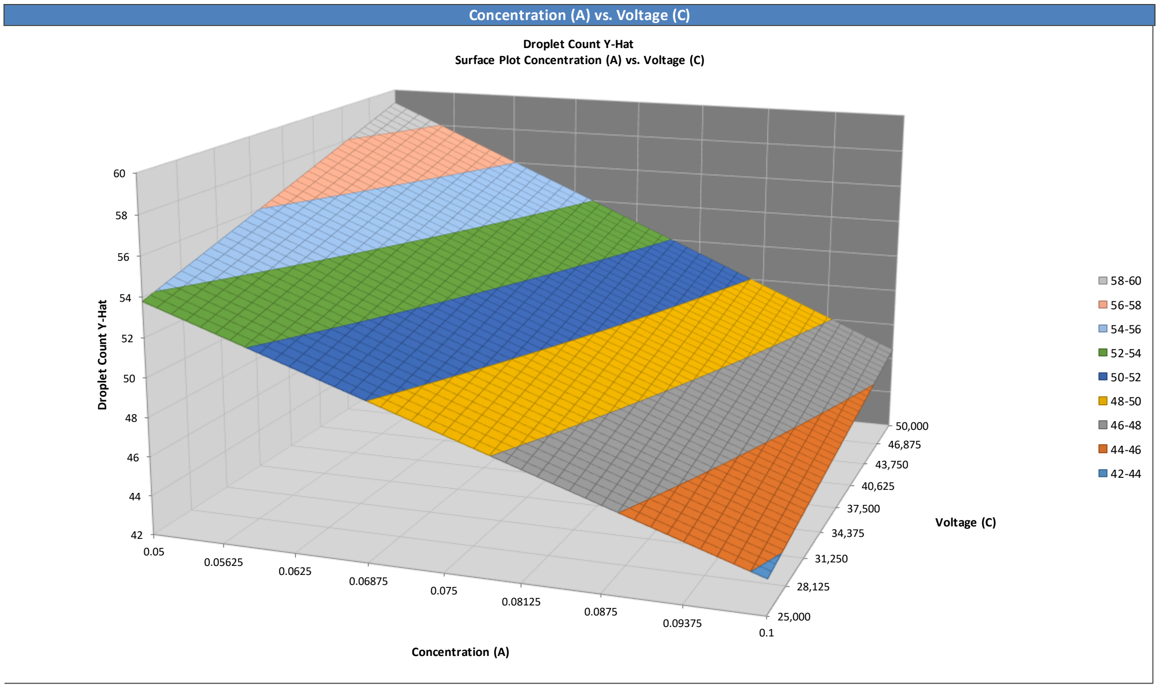

Figure 41: Surface Chart - Concentration vs Voltage for Droplet Count h-hat (Palm oil, Soy Lecithin, 19ga Capillary)

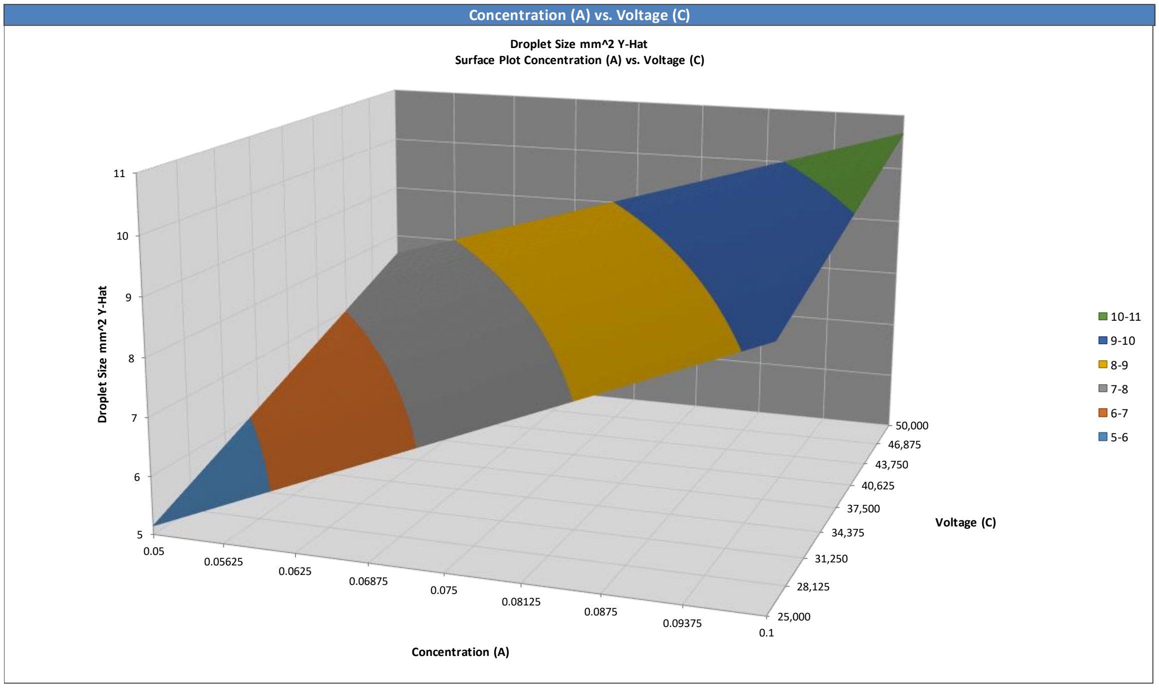

Figure 42: Surface Chart - Concentration vs Voltage for Droplet Size h-hat (Palm oil, Soy Lecithin, 19ga Capillary)

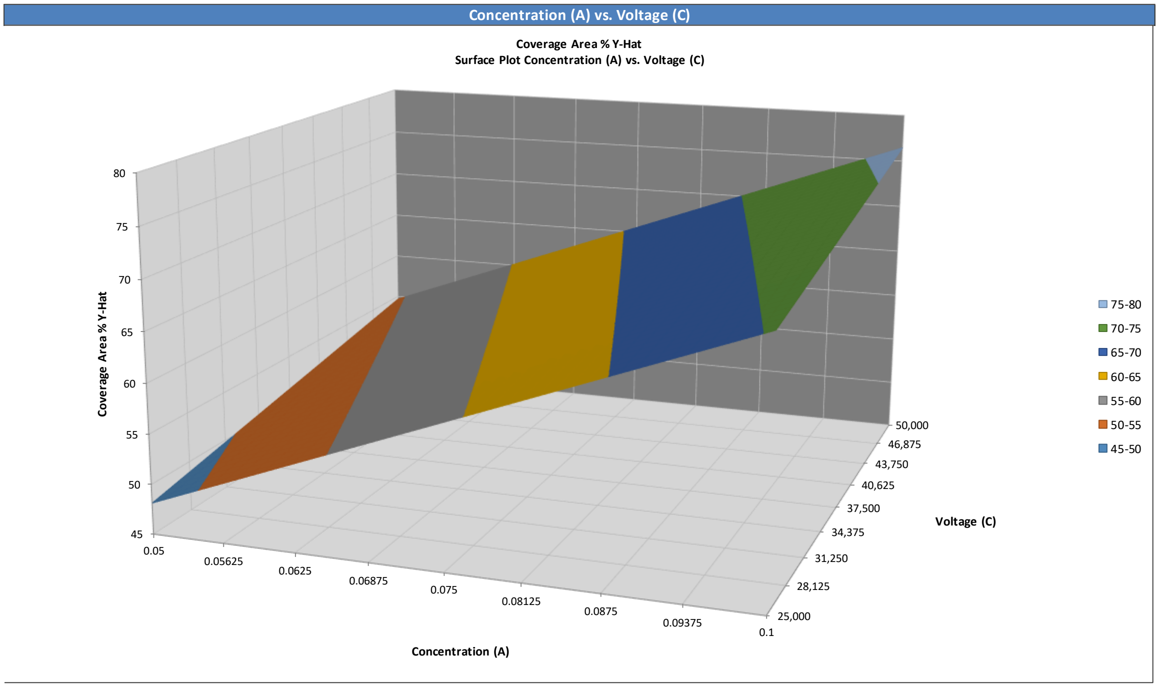

Figure 43: Surface Chart - Concentration vs Voltage for Coverage Area h-hat (Palm oil, Soy Lecithin, 19ga Capillary)

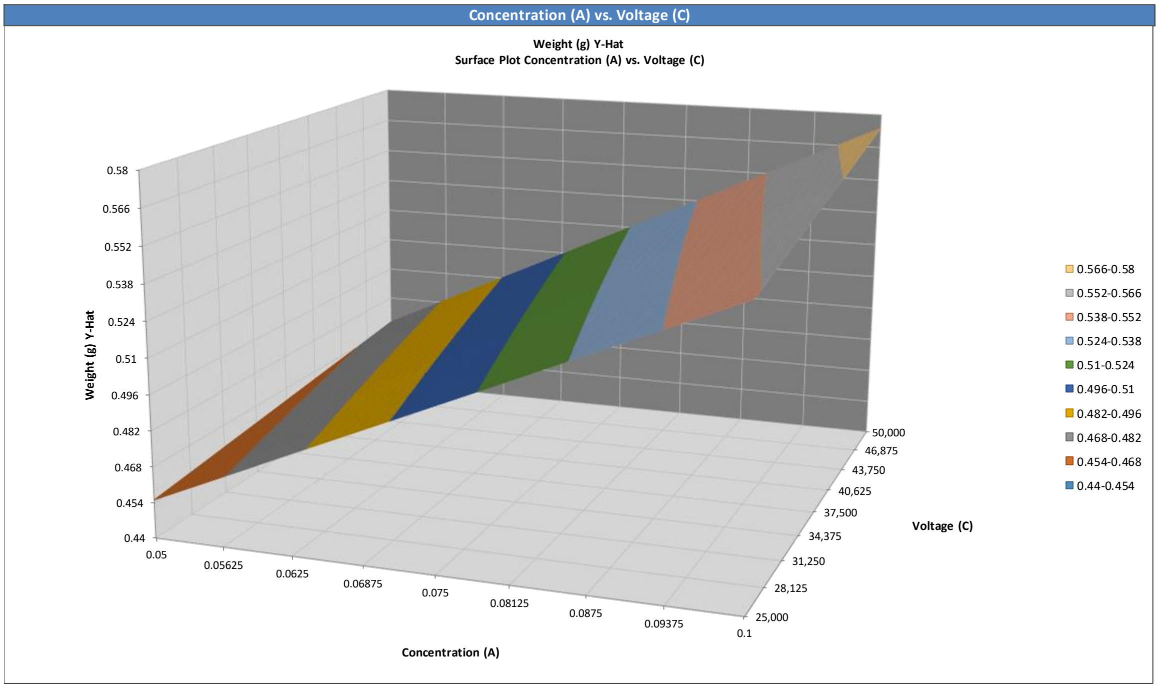

Figure 44: Surface Chart - Concentration vs Voltage for Sample Weight h-hat (Palm oil, Soy Lecithin, 19ga Capillary)

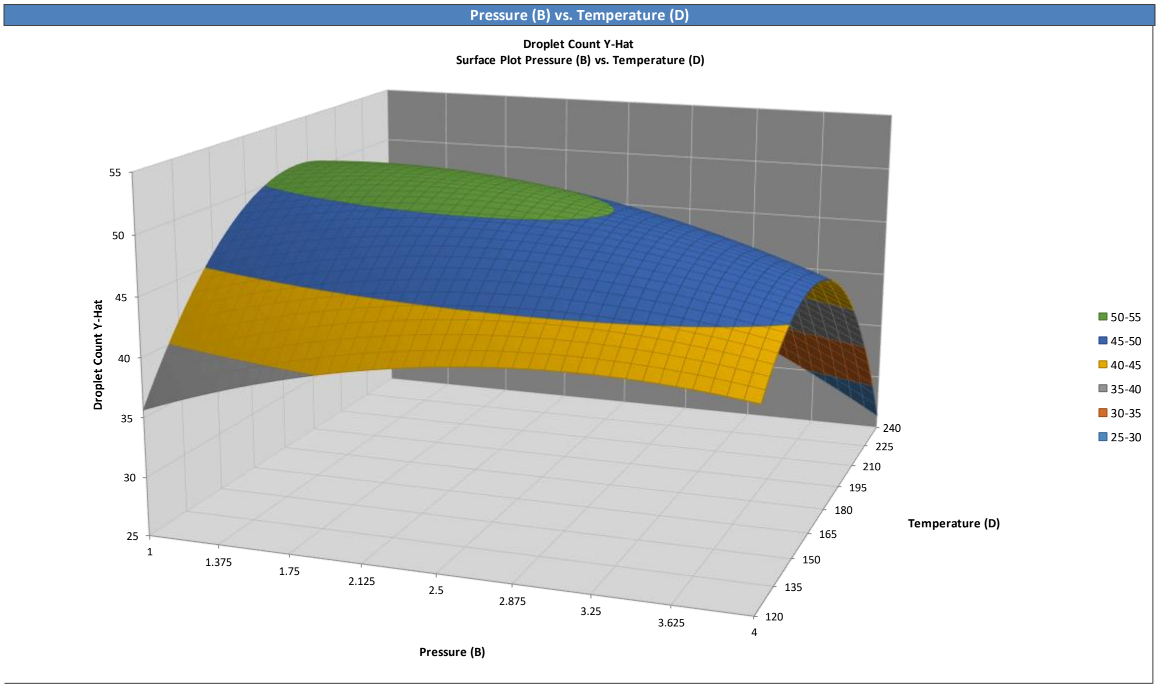

Figure 45: Surface Chart – Pressure vs Temperature for Droplet Count h-hat (Palm oil, Soy Lecithin, 19ga Capillary)

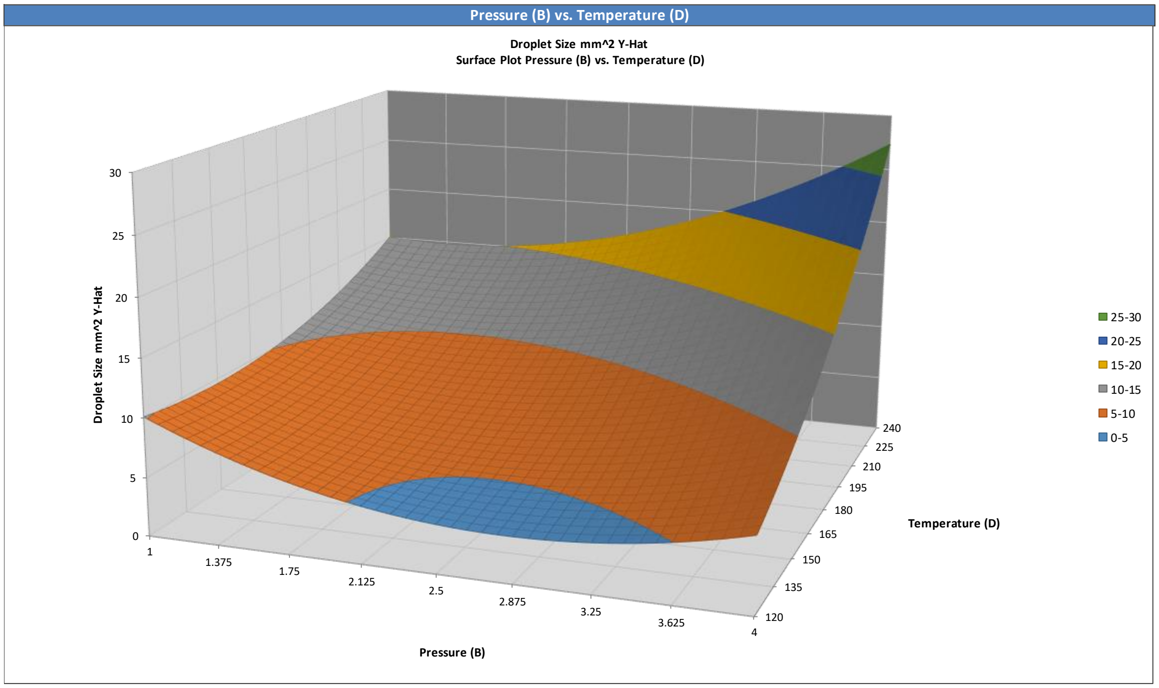

Figure 46: Surface Chart – Pressure vs Temperature for Droplet Size h-hat (Palm oil, Soy Lecithin, 19ga Capillary)

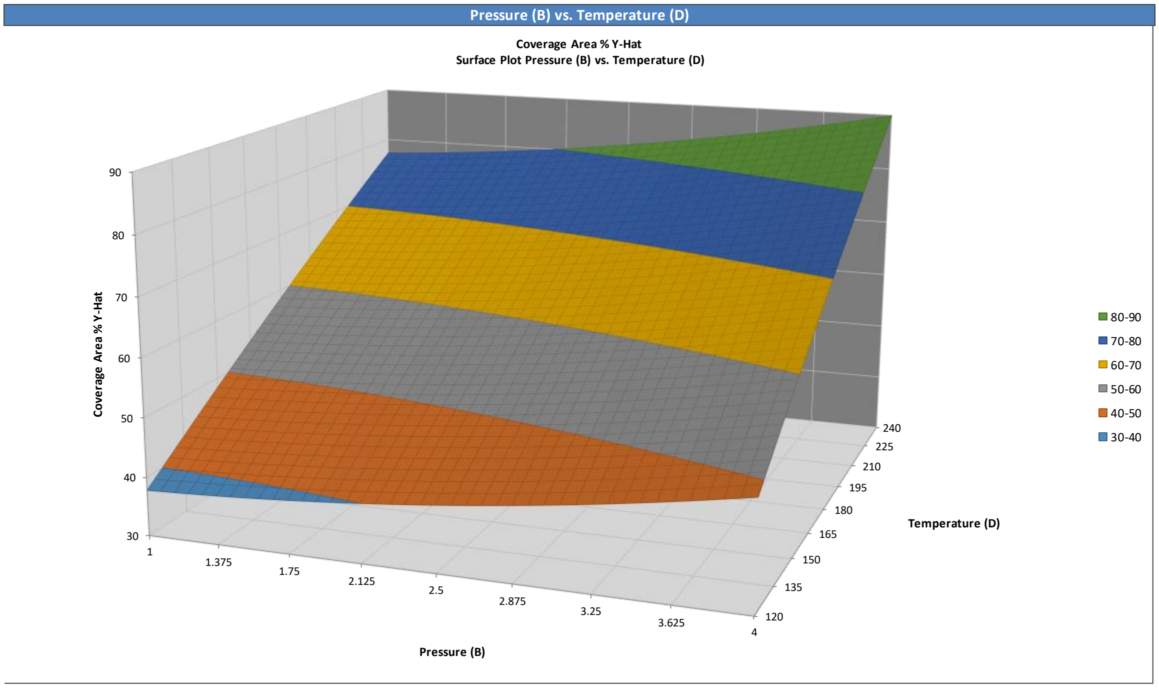

Figure 47: Surface Chart – Pressure vs Temperature for Coverage Area h-hat (Palm oil, Soy Lecithin, 19ga Capillary)

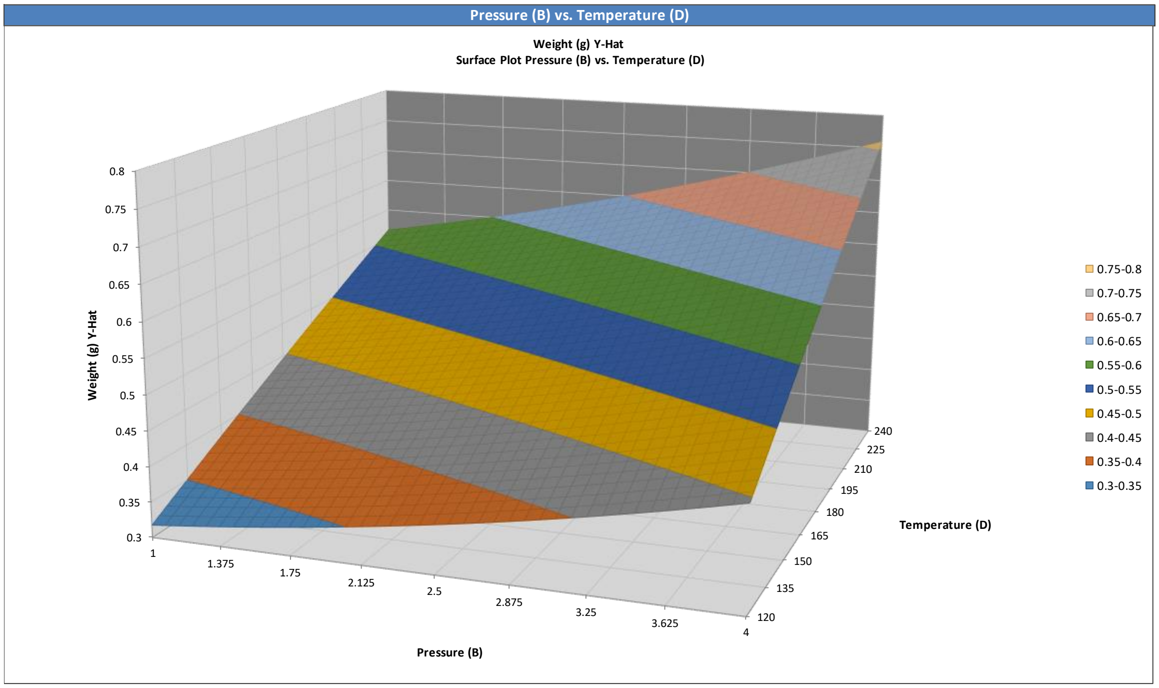

Figure 48: Surface Chart – Pressure vs Temperature for Sample Weight h-hat (Palm oil, Soy Lecithin, 19ga Capillary)

5.1.2. Soy Lecithin with 22 Gauge Capillary

Table 5: Main Effects Plot for Palm Oil & Soy Lecithin @ 22ga Capillary

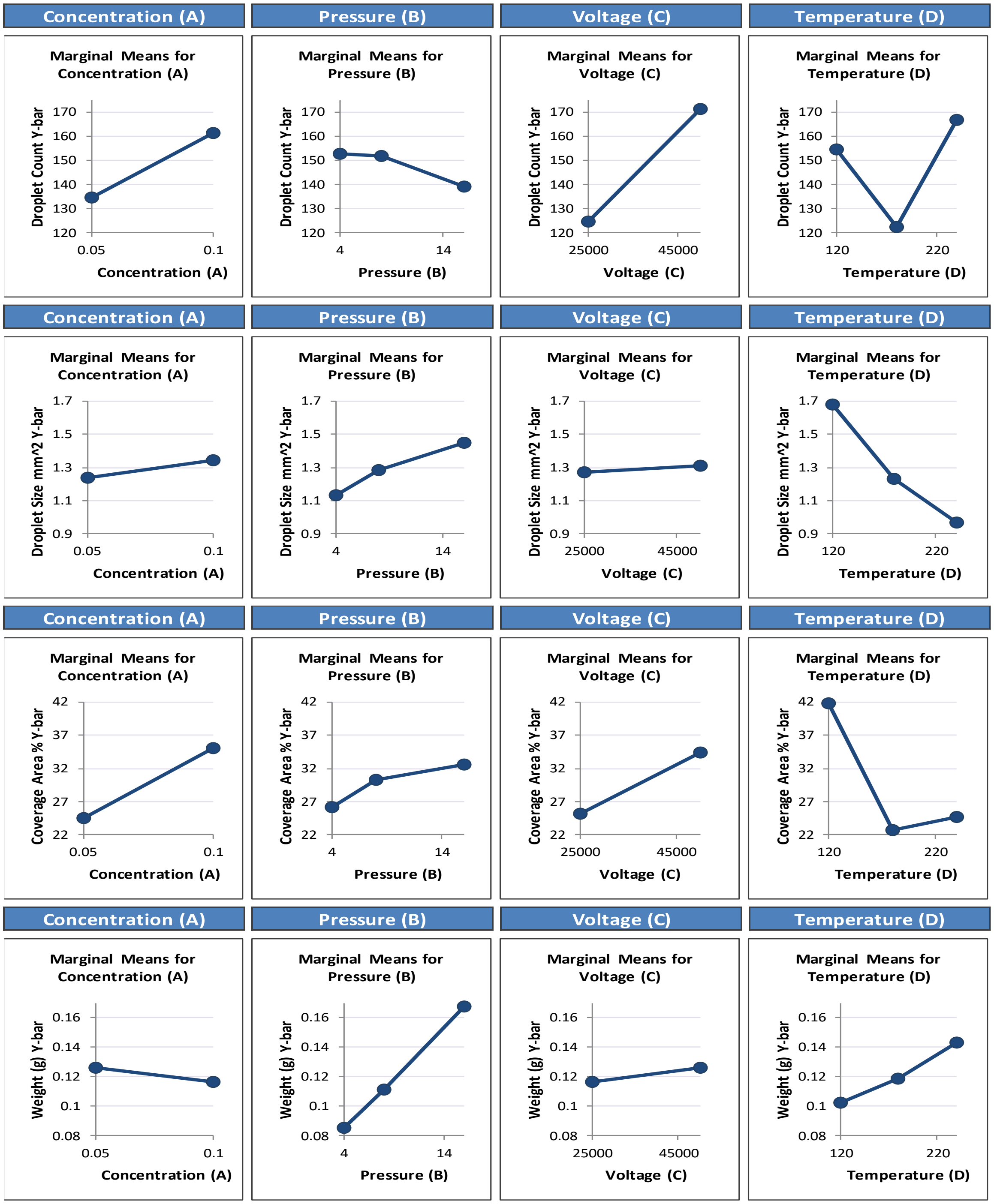

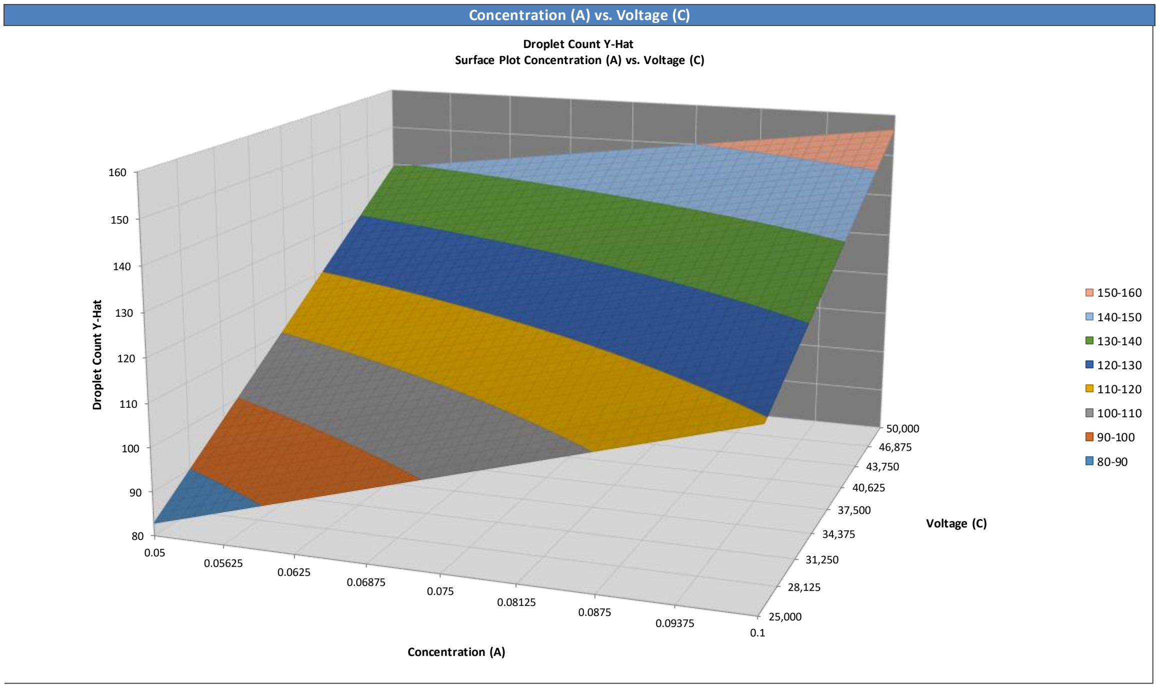

Figure 49: Surface Chart - Concentration vs Voltage for Droplet Count h-hat (Palm oil, Soy Lecithin, 22ga Capillary)

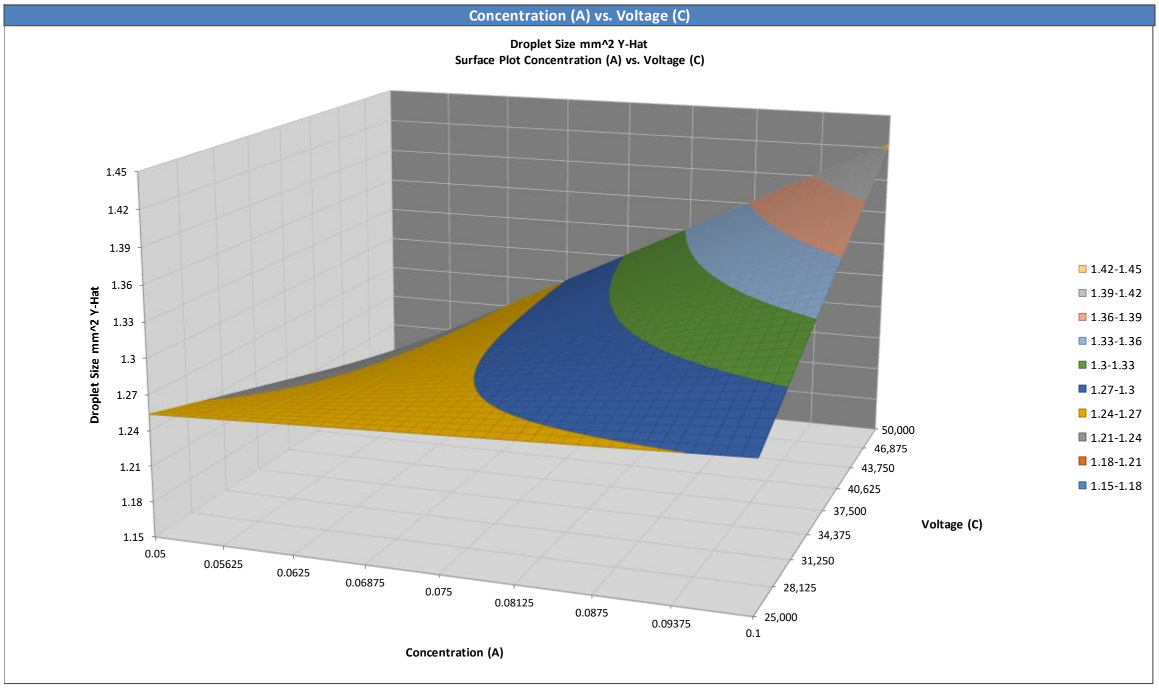

Figure 50: Surface Chart - Concentration vs Voltage for Droplet Size h-hat (Palm oil, Soy Lecithin, 22ga Capillary)

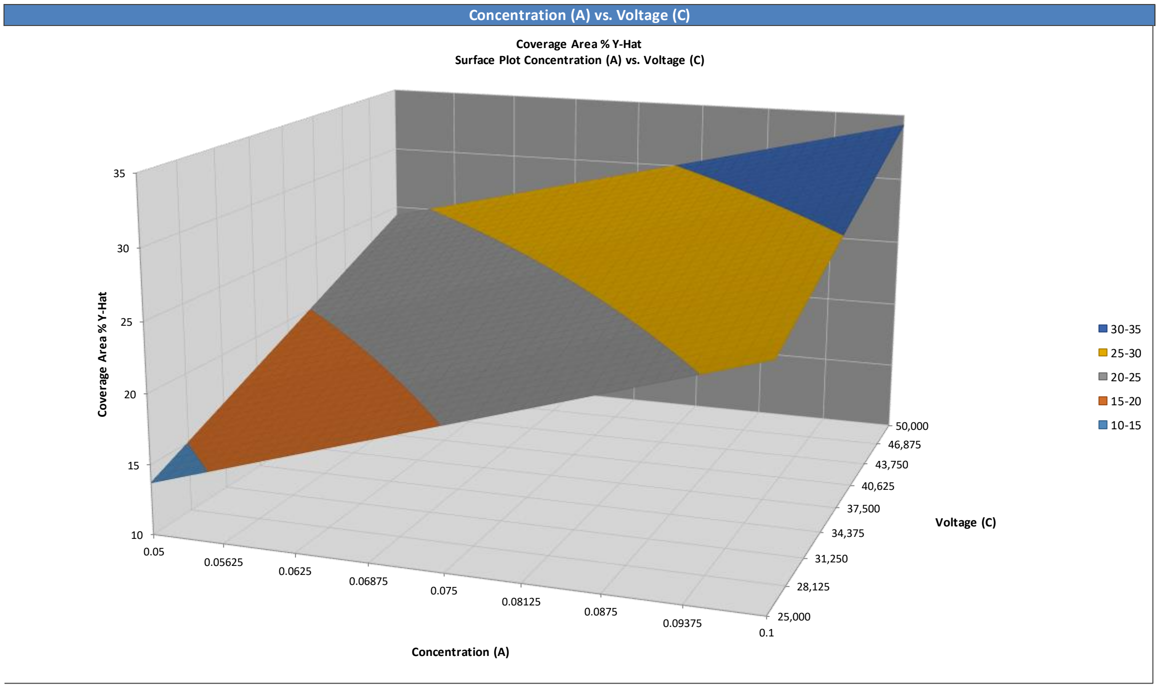

Figure 51: Surface Chart - Concentration vs Voltage for Coverage Area h-hat (Palm oil, Soy Lecithin, 22ga Capillary)

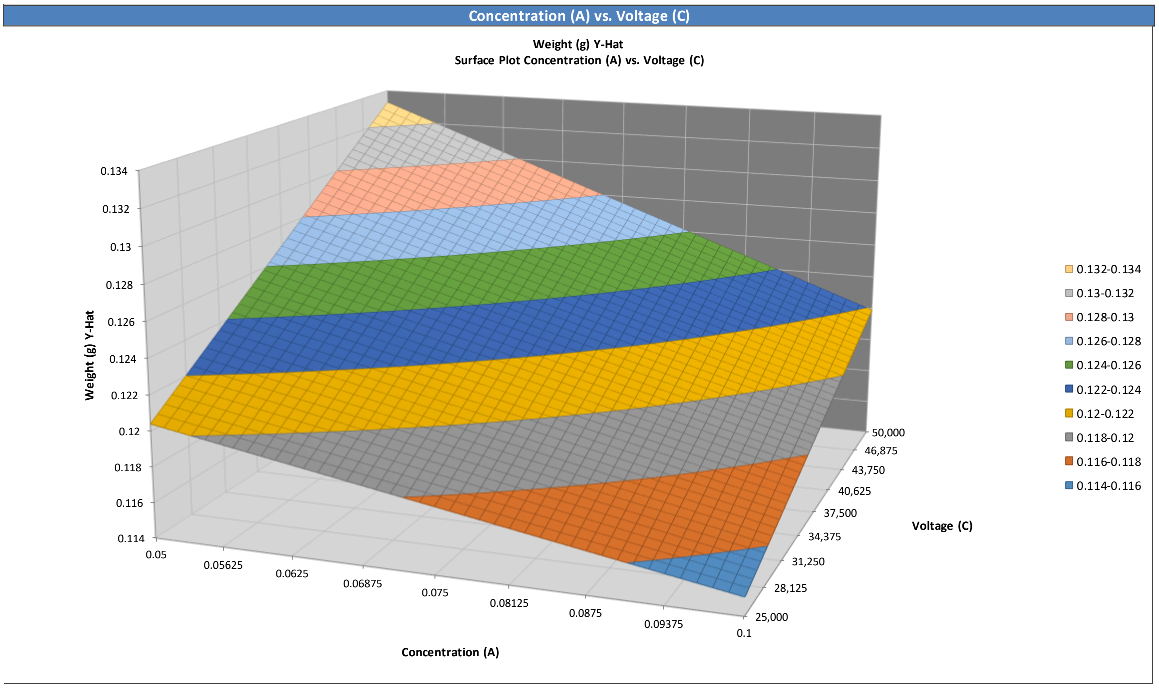

Figure 52: Surface Chart - Concentration vs Voltage for Sample Weight h-hat (Palm oil, Soy Lecithin, 22ga Capillary)

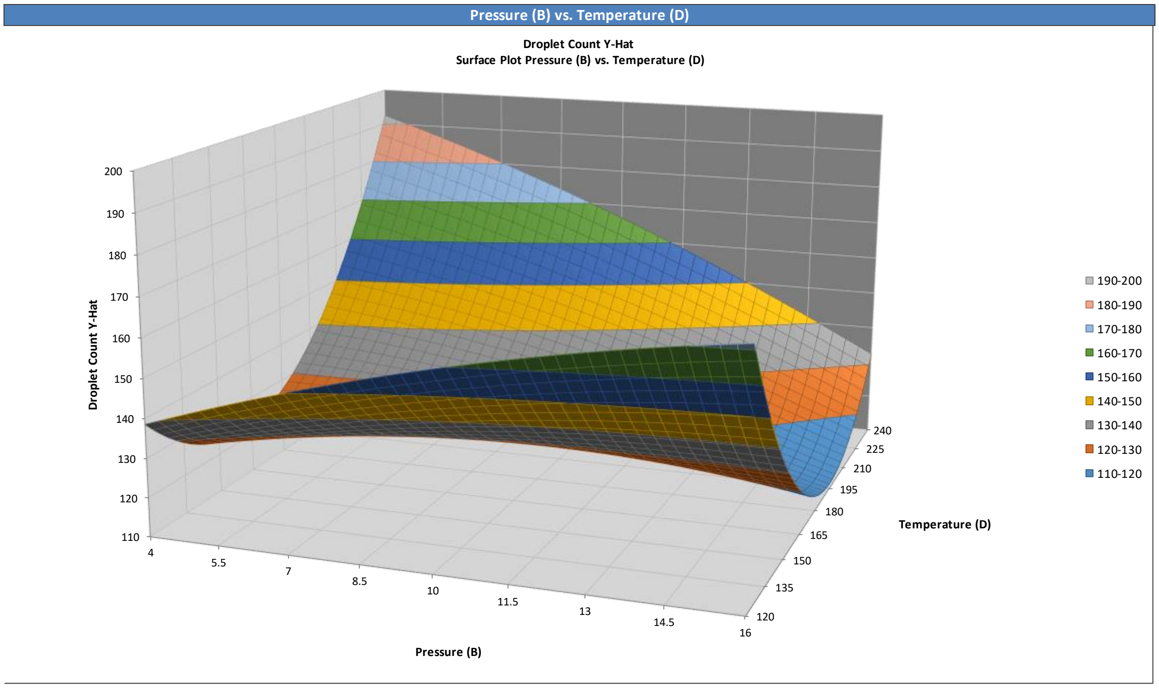

Figure 53: Surface Chart – Pressure vs Temperature for Droplet Count h-hat (Palm oil, Soy Lecithin, 22ga Capillary)

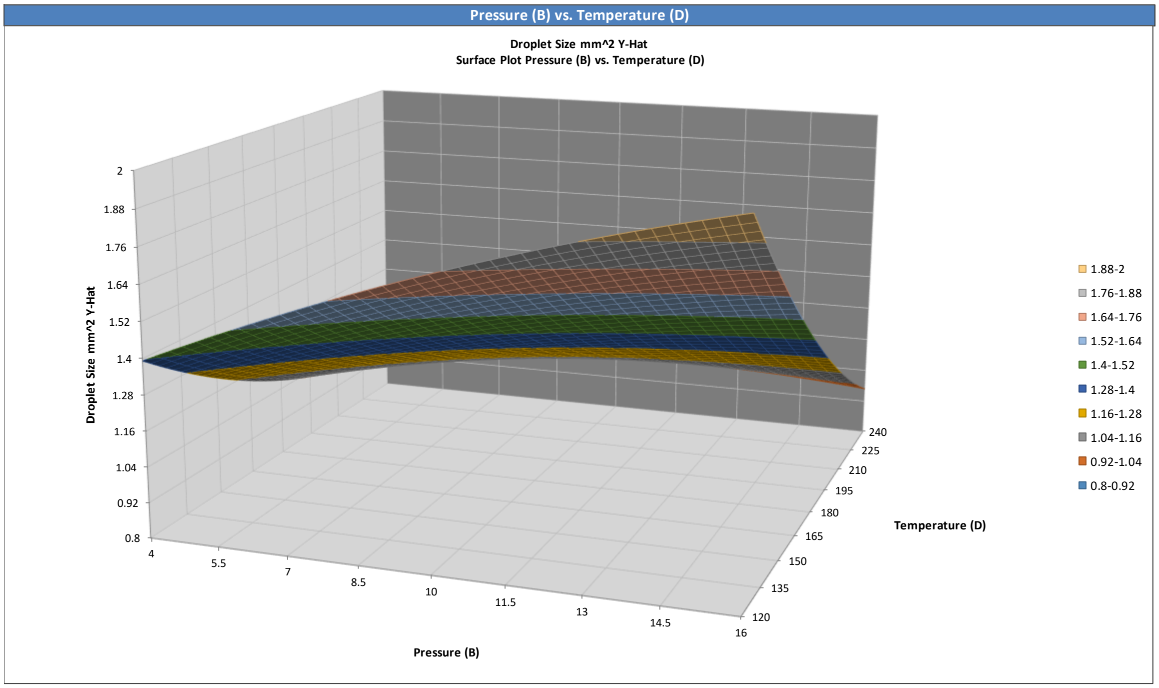

Figure 54: Surface Chart – Pressure vs Temperature for Droplet Size h-hat (Palm oil, Soy Lecithin, 22ga Capillary)

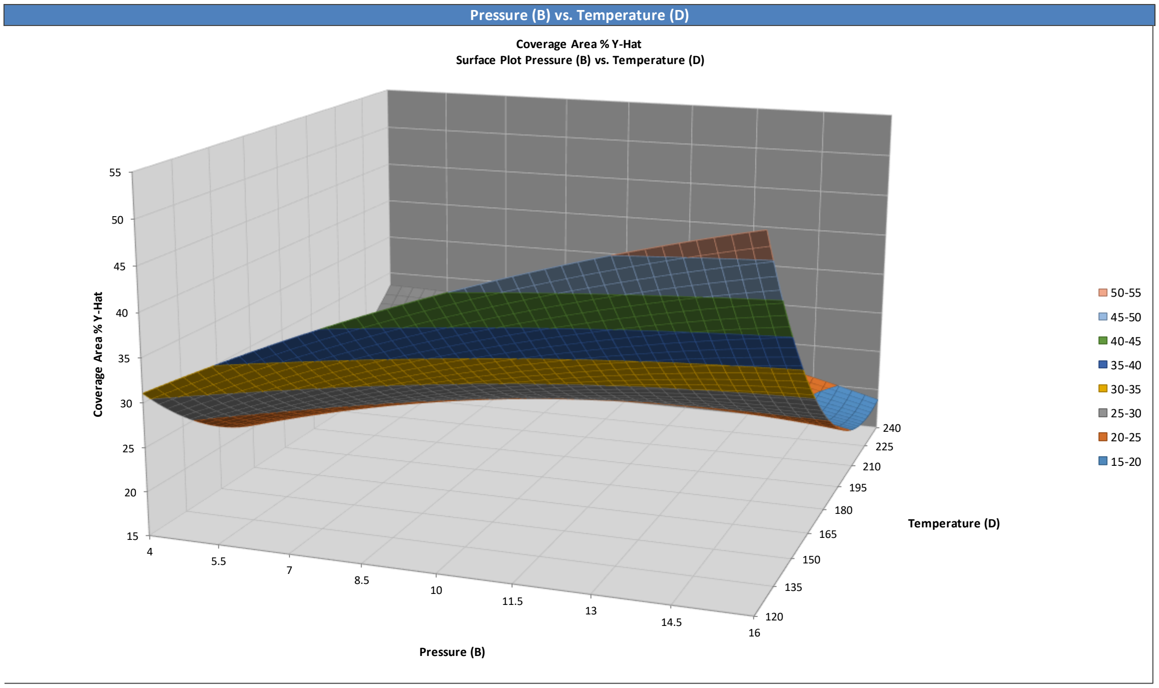

Figure 55: Surface Chart – Pressure vs Temperature for Coverage Area h-hat (Palm oil, Soy Lecithin, 22ga Capillary)

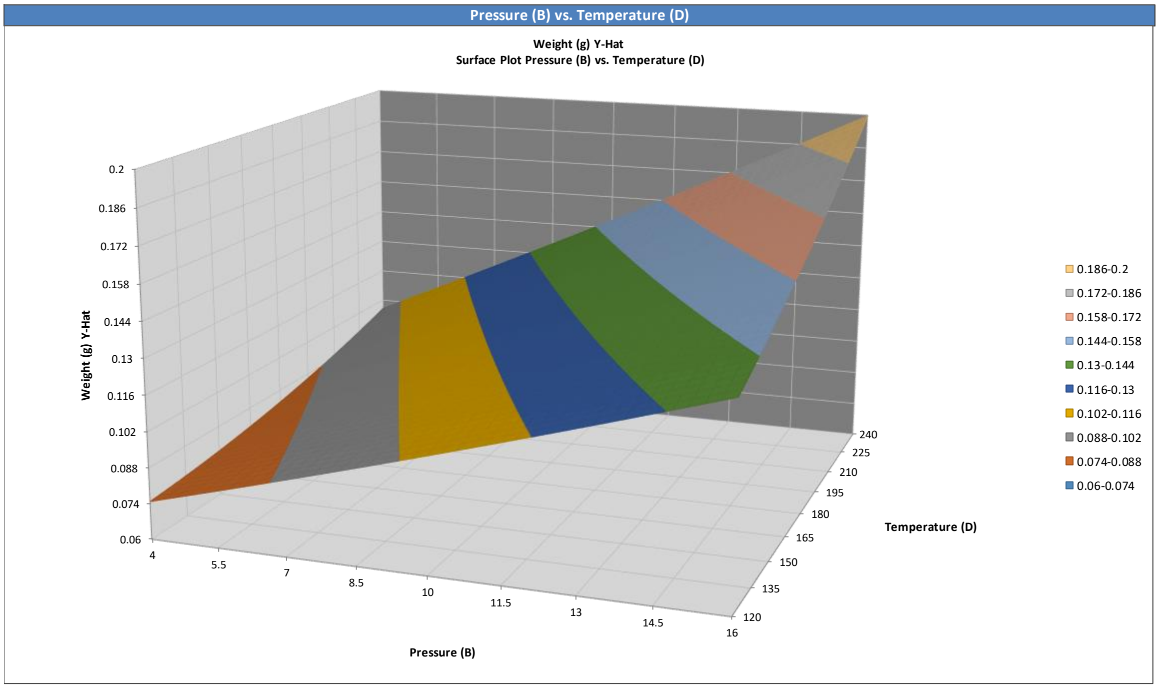

Figure 56: Surface Chart – Pressure vs Temperature for Sample Weight h-hat (Palm oil, Soy Lecithin, 22ga Capillary)

5.1.3. Polysorbate 80 with 19 Gauge Capillary

Table 6: Main Effects Plot for Palm Oil & Polysorbate 80 @ 19ga Capillary

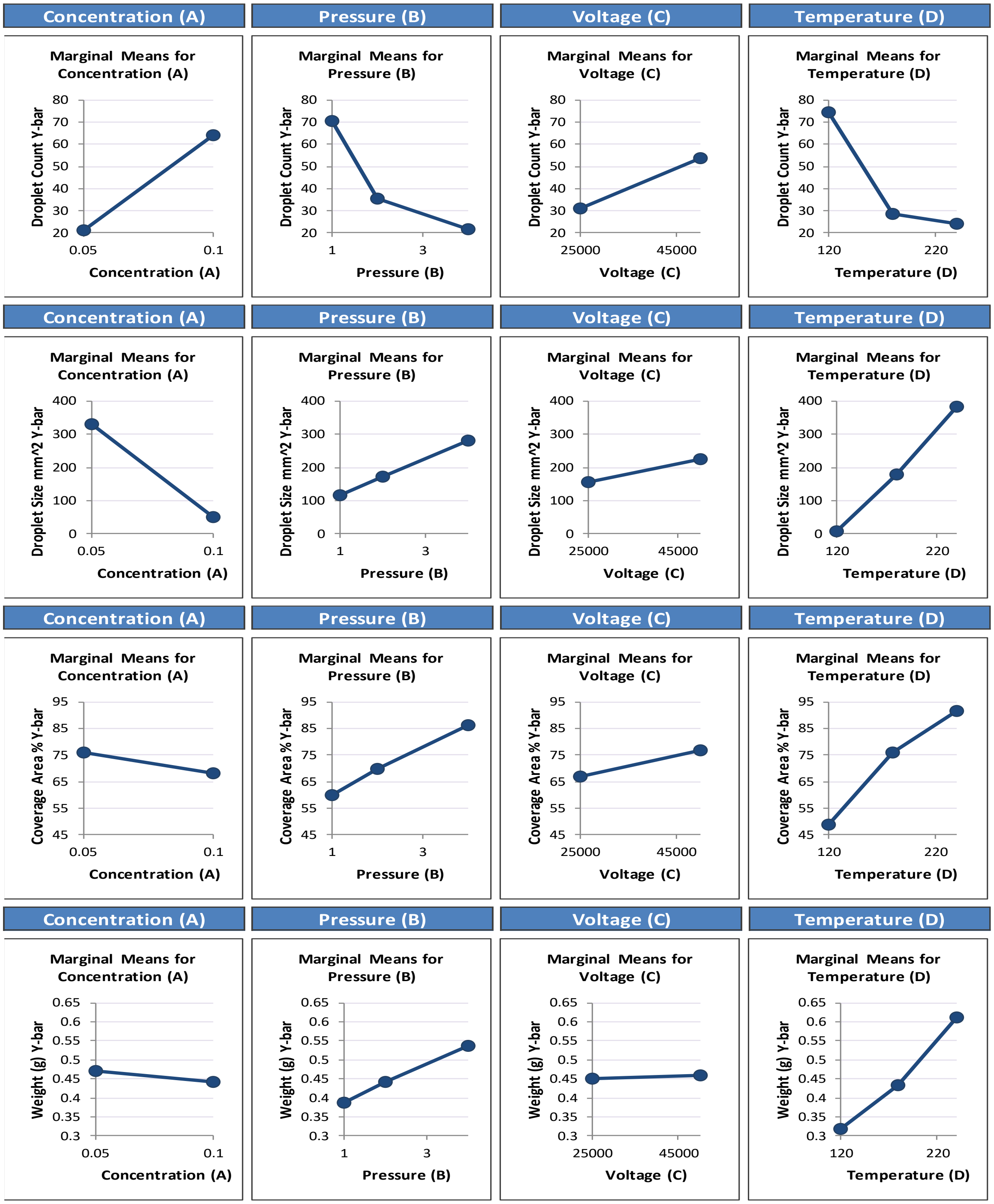

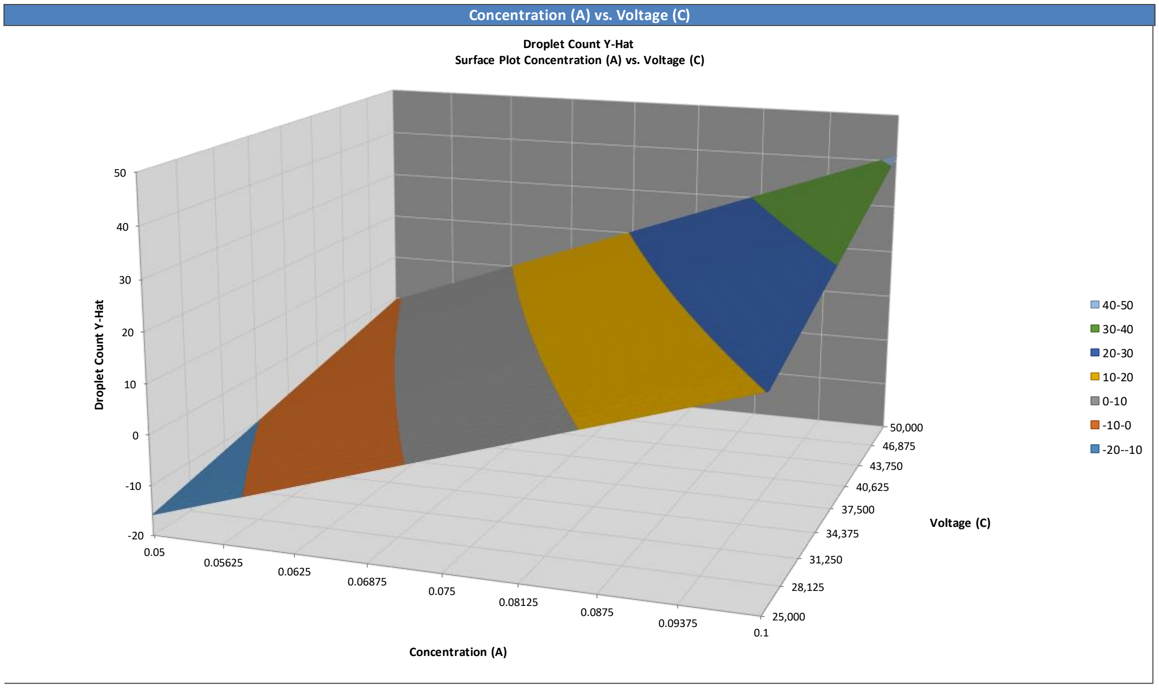

Figure 57: Surface Chart - Concentration vs Voltage for Droplet Count h-hat (Palm oil, Polysorbate 80, 19ga Capillary)

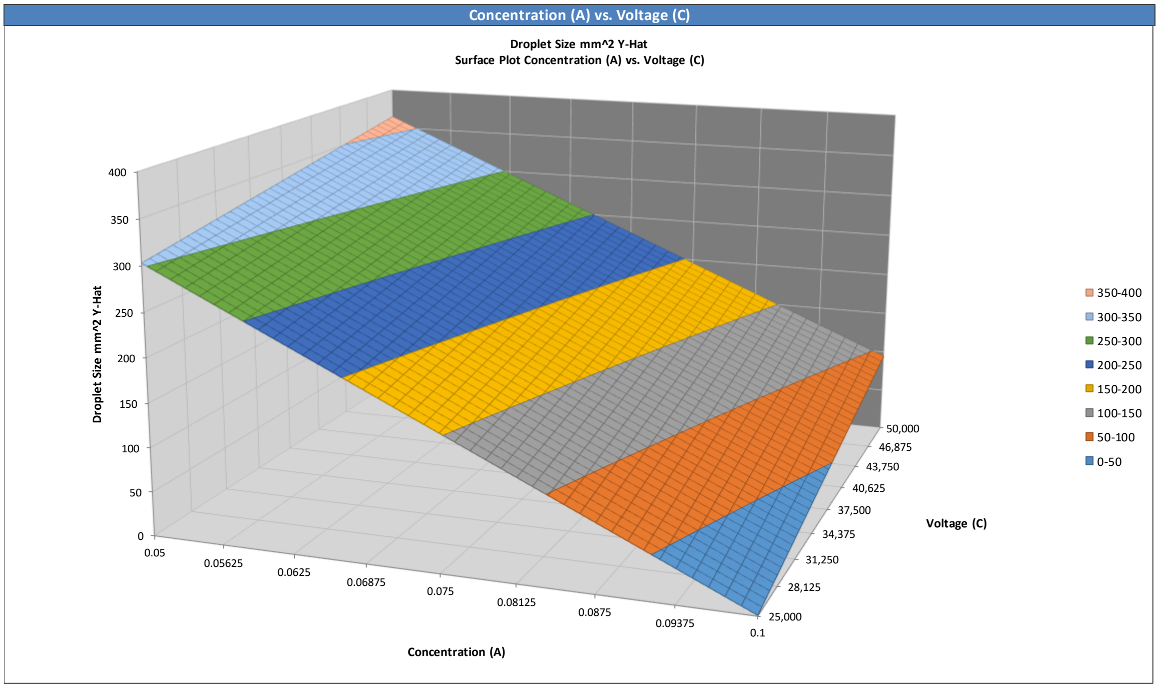

Figure 58: Concentration vs Voltage for Droplet Size h-hat (Palm oil, Polysorbate 80, 19ga Capillary)

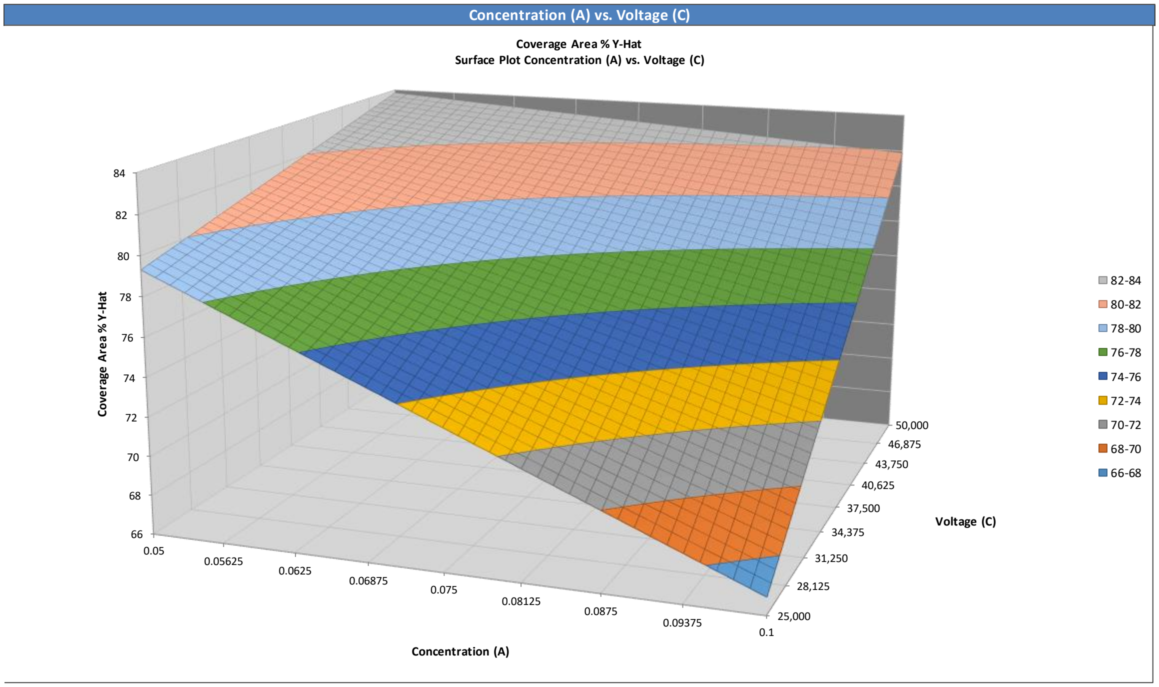

Figure 59: Concentration vs Voltage for Coverage Area h-hat (Palm oil, Polysorbate 80, 19ga Capillary)

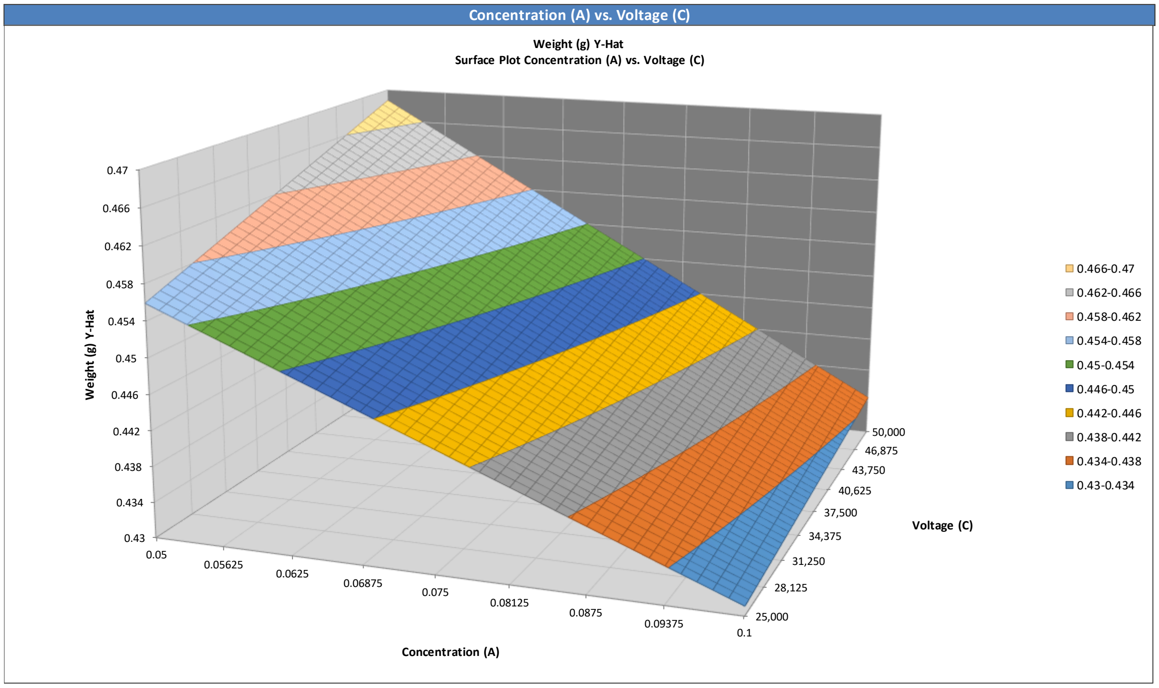

Figure 60: Concentration vs Voltage for Sample Weight h-hat (Palm oil, Polysorbate 80, 19ga Capillary)

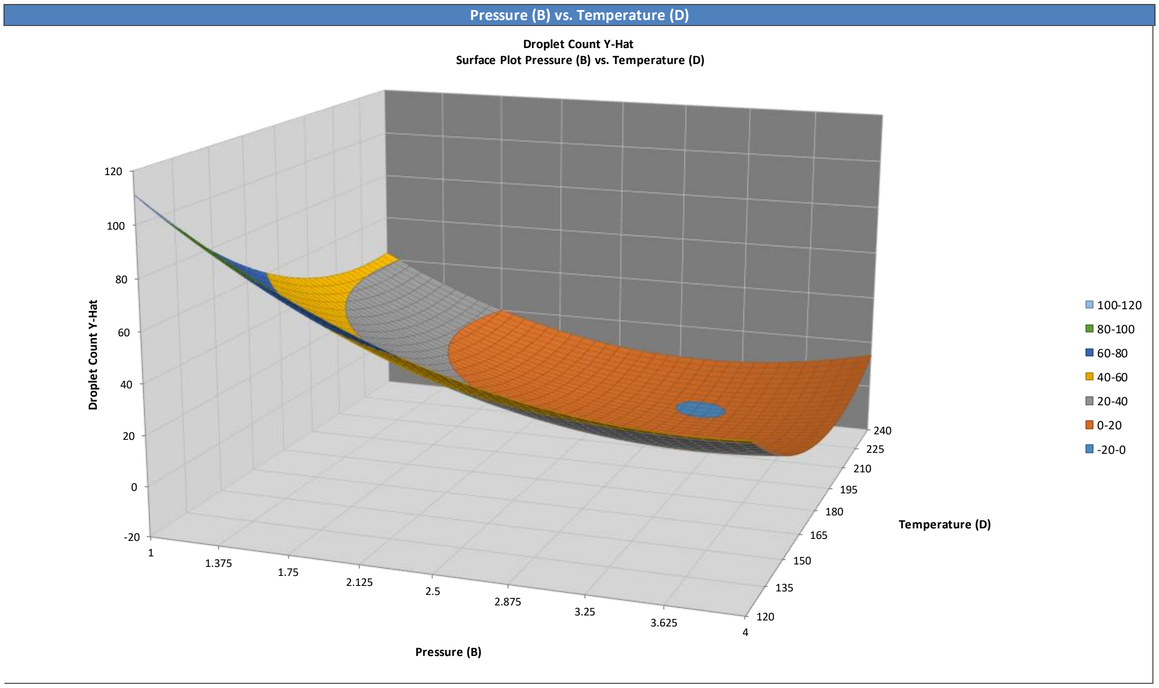

Figure 61: Surface Chart – Pressure vs Temperature for Droplet Count h-hat (Palm oil, Polysorbate 80, 19ga Capillary)

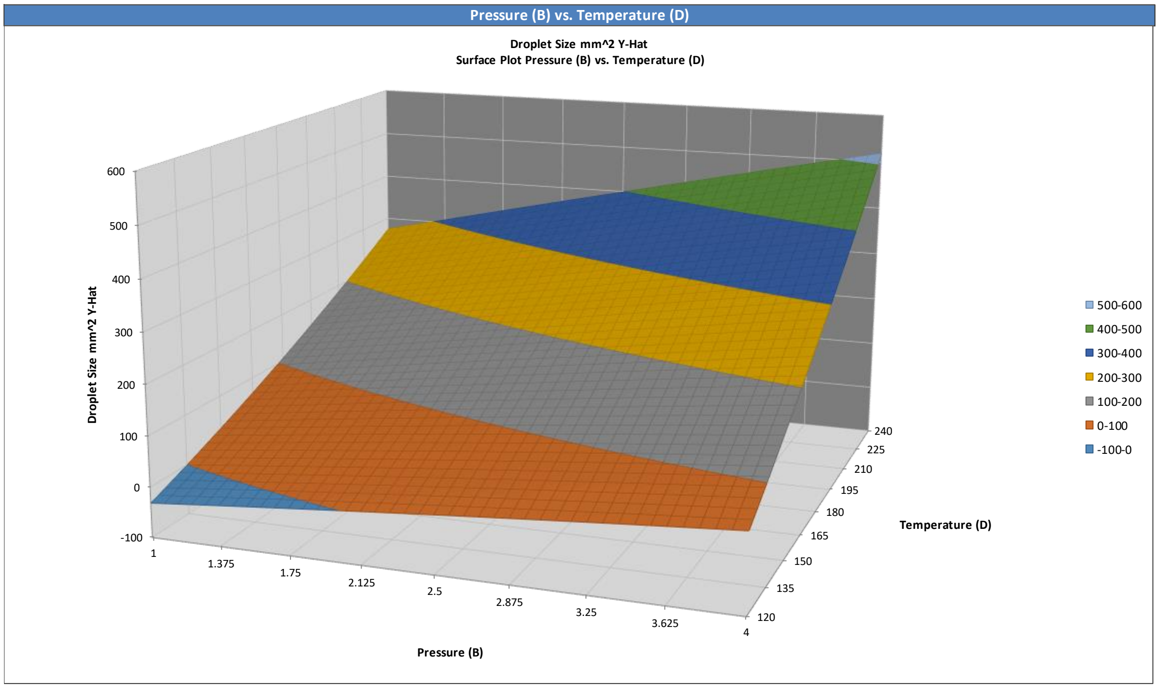

Figure 62: Surface Chart – Pressure vs Temperature for Droplet Size h-hat (Palm oil, Polysorbate 80, 19ga Capillary)

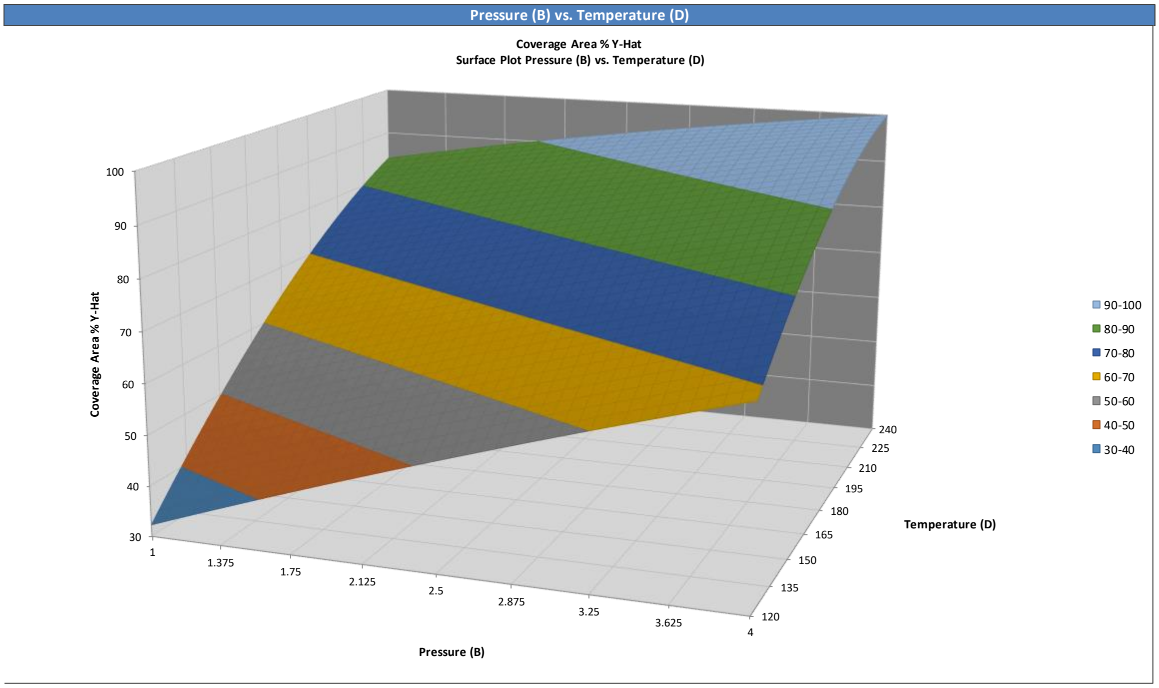

Figure 63: Surface Chart – Pressure vs Temperature for overage Area h-hat (Palm oil, Polysorbate 80, 19ga Capillary)

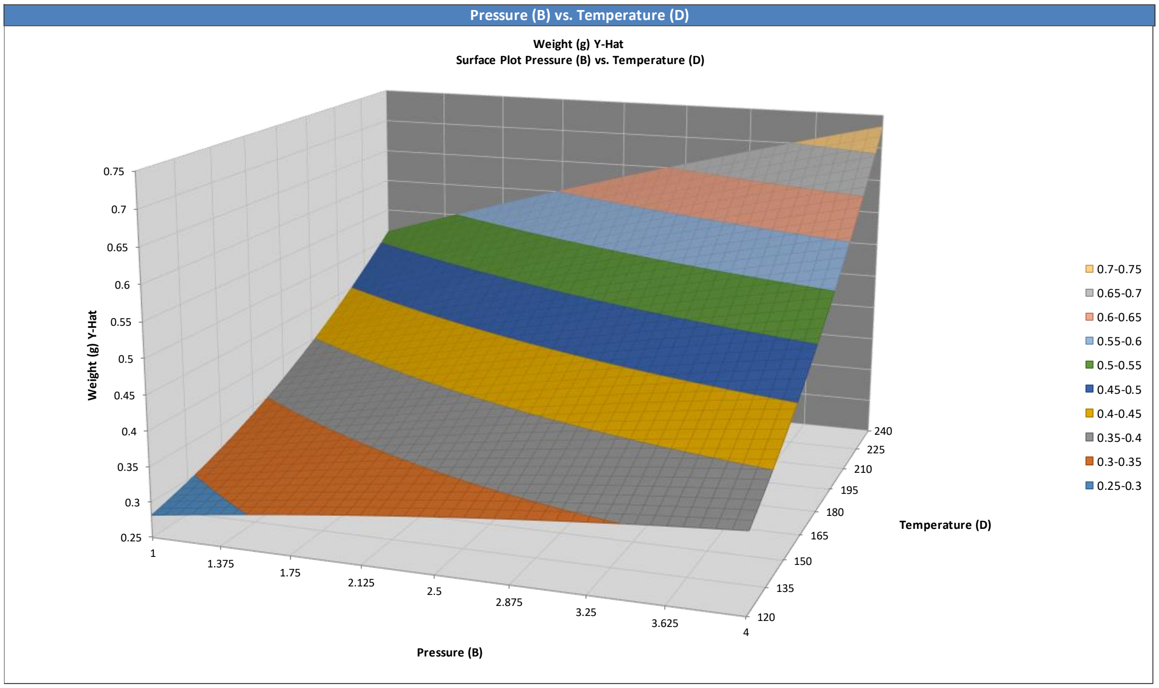

Figure 64: Surface Chart – Pressure vs Temperature for Sample Weight h-hat (Palm oil, Polysorbate 80, 19ga Capillary)

5.1.4. Polysorbate 80 with 22 Gauge Capillary

Table 7: Main Effects Plot for Palm Oil & Polysorbate 80 @ 22ga Capillary

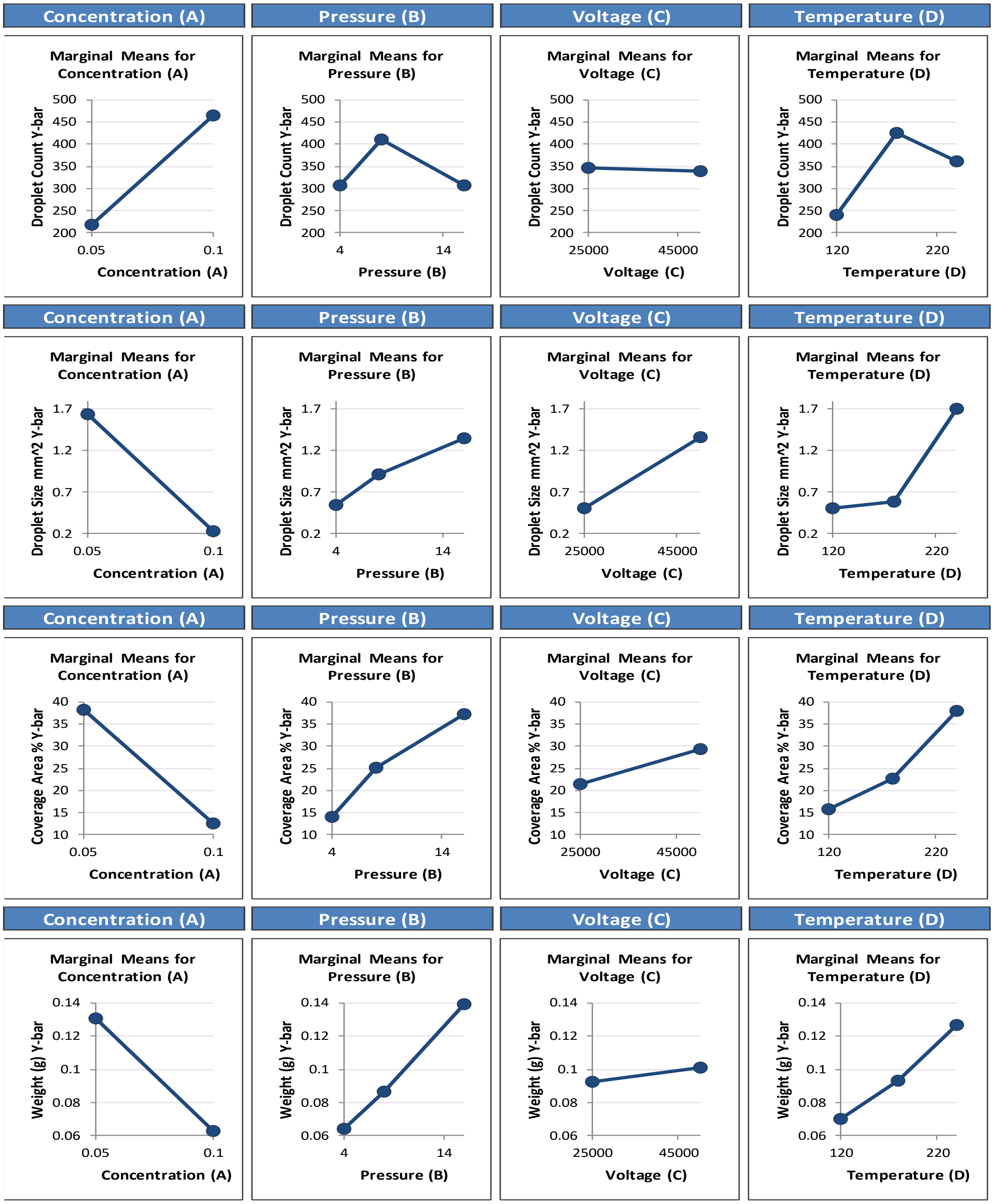

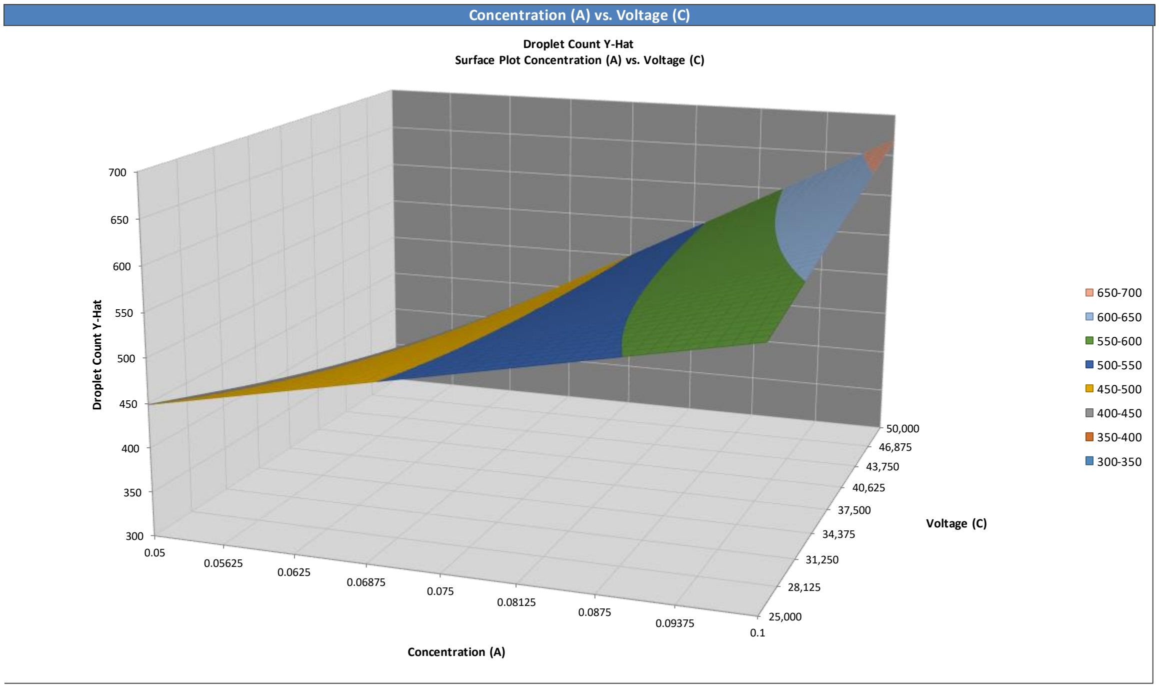

Figure 65: Surface Chart - Concentration vs Voltage for Droplet Count h-hat (Palm oil, Polysorbate 80, 22ga Capillary)

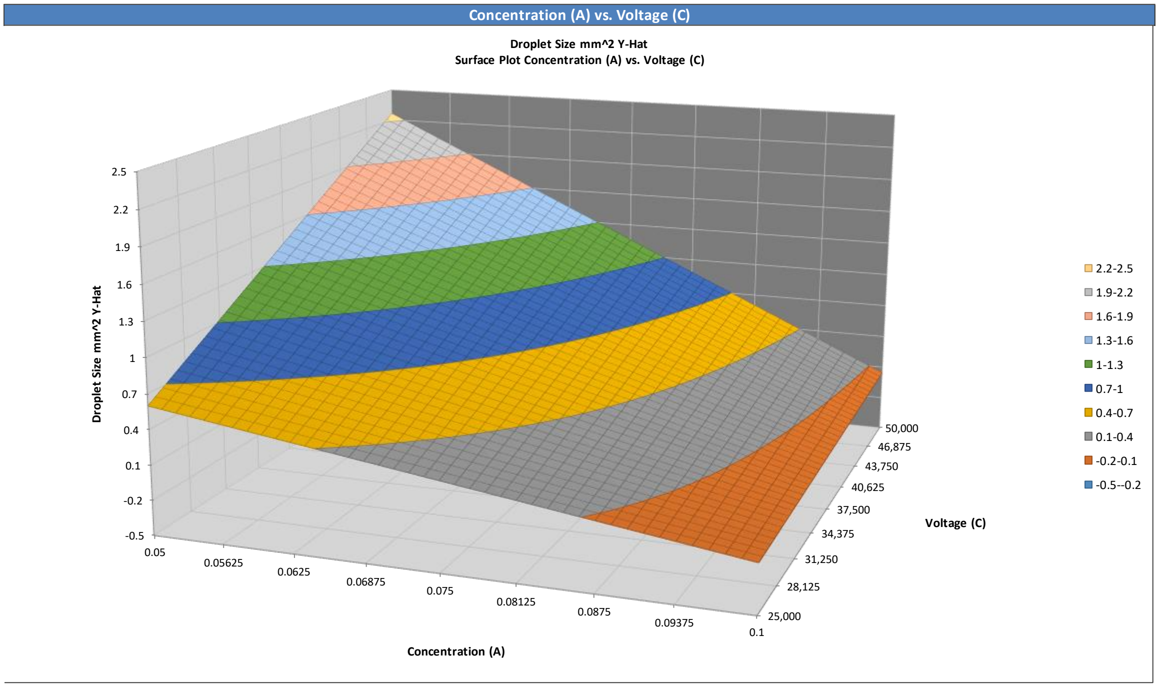

Figure 66: Surface Chart - Concentration vs Voltage for Droplet Size h-hat (Palm oil, Polysorbate 80, 22ga Capillary)

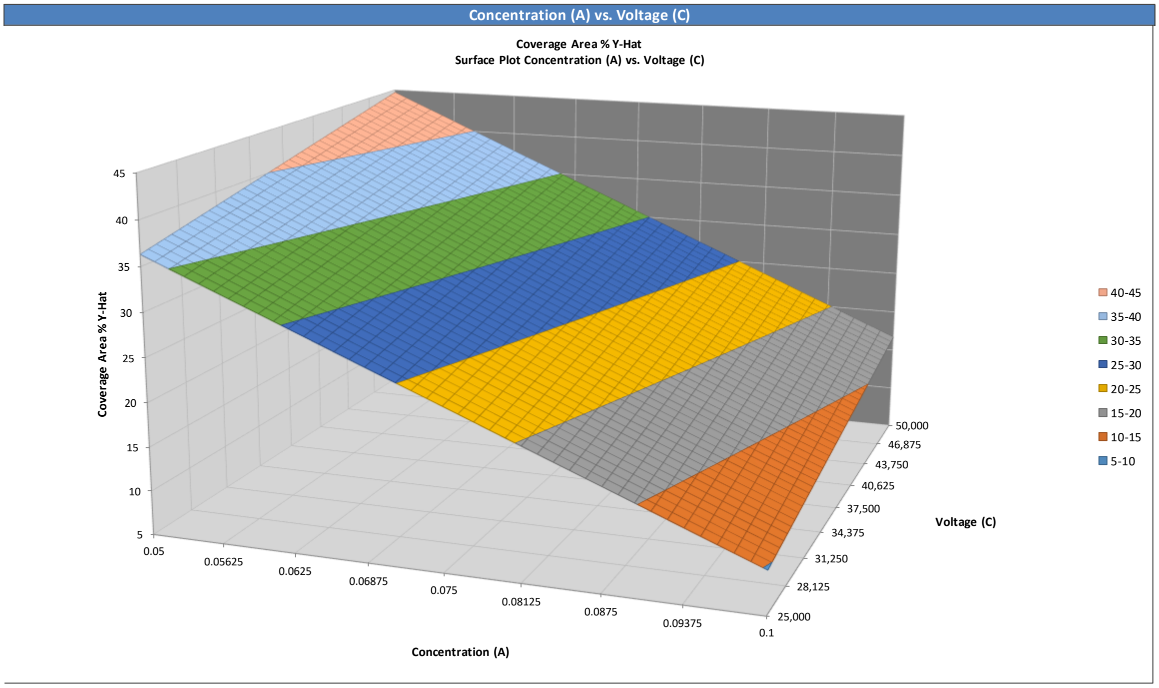

Figure 67: Surface Chart - Concentration vs Voltage for Coverage Area h-hat (Palm oil, Polysorbate 80, 22ga Capillary)

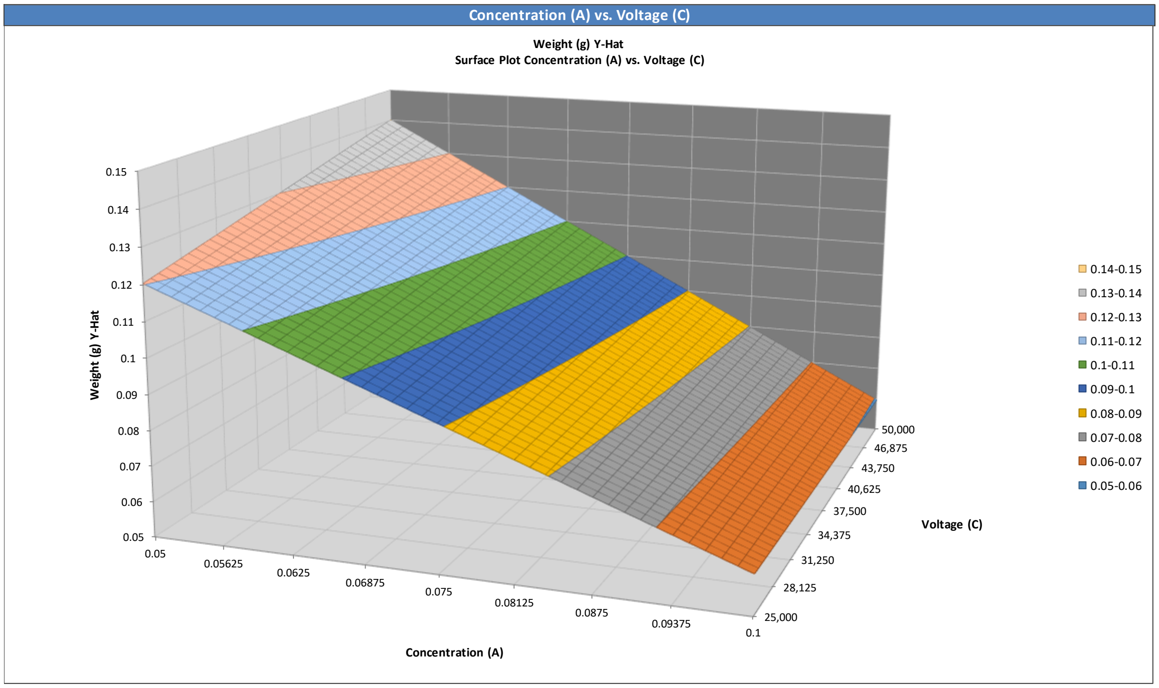

Figure 68: Surface Chart - Concentration vs Voltage for Sample Weight h-hat (Palm oil, Polysorbate 80, 22ga Capillary)

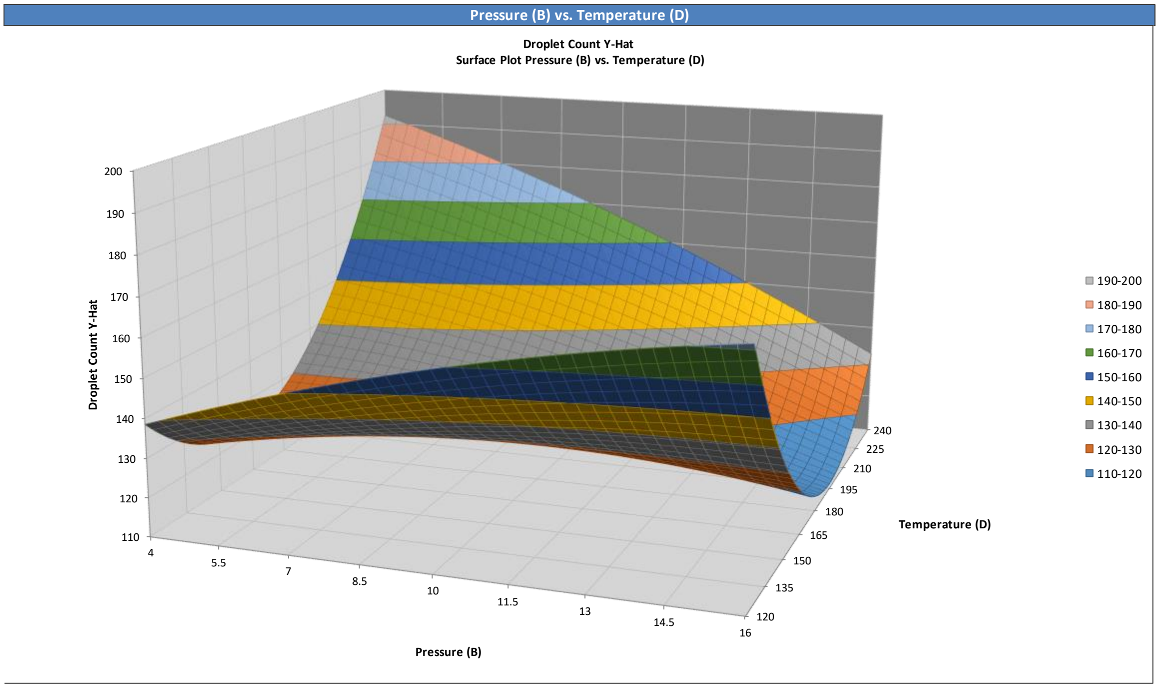

Figure 69: Surface Chart – Pressure vs Temperature for Droplet Count h-hat (Palm oil, Polysorbate 80, 22ga Capillary)

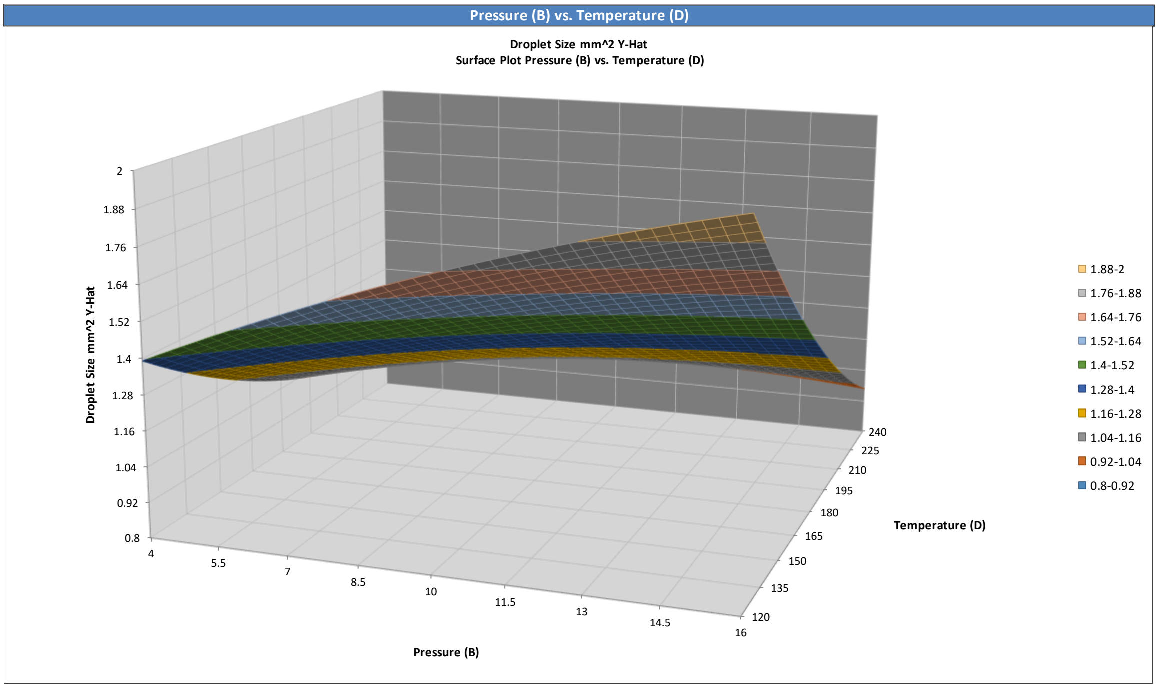

Figure 70: Surface Chart – Pressure vs Temperature for Droplet Size h-hat (Palm oil, Polysorbate 80, 22ga Capillary)

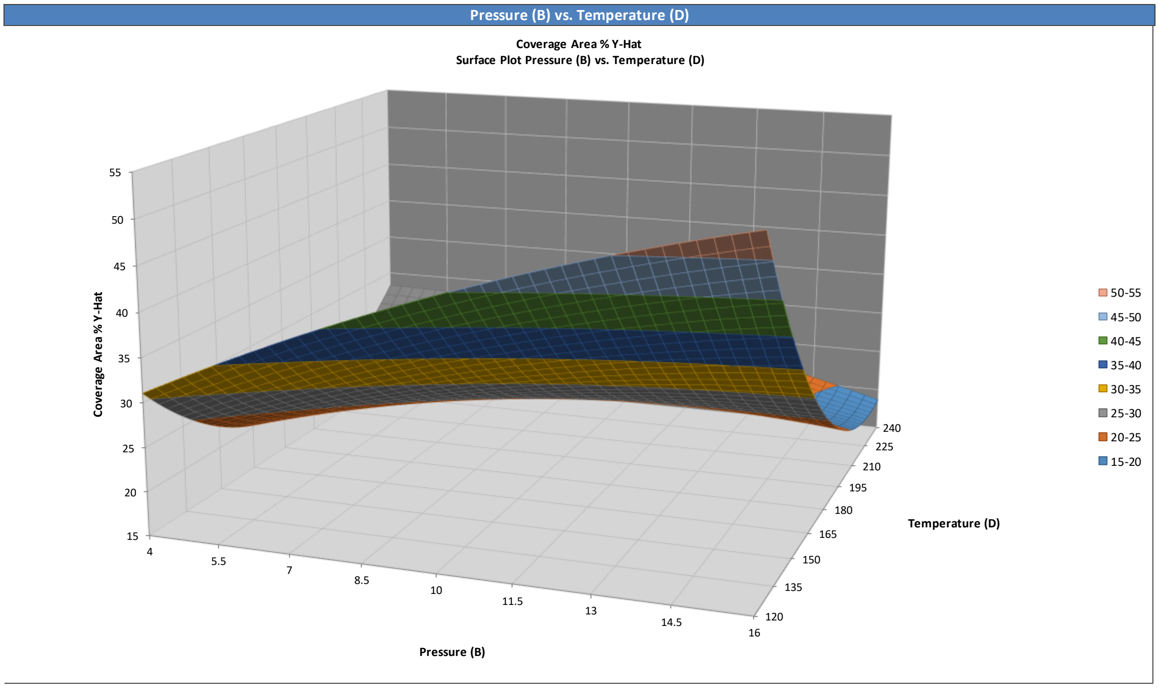

Figure 71: Surface Chart – Pressure vs Temperature for Coverage Area h-hat (Palm oil, Polysorbate 80, 22ga Capillary)

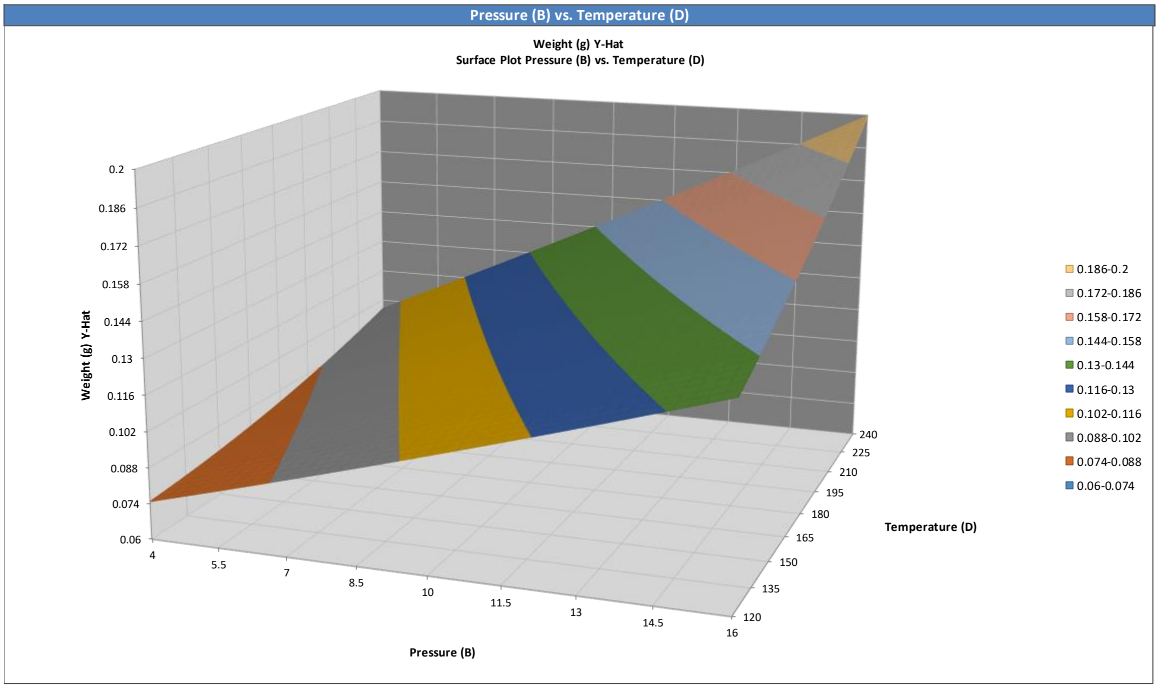

Figure 72: Surface Chart – Pressure vs Temperature for Sample Weight h-hat (Palm oil, Polysorbate 80, 22ga Capillary)

5.1.5. Propylene Glycol with 19 Gauge Capillary

Table 8: Main Effects Plot for Palm Oil & Propylene Glycol @ 19ga Capillary

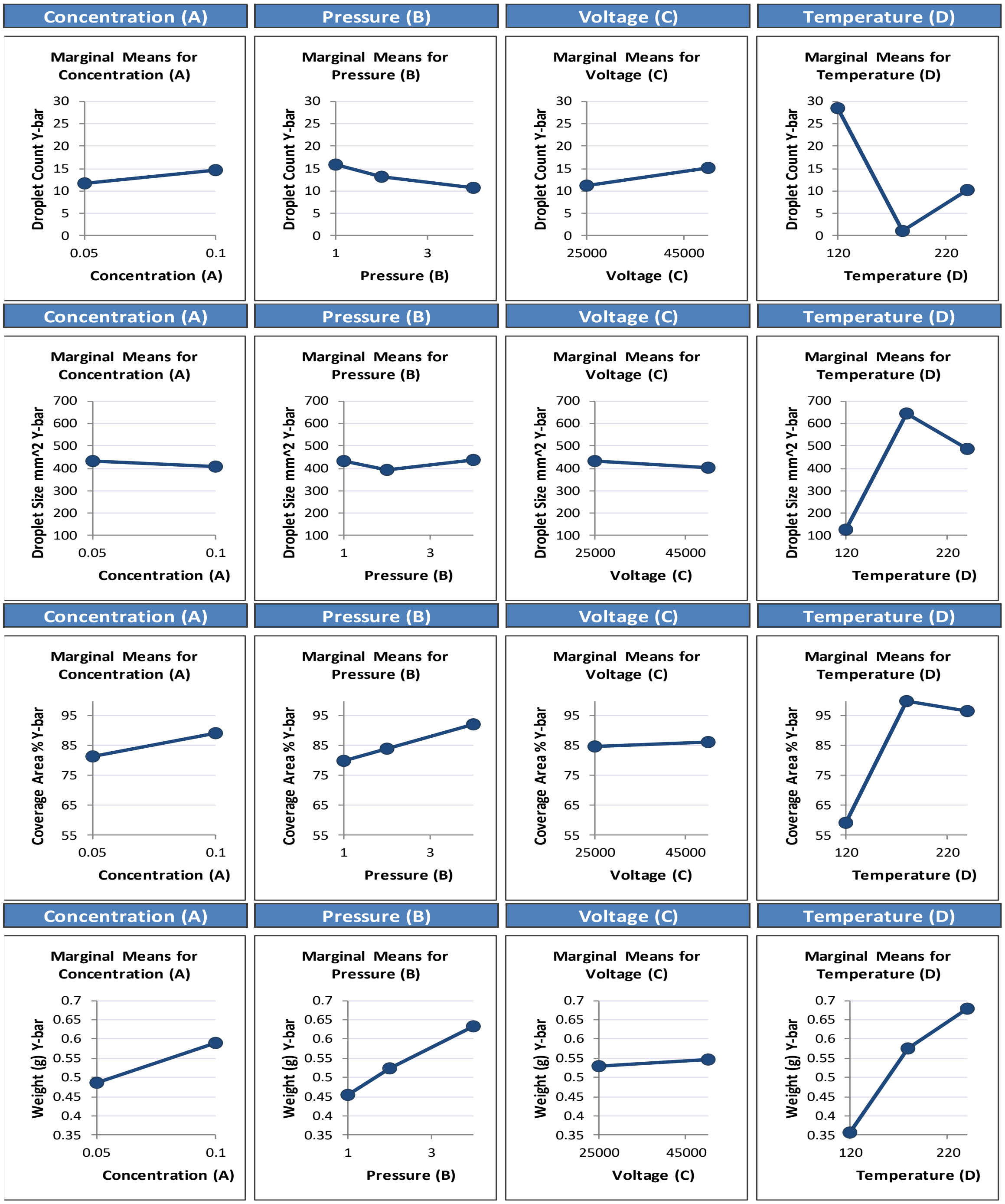

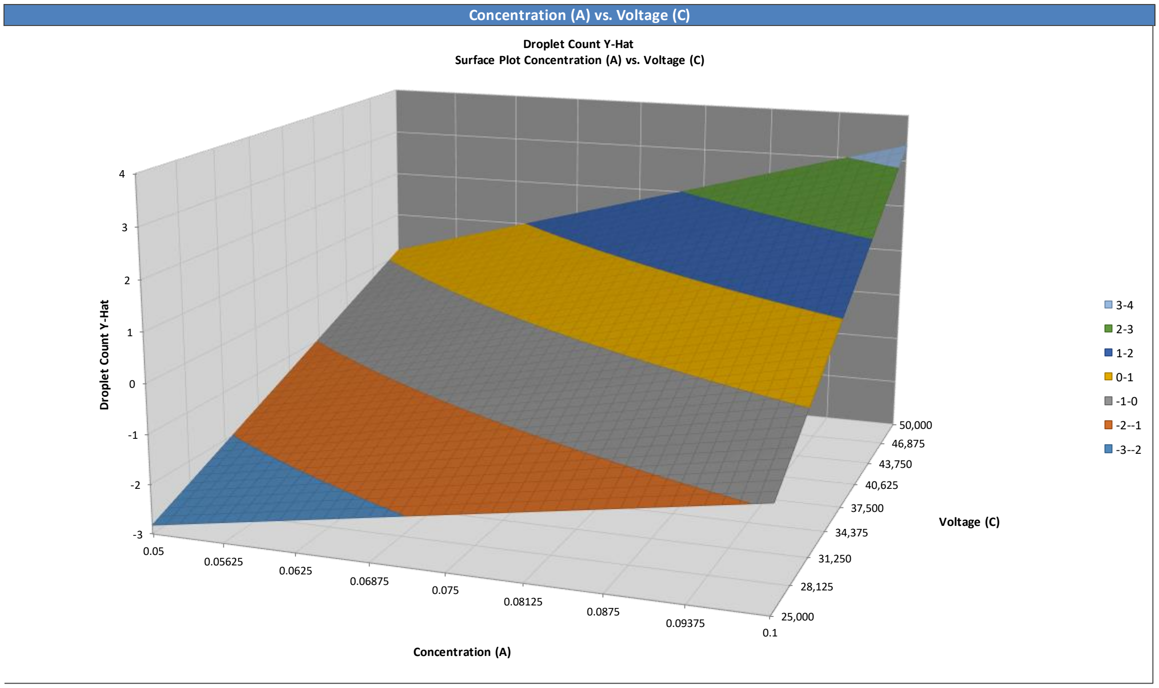

Figure 73: Surface Chart - Concentration vs Voltage for Droplet Count h-hat (Palm oil, Propylene Glycol, 19ga Capillary)

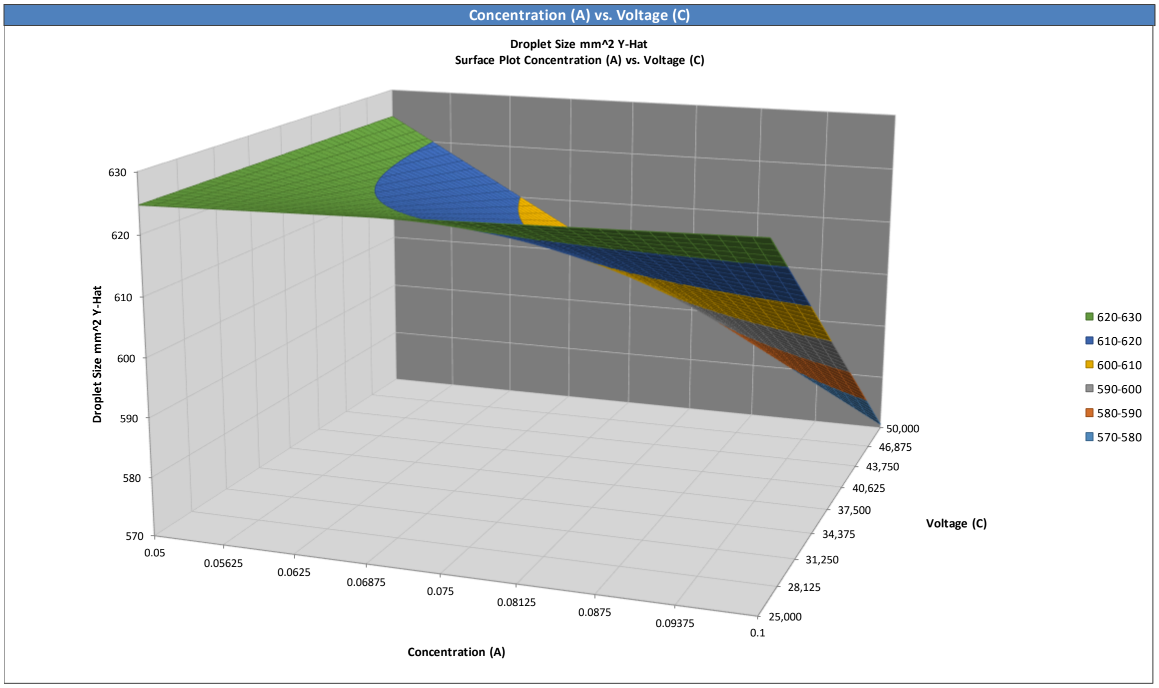

Figure 74: Surface Chart - Concentration vs Voltage for Droplet Size Y-hat (Palm oil, Propylene Glycol, 19ga Capillary)

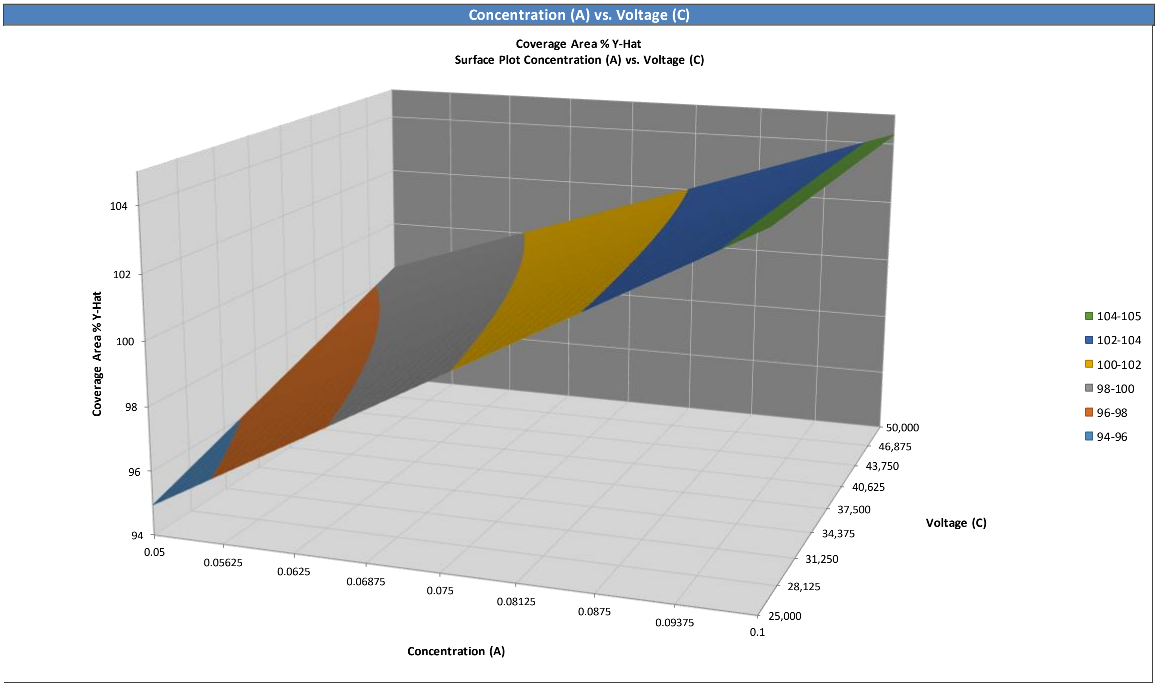

Figure 75: Surface Chart - Concentration vs Voltage for Coverage Area Y-hat (Palm oil, Propylene Glycol, 19ga Capillary)

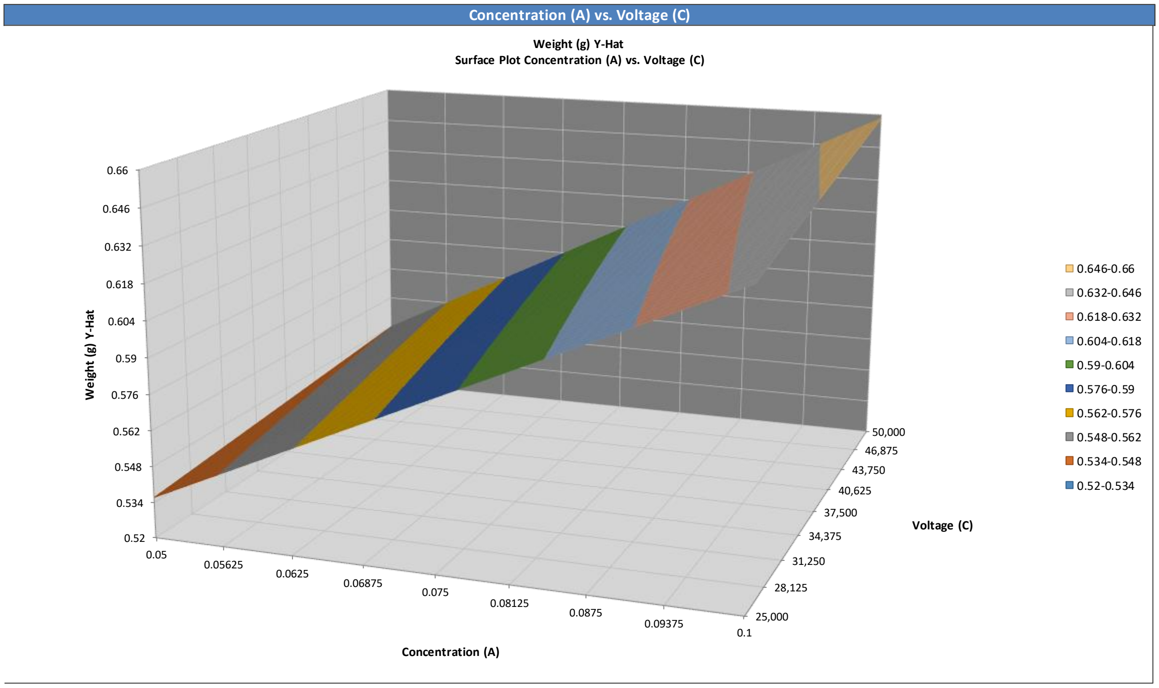

Figure 76: Surface Chart - Concentration vs Voltage for Sample Weight Y-hat (Palm oil, Propylene Glycol, 19ga Capillary)

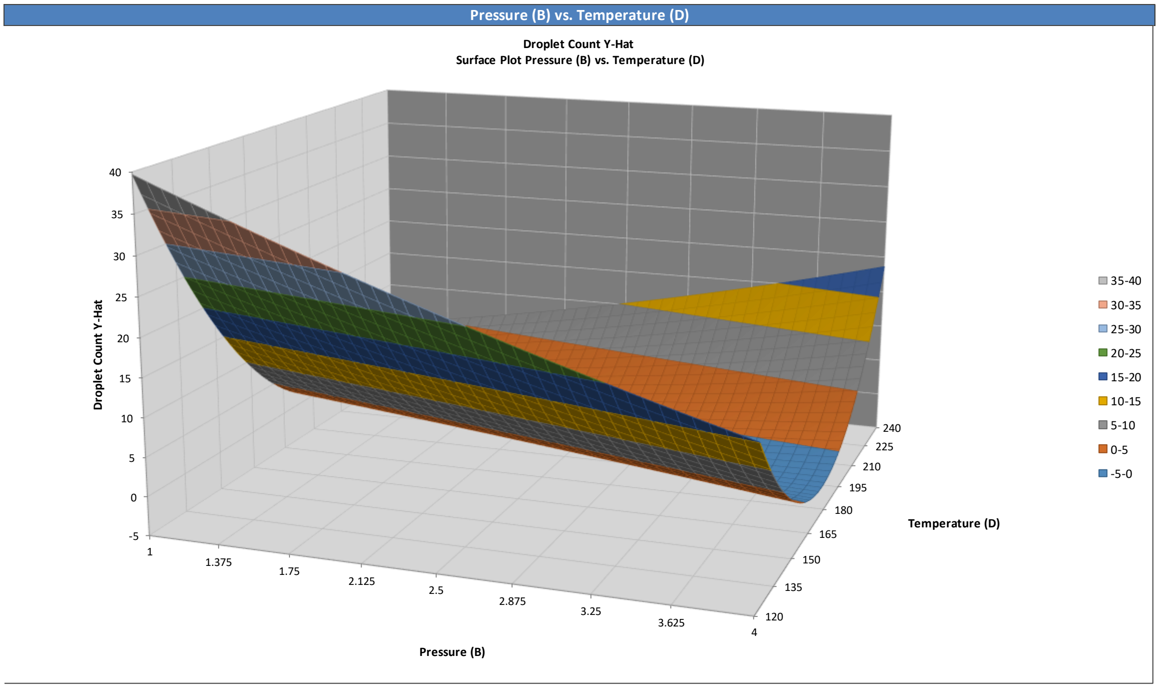

Figure 77: Surface Chart - Pressure vs Temperature for Droplet Count h-hat (Palm oil, Propylene Glycol, 19ga Capillary)

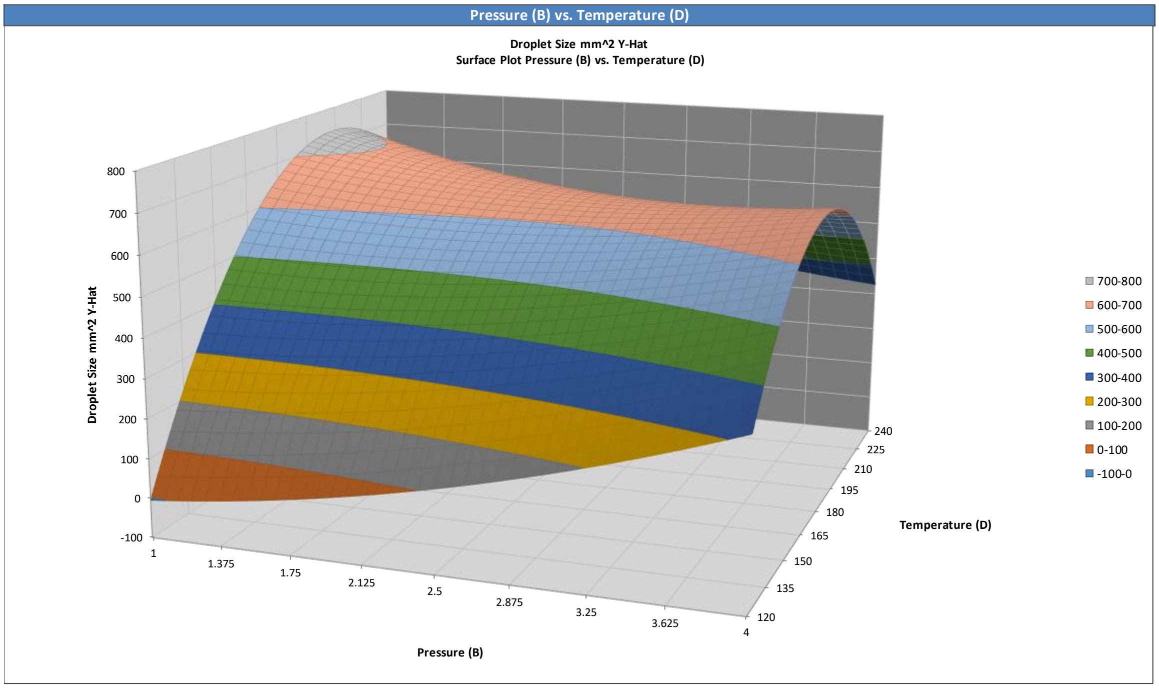

Figure 78: Surface Chart - Pressure vs Temperature for Droplet Size h-hat (Palm oil, Propylene Glycol, 19ga Capillary)

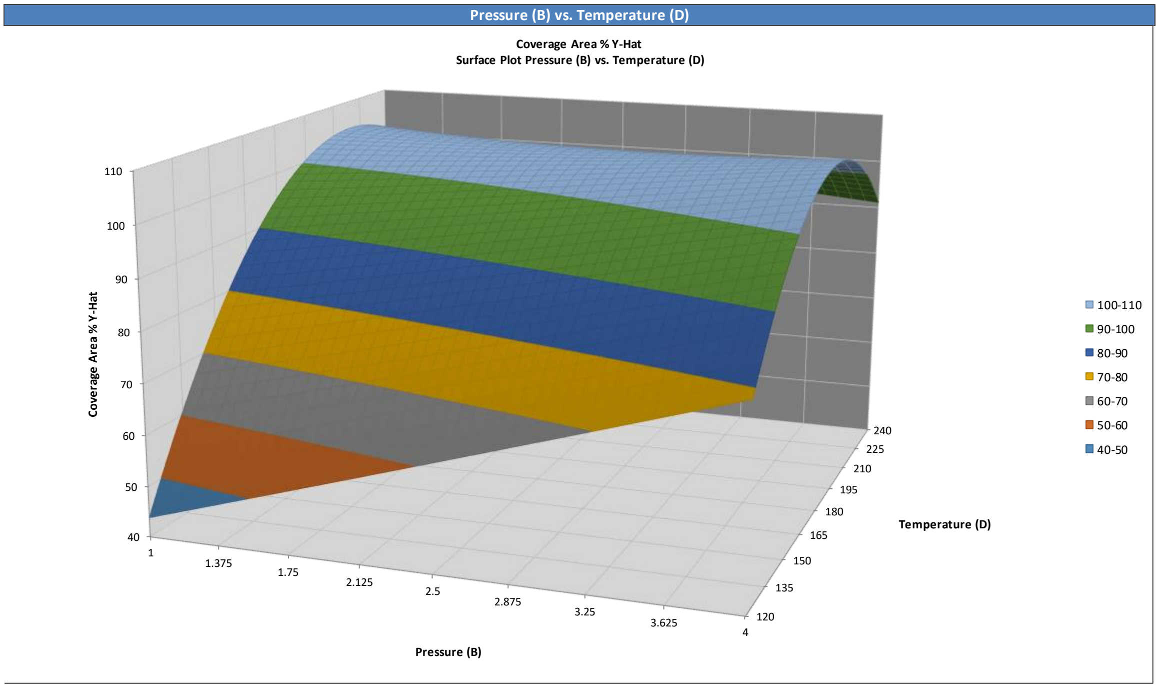

Figure 79: Surface Chart - Pressure vs Temperature for Coverage Area h-hat (Palm oil, Propylene Glycol, 19ga Capillary)

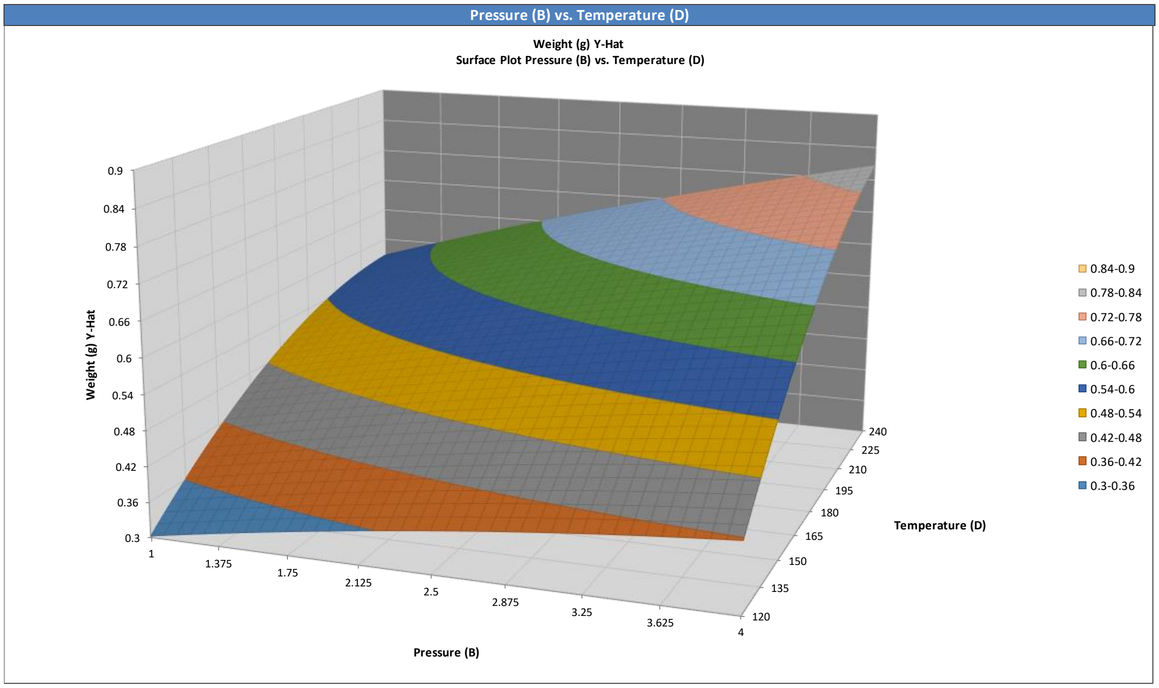

Figure 80: Surface Chart - Pressure vs Temperature for Sample Weight h-hat (Palm oil, Propylene Glycol, 19ga Capillary)

5.1.6. Propylene Glycol with 22 Gauge Capillary

Table 9: Main Effects Plot for Palm Oil & Propylene Glycol @ 22ga Capillary

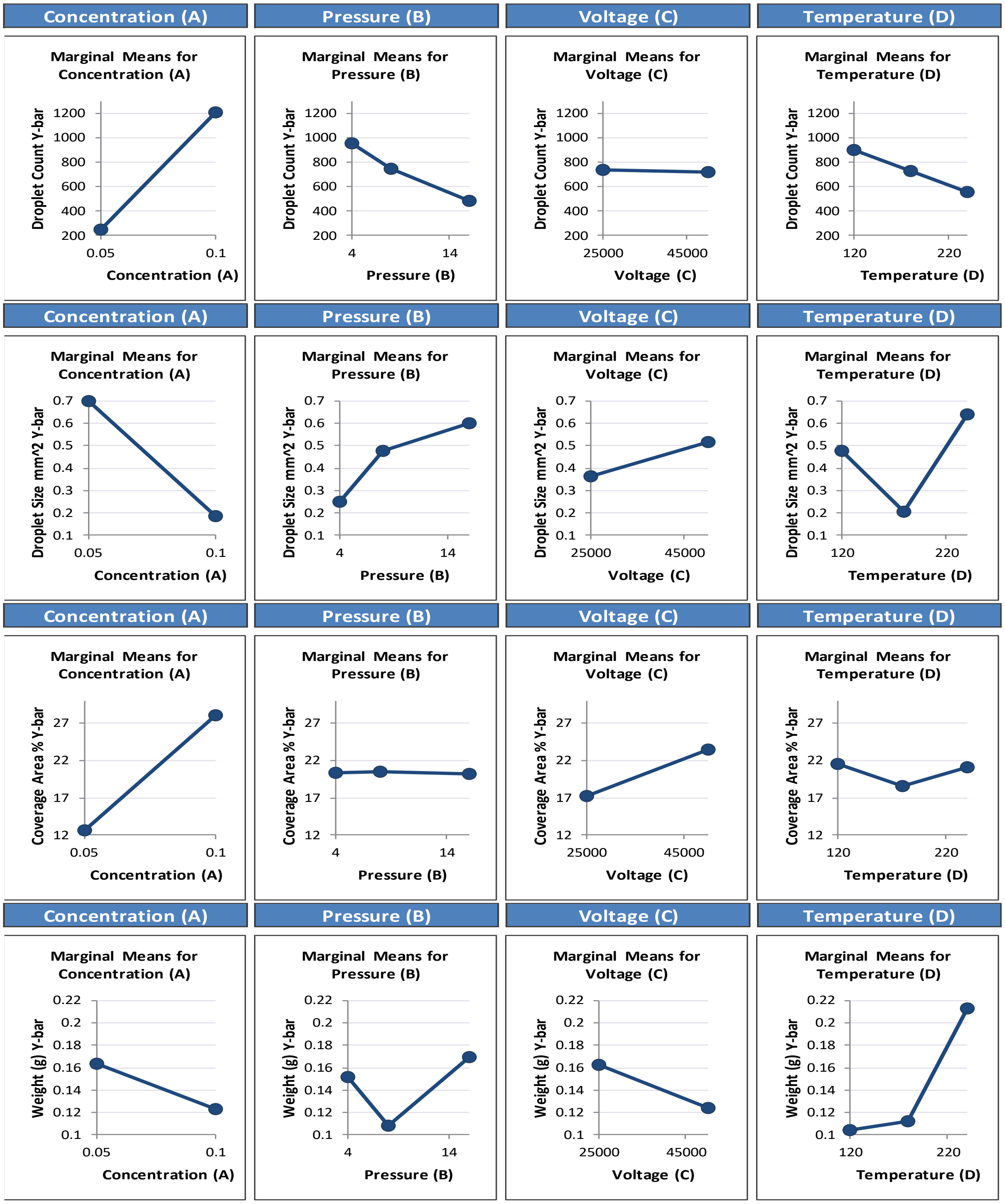

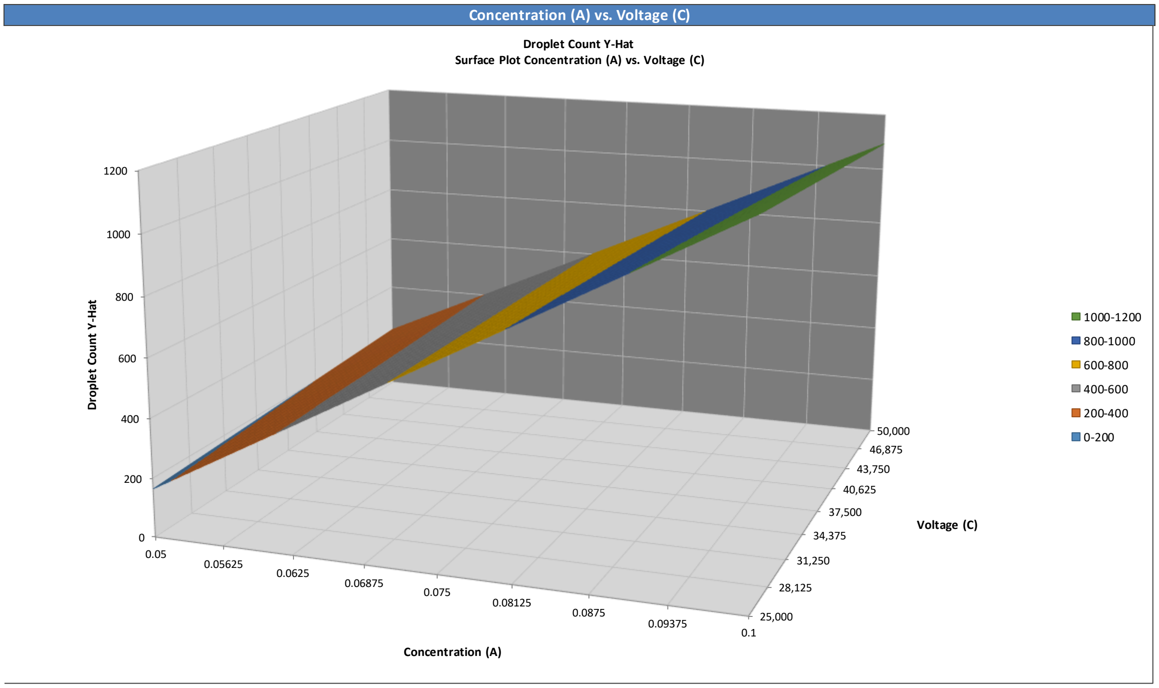

Figure 81: Surface Chart - Concentration vs Voltage for Droplet Count Y-hat (Palm oil, Propylene Glycol, 22ga Capillary)

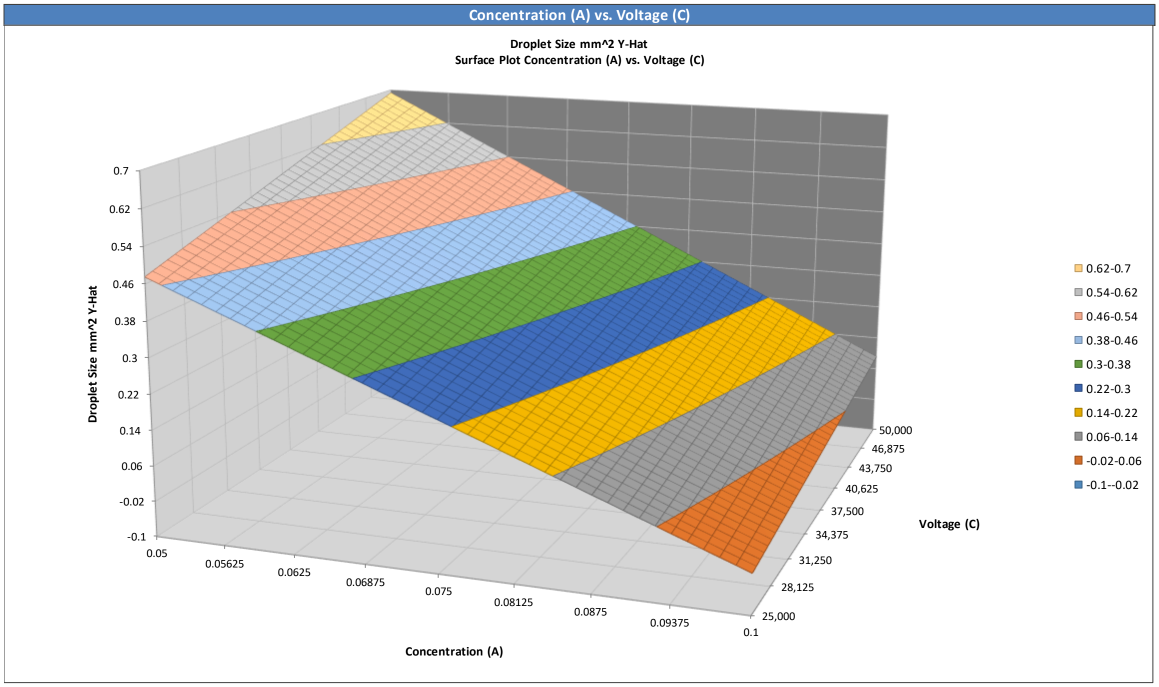

Figure 82: Surface Chart - Concentration vs Voltage for Droplet Size Y-hat (Palm oil, Propylene Glycol, 22ga Capillary)

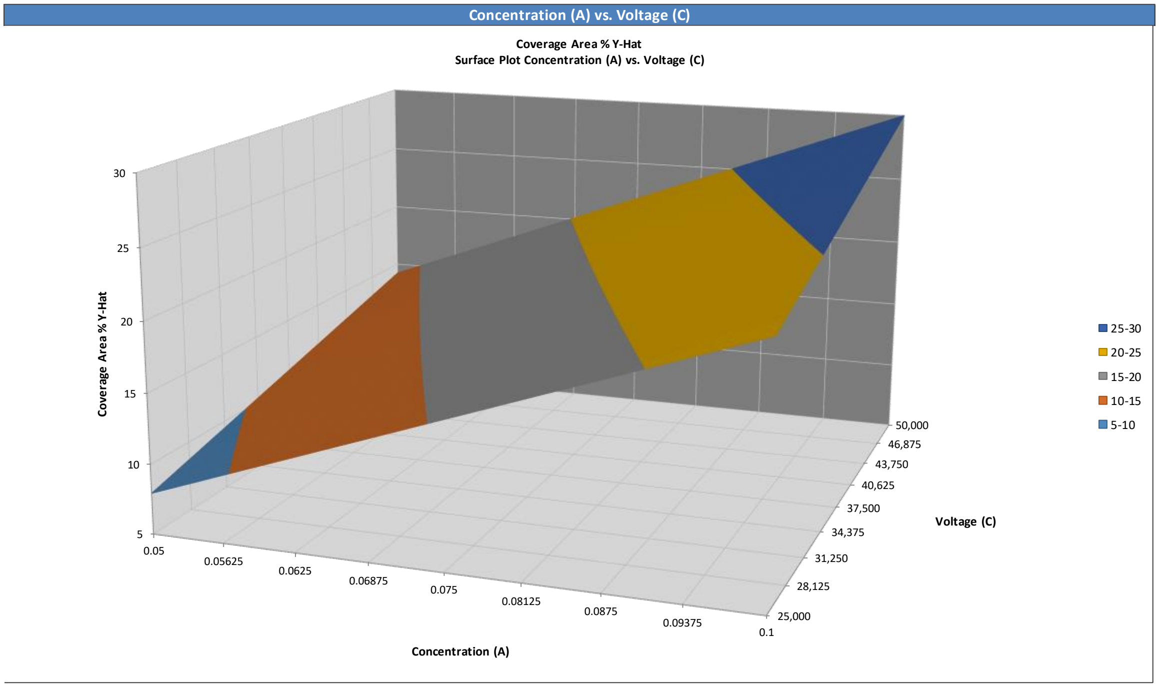

Figure 83: Surface Chart - Concentration vs Voltage for Coverage Area Y-hat (Palm oil, Propylene Glycol, 22ga Capillary)

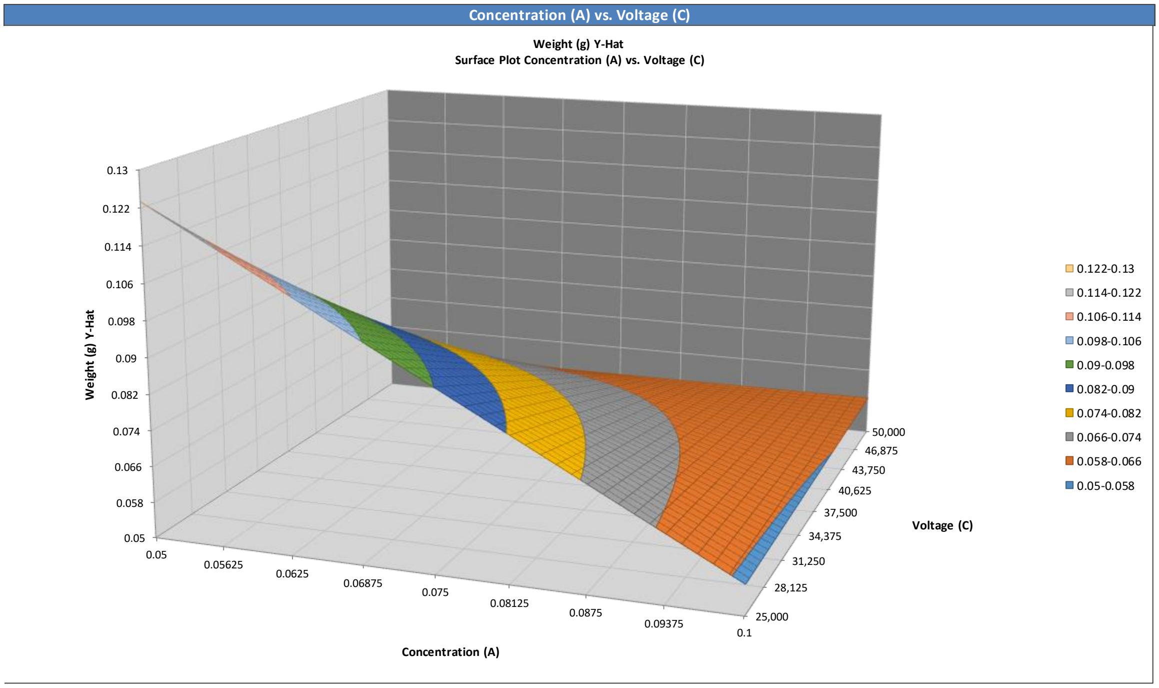

Figure 84: Surface Chart - Concentration vs Voltage for Sample Weight Y-hat (Palm oil, Propylene Glycol, 22ga Capillary)

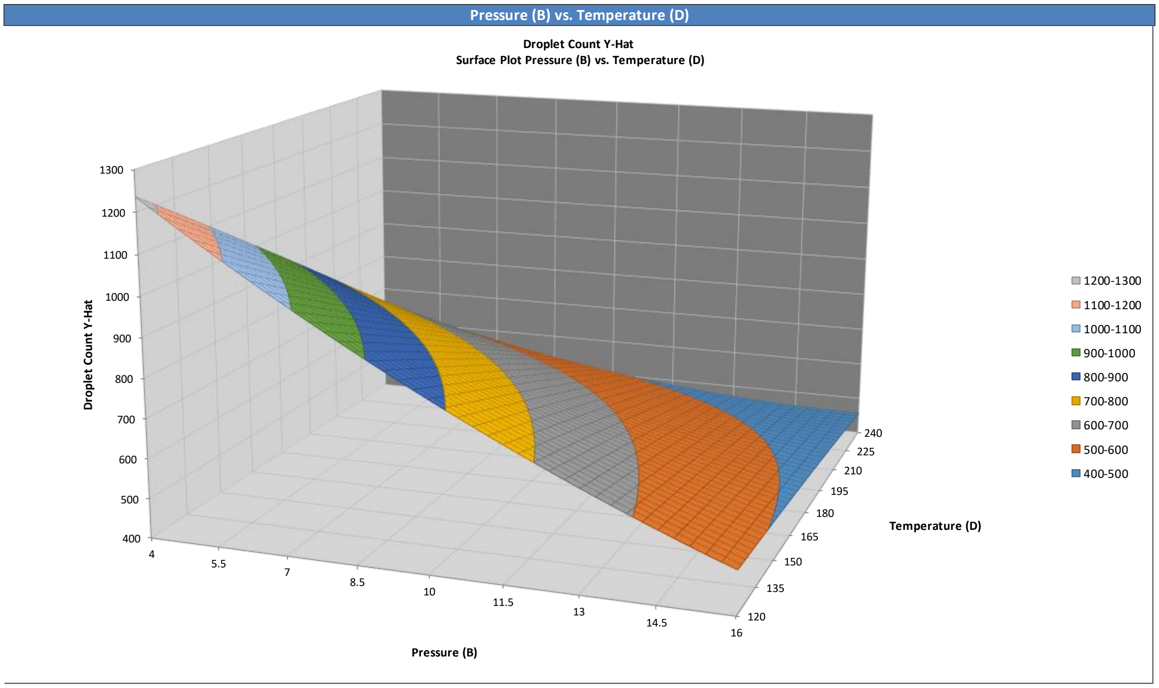

Figure 85: Surface Chart – Pressure vs Temperature for Droplet Count Y-hat (Palm oil, Propylene Glycol, 22ga Capillary)

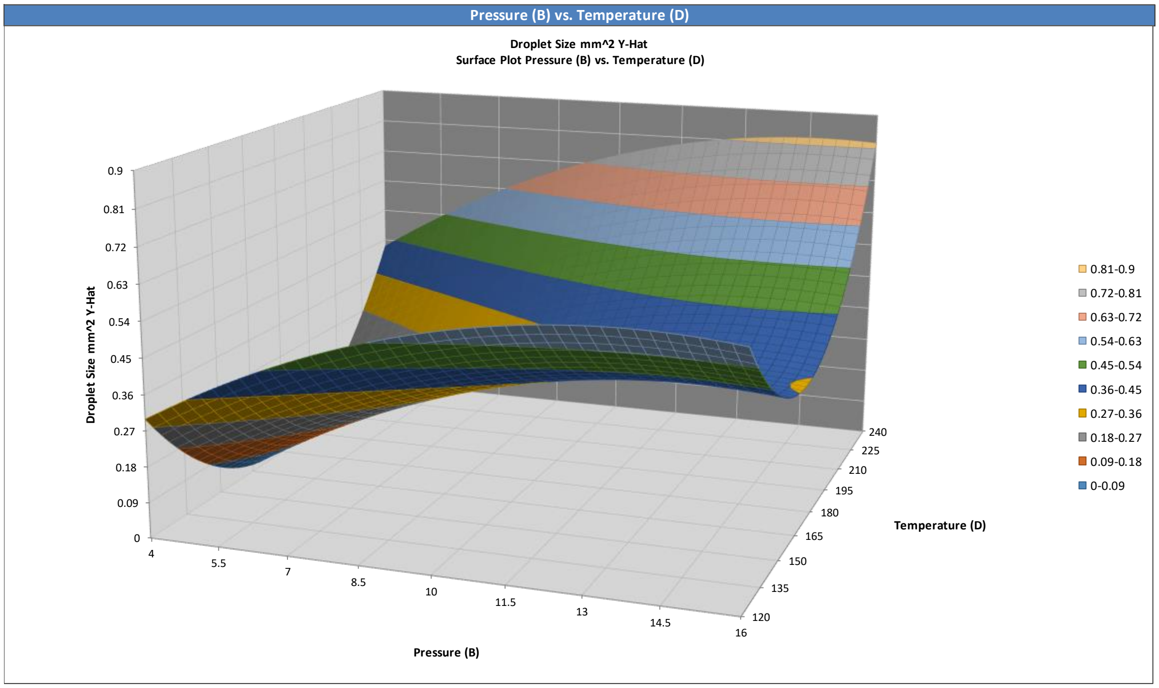

Figure 86: Surface Chart – Pressure vs Temperature for Droplet Size Y-hat (Palm oil, Propylene Glycol, 22ga Capillary)

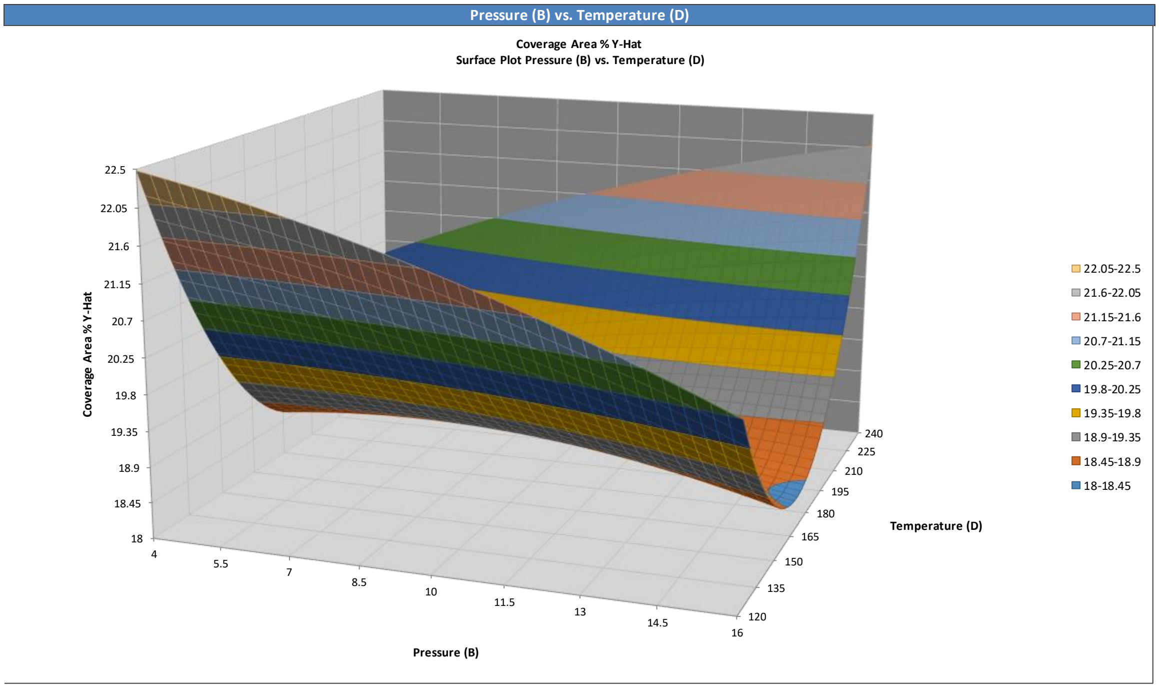

Figure 87: Surface Chart – Pressure vs Temperature for Coverage Area Y-hat (Palm oil, Propylene Glycol, 22ga Capillary)

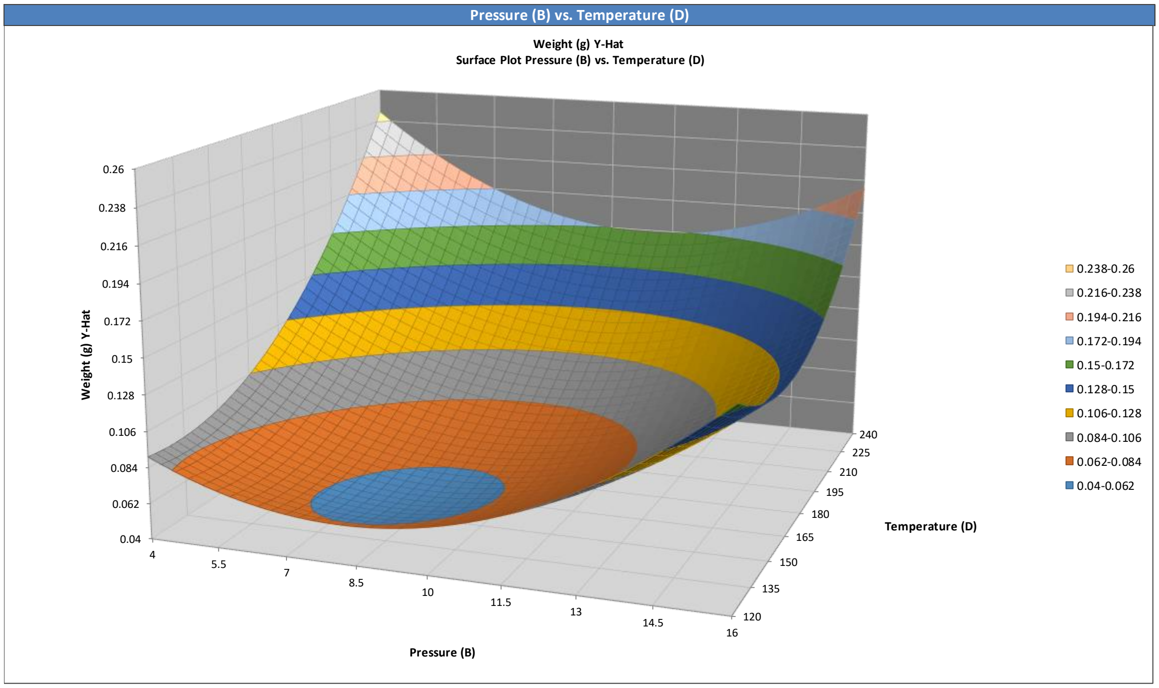

Figure 88: Surface Chart – Pressure vs Temperature for Sample Weight Y-hat (Palm oil, Propylene Glycol, 22ga Capillary)

5.2. SOYBEAN OIL

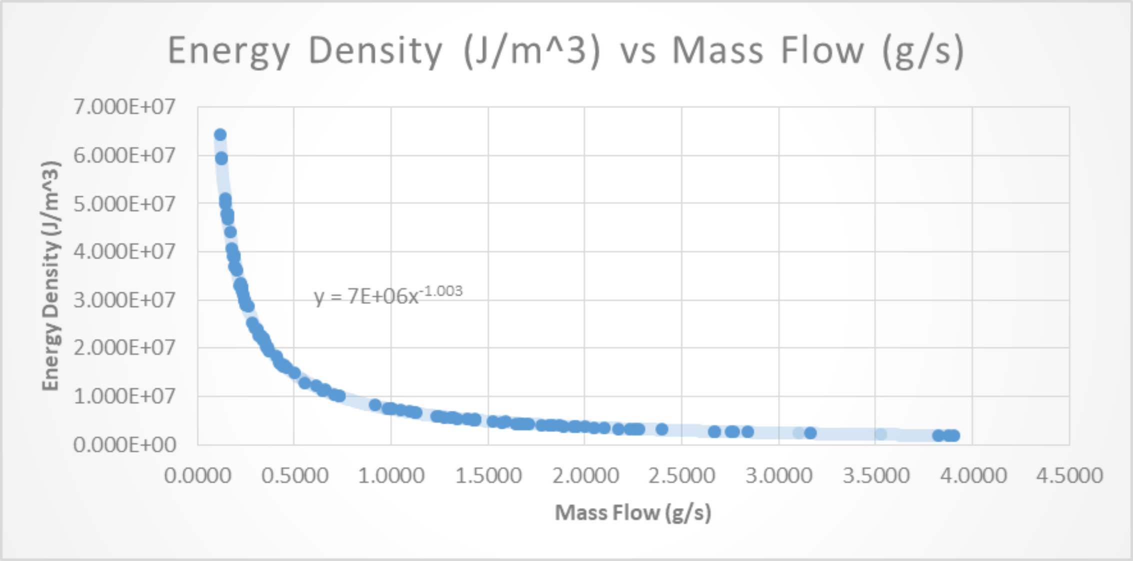

Figure 89: Soybean Oil Energy Density vs Mass Flow Chart 25kV

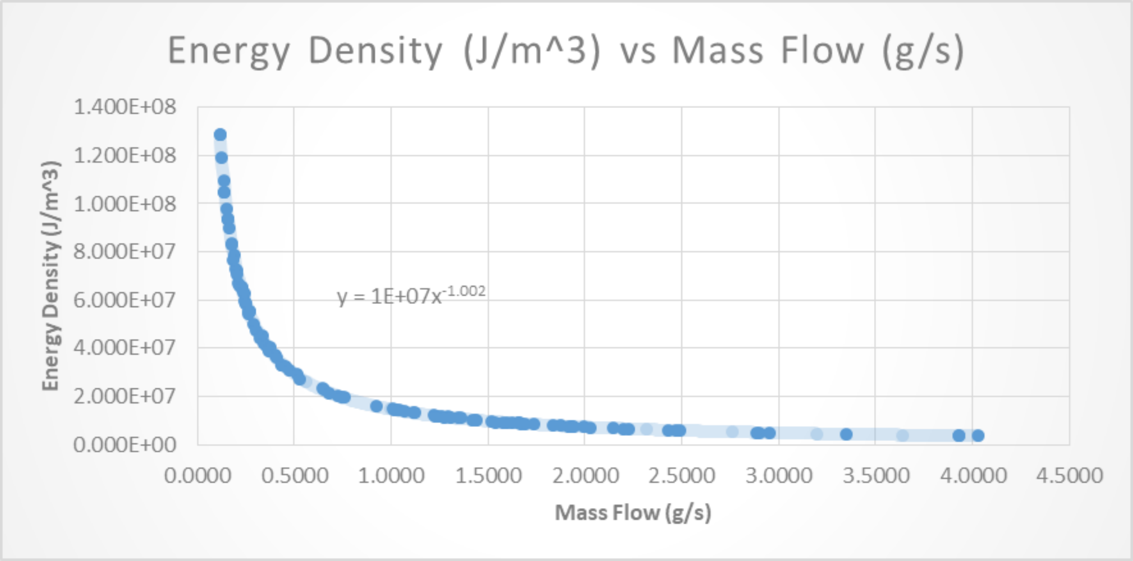

Figure 90: Soybean Oil Energy Density vs Mass Flow Chart 50kV

5.2.1. Soy Lecithin with 19 Gauge Capillary

Table 10: Main Effects Plot for Soybean Oil & Soy Lecithin @ 19ga Capillary

Concentration (A)

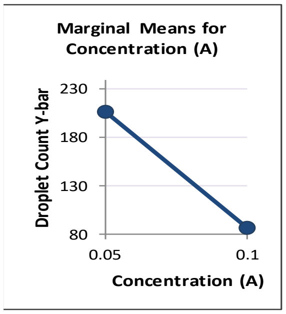

Pressure (B)

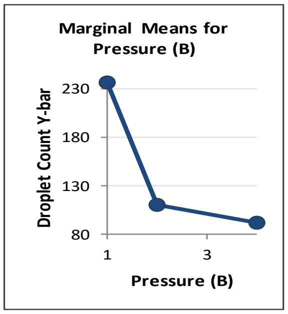

Voltage (C)

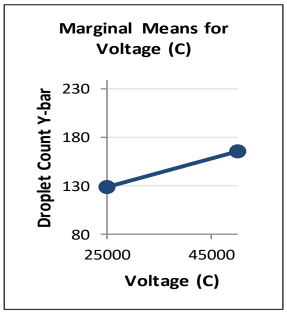

Temperature (D)

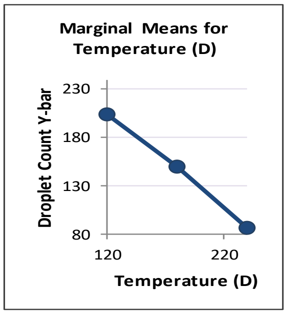

Concentration (A)

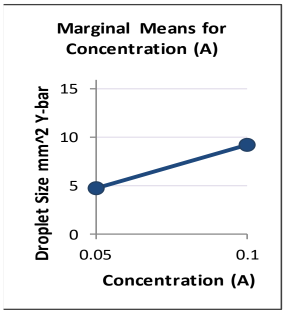

Pressure (B)

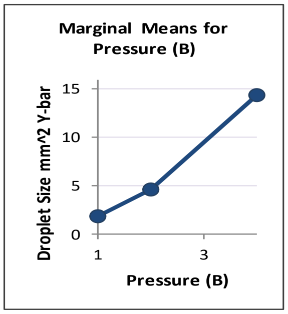

Voltage (C)

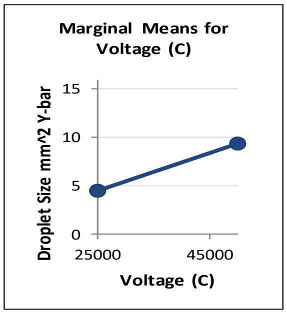

Temperature (D)

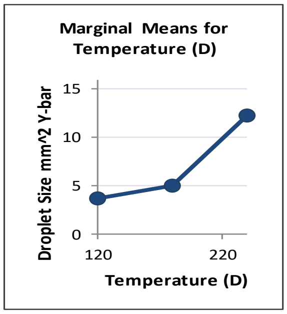

Concentration (A)

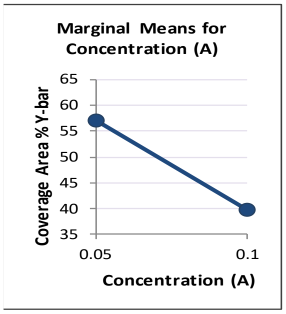

Pressure (B)

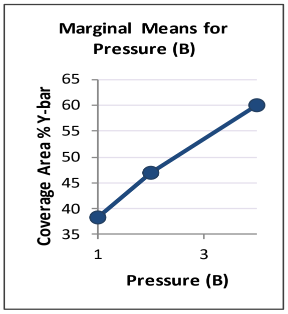

Voltage (C)

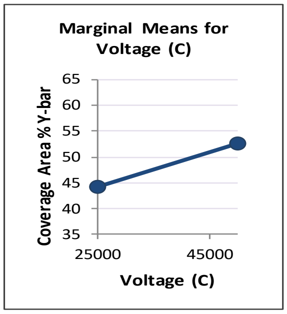

Temperature (D)

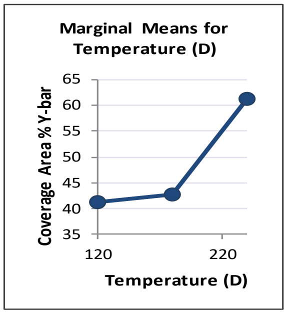

Concentration (A)

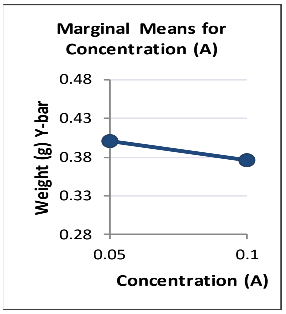

Pressure (B)

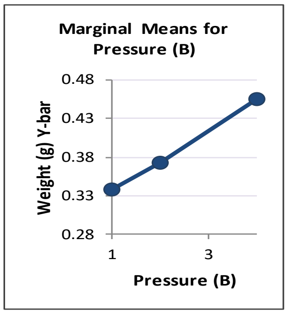

Voltage (C)

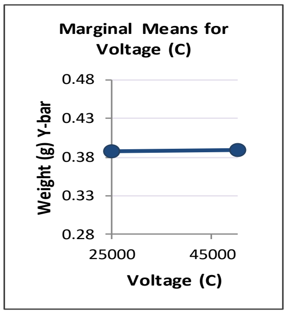

Temperature (D)

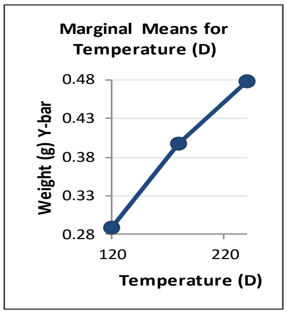

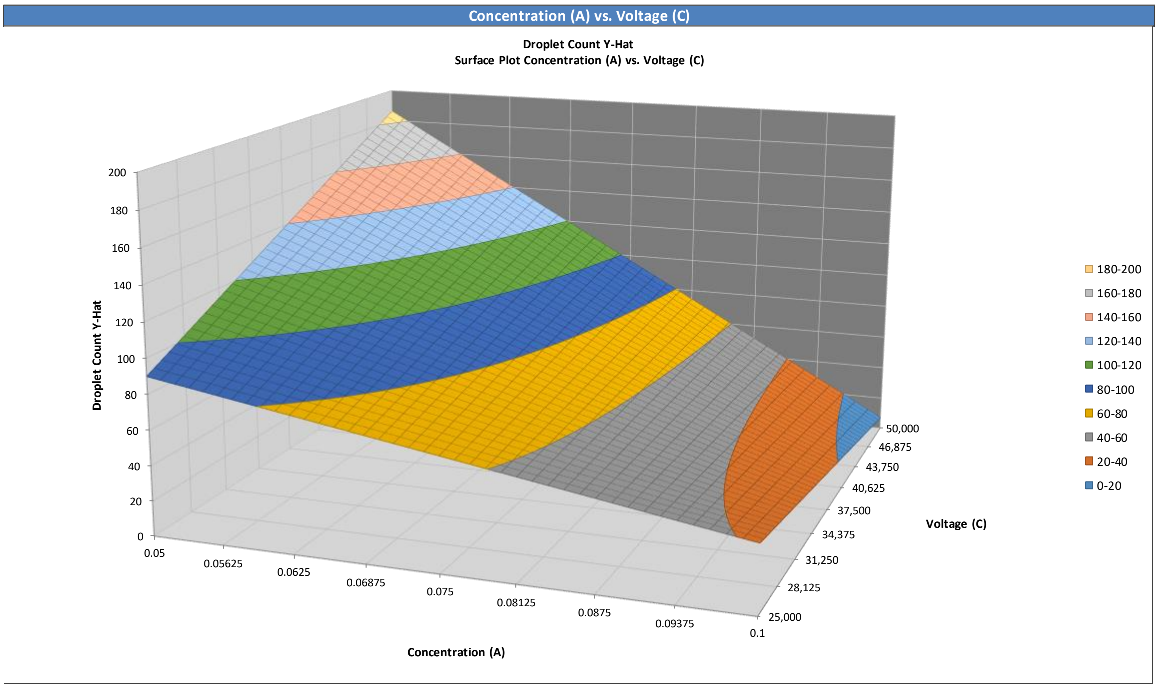

Figure 91: Surface Chart - Concentration vs Voltage for Droplet Count h-hat (Soybean oil, Soy Lecithin, 19ga Capillary)

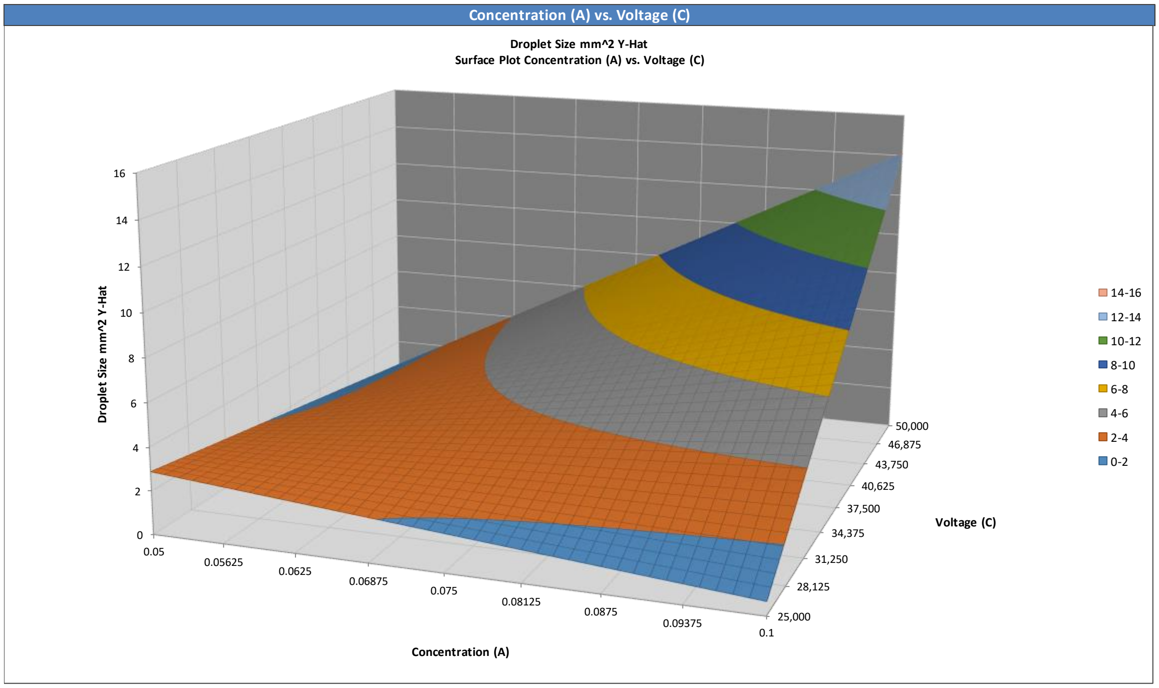

Figure 92: Surface Chart - Concentration vs Voltage for Droplet Size h-hat (Soybean oil, Soy Lecithin, 19ga Capillary)

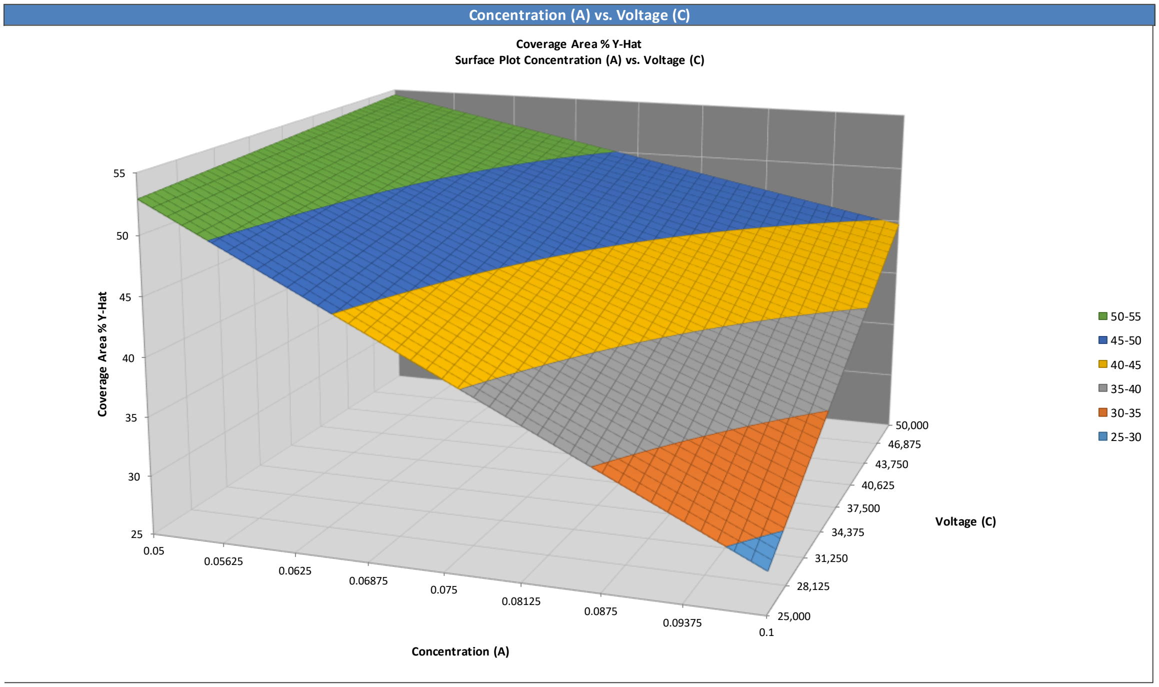

Figure 93: Surface Chart - Concentration vs Voltage for Coverage Area h-hat (Soybean oil, Soy Lecithin, 19ga Capillary)

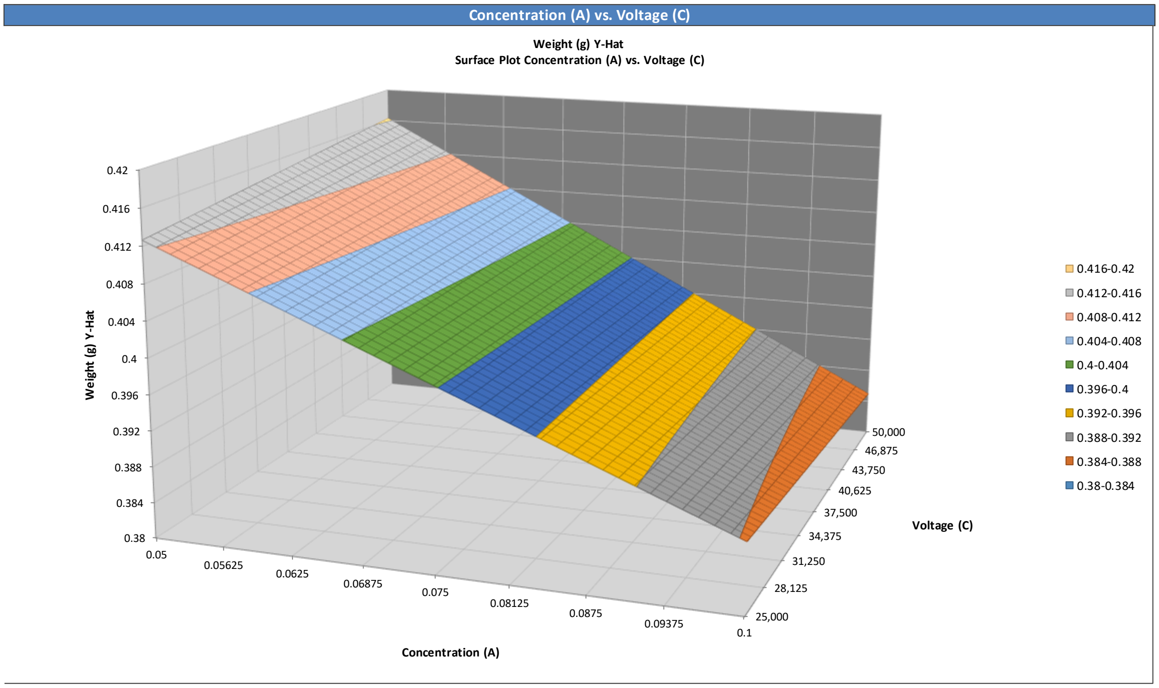

Figure 94: Surface Chart - Concentration vs Voltage for Sample Weight h-hat (Soybean oil, Soy Lecithin, 19ga Capillary)

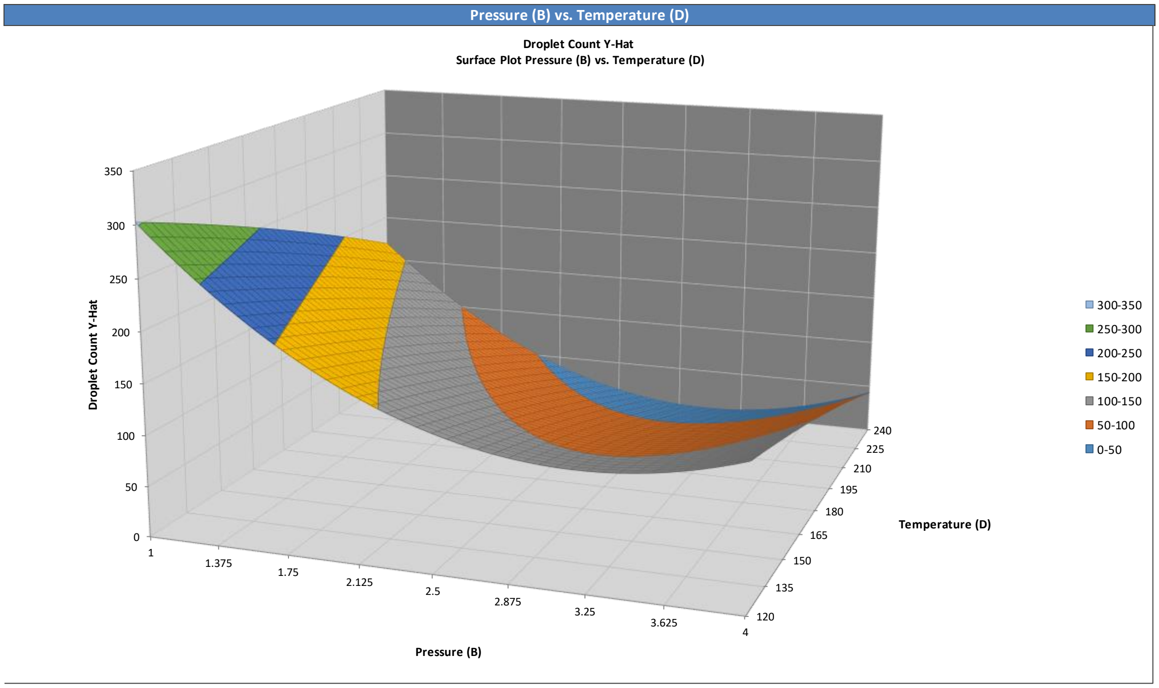

Figure 95: Surface Chart – Pressure vs Temperature for Droplet Count h-hat (Soybean oil, Soy Lecithin, 19ga Capillary)

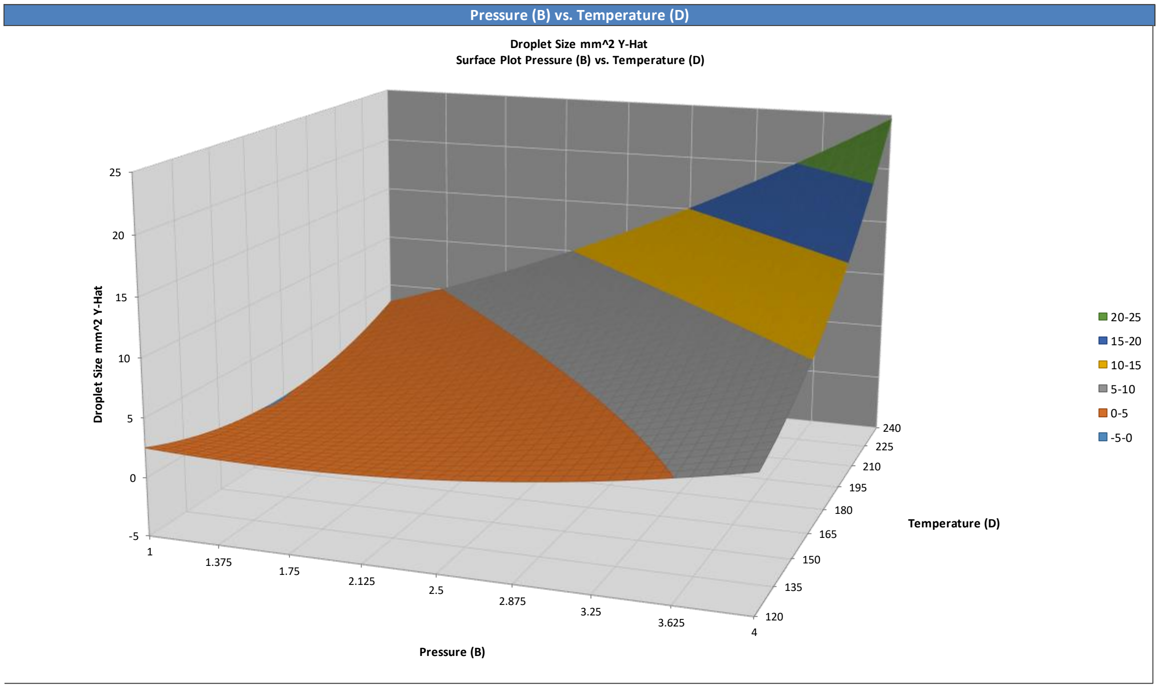

Figure 96: Surface Chart – Pressure vs Temperature for Droplet Size h-hat (Soybean oil, Soy Lecithin, 19ga Capillary)

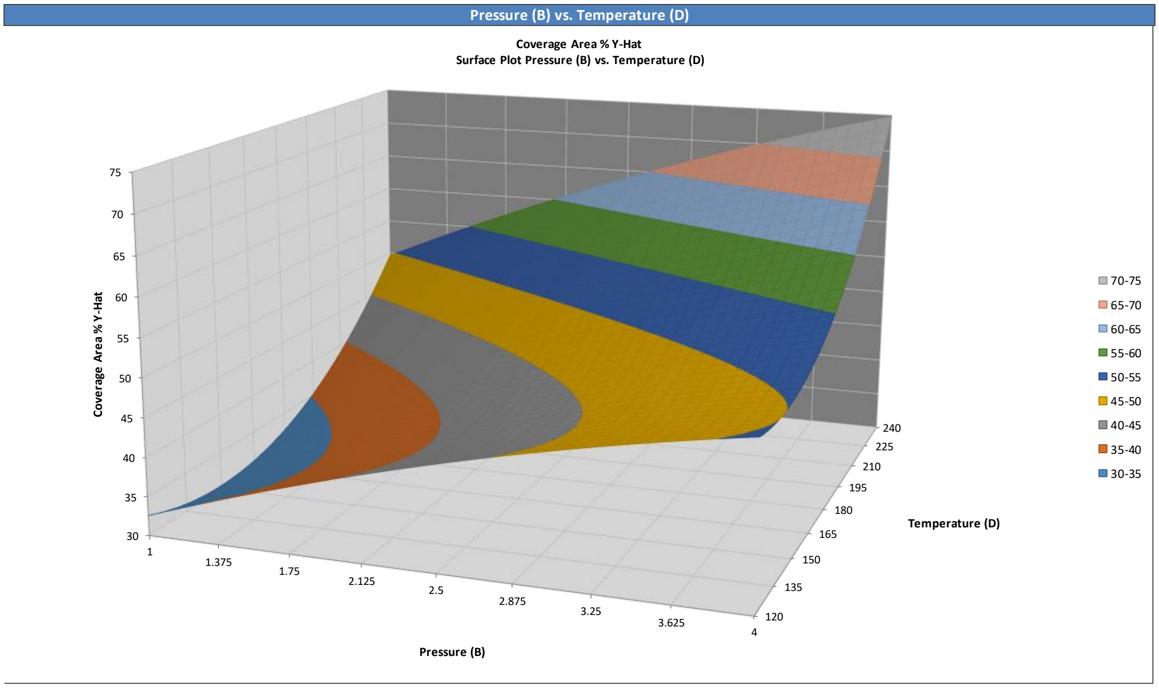

Figure 97: Surface Chart – Pressure vs Temperature for Coverage Area h-hat (Soybean oil, Soy Lecithin, 19ga Capillary)

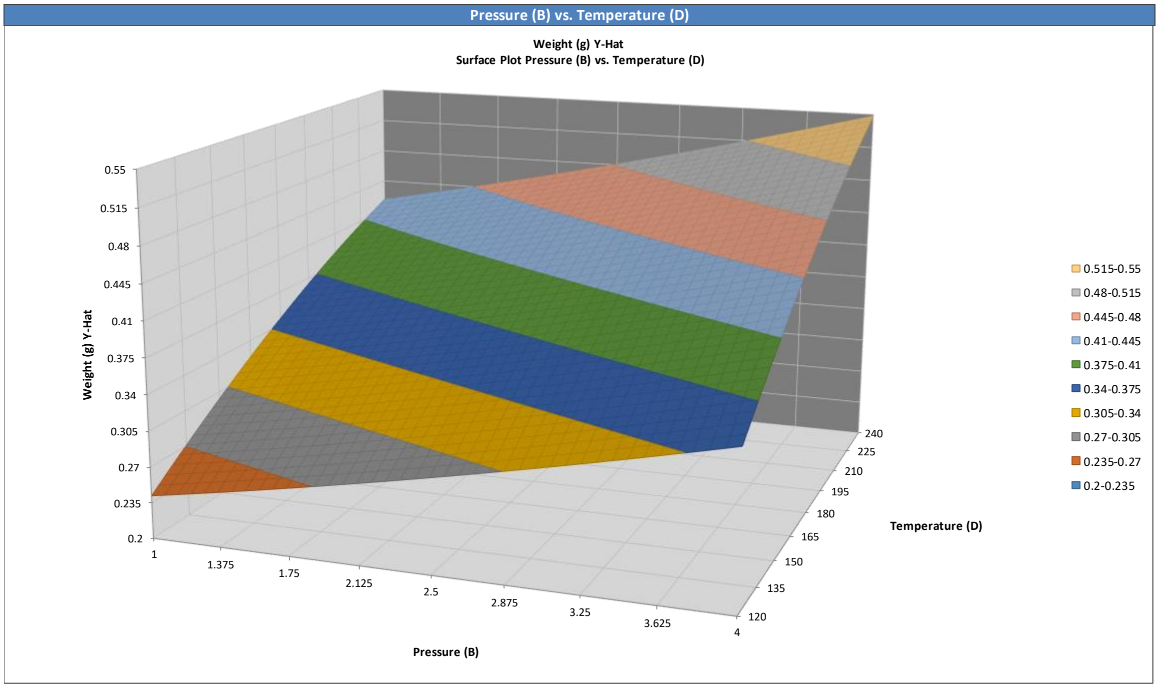

Figure 98: Surface Chart – Pressure vs Temperature for Sample Weight h-hat (Soybean oil, Soy Lecithin, 19ga Capillary)

5.2.2. Soy Lecithin with 22 Gauge Capillary

Table 11: Main Effects Plot for Soybean Oil & Soy Lecithin @ 22g Capillary

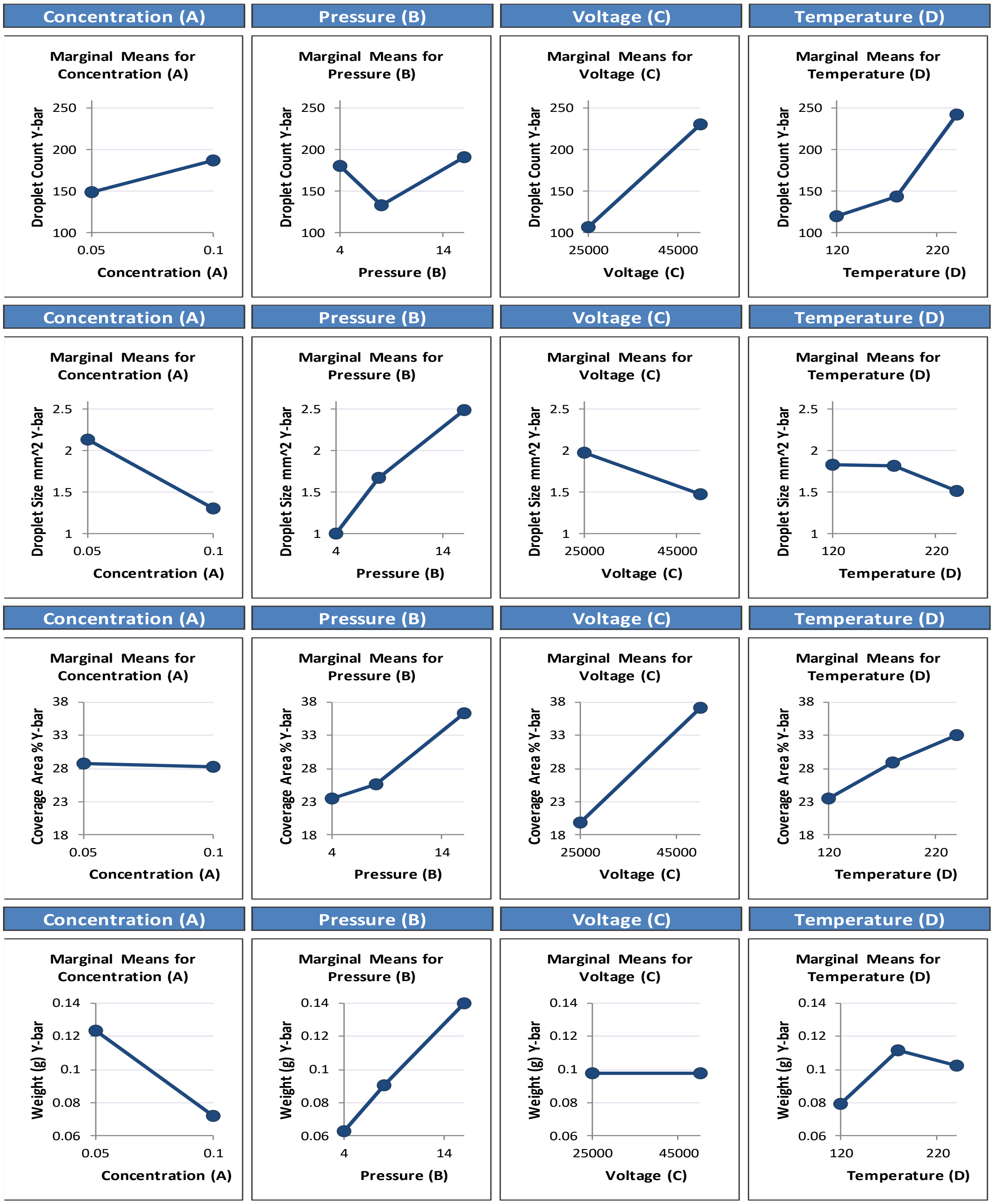

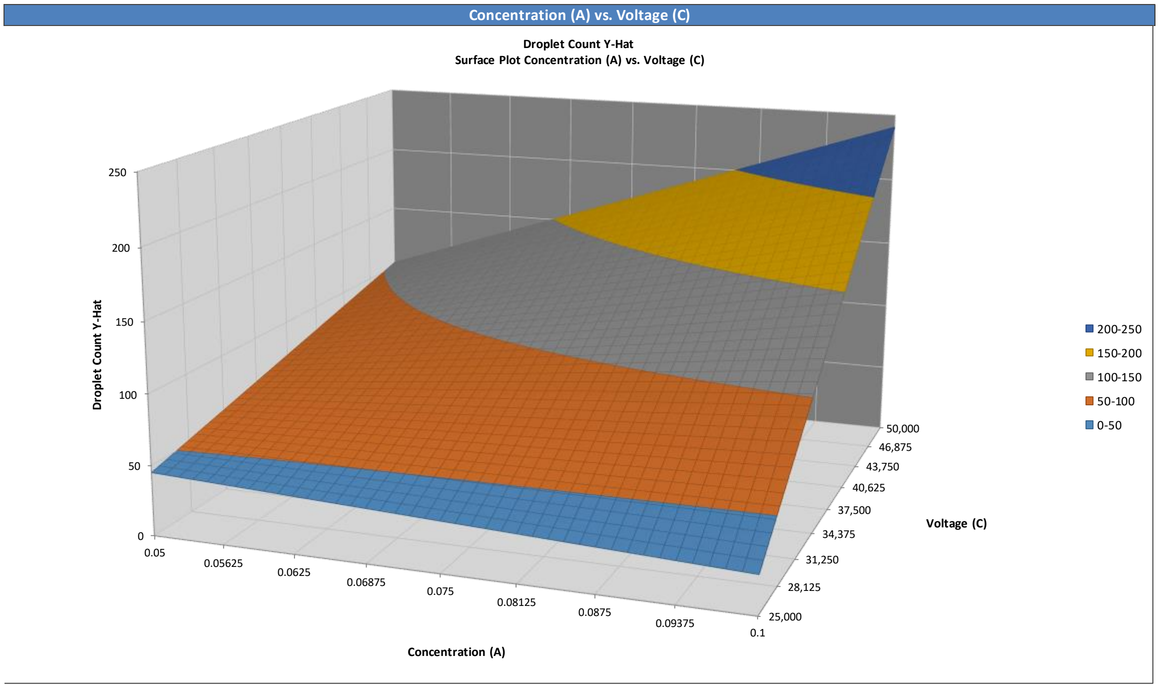

Figure 99: Surface Chart - Concentration vs Voltage for Droplet Count h-hat (Soybean oil, Soy Lecithin, 22ga Capillary)

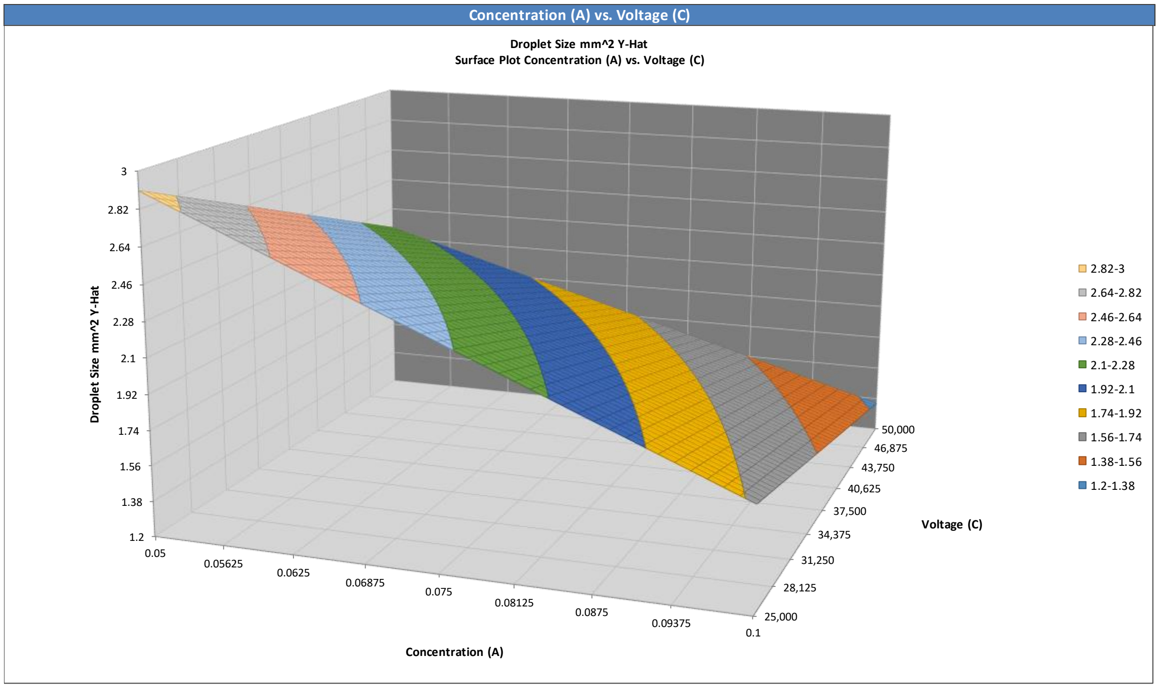

Figure 100: Surface Chart - Concentration vs Voltage for Droplet Size h-hat (Soybean oil, Soy Lecithin, 22ga Capillary)

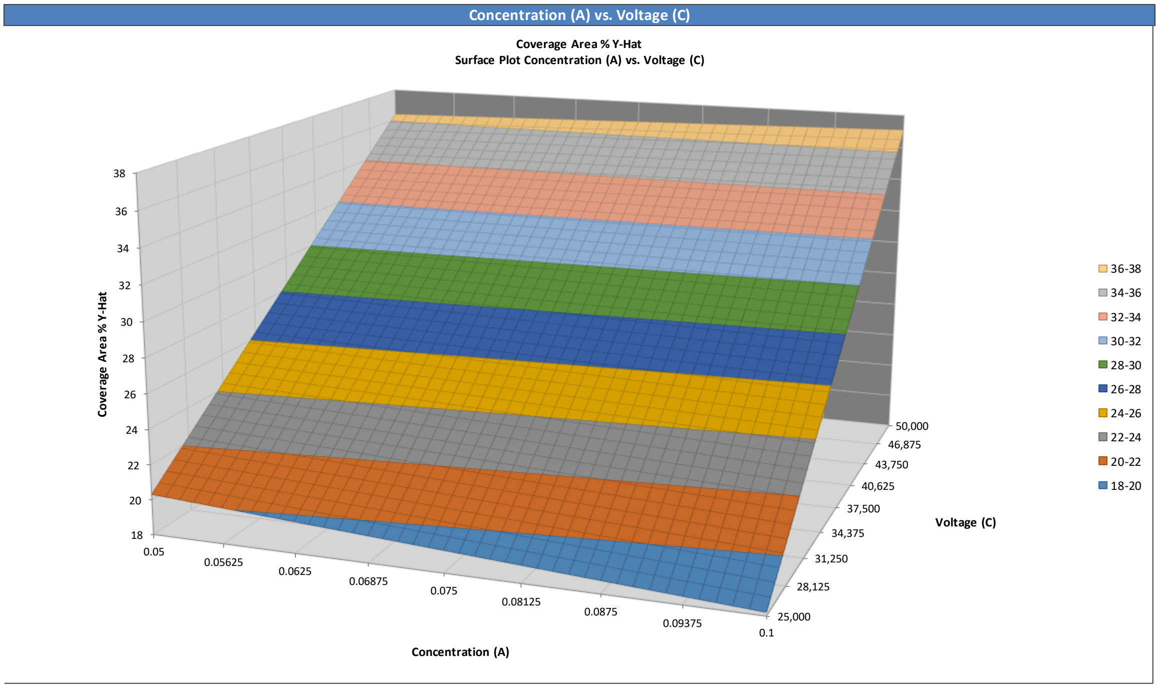

Figure 101: Surface Chart - Concentration vs Voltage for Coverage Area h-hat (Soybean oil, Soy Lecithin, 22ga Capillary)

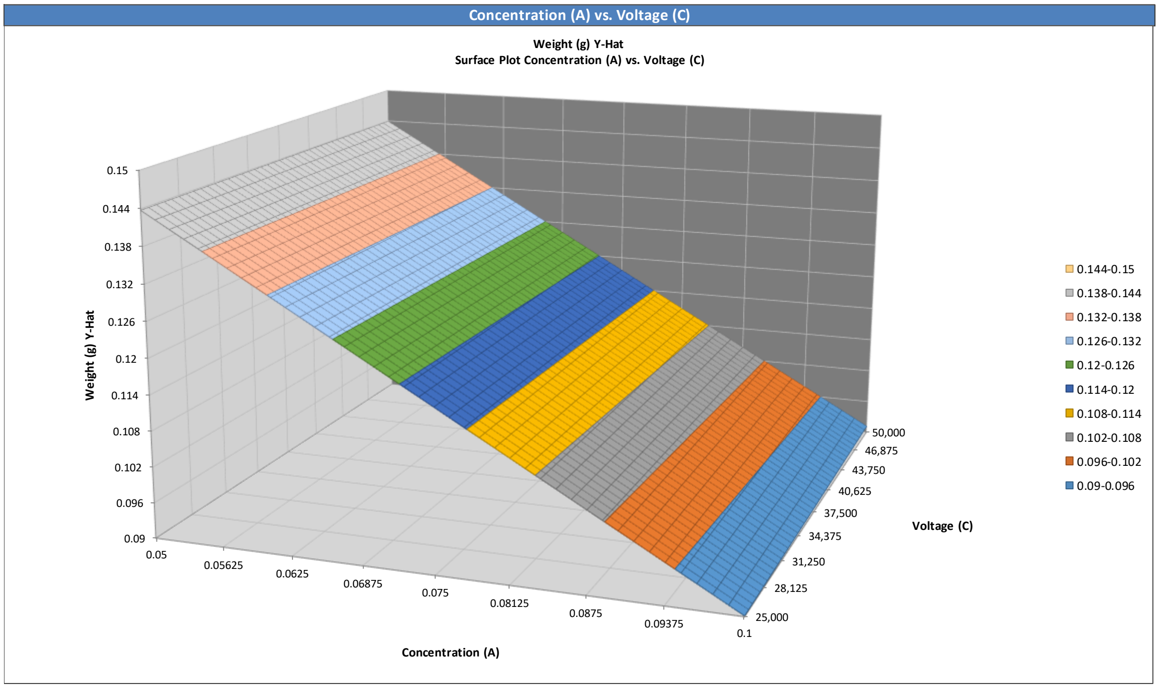

Figure 102: Surface Chart - Concentration vs Voltage for Sample Weight h-hat (Soybean oil, Soy Lecithin, 22ga Capillary)

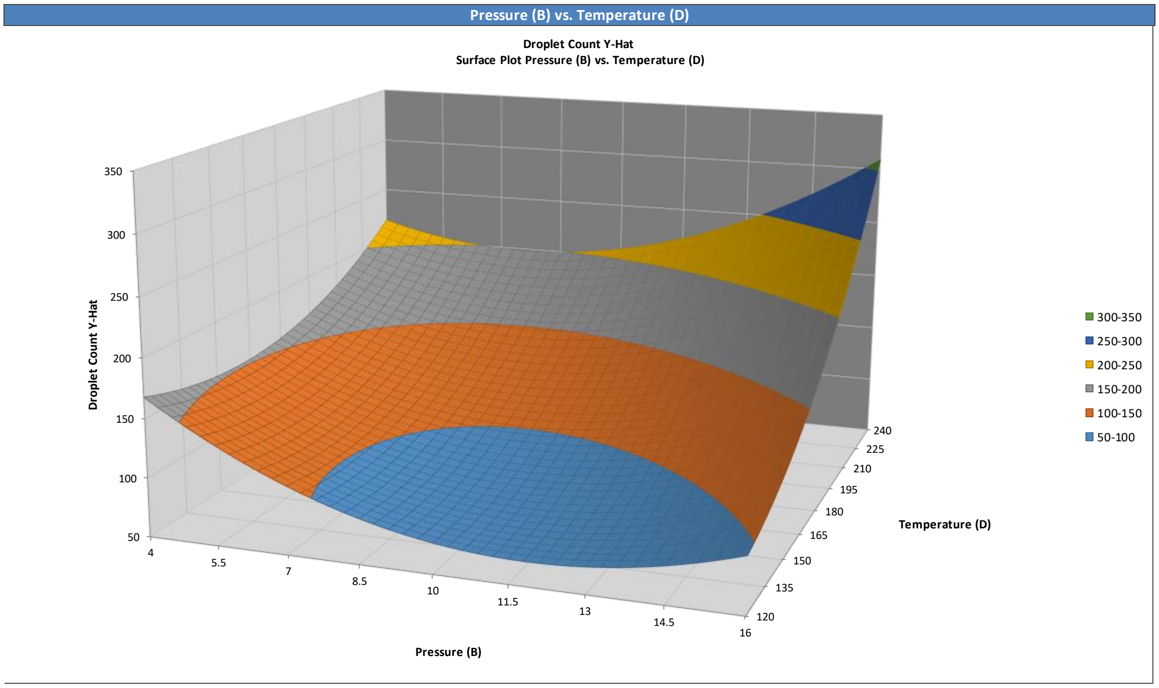

Figure 103: Surface Chart – Pressure vs Temperature for Droplet Count h-hat (Soybean oil, Soy Lecithin, 22ga Capillary)

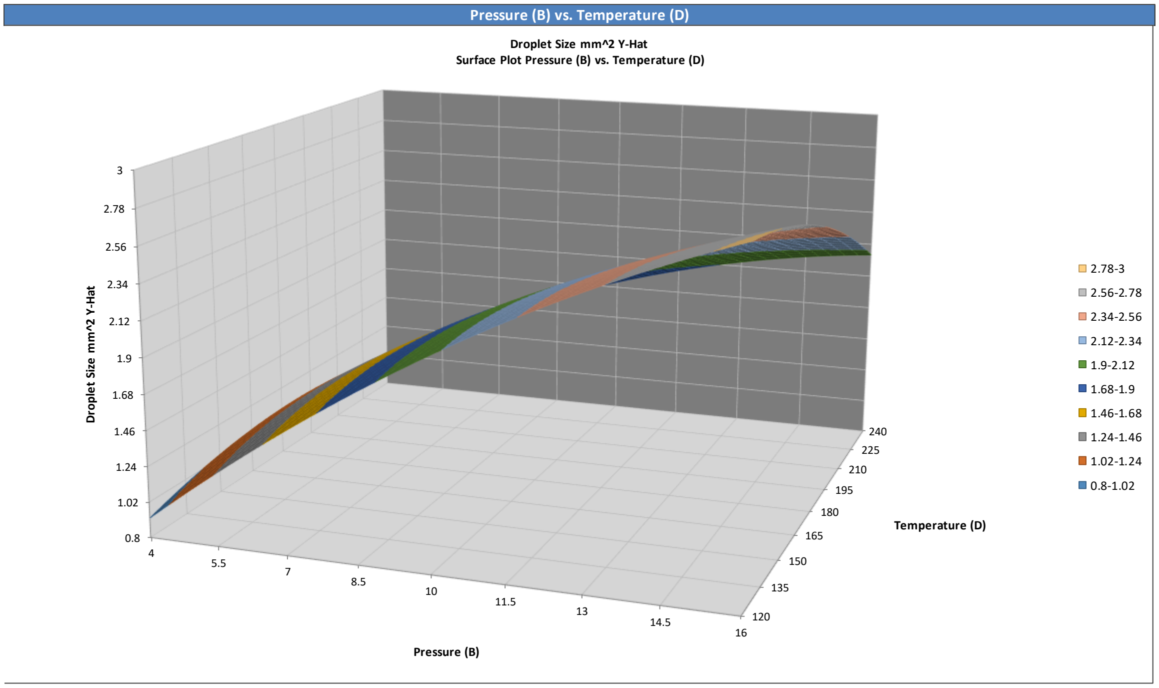

Figure 104: Surface Chart – Pressure vs Temperature for Droplet Size h-hat (Soybean oil, Soy Lecithin, 22ga Capillary)

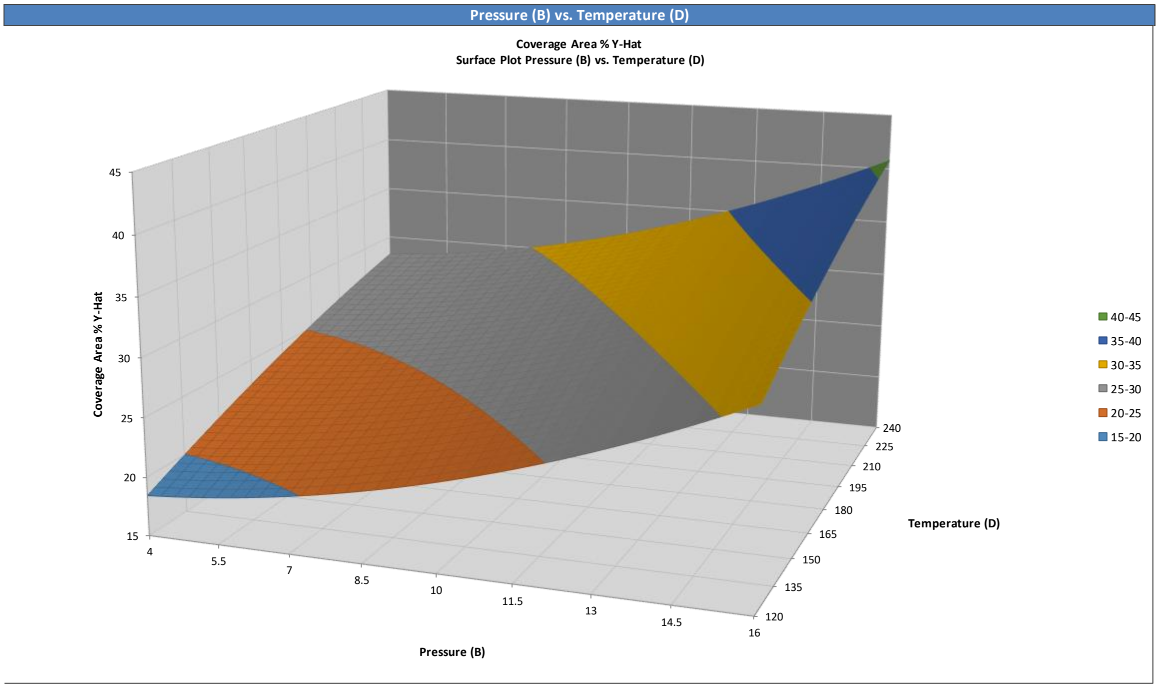

Figure 105: Surface Chart – Pressure vs Temperature for Coverage Area h-hat (Soybean oil, Soy Lecithin, 22ga Capillary)

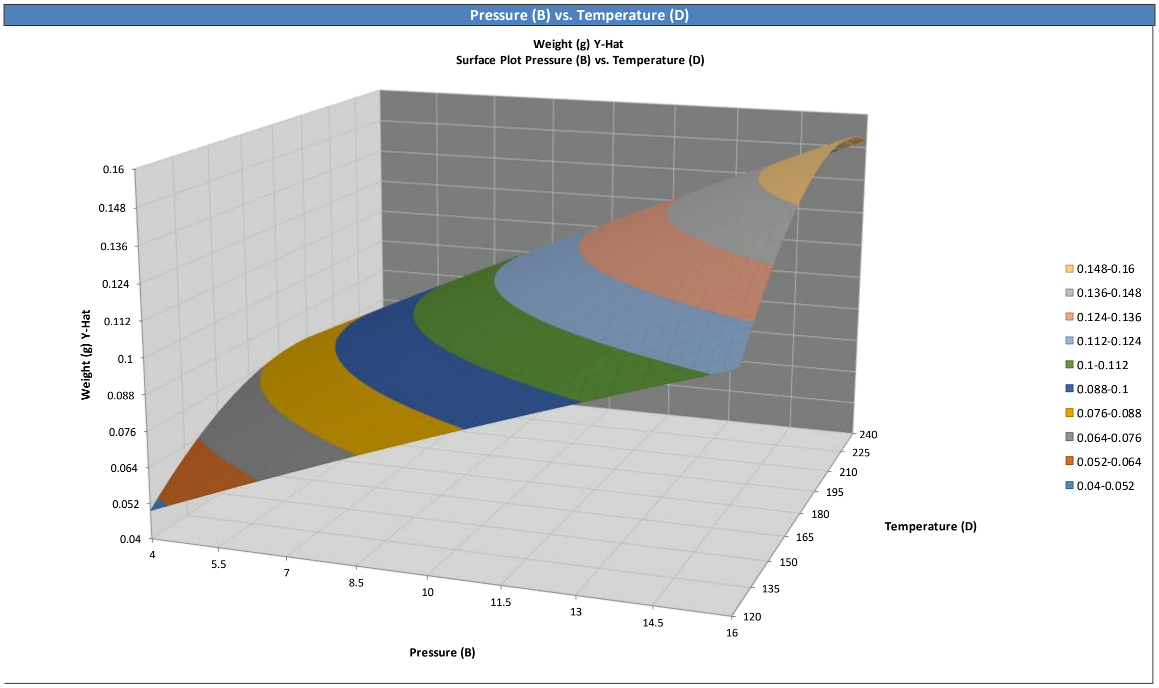

Figure 106: Surface Chart – Pressure vs Temperature for Sample Weight h-hat (Soybean oil, Soy Lecithin, 22ga Capillary)

5.2.3. Polysorbate 20 with 19 Gauge Capillary

Table 12: Main Effects Plot for Soybean Oil & Polysorbate 20 @ 19ga Capillary

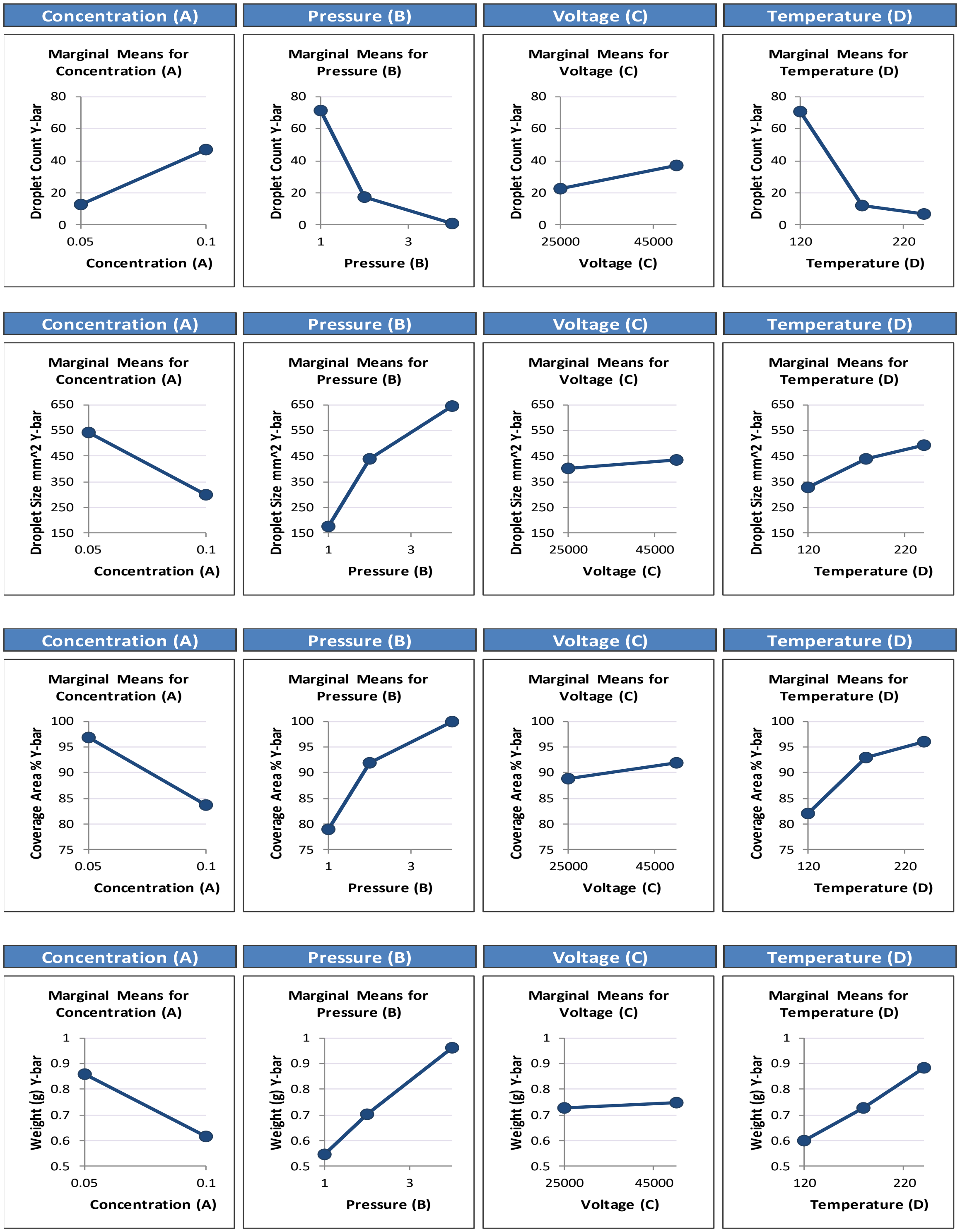

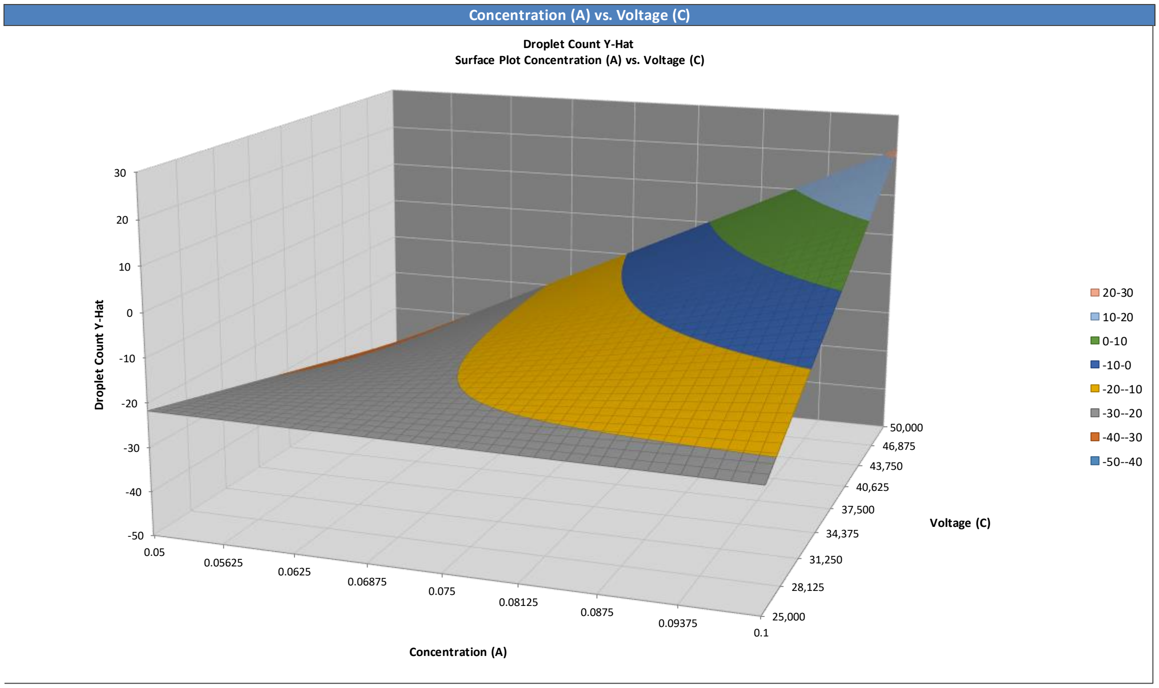

Figure 107: Surface Chart - Concentration vs Voltage for Droplet Count h-hat (Soybean oil, Polysorbate 20, 19ga Capillary)

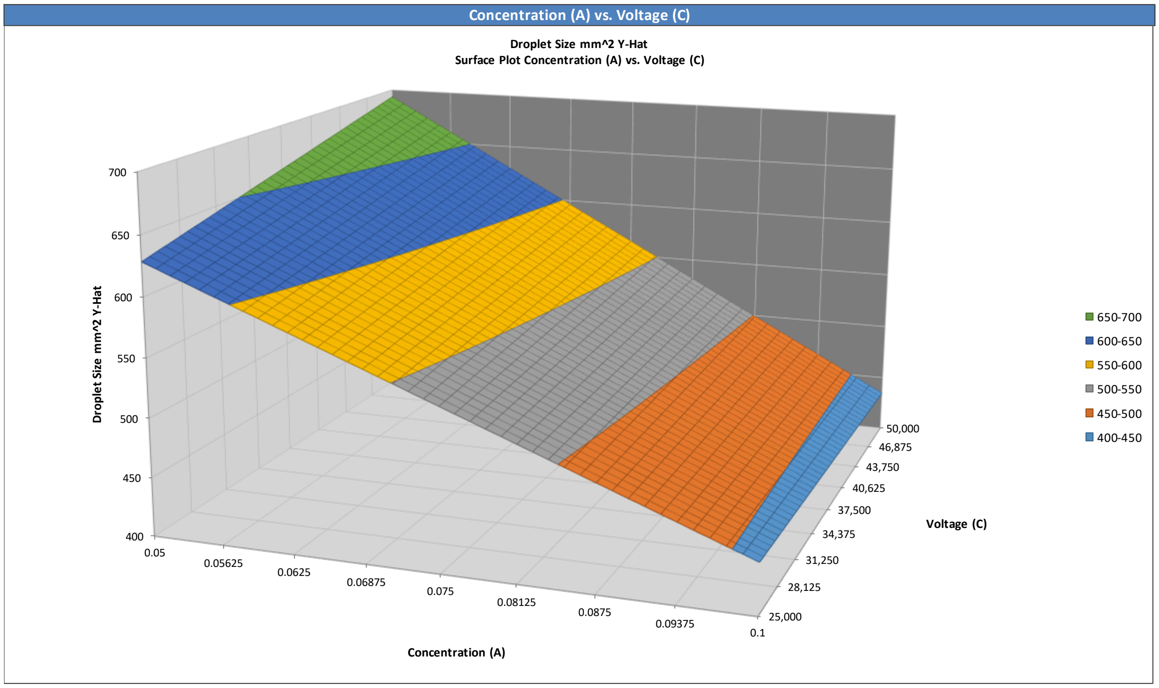

Figure 108: Surface Chart - Concentration vs Voltage for Droplet Size h-hat (Soybean oil, Polysorbate 20, 19ga Capillary)

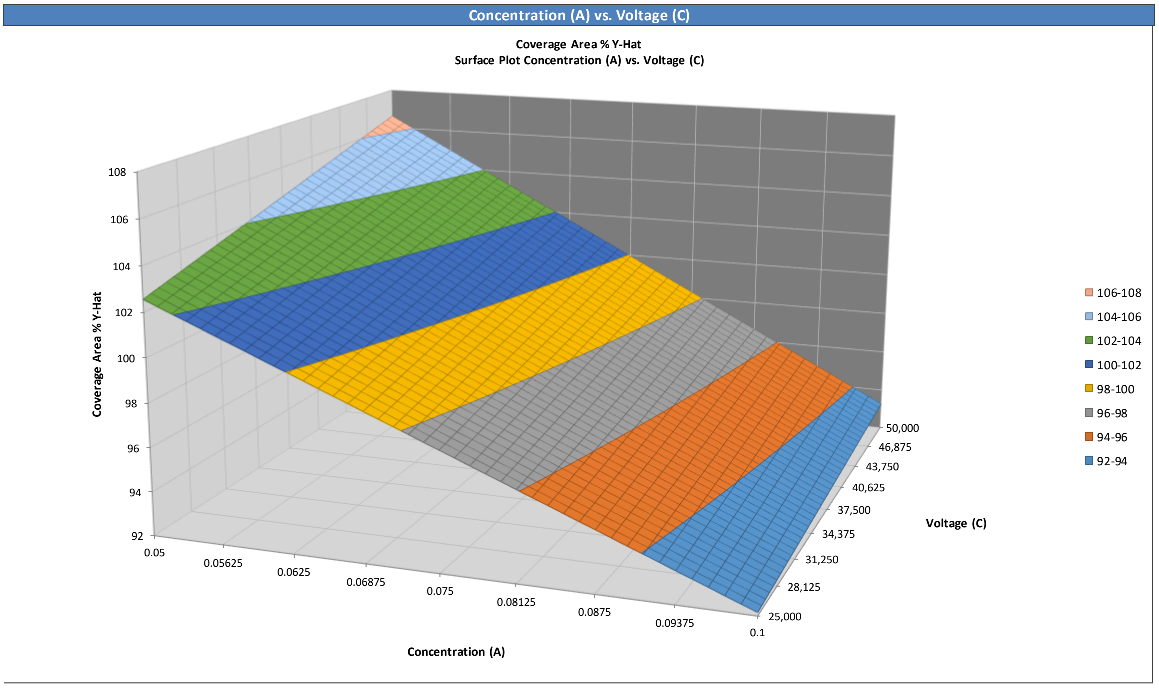

Figure 109: Surface Chart - Concentration vs Voltage for Coverage Area h-hat (Soybean oil, Polysorbate 20, 19ga Capillary)

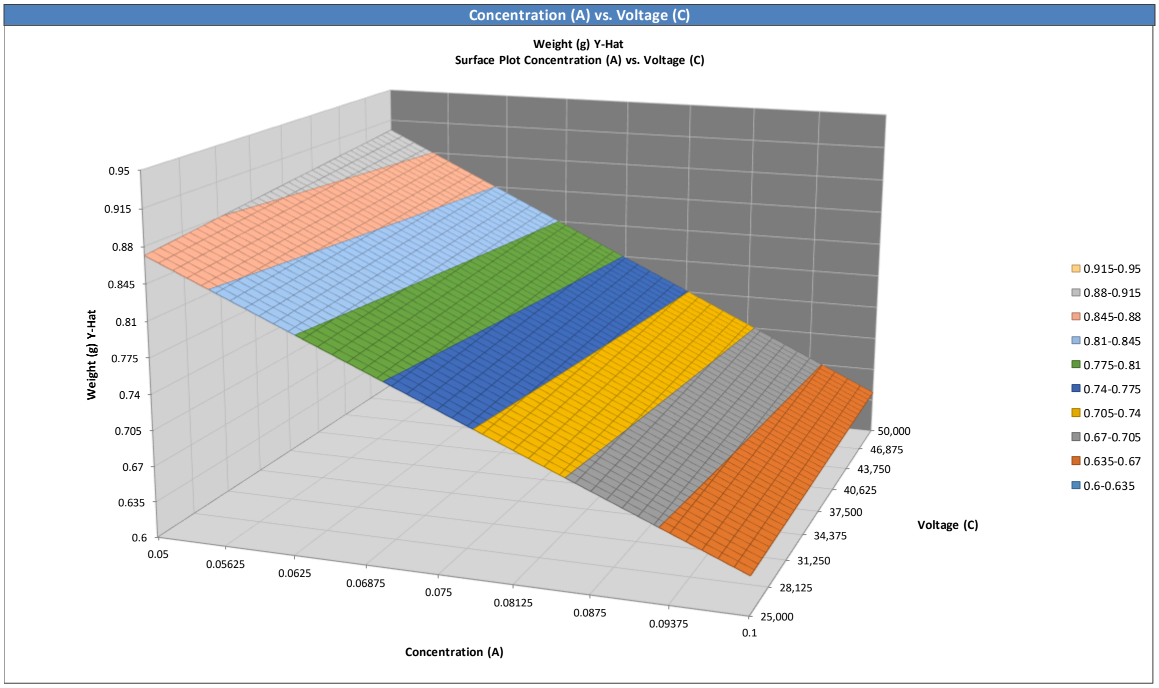

Figure 110: Surface Chart - Concentration vs Voltage for Sample Weight h-hat (Soybean oil, Polysorbate 20, 19ga Capillary)

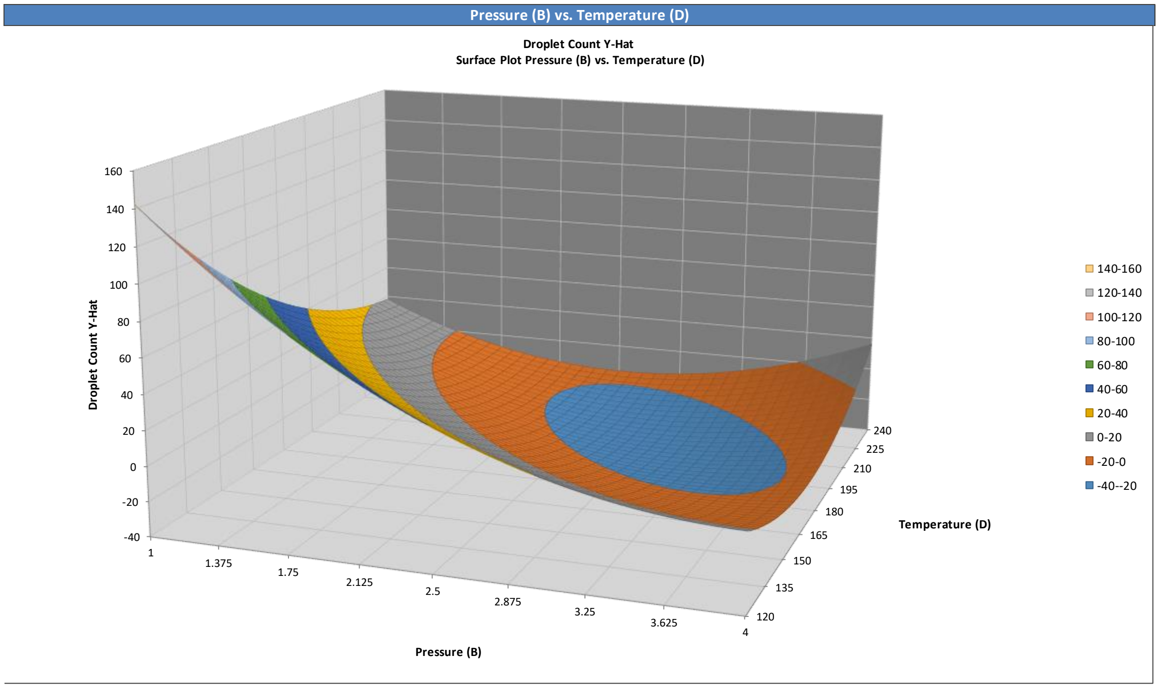

Figure 111: Surface Chart – Pressure vs Temperature for Droplet Count h-hat (Soybean oil, Polysorbate 20, 19ga Capillary)

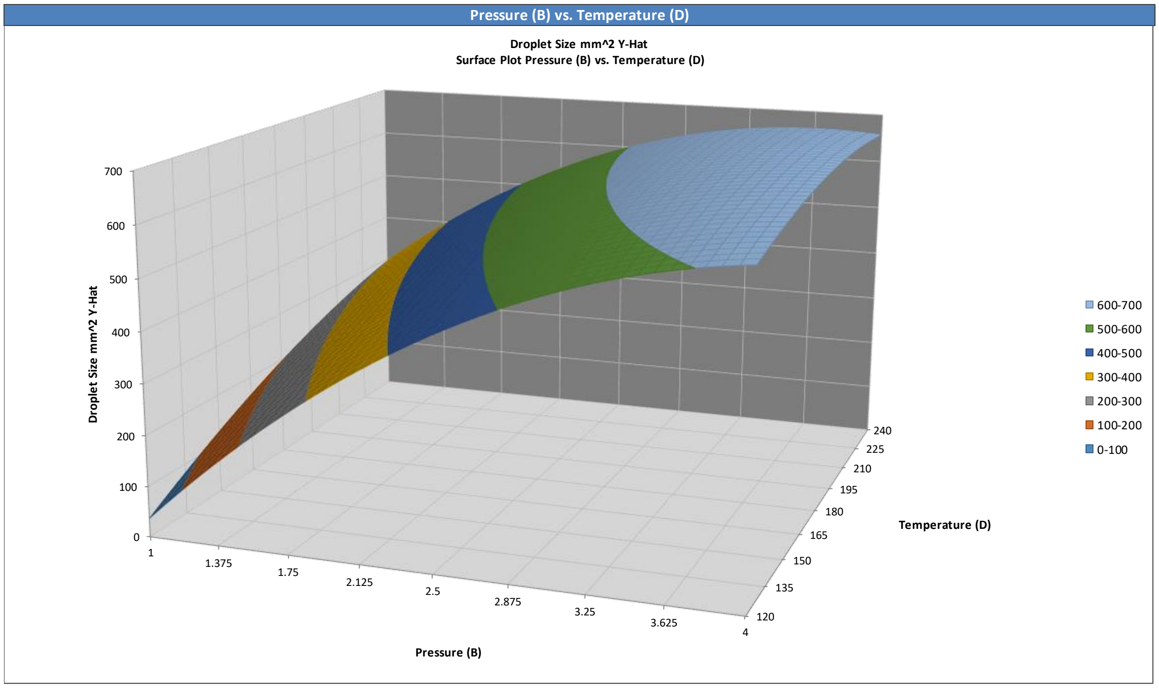

Figure 112: Surface Chart – Pressure vs Temperature for Droplet Size h-hat (Soybean oil, Soy Polysorbate 20, 19ga Capillary)

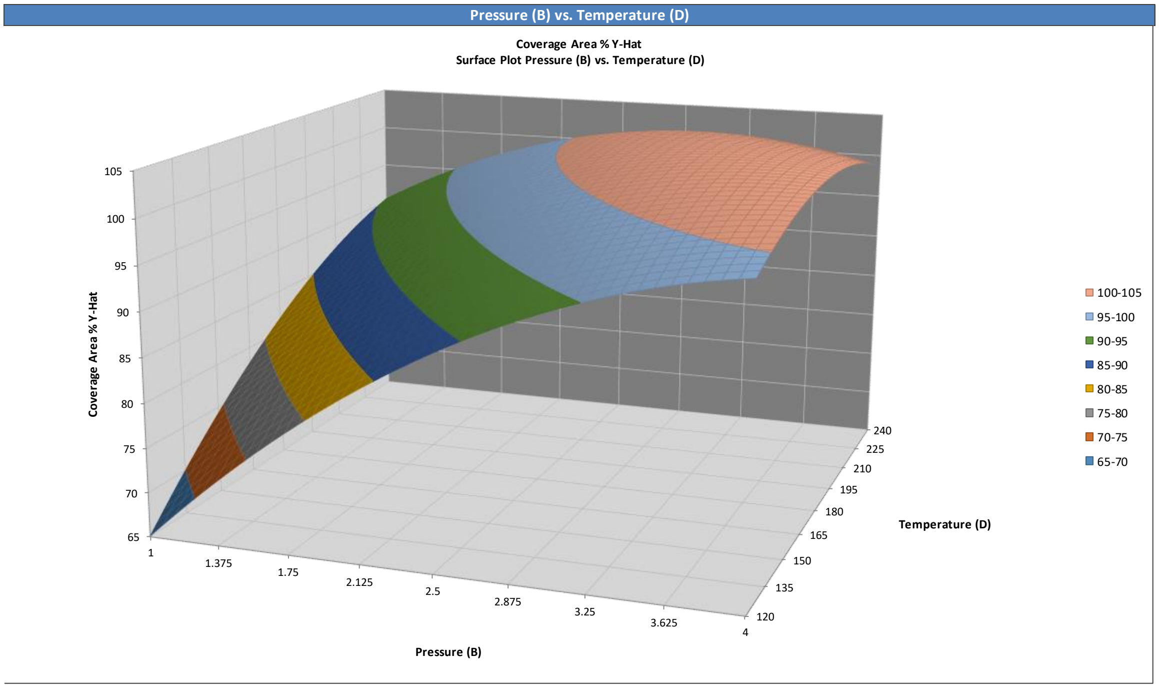

Figure 113: Surface Chart – Pressure vs Temperature for Coverage Area h-hat (Soybean oil, Soy Polysorbate 20, 19ga Capillary)

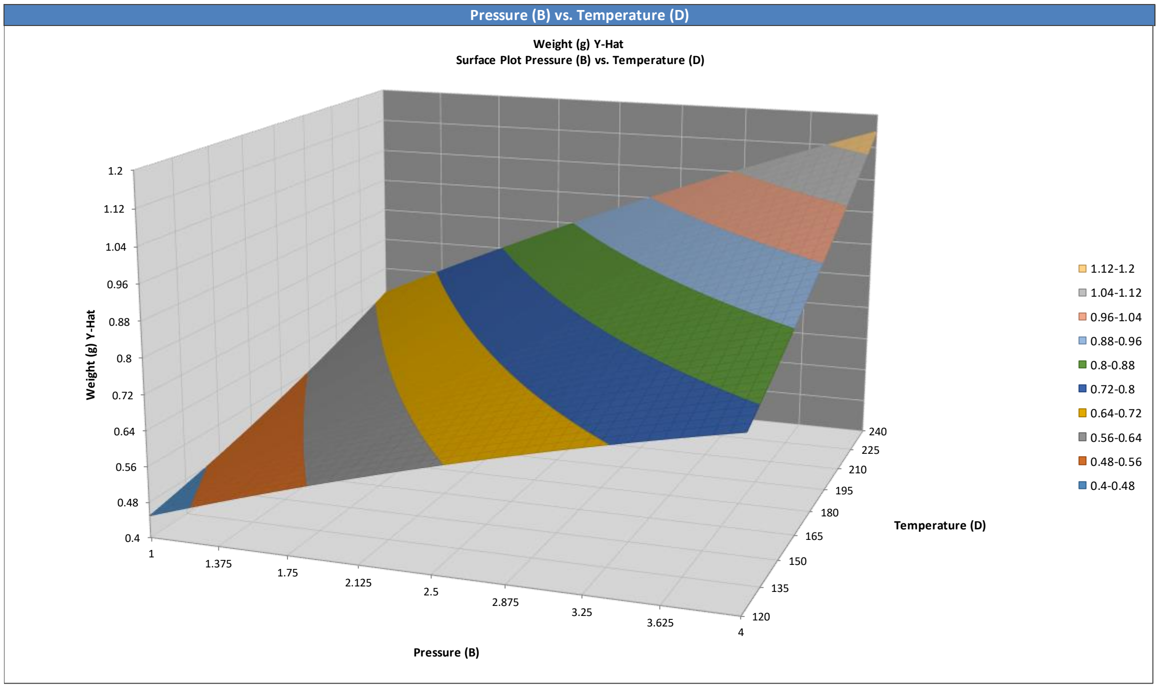

Figure 114: Surface Chart – Pressure vs Temperature for Sample Weight h-hat (Soybean oil, Soy Polysorbate 20, 19ga Capillary)

5.2.4. Polysorbate 20 with 22 Gauge Capillary

Table 13: Main Effects Plot for Soybean Oil & Polysorbate 20 @ 22g Capillary

Concentration (A)

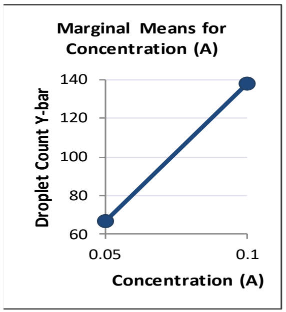

Pressure (B)

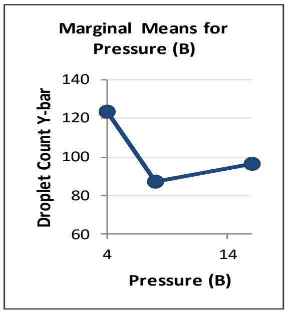

Voltage (C)

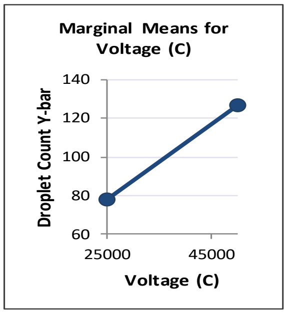

Temperature (D)

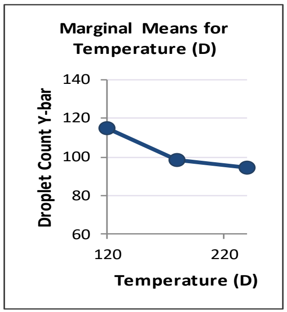

Concentration (A)

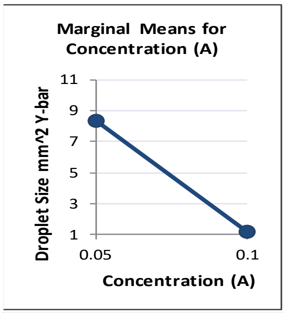

Pressure (B)

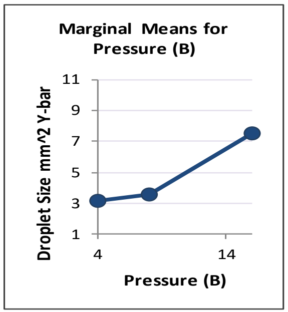

Voltage (C)

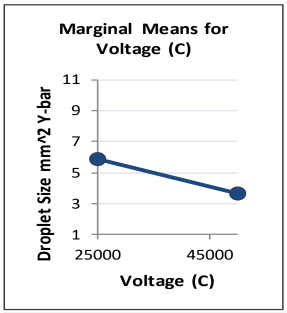

Temperature (D)

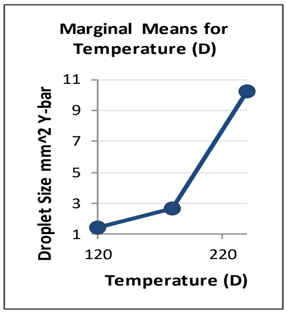

Concentration (A)

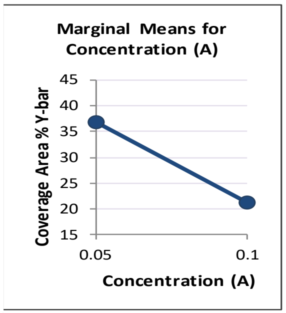

Pressure (B)

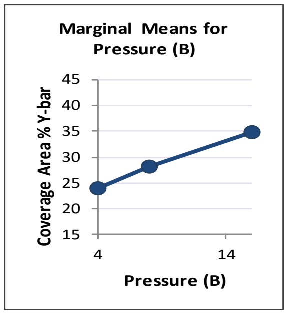

Voltage (C)

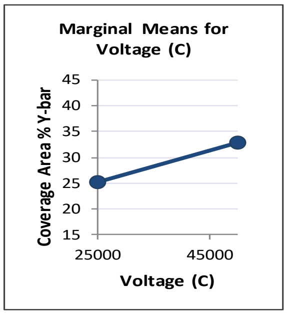

Temperature (D)

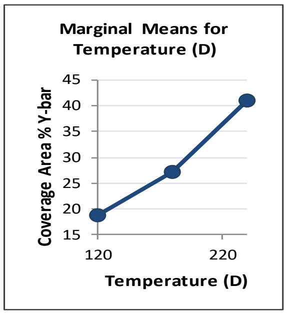

Concentration (A)

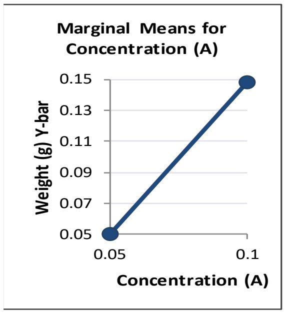

Pressure (B)

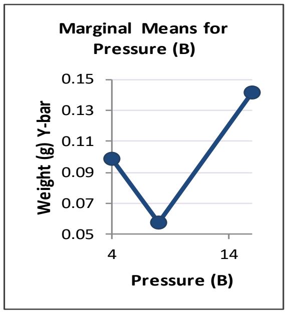

Voltage (C)

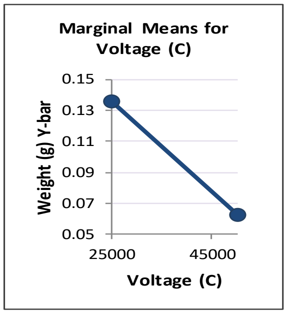

Temperature (D)

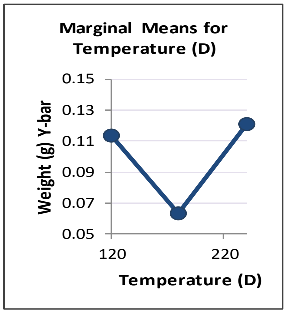

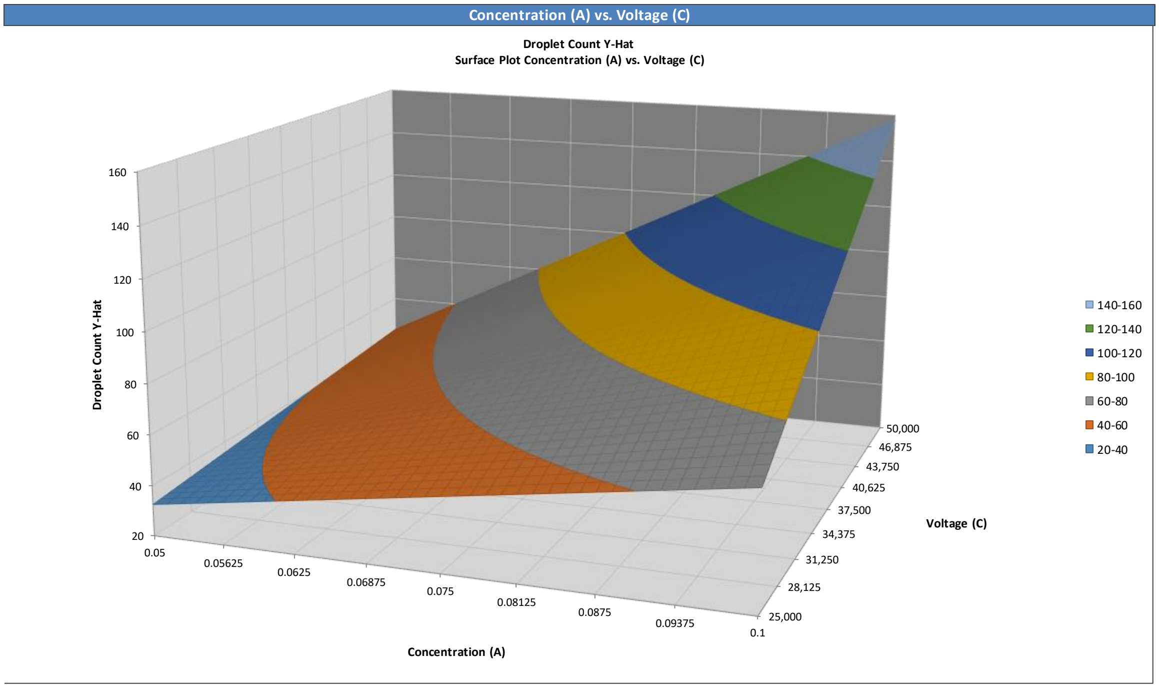

Figure 115: Surface Chart - Concentration vs Voltage for Droplet Count h-hat (Soybean oil, Polysorbate 20, 22ga Capillary)

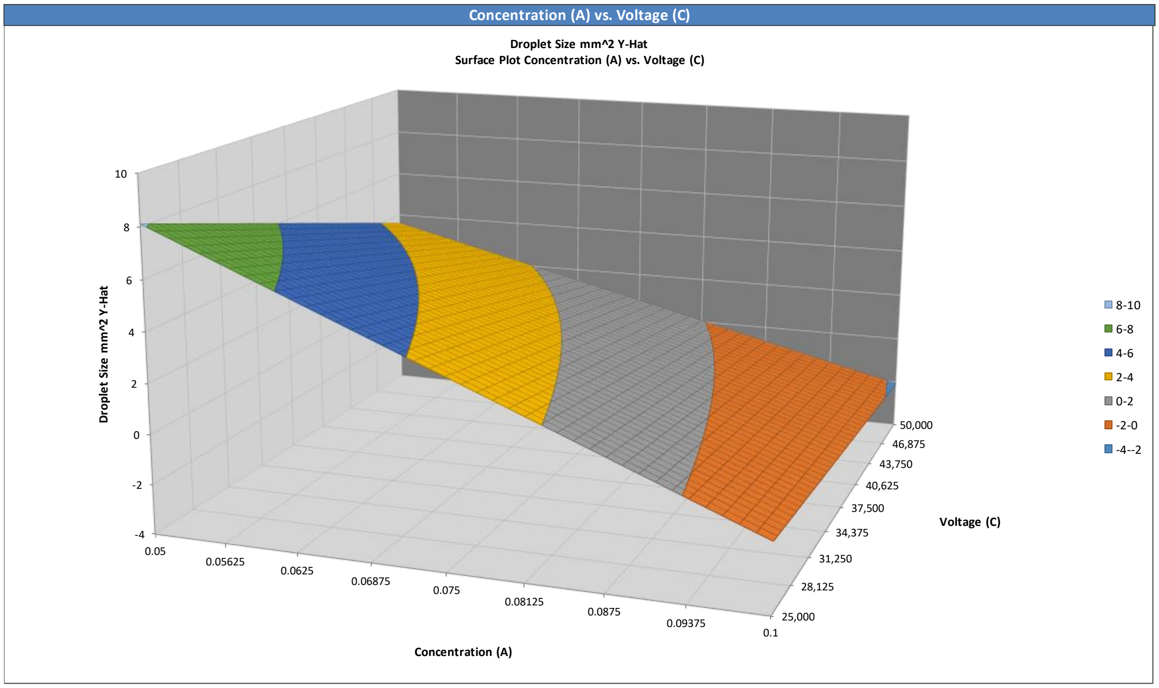

Figure 116: Surface Chart - Concentration vs Voltage for Droplet Count h-hat (Soybean oil, Polysorbate 20, 22ga Capillary)

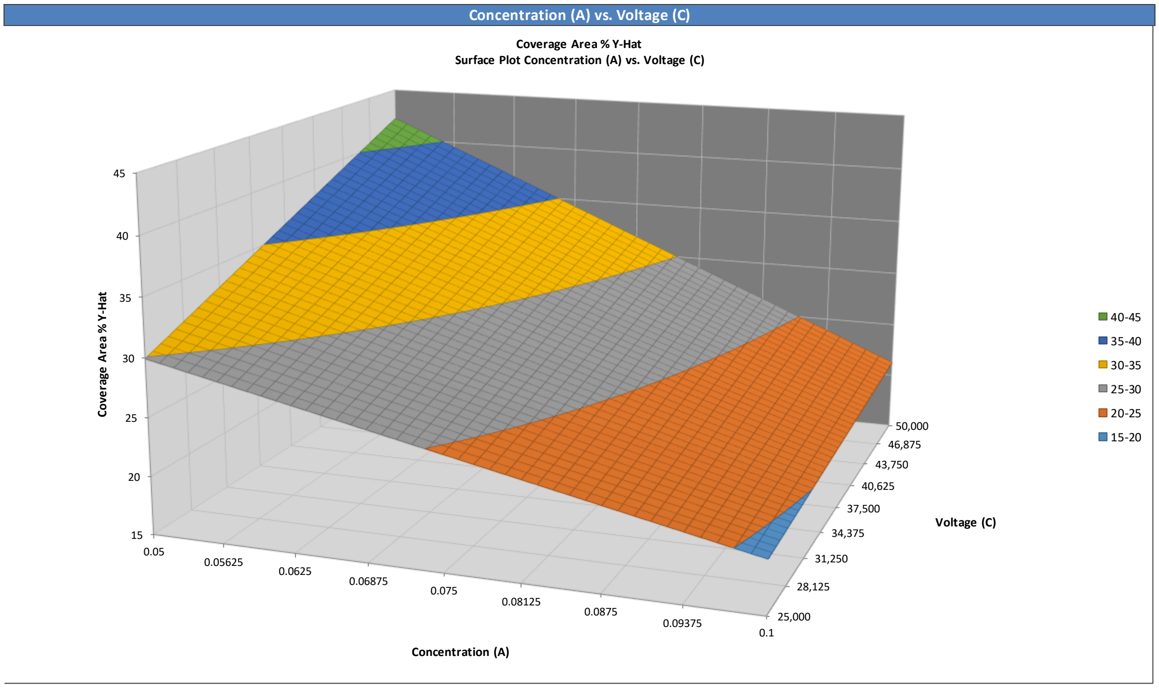

Figure 117: Surface Chart - Concentration vs Voltage for Droplet Area h-hat (Soybean oil, Polysorbate 20, 22ga Capillary)

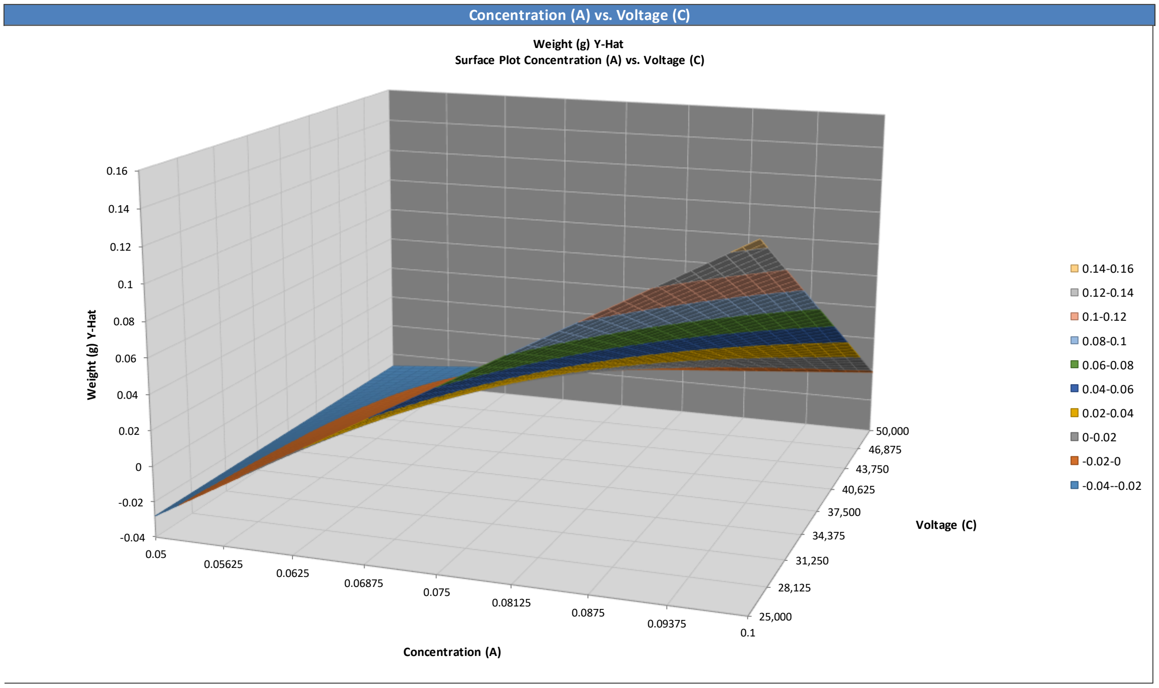

Figure 118: Surface Chart - Concentration vs Voltage for Sample Weight h-hat (Soybean oil, Polysorbate 20, 22ga Capillary)

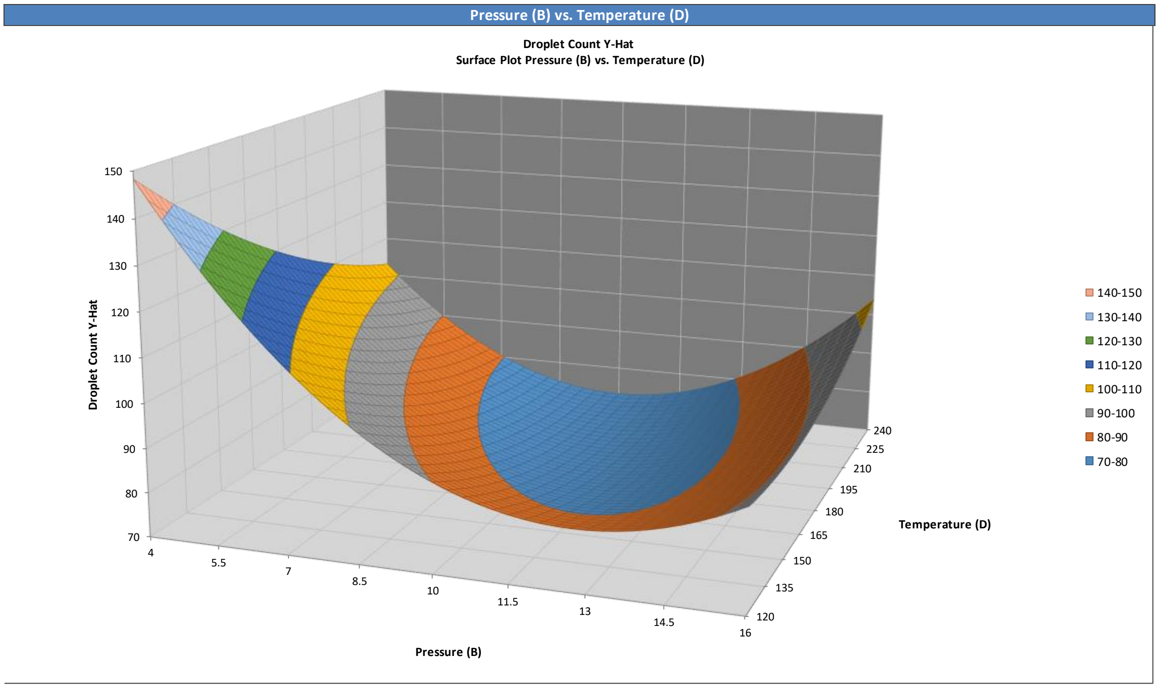

Figure 119: Surface Chart – Pressure vs Temperature for Droplet Count h-hat (Soybean oil, Polysorbate 20, 22ga Capillary)

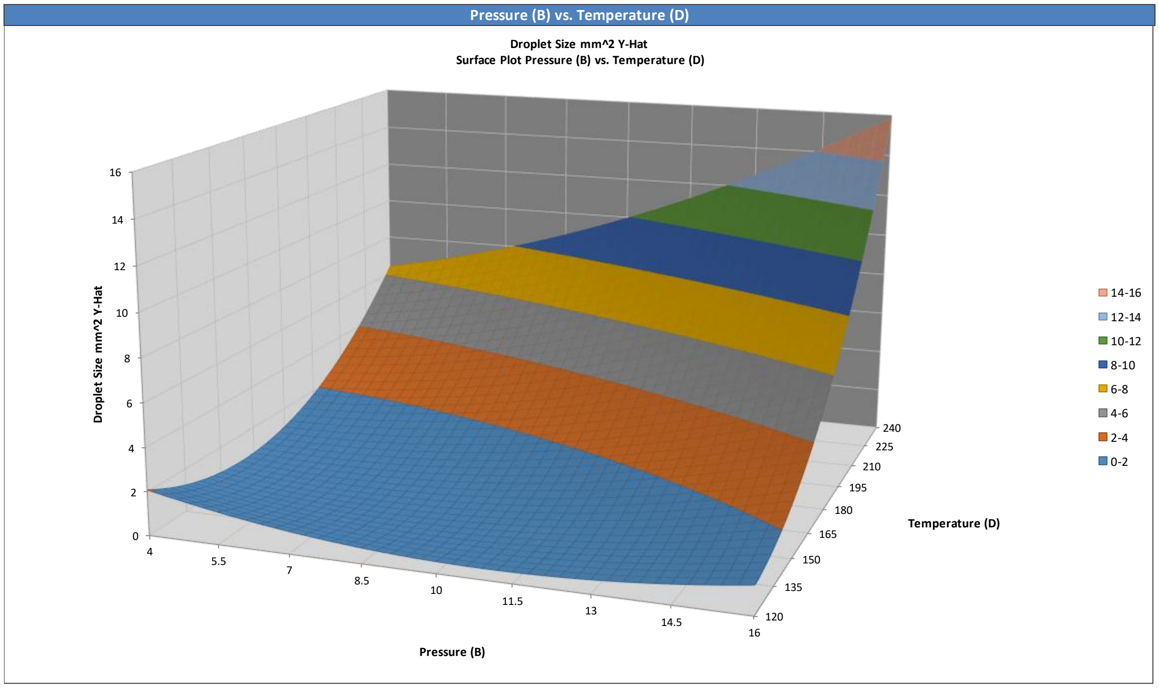

Figure 120: Surface Chart – Pressure vs Temperature for Droplet Size h-hat (Soybean oil, Polysorbate 20, 22ga Capillary)

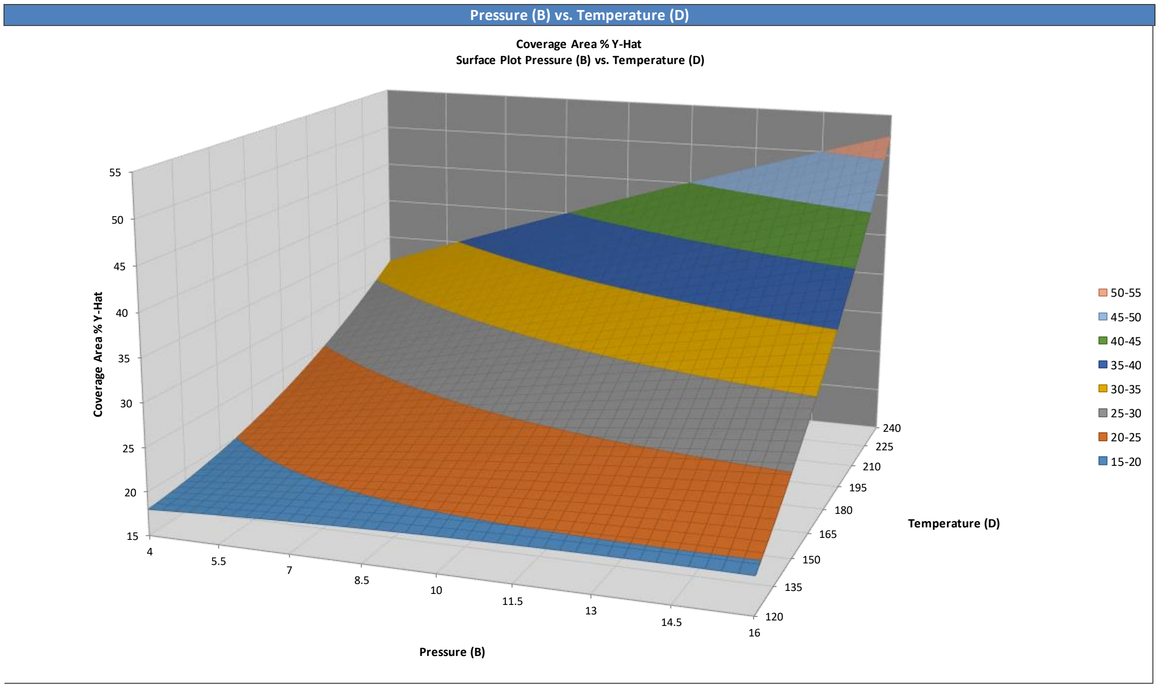

Figure 121: Surface Chart – Pressure vs Temperature for Coverage Area h-hat (Soybean oil, Polysorbate 20, 22ga Capillary)

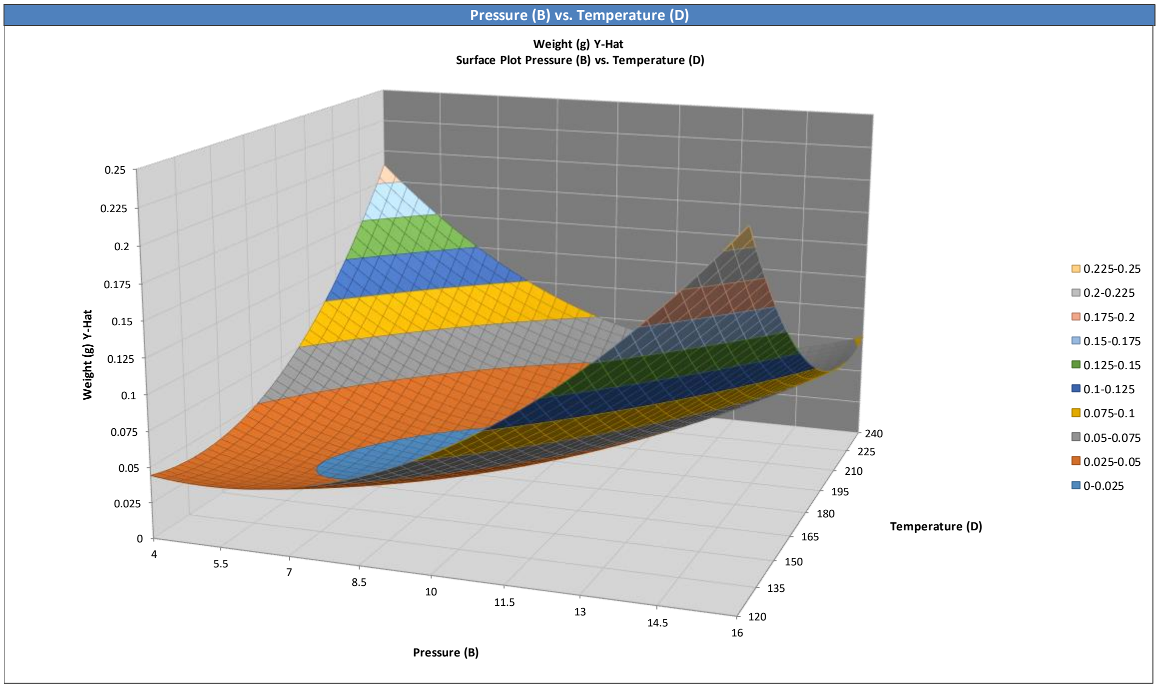

Figure 122: Surface Chart – Pressure vs Temperature for Sample Weight h-hat (Soybean oil, Polysorbate 20, 22ga Capillary)

5.2.5. Propylene Glycol with 19 Gauge Capillary

Table 14: Main Effects Plot for Soybean Oil & Propylene Glycol @ 19ga Capillary

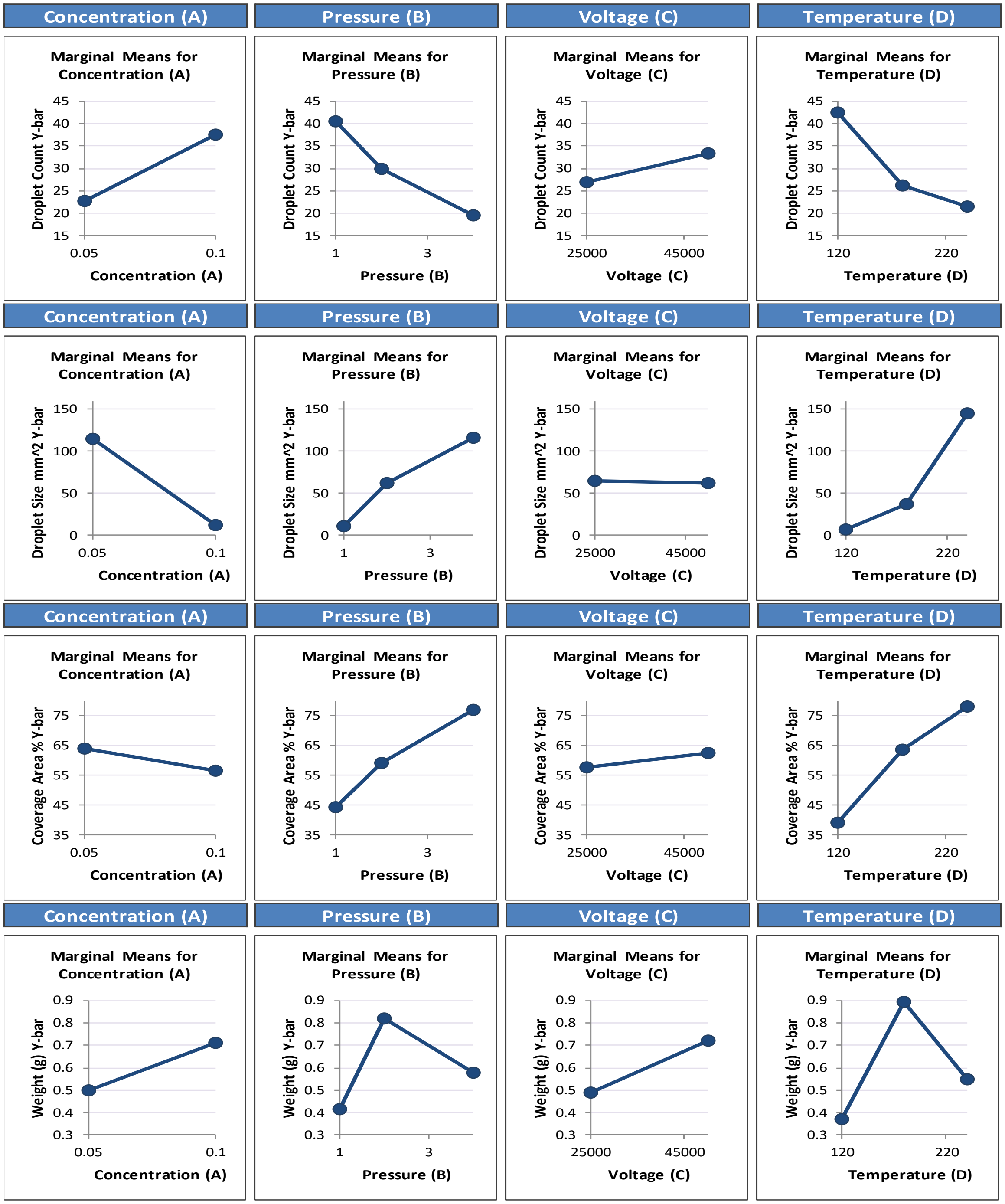

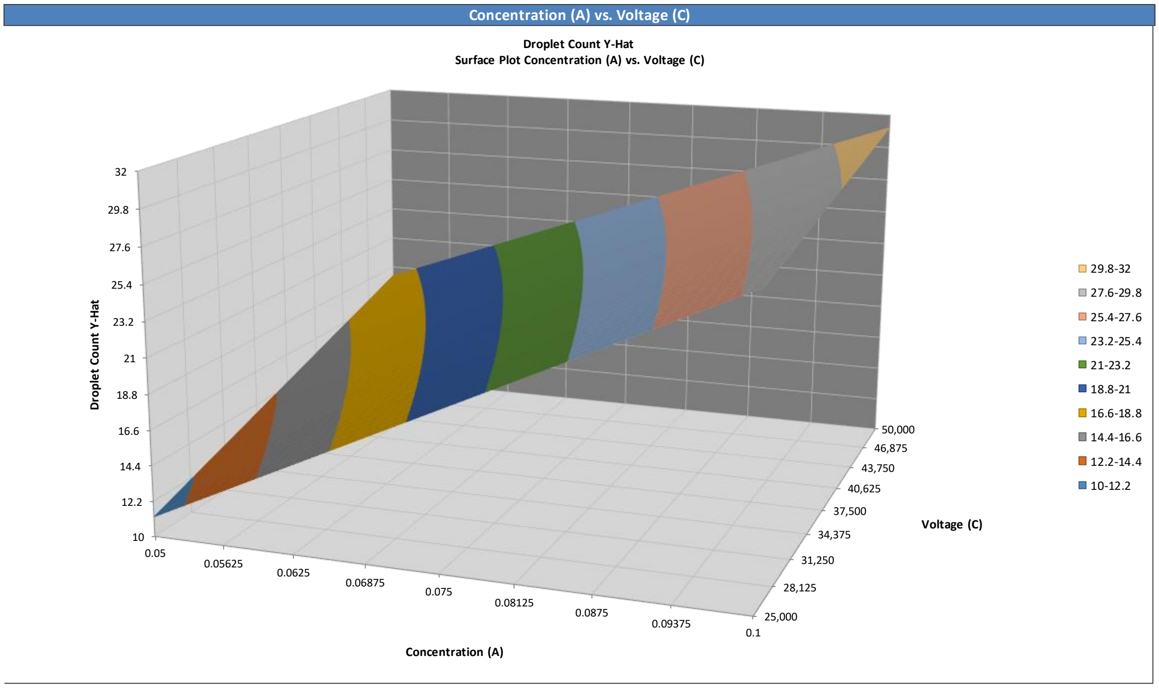

Figure 123: Surface Chart - Concentration vs Voltage for Droplet Count h-hat (Soybean oil, Propylene Glycol, 19ga Capillary)

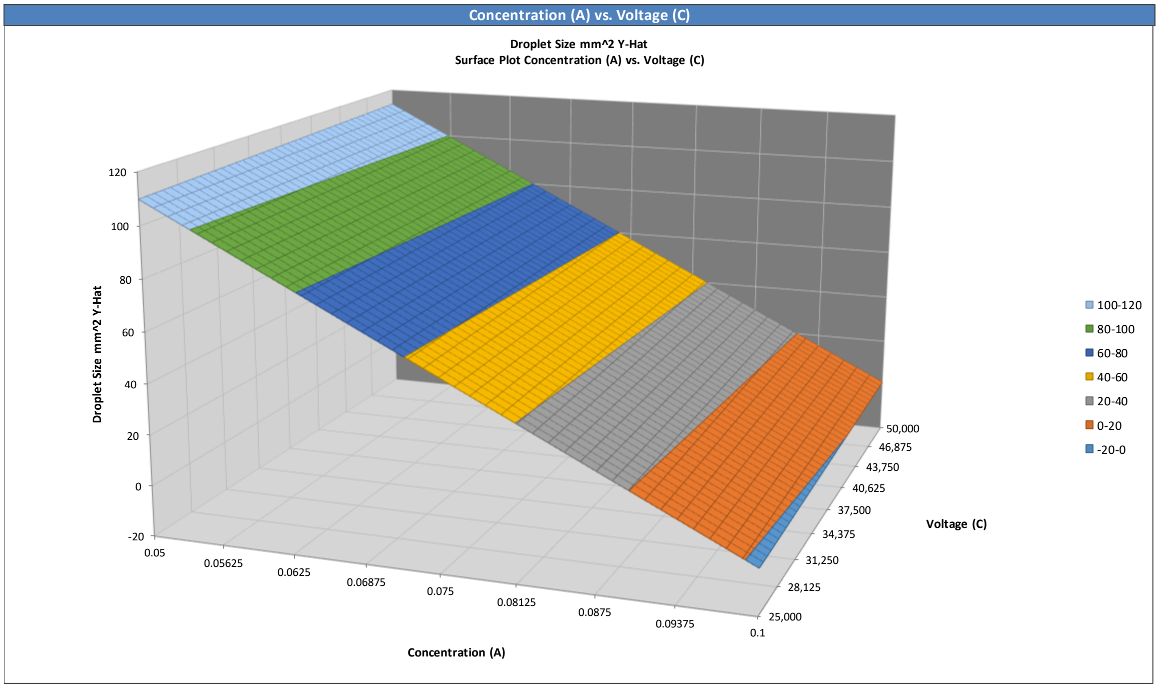

Figure 124: Surface Chart - Concentration vs Voltage for Droplet Size h-hat (Soybean oil, Propylene Glycol, 19ga Capillary)

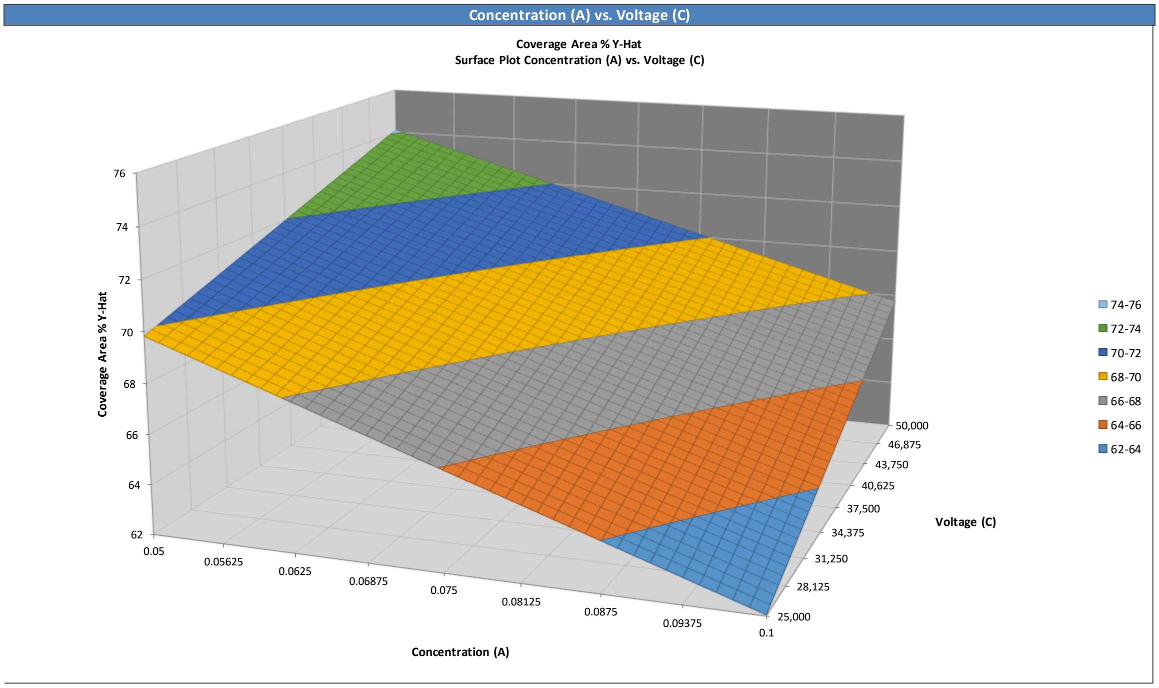

Figure 125: Surface Chart - Concentration vs Voltage for Coverage Area h-hat (Soybean oil, Propylene Glycol, 19ga Capillary)

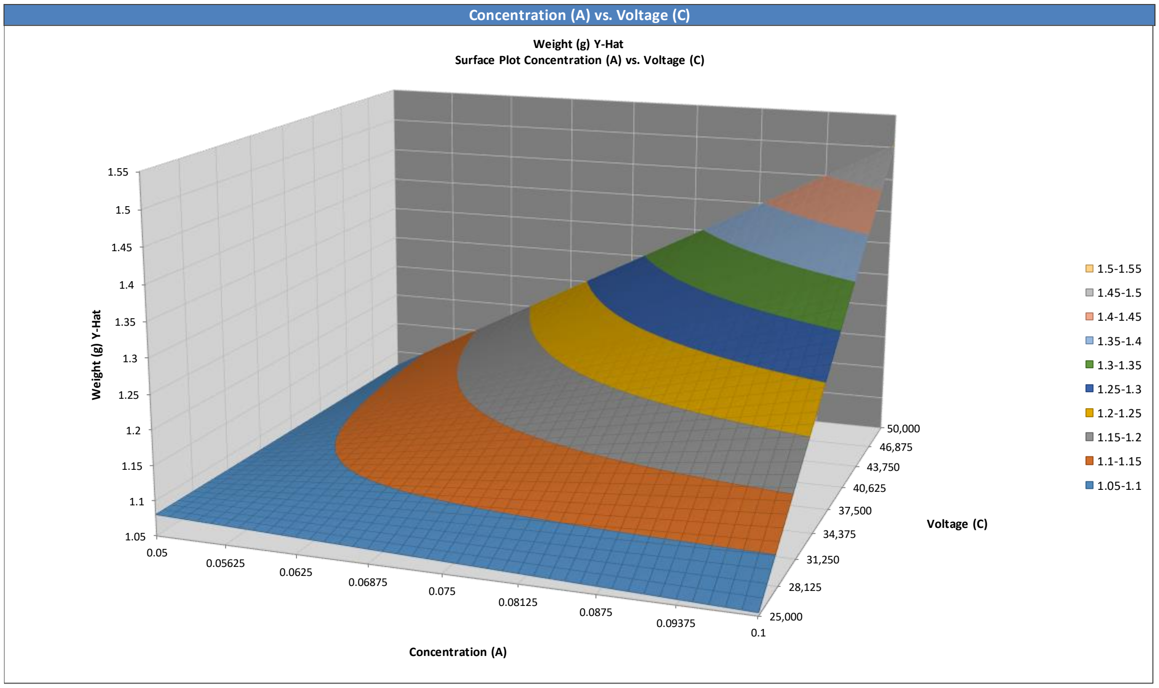

Figure 126: Surface Chart - Concentration vs Voltage for Sample Weight h-hat (Soybean oil, Propylene Glycol, 19ga Capillary)

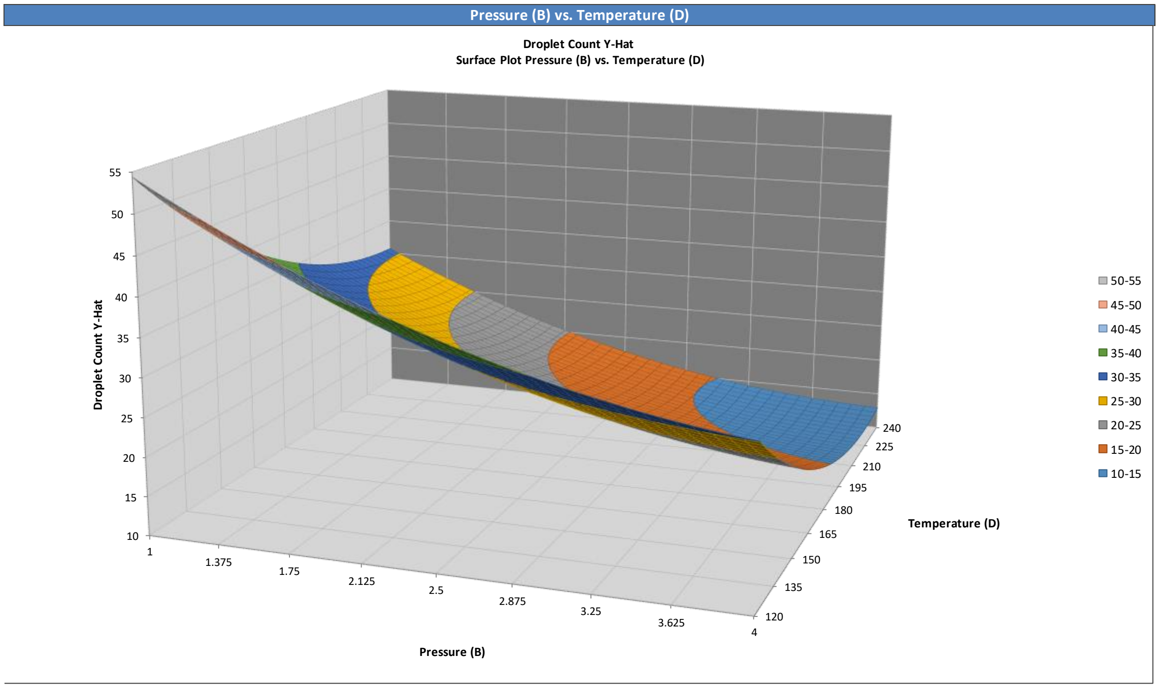

Figure 127: Surface Chart – Pressure vs Temperature for Droplet Count h-hat (Soybean oil, Propylene Glycol, 19ga Capillary)

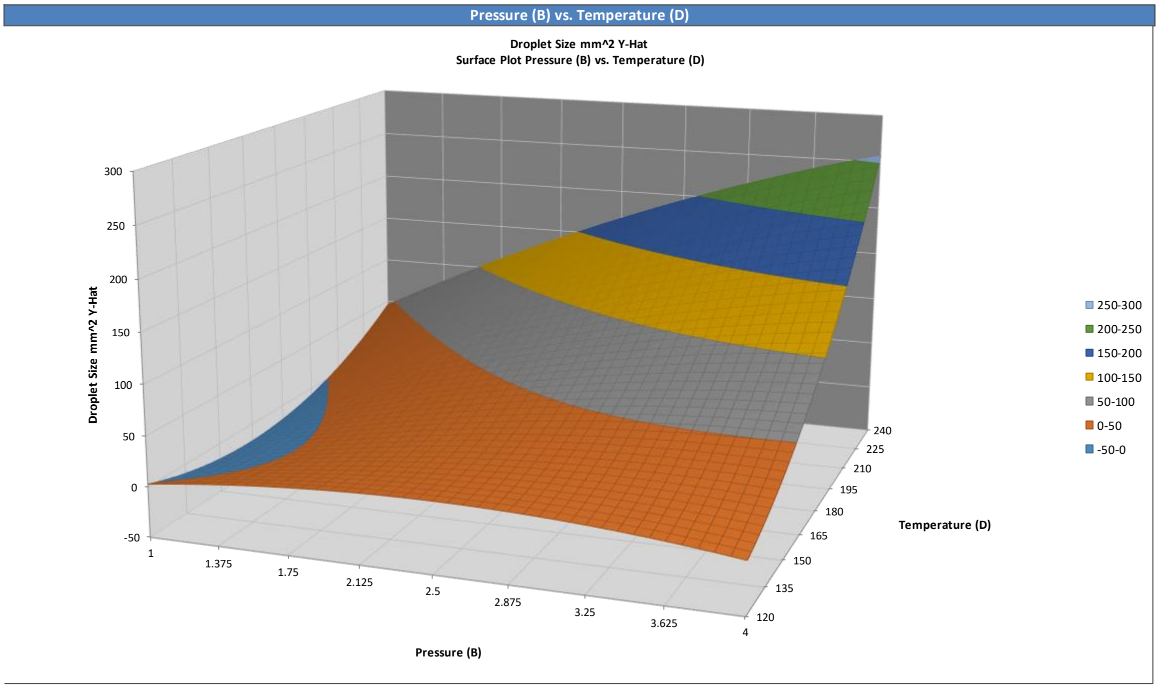

Figure 128: Surface Chart – Pressure vs Temperature for Droplet Size h-hat (Soybean oil, Propylene Glycol, 19ga Capillary)

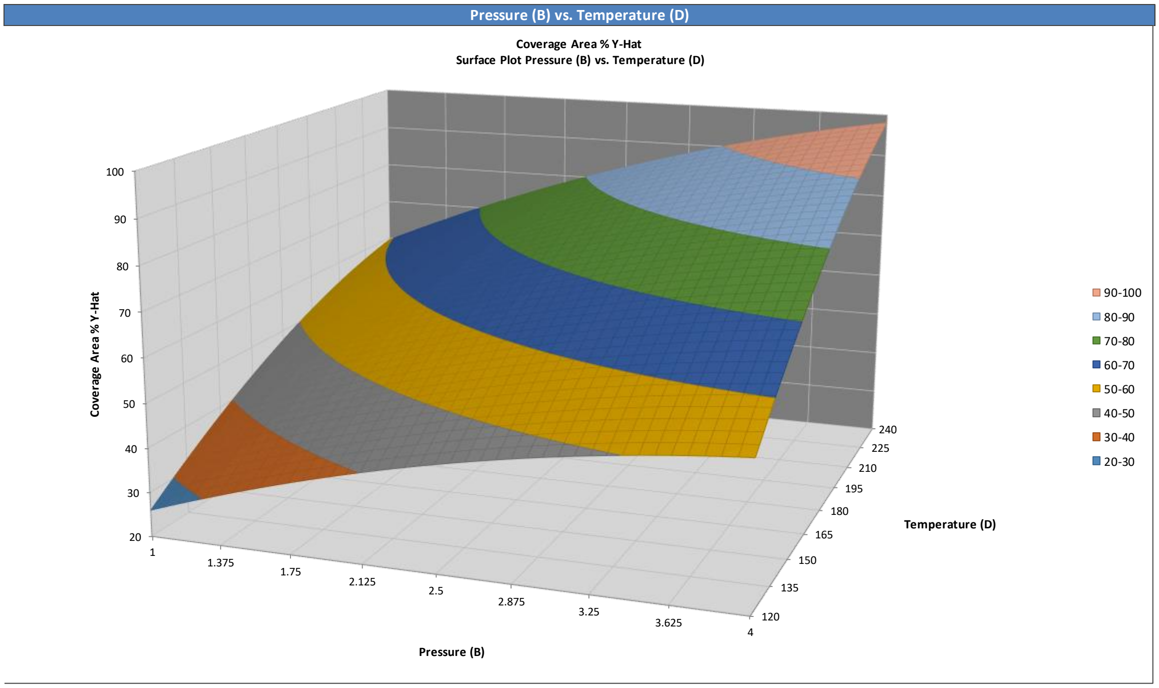

Figure 129: Surface Chart – Pressure vs Temperature for Coverage Area h-hat (Soybean oil, Propylene Glycol, 19ga Capillary)

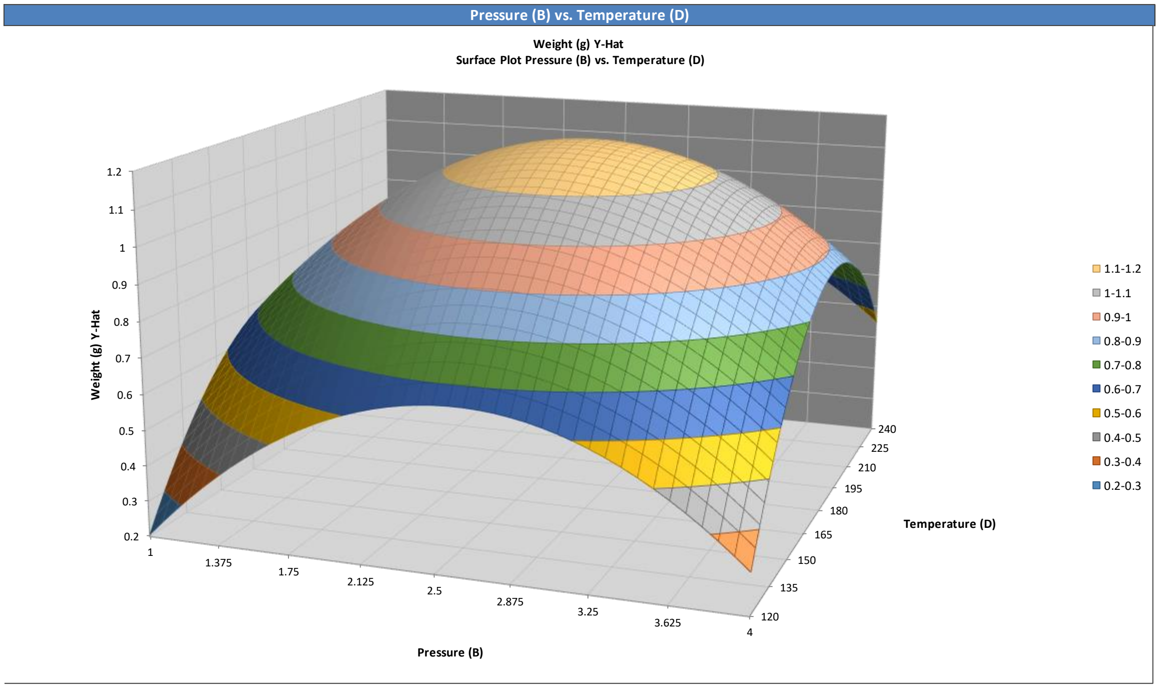

Figure 130: Surface Chart – Pressure vs Temperature for Sample Weight h-hat (Soybean oil, Propylene Glycol, 19ga Capillary)

5.2.6. **Propylene Glycol with 22 Gauge Capillary**

Table 15: Main Effects Plot for Soybean Oil & Propylene Glycol @ 22g Capillary

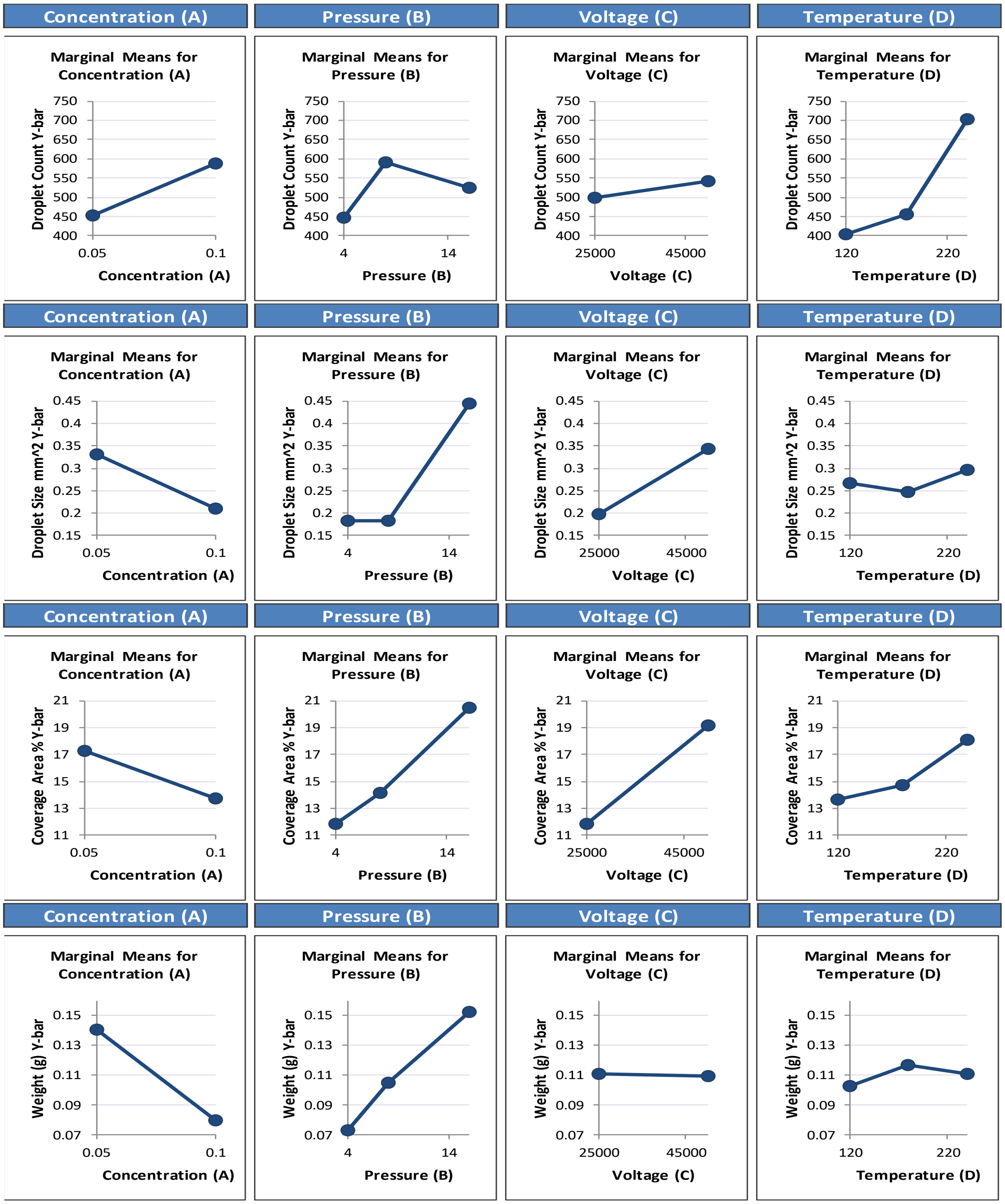

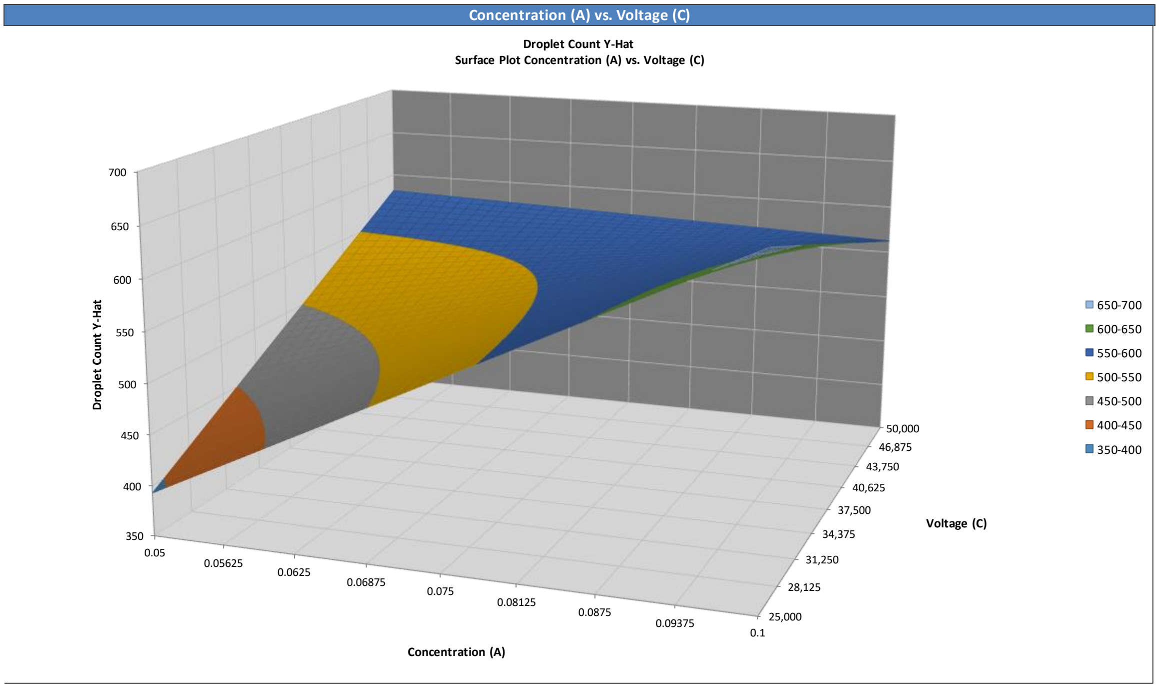

Figure 131: Surface Chart - Concentration vs Voltage for Droplet Count h-hat (Soybean oil, Propylene Glycol, 22ga Capillary)

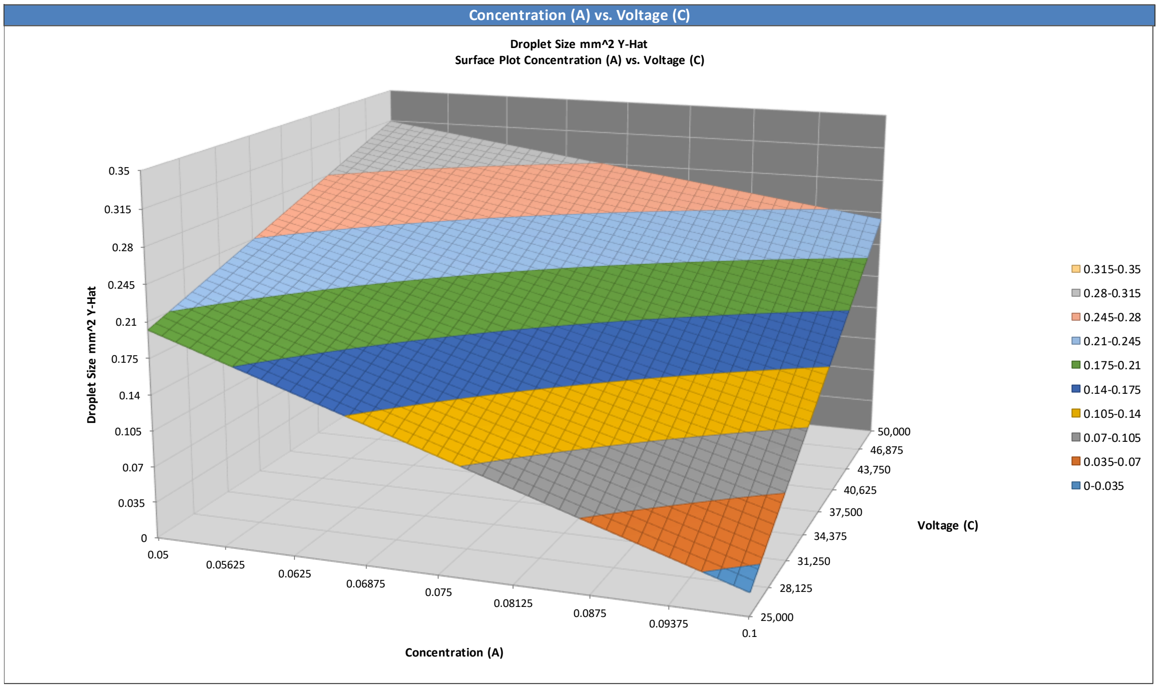

Figure 132: Surface Chart - Concentration vs Voltage for Droplet Size h-hat (Soybean oil, Propylene Glycol, 22ga Capillary)

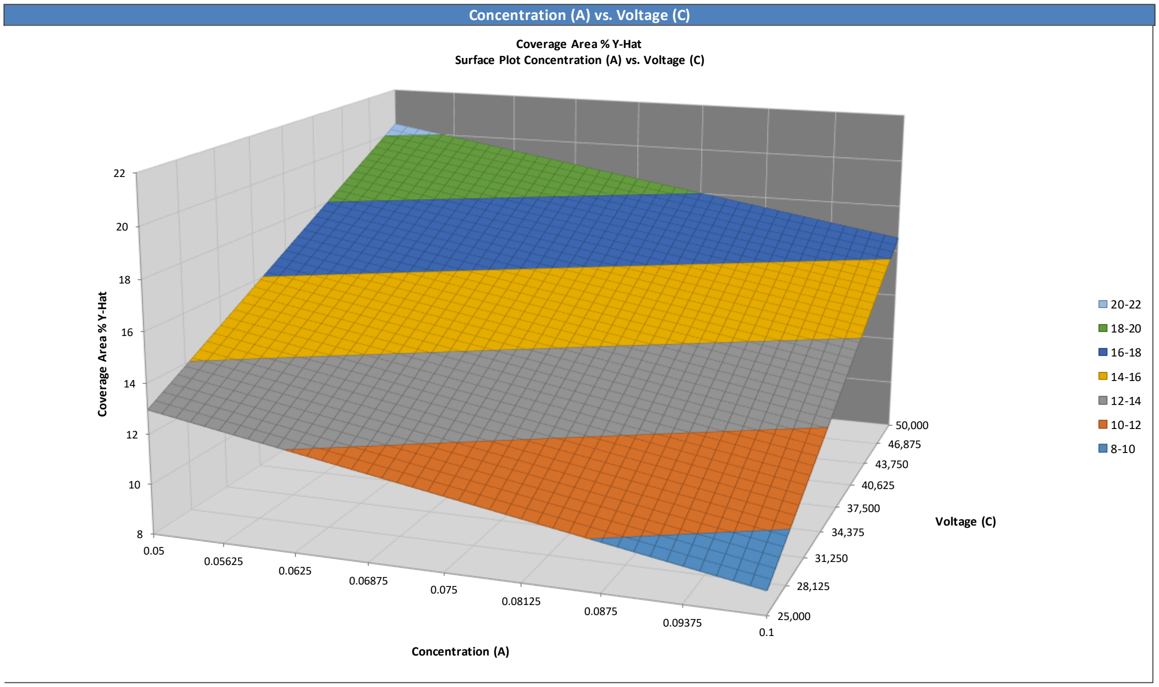

Figure 133: Surface Chart - Concentration vs Voltage for Droplet Area h-hat (Soybean oil, Propylene Glycol, 22ga Capillary)

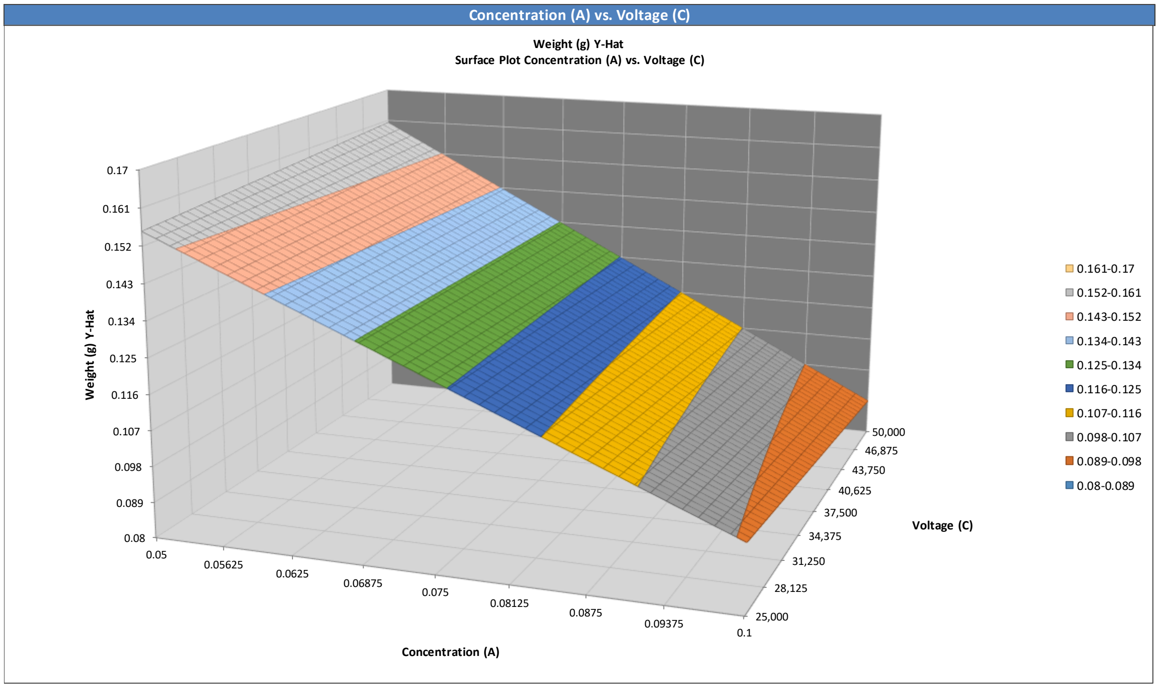

Figure 134: Surface Chart - Concentration vs Voltage for Sample Weight h-hat (Soybean oil, Propylene Glycol, 22ga Capillary)

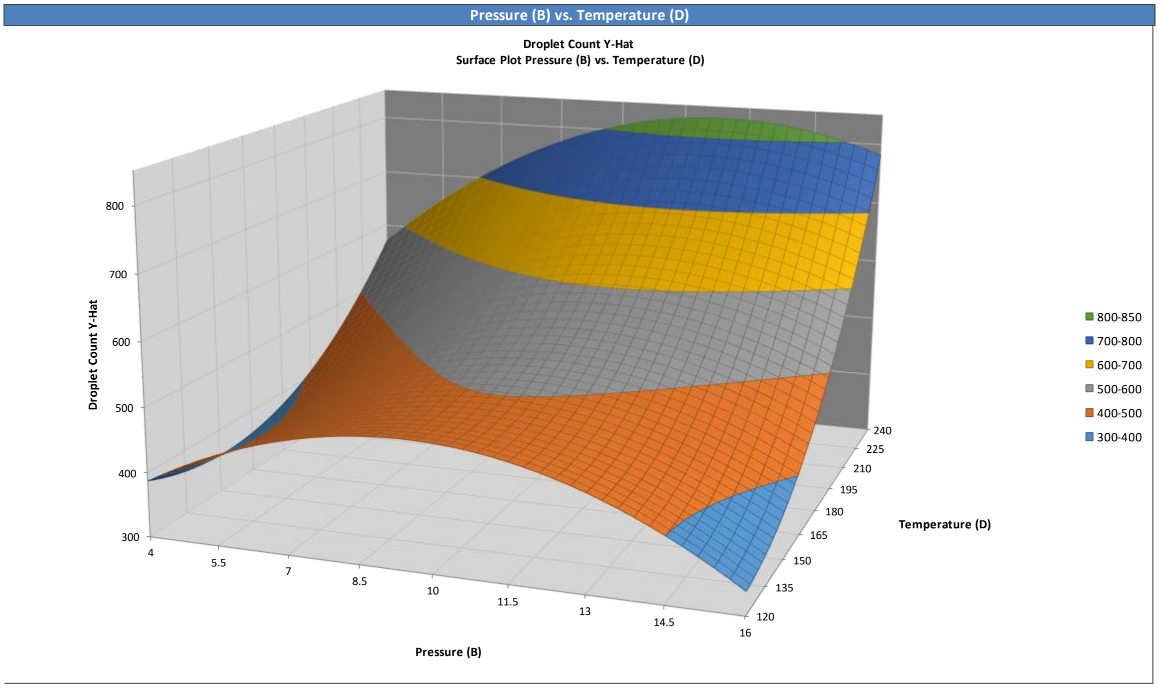

Figure 135: Surface Chart – Pressure vs Temperature for Droplet Count h-hat (Soybean oil, Propylene Glycol, 22ga Capillary)

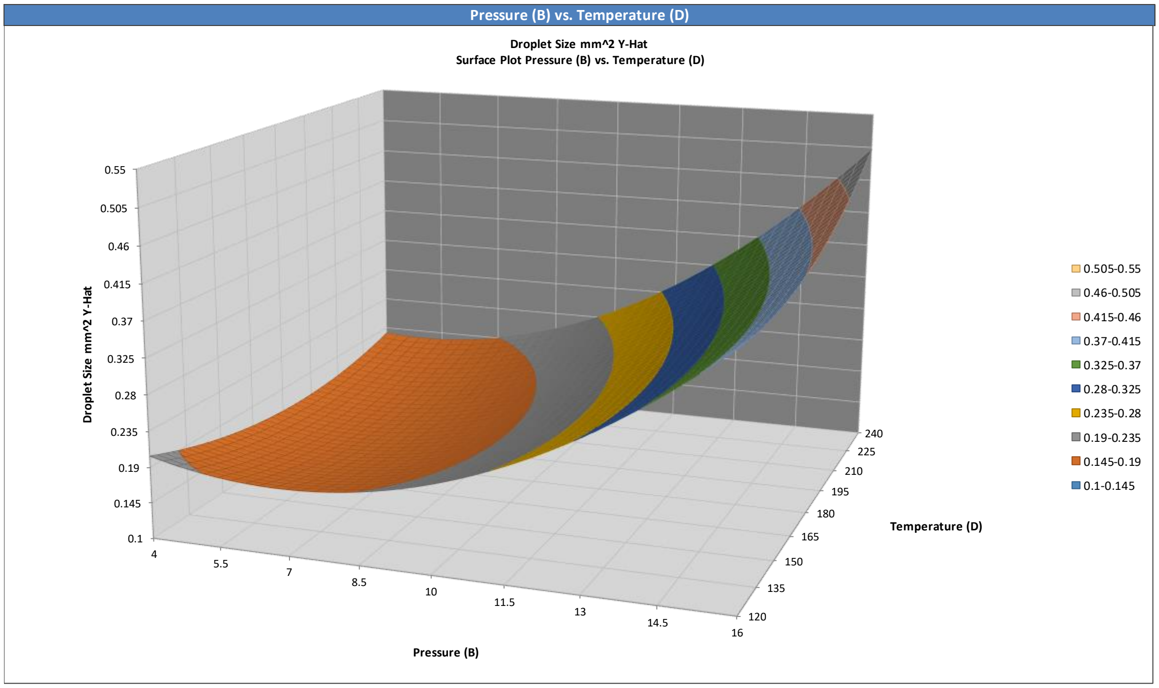

Figure 136: Surface Chart – Pressure vs Temperature for Droplet Size h-hat (Soybean oil, Propylene Glycol, 22ga Capillary)

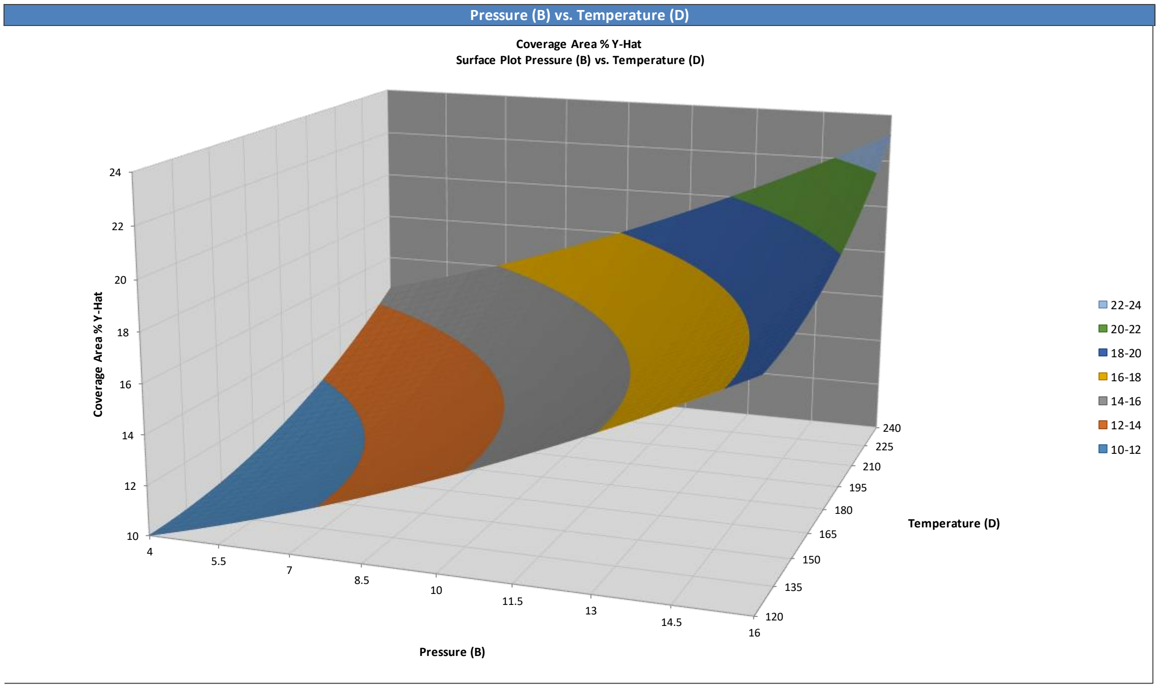

Figure 137: Surface Chart – Pressure vs Temperature for Coverage Area h-hat (Soybean oil, Propylene Glycol, 22ga Capillary)

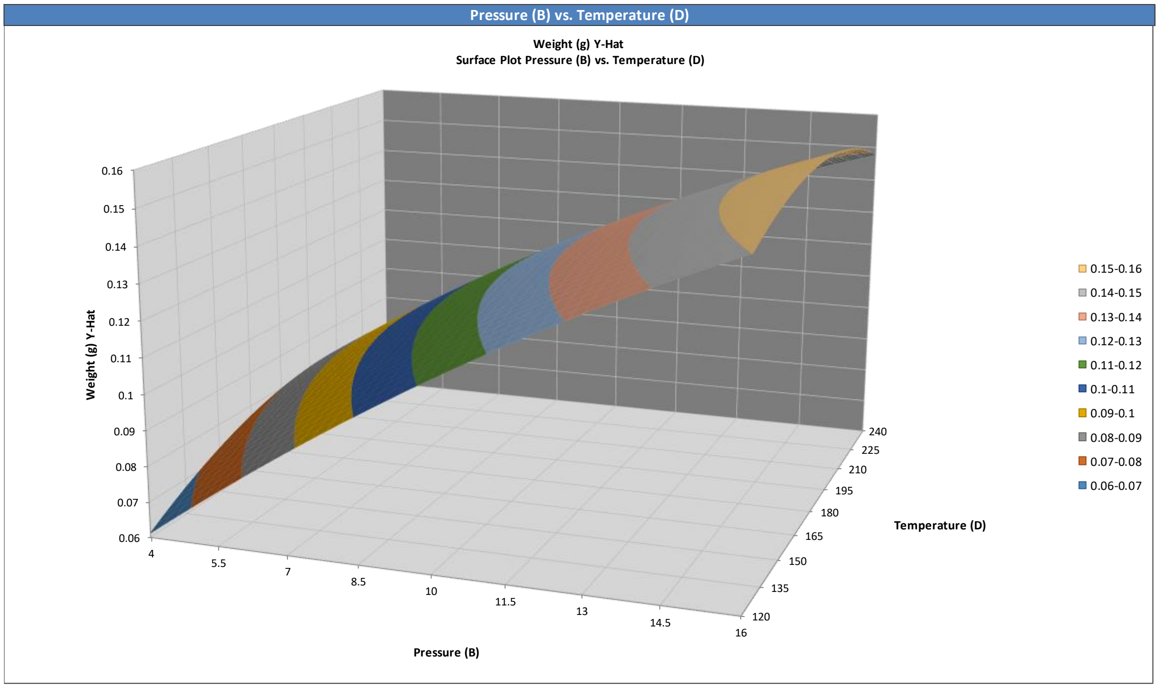

Figure 138: Surface Chart – Pressure vs Temperature for Sample Weight h-hat (Soybean oil, Propylene Glycol, 22ga Capillary)

5.3. RAPESEED (Canola) OIL

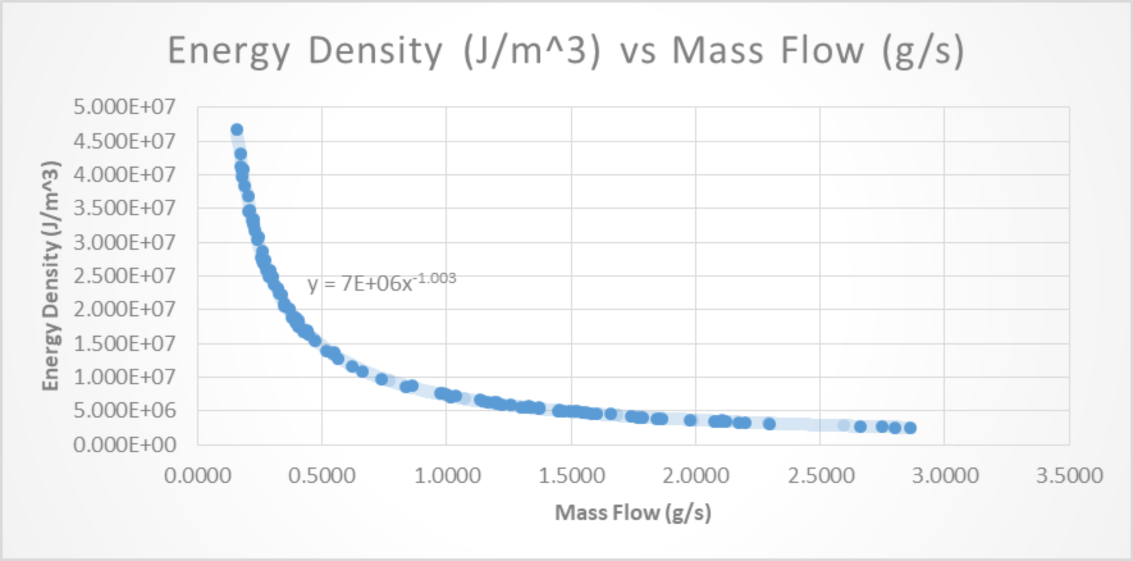

Figure 139: Rapeseed Oil Energy Density vs Mass Flow Chart 25kV

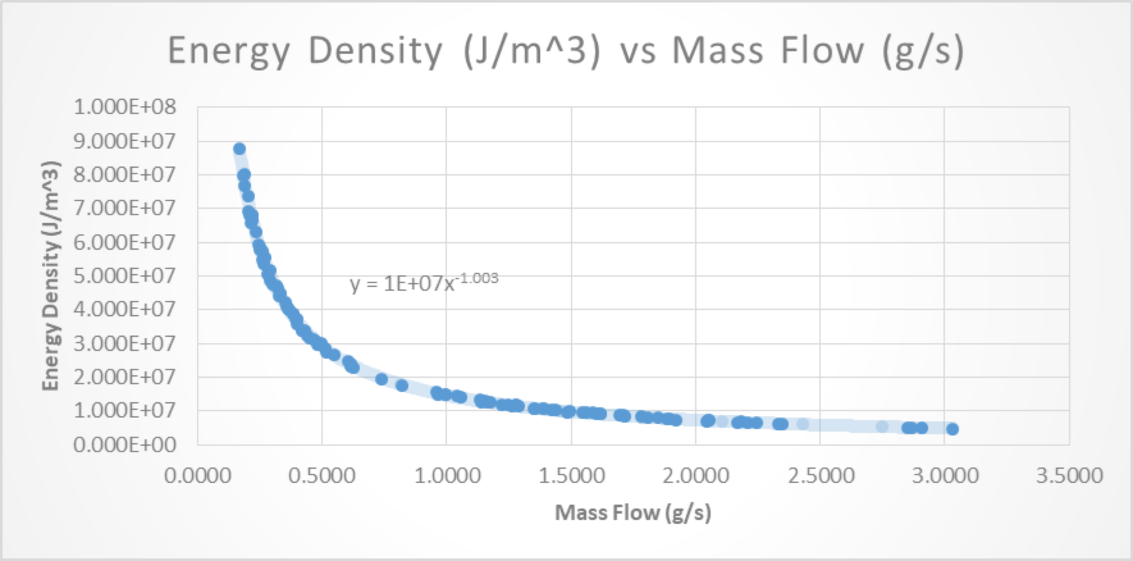

Figure 140: Rapeseed Oil Energy Density vs Mass Flow Chart 50kV

5.3.1. **Sunflower Lecithin with 19 Gauge Capillary**

Table 16: Main Effects Plot for Rapeseed Oil & Sunflower Lecithin @ 19ga Capillary

Concentration (A) | **Pressure (B)** | **Voltage (C)** | **Temperature (D)**

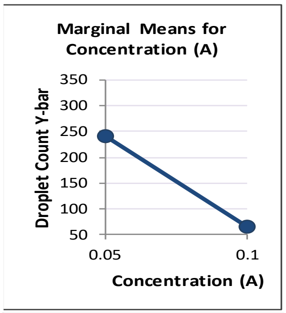

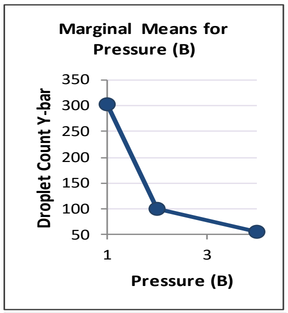

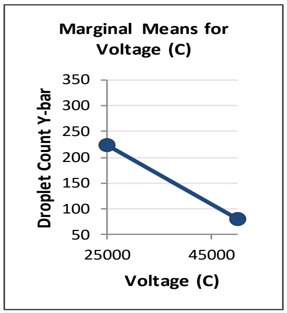

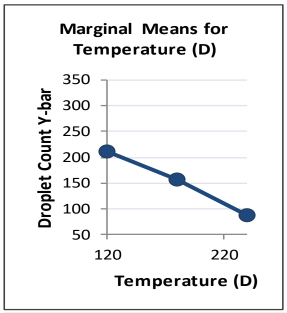

Concentration (A) | **Pressure (B)** | **Voltage (C)** | **Temperature (D)**

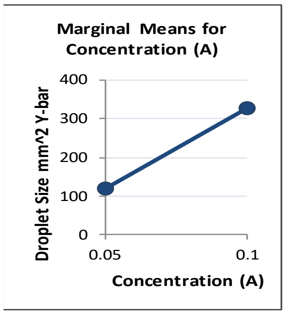

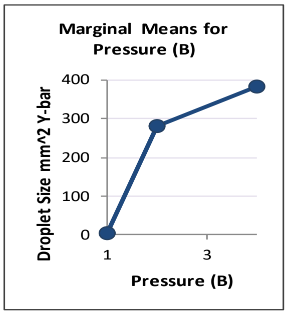

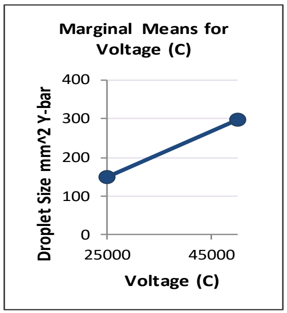

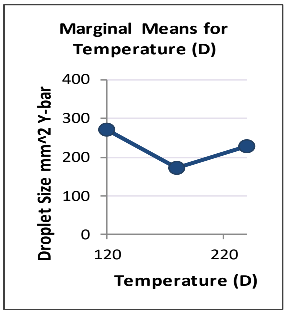

Concentration (A) | **Pressure (B)** | **Voltage (C)** | **Temperature (D)**

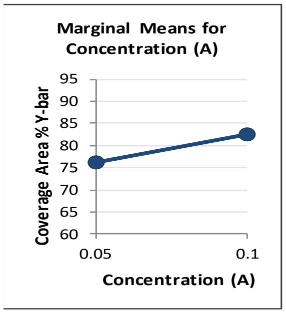

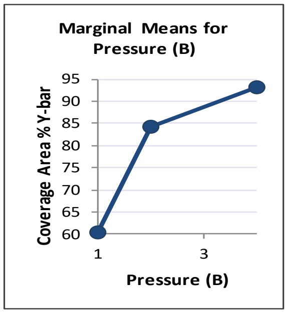

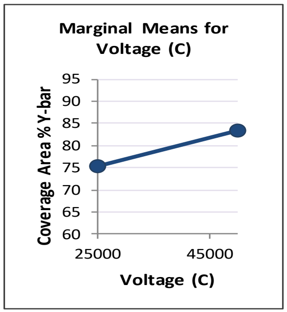

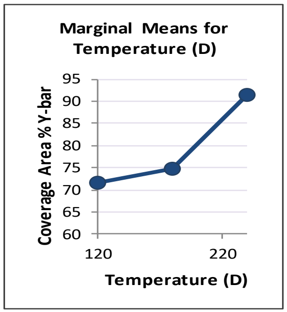

Concentration (A) | **Pressure (B)** | **Voltage (C)** | **Temperature (D)**

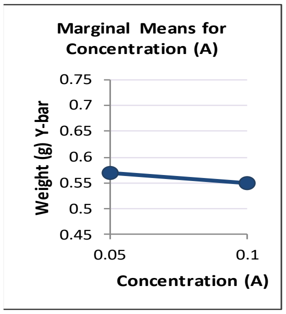

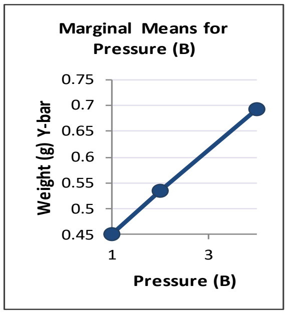

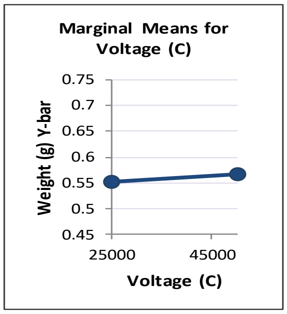

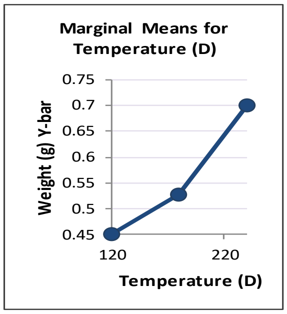

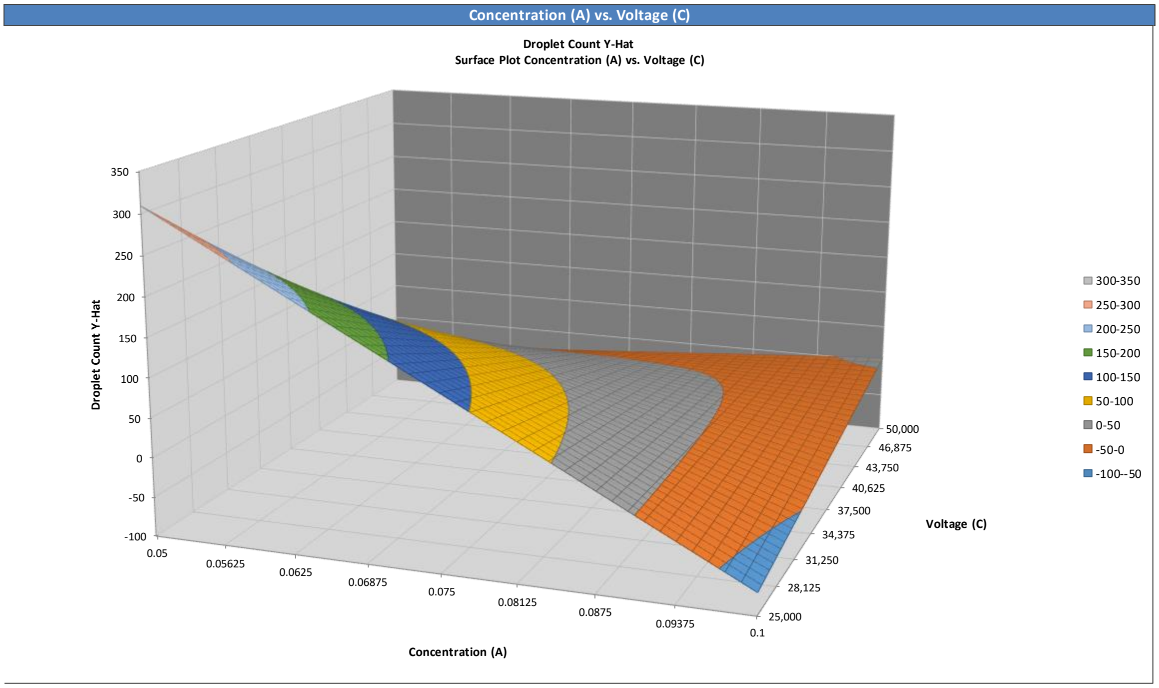

Figure 141: Surface Chart - Concentration vs Voltage for Droplet Count h-hat (Rapeseed oil, Sunflower Lecithin, 19ga Capillary)

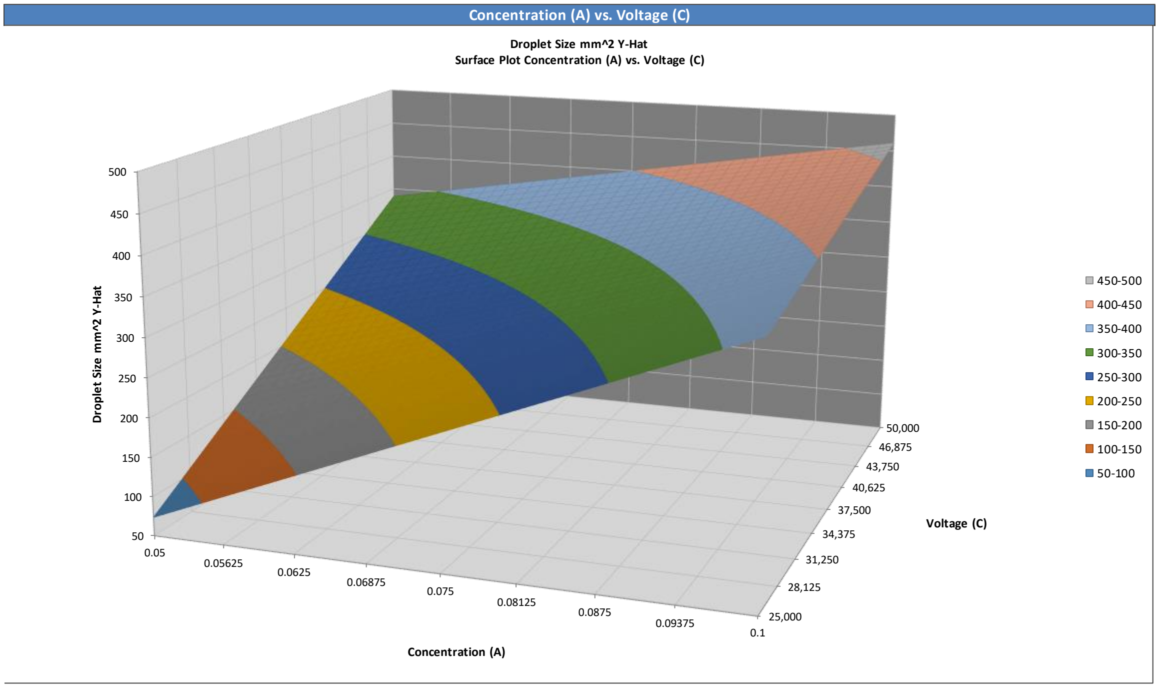

Figure 142: Surface Chart - Concentration vs Voltage for Droplet Size h-hat (Rapeseed oil, Sunflower Lecithin, 19ga Capillary)

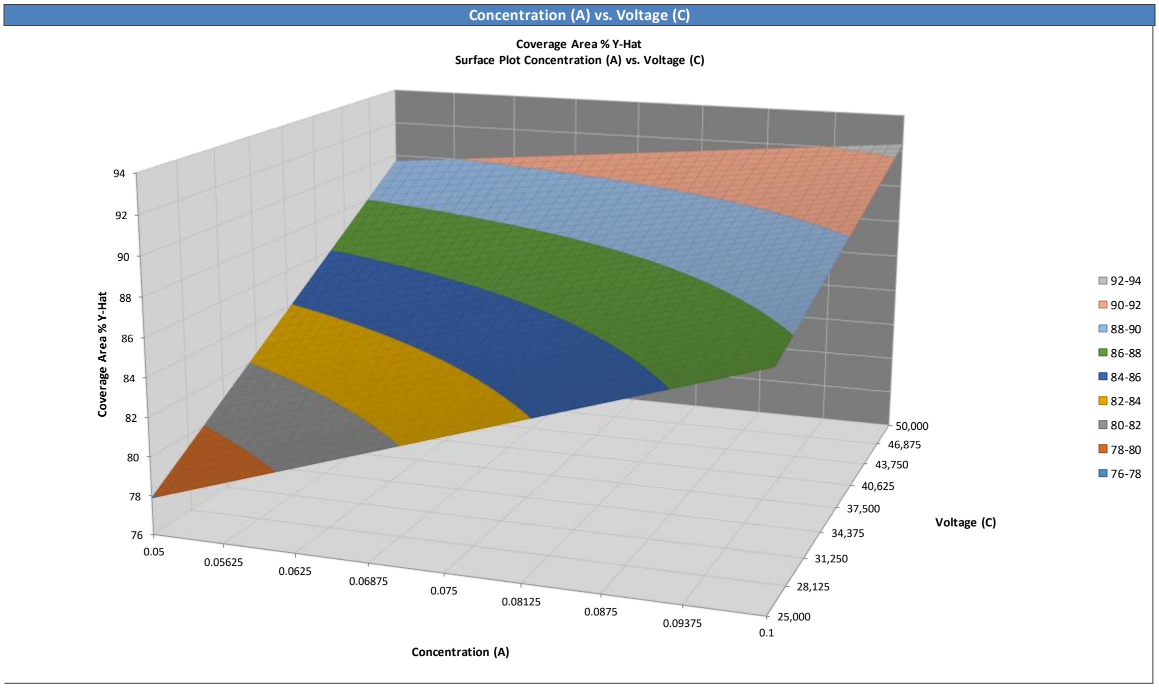

Figure 143: Surface Chart - Concentration vs Voltage for Coverage Area h-hat (Rapeseed oil, Sunflower Lecithin, 19ga Capillary)

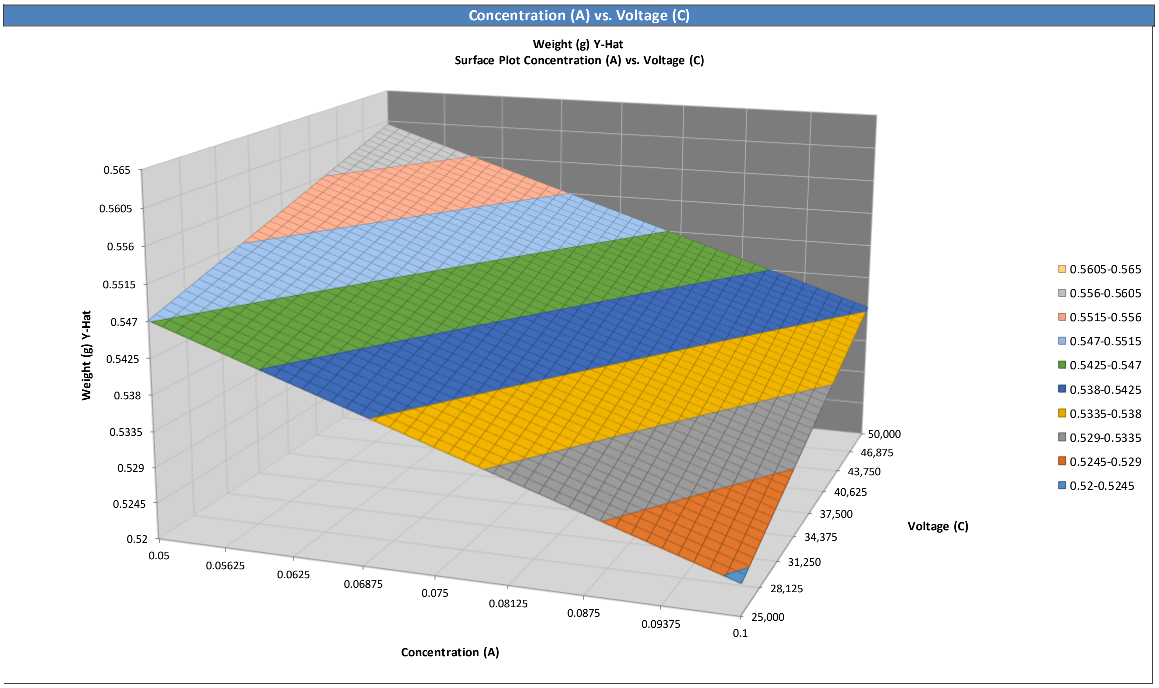

Figure 144: Surface Chart - Concentration vs Voltage for Sample Weight h-hat (Rapeseed oil, Sunflower Lecithin, 19ga Capillary)

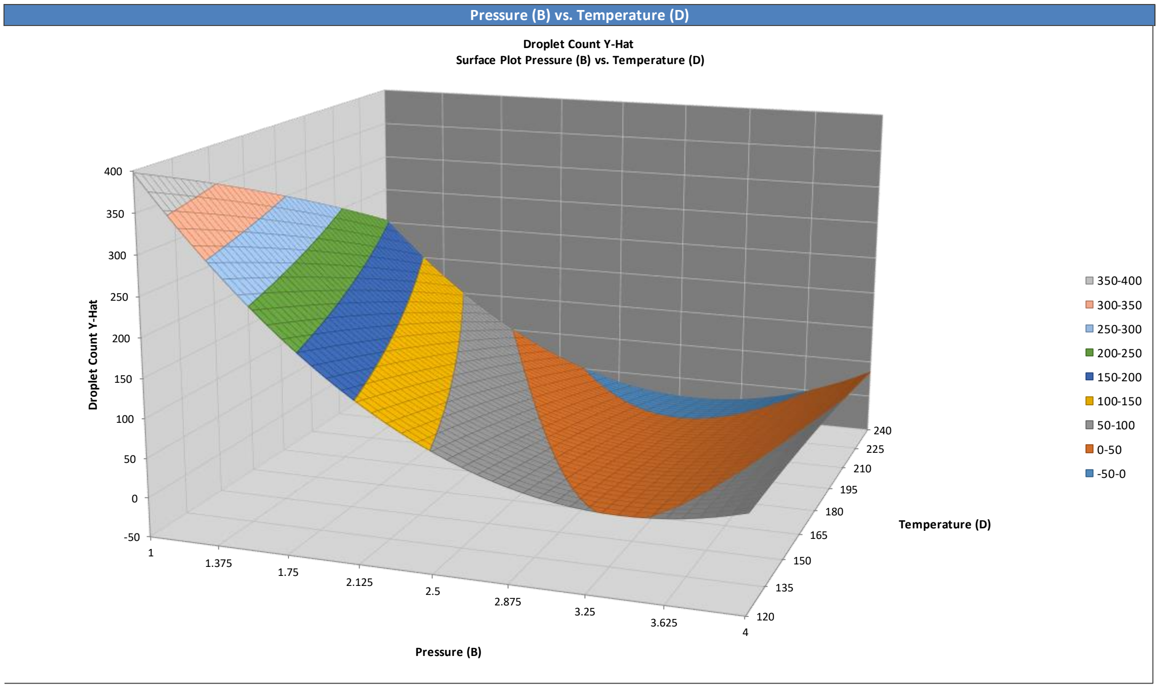

Figure 145: Surface Chart – Pressure vs Temperature for Droplet Count h-hat (Rapeseed oil, Sunflower Lecithin, 19ga Capillary)

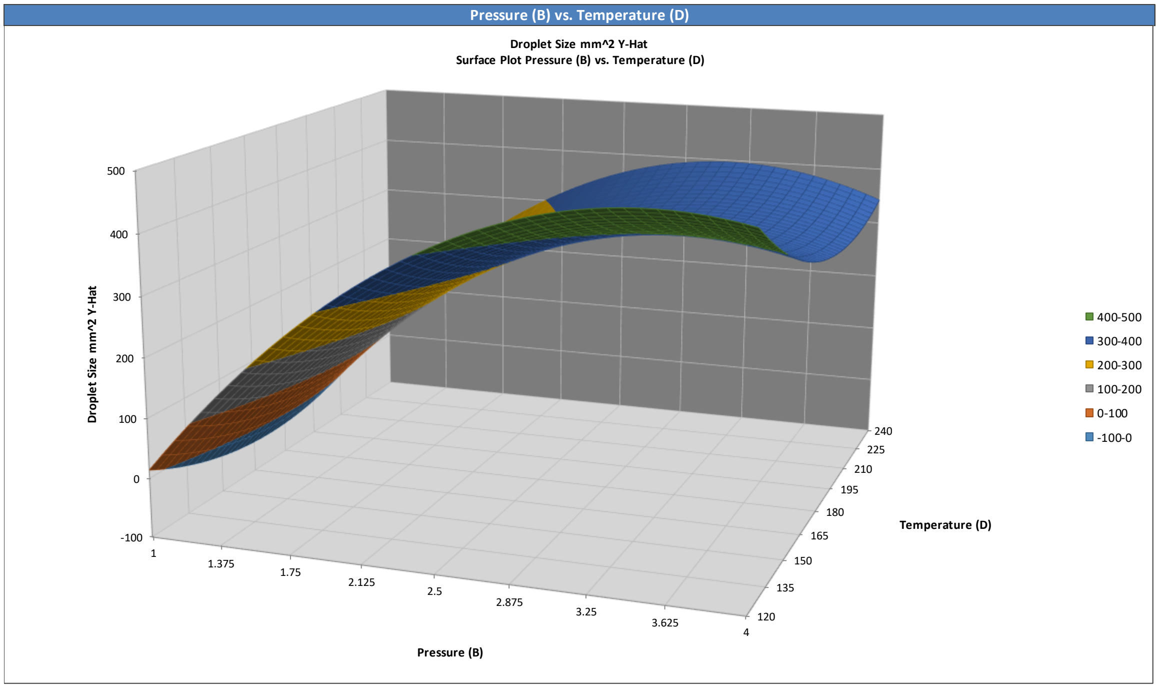

Figure 146: Surface Chart – Pressure vs Temperature for Droplet Size h-hat (Rapeseed oil, Sunflower Lecithin, 19ga Capillary)

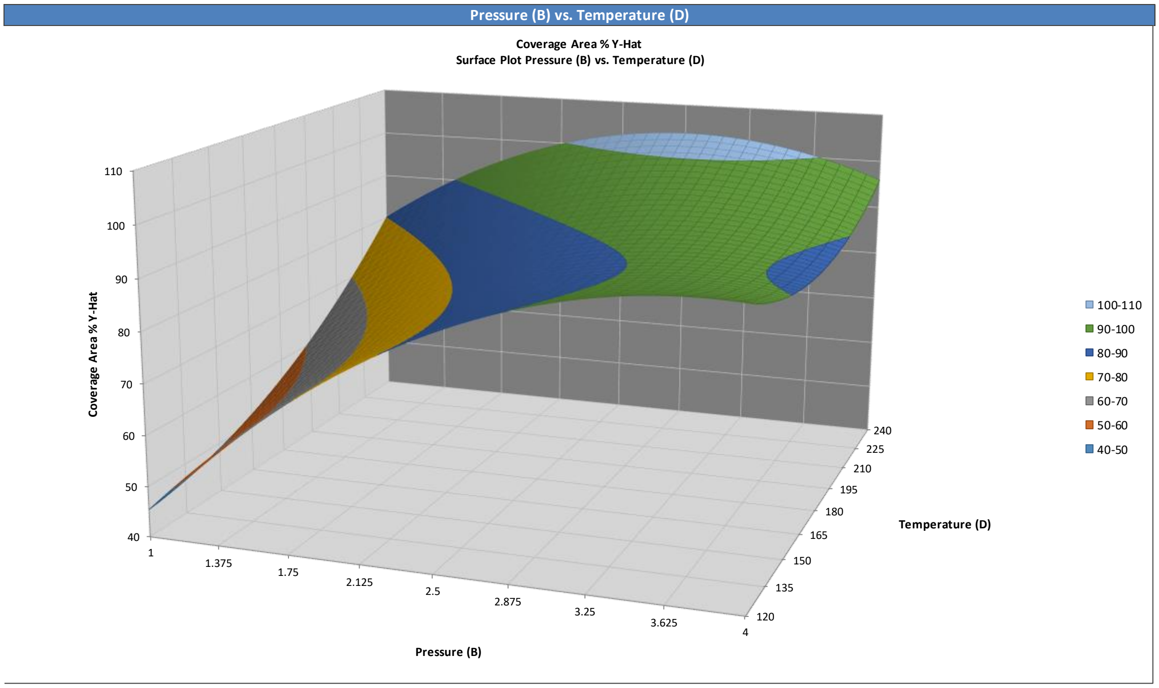

Figure 147: Surface Chart – Pressure vs Temperature for Coverage Area h-hat (Rapeseed oil, Sunflower Lecithin, 19ga Capillary)

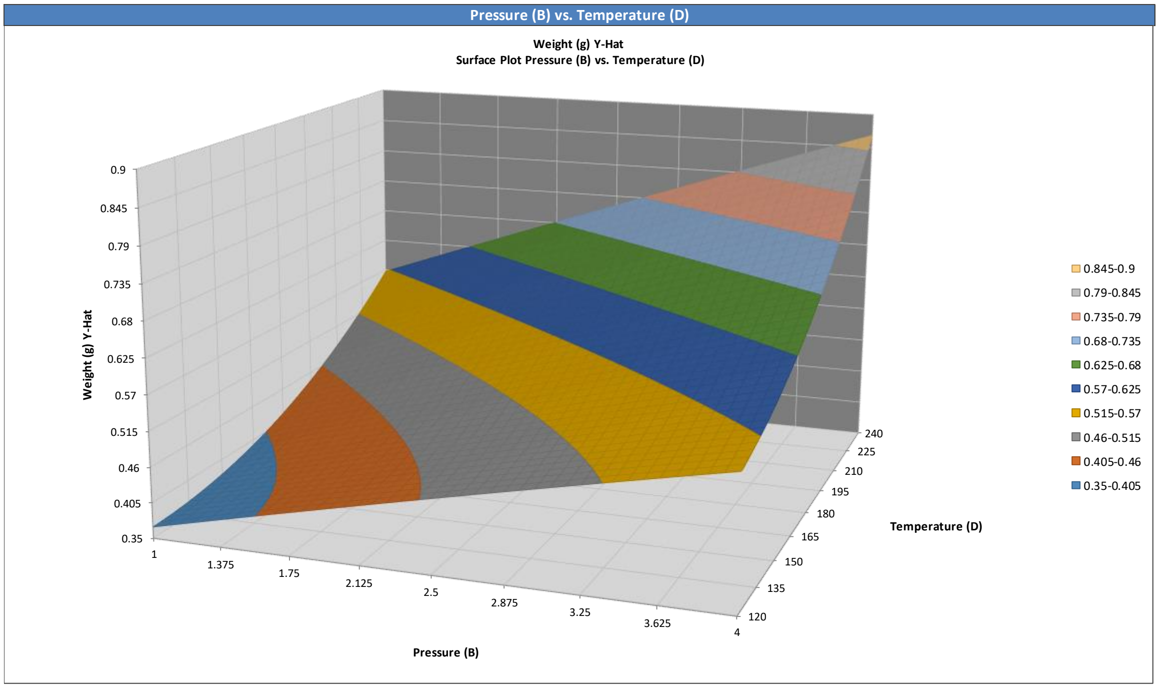

Figure 148: Surface Chart – Pressure vs Temperature for Sample Size h-hat (Rapeseed oil, Sunflower Lecithin, 19ga Capillary)

5.3.2. Sunflower Lecithin with 22 Gauge Capillary

Table 17: Main Effects Plot for Rapeseed Oil & Sunflower Lecithin @ 22ga Capillary

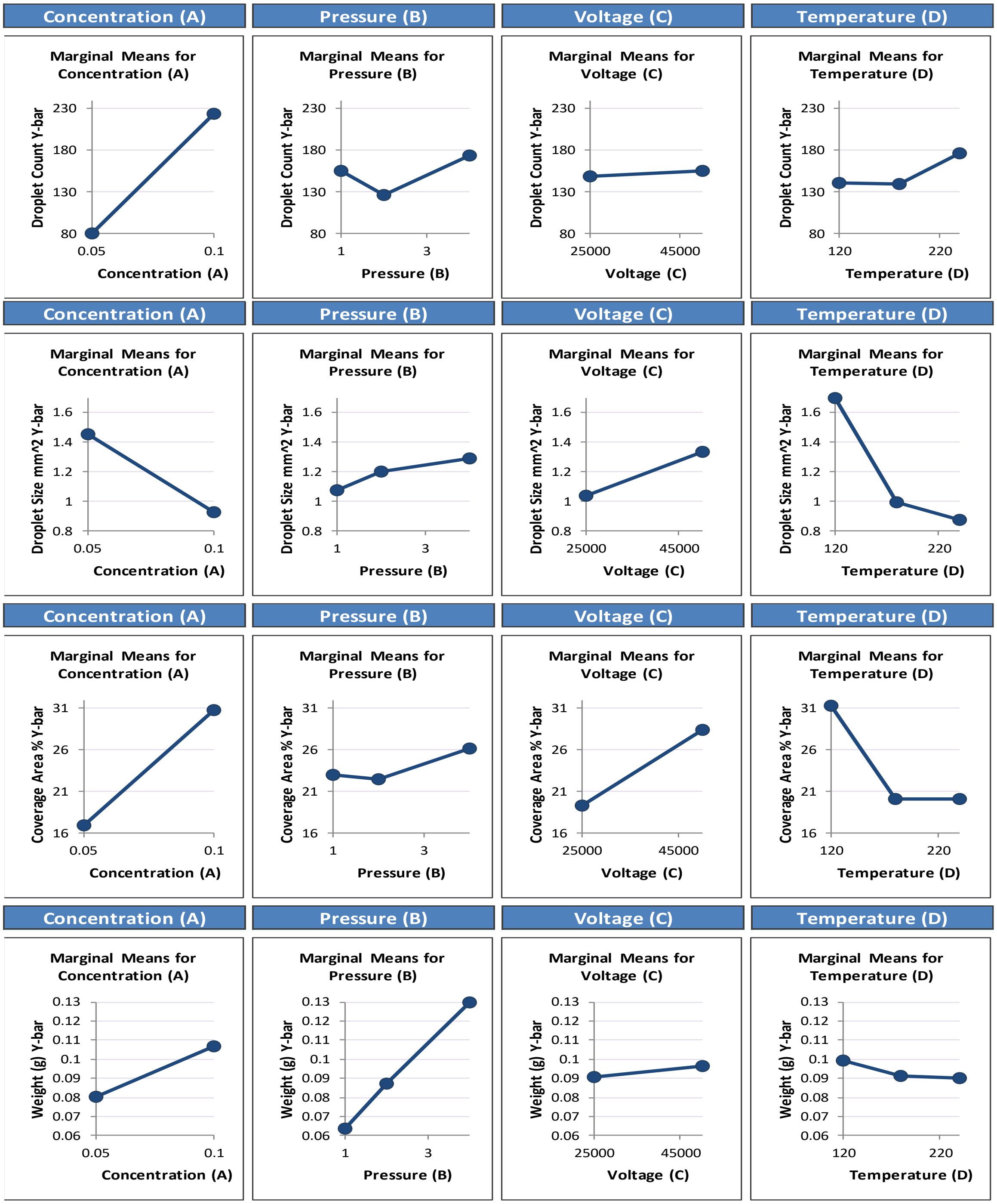

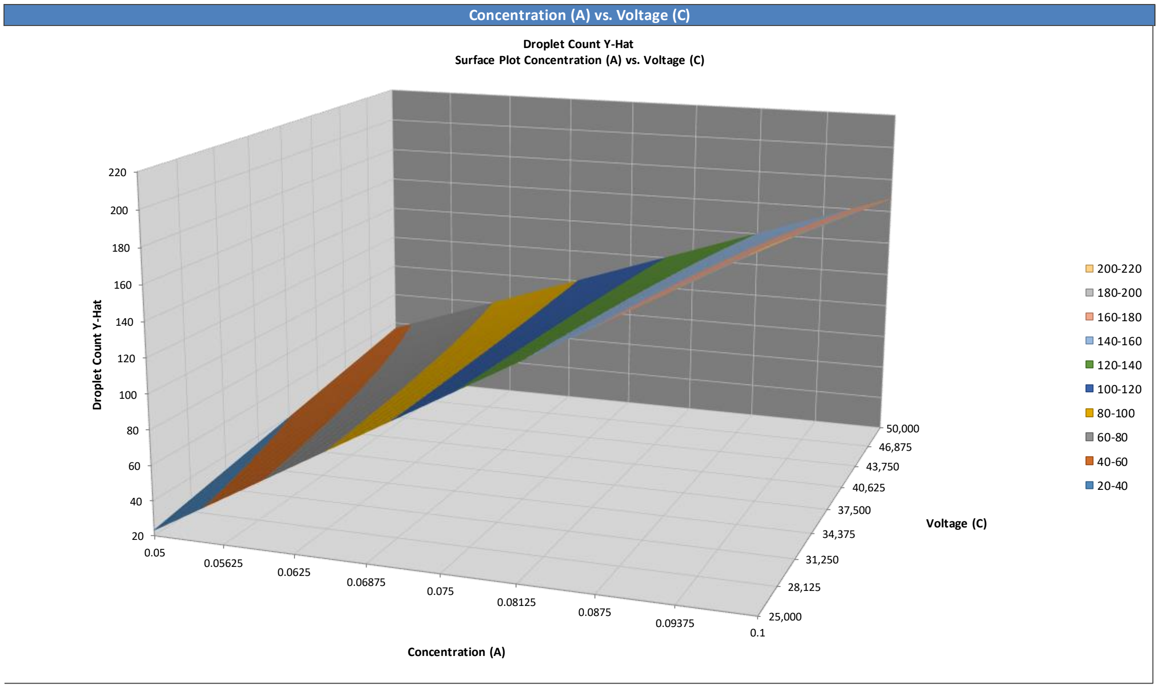

Figure 149: Surface Chart - Concentration vs Voltage for Droplet Count h-hat (Rapeseed oil, Sunflower Lecithin, 22ga Capillary)

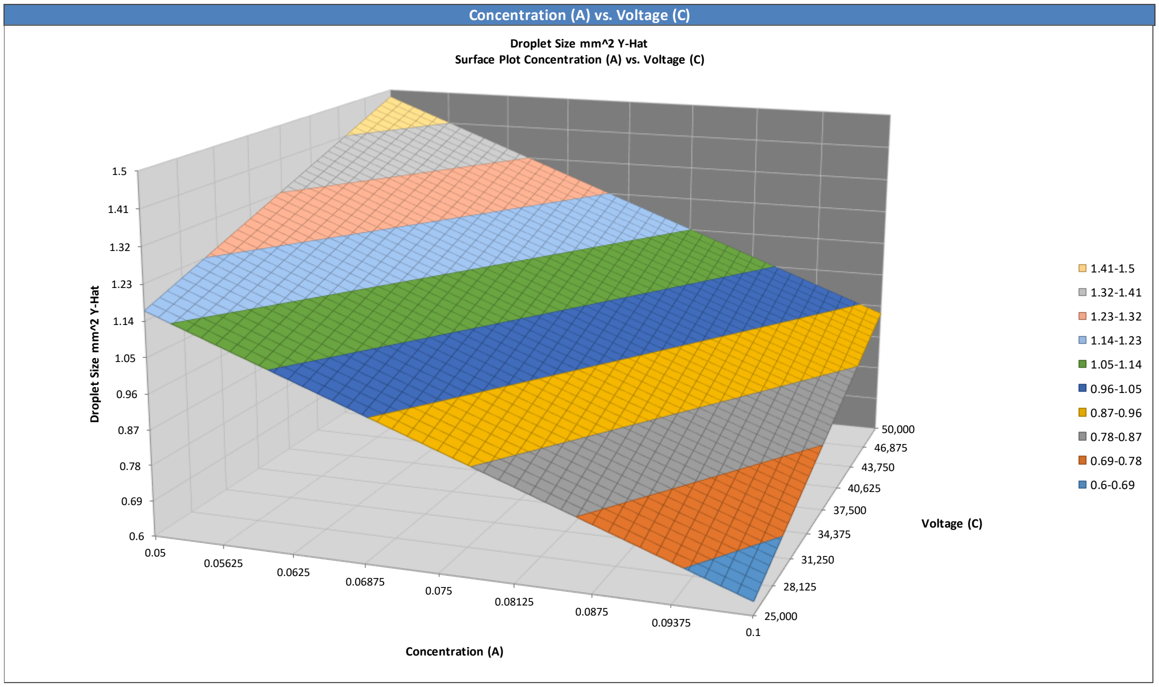

Figure 150: Surface Chart - Concentration vs Voltage for Droplet Size h-hat (Rapeseed oil, Sunflower Lecithin, 22ga Capillary)

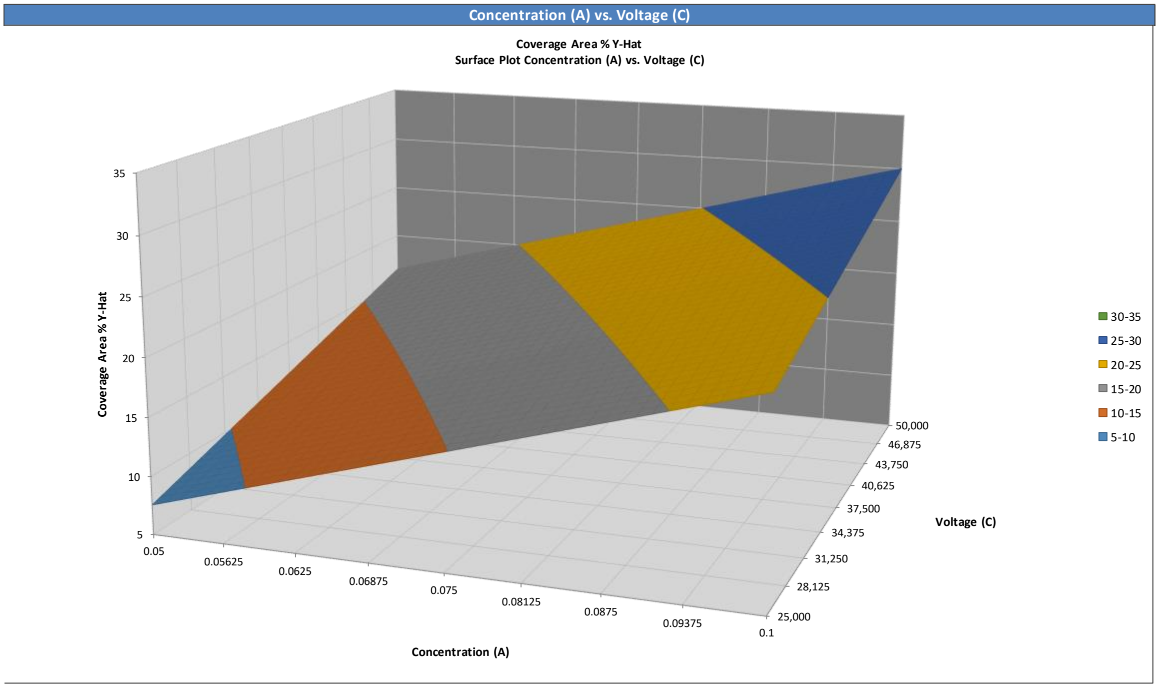

Figure 151: Surface Chart - Concentration vs Voltage for Coverage Area h-hat (Rapeseed oil, Sunflower Lecithin, 22ga Capillary)

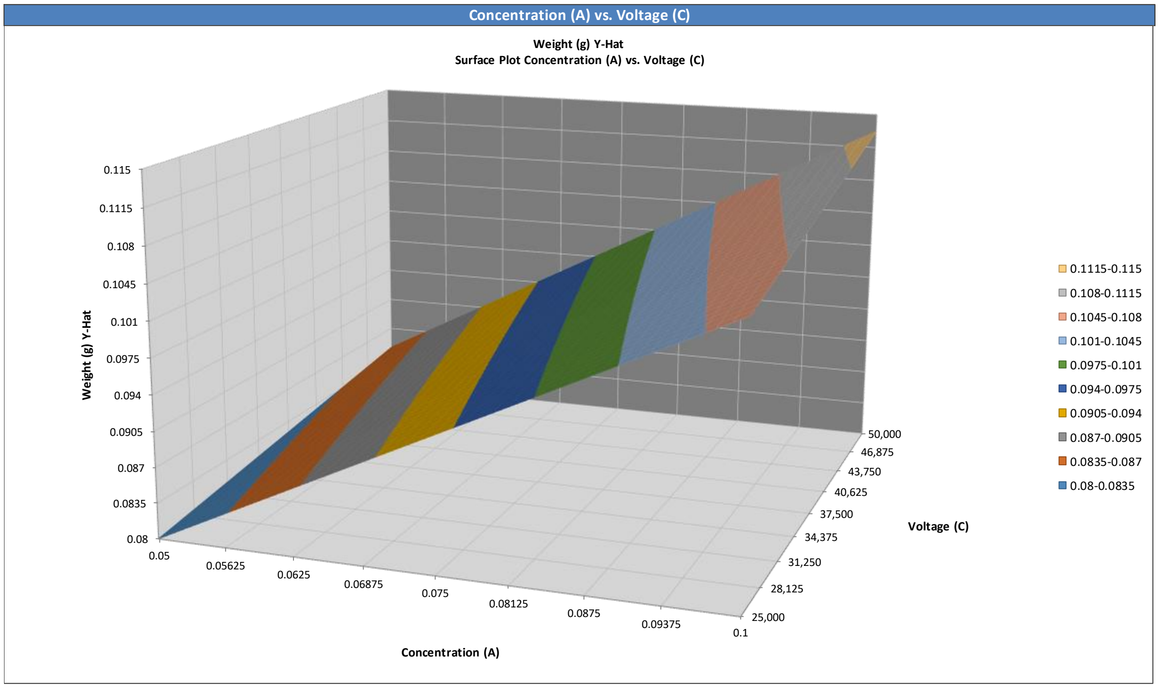

Figure 152: Surface Chart - Concentration vs Voltage for Sample WT h-hat (Rapeseed oil, Sunflower Lecithin, 22ga Capillary)

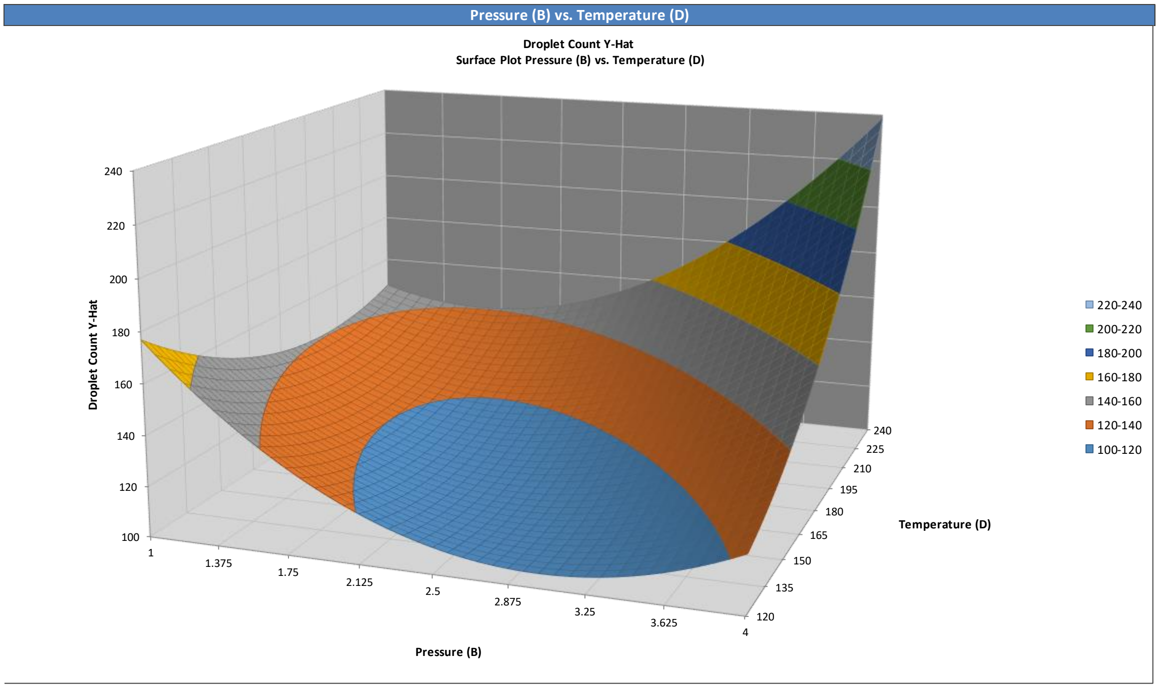

Figure 153: Surface Chart – Pressure vs Temperature for Droplet Count h-hat (Rapeseed oil, Sunflower Lecithin, 22ga Capillary)

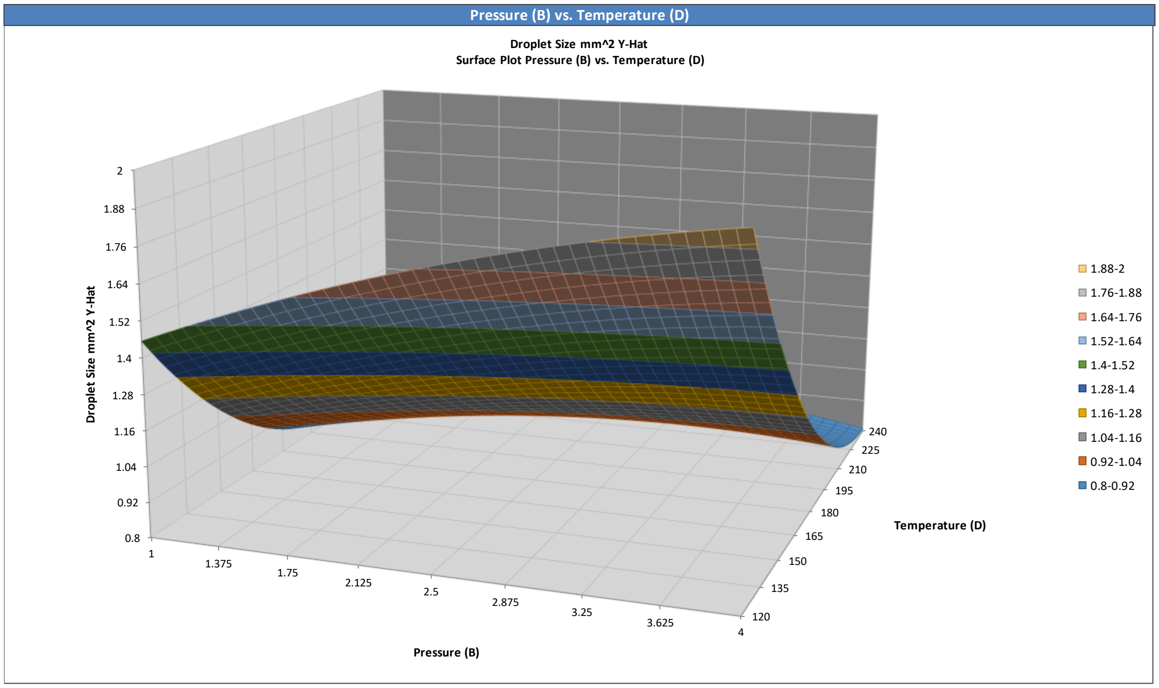

Figure 154: Surface Chart – Pressure vs Temperature for Droplet Size h-hat (Rapeseed oil, Sunflower Lecithin, 22ga Capillary)

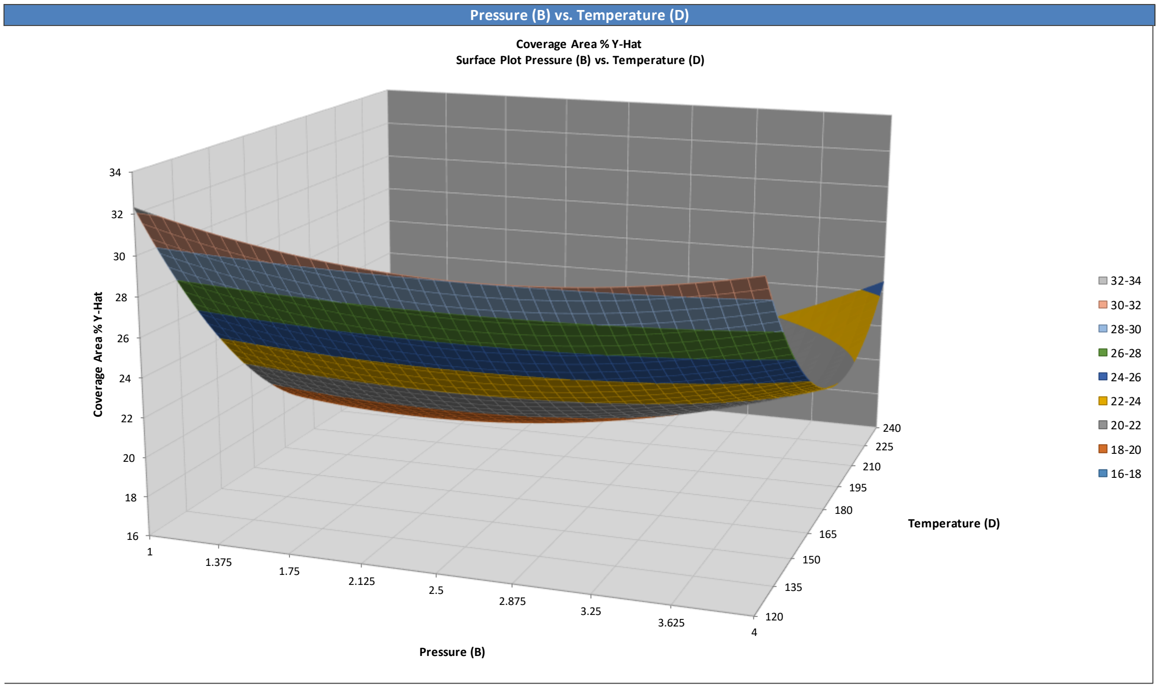

Figure 155: Surface Chart – Pressure vs Temperature for Coverage Area h-hat (Rapeseed oil, Sunflower Lecithin, 22ga Capillary)

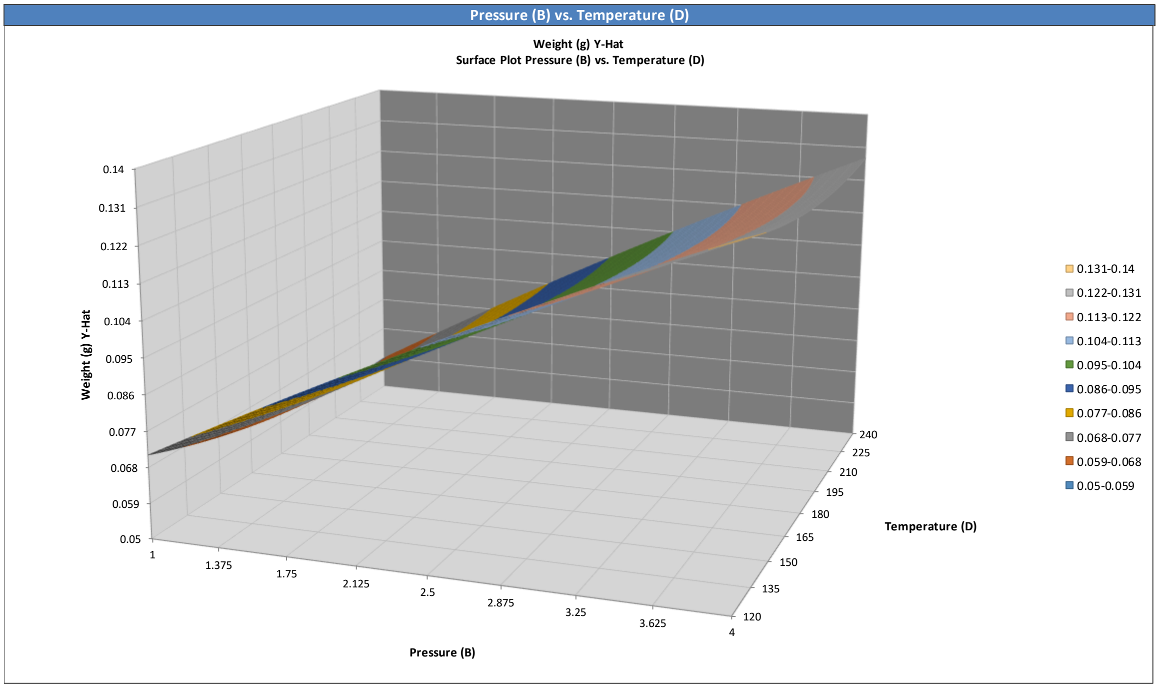

Figure 156: Surface Chart – Pressure vs Temperature for Sample Weight h-hat (Rapeseed oil, Sunflower Lecithin, 22ga Capillary)

5.3.3. Polysorbate 20 with 19 Gauge Capillary

Table 18: Main Effects Plot for Rapeseed Oil & Polysorbate 20 @ 19ga Capillary

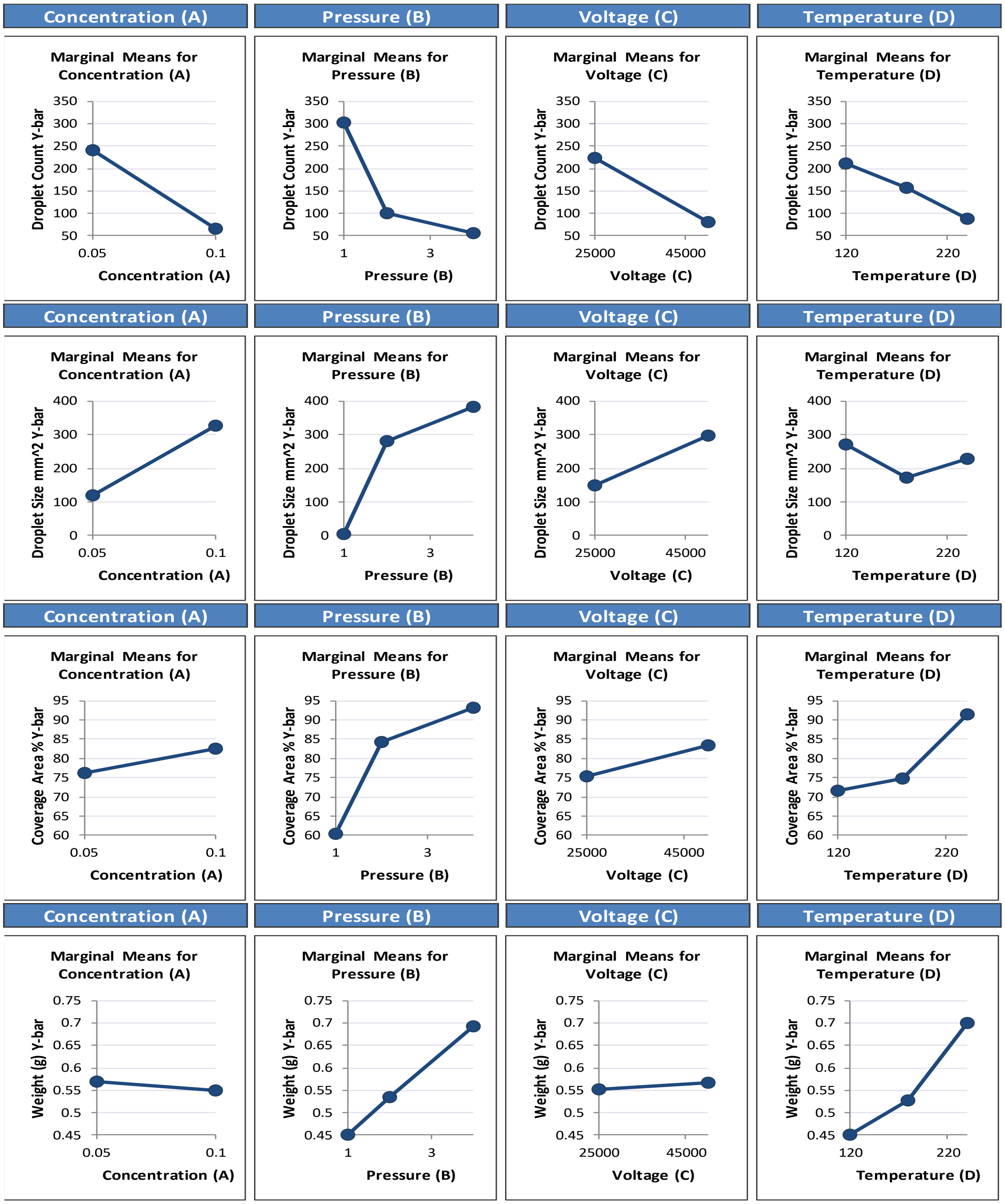

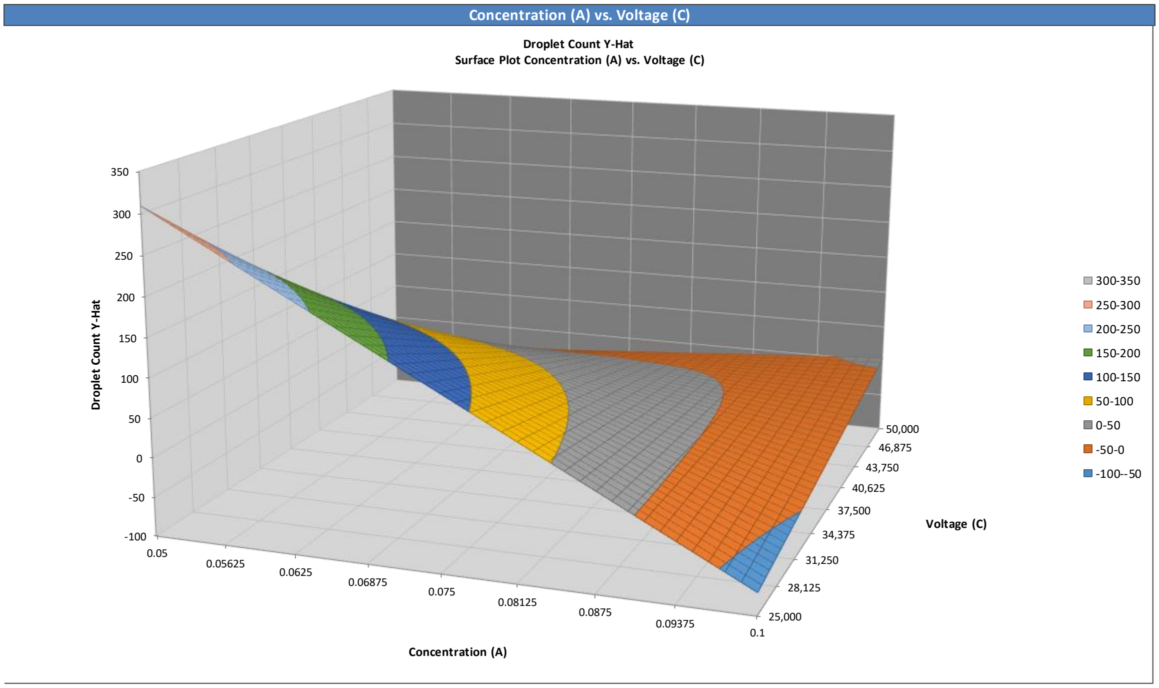

Figure 157: Surface Chart - Concentration vs Voltage for Droplet Count h-hat (Rapeseed oil, Polysorbate 20, 19ga Capillary)

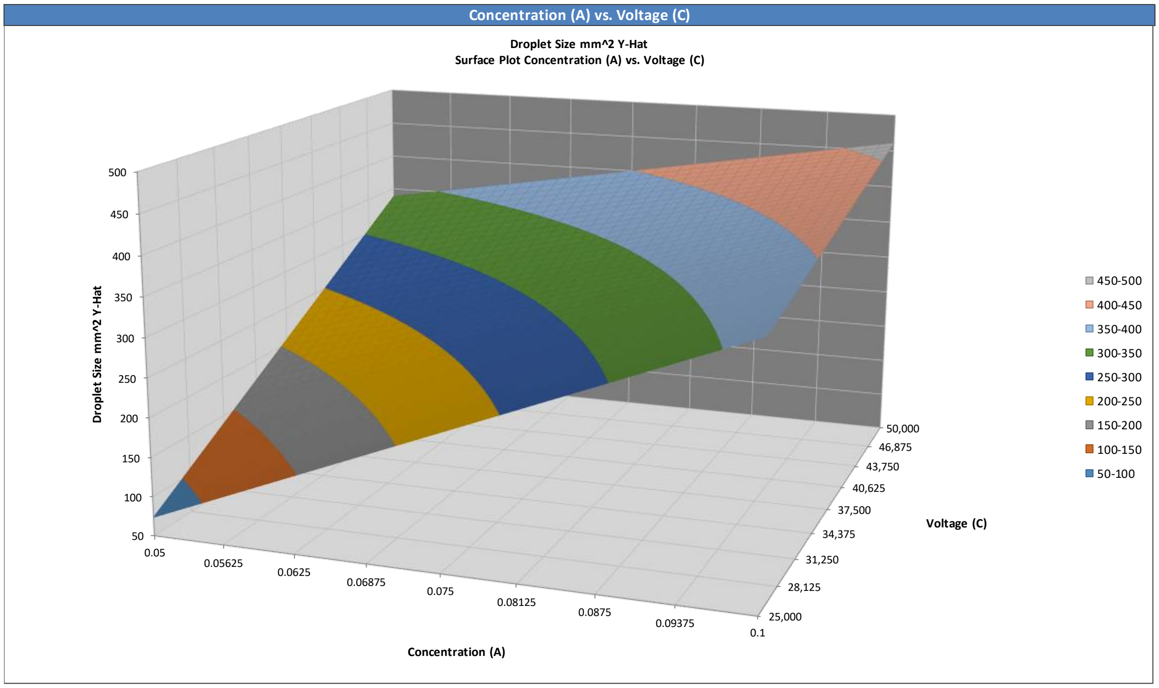

Figure 158: Surface Chart - Concentration vs Voltage for Droplet Size h-hat (Rapeseed oil, Polysorbate 20, 19ga Capillary)

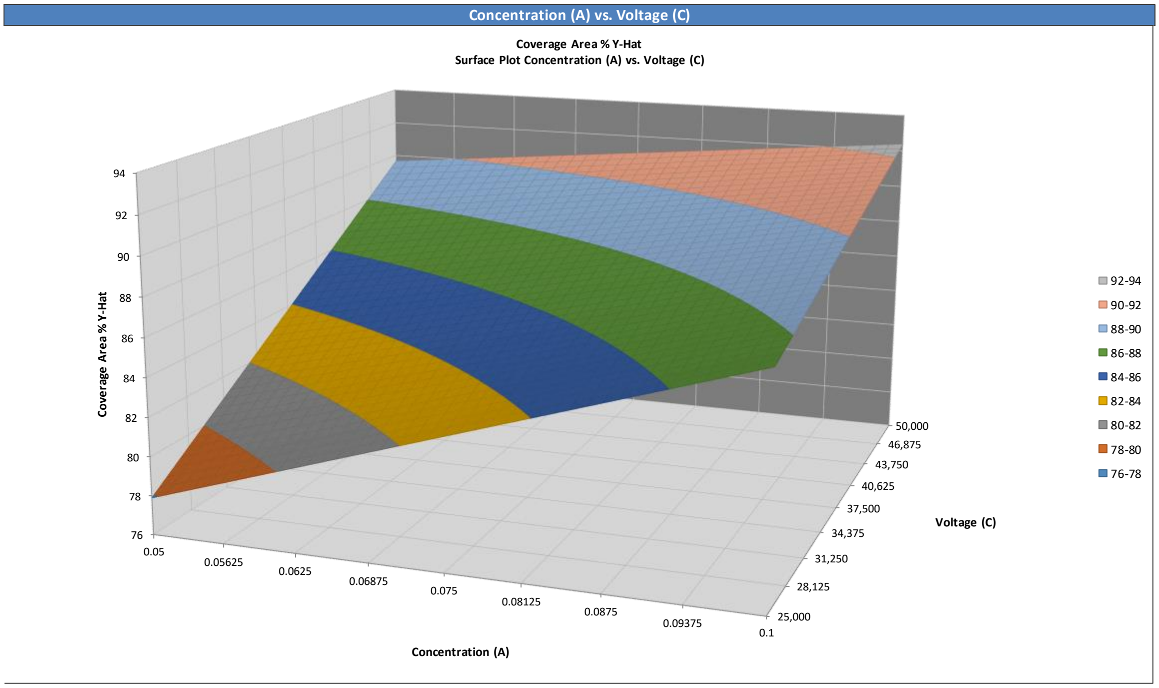

Figure 159: Surface Chart - Concentration vs Voltage for Coverage Area h-hat (Rapeseed oil, Polysorbate 20, 19ga Capillary

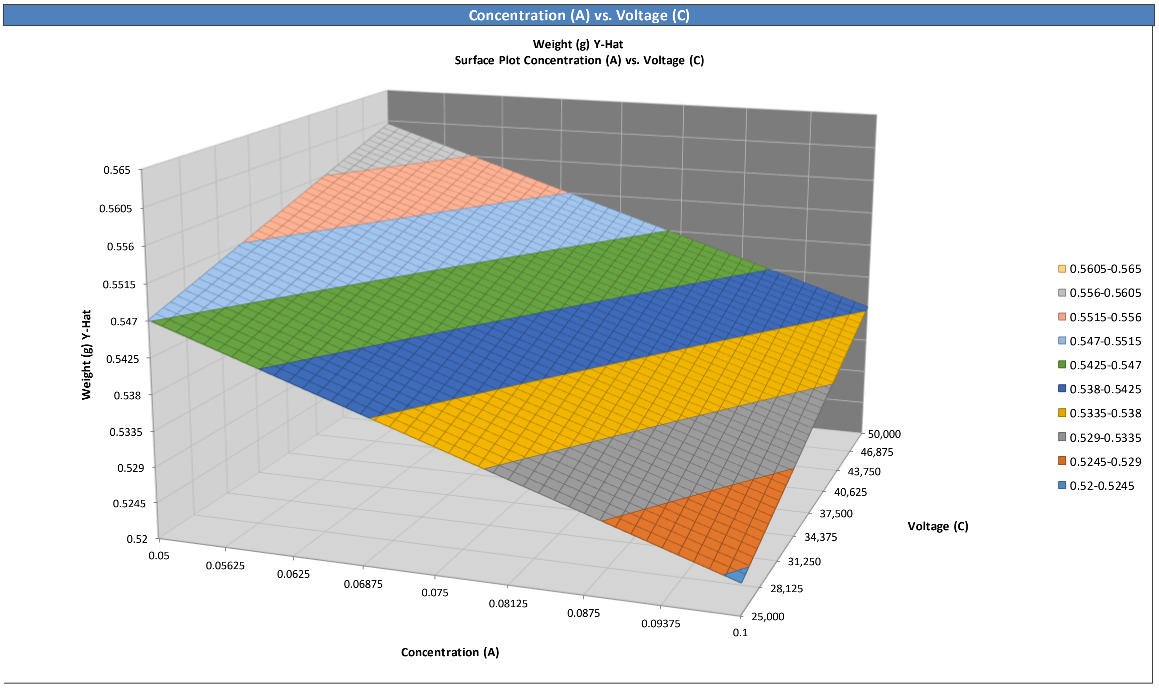

Figure 160: Surface Chart - Concentration vs Voltage for Sample Weight h-hat (Rapeseed oil, Polysorbate 20, 19ga Capillary)

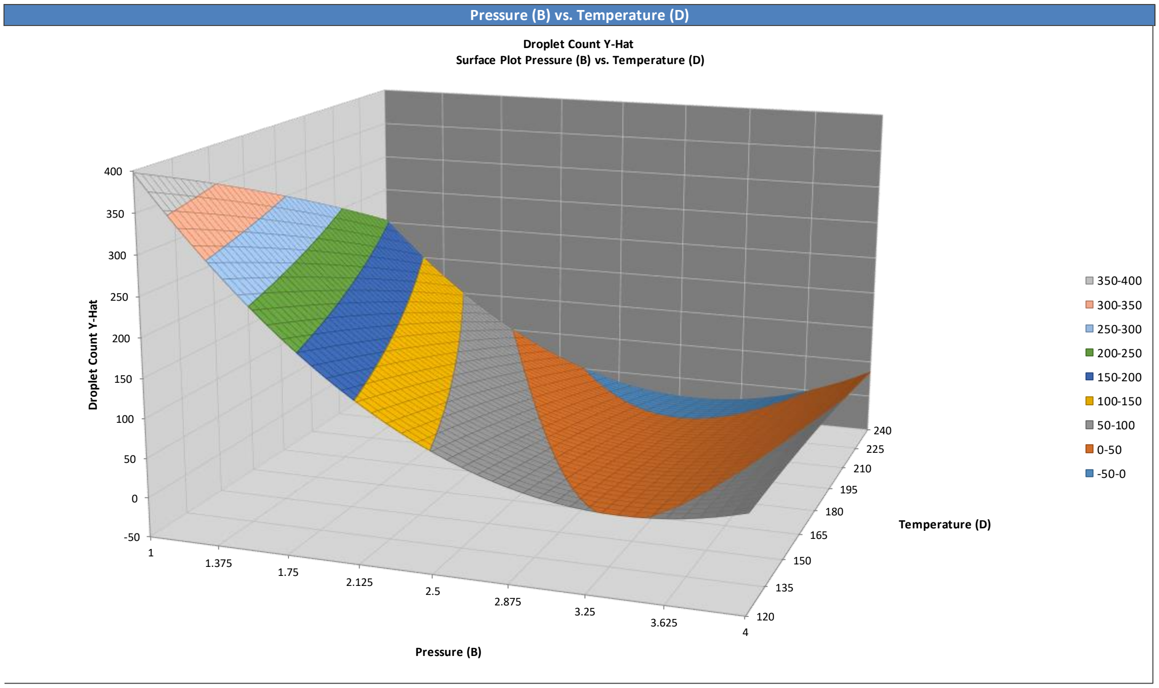

Figure 161: Surface Chart – Pressure vs Temperature for Droplet Count h-hat (Rapeseed oil, Polysorbate 20, 19ga Capillary)

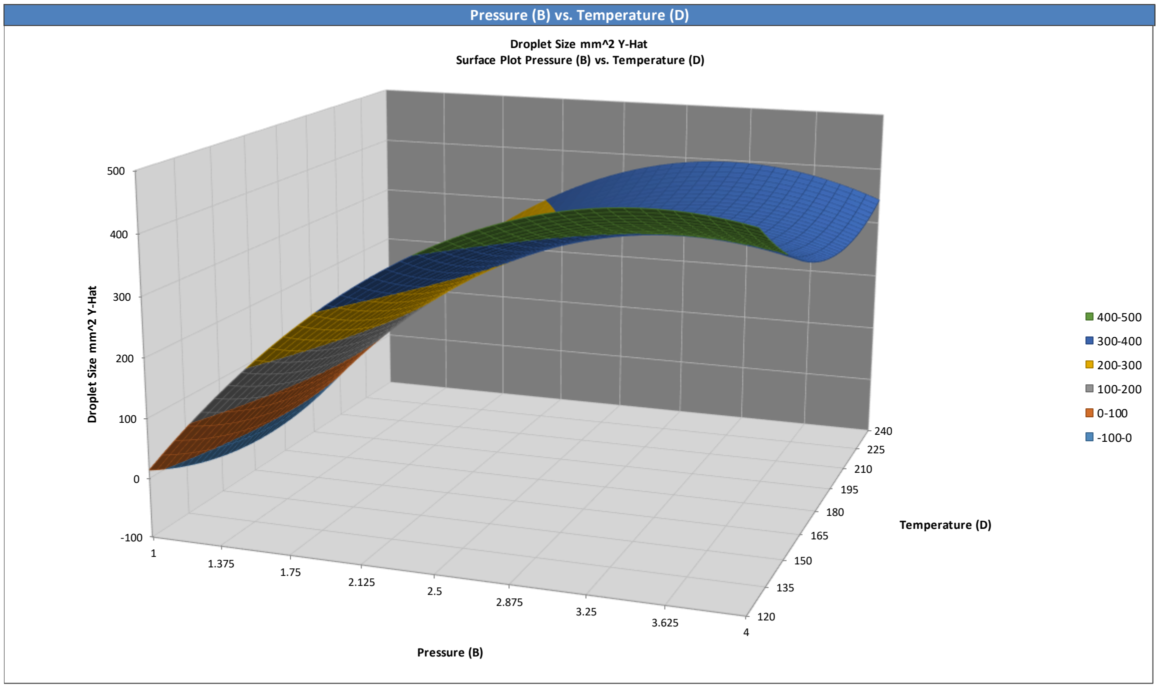

Figure 162: Surface Chart – Pressure vs Temperature for Droplet Size h-hat (Rapeseed oil, Polysorbate 20, 19ga Capillary)

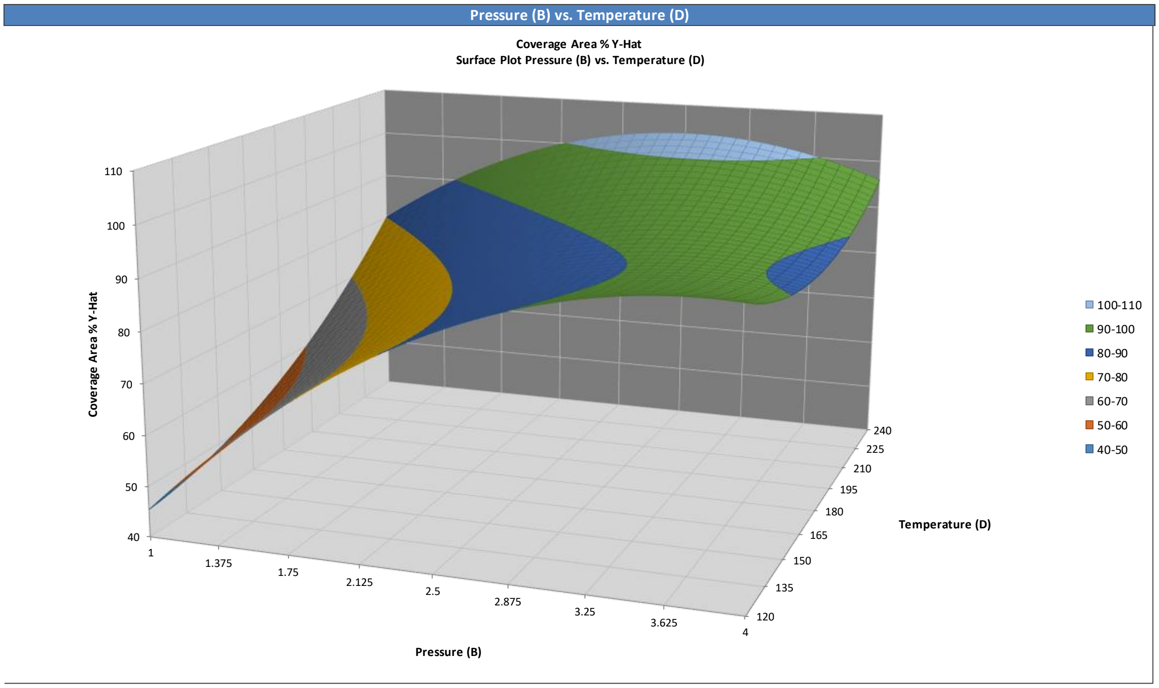

Figure 163: Surface Chart – Pressure vs Temperature for Coverage Area h-hat (Rapeseed oil, Polysorbate 20, 19ga Capillary)

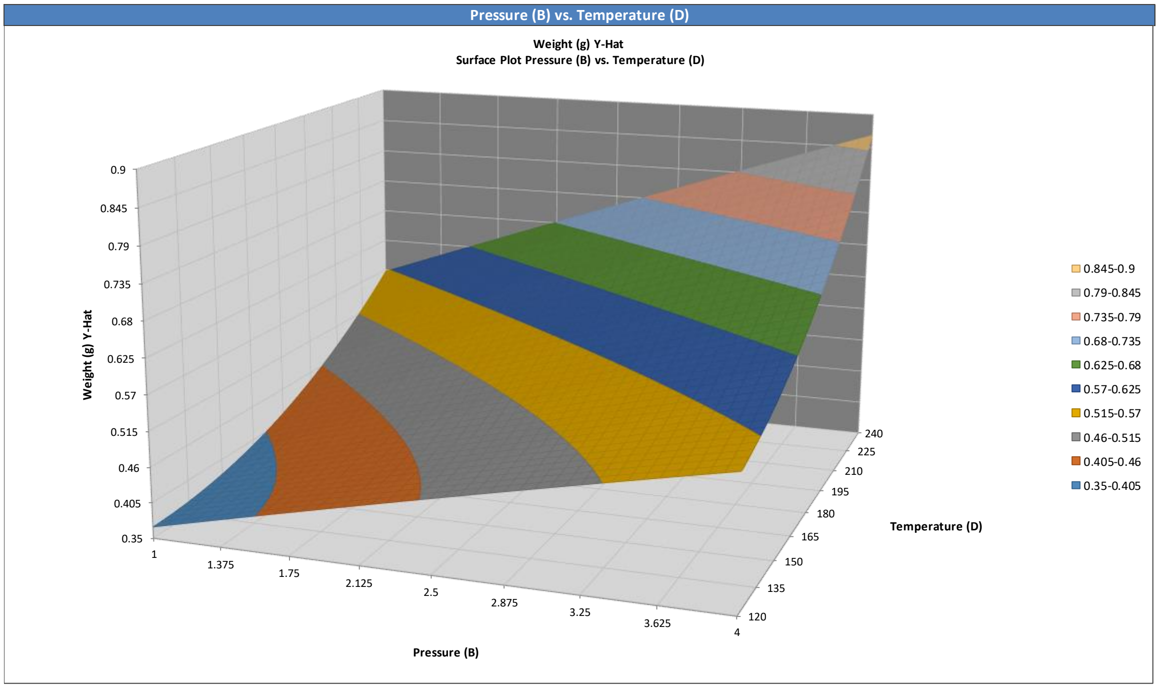

Figure 164: Surface Chart – Pressure vs Temperature for Sample Weight h-hat (Rapeseed oil, Polysorbate 20, 19ga Capillary)

5.3.4. Polysorbate 20 with 22 Gauge Capillary

Table 19: Main Effects Plot for Rapeseed Oil & Polysorbate 20 @ 22ga Capillary

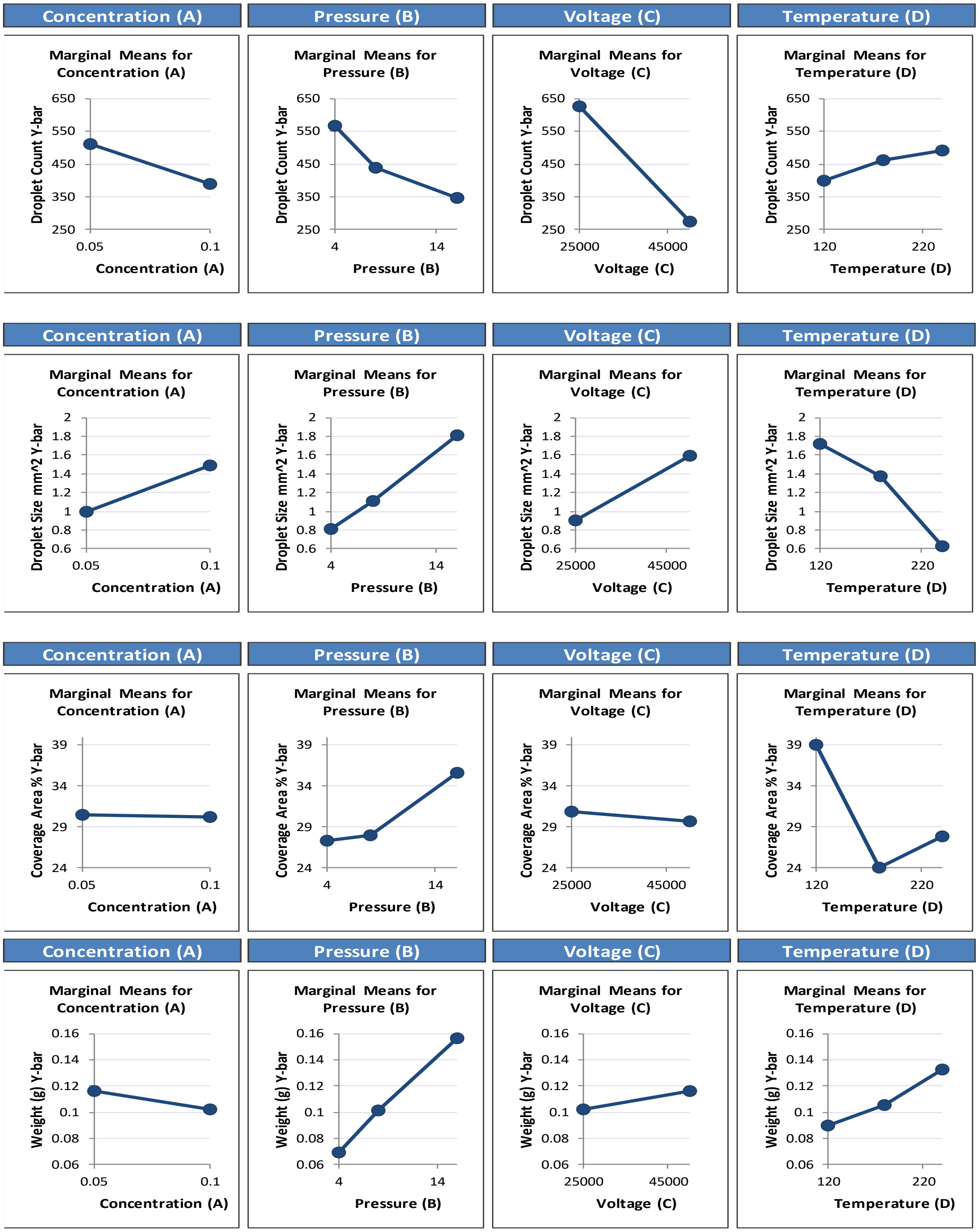

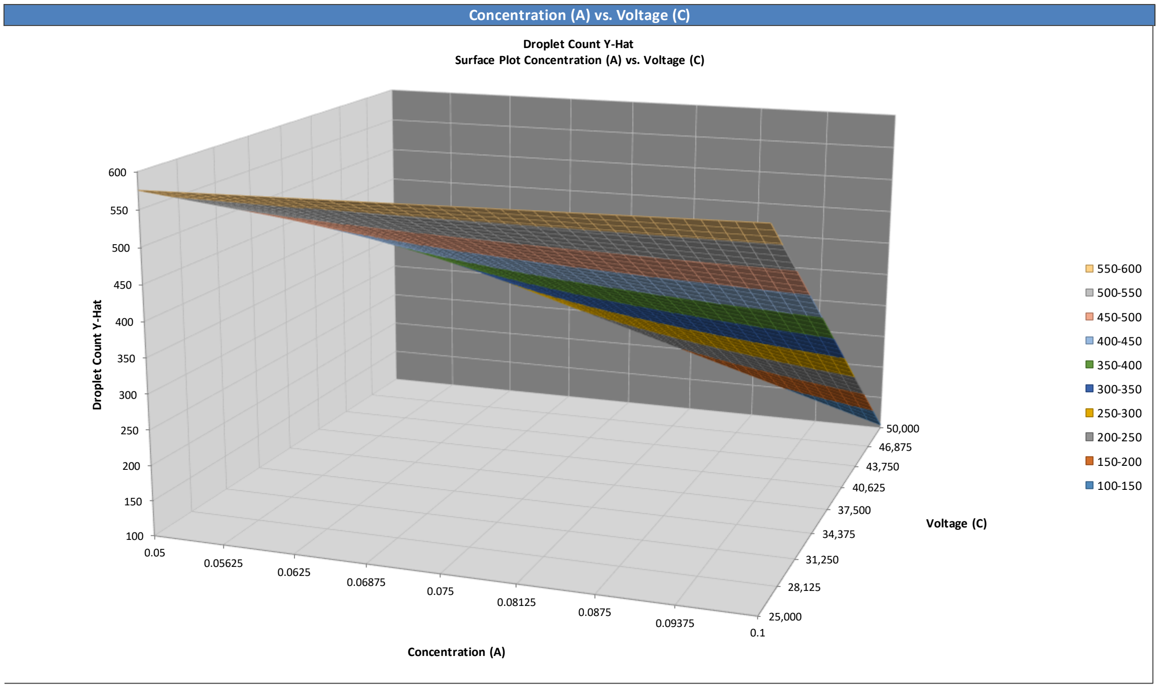

Figure 165: Surface Chart - Concentration vs Voltage for Droplet Count h-hat (Rapeseed oil, Polysorbate 20, 22ga Capillary)

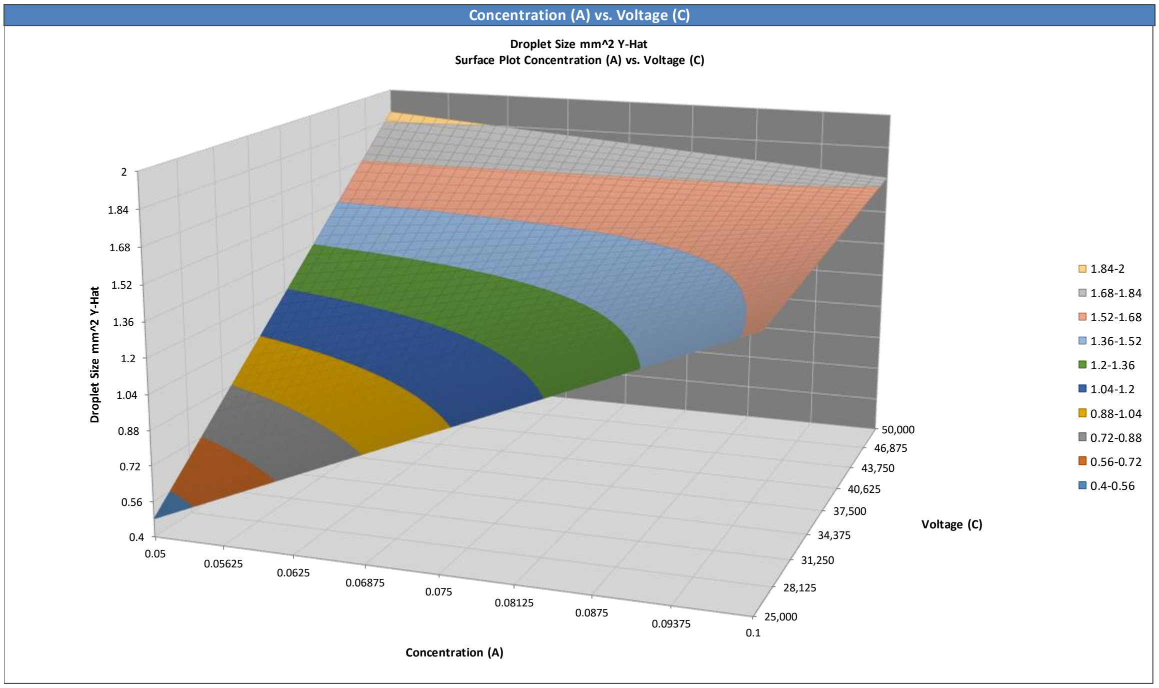

Figure 166: Surface Chart - Concentration vs Voltage for Droplet Size h-hat (Rapeseed oil, Polysorbate 20, 22ga Capillary)

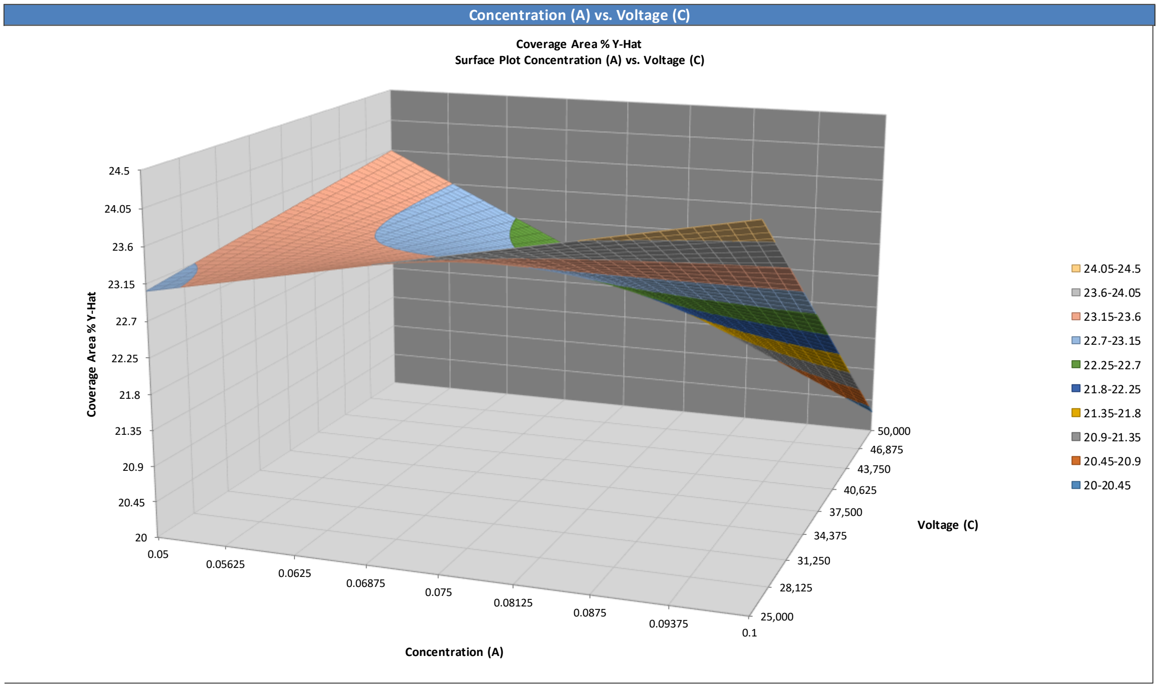

Figure 167: Surface Chart - Concentration vs Voltage for Coverage Area h-hat (Rapeseed oil, Polysorbate 20, 22ga Capillary)

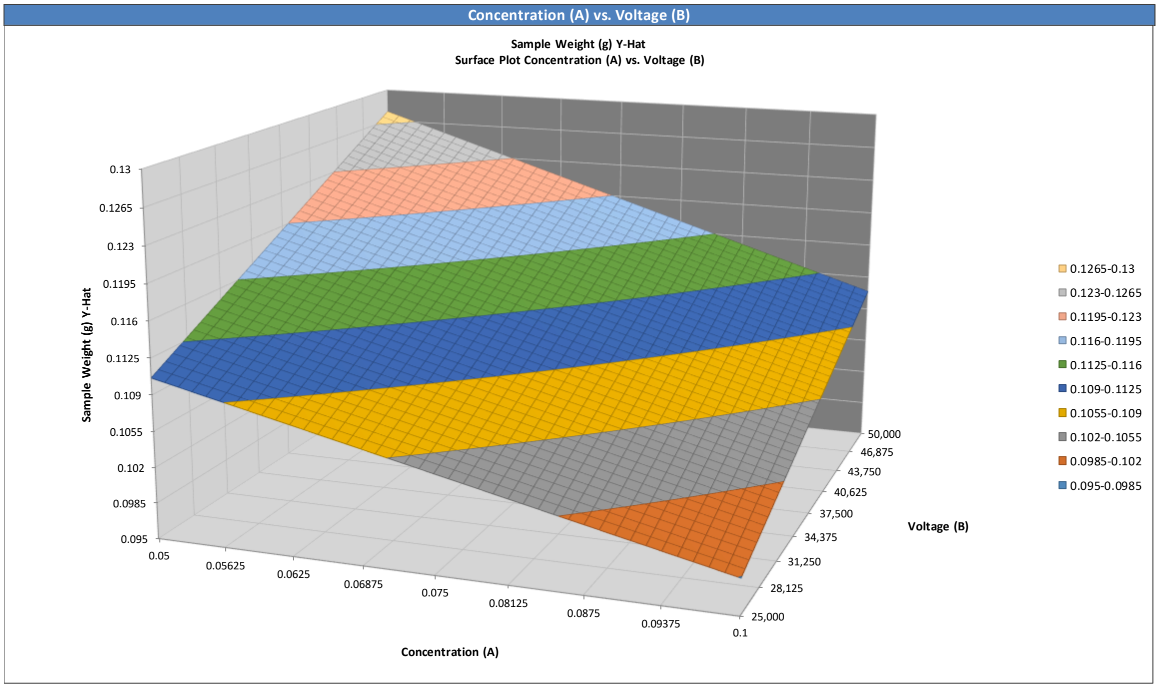

Figure 168: Surface Chart - Concentration vs Voltage for Sample Weight h-hat (Rapeseed oil, Polysorbate 20, 22ga Capillary)

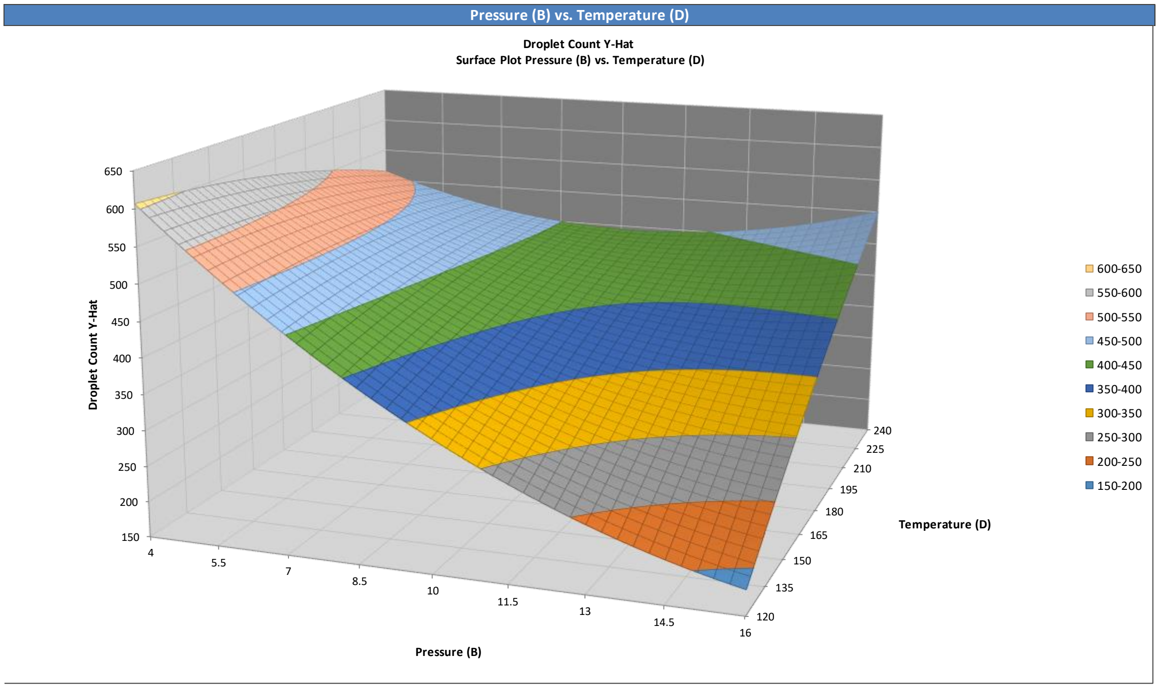

Figure 169: Surface Chart – Pressure vs Temperature for Droplet Count h-hat (Rapeseed oil, Polysorbate 20, 22ga Capillary)

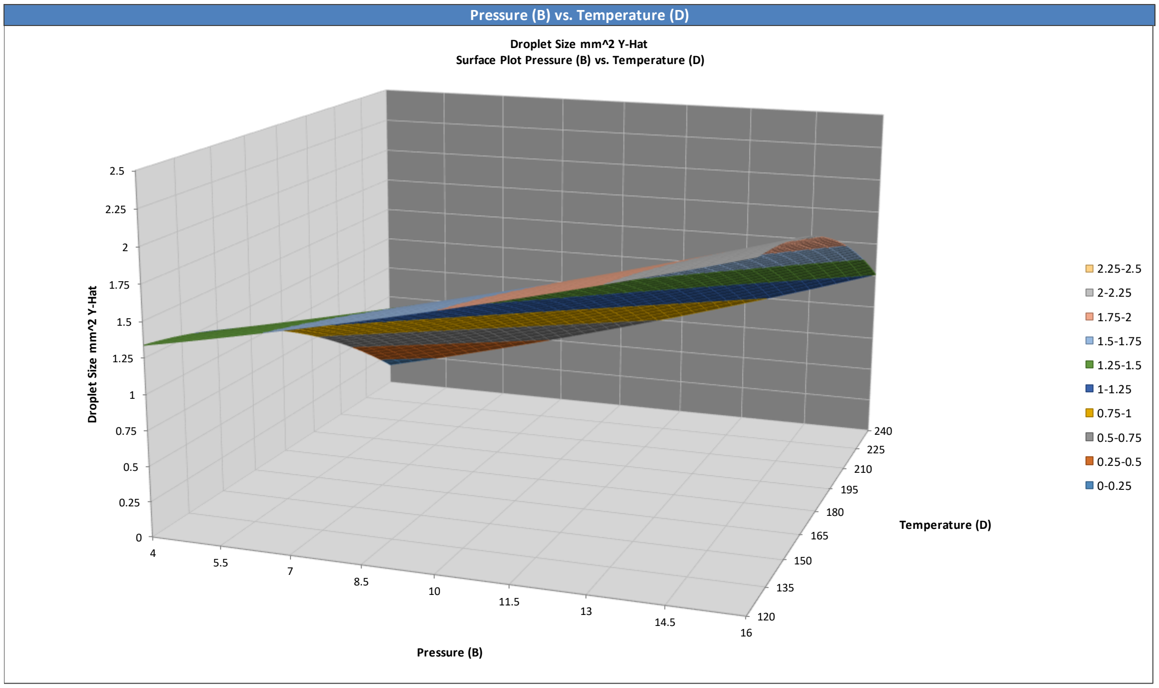

Figure 170: Surface Chart – Pressure vs Temperature for Droplet Size h-hat (Rapeseed oil, Polysorbate 20, 22ga Capillary)

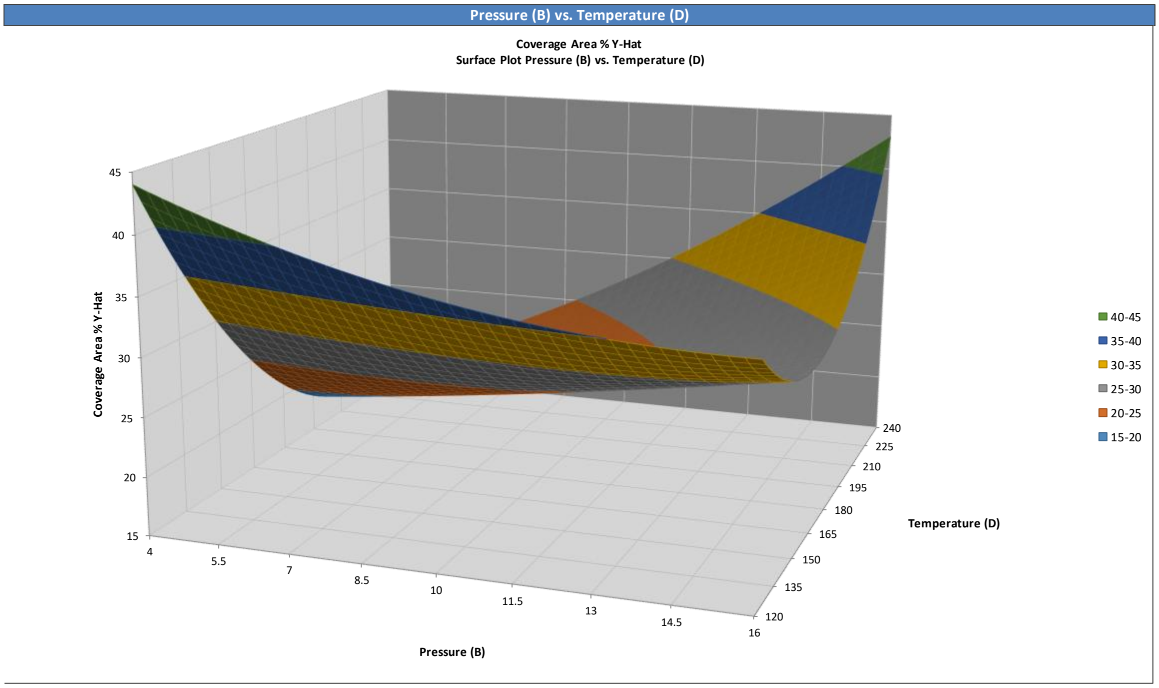

Figure 171: Surface Chart – Pressure vs Temperature for Coverage Area h-hat (Rapeseed oil, Polysorbate 20, 22ga Capillary)

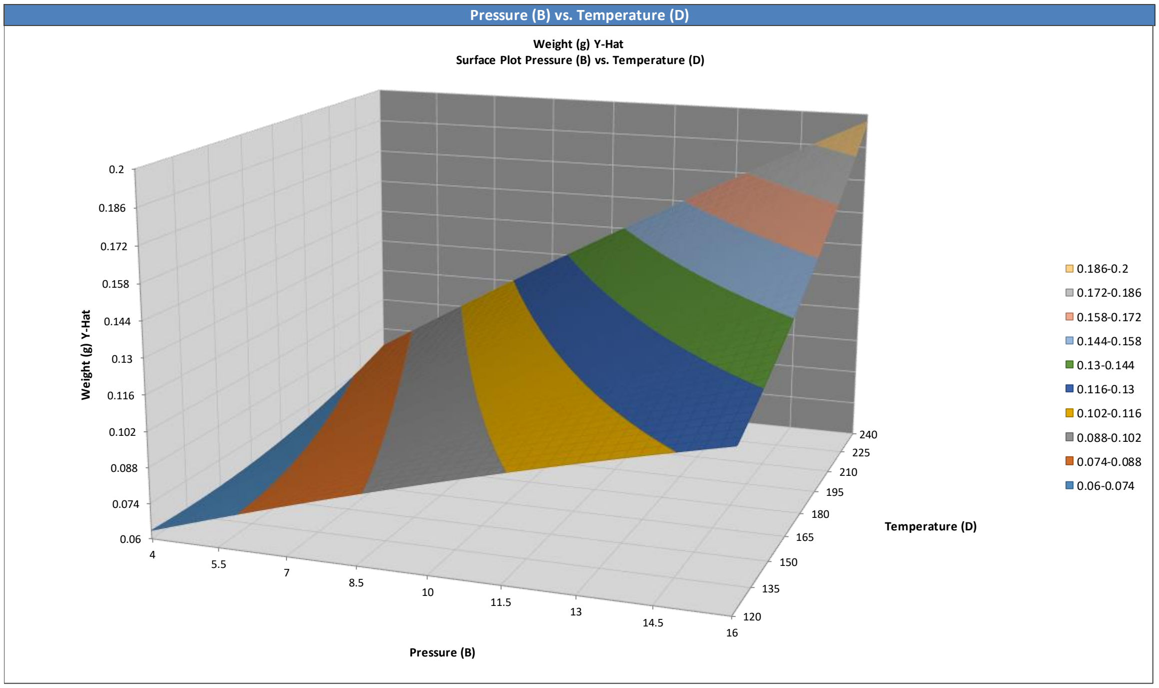

Figure 172: Surface Chart – Pressure vs Temperature for Sample Weight h-hat (Rapeseed oil, Polysorbate 20, 22ga Capillary)

5.3.5. Propylene Glycol with 19 Gauge Capillary

Table 20: Main Effects Plot for Rapeseed Oil & Propylene Glycol @ 19ga Capillary

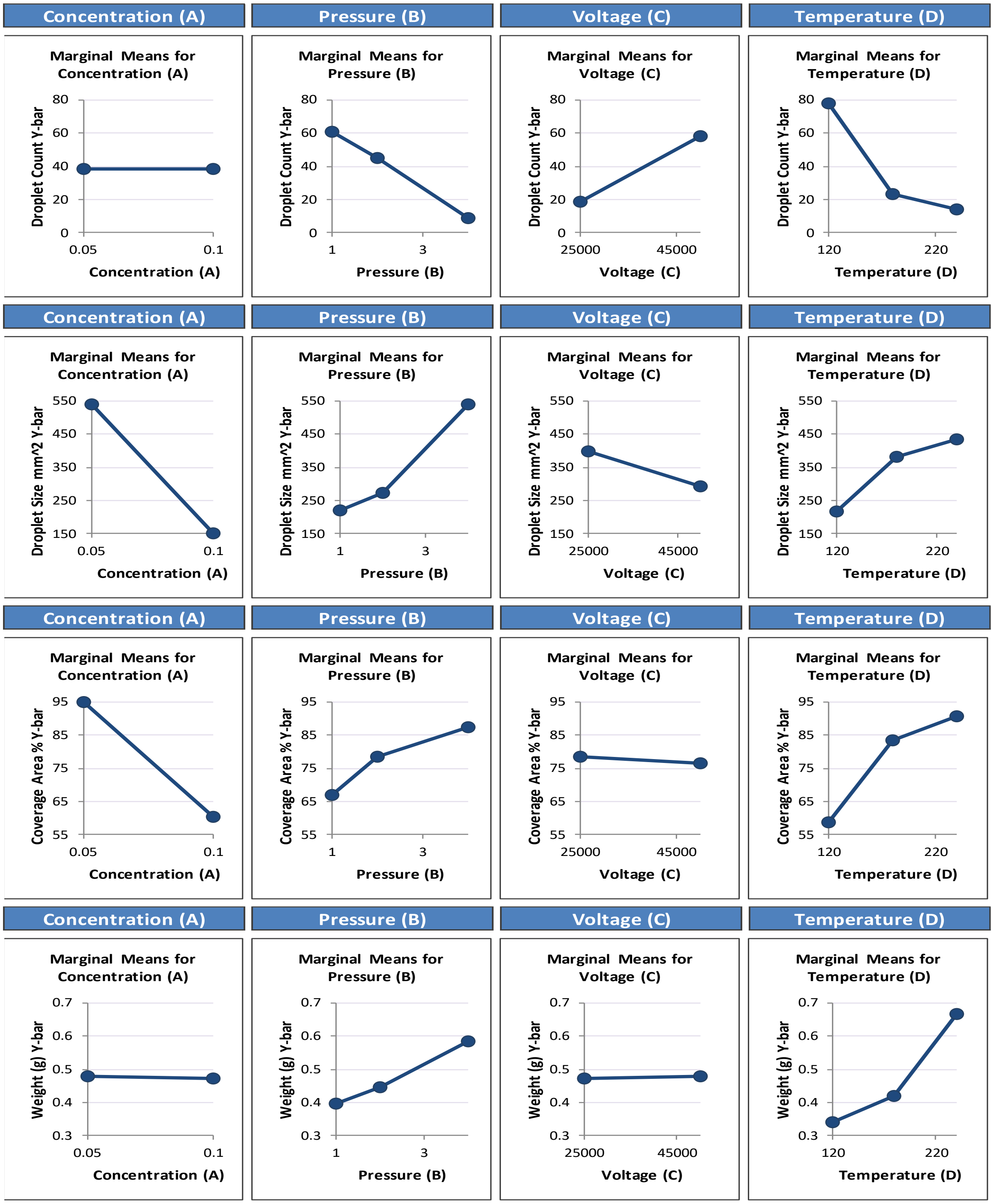

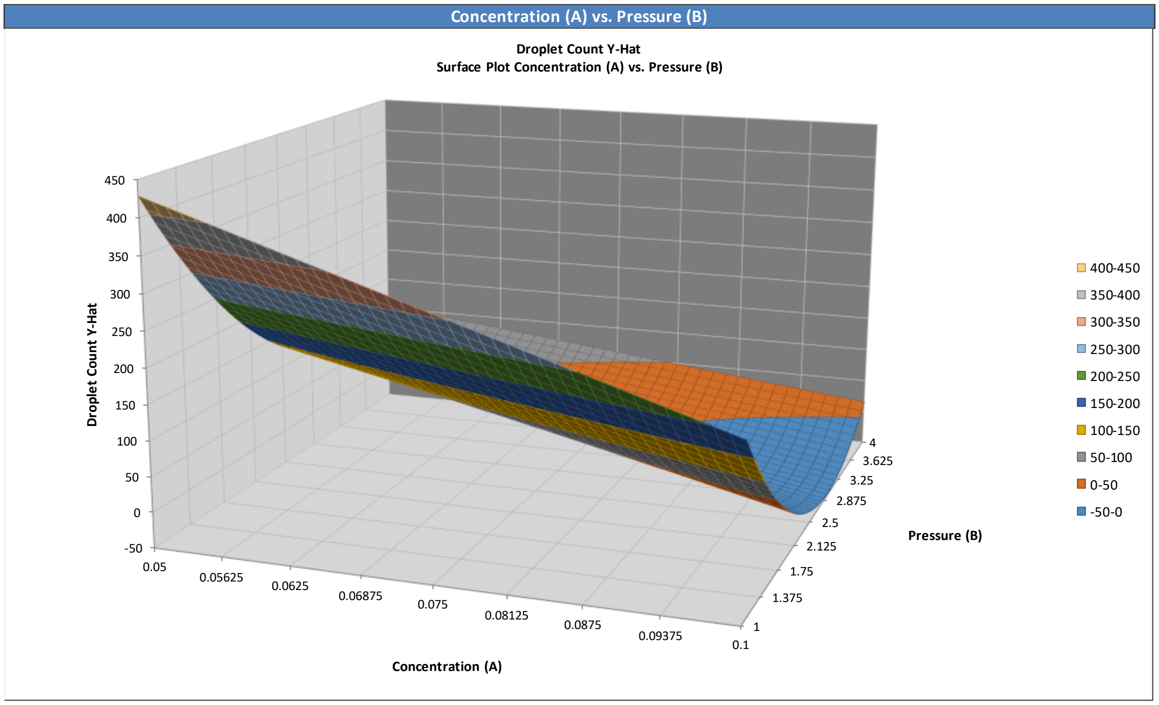

Figure 173: Surface Chart - Concentration vs Voltage for Droplet Count h-hat (Rapeseed oil, Propylene Glycol, 19ga Capillary)

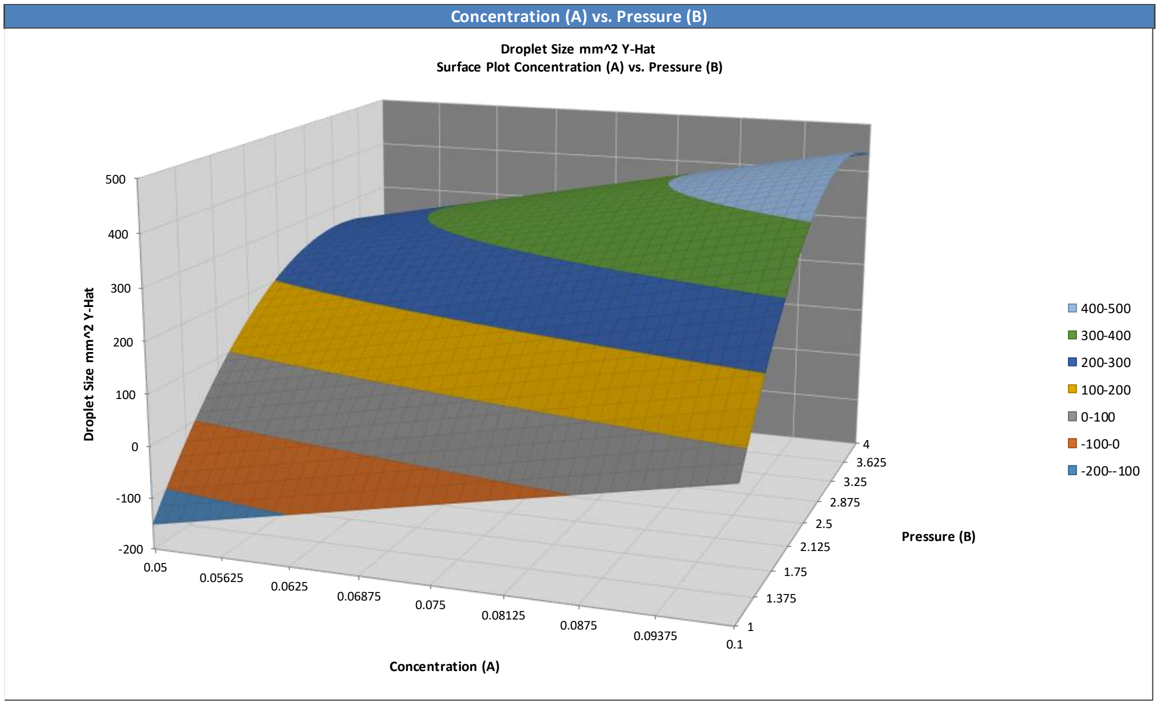

Figure 174: Surface Chart - Concentration vs Voltage for Droplet Size h-hat (Rapeseed oil, Propylene Glycol, 19ga Capillary)

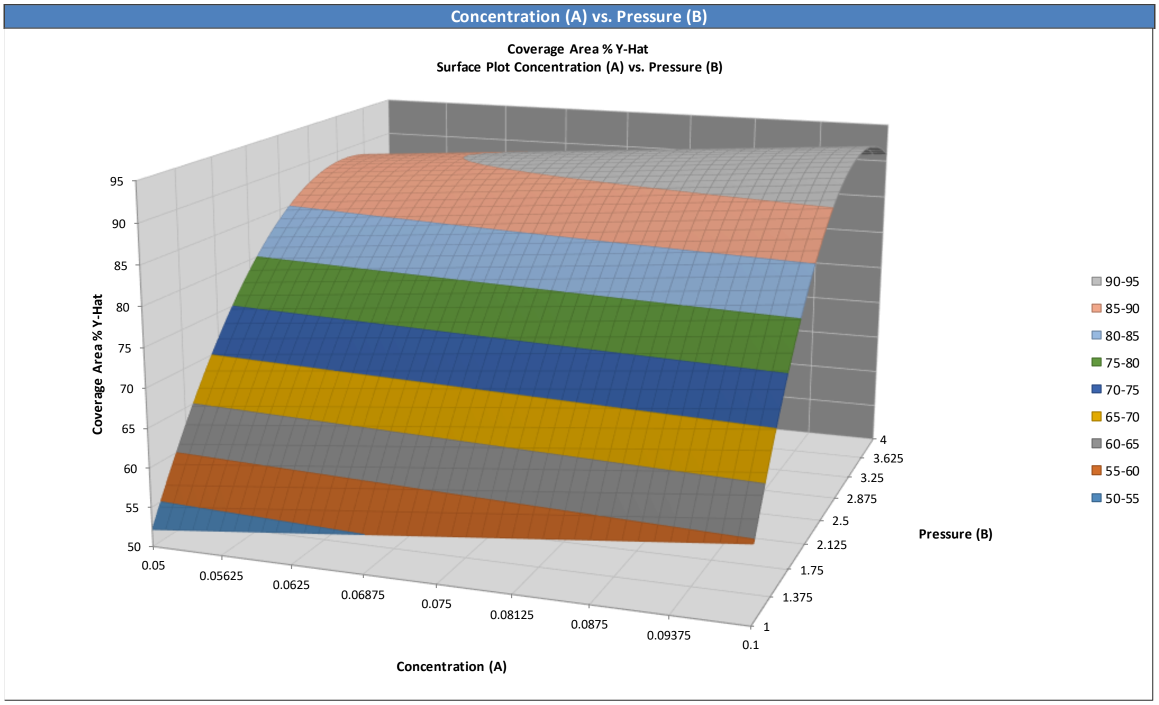

Figure 175: Surface Chart - Concentration vs Voltage for Coverage Area h-hat (Rapeseed oil, Propylene Glycol, 19ga Capillary)

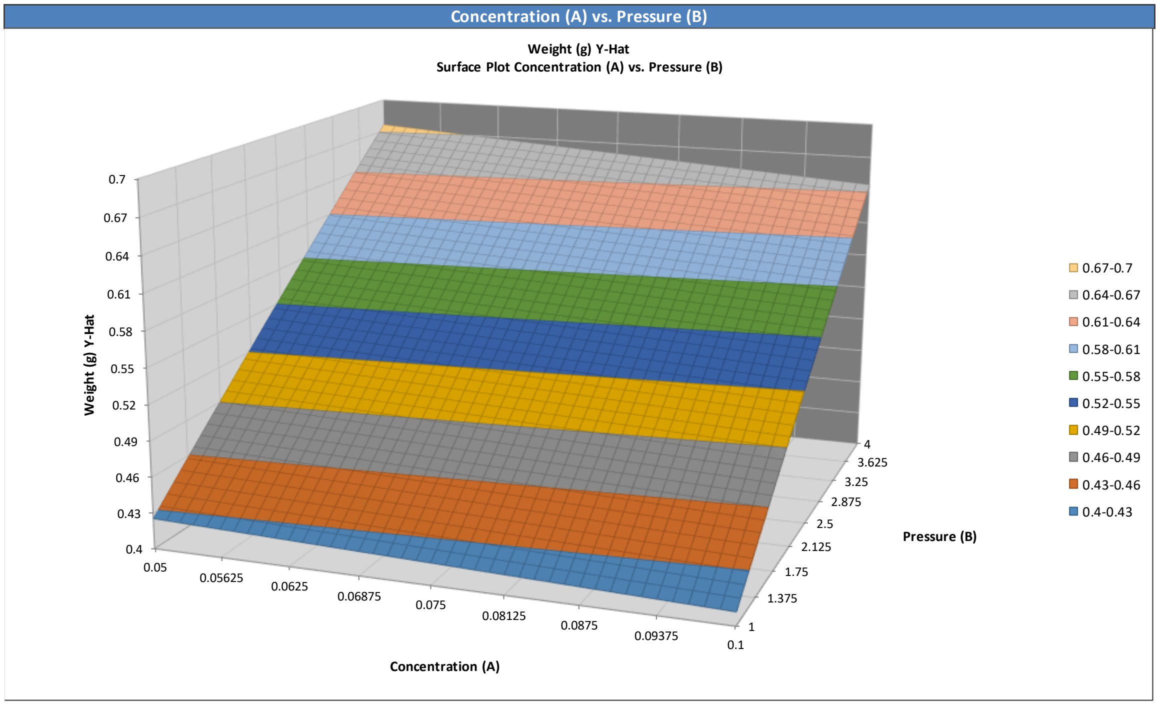

Figure 176: Surface Chart - Concentration vs Voltage for Sample Weight h-hat (Rapeseed oil, Propylene Glycol, 19ga Capillary)

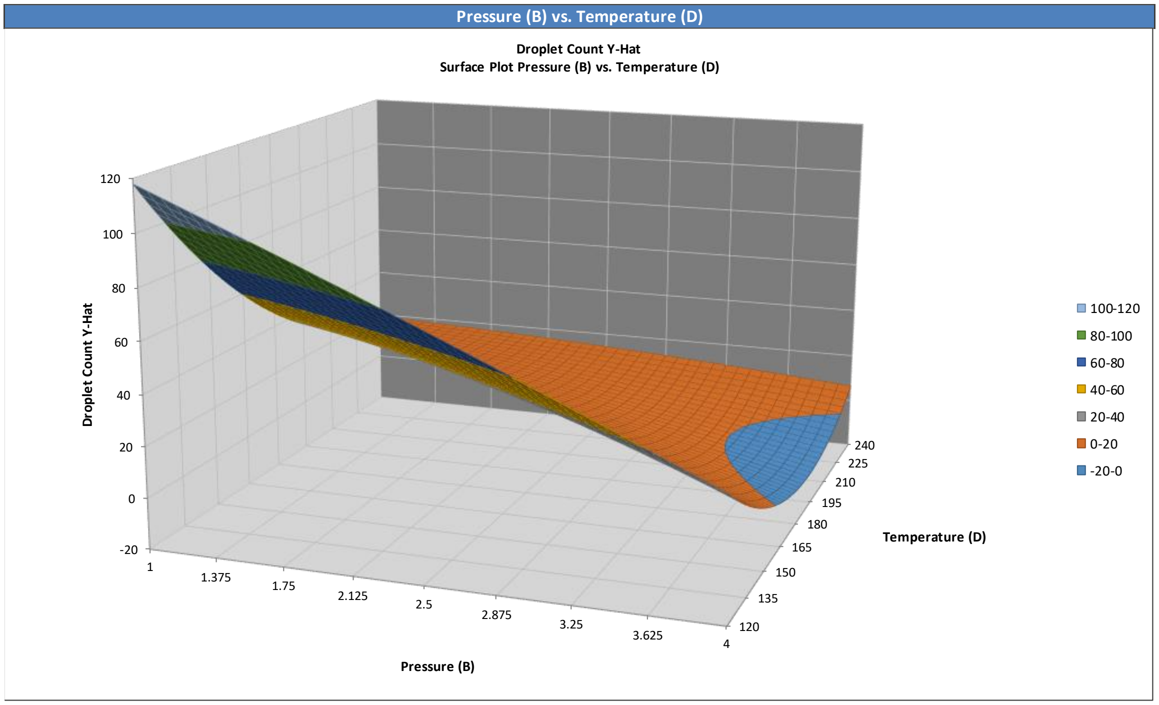

Figure 177: Surface Chart – Pressure vs Temperature for Droplet Count h-hat (Rapeseed oil, Propylene Glycol, 19ga Capillary)

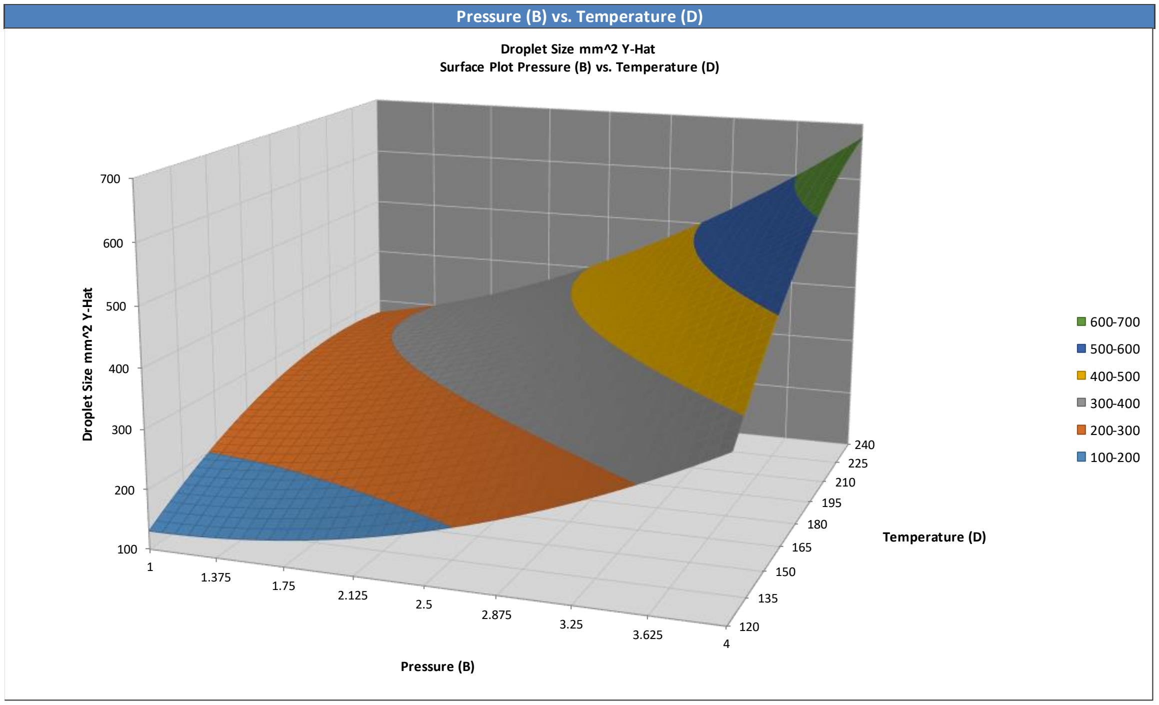

Figure 178: Surface Chart – Pressure vs Temperature for Droplet Size h-hat (Rapeseed oil, Propylene Glycol, 19ga Capillary)

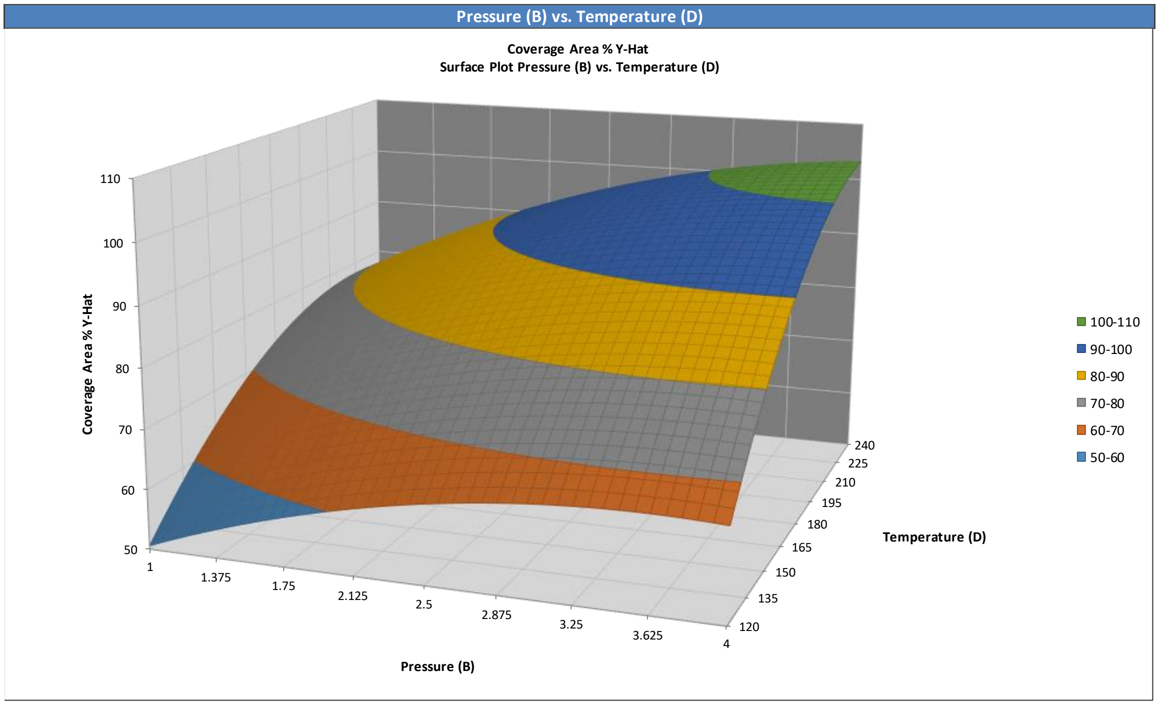

Figure 179: Surface Chart – Pressure vs Temperature for Coverage Area h-hat (Rapeseed oil, Propylene Glycol, 19ga Capillary)

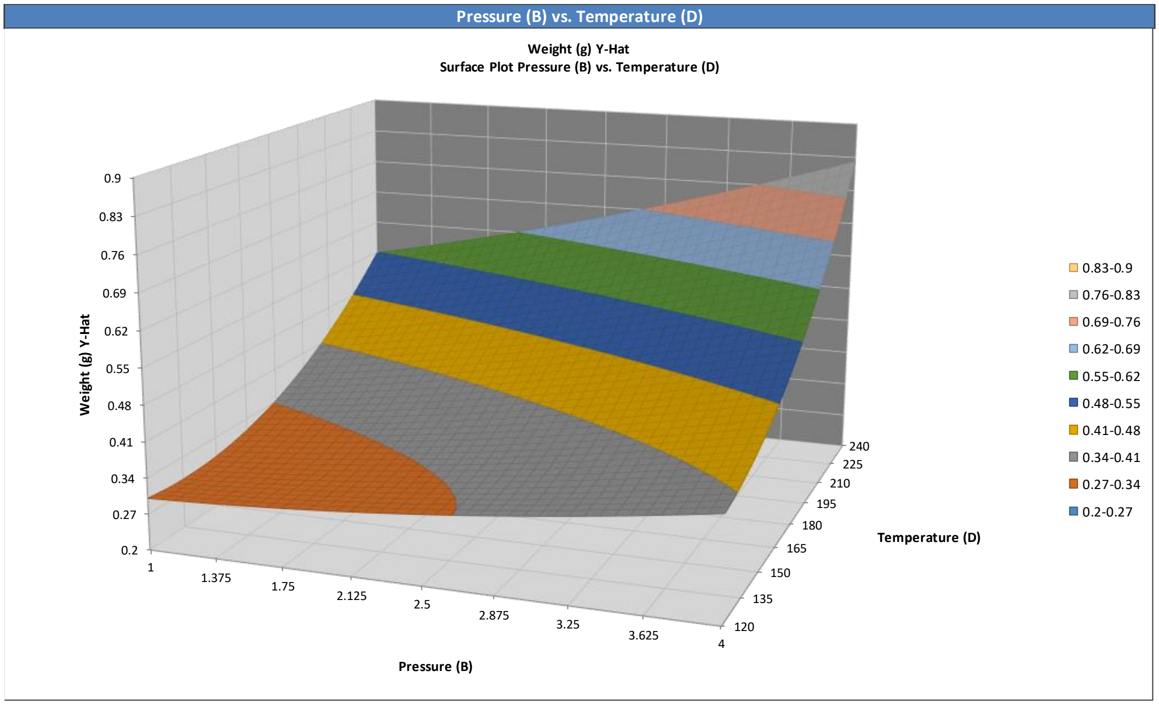

Figure 180: Surface Chart – Pressure vs Temperature for Sample Weight h-hat (Rapeseed oil, Propylene Glycol, 19ga Capillary)

5.3.6. Propylene Glycol with 22 Gauge Capillary

Table 21: Main Effects Plot for Rapeseed Oil & Propylene Glycol @ 22ga Capillary

Concentration (A) **Pressure (B)** **Voltage (C)** **Temperature (D)**

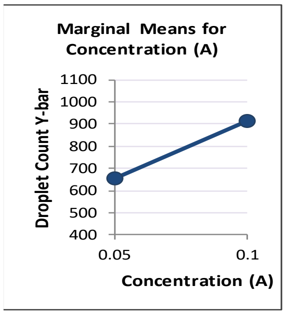

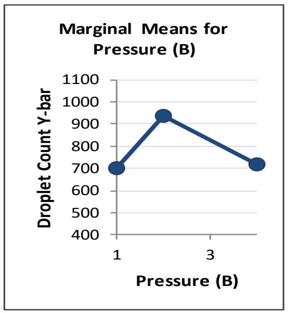

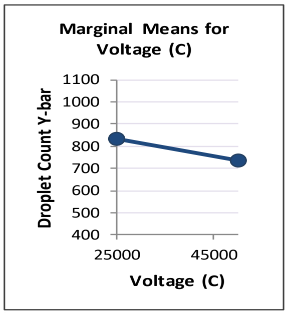

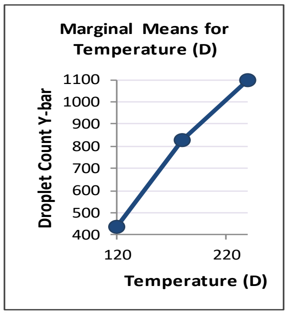

Concentration (A) **Pressure (B)** **Voltage (C)** **Temperature (D)**

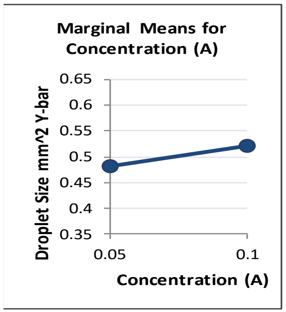

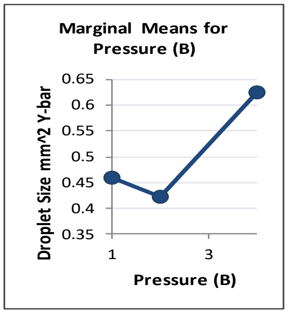

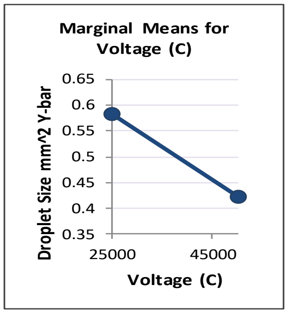

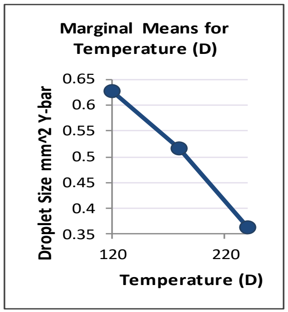

Concentration (A) **Pressure (B)** **Voltage (C)** **Temperature (D)**

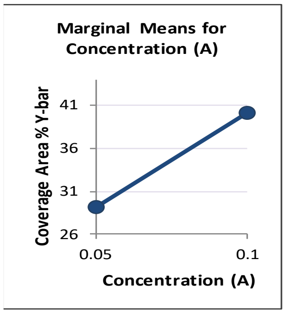

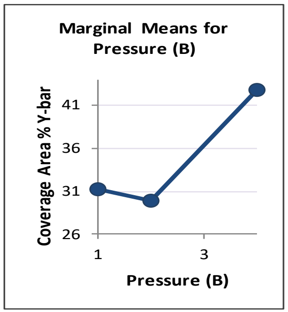

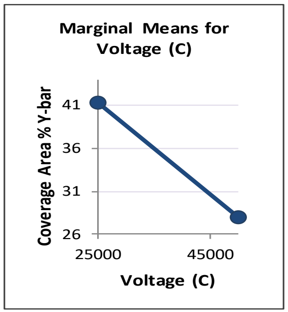

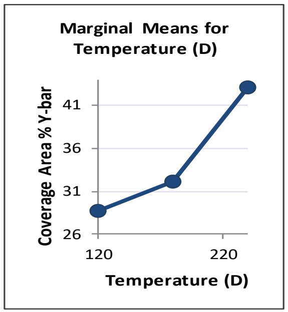

Concentration (A) **Pressure (B)** **Voltage (C)** **Temperature (D)**

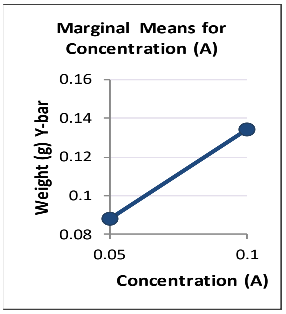

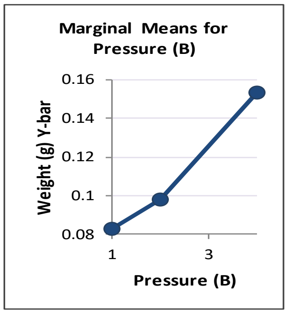

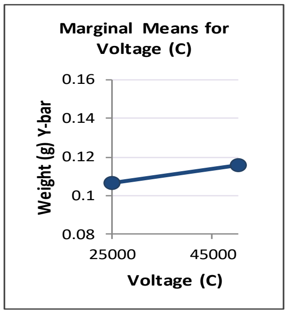

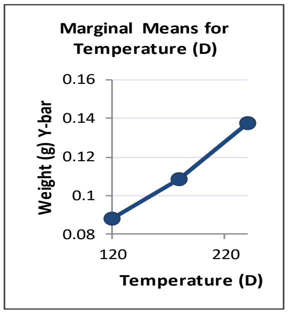

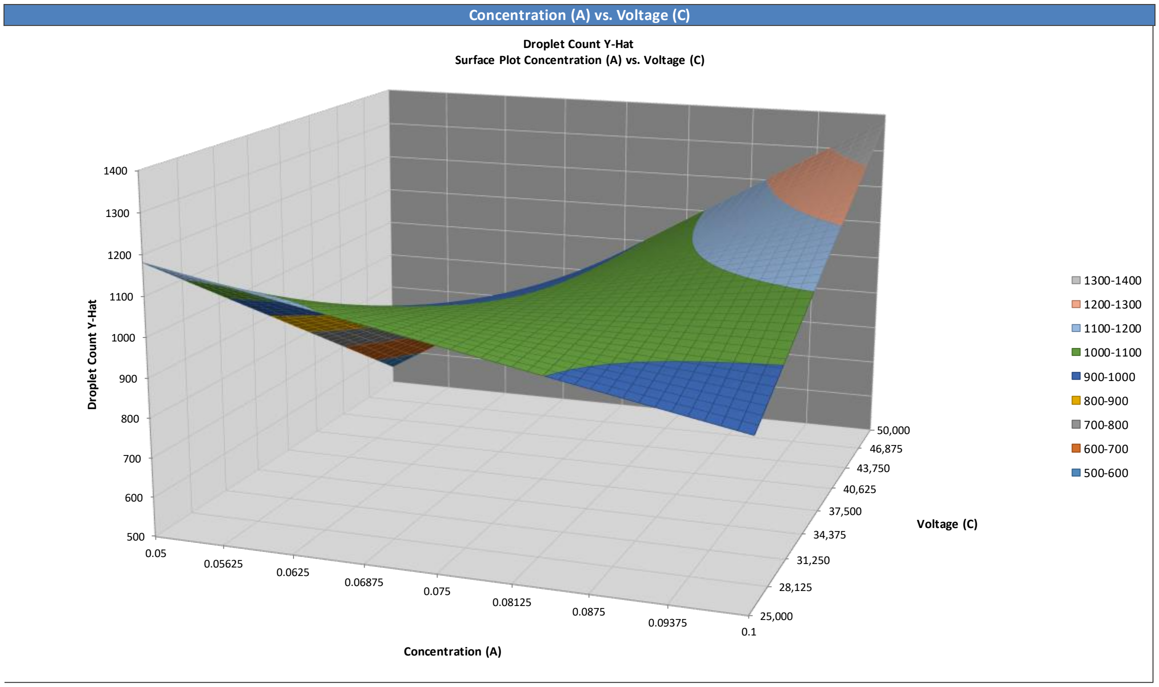

Figure 181: Surface Chart - Concentration vs Voltage for Droplet Count h-hat (Rapeseed oil, Propylene Glycol, 22ga Capillary)

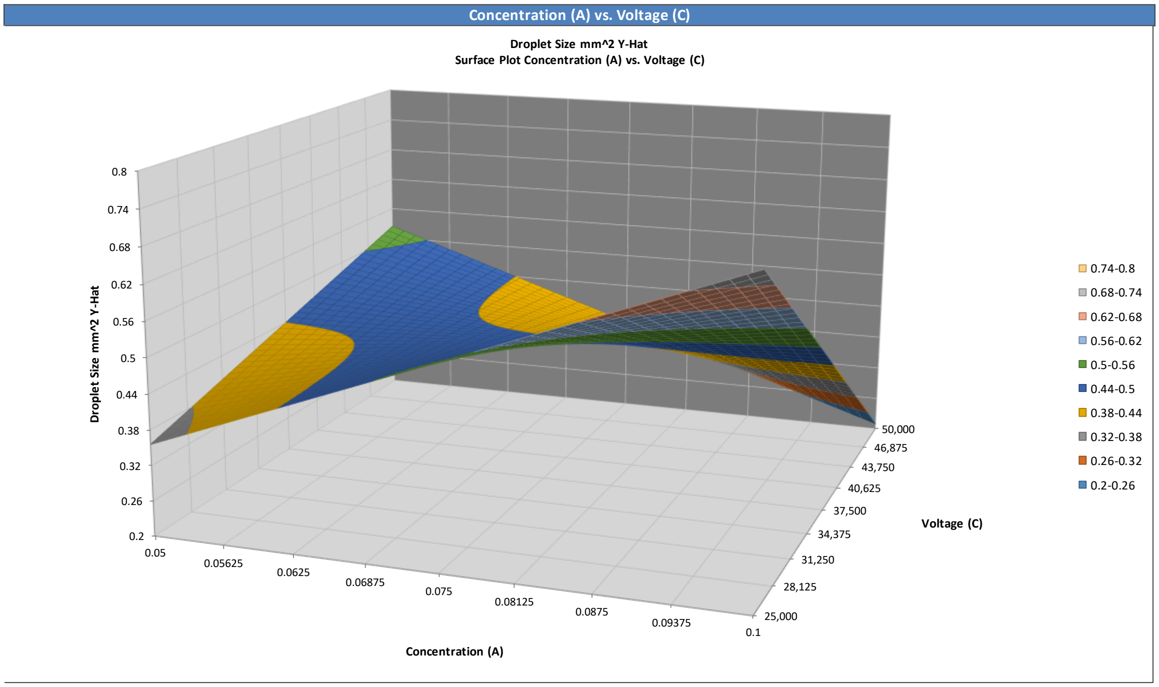

Figure 182: Surface Chart - Concentration vs Voltage for Droplet Size h-hat (Rapeseed oil, Propylene Glycol, 22ga Capillary)

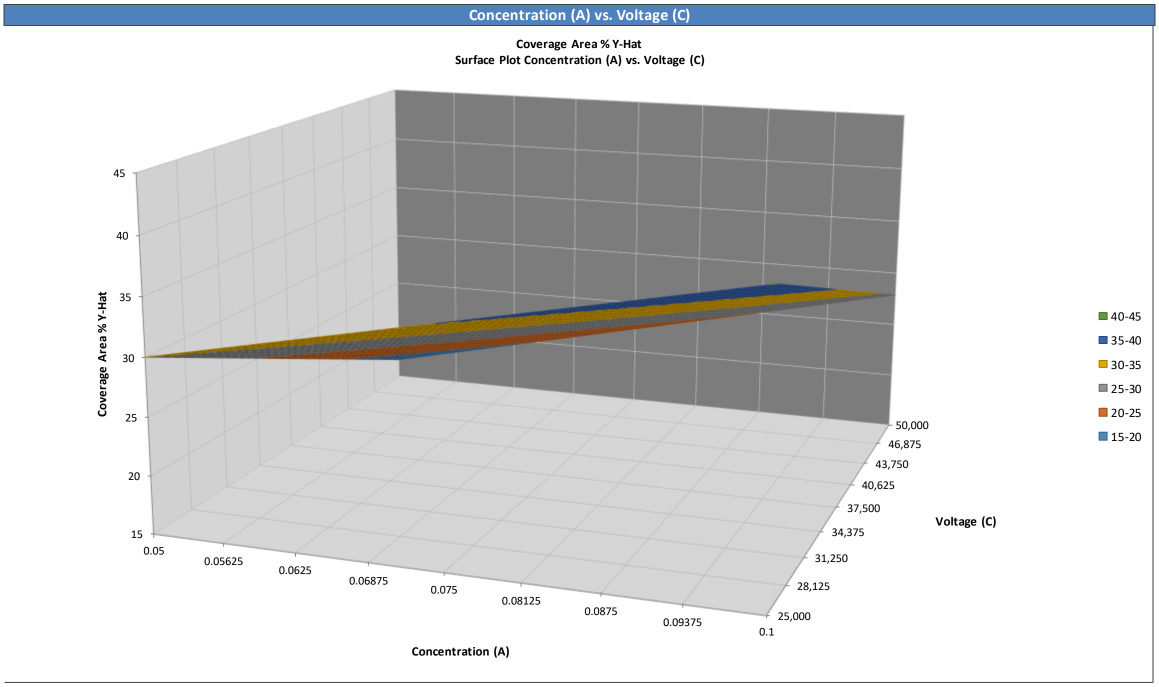

Figure 183: Surface Chart - Concentration vs Voltage for Coverage Area h-hat (Rapeseed oil, Propylene Glycol, 22ga Capillary)

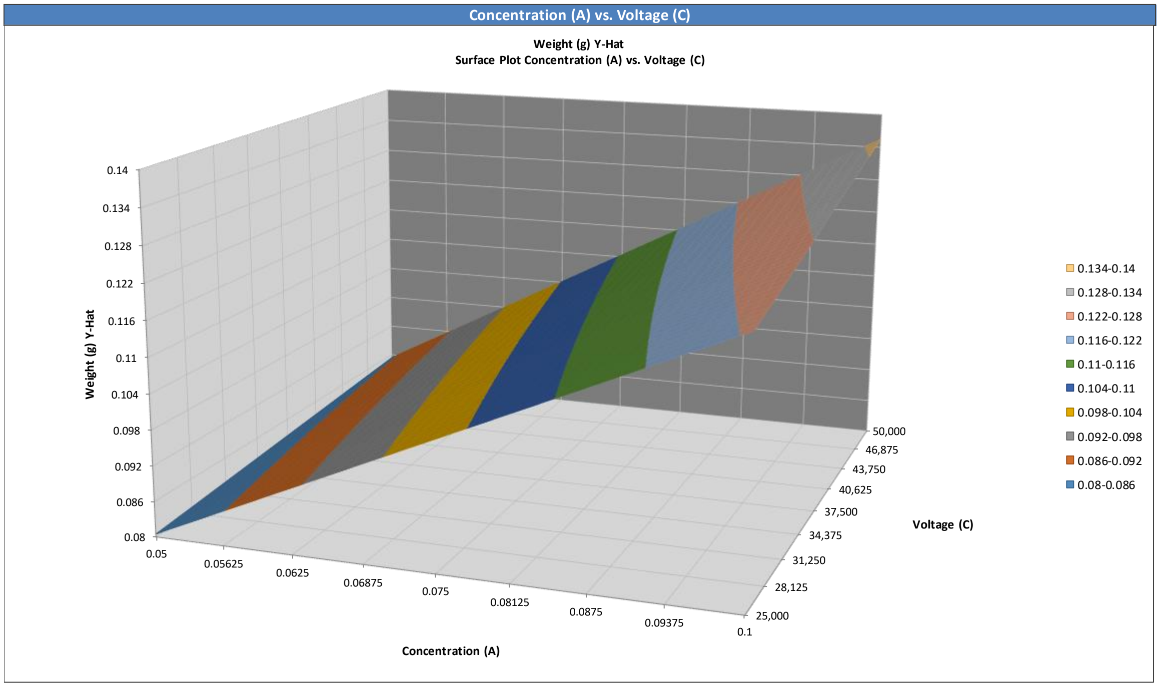

Figure 184: Surface Chart - Concentration vs Voltage for Sample Weight h-hat (Rapeseed oil, Propylene Glycol, 22ga Capillary)

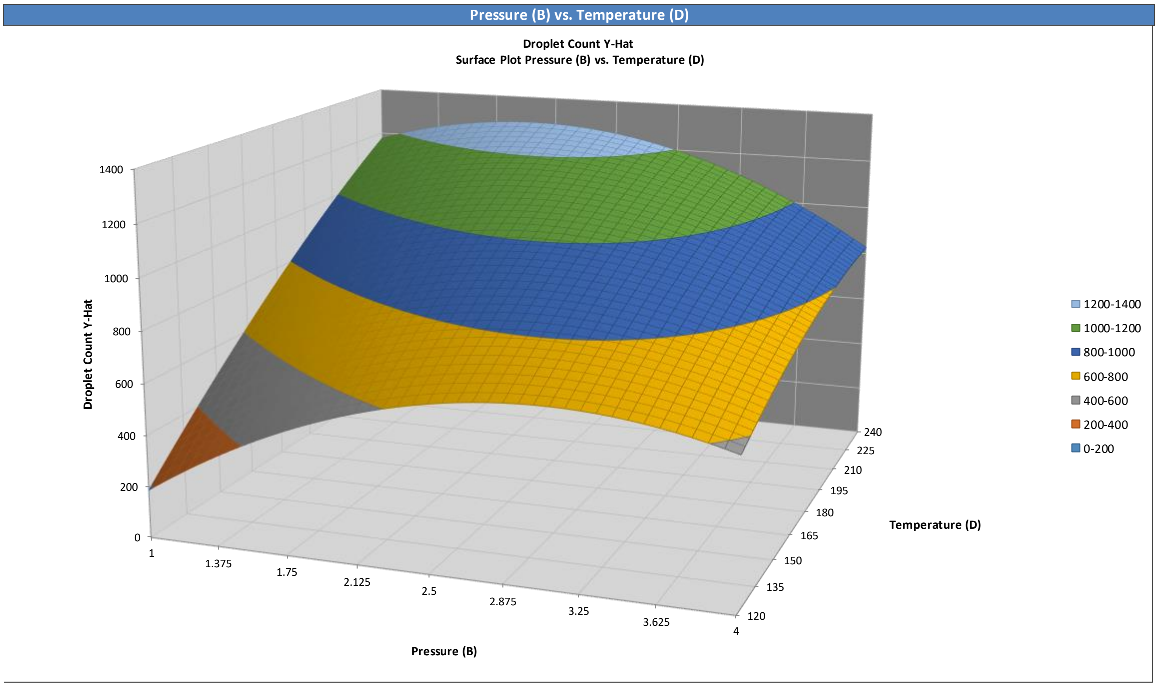

Figure 185: Surface Chart – Pressure vs Temperature for Droplet Count h-hat (Rapeseed oil, Propylene Glycol, 19ga Capillary)

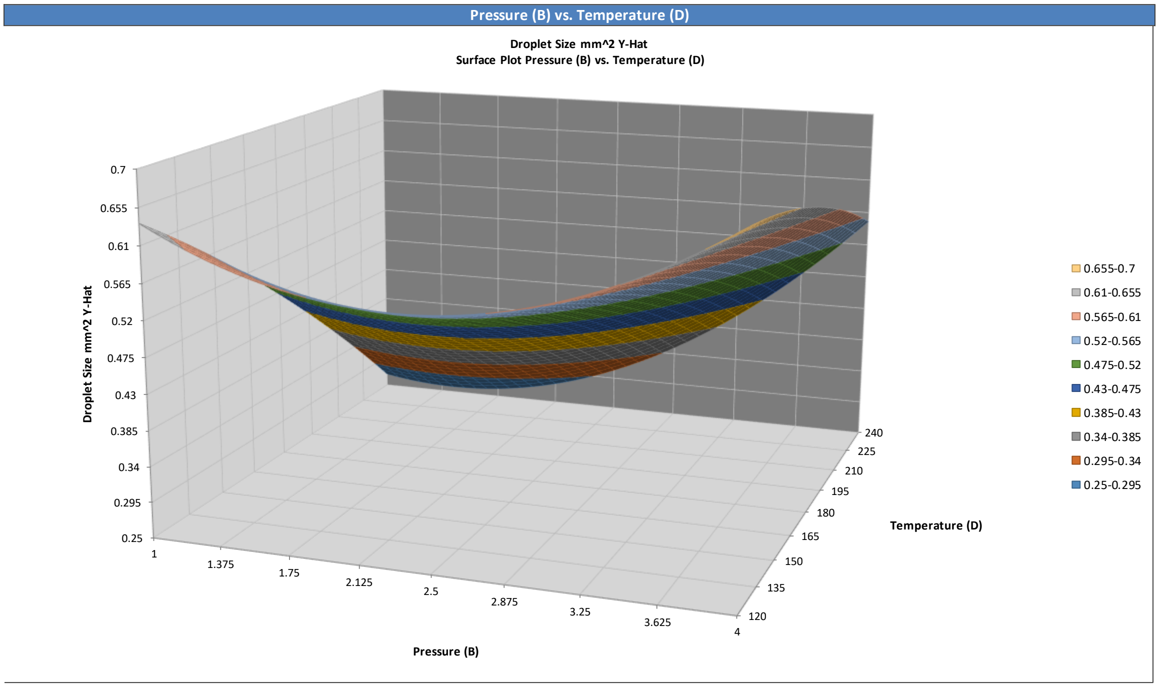

Figure 186: Surface Chart – Pressure vs Temperature for Droplet Size h-hat (Rapeseed oil, Propylene Glycol, 19ga Capillary)

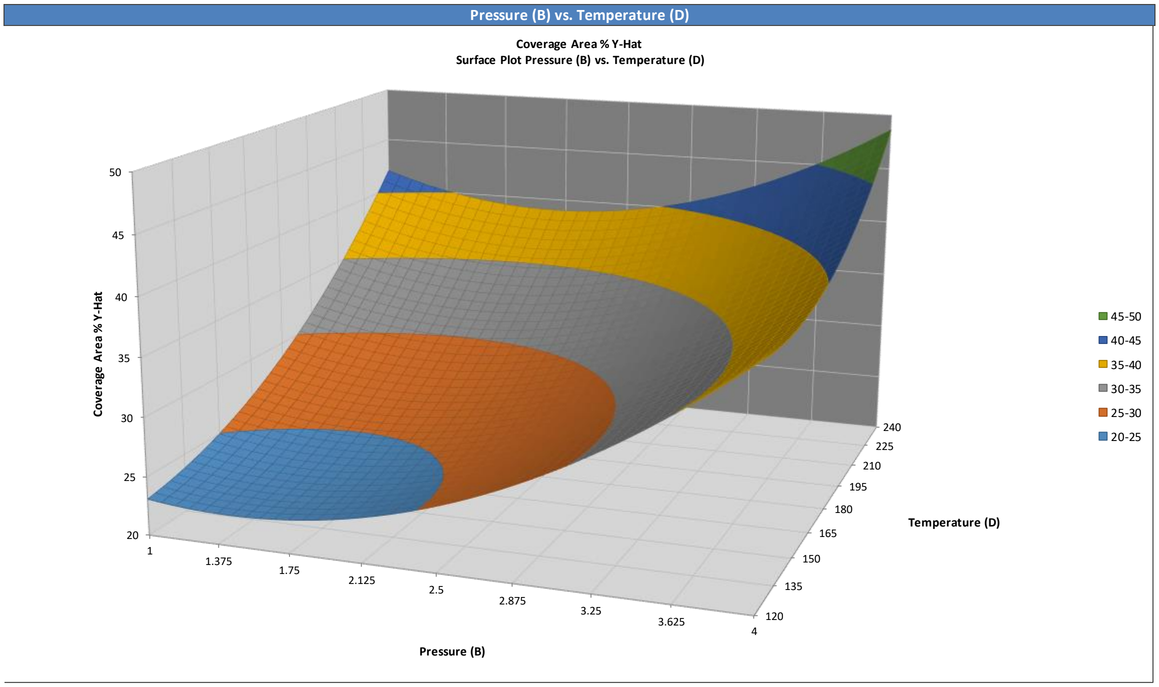

Figure 187: Surface Chart – Pressure vs Temperature for Coverage Area h-hat (Rapeseed oil, Propylene Glycol, 19ga Capillary)

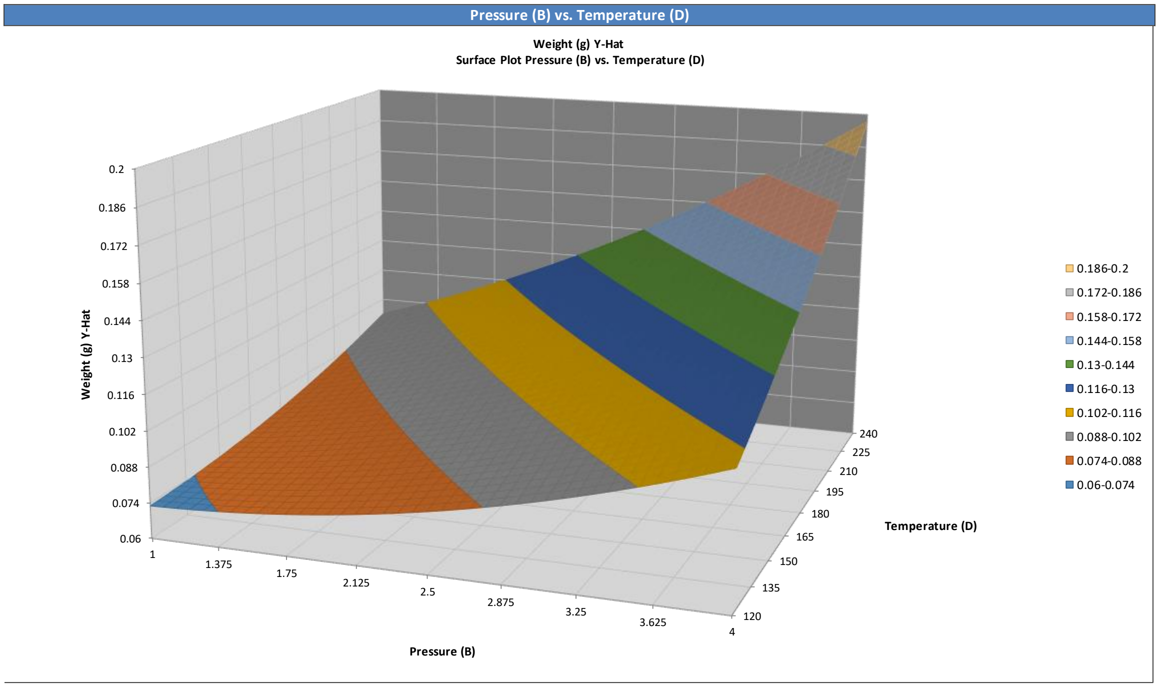

Figure 188: Surface Chart – Pressure vs Temperature for Sample Weight h-hat (Rapeseed oil, Propylene Glycol, 19ga Capillary)

5.4. SUNFLOWER OIL

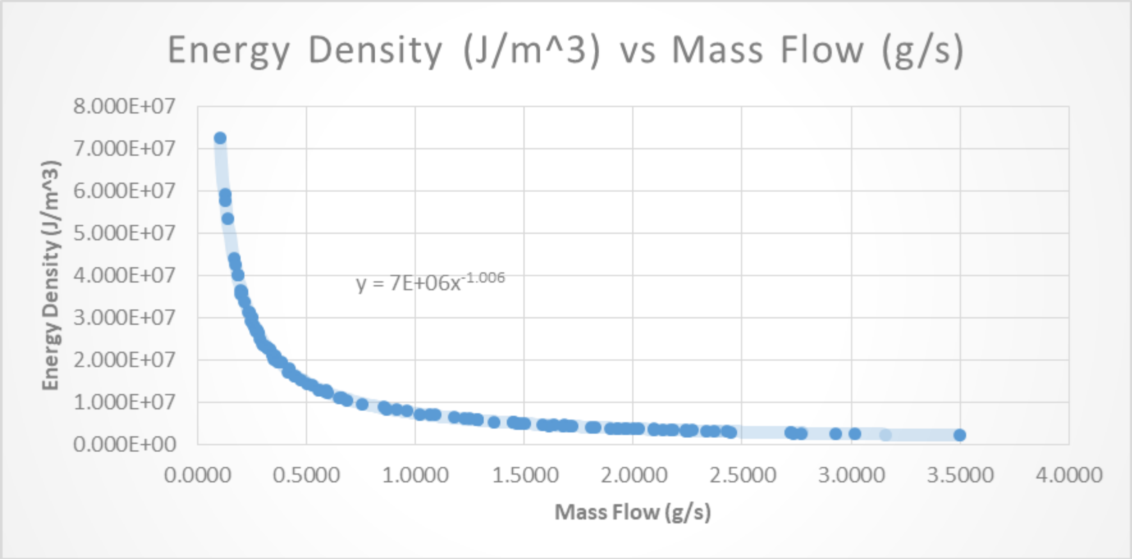

Figure 189: Sunflower Oil Energy Density vs Mass Flow Chart 25kV

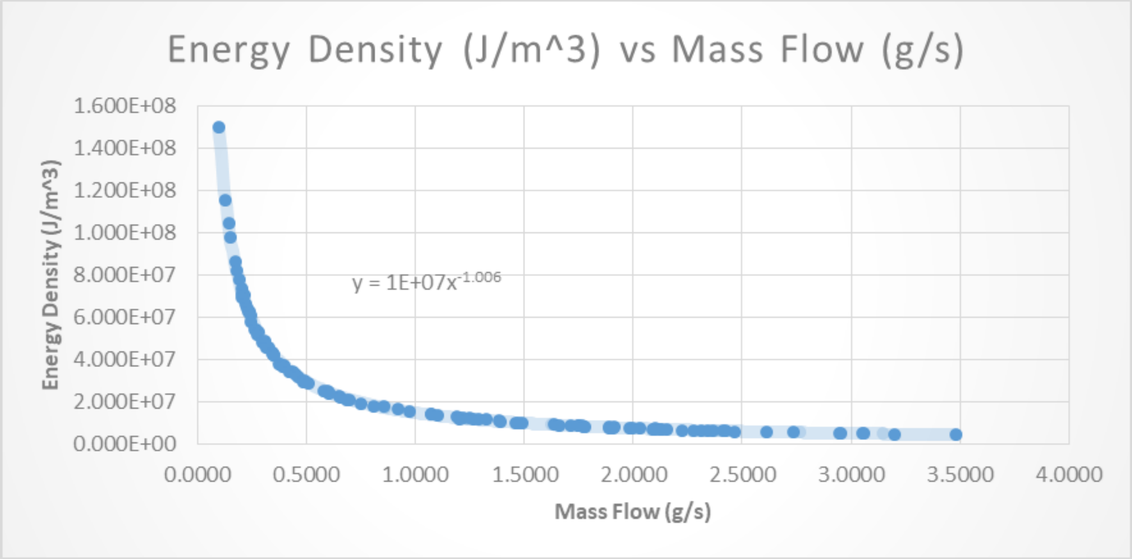

Figure 190: Sunflower Oil Energy Density vs Mass Flow Chart 50kV

5.4.1. Sunflower Lecithin with 19 Gauge Capillary

Table 22: Main Effects Plot for Sunflower Oil & Sunflower Lecithin @ 19ga Capillary

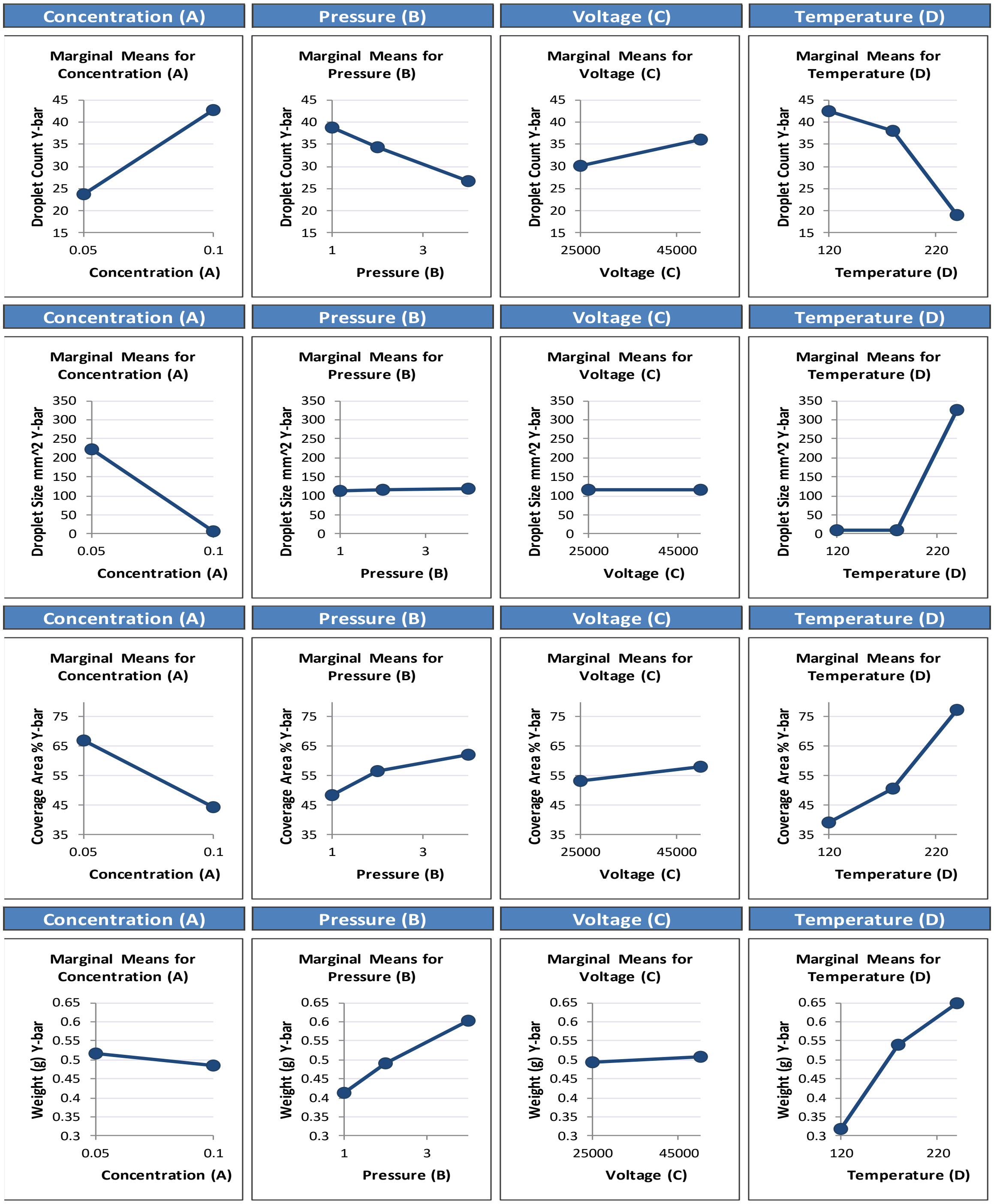

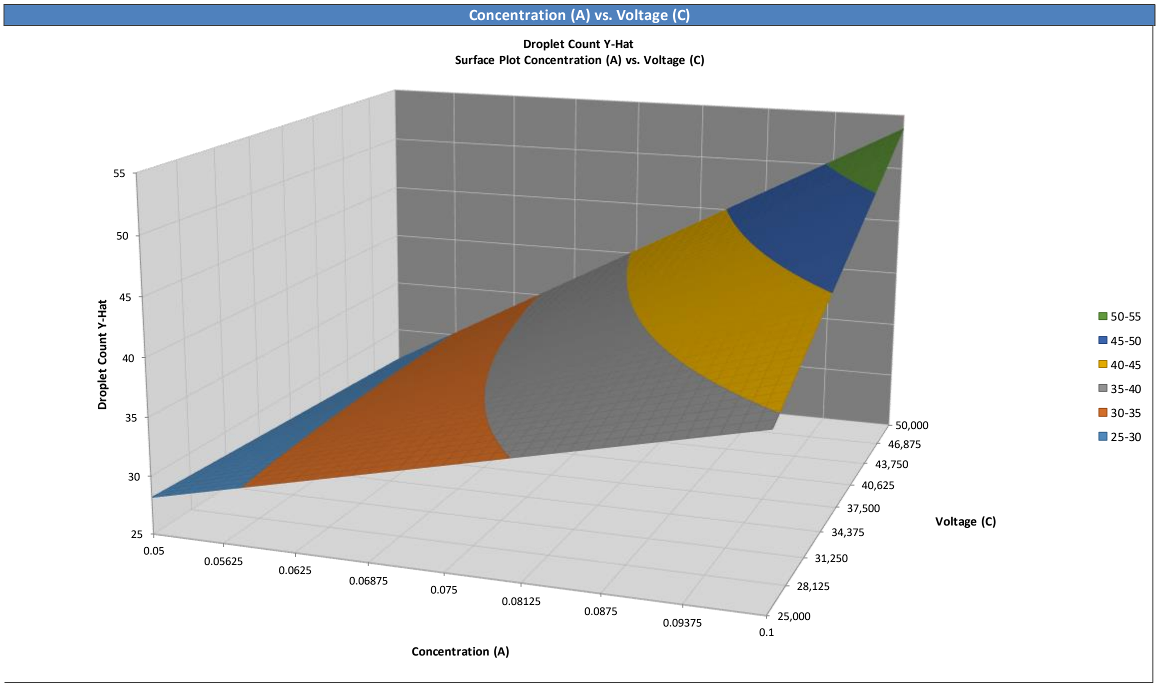

Figure 191: Surface Chart - Concentration vs Voltage for Droplet Count h-hat (Sunflower oil, Sunflower Lecithin, 19ga Capillary)

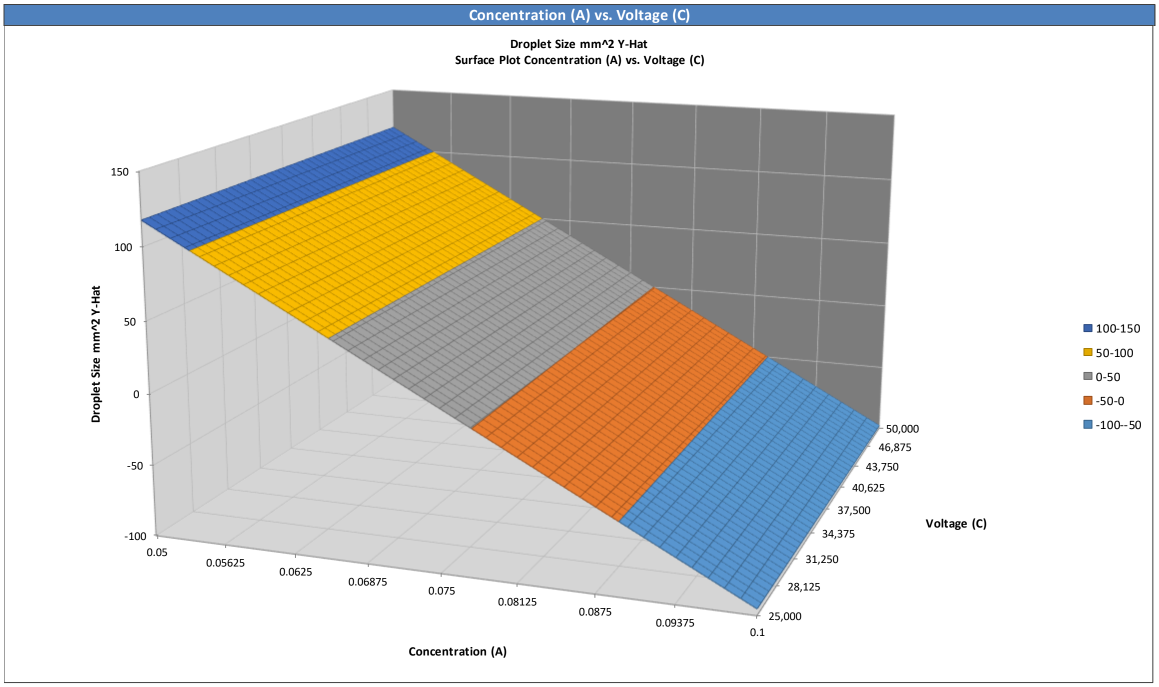

Figure 192: Surface Chart - Concentration vs Voltage for Droplet Size h-hat (Sunflower oil, Sunflower Lecithin, 19ga Capillary)

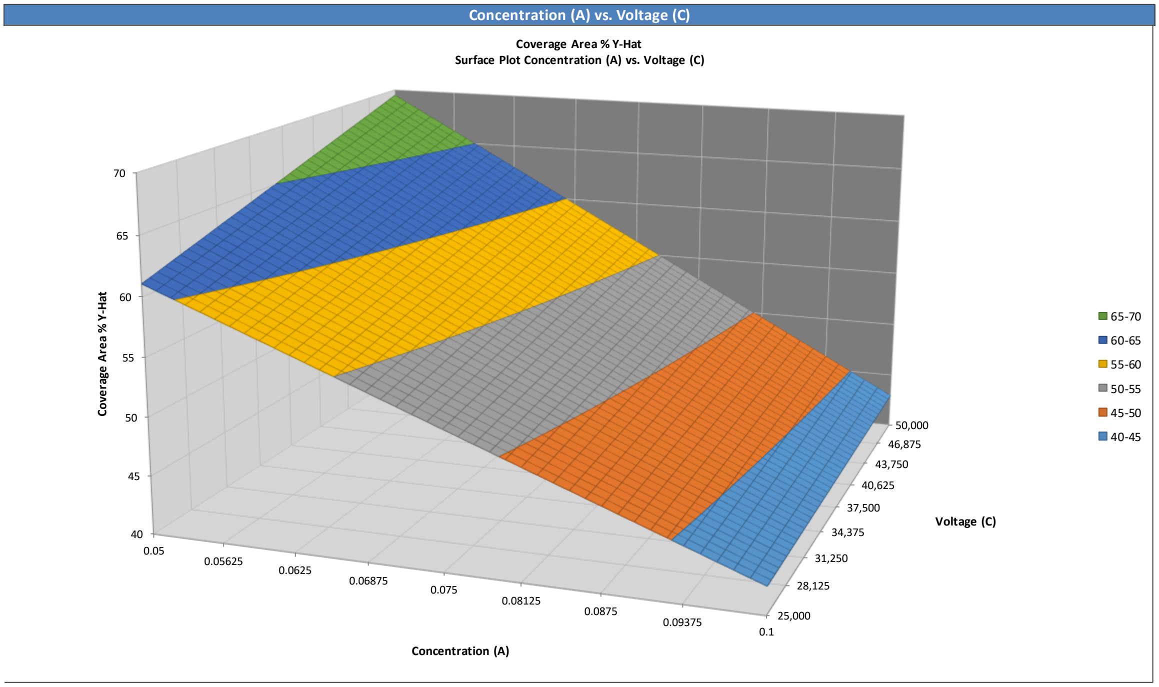

Figure 193: Surface Chart - Concentration vs Voltage for Coverage Area h-hat (Sunflower oil, Sunflower Lecithin, 19ga Capillary)

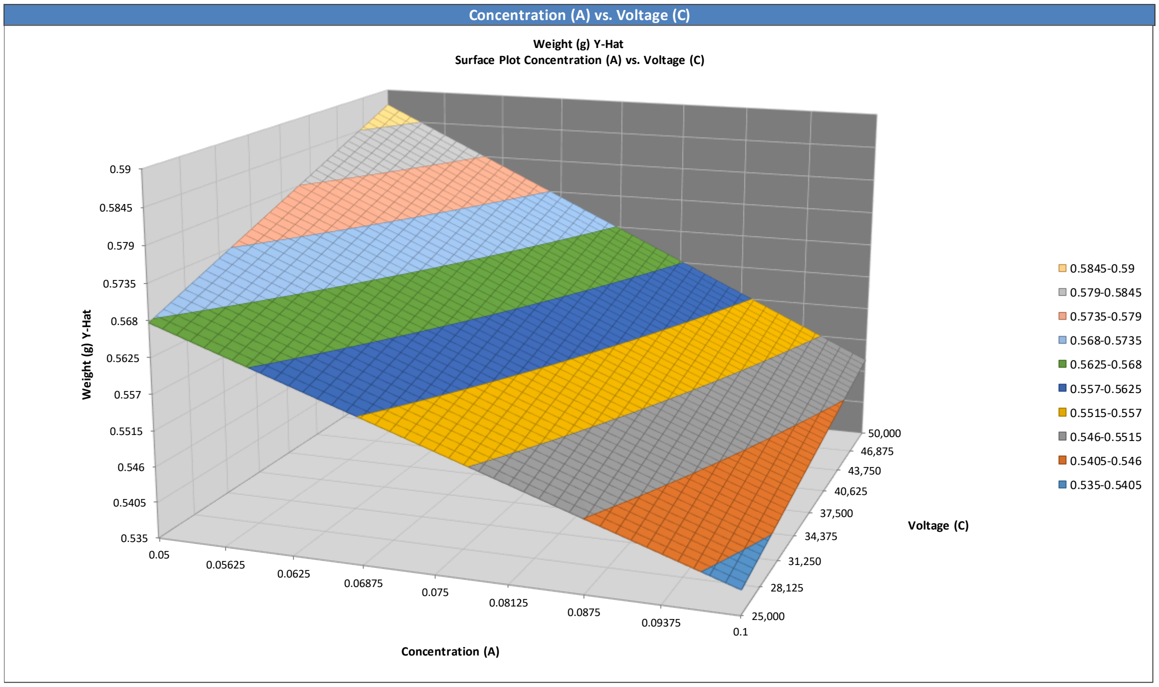

Figure 194: Surface Chart - Concentration vs Voltage for Sample Weight h-hat (Sunflower oil, Sunflower Lecithin, 19ga Capillary)

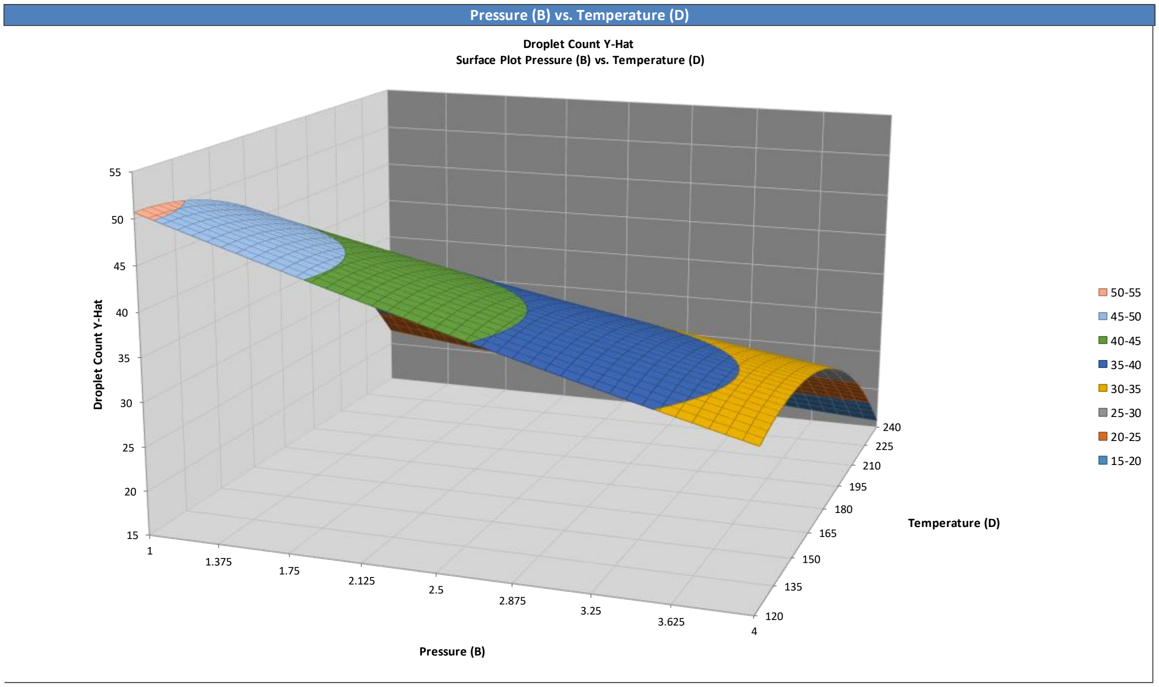

Figure 195: Surface Chart – Pressure vs Temperature for Droplet Count h-hat (Sunflower oil, Sunflower Lecithin, 19ga Capillary)

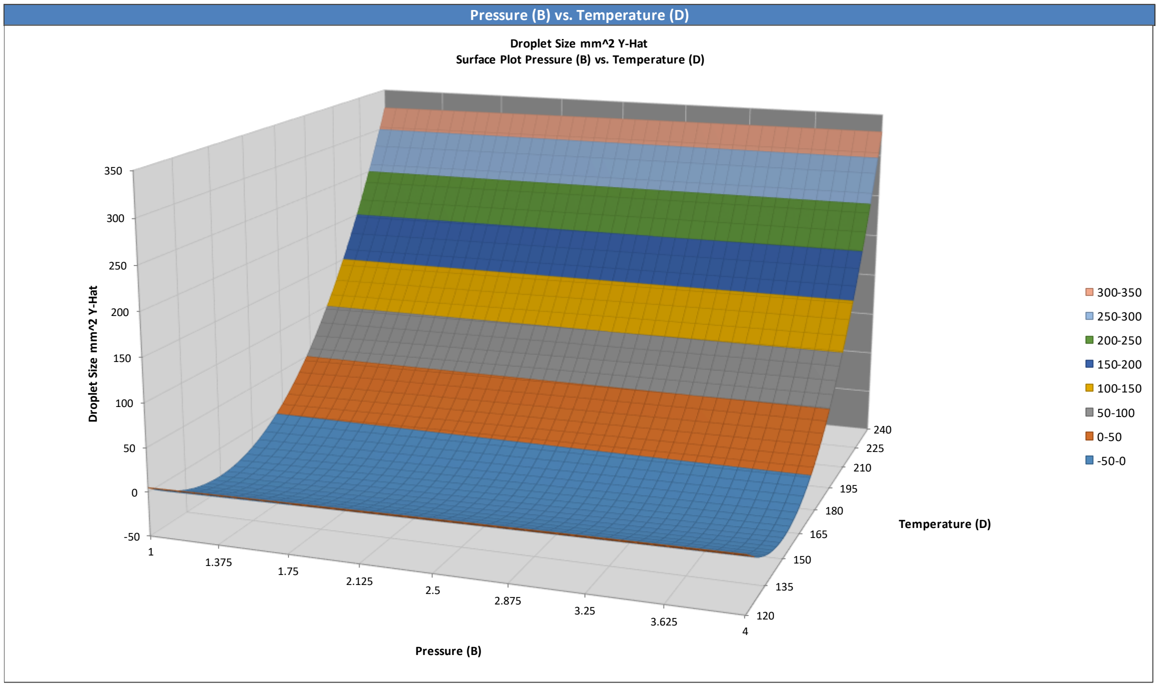

Figure 196: Surface Chart – Pressure vs Temperature for Droplet Size h-hat (Sunflower oil, Sunflower Lecithin, 19ga Capillary)

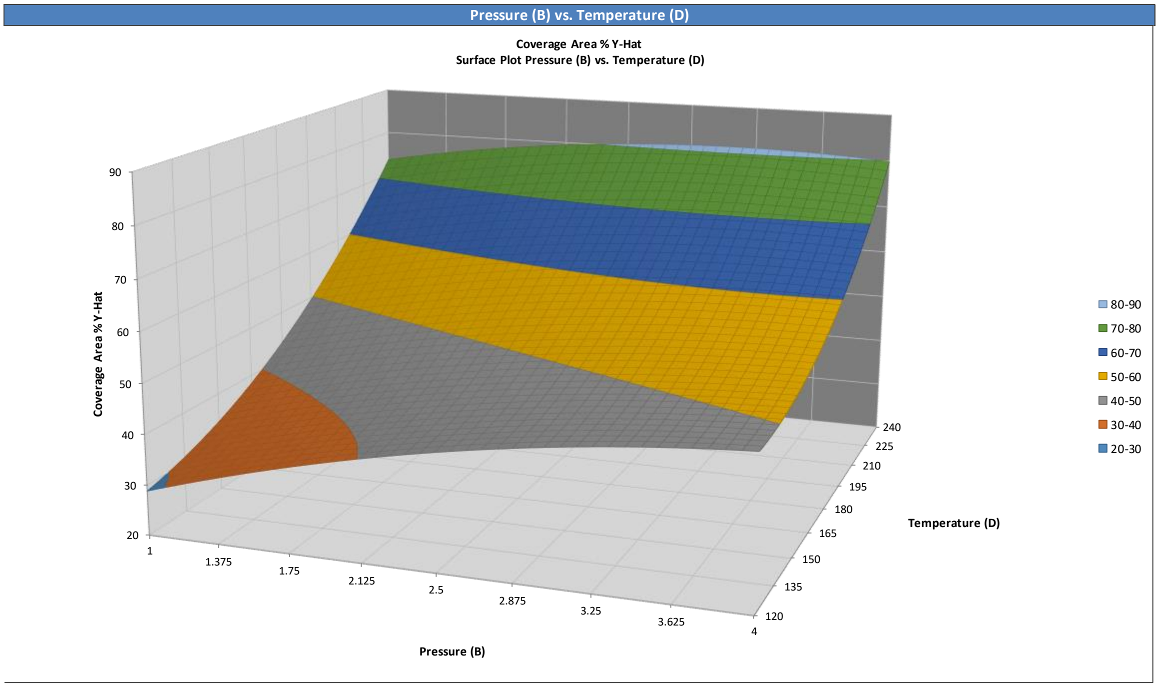

Figure 197: Surface Chart – Pressure vs Temperature for Coverage Area h-hat (Sunflower oil, Sunflower Lecithin, 19ga Capillary)

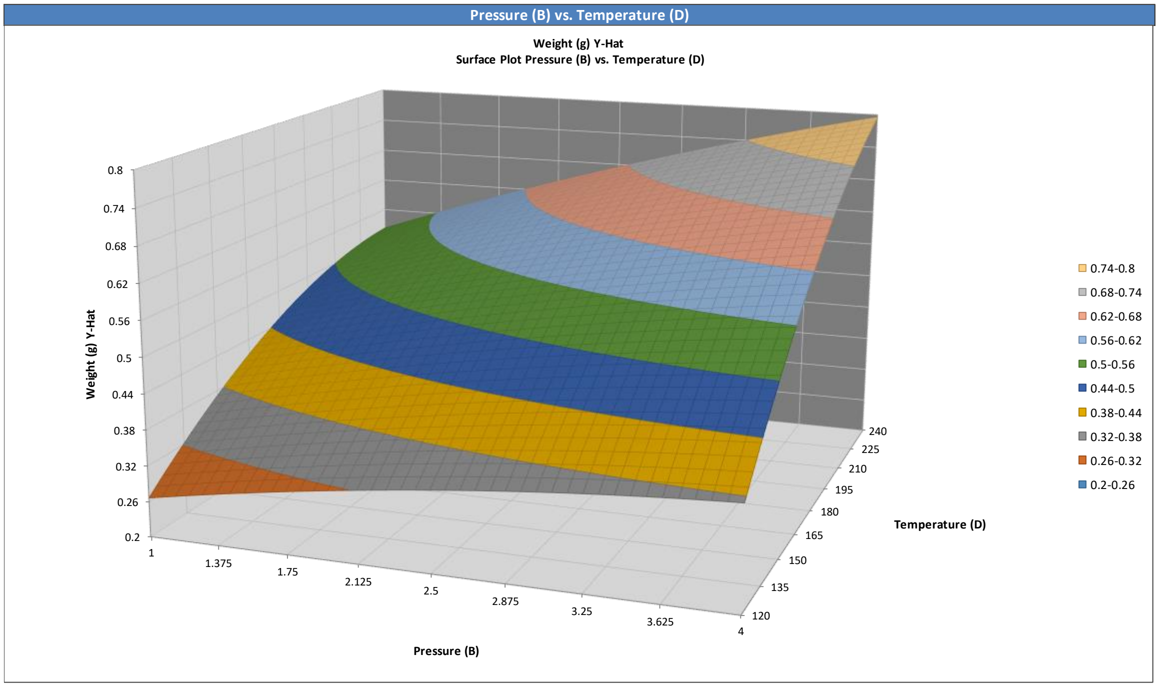

Figure 198: Surface Chart – Pressure vs Temperature for Sample Weight h-hat (Sunflower oil, Sunflower Lecithin, 19ga Capillary)

5.4.2. Sunflower Lecithin with 22 Gauge Capillary

Table 23: Main Effects Plot for Sunflower Oil & Sunflower Lecithin @ 22ga Capillary

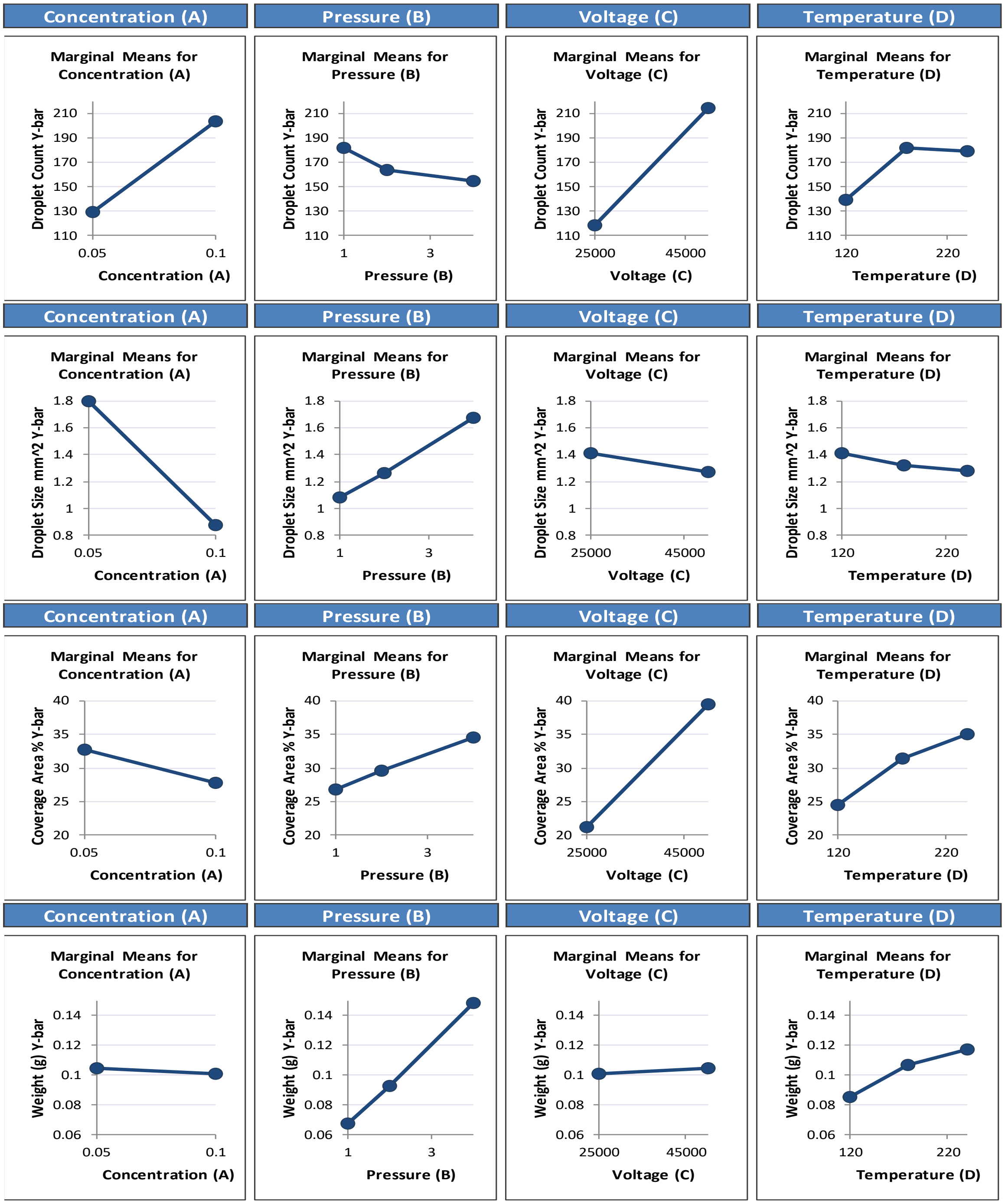

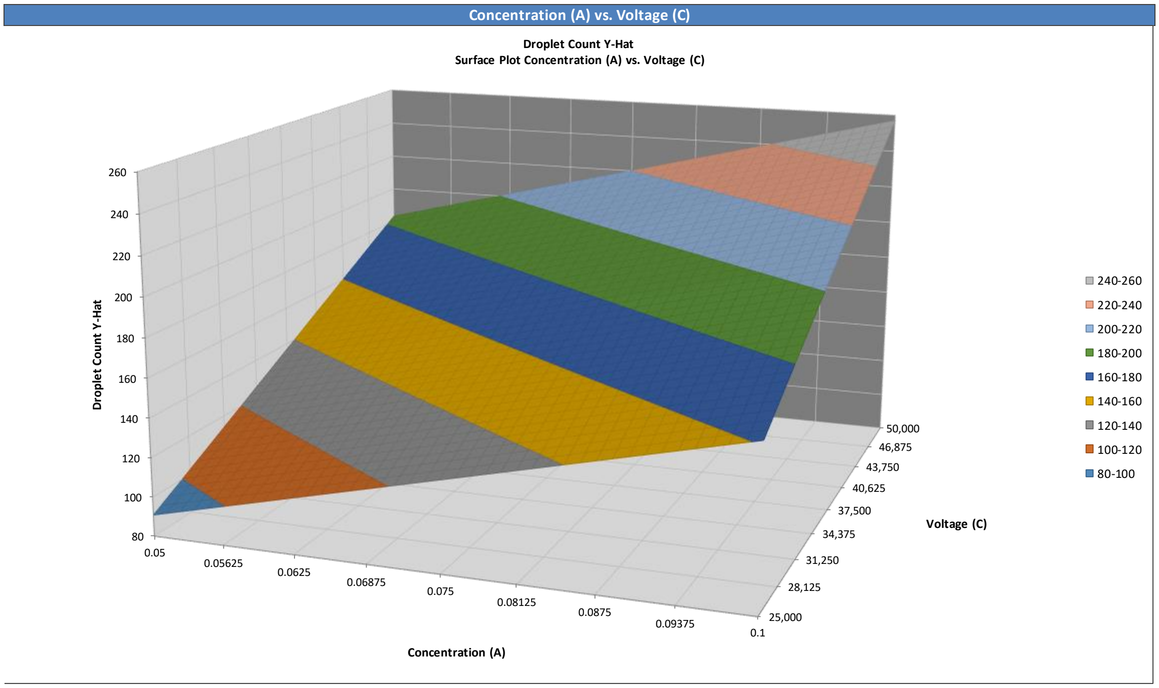

Figure 199: Surface Chart - Concentration vs Voltage for Droplet Count h-hat (Sunflower oil, Sunflower Lecithin, 22ga Capillary)

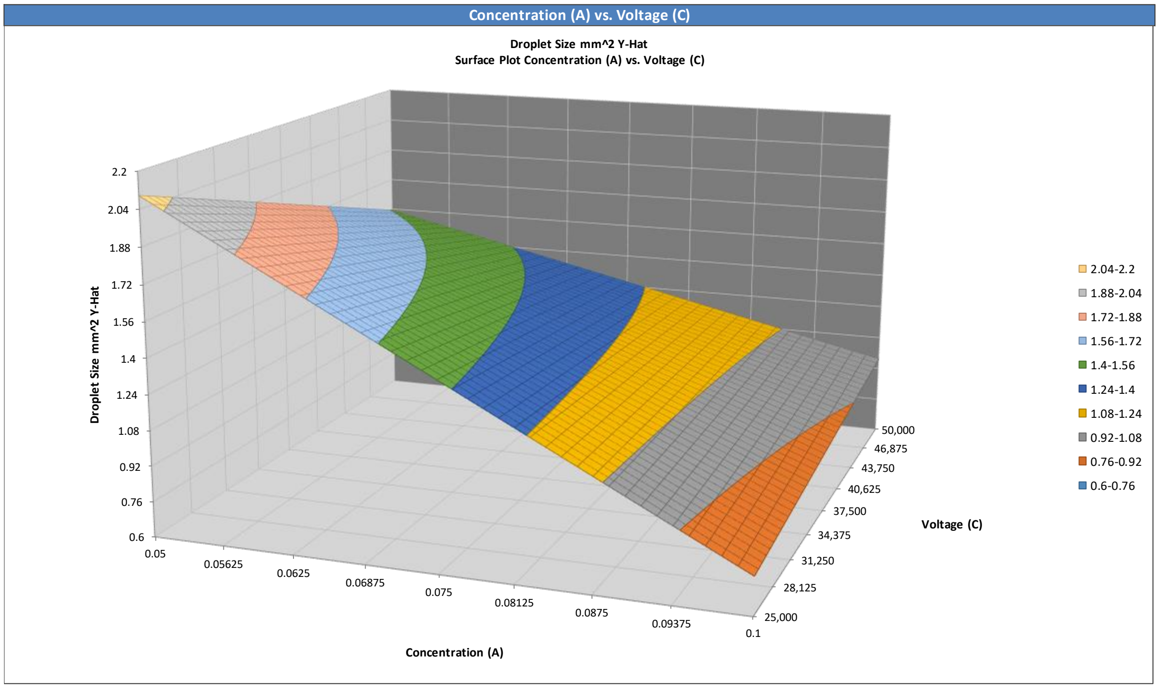

Figure 200: Surface Chart - Concentration vs Voltage for Droplet Size h-hat (Sunflower oil, Sunflower Lecithin, 22ga Capillary)

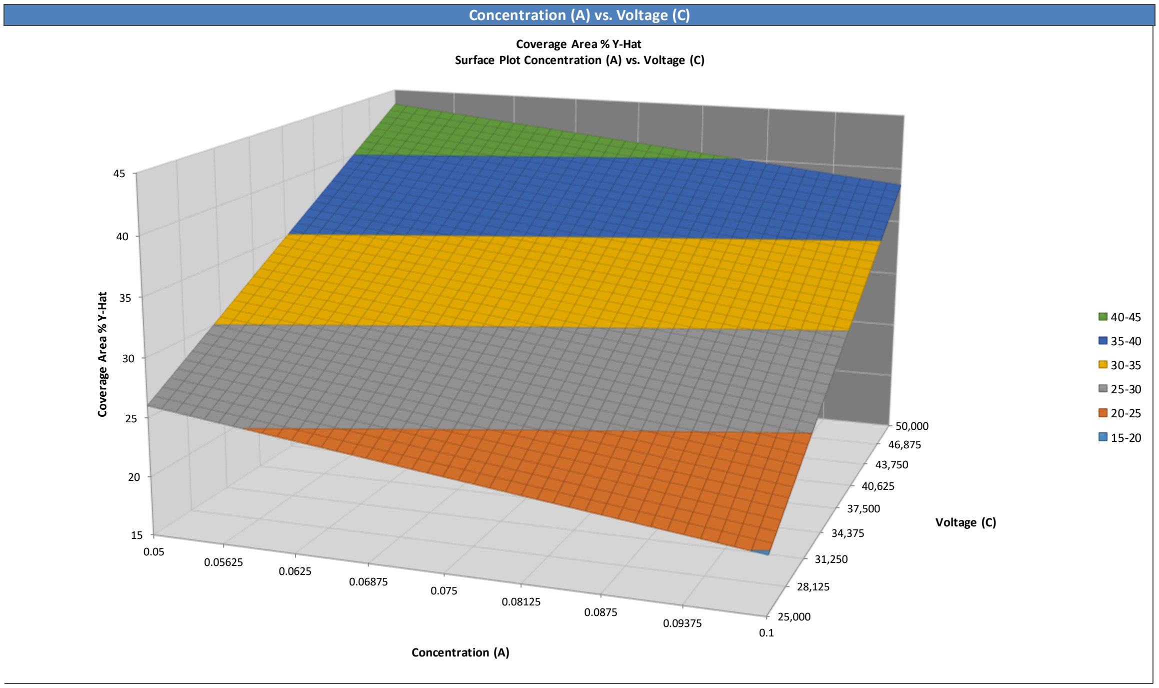

Figure 201: Surface Chart - Concentration vs Voltage for Coverage Area h-hat (Sunflower oil, Sunflower Lecithin, 22ga Capillary)

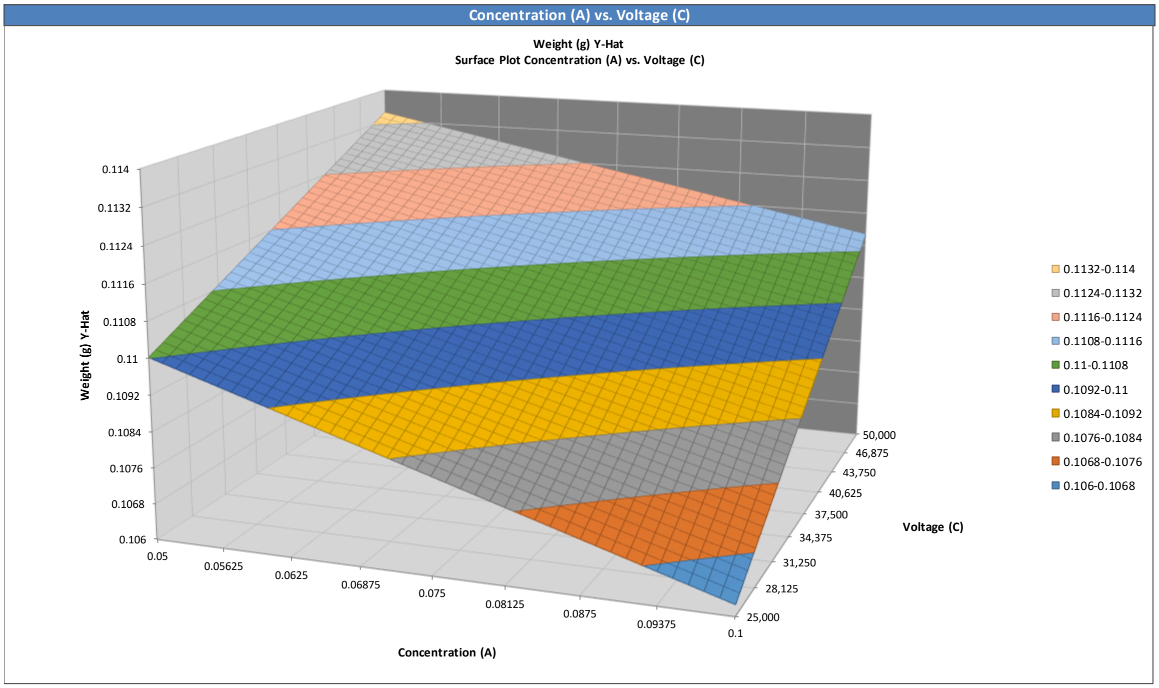

Figure 202: Surface Chart - Concentration vs Voltage for Sample Weight h-hat (Sunflower oil, Sunflower Lecithin, 22ga Capillary)

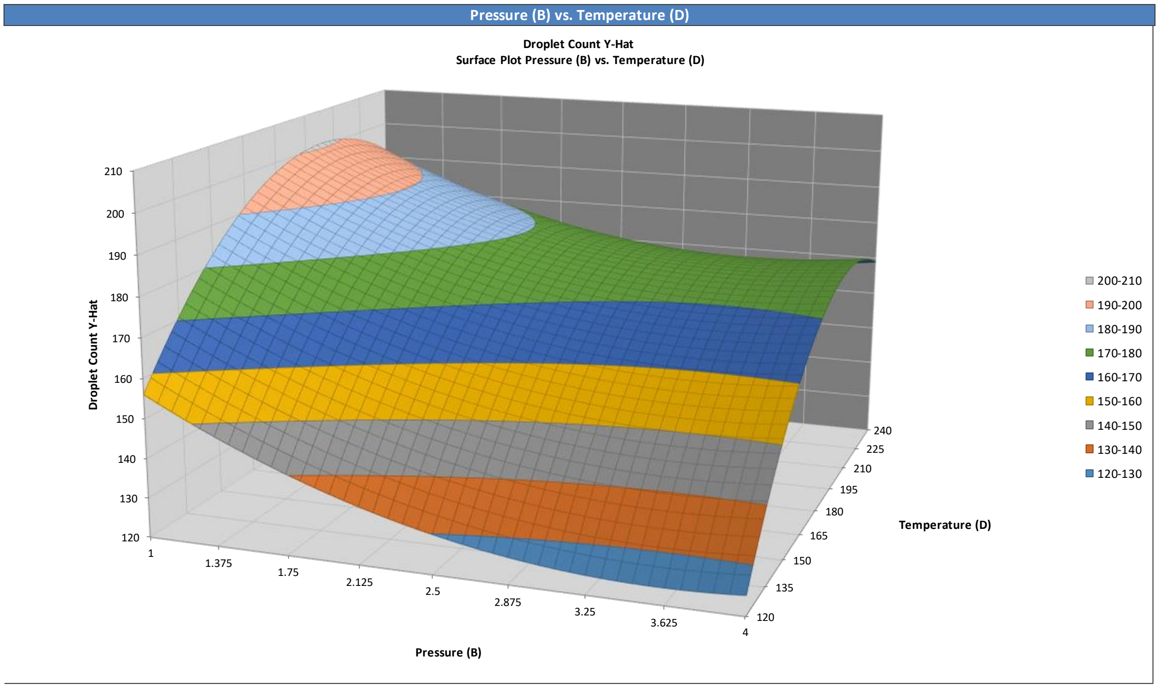

Figure 203: Surface Chart – Pressure vs Temperature for Droplet Count h-hat (Sunflower oil, Sunflower Lecithin, 22ga Capillary)

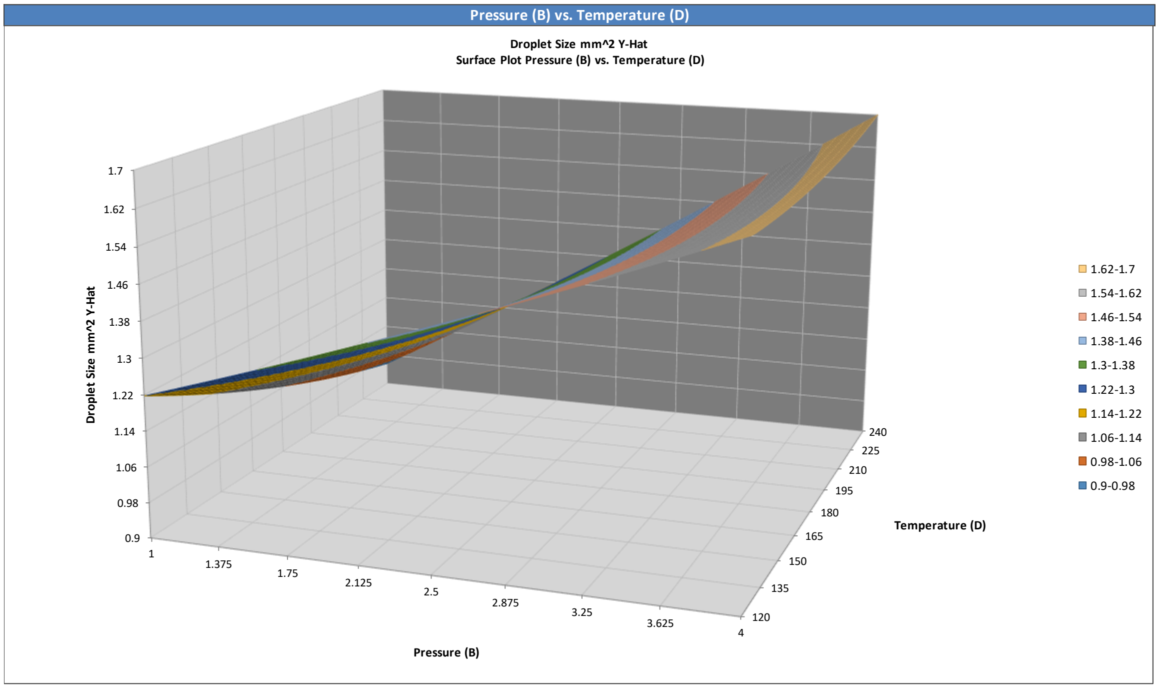

Figure 204: Surface Chart – Pressure vs Temperature for Droplet Size h-hat (Sunflower oil, Sunflower Lecithin, 22ga Capillary)

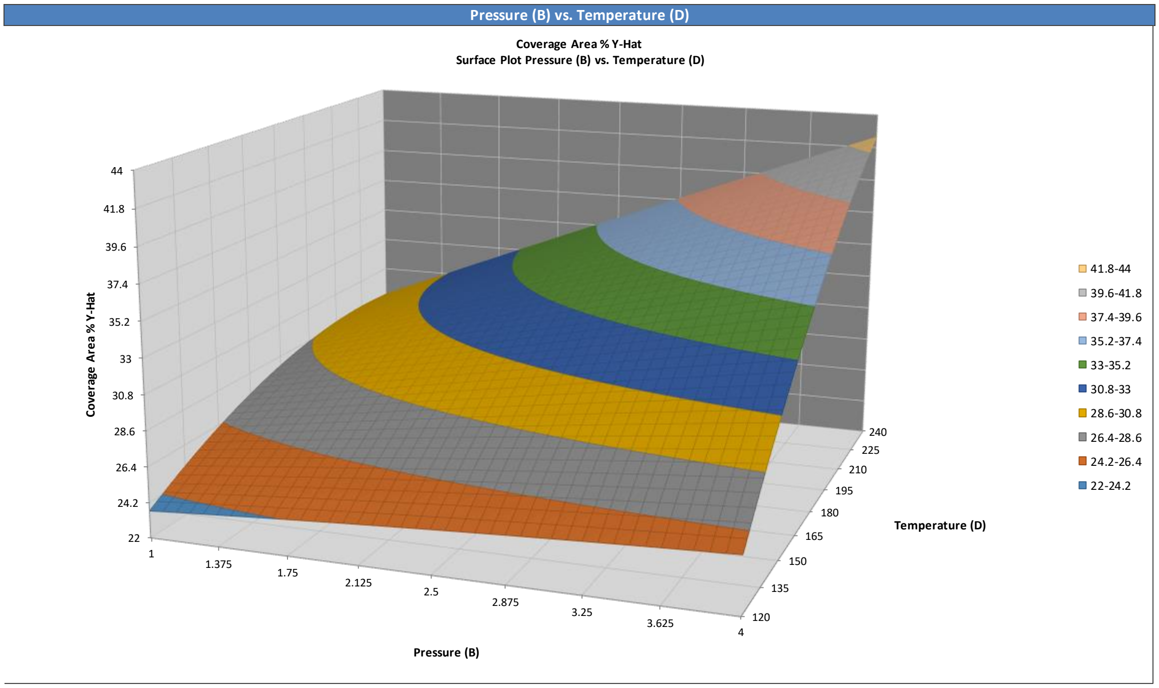

Figure 205: Surface Chart – Pressure vs Temperature for Coverage Area h-hat (Sunflower oil, Sunflower Lecithin, 22ga Capillary)

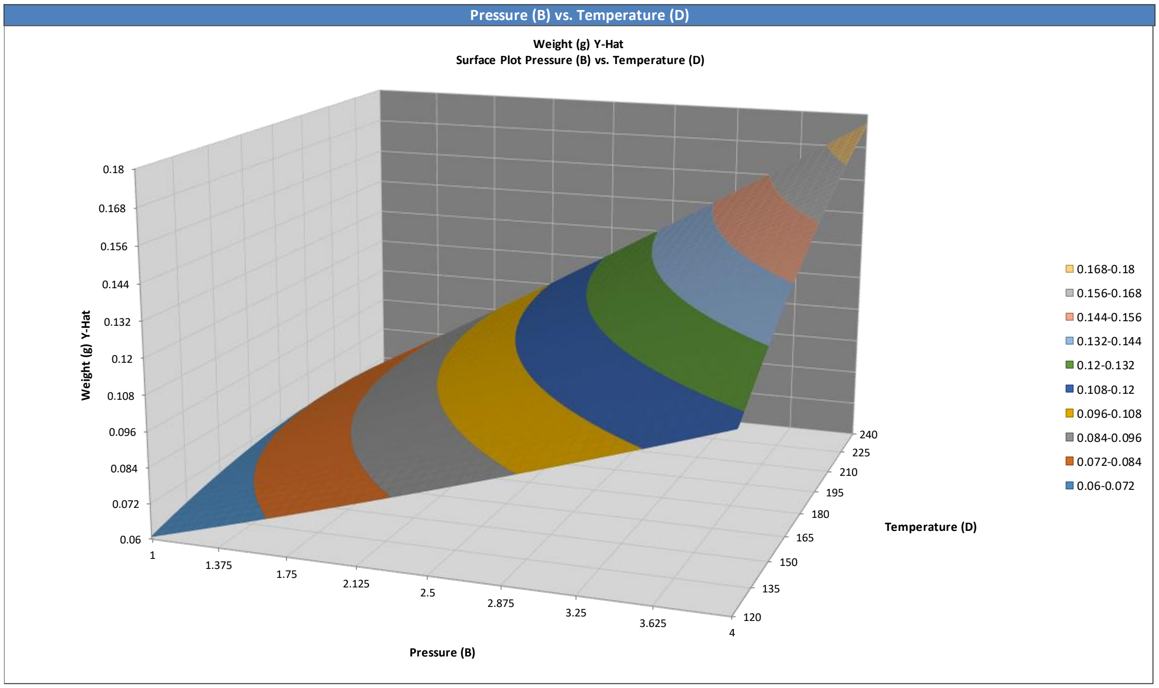

Figure 206: Surface Chart – Pressure vs Temperature for Sample Weight h-hat (Sunflower oil, Sunflower Lecithin, 22ga Capillary)

5.4.3. Polysorbate 80 with 19 Gauge Capillary

Table 24: Main Effects Plot for Sunflower Oil & Polysorbate 80 @ 19ga Capillary

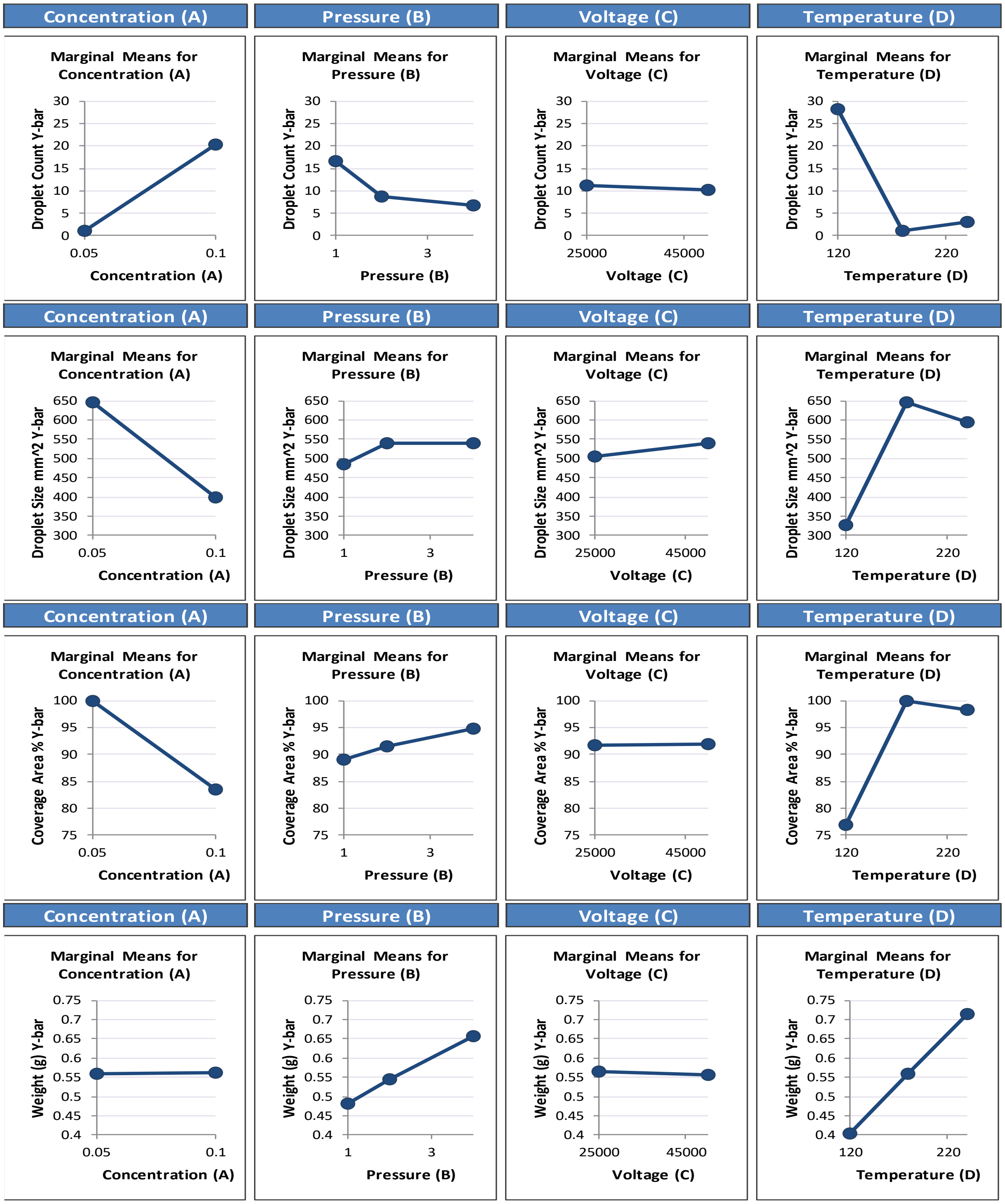

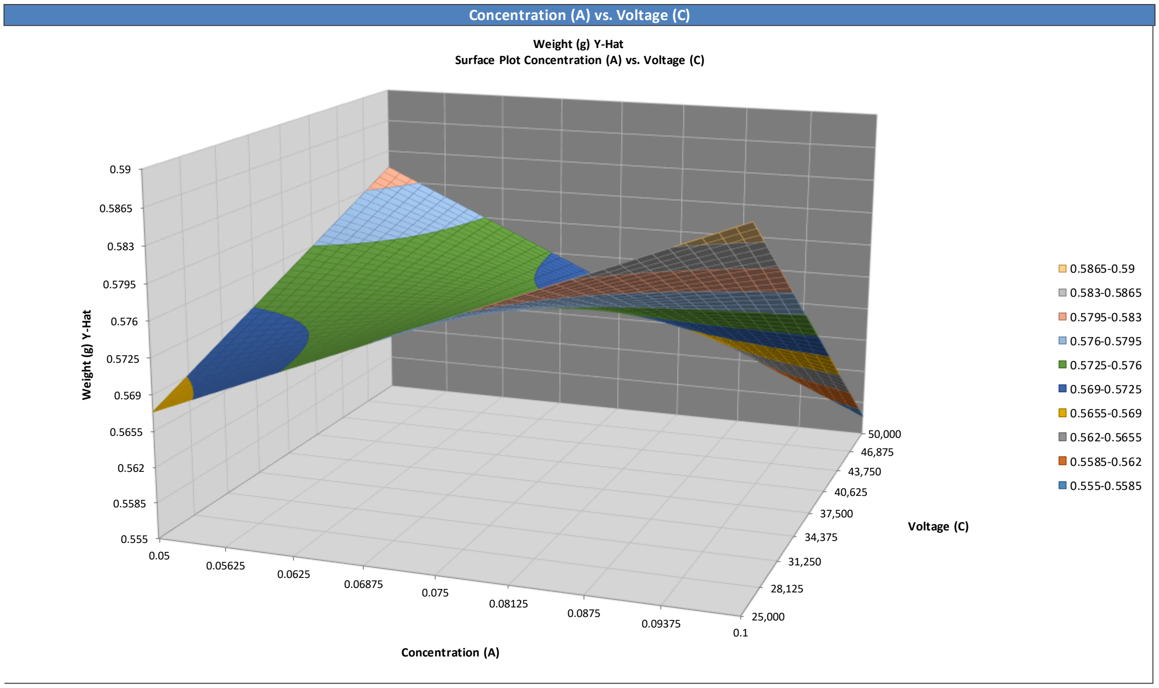

Figure 207: Surface Chart - Concentration vs Voltage for Droplet Count h-hat (Sunflower oil, Polysorbate 80, 19ga Capillary)

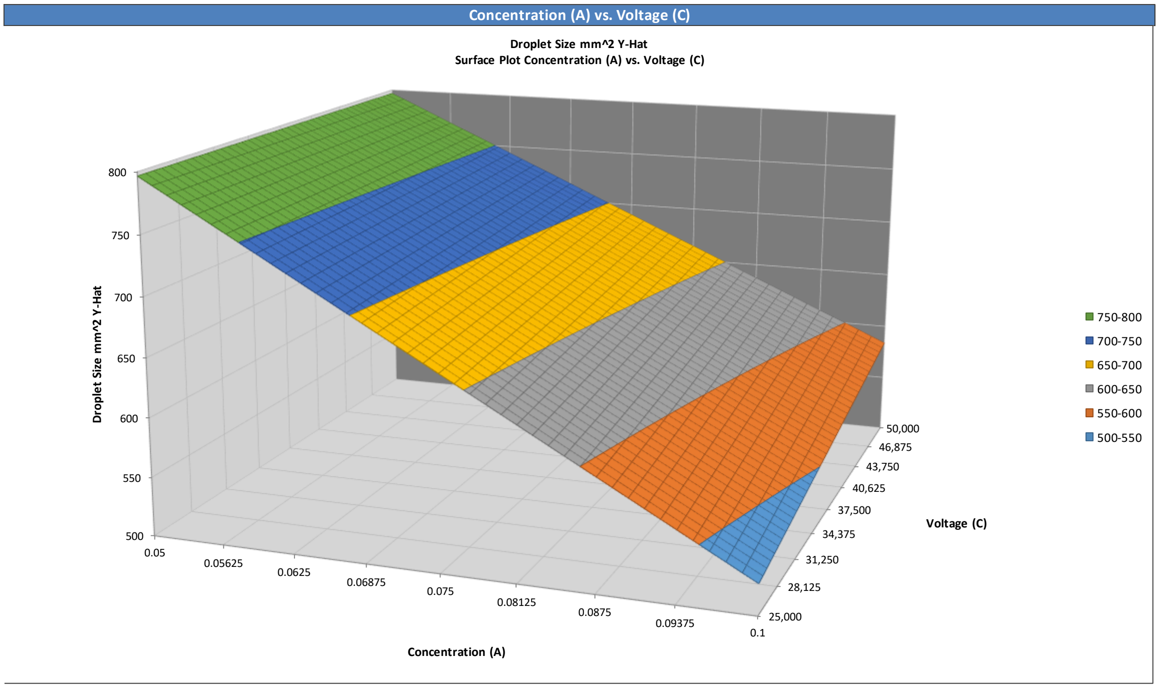

Figure 208: Surface Chart - Concentration vs Voltage for Droplet Size h-hat (Sunflower oil, Polysorbate 80, 19ga Capillary)

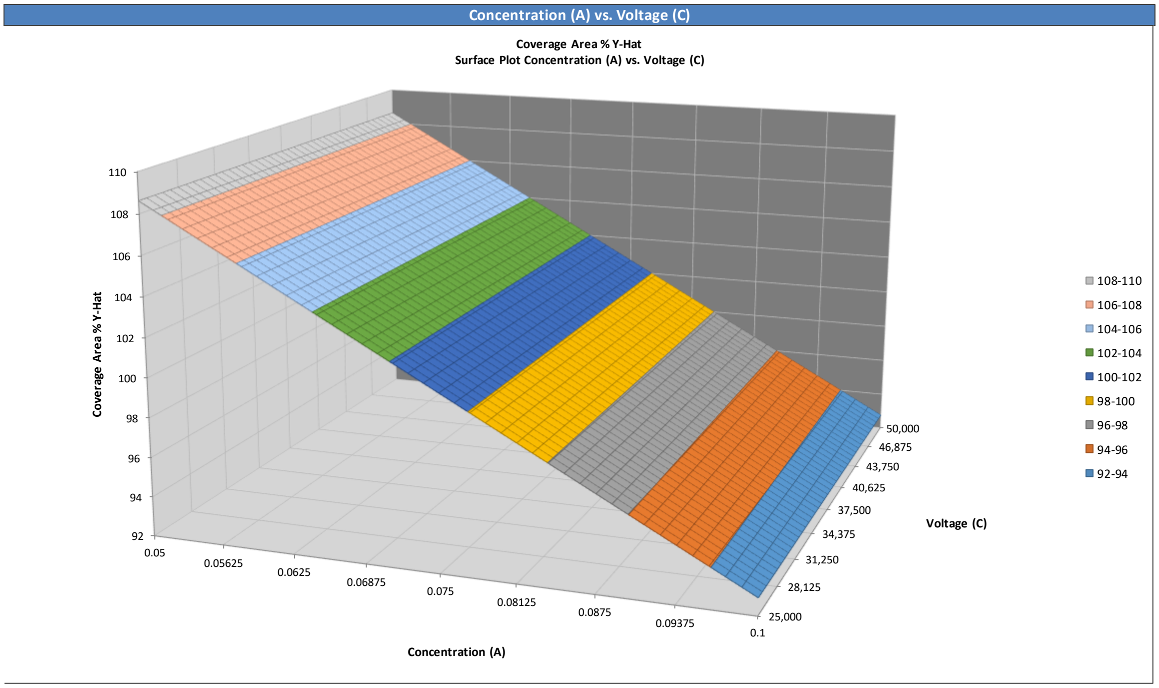

Figure 209: Surface Chart - Concentration vs Voltage for Coverage Area h-hat (Sunflower oil, Polysorbate 80, 19ga Capillary)

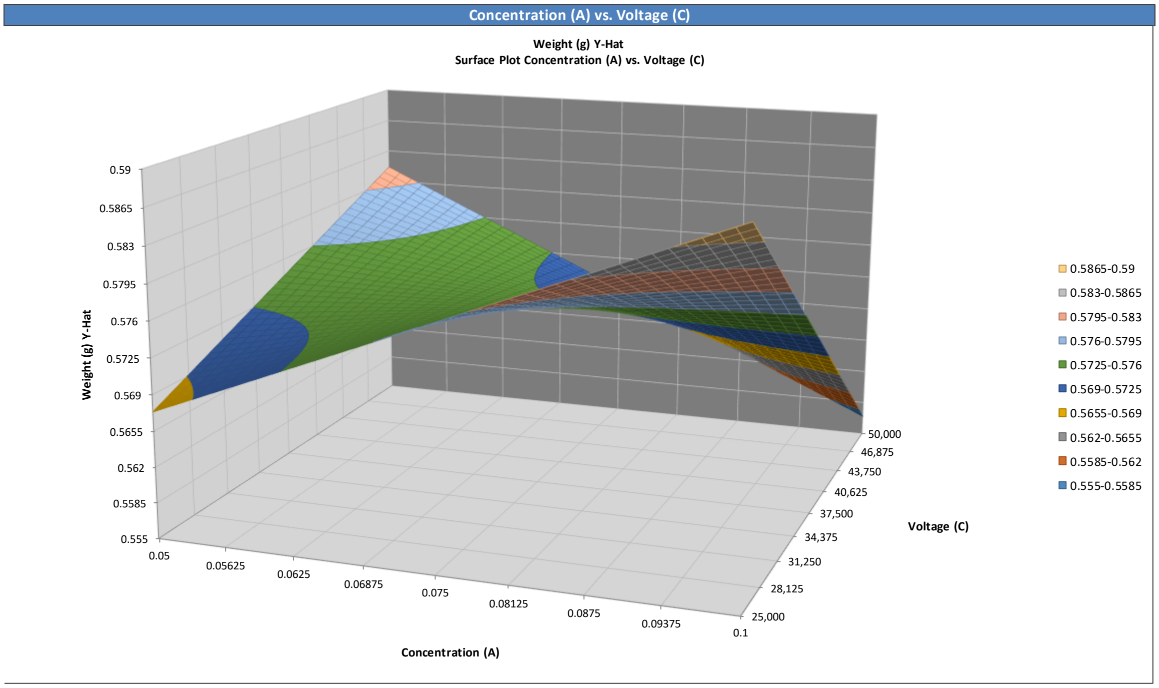

Figure 210: Surface Chart - Concentration vs Voltage for Sample Weight h-hat (Sunflower oil, Polysorbate 80, 19ga Capillary)

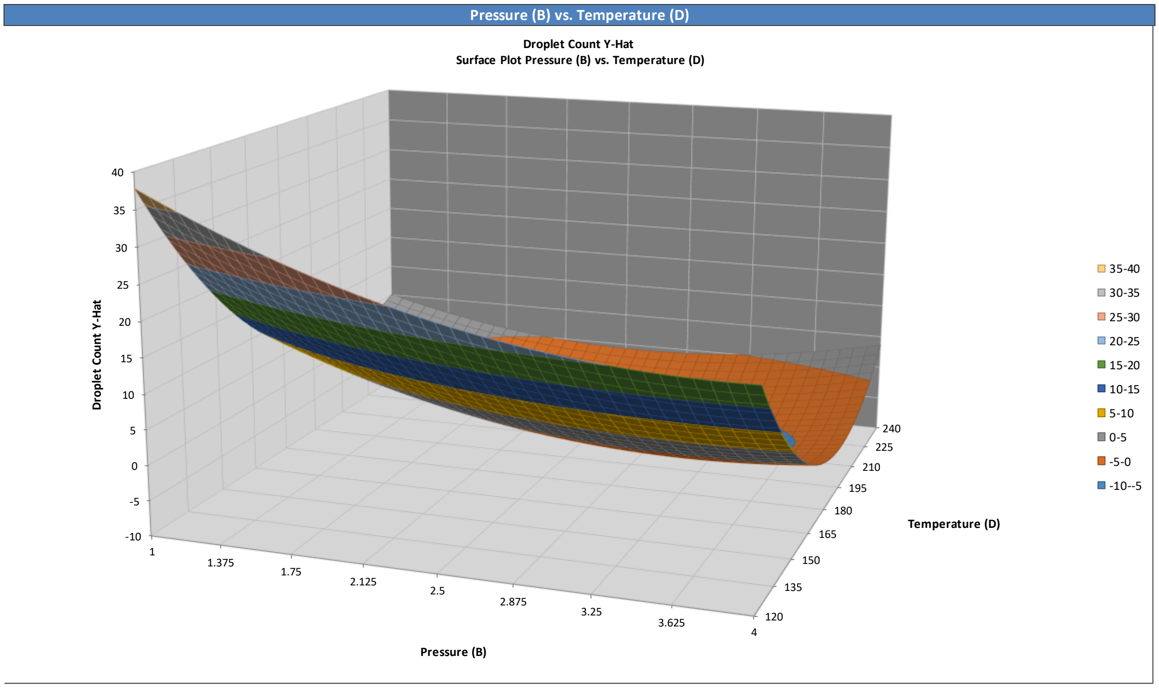

Figure 211: Surface Chart – Pressure vs Temperature for Droplet Count h-hat (Sunflower oil, Polysorbate 80, 19ga Capillary)

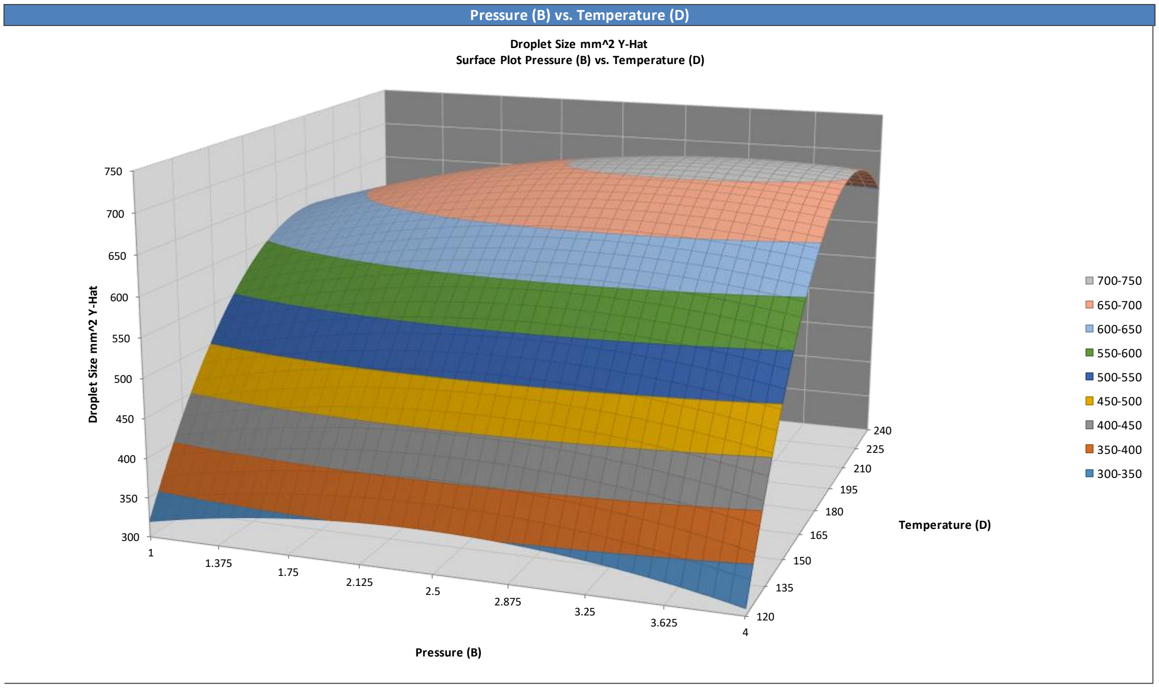

Figure 212: Surface Chart – Pressure vs Temperature for Droplet Size h-hat (Sunflower oil, Polysorbate 80, 19ga Capillary)

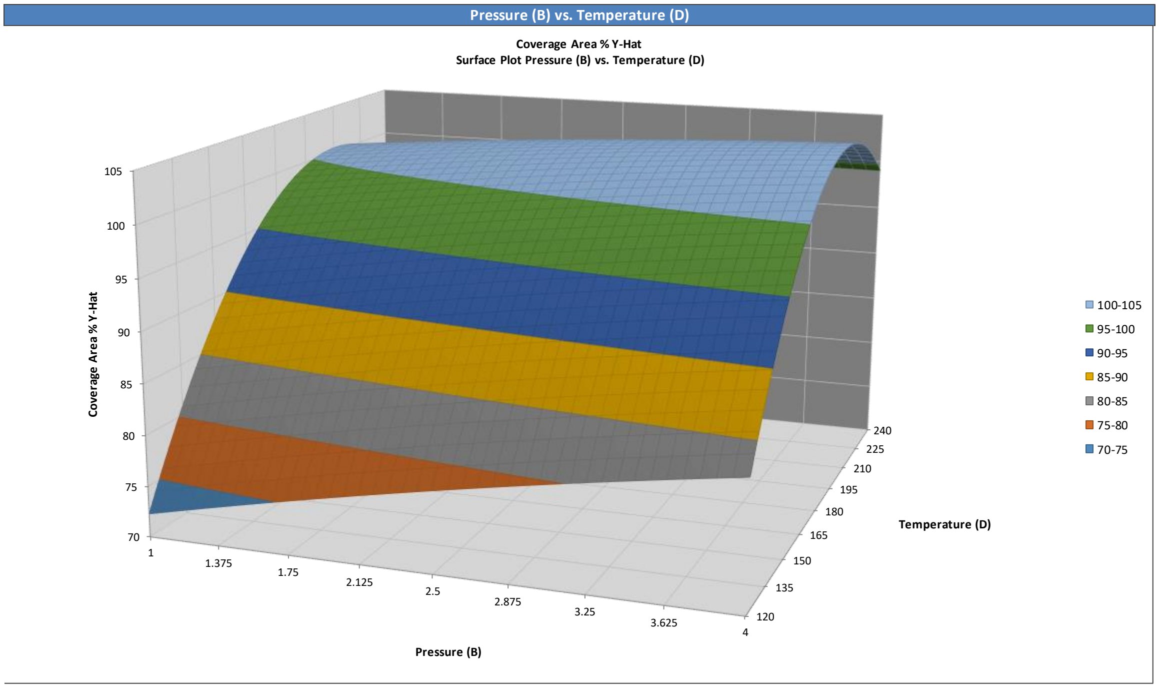

Figure 213: Surface Chart – Pressure vs Temperature for Coverage Area h-hat (Sunflower oil, Polysorbate 80, 19ga Capillary)

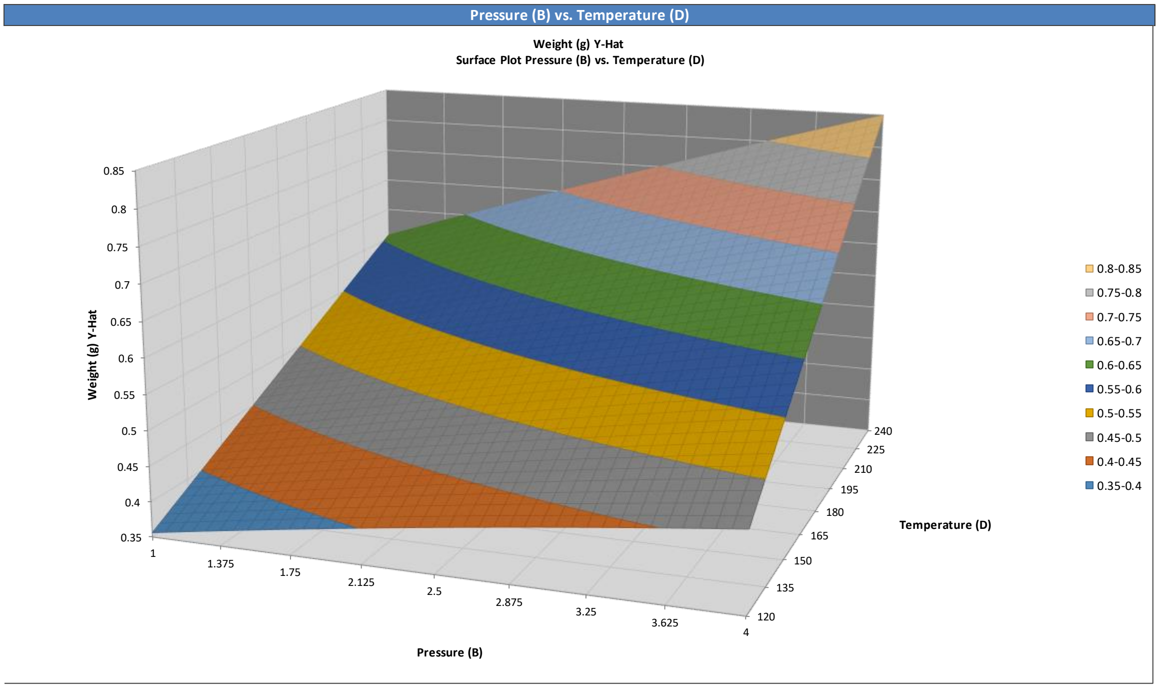

Figure 214: Surface Chart – Pressure vs Temperature for Sample Weight h-hat (Sunflower oil, Polysorbate 80, 19ga Capillary)

5.4.4. Polysorbate 80 with 22 Gauge Capillary

Table 25: Main Effects Plot for Sunflower Oil & Polysorbate 80 @ 22ga Capillary

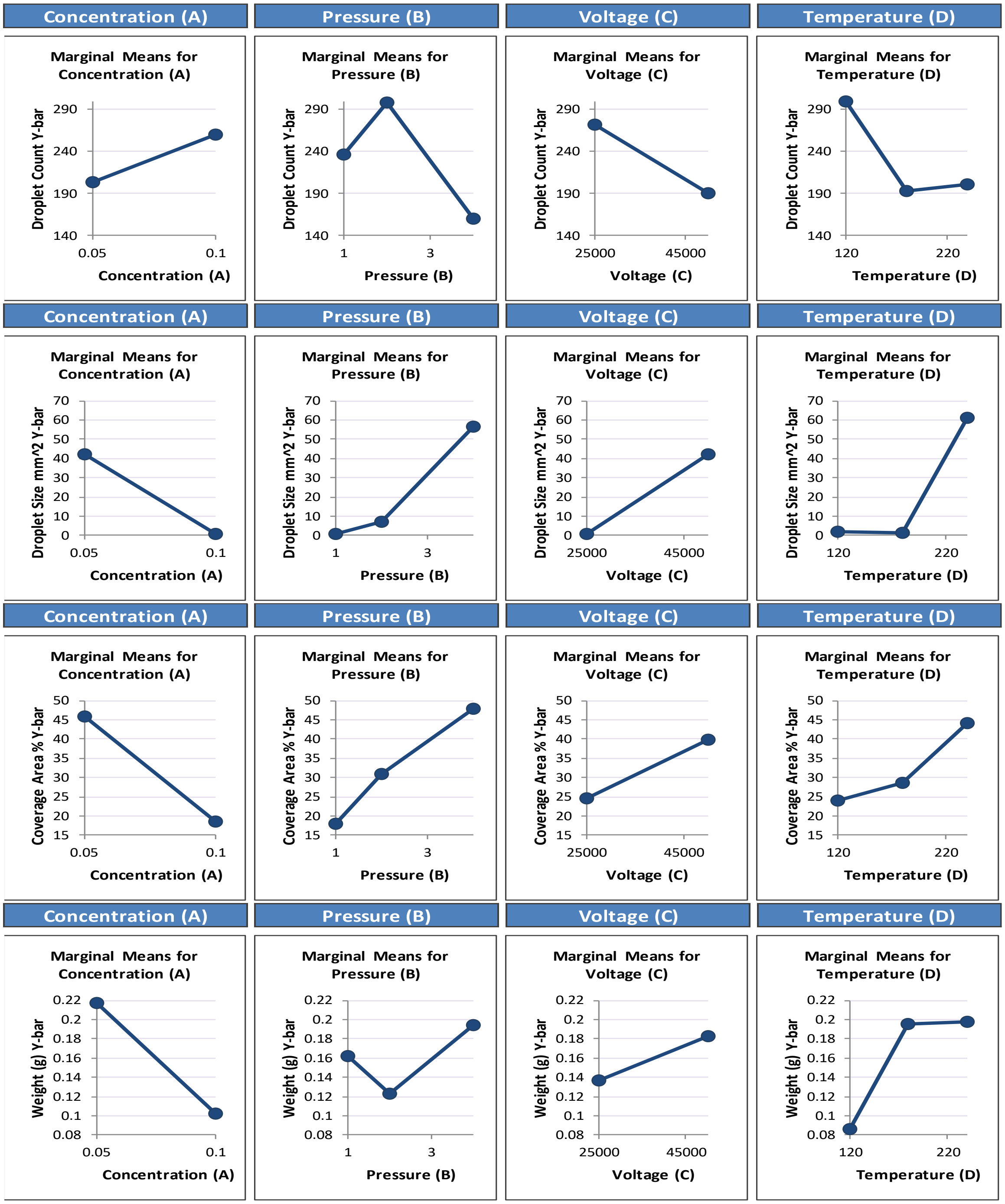

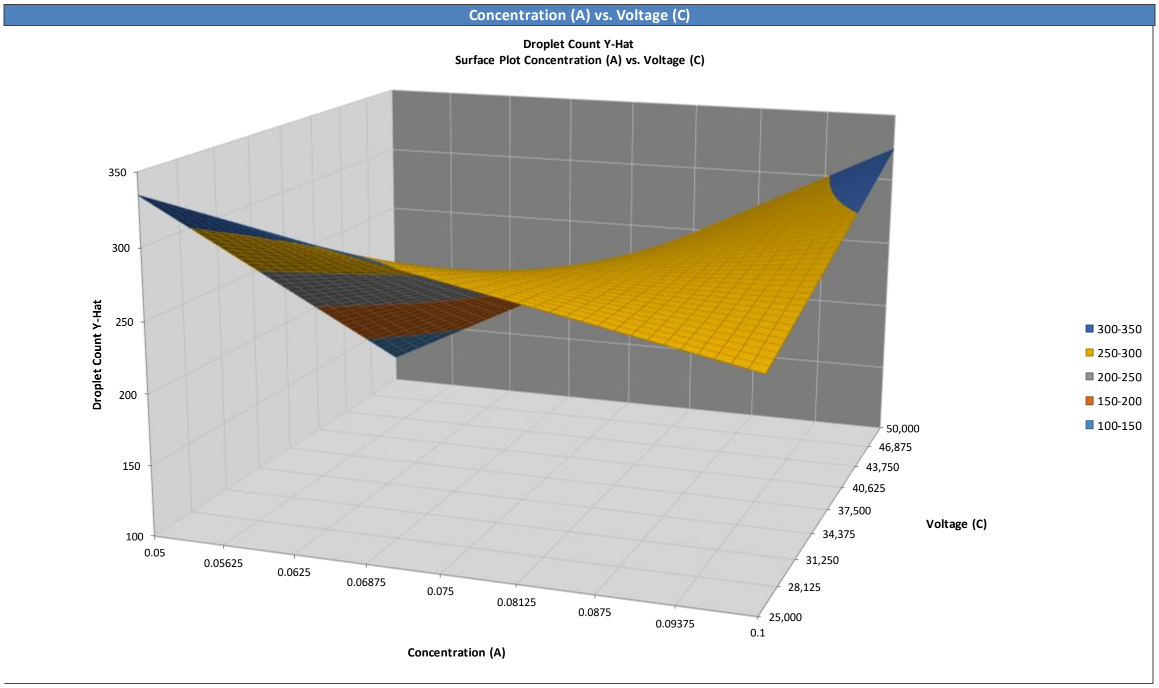

Figure 215: Surface Chart - Concentration vs Voltage for Droplet Count h-hat (Sunflower oil, Polysorbate 80, 22ga Capillary)

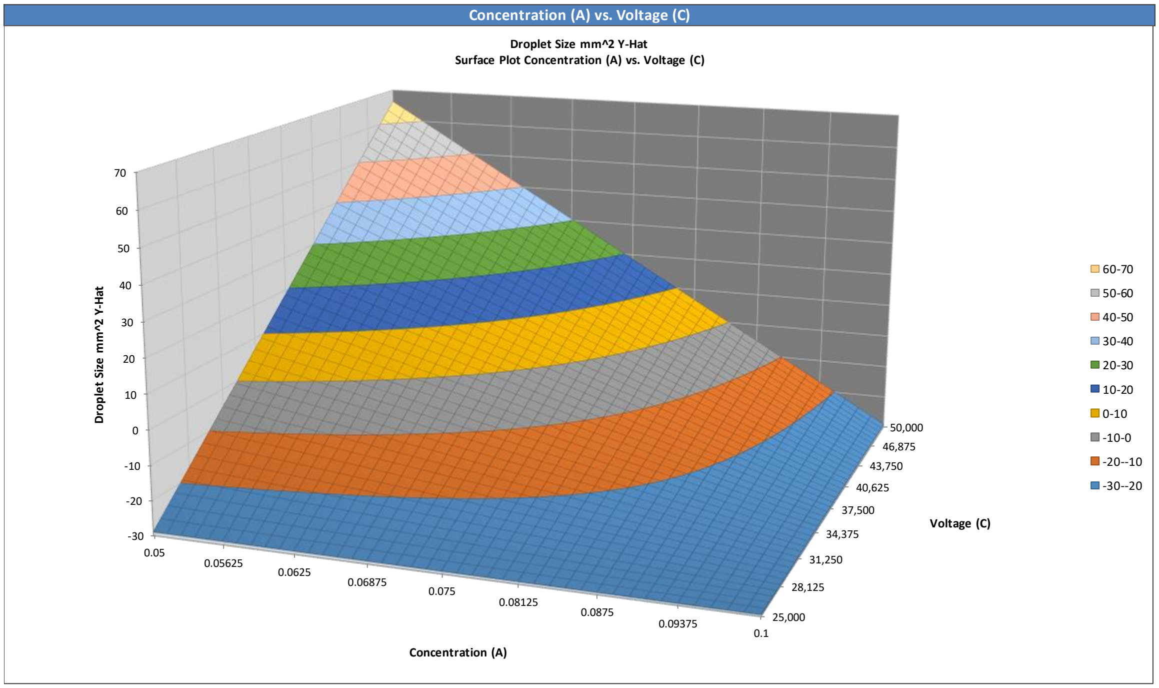

Figure 216: Surface Chart - Concentration vs Voltage for Droplet Size h-hat (Sunflower oil, Polysorbate 80, 22ga Capillary)

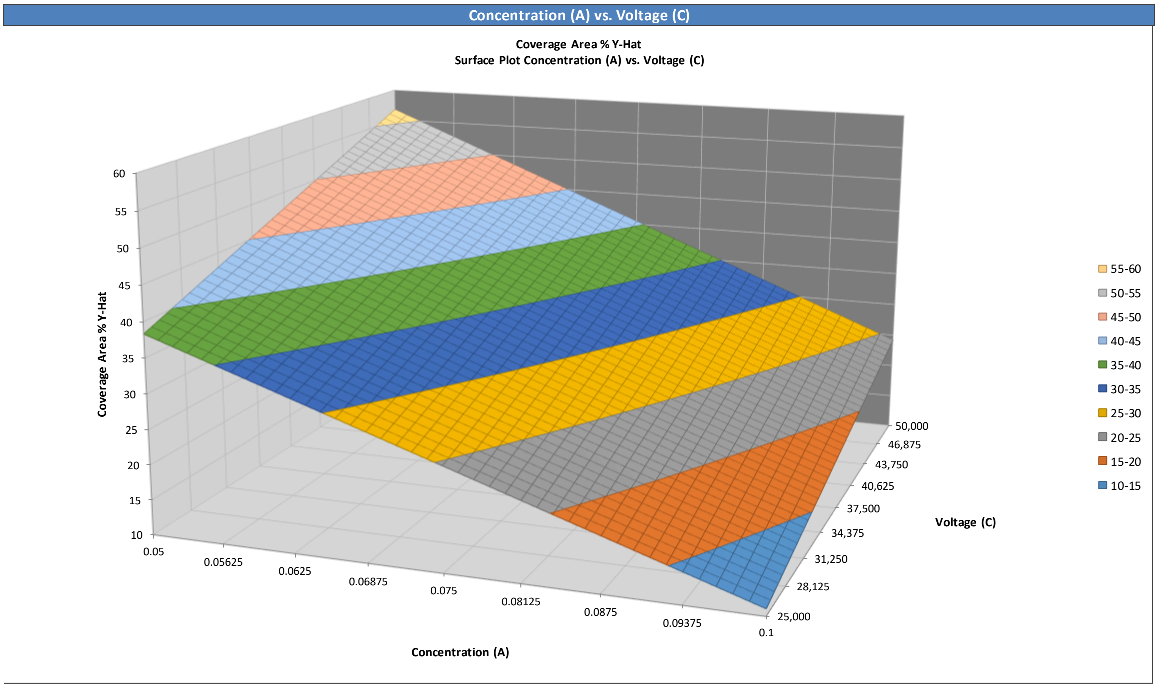

Figure 217: Surface Chart - Concentration vs Voltage for Coverage Area h-hat (Sunflower oil, Polysorbate 80, 22ga Capillary)

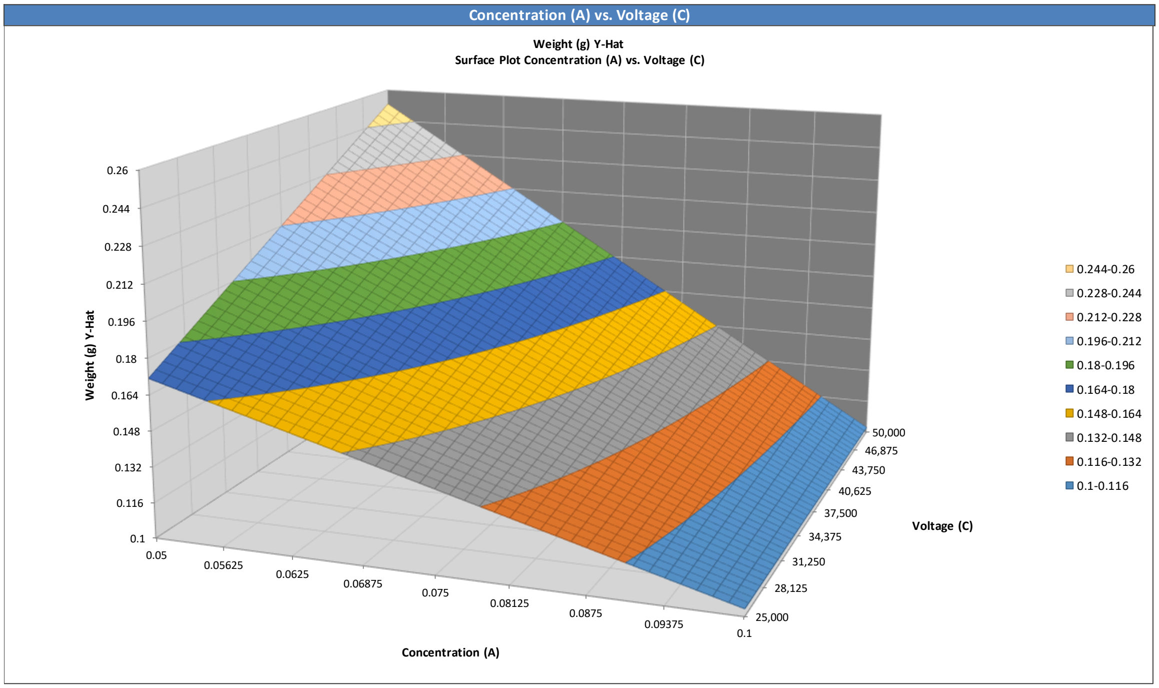

Figure 218: Surface Chart - Concentration vs Voltage for Sample Weight h-hat (Sunflower oil, Polysorbate 80, 22ga Capillary)

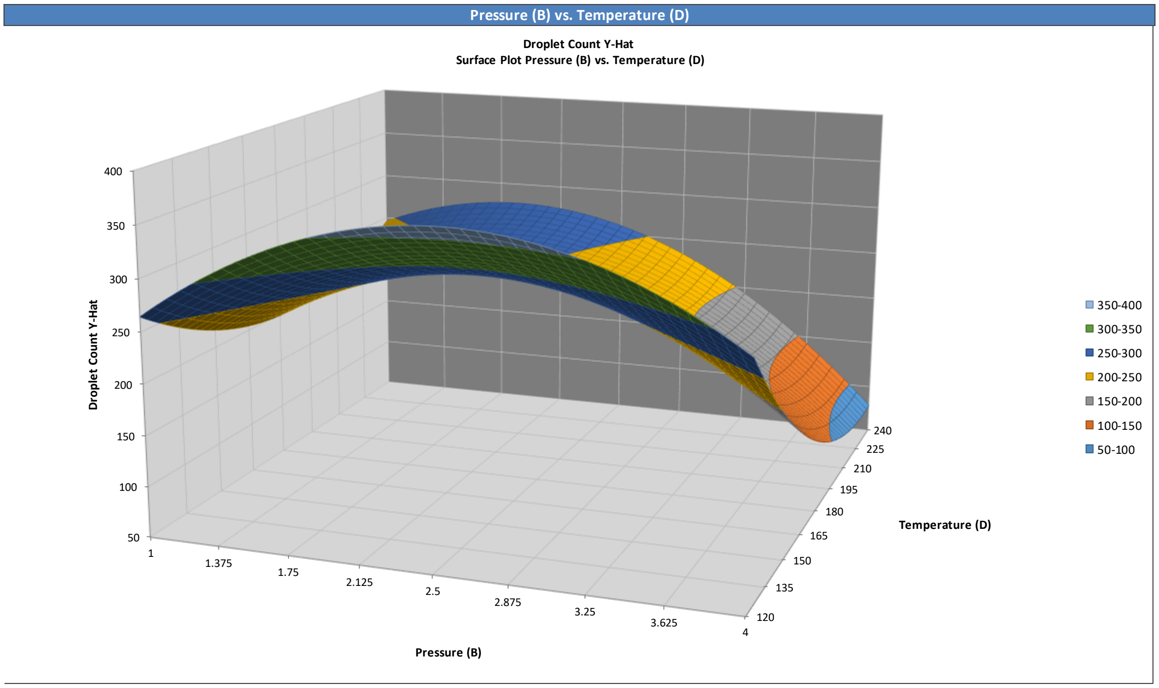

Figure 219: Surface Chart – Pressure vs Temperature for Droplet Count h-hat (Sunflower oil, Polysorbate 80, 22ga Capillary)

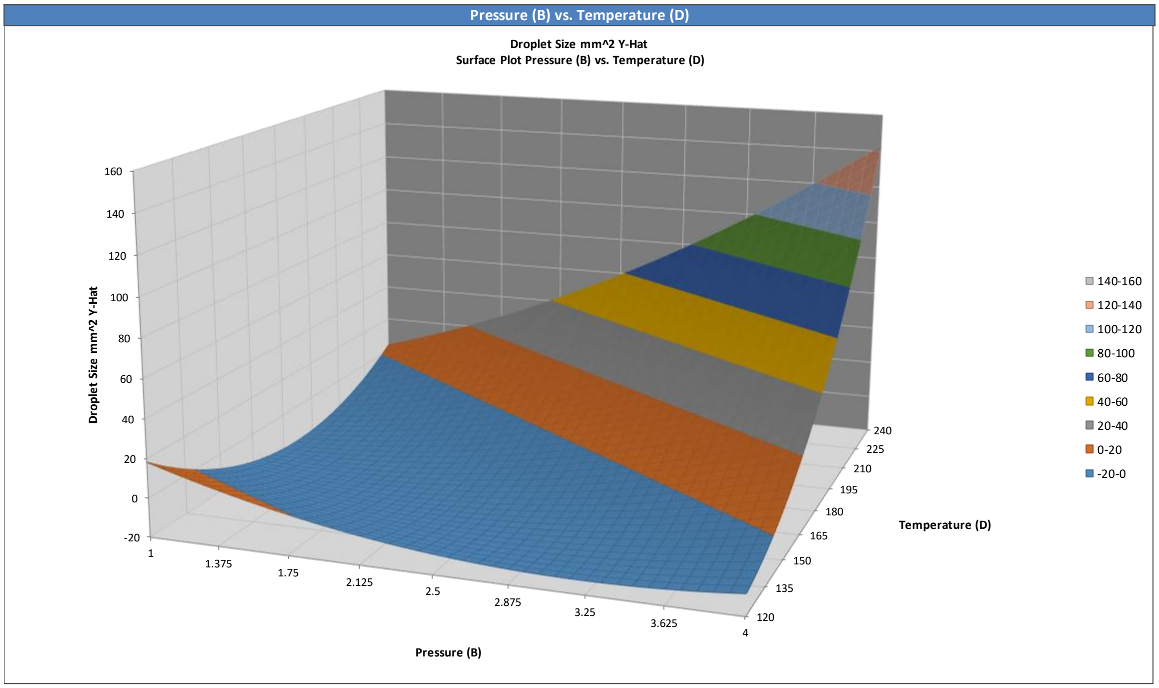

Figure 220: Surface Chart – Pressure vs Temperature for Droplet Size h-hat (Sunflower oil, Polysorbate 80, 22ga Capillary)

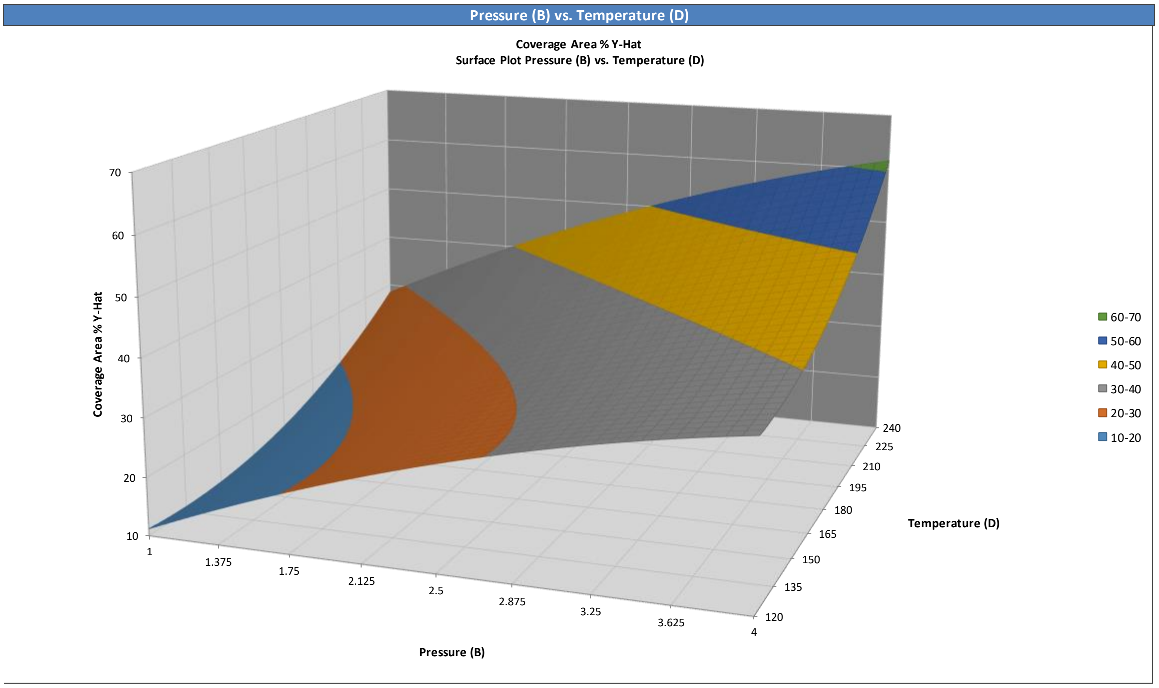

Figure 221: Surface Chart – Pressure vs Temperature for Coverage Area h-hat (Sunflower oil, Polysorbate 80, 22ga Capillary)

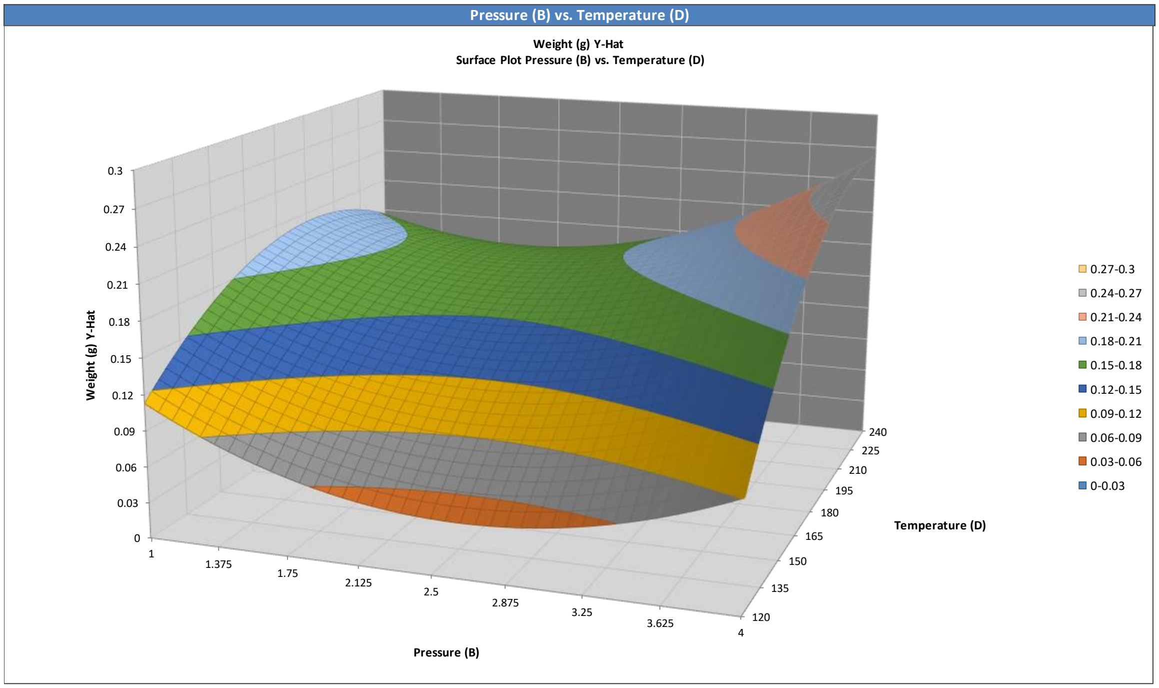

Figure 222: Surface Chart – Pressure vs Temperature for Sample Weight h-hat (Sunflower oil, Polysorbate 80, 22ga Capillary)

5.4.5. Propylene Glycol with 19 Gauge Capillary

Table 26: Main Effects Plot for Sunflower Oil & Propylene Glycol @ 19ga Capillary

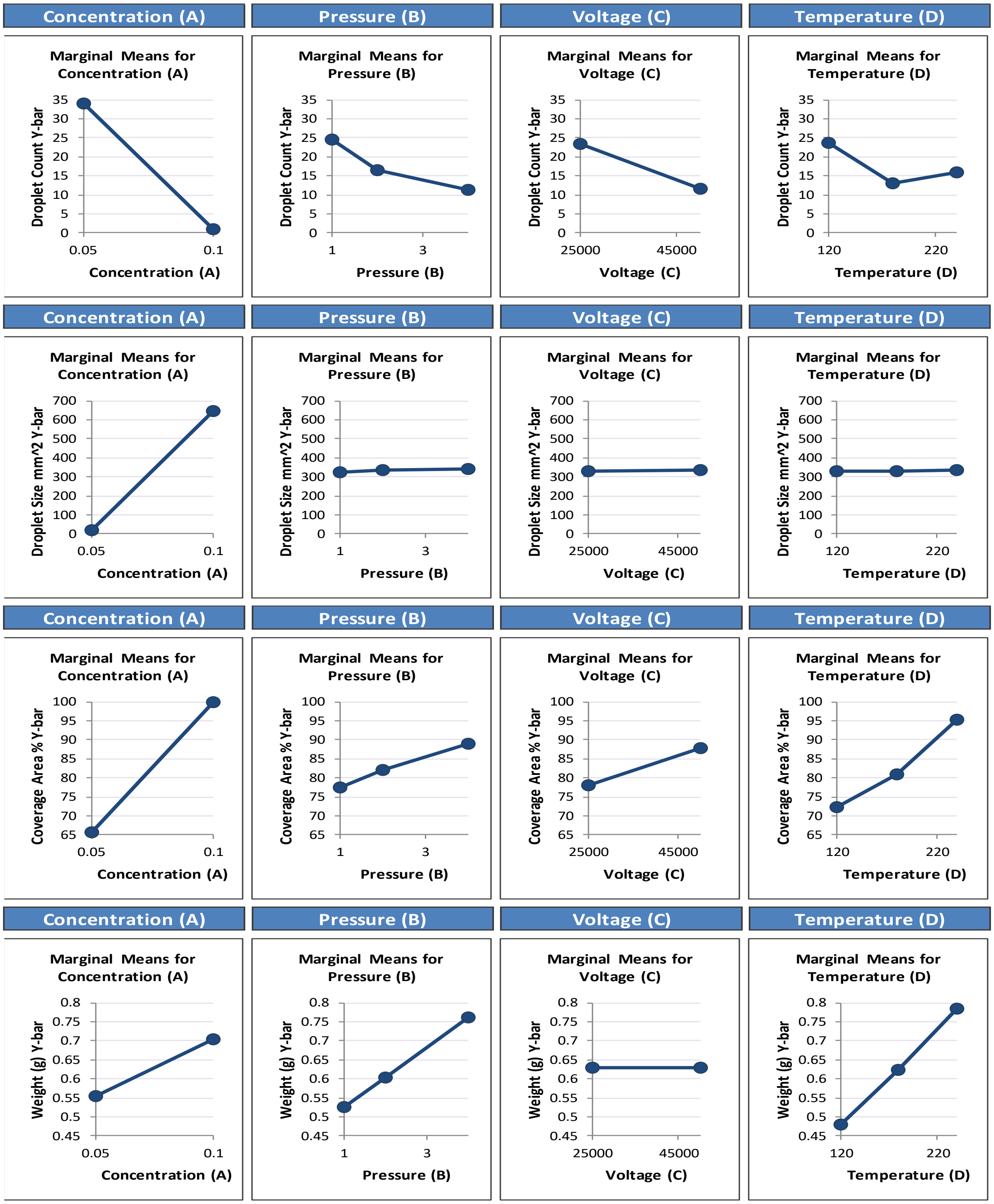

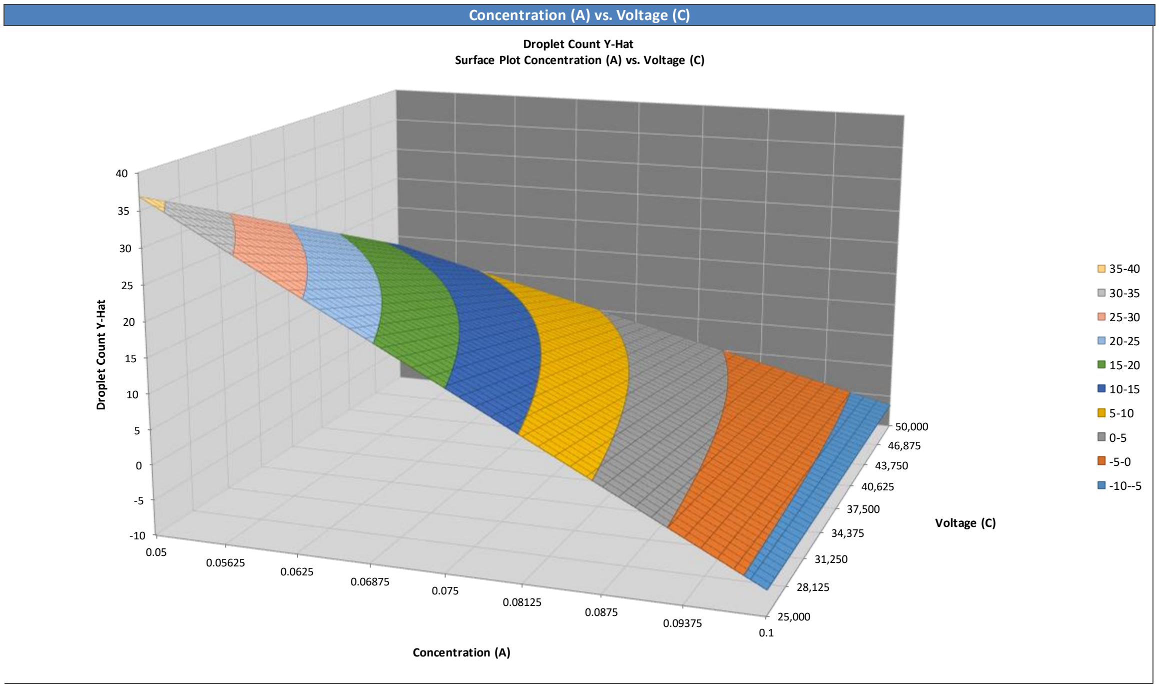

Figure 223: Surface Chart - Concentration vs Voltage for Droplet Count h-hat (Sunflower oil, Propylene Glycol, 19ga Capillary)

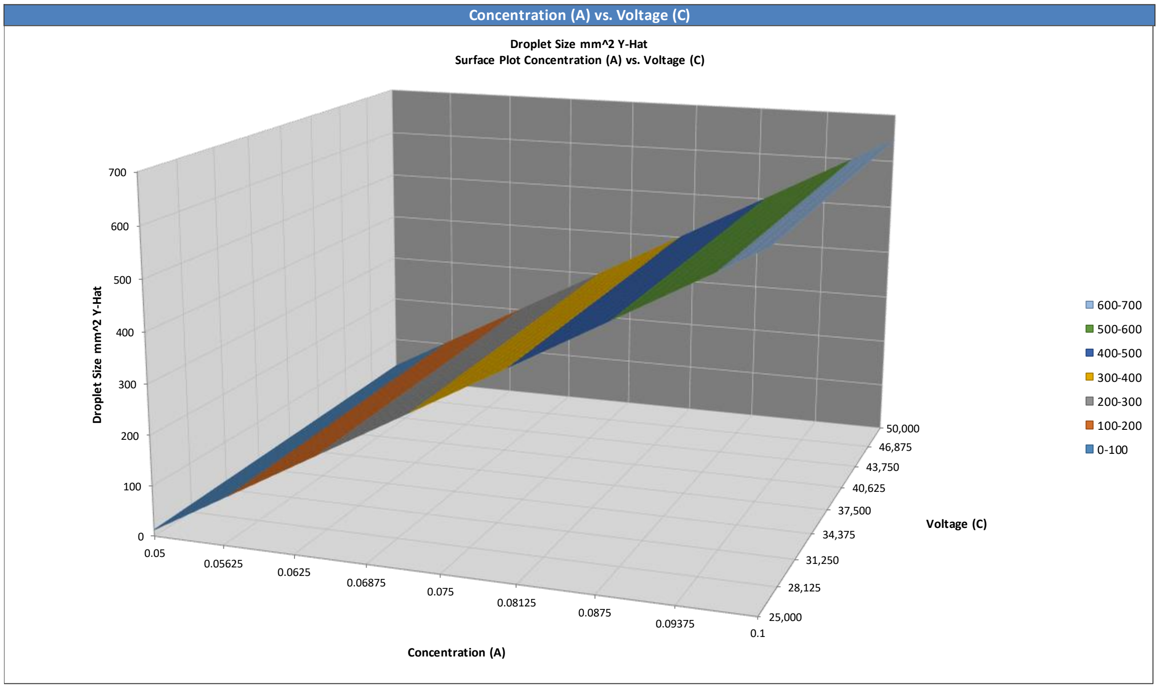

Figure 224: Surface Chart - Concentration vs Voltage for Droplet Size h-hat (Sunflower oil, Propylene Glycol, 19ga Capillary)

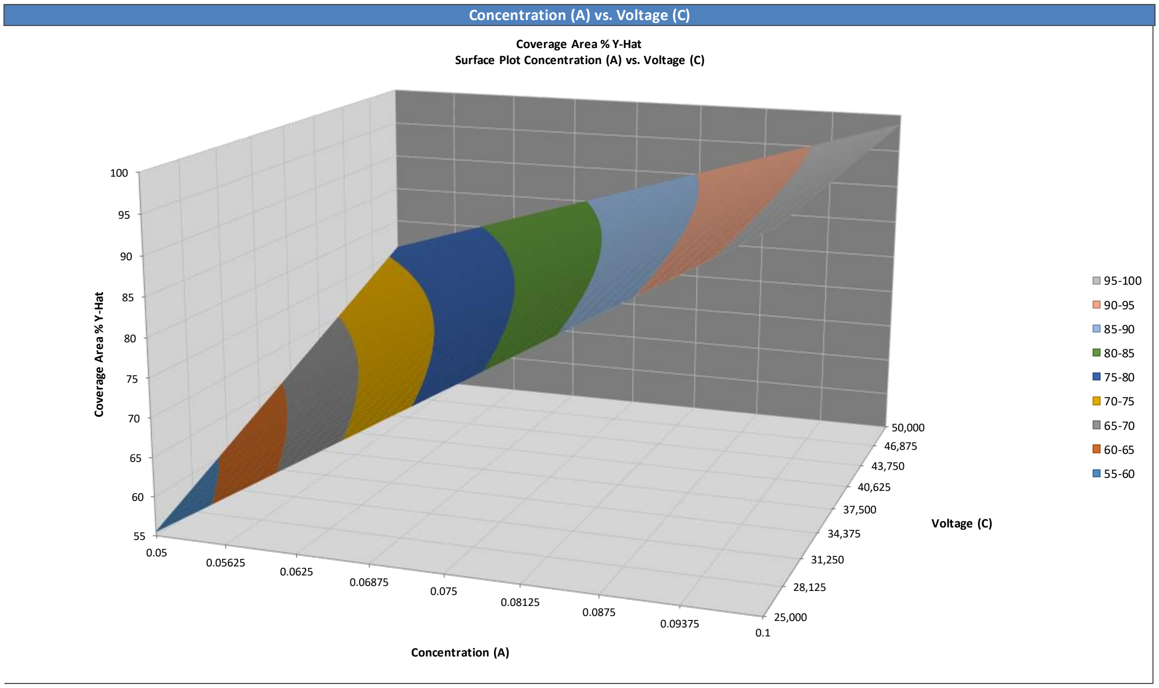

Figure 225: Surface Chart - Concentration vs Voltage for Coverage Area h-hat (Sunflower oil, Propylene Glycol, 19ga Capillary)

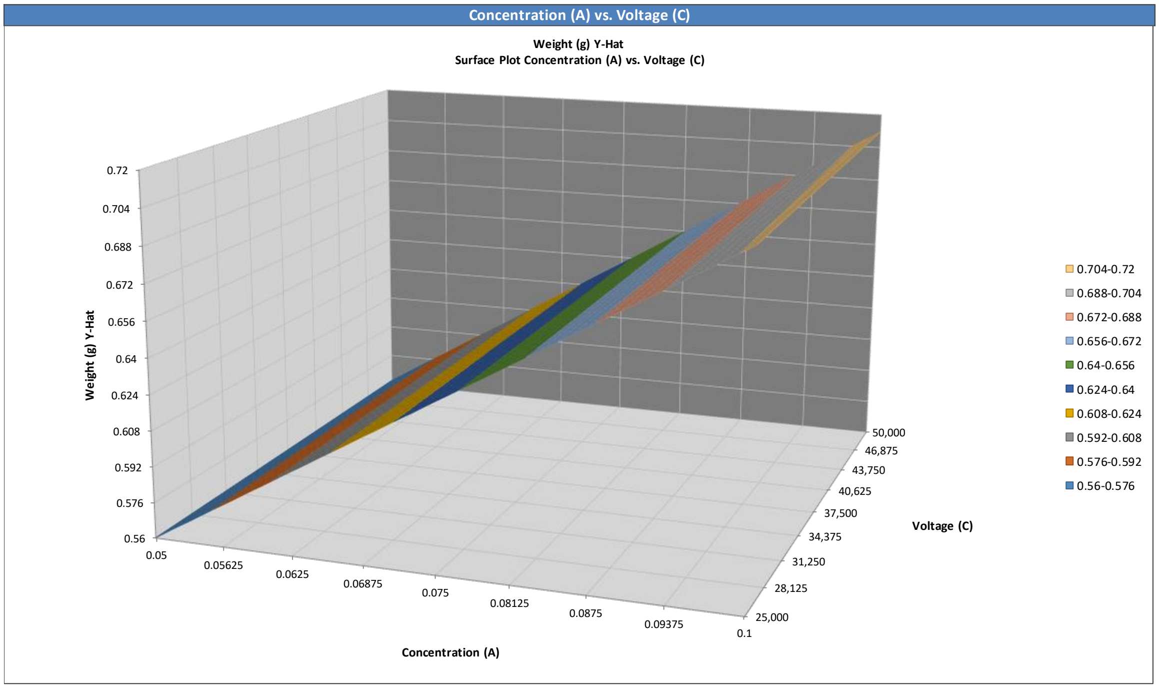

Figure 226: Surface Chart - Concentration vs Voltage for Sample Size h-hat (Sunflower oil, Propylene Glycol, 19ga Capillary)

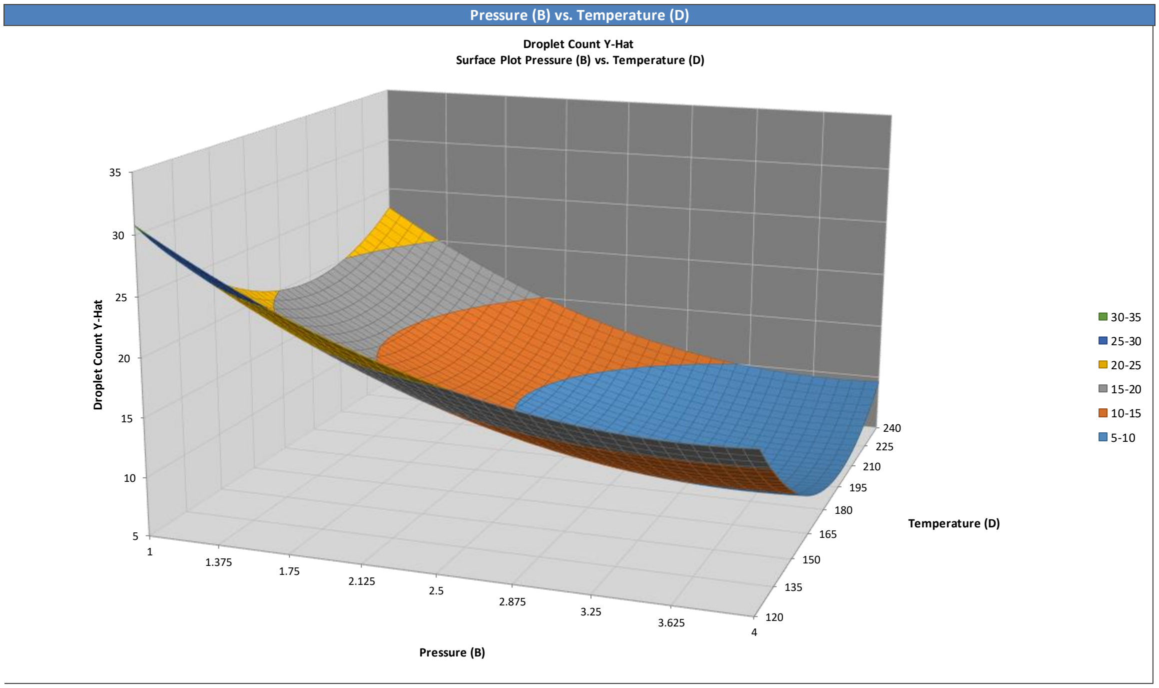

Figure 227: Surface Chart – Pressure vs Temperature for Droplet Count h-hat (Sunflower oil, Propylene Glycol, 19ga Capillary)

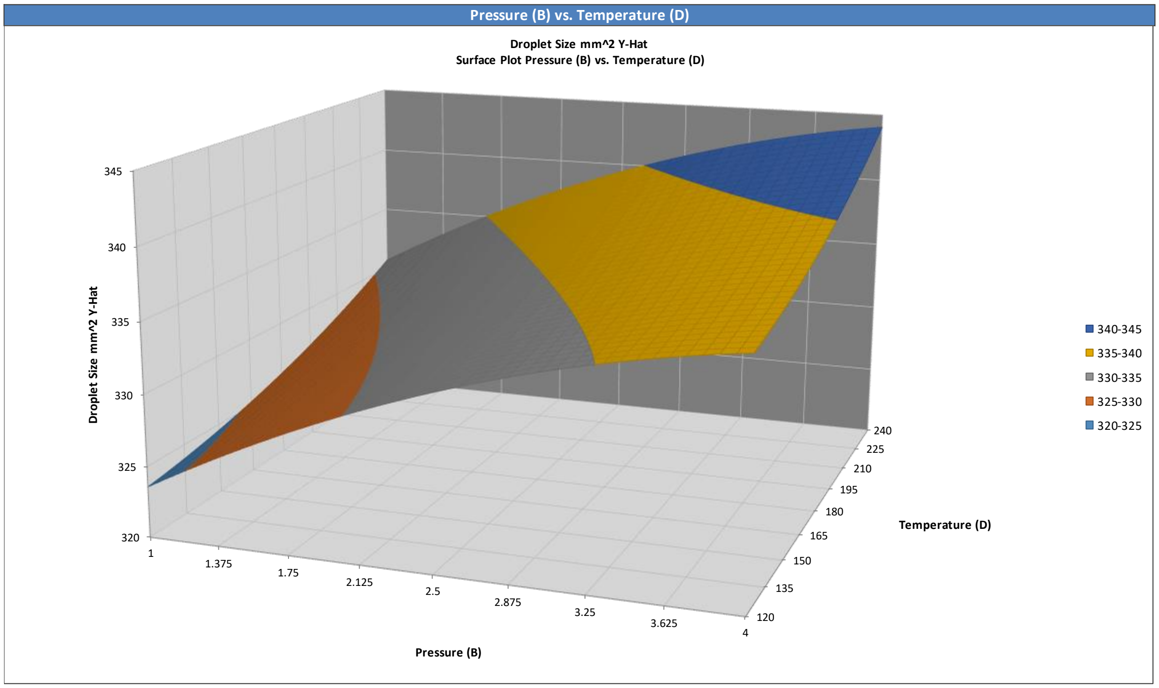

Figure 228: Surface Chart – Pressure vs Temperature for Droplet Size h-hat (Sunflower oil, Propylene Glycol, 19ga Capillary)

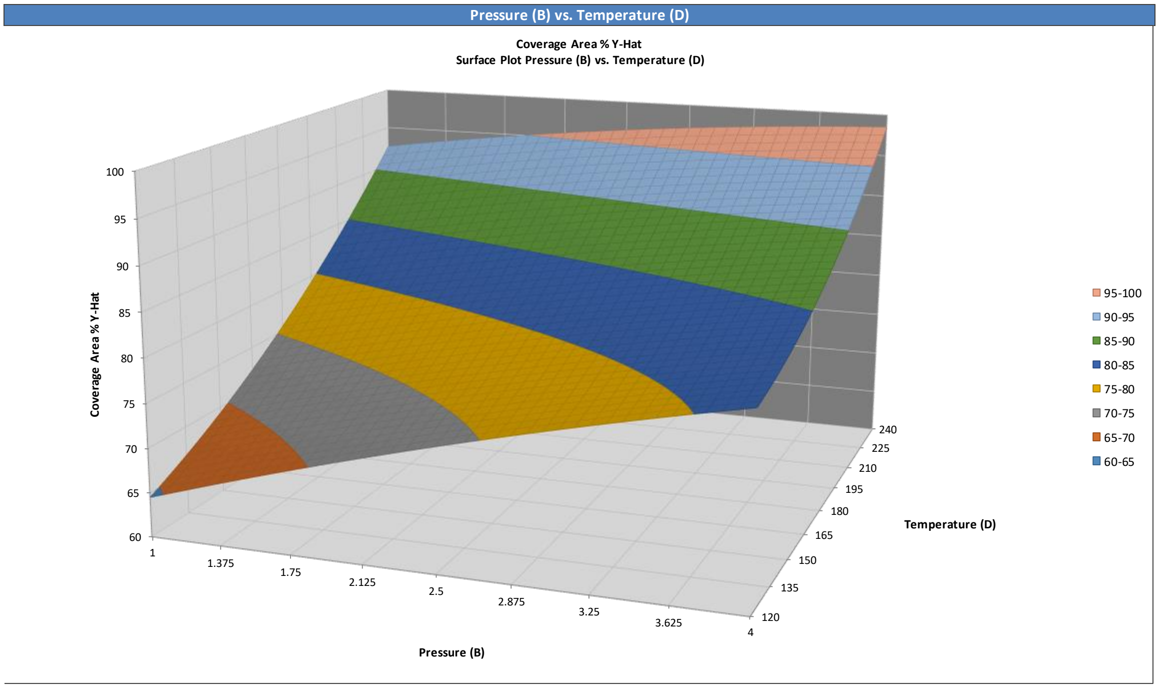

Figure 229: Surface Chart – Pressure vs Temperature for Coverage Area h-hat (Sunflower oil, Propylene Glycol, 19ga Capillary)

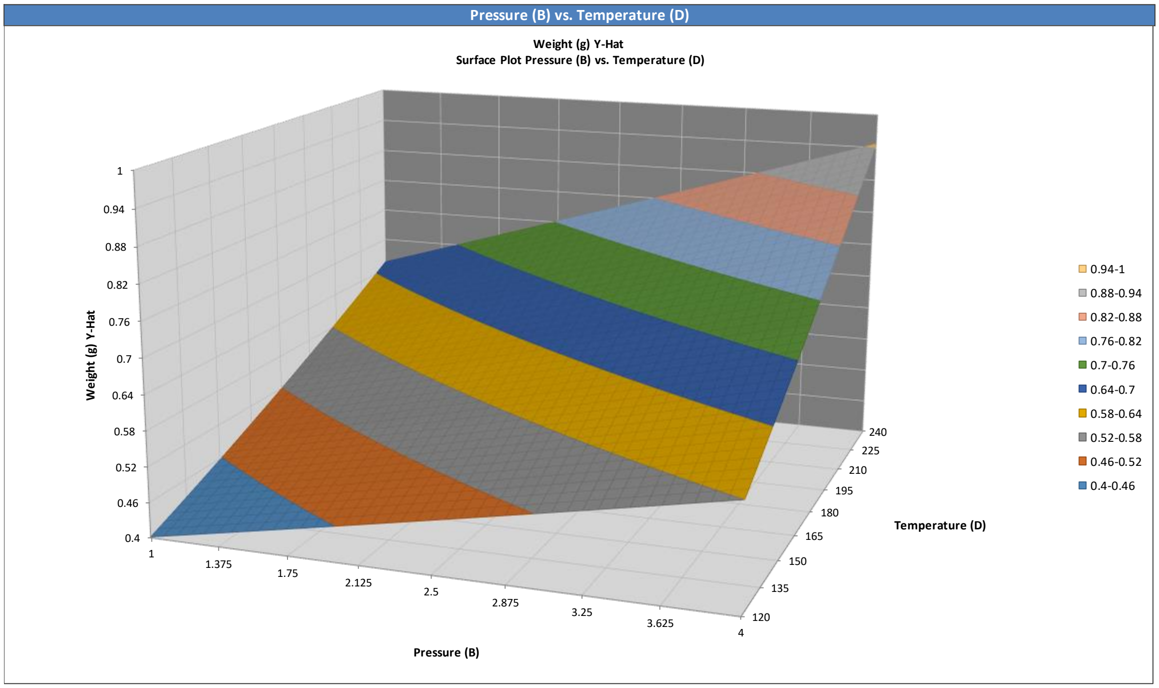

Figure 230: Surface Chart – Pressure vs Temperature for Sample Weight h-hat (Sunflower oil, Propylene Glycol, 19ga Capillary)

5.4.6. Propylene Glycol with 22 Gauge Capillary

Table 27: Main Effects Plot for Sunflower Oil & Propylene Glycol @ 22ga Capillary

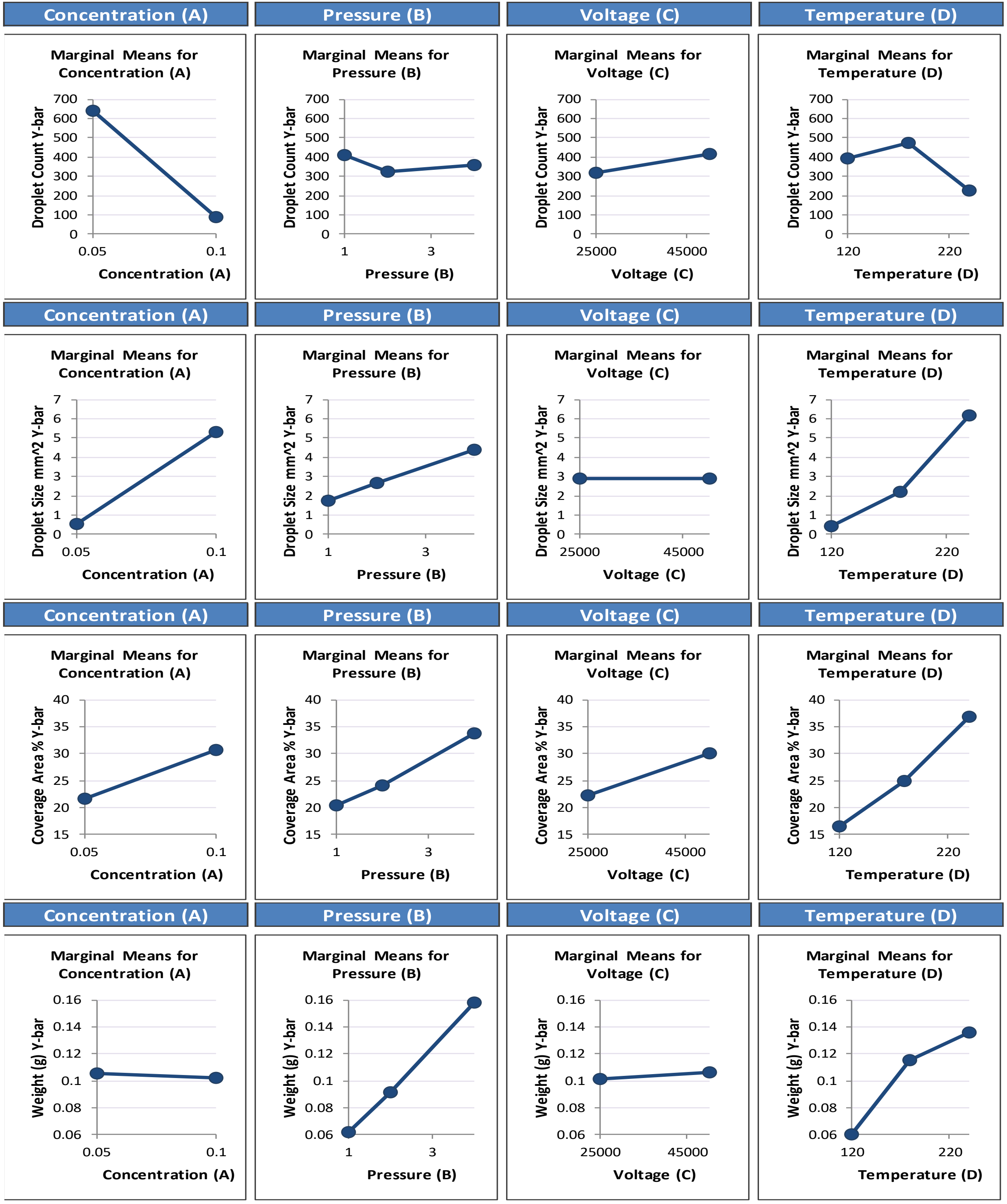

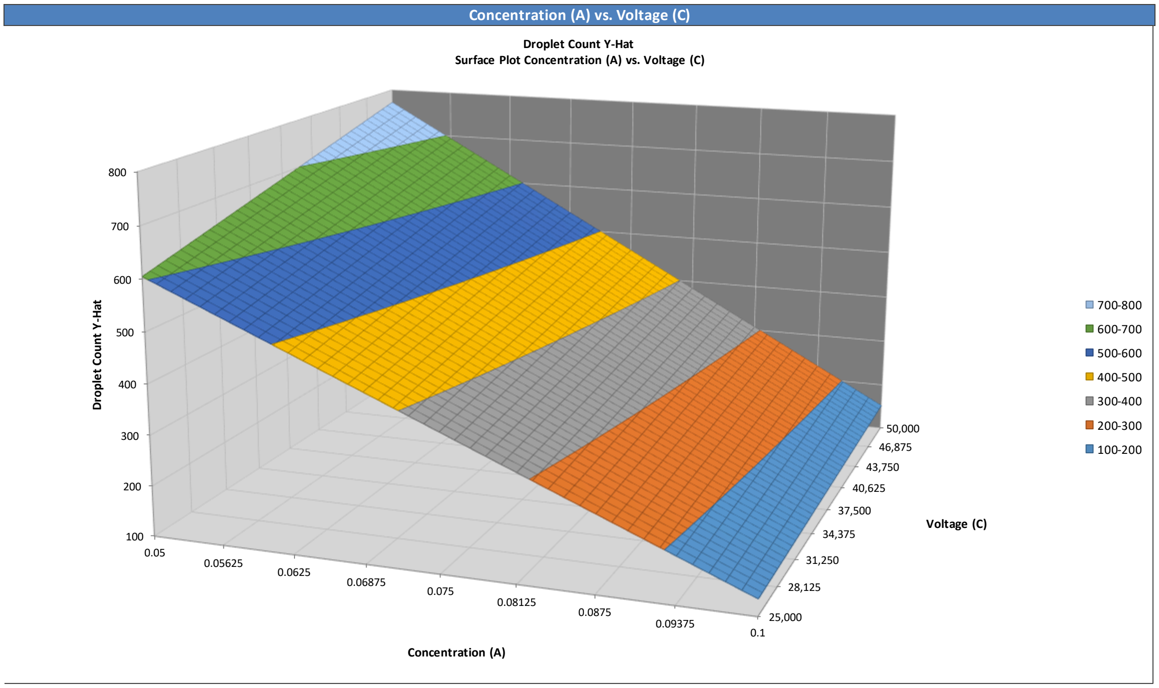

Figure 231: Surface Chart - Concentration vs Voltage for Droplet Count h-hat (Sunflower oil, Propylene Glycol, 22ga Capillary)

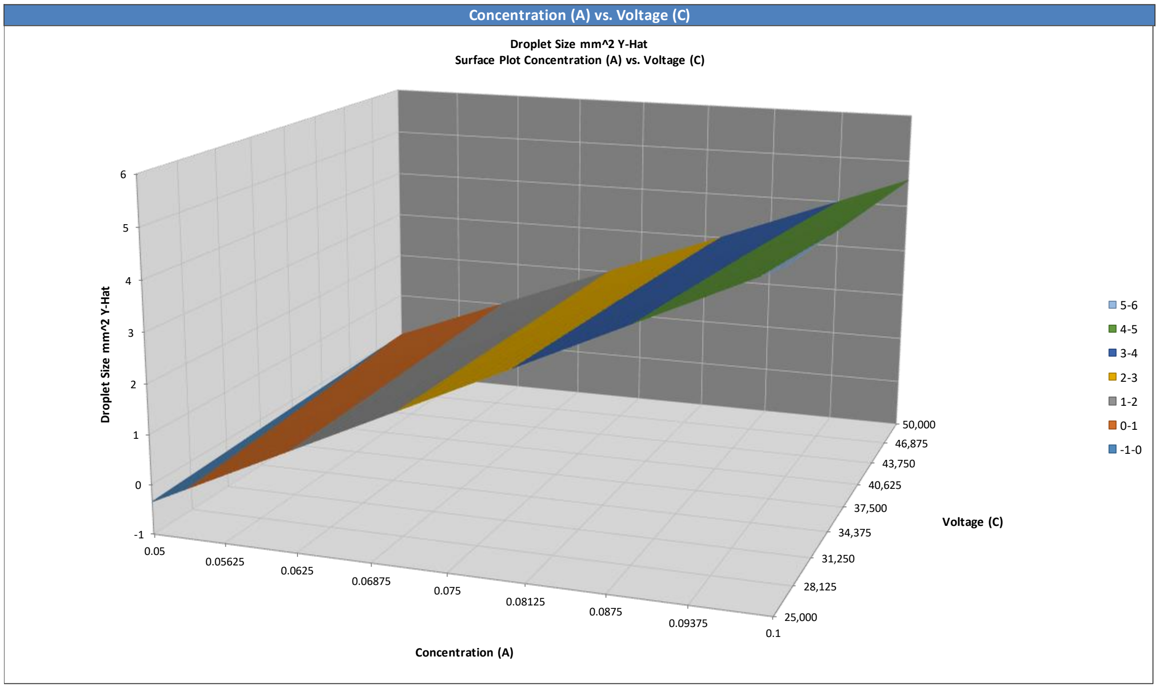

Figure 232: Surface Chart - Concentration vs Voltage for Droplet Size h-hat (Sunflower oil, Propylene Glycol, 22ga Capillary)

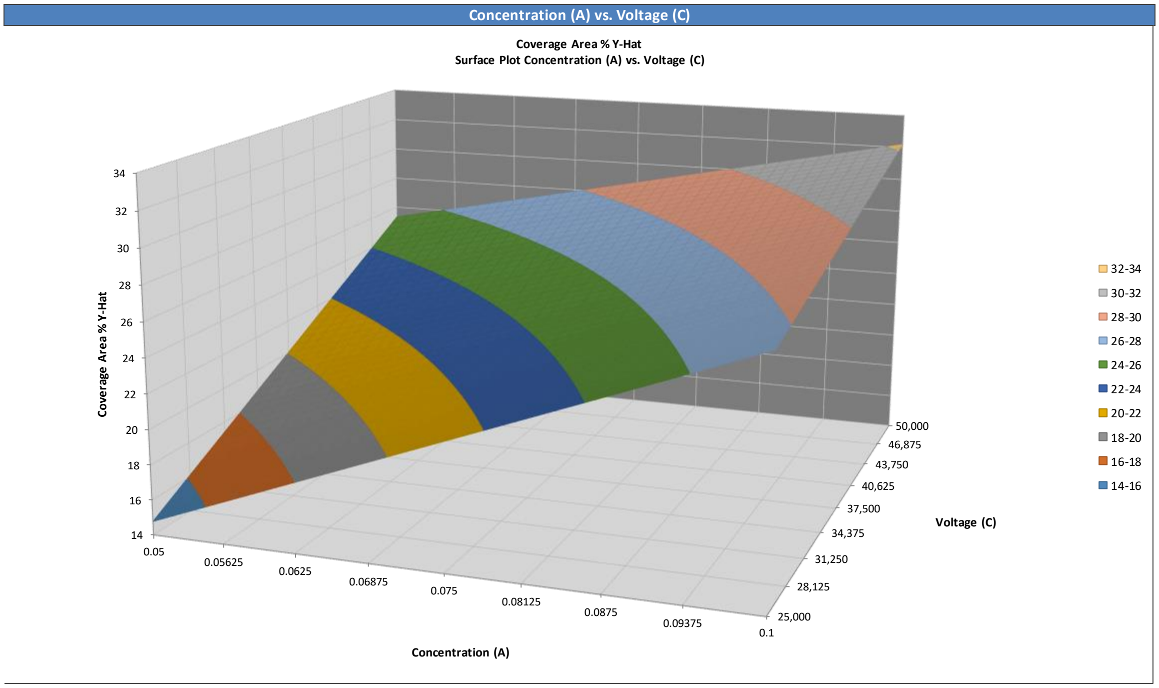

Figure 233: Surface Chart - Concentration vs Voltage for Coverage Area h-hat (Sunflower oil, Propylene Glycol, 22ga Capillary)

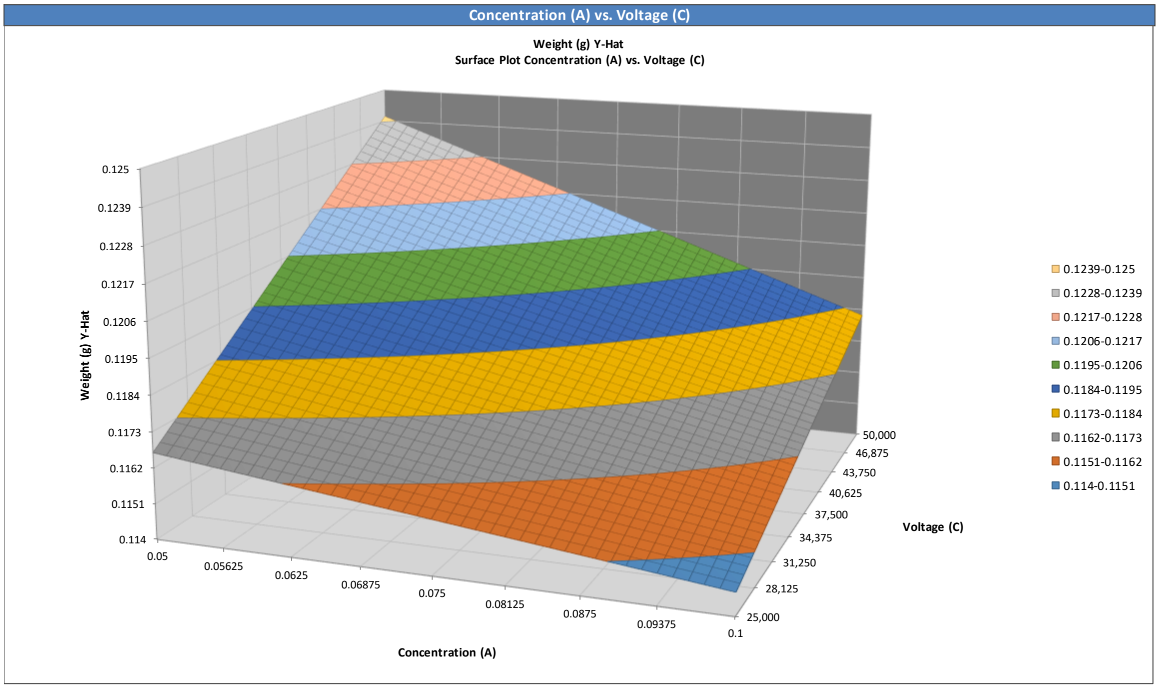

Figure 234: Surface Chart - Concentration vs Voltage for Sample Weight h-hat (Sunflower oil, Propylene Glycol, 22ga Capillary)

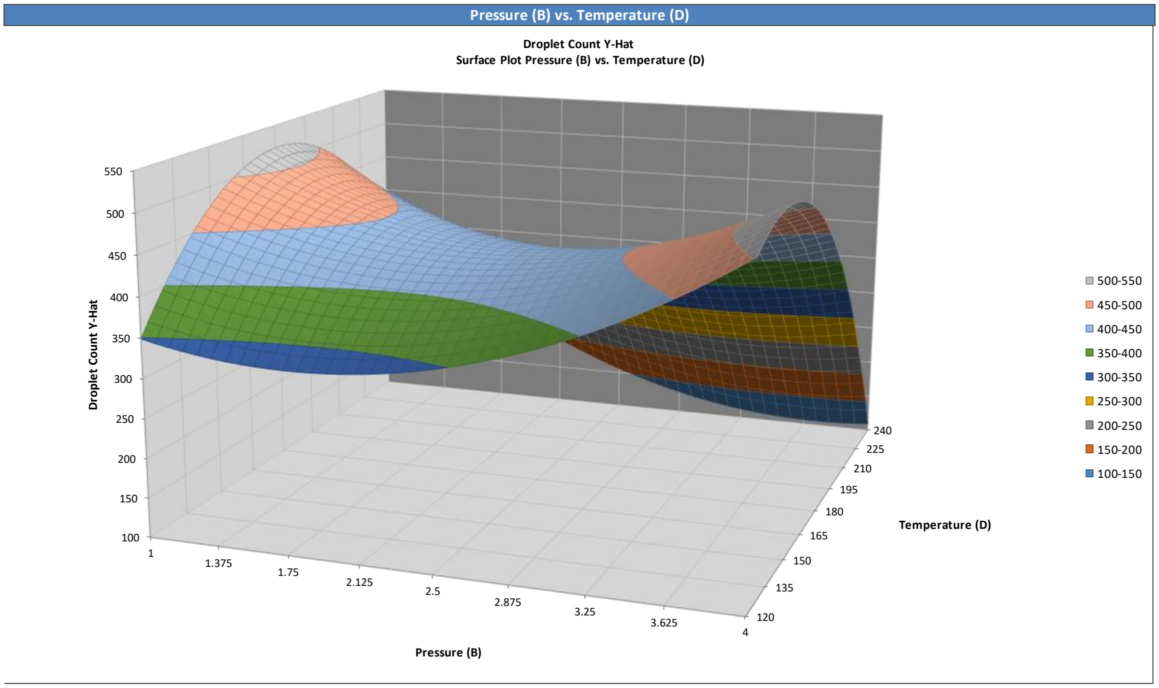

Figure 235: Surface Chart – Pressure vs Temperature for Droplet Count h-hat (Sunflower oil, Propylene Glycol, 22ga Capillary)

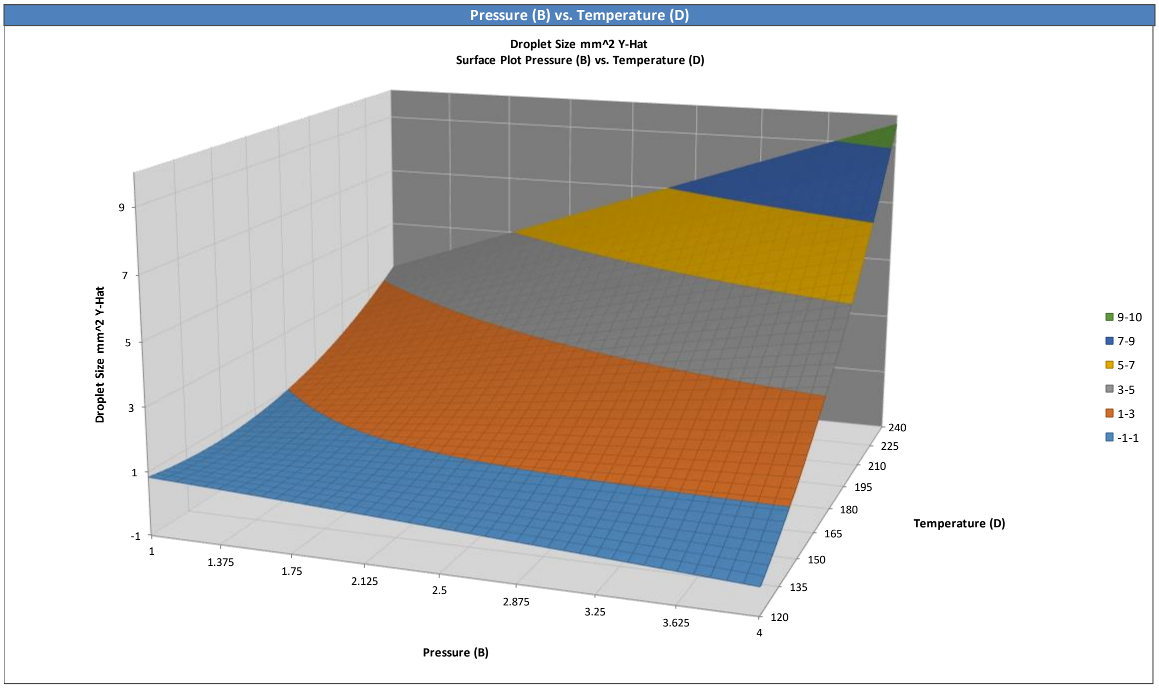

Figure 236: Surface Chart – Pressure vs Temperature for Droplet Size h-hat (Sunflower oil, Propylene Glycol, 22ga Capillary)

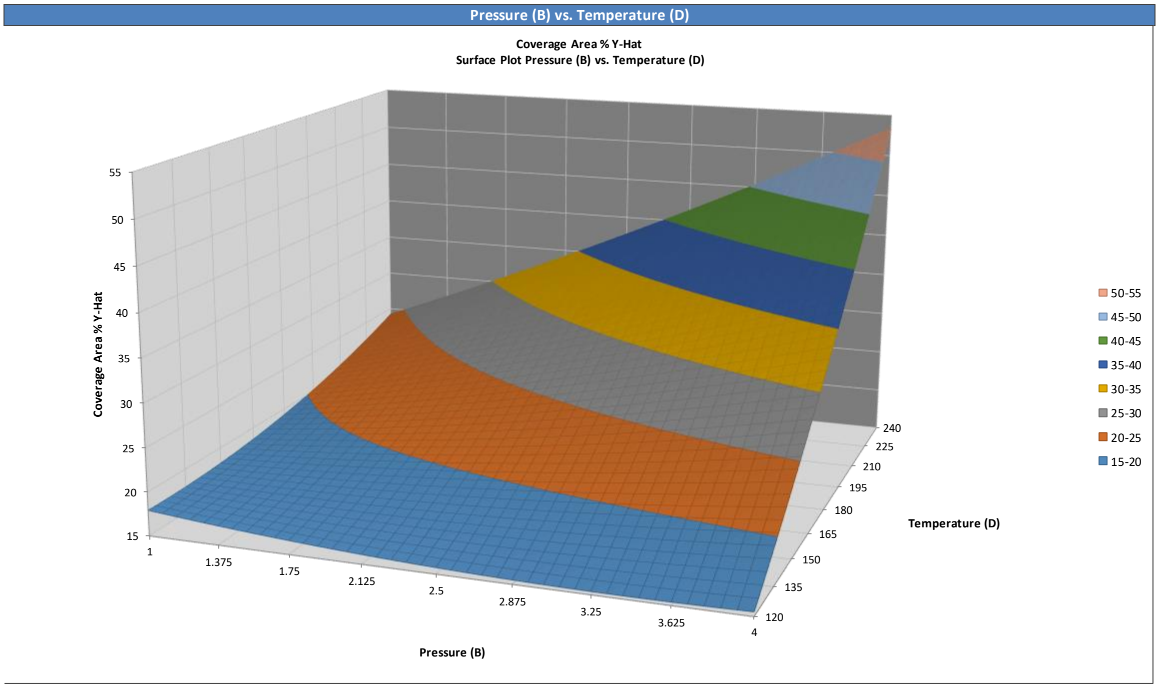

Figure 237: Surface Chart – Pressure vs Temperature for Coverage Area h-hat (Sunflower oil, Propylene Glycol, 22ga Capillary)

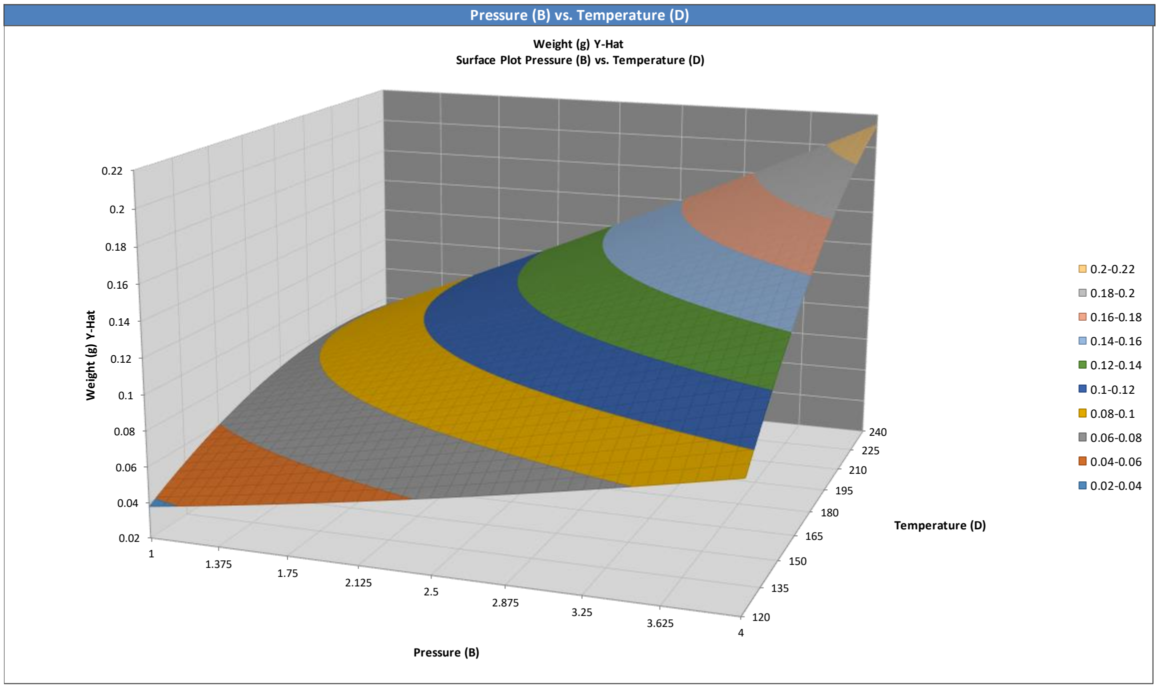

Figure 238: Surface Chart – Pressure vs Temperature for Sample Weight h-hat (Sunflower oil, Propylene Glycol, 22ga Capillary)

CHAPTER VI

6. EXPERIMENT CONCLUSIONS

From the Problem Statement for this research, it was determined that three separate criteria needed to be satisfied to answer the question, “Knowing that vegetable oil is generally considered an electrical insulator, is it possible to spot-spray vegetable oil using electro-hydrodynamic technology if a surfactant is added to the base oil?” In order to validate this notion and to prove the technology viable for use in coating applications in industrial baking, it was necessary to:

1. Develop a technology and methodology to spot-spay while electrically charging the fluid pathway with high voltage (25kV and 50kV). Additionally, this process needed to exceed a mass flow rate of >15g/minute.
2. Determine if the top four (4) commercially available vegetable oils could be made to carry a charge by the addition of a variety of emulsifiers (surfactants).
3. Achieve a sufficiently small enough droplet size with a sufficiently dense enough droplet pattern to provide adequate coverage for use in pan coating.

From this Problem Statement, several research questions were posed. Can the top four (4) commercially available vegetable oils be made to carry a charge with the addition of food grade surfactants? Can spot-spray technology be made to work with EHD spraying? Can mass flow rates of EHD atomization meet the >15g/min mark needed for industrial bakery applications? Can emulsifiers other than Lecithin be used as a surfactant in lowering surface tension of vegetable oils? Does higher voltage mean better atomization? What is the relationship between the different input variables and outputs?

From the experiment, each of the three criteria were successfully attended. Technology was developed, patent pending, to spot-spray EHD charged fluid. For each oil type, six (6) separate experiments were performed. The technology was used in the test fixture to successfully EHD spray a total of 865 samples of the four commercially available food grade vegetable oils (Palm, Soybean, Rapeseed, and Sunflower). For each test, vegetable oil was blended with an emulsifier and sprayed onto a test swatch. From the test swatches, data was generated that could feed the DOE statistical model and ANOVA was performed. From this model, the relationship between each input and subsequent outputs was presented graphically (see Chapter V).

6.1. PATTERN ANALYSIS

Results from the experiment were varied and produced an entire range of droplet counts, sizes, and pattern densities. Pattern density can be described as the relationship between droplet count and coverage area and is demonstrated in Figure 223. In the example presented in this Figure, coverage area (the percentage of sample covered by the oil/emulsifier blend after spraying) is presented from 0% to 100% in increments of 10%.

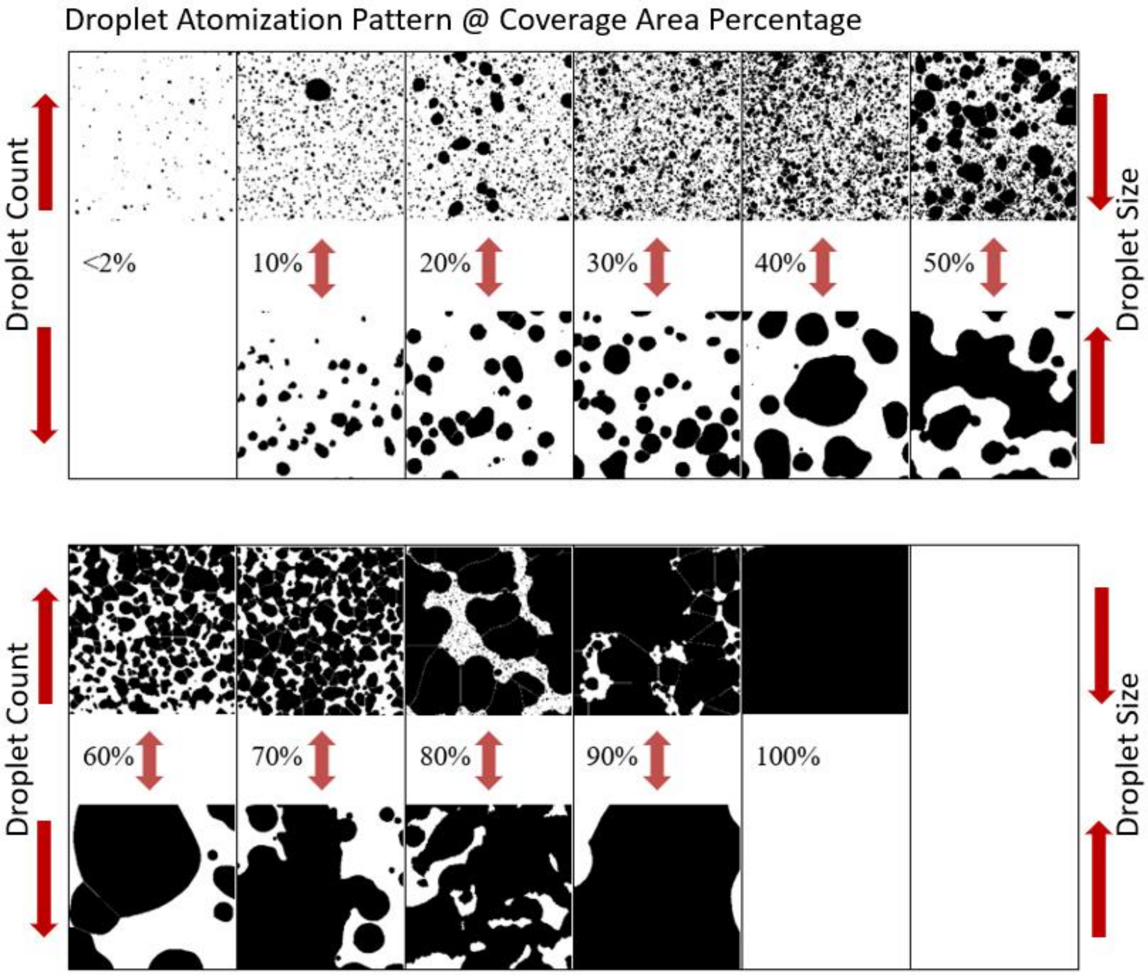

Figure 239: Droplet Atomization Patterns @ Coverage Percentages

The upper row demonstrates an example of a high droplet count and the lower row demonstrates a low droplet count. Subsequently, low coverage area percentages are also indicative of lower mass flow (measured in weight) through the system while higher coverage area percentages correlates to higher mass flows. This exemplifies the four outputs from the experiment (Droplet Count, Droplet Size, Coverage Area %, and Sample Weight) and the relationship between them. In each set of experiments, statistical patterns formed that modeled the behavior of the physical test samples.

The goal of the experiment was to produce a high coverage area with a high droplet count of small diameter droplets. For optimal range, a coverage area of between 15%-60% and a droplet count of greater than 200 droplets/inch is desirable. It was observed that as the droplet count increased, the droplet sized decreased and vice versa (see Figure 239).

6.1.1. Droplet Count

The number of droplets per unit area is a clear indicator of EHD spray performance. Because the capillary tube generates a laminar flow under non-charged conditions or any condition less than the Rayleigh limit, any droplets formed from EHD spraying were directly resultant to the applied charge. Propylene Glycol, in general, performed generated the highest Droplet Count of any emulsifier. When mixed with Palm or Rapeseed oil, sprayed through a 22ga capillary, at generally low temperature and pressure, Propylene Glycol produced droplet counts as high as 2644 droplets/in^2. Conversely, 132 tests (15.25%) produced a droplet count of one (1). This ‘blind’ condition is indicative of an EHD failure (failure to exceed the Rayleigh limit). These failures were seen across all four (4) oils, yet almost exclusive to Polysorbate 20 & 80 and Propylene Glycol and were all exclusive to tests performed with a 19ga capillary tube. These failures all occurred at mass flow rates greater than 1.2 g/s, with the greatest number of failures (66%) occurring at mass flow rates in excess of 2 g/s or 120 g/minute.

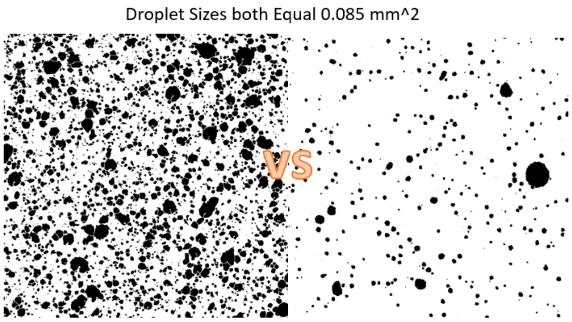

Figure 240: Droplet Size Comparison per Unit Measure

While a relationship exists between droplet count and droplet size, it is a correlation at best. In order for droplet counts to be on the higher end of the spectrum, droplet size must be sufficiently small. However, this droplet density does not hold true in every case. Plenty of samples had significantly small droplet sizes but also had low droplet counts. In the example in Figure 240, both samples produces a reletivly equal droplet size (0.085mm^2), however, the droplet count on the left is 2089 and the droplet count on the right is 384 covering 30% and 5.25% respectively. The left side is Palm and Propylene Glycol (10% @ 22ga, 50kV, 120F,8psi) and the right is Palm and Polysorbate 80 (10% @ 22ga, 25kV, 180F, 8psi).

6.1.2. Droplet Size

Droplet size is a determination of the efficiency of EHD atomization. If a liquid's surface tension is too high, or if it's resistivity is too high, or if the charge is inadequate to exceed the Rayleigh limit, atomization will not occur (see equation 5&6) (Gaultney et al., 1987) (Abu-Ali & Barringer, 2008) (Wang, 2012). Large droplets are undesirable in a pan oiling application due to the fact that not all surfaces receive adequate coverage and 'oil pooling' potentially causes a 'frying' effect on the product.

Table 28: Cone Jet Characteristics at Varying Pressures

Soybean & Soy Lecithin @ 22ga, 25kV, 120F,
and 4psi, 8psi, 16psi

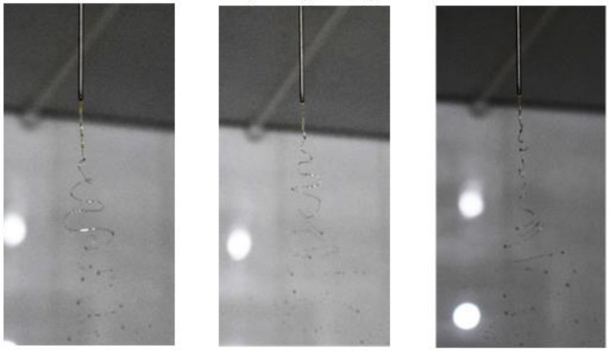

Sunflower & Propylene Glycol @ 19ga, 50kV, 120F,
and 1psi, 2psi, 4psi

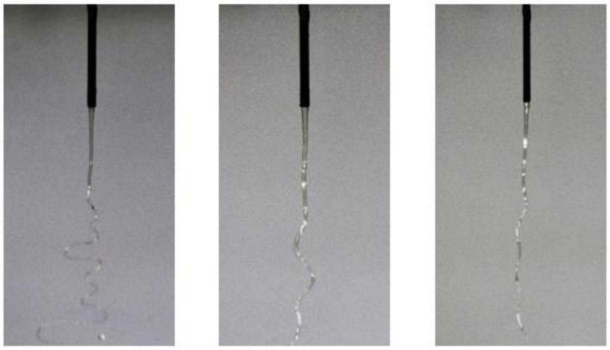

An increase in droplet size, from the data given, is largely contributed to an increase in the Mass Flow of the test samples. This is likely due to a change in charge density as the voltage (25kV or 50kV) and amperage (0.1mA) used in the experiment was constant. As more material passes the charging rod at a given time, the amount of charge per unit decreases. Assuming the liquid atomized well at low mass flow rates, this phenomenon might likely be corrected by increasing the amperage applied at higher mass flow rates.

The system operated in a cone-jet mode during both small droplet and large droplet tests (see Table 28) but the instability moved from kink to varicose as charge density decreased. It was also observed that, in certain low volume but higher pressure testing, the initial kink instabilities were present during the spray operation but that further breakdown of droplets into smaller sized did not occur or occurred intermittently. This gave a mixture of small and larger droplets within the same test sample. This demonstrates the importance of charge density in the secondary breakdown of droplets during EHD atomization. The cone jet elongates at low pressure releasing smaller segments of liquid in the process. The kink instability diminishes as the charge density decreases until the point where it converts back to a varicose instability. All of this had a significant impact on droplet size.

6.1.3. Coverage Area %

Coverage area, defined as the percentage of the test swatch covered by the oil/emulsifier blend after spraying, is important to the experiments findings for two reasons. First, it is a determination of the ability of the fluid to adequately coat the surface to which it is applied. In differing test circumstances, a test sample may contain droplets of the same size but with different coverage areas. The less dense patterns tended to have an overall larger pattern area. The denser patterns, however, would provide better coating ability. Second, coverage area helps determine if a sample is statistically 'blind' or not. That is to say, test samples with high coverage areas but low droplet counts indicate a condition where the charge density was not sufficient enough to exceed the Rayleigh point (see equations 5 & 6). In these cases, we see high mass flow rates (measured as sample weight) and a breakdown of the cone-jet mode (see Table 28).

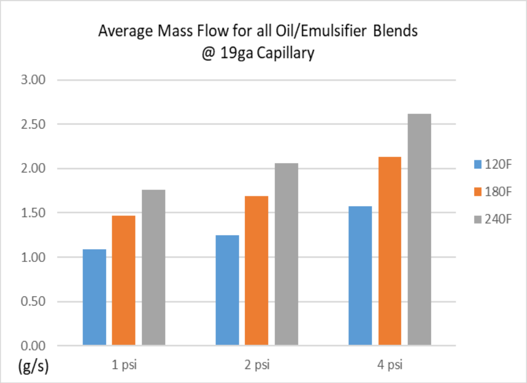

Figure 242: Average Mass Flow for all Blends @ 19ga

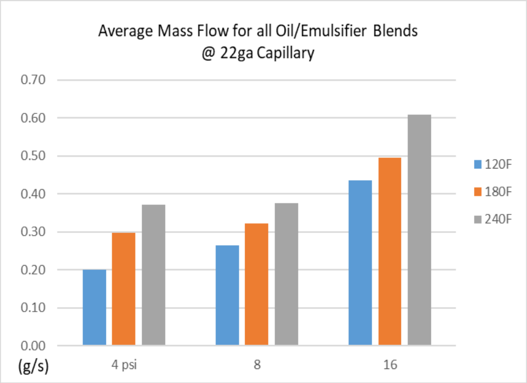

Figure 241: Average Mass Flow for All blends @ 22ga

6.1.4. Weight (Mass Flow)

Measuring the weight of each sample run allowed for an understanding of the different variables and their impact on Mass Flow. It was hypothesized that mass flow would increase as temperature and pressure increased. This was proven universally true across all combinations of oil and emulsifier. It was also proven that voltage had little to no impact on the mass flow rate. Mass flow was calculated from the weight of each sample and the spray time for each sample run.

The impact of mass flow (measured as sample weight) on the experiment was proportional to droplet size. As mass flow increased, droplet size also increased. This phenomenon was less pronounced in the 22gauge capillary tests but this is likely due to the overall lower mass flow rate of these tests. In fact, performance continued to improve in the 22ga test runs. The overall droplet density may continue to improve at even higher system pressures, and resultant mass flow rates, than the 16psi maximum pressure for this experiment group.

6.1.5. Energy Density

The energy density of the test samples is the amount of energy per unit measure of the various blends. An exponential relationship exists between the energy density (J/m^3) and the Mass Flow (g/s). This exists due to the change in dynamic viscosity and density of the blends as they gain temperature and as the overall volumetric flow rate changes at different pressures. Because the voltage (25kV and 50kV), amperage (0.1A), and cycle time (300ms) were fixed for every experiment, and because the differences in dynamic viscosity and density were trivial between each of the four base oils, the relationship between mass flow and energy density can be graphed as a continuous equation.

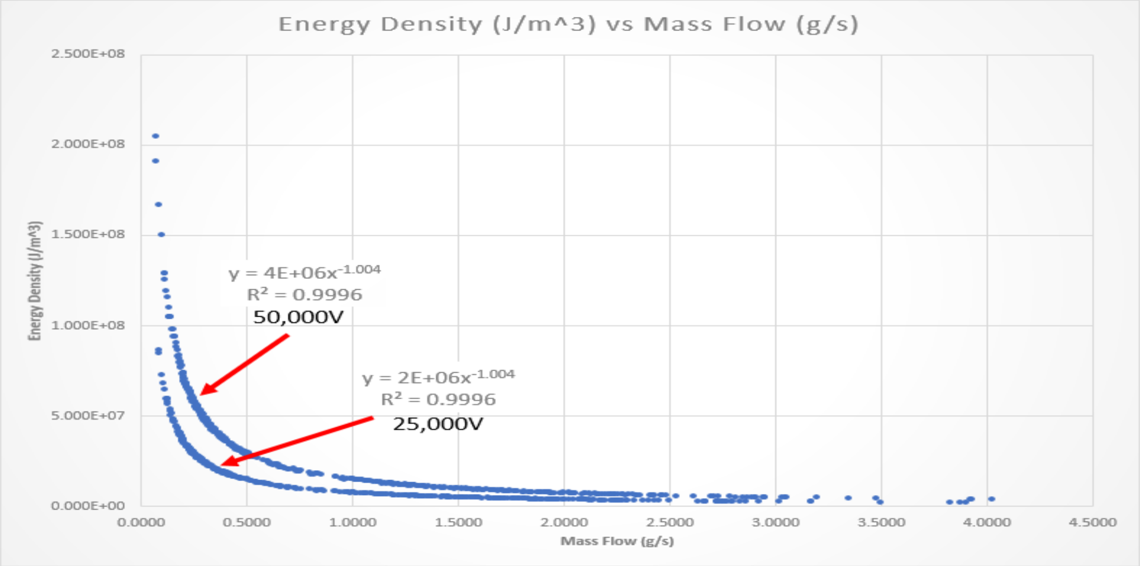

Figure 243: Energy Density vs Sample Weight for all Test Samples

Figure 243 demonstrates how every single datum from the various experiments falls on either the 25kV regression or the 50kV regression. This is a function of two different energy levels. At 25kV and 0.1mA for 0.3 seconds, 2.5 Joules of energy are introduced to the fluid. At 50kv and 0.1ma for 0.3 seconds, 5 Joules of energy are introduced to the fluid. It also shows why low mass flows, and subsequent low sample weights, have higher energy densities and vice versa. This is a critical factor in droplet development. In experiments with high mass flows (19ga capillary, higher temperature, and higher pressures), droplets tend to be larger. It also demonstrates why higher voltage tends to produce smaller droplets. Per the regression, energy densities, E_d, can be modeled for 25kV and 50kV as:

Equation 28: Energy Density Regression for 25kV (all oils)

$$E_d = 6\dot{m}^{-1.004} * 10^2 \tag{28}$$

Equation 29: Energy Density Regression for 50kV (all oils)

$$E_d = 6\dot{m}^{-1.004} * 10^4 \tag{29}$$

6.2. SPOT SPRAY

The spot spray concept went through several iterations in the design process that included both inductive and conductive charging. The final design settled on creating a fluid chamber internal to the valve and using the valve stem as a charging rod for the fluid. The valve stem created a plug for the top of the capillary and sealed off the fluid flow while creating a vacuum for the liquid remaining in the capillary tube. The valve had an 8.5ms actuation rate. The 24VDC solenoid provided approximately 1925 grams of pulling force. Of the 865 individual tests performed, the EHD valve performed as expected 100% of the time. Patent protection was filed for the EHD valve and EHD oiling assembly to prior to publishing this paper.

The EHD spray valve performed well but did have a few issues. First, the valve was electrically actuated with a spring return. The valve developed a slight drip when fluid temperatures were at the 240F mark. While this didn’t negatively affect the experiment, a stronger return spring or different geometry where the valve stem seats above the capillary tube would mitigate this problem. Also, the system would occasionally arc to the solenoid when the charging rod was electrified. Again, this didn’t provide any problems with the experiment, but could be mitigated by increasing the distance between the top of the charging rod and the bottom of the solenoid valve.

Overall actuation time was sufficient for a pan oiling operation. Virtually no overspray was observed during any of the 865 test runs. At the tested mass flow rates, in very high-speed operations (bun and roll), it might be necessary to use two separate valves inline to account for the increased throughput. This could be easily handled through sequencing, but such configuration was not tested as part of this experiment. Another consideration not tested is the impact of using the complex geometry of a bakery pan as a collector.

6.3. PALM OIL

Six separate experiments were performed with Palm oil as the base. Every combination resulted in EHD atomization utilizing the 22ga capillary. With the 19ga capillary tube, many of the tests at higher pressure and temperature resulted in a ‘blind’ (no discernable electrostatic atomization) condition. Results for tests performed using the 19ga capillary were poor-to-bad. However, many of these same combinations performed much better using the 22ga capillary. This is likely due to the much lower mass flow rates, and subsequent higher energy density, associated with the 22ga capillary. Tests such as Soy Lecithin that performed poor with a 19ga capillary might well perform better with an intermediate capillary size. Results for tests performed using the 22ga capillary tube were markedly better ranging from fair-to-superior. Surprisingly, Propylene Glycol performed the best of all of the tests at 10% concentration with a droplet count of >1,200/in^2. Palm oil received a score of 17 out of 30 for EHD performance.

6.3.1. **Soy Lecithin with 19ga Capillary**

This test, overall, produced poor results. While EHD atomization did occur, average droplet counts were low at both the 5% and 10% concentrations. Average droplet counts actually decreased from 48/in^2 to 38/in^2 as concentration increased. Average droplet sizes increased from 10mm^2 to almost 15mm^2 as concentration increased. Average coverage area percentages increased from just over 50% to almost 75%. Average sample weights rose almost 21% as concentration increased.

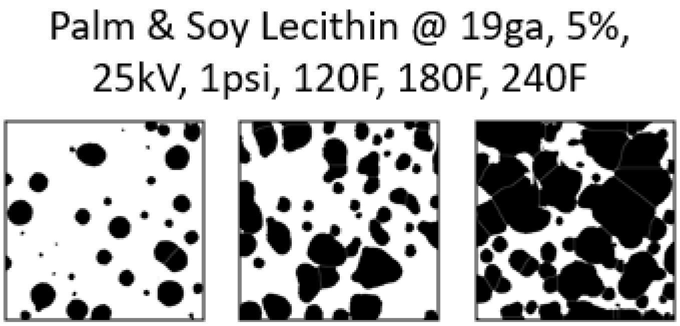

Figure 244: Palm and Soy Lecithin 19ga Pattern Sample

Desirably, as voltage increased, average droplet count increased approximately 12%. However, average droplet size also increased in an undesirable fashion with the voltage increase. Concentration, pressure, and temperature all produced an increase in average sample weight. Average coverage area percentages moved from just over 40% to over 80% as temperature reached 240F. Higher temperature and pressure resulted in higher average sample weights (and mass flow) and an overall lower charge density. The test produced a large swing in energy density with a low of 2.618E+06 J/m^3 and a high of 1.023E+07 J/m^3 but both values were on the low end of the spectrum. Conversely, mass flow was high with a range of 0.73 g/s to 2.73 g/s. Many of the samples produced 'blind' as a result.

6.3.2. **Soy Lecithin with 22ga Capillary**

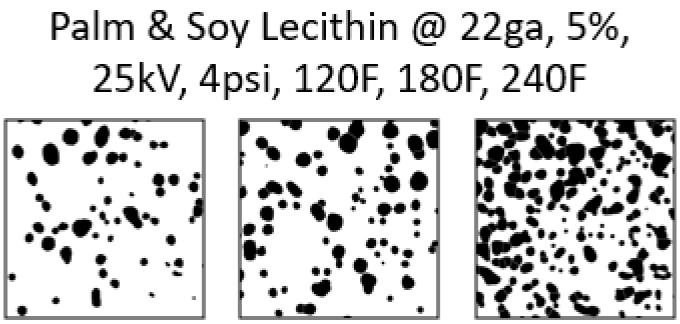

Figure 245: Palm and Soy Lecithin 22ga Pattern Sample

This test, overall, produced fair-to-good results with both high average droplet counts and good average coverage area percentage at the 10% concentration level. Average droplet count saw a significant increase with an increase in concentration (~134/in^2 to ~162/in^2) and voltage (~125/in^2 to ~172/in^2). Average droplet size saw only a marginal increases with increased concentration (~1.25mm^2 to ~1.32mm^2). Average droplet size experienced a significant size reduction with increased temperature (~1.68 mm^2 to ~0.98mm^2). This is counter to expected results. As expected, average sample weights increased with both pressure and temperature. Energy density fell in the low-to-mid range with a low of 1.025E+07 J/m^3)and a high of 3.169E+07 J/m^3. Mass Flow averaged 0.70 g/s. Using least squares regression as a predictive tool, an average droplet count of 224/in^2 could be potentially achieved by decreasing temperature to 80F.

6.3.3. **Polysorbate 80 with 19ga Capillary**

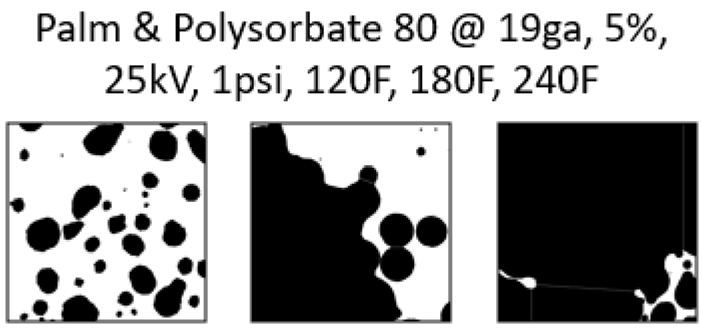

Figure 246: Palm and Polysorbate 80 19ga Pattern Sample

This test presents a unique set of circumstances where the overall performance of the test is rated as poor, but the trends in certain interactions moved in the right direction. Surprisingly, average droplet count improves with an increase in concentration from ~20/in^2 to ~65/in^2. Average droplet size moves downward with an increase in concentration from ~330mm^2 to ~65mm^2. Both trends, while not in an acceptable range for pan oiling, represent movement in a favorable direction. Other interactions, however, perform as expected. Average coverage area percentage moved downward from ~75% to ~67%. Pressure and temperature still provide an increase in average droplet size, coverage area percentage, and weight. Energy density was on the low side (2.711E+06 J/m^3) and didn't move that high relative to other blends (9.072E+06 J/m^3). Mass flow ranged from 0.83 g/s to 2.63 g/s. At lower pressure and at higher surfactant concentration, the pattern was borderline acceptable for a pan coating application. It is likely that the pattern could be improved with a higher energy density (voltage or amperage).

6.3.4. **Polysorbate 80 with 22ga Capillary**

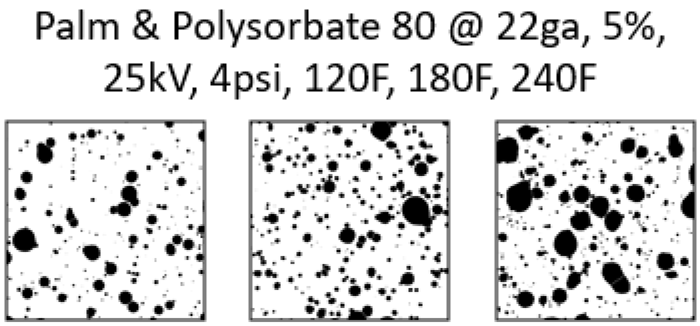

Figure 247: Palm and Polysorbate 80 22ga Pattern Sample

Overall, this test performed exceptionally well with good overall performance at 5% concentration and superior performance at 10% concentration. Average droplet count moved from ~220/in^2 at 5% concentration to ~465/in^2 at 10% concentration. Moreover, average droplet size decreased from ~1.68mm^2 to ~0.25mm^2. Temperature produced an increase in average droplet count from ~245/in to ~320/in. Pressure and Temperature both roughly doubled average sample weight. Average coverage area percentage moved from ~15% to ~38% with pressure, temperature and voltage. With average coverage hovering around ~15% at 4psi and 120F, this is a candidate for higher pressure testing (240F is likely top of the mark in temperature). Energy density ranged from 1.115E+07 J/m^3 to 8.653E+07 J/m^3 and mass flow ranged from 0.087 g/s to 0.64 g/s. It is likely that with a higher pressure and greater energy density that the coverage could improve greatly. Using least squares regression as a predictive tool, an average droplet count of 1090/in^2 could be potentially achieved by increasing concentration to 20%.

6.3.5. **Propylene Glycol with 19ga Capillary**

This test provided results that were generally bad but relatively unmoving between many varying input conditions. Average droplet count was a very low ~12/in^2 at 5% concentration and only moved up to ~15/in^2 at 10% concentration. Average droplet size (~420mm^2), while high, remained relatively unmoved by changes in concentration, pressure, or voltage. Average coverage area percentage was the most greatly influenced by temperature moving from ~57% to ~96%. This is indicative of a 'bling' condition. Average sample weight, as expected, increased with an increase in pressure and/or temperature. Energy density, again, was on the low side with a range of 2.555E+06 J/m^3 to 1.023E+07 J/m^3. Mass flow was on the high side with a range of 0.73 g/s to 2.79 g/s. Low side performance was in the acceptable range for pan oiling but quickly moved to a 'blind' state. This blend might benefit from lower pressure and higher energy density. This particular test showed promise on the low-pressure side with good droplet dispersion.

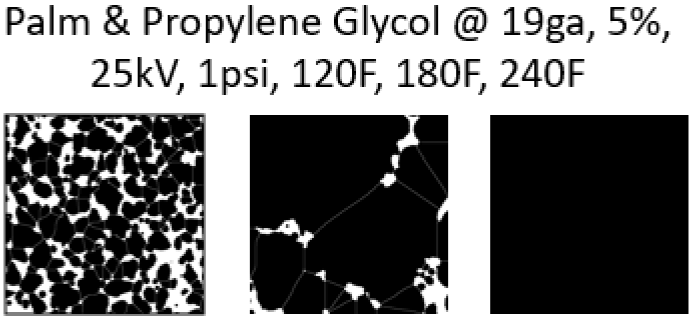

Figure 248: Palm and Propylene Glycol 19ga Pattern Sample

6.3.6. **Propylene Glycol with 22ga Capillary**

This test provided superior results. An increase in concentration provided the largest changes in the output values of all of the tests with Palm oil. Average droplet count remained flat between voltages but moved from ~225/in^2 to ~1,200/in^2 as concentration moved from 5% to 10%. Average droplet size moved from ~0.7mm^2 to ~0.2mm^2. Average coverage area percentage moved from ~13% to ~30%. Increasing pressure from 1psi to 16psi increased average weight 11%. Temperature almost doubled average weight from 0.11g to 0.22g. Average coverage area percentages were low at 5% concentration but excellent (~30%) at 10% concentration. This test had an overall high energy density with a range of 2.254E+06 J/m^3 to 3.879E+07 J/m^3. Mass flow had a range of 0.85 g/s to 0.89 g/s. This was the tightest range of all of the Palm tests and indicates that droplet density is likely a function of Coulombic repusion at lower mass flows due to higher energy densities. Using least squares regression as a predictive tool, an average droplet count of 3050/in^2 could be potentially achieved by increasing concentration to 20%.

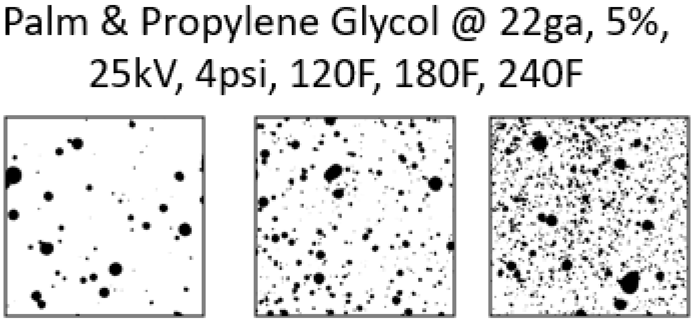

Figure 249: Palm and Propylene Glycol 22ga Pattern Sample

6.4. SOYBEAN OIL

Six separate experiments were performed using Soybean oil as the base. Every combination resulted in EHD atomization utilizing the 22ga capillary. With the 19ga capillary tube, many of the tests at higher pressure and temperature resulted in a ‘blind’ (no discernable electrostatic atomization) condition. Results for tests performed using the 19ga capillary were poor-to-good. Many of these same combinations performed much better using the 22ga capillary. This is likely due to the much lower mass flow rates, and subsequent higher energy density associated with the 22ga capillary. Tests such as Propylene Glycol that performed poor with a 19ga performed superior with a 22ga capillary. Results for tests performed using the 22ga capillary tube were markedly better ranging from fair-to-superior. Surprisingly, Propylene Glycol performed the best of all of the tests at 10% concentration with a droplet count of >1,269/in2. Soybean oil received a score of 20 out of 30 for EHD performance.

6.4.1. **Soy Lecithin with 19ga Capillary**

This test showed good results at low pressure and low temperature. Average droplet counts were as high as ~235/in^2 at 1psi but dropped to ~85/in^2 at 4psi. Temperature also caused an approximate ~67% reduction in average droplet count. Pressure also negatively influenced average droplet size with a ~2.2mm^2 size at 1psi and a ~14.6mm^2 size at 4psi. Average coverage area percentage dropped with an increase in concentration from ~57% to ~39.5%. Both, however were in the acceptable range. Overall average coverage area percentage climbed to ~61% with an increase in either temperature or pressure. Voltage contributed favorably to average count by moving the average from ~130/in^2 to ~165/in^2. This moderate gain is

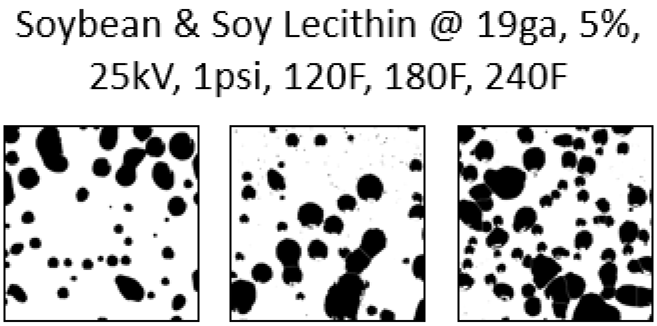
Soybean & Soy Lecithin @ 19ga, 5%, 25kV, 1psi, 120F, 180F, 240F

Figure 250: Soybean and Soy Lecithin 19ga Pattern Sample

an indicator that the overall performance might be improved with an increase in voltage or amperage. Energy density saw a low of 3.206E+06 J/m^3 and a high of 5.947E+07 J/m^3. This is on the high side of all of the 19ga tests. Mass flow has a wide span that ranged from 0.1267 g/s to 2.6667 g/s. This test, like most of the 19ga tests, could benefit from a higher energy density. Given the performance at high mass flow, this combination has the potential to be an excellent EHD spray option for pan oiling. Using least squares regression as a predictive tool, an average droplet count of 333/in^2 could be potentially achieved by decreasing pressure to 0.5psi.

6.4.2. **Soy Lecithin with 22ga Capillary**

This test showed good results with average droplet counts as high as ~245/in^2 and droplet size as low as 1mm^2. The increase in concentration showed favorable results with average droplet size lowering from ~2.2mm^2 to ~1.4mm^2 and average droplet count increasing from ~150/in^2 to ~180/in^2. Average coverage area remained flat at roughly ~28%. The increase in pressure from 1psi to 16psi more than doubled the average sample weight from 0.06g to 0.14g. Increases in Voltage and Temperature both raised the average droplet count from roughly 100/in^2 to ~245/in^2. The average coverage area peaked at ~37% at the 50kV mark. Temperature lowered the average droplet size from ~1.7mm^2 to ~1.5mm^2. Energy density ranged from 1.286E+07 J/m^3 to 6.432E+07 J/m^3. Mass flow for the test ranged from 0.16 g/s to 0.71 g/s. This is promising on both ends of the spectrum.

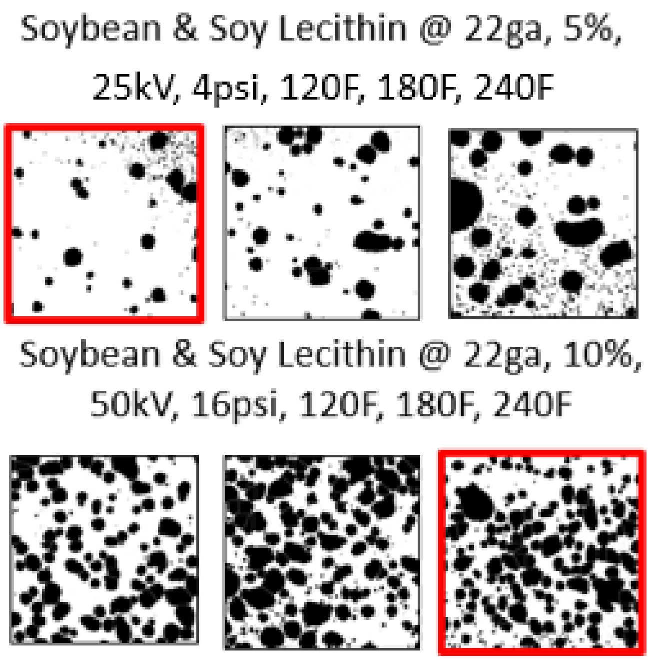

Figure 251: Comparison of Pattern Quality between the Minimum and Maximum Values in the Soybean @ Soy Lecithin 22ga Test Group

This test indicates that performance could further be improved by moving to an intermediate capillary size and increasing temperature or voltage. Figure 234 shows the difference between the low end of the spectrum (low pressure, concentration, and voltage) and the high end of the spectrum. Droplet count at the high end (10%, 50k, 16psi, and 240F) was 978/in^2 and droplet size was 0.296mm^2. This is an excellent example of how, while the average is mediocre with respect to potential pan coating, one extreme or the other may prove excellent for the application. Using least squares regression as a predictive tool, an average droplet count of 884/in^2 could be potentially achieved by increasing pressure to 32psi.

6.4.3. **Polysorbate 20 with 19ga Capillary**

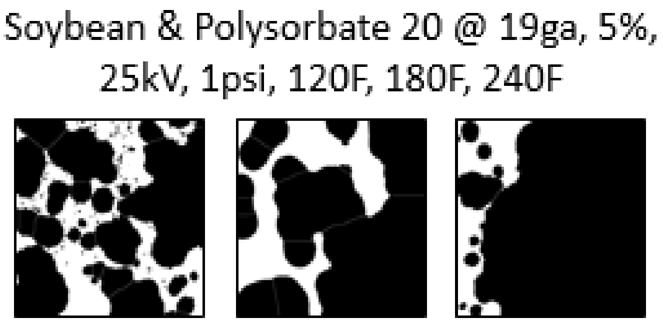

Figure 252:Soybean and Polysorbate 20 19ga Pattern Sample

This test showed poor performance but with some positive trends. That is to say that while average droplet count and average droplet size were low and average coverage area was high, performance indicators moved in the right direction with increases in concentration and voltage. Average droplet count was ~18/in2 at 5% concentration but moved to ~45/in^2 at 10% concentration. Additionally, average droplet size dropped from ~550mm2 to ~300mm^2 and average coverage area dropped from ~97% to ~84%. With an increase in voltage from 20kV to 50kV, average droplet size moved from ~20/in2 to ~40/in^2, average droplet size remained relatively flat moving from ~350mm2 to ~390mm2, and average coverage area moved unfavorably from ~89% to ~92%. Increases in temperature and pressure both negatively influenced performance moving droplet count from ~72/in2 to <5/in^2. The increase in concentration percentage pushed average sample weight down from ~0.86g to ~0.62g, but pressure and temperature each pushed it up to ~0.96g and ~0.89g respectively. Energy density ranged between 1.834E+06 J/m^3 and 7.479E+06 J/m^3 with mass flow ranging between 1.03 g/s and 3.9 g/s. The data between these relationships tends to indicate that the performance was negatively impacted by exceptionally high mass flow rates and that either an increase in energy density or a smaller cross-sectional capillary diameter might correct this problem.

6.4.4. **Polysorbate 20 with 22ga Capillary**

This test product poor-to-fair results with high heterogeneous blend of droplet sizes. From the DOE data, most of the relationships performed as expected for a 22ga test, however, droplet size remained on the large size throughout the test. While concentration seemingly pushed

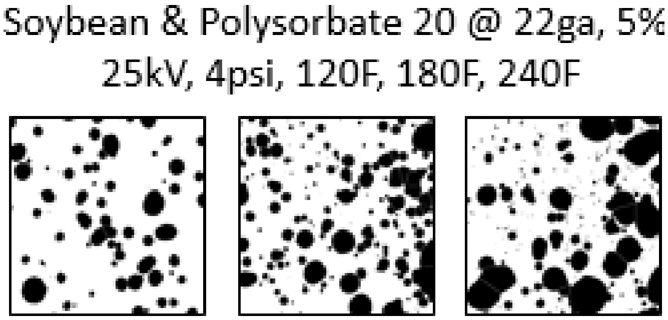
Soybean & Polysorbate 20 @ 22ga, 5%
25kV, 4psi, 120F, 180F, 240F

Figure 253: Soybean and Polysorbate 20 22ga Pattern Sample

average droplet size downwards, this is somewhat misleading as the heterogeneous mix included a heavy blending of a few very large droplets with numerous very small droplets. Having said that, as concentration percentages moved from 5% to 10%, average droplet count moved from ~66/in2 to ~138/in^2. Average droplet size moved downward from ~8.4mm^2 to ~1.4mm^2. Coverage area also trended downward with increased concentration from a solid ~36% to an unfavorable ~22%. Voltage increases droplet count from ~79/in^2 to ~129/in^2 and decreased droplet size from ~5.8mm^2 to ~3.7mm^2 and decreased weight from ~0.135g to ~0.08g. Like the 19ga test, all of the averages moved in favorable directs, but the final results were generally undesirable. As such, Polysorbate 20 would not be recommended as a surfactant of choice when blended with soybean oil. Using least squares regression as a predictive tool, an average droplet count of 259/in^2 could be potentially achieved by increasing concentration to 20%.

6.4.5. **Propylene Glycol with 19ga Capillary**

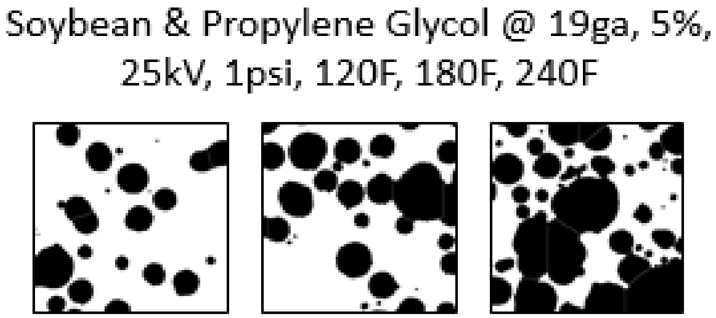

Figure 254: Soybean and Propylene Glycol 19ga Pattern Sample

Performance in this test moved from fair to poor. Average droplet count was low but climbed with concentration from ~22/in2 to ~38/in2. Average droplet size was pushed up from a low of ~11mm2 to a high of ~145/in2 with increases in temperature from 120F to 240. Pressure also had a negative effect on droplet size, pushing it to ~112mm2. Voltage showed an improvement from ~27mm2 to ~38mm2. All four input variables pushed weight up from a low of 0.375g to a high of 0.8g. Energy density was on the low side and ranged from 3.685E+06 J/m3 to 7.479E+06 J/m3. This was likely due to higer mass flows ranging from 1.25g/s to 2.67g/s. Coverage area ranged from 35.85% on the low side to 97.38% on the high size with an average coverage of 63.89%. With no tests reaching the ‘blind’ point, improving energy density should improve spray performance.

6.4.6. **Propylene Glycol with 22ga Capillary**

This test provided superior results. As with Palm oil, an increase in concentration provided the largest changes in the output values of all of the tests with Soybean oil. Average droplet count remained increased between voltages but moved from ~450/in2 to ~580/in2 as concentration moved from 5% to 10%. Average droplet size moved from ~0.32mm2 to ~0.21mm2. Average coverage area percentage moved from ~13% to ~20% when pressure moved from 4psi to 16psi with a high mark of 24% Temperature only slightly moved average sample weight from 0.09g to 0.11g. This test had an overall high energy density with a range of 1.005E+07 J/m3 to 4.414E+07 J/m3. Mass flow had a range of 0.17 g/s to 0.73 g/s. Droplets were highly heterogeneous with a blend of large and small droplets present in the sample area. Using least squares regression as a predictive tool, an average droplet count of 878/in^2 could be potentially achieved by increasing concentration to 20%.

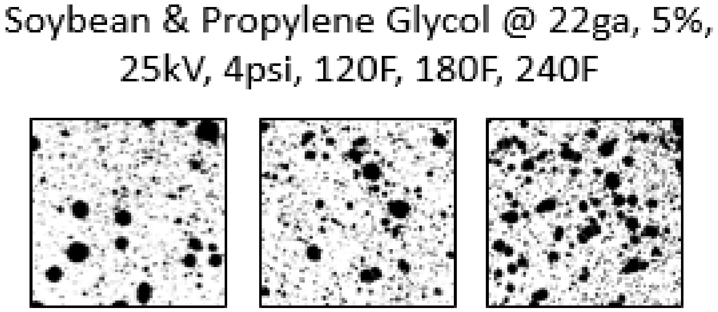

Figure 255: Soybean and Propylene Glycol 22ga Pattern Sample

6.5. RAPESEED (Canola) OIL

Six separate experiments were performed using Rapeseed oil as the base. Every combination resulted in EHD atomization utilizing the 22ga capillary. With the 19ga capillary tube, many of the tests at higher pressure and temperature resulted in a ‘blind’ (no discernable electrostatic atomization) condition. Results for tests performed using the 19ga capillary were fair-to-bad. Many of these same combinations performed much better using the 22ga capillary. This is likely due to the much lower mass flow rates, and subsequent higher energy density associated with the 22ga capillary. Tests such as Propylene Glycol that performed bad with a 19ga performed superior with a 22ga capillary. Results for tests performed using the 22ga capillary tube were markedly better ranging from fair-to-superior. Surprisingly, Propylene Glycol performed the best of all of the tests at 10% concentration with a droplet count of 2644/in2. Rapeseed oil received a score of 22 out of 30 for EHD performance. This was the highest score of all four vegetable oils tested.

6.4.7. **Sunflower Lecithin with 19ga Capillary**

The test produced results that ranged from good-to-bad. Average droplet count at low concentration (5%) moved from an good ~245/in^2 to a poor ~58/in^2 at 10% concentration. Average droplet size increased, respectively, from ~105mm^2 to ~324mm^2. Coverage area moved from the mid 75% range to the high 80% range as concentration moved from 5% to 10% and/or as voltage moved from 25kV to 50kV. Coverage area peaked out in the mid 90% range with increases in pressure from 1psi to 4 psi and/or temperature from 120F to 240F. As expected, average sample weight increased as both temperature and pressure increased moving from ~0.45g to ~0.7g. Energy density was higher than with other sample

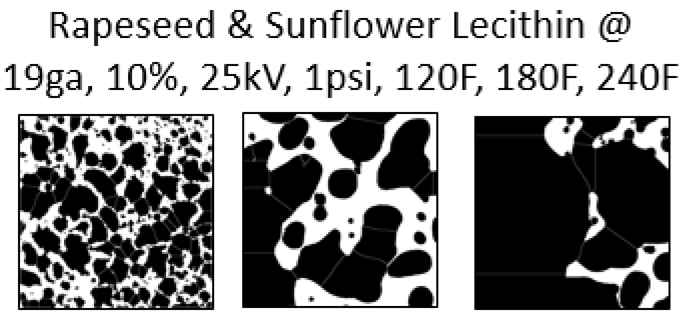

Figure 256: Rapeseed and Sunflower Lecithin 19ga Pattern Sample

groups tested using a 19ga capillary, but still on the low side with the lowest value coming in at 4.865E+06 J/m^3 and the highest value at 1.151E+07 J/m^3. Mass flow rates ranged from 1.067g/s to 2.196g/s. Droplet dispersion was relatively uniform across all tests. Energy density and lower mass flow rates provided EHD atomization that would be acceptable in pan oiling at the low temperature and low-pressure ranges. A higher energy density could easily push these values into the superior range.

6.4.8. Sunflower Lecithin with 22ga Capillary

This experiment produced good to superior results. Average droplet count moved from ~80/in^2 to ~225/in^2 as concentration moved from 5% to 10%. In doing so, average droplet size dropped from ~1.45mm2 to ~0.094mm2. An increase in concentration percentage also produced an increase in average coverage area from ~17% to ~31% and an increase in average sample weight from ~0.08g to ~0.10g. As pressure moved from 1psi to 4psi, average droplet count increased from ~150/in^2 to ~175/in^2, average droplet size increased from ~1.08mm^2 to ~2.25mm^2, and average sample weight rose from 0.065g to 0.13g. As voltage

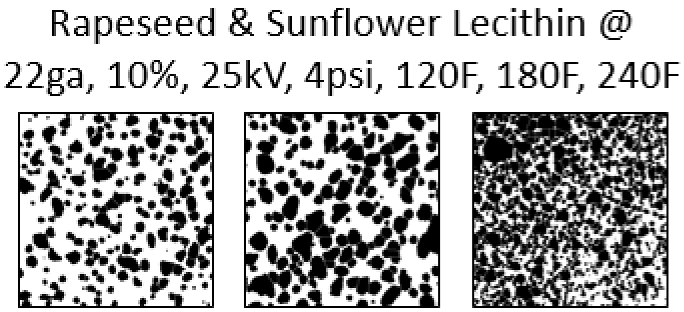

Figure 257:Rapeseed and Sunflower Lecithin 22ga Pattern Sample

increased from 25kV to 50kV, average droplet count remained relatively flat at ~135in/^{2}, average droplet size moved from ~1mm^2 to ~1.35mm^2, average coverage area moved from ~19% to ~28.5%, and average sample weight remained relatively flat at ~0.095g. Temperature (120F to 240F) pushed average droplet count up from ~135/in^2 to ~175/in^2 while driving droplet size down from ~1.7mm^2 to 0.88mm^2. Energy density varied from a low of 1.367E+07 J/m^3 to a high of 4.672E+07 J/m^3 mass flow moved from 0.16g/s to 0.55g/s. Coverage, overall, was a little light on the lower end of the spectrum but superior in the middle and upper ranges. Using a least square regression as a predictive tool, an average droplet count of 480/in^2 could be potentially achieved by increasing concentration to 20%.

6.4.9. **Polysorbate 20 with 19ga Capillary**

The test produced fair-to-poor results with some misleading average droplet counts at low test parameters. Samples tested at the 5% concentration levels produced highly heterogeneous results with high droplet counts consisting of very large droplets and very small droplets blended in the same sample. This phenomenon resulted in what could be described as fair coverage on the low pressure, low temperature samples. It seemed to resolve itself at high concentration (10%) and produced poor results.

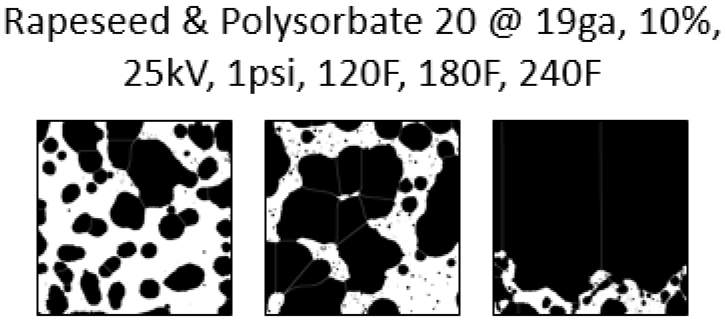
Rapeseed & Polysorbate 20 @ 19ga, 10%, 25kV, 1psi, 120F, 180F, 240F

Figure 258: Rapeseed and Polysorbate 20 19ga Pattern Sample

Because of the high droplet count in the 5% concentration range, overall average droplet count comes in high at ~245in^2 and drops to ~58/in^2. With the high average droplet counts, 28% of test samples produced a droplet count of 1/in2 or a 'blind' condition. Average droplet size rose with concentration from ~110mm^2 to ~325mm^2 while average coverage area remained flat between ~75% and ~85%. Average sample weight also remained somewhat flat (~0.575g to ~0.55g) as concentration rose. A change in pressure (1psi to 4psi) caused an expected decrease in average droplet count (~300/in2 to ~55/in2), an increase in average droplet size from ~0.85mm^2 to ~385 mm^2, an increase in average coverage area from ~6027% to ~98%, and average sample weight moved from 0.45g to 0.69g. A change in voltage, on the other hand, resulted in an unexpected drop in average droplet count (~225/in^2 to ~78/in^2) while resulting in an increase in average droplet size (~150mm^2 to ~300mm^2). A change in temperature also resulted in an expected decrease in average droplet size (~216/in^2 to ~86/in^2) while driving average droplet size down from ~272mm^2 to ~228mm^2. Again, these results are deceptive in comparison to other tests as the appearance of fine mist blended with larger droplets resulting in artificially high average droplet counts and artificially low average droplet sizes. Mass flow for the sample was in line with other tests with similar input parameters at 1.15g/s on the low end and 2.83g/s on the high end. Energy density was on the low side of the spectrum but in line with other test of similar input parameters at 2.492E+06 J/m^3 at the low end and 6.519E+06 J/m^3 at the high end. Using least squares regression as a predictive tool, an average droplet count of 453/in^2 could be potentially achieved by decreasing pressure to 0.5psi.

6.4.10. **Polysorbate 20 with 22ga Capillary**

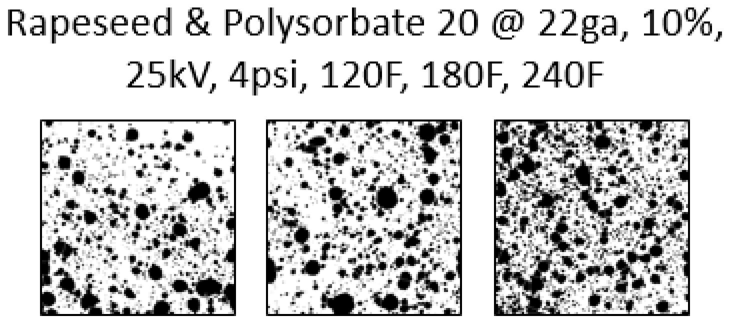

Figure 259: Rapeseed and Polysorbate 20 22ga Pattern Sample

This test produced superior results. Droplets were generally small with slight heterogeneity. Average droplet counts were high across all input variables. Average coverage area was also consistent across all input variables. Average droplet count at 5% concentration average just over ~510/in^2 and lowered to ~390/in^2 at 10% concentration. Droplet size moved from ~1mm^2 to ~1.5mm^2 as concentration increased. Coverage area was flat at ~30% for both concentrations and average sample weight dropped slightly from ~0.115g to ~0.11g. Voltage changes (25kV to 50kV) induced a decrease in the average droplet count from ~640/in^2 to ~265/in^2 whine increasing droplet size from ~0.85mm^2 to ~1.65mm^2 and coverage area from ~27% to ~33.5%. Temperature and pressure increased had the effect of increasing average sample weight (~0.09g to ~0.13g as temperature moved from 120F to 240F and ~0.07g to ~0.158g as pressure moved from 4psi to 16psi). Mass flow increased with pressure from 0.17g/s at 4psi to 0.85g/s at 16psi. Inversely, energy density dropped from 4.313E+07 J/m^3 at 4psi to 1.076E+07 J/m^3 at 16psi. As average droplet count improved with pressure, the overall results might improve by increasing pressure. Using least squares regression as a predictive tool, an average droplet count of 851/in^2 could be potentially achieved by increasing pressure to 32psi.

6.4.11. **Propylene Glycol with 19ga Capillary**

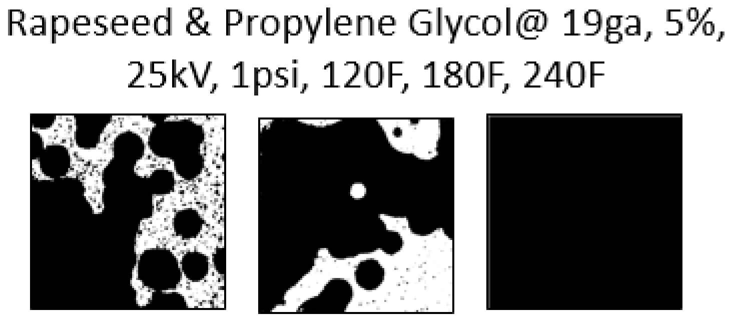

Figure 260: Rapeseed and Propylene Glycol 19ga Pattern Sample

Overall, this test performed poor-to-bad. Changes in concentration had no net effect on average droplet count (~41/in^2), as such, concentration had no effect on average sample weight (~0.48g). Average droplet size dropped from ~61/in2 to ~8/in2 as pressure was increased from 1psi to 4psi and coverage area rose from ~66.5% to ~87%. Temperature changes (120F to 240F) caused a decrease in droplet count from ~79/in2 to ~17/in2 while increasing average droplet size (~212mm2 to ~410mm2), average coverage area (~57% to ~91%), and average sample weight (~0.34g to ~0.68g). Voltage increases (25kV to 50kV) resulted in an increase in average droplet count (~20/in2 to ~59/in2). Mass flow was high for this test with a low of 0.86g/s and a high of 2.75g/s. Energy density was inversely proportional to mass flow with a low value of 2.595E+06 J/m3 and a high value of 8.692E+06 J/m3.

6.4.12. **Propylene Glycol with 22ga Capillary**

This test produced good-to-superior results. Droplet counts ranged from a low of 133/in^2 to t a high of 2644/in^2. The test produces some heterogeneous droplet sizes with very find droplets blended with very large droplets. This was consistent throughout the test. Increasing concentration from 5% to 10% had the effect of increasing average droplet count

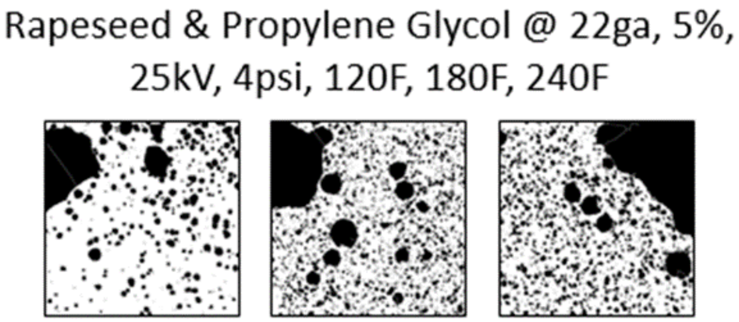

Figure 261: Rapeseed and Propylene Glycol 22ga Pattern Sample

from ~650/in2 to ~910/in^2, increasing droplet size slightly from ~0.485mm2 to ~0.52mm2, increasing average coverage area from ~29% to ~40%, and increasing average sample weight from ~0.09g to ~0.135g. Changes in pressure (4psi to 16psi) had little effect on droplet count, but increased droplet size from ~0.46mm2 to ~0.63mm2, increasing coverage area from ~31% to ~43%, and increase average sample weight from ~0.085g to ~0.155g. Increasing voltage lowered droplet count from ~825/in^2 to ~745/in^2 and lowered average coverage area from ~41% to ~27.4%. Raising the temperature of the samples from 120F to 240F increased the average droplet count from ~425/in^2 to ~1100/in^2, decreased the average droplet size from ~0.63mm2 to ~0.36mm2, and raised sample weight from ~0.09g to ~0.13g. Mass flow ranged from 0.18g/s to 0.96g/s and the energy density ranged from 1.481E+07 J/m^3 at 16psi to 1.481E+07 J/m^3 at 4psi. Using least squares regression as a predictive tool, an average droplet count of 1717/in^2 could be potentially achieved by increasing concentration to 20%.

6.5. SUNFLOWER OIL

Six separate experiments were performed using Sunflower oil as the base. Every combination resulted in EHD atomization utilizing the 22ga capillary. With the 19ga capillary tube, many of the tests at higher pressure and temperature resulted in a ‘blind’ (no discernable electrostatic atomization) condition. Results for tests performed using the 19ga capillary were all rated as ‘bad’. This oil type performed the worst of all four tested. Many of these same combinations, however, performed much better using the 22ga capillary. This is likely due to the much lower mass flow rates, and subsequent higher energy density associated with the 22ga capillary. Tests such as Propylene Glycol that performed ‘bad’ with a 19ga performed ‘superior’ with a 22ga capillary. Results for tests performed using the 22ga capillary tube were markedly better ranging from good-to-superior. Sunflower oil was a top performer in the 22ga category, coming in second only to Rapeseed oil. Propylene Glycol performed the best of all of the tests at 10% concentration with a droplet count of 1553/in2. Sunflower oil received a score of 16 out of 30 for EHD performance. This was the lowest score of all four vegetable oils tested.

6.5.1. **Soy Lecithin with 19ga Capillary**

This test produced poor-to-bad results but increased in concentration and voltage pushed average droplet counts towards a favorable direction. Average droplet count increased with concentration (5% to 10%) from ~24/in^2 to ~43/in^2 and with voltage increases (25kV to 50kV) from ~30/in^2 to ~36/in^2. Pressure (1psi to 4psi) and temperature (120F to 240F) pushed down average droplet counts with three (3) tests returning ‘blind’ results at 240F. Pressure and temperature increased average sample weights from ~0.42g to ~0.61g for pressure and ~0.32g to ~0.65g for temperature. Increases in concentration had the effect

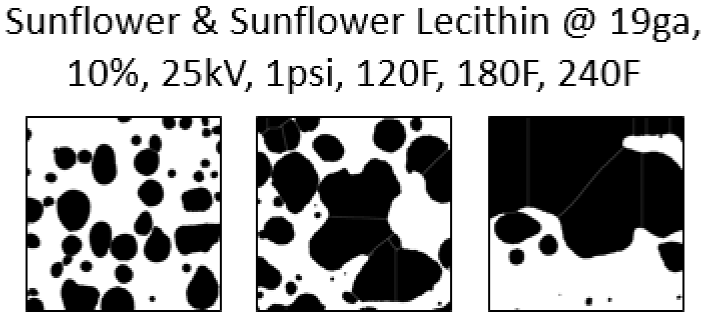

Figure 262: Sunflower and Sunflower Lecithin 19ga Pattern Sample

of lowering average droplet size (~220mm^2 to ~27mm^2) and average coverage area (~66% to ~44%). Mass flow varied from a low of 0.63g/s at 1psi to a high of 3.05g/s at 4psi while energy density responded inversely at 2.277E+07 J/m^3 at 1psi and 4.681E+06 J/m^3 at 4psi.

6.5.2. **Soy Lecithin @ 22ga Capillary**

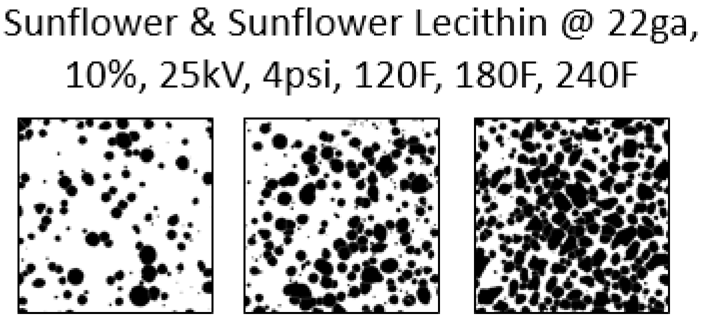

Figure 263: Sunflower and Sunflower Lecithin 22ga Pattern Sample

This test produce fair to good results. Droplet sizes were a little on the larger size, but pattern density was excellent. As concentration moved from 5% to 10%, average droplet count increased from ~130/in^2 to ~205/in^2, droplet size dropped from ~1.8mm^2 to ~0.85mm2, and coverage area lowered from ~32% to ~28%. Average sample weight remained flat at ~0.1g. As pressure rose from 4psi to 16psi, average droplet count fell (~182/in^2 to ~155/in^2), average droplet size increased (~1.1mm^2 to ~1.65mm^2), average coverage area increased from ~16^ to ~34%, and average sample weight rose from ~0.065g to ~0.16g. Voltage had a significant impact on average droplet count. As voltage rose from 25kV to 50kV, average droplet count also rose from ~115/in^2 to ~210/in^2 while average droplet size remained relatively flat at 1.43mm^2 to 1.3mm^2. Coverage area rose significantly with voltage from ~21% to ~39% while average sample weight stayed at the ~0.1g mark. Mass flow ranged from 0.18g/s at 4psi to 0.85g/s at 16psi. Energy density followed the opposing track at 1.267E+07 J/m^3 at 16psi to 8.181E+07 J/m^3 at 4psi. Using least squares regression as a predictive tool, an average droplet count of 314/in^2 and average droplet size of 1.08mm^2 could be potentially achieved by increasing voltage to 75kV.

6.5.3. **Polysorbate 80 with 19ga Capillary**

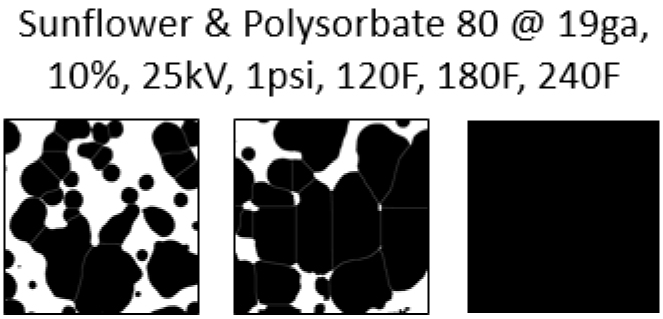

Figure 264: Sunflower and Polysorbate 80 19ga Pattern Sample

This test produced poor-to-bad results. Average droplet count moved from ~1/in^2 to ~20/in^2 as concentration moved from 5% to 10%. Average droplet size improved with increased concentration moving from ~650mm^2 (blind condition) to ~400mm^2. Average coverage area never dropped below ~75% for any input. Average droplet count reached a high of ~28/in^2 at 120F. Mass flow for this test ranged from 1.07g/s at 1psi to 3.05g/s at 4psi. Energy density ranged from 2.439E+06 J/m^3 to 1.397E+07 J/m^3. The maximum droplet count for this test was 94/in^2 at 120f, 1psi, 50kV and 10% solution. 29 of the 36 tests in this series returned ‘blind’. Polysorbate 80 is not a viable emulsifier to use with this capillary size.

6.5.4. **Polysorbate 80 with 22ga Capillary**

Unlike the 19ga sample group, this test returned results that ranged from good-to-fair. As concentration moved from 5% to 10%, average droplet count increased from ~200.in^2 to

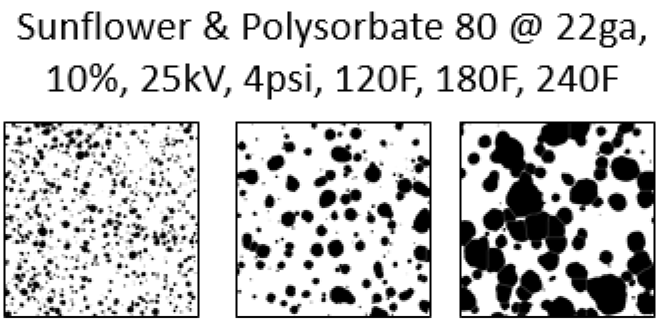

Figure 265: Sunflower and Polysorbate 80 22ga Pattern Sample

~260/in^2, average droplet size dropped from ~41mm^2 to 0.52mm^2, average coverage area dropped from ~46% to ~19%, and average sample weight dropped from ~0.22g to ~0.11g. A change in pressure (4psi to 16psi) resulted in a drop in average droplet count (~240/in^2 to ~155/in^2), an increase in droplet size from ~0.5mm^2 to ~58mm^2, average coverage area gains from ~17% to ~48%, and a gain in average sample weight from ~0.16g to ~0.19g. Temperature (120F to 240F) pushed down average droplet count (~300/in^2 to ~194/in^2) while pushing up average coverage area (~24% to ~44%) and average sample weight (~0.09g to ~0.115g). Mass flow ranged from a low of 0.13g/s to a high of 1.2g/s while energy density ranged from 4.576E+06 J/m^3 at 16psi to 1.500E+08 J/m^3 at 4psi. Using least squares regression as a predictive tool, an average droplet count of 412/in^2 could be potentially achieved by increasing concentration to 20%.

6.5.5. **Propylene Glycol with 19ga Capillary**

This test returned bad coverage results with over half of the test runs returning blind results. This has been a theme with Propylene Glycol where tests at high mass flow and low energy density produce really

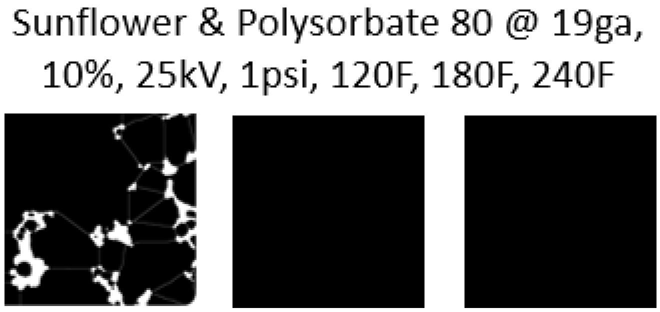

Figure 266: Sunflower and Polysorbate 80 19ga Pattern Sample

bad results and tests at higher energy densities and lower mass flows produce really good results. Average droplet count never rose above ~35/in^2 for any input. Average droplet size was above ~300mm^2 for every input. Average coverage area was above ~65% for every input, and average sample weight were above ~0.45g for every sample. Energy density maxed out at 1.260E+07 J/m^3 at 1psi.

6.5.6. **Propylene Glycol with 22ga Capillary**

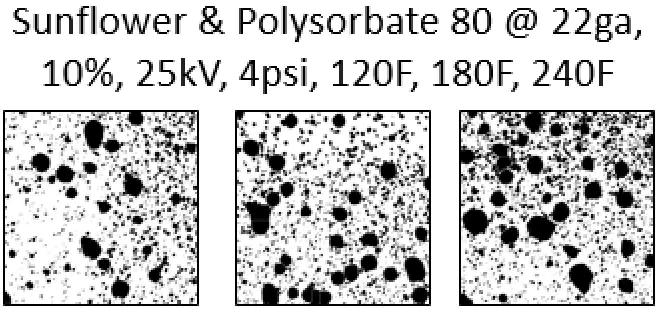

Figure 267: Sunflower and Propylene Glycol 22ga Pattern Sample

This test produce fair-to-good results. An increase in voltage (25kV to 50kV) produced the most appreciable increase in average droplet count ~314/in^2 to ~407/in^2. Increases in concentration (from 5% to 10%) lowered droplet count from ~540/in^2 to ~97/in^2 while raising average droplet size from ~0.45mm2 to ~5.4mm2. Average coverage area was highest at 240F with a value of ~37%. As expected temperature (120F to 240F) and pressure (4psi to 16psi) drove down average droplet counts (~405/in^2 to ~377/in^2 for pressure and ~399/in^2 to ~223/in^2 for temperature) while raising average sample weights (~0.06g to ~0.16g for pressure and ~0.06g to ~0.135g for temperature) and average coverage areas (~20% to ~34% for pressure and ~16% to ~36% for temperature). Mass flow ranged from 0.12g/s at 4 psi to 0.85g/s at 16psi. Energy density ranged from 1.039E+07 J/m^3 at 16psi to 1.154E+08 J/m^3 at 4psi. Using least squares regression as a predictive tool, an average droplet count of 1400/in2 could be potentially achieved by increasing voltage to 75kV.

6.6. CONCLUSION

The path to determining the viability of Electro-hydrodynamic spot spraying of food grade vegetable oils as a release agent in baking is multi-faceted. First, the hurdle of developing a technology capable of spot spraying in an EHD spraying mode had to be overcome. Second, a determination had to be made regarding the four major commercially available vegetable oils and their ability to carry a charge that exceeded the Rayleigh point so that EHD was possible (Bailey, 1974). Next, knowing that soy lecithin has been used to lower the surface tension and allow soybean oil to reach the critical point, it was determined that other various surfactants could be used to accomplish the same thing across each of the four commercially available vegetable oils (Palm, Soybean, Rapeseed, and Sunflower). Finally, understanding Electro-hydrodynamic spraying performance across multiple oil/emulsifier solutions required understanding the dynamic interactions between several input variables.

6.6.1. Answers to Research Questions

Can the top four (4) commercially available vegetable oils (Soybean, Rapeseed, Sunflower, and Palm) be made to carry a charge with the addition of food grade surfactants?

The experiment was successful in achieving a charge and electro-hydrodynamically spot-spraying each of the twenty-four vegetable oils blends, whereas, the control state of each of the vegetable oils did not carry a charge. To quantify the performance of each oil/emulsifier blend, a full factor ANOVA was developed based on a Design of Experiments (DOE). Experiments were conducted, and an analysis of the results determined that each vegetable oil and emulsifier blend lowered the surface tension such that the charge, when testing with the 22ga capillary, exceeded the Rayleigh limit and EHD spraying occurred in the cone-jet mode (see Table 28) producing kink instabilities. Tests with the 19ga capillary were generally successful at achieving kink instabilities at low pressure and low temperature (lower mass flows) but tended to revert back to varicose instabilities at higher pressures and temperatures (higher mass flows) and often resulted in a 'blind' condition.

For the experiment, several food grade emulsifiers with surfactant properties (based on HBL scale) were identified and input parameters were developed for the experiment. For each of the four vegetable oils, three emulsifiers and two capillary sizes were selected. Four inputs were identified for the experiment (temperature, pressure, concentration, and voltage). A DOE was constructed and, based on potential interactions, 865 individual tests were performed. Performance criteria was developed to determine EHD performance of each test and a statistical treatment was applied to the results.

Based on performance criteria and the 'Grade Scale' developed and outlined in Table 29, each of the four oil types and the three major emulsifier types were graded from 'bad' with a score of 1, to 'Superior' with a score of '5'. In order to achieve a 'good' rating, droplet counts must have exceeded 200/in2, droplet size must have been smaller than 1.25mm2, Coverage area must have been between 15% and 60%, and weight must have been greater than 0.2g. Of the four vegetable oils, Rapeseed, scored the highest score with superior rating in each of the three 22ga tests and 'fair' in two (2) of the three (3) 19ga tests. Soybean oil followed closely behind with a score of 20. However, Soybean oil underperformed in the 22ga Polysorbate tests. Sunflower oil performed the worst of all of the oils with a score of 16. This is largely due to 'bad' scores for each of the 19ga tests. When evaluating the emulsifiers, Propylene Glycol scored the highest score among 22ga tests and the lowest score among 19ga test. It also scored a 25, the second best overall (combination of the two tests) behind Lecithin. Lecithin came first with a score of 26. Both Lecithin and Polysorbate only had one 'bad' rating (both for Sunflower blends).

Table 29: EHD Performance Chart

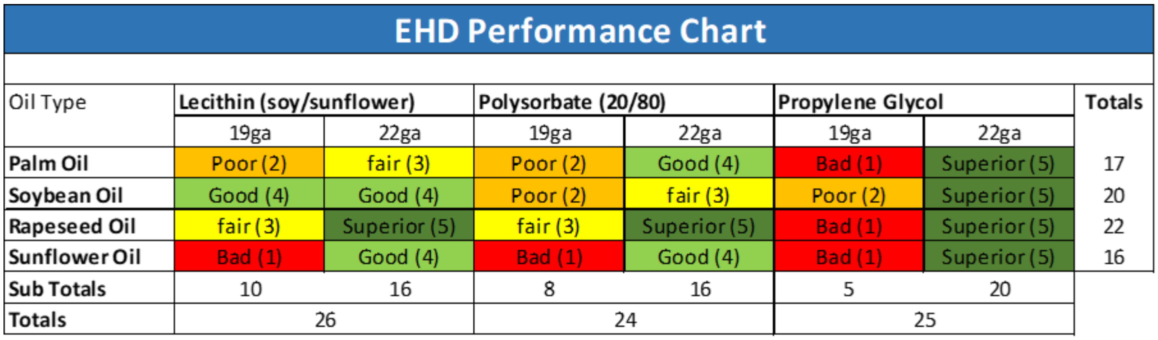

EHD Performance Chart

Oil Type	**Lecithin (soy/sunflower)**		**Polysorbate (20/80)**		**Propylene Glycol**		**Totals**
	19ga	22ga	19ga	22ga	19ga	22ga	
Palm Oil	Poor (2)	fair (3)	Poor (2)	Good (4)	Bad (1)	Superior (5)	17
Soybean Oil	Good (4)	Good (4)	Poor (2)	fair (3)	Poor (2)	Superior (5)	20
Rapeseed Oil	fair (3)	Superior (5)	fair (3)	Superior (5)	Bad (1)	Superior (5)	22
Sunflower Oil	Bad (1)	Good (4)	Bad (1)	Good (4)	Bad (1)	Superior (5)	16
Sub Totals	10	16	8	16	5	20	
Totals	26		24		25		

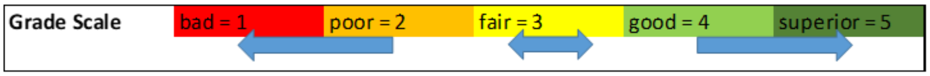

Grade Scale	bad = 1	poor = 2	fair = 3	good = 4	superior = 5

Hypothesis one (1) held true in that the tested vegetable oils have common enough physical characteristics so that the addition of a tested surfactants lowered the surface tension and resistivity enough to carry a charge. Hypothesis two (2) was proven untrue. Palm oil performed in the middle of the pack in overall performance and thus kinematic viscosity was not a factor in determining the viability EHD atomization in the experiment.

Can spot spray technology can be made to work with EHD atomization?

While EHD atomization failed with known fast acting spray valve technologies, EHD spot spraying was achieved for this experiment. To meet this hurdle, a proprietary

EHD spray valve was designed and intellectual property was developed (appendix A - patent pending P2512US00). This design provided protection between the fluid path and earth ground, a fluid chamber in the valve assembly, and a charging rod/valve stem to charge the fluid path. The valve, when actuated by a 24VDC solenoid, sent charged fluid through a capillary valve and sprayed laminar flow into the test area. A high voltage power supply was attached to the charging rod and voltage was applied to the fluid prior to exiting the valve. The result was a valve that sprayed fluid up to 5g/s and charged the fluid with 25kVDC or 50kVDC at 0.1mA. The valve also created an electrical field inside the test fixture between the capillary tube (positively charged) and the collector plate of the test fixture (negatively charged). The result was a design that generated electrically charged intermitted spray (spot-spray) with at 8.5ms actuation time. When the energy density of the liquid was sufficiently high

Hypothesis one (1) proved to be true. EHD atomization did occur, without lag, in spot spray mode where initial velocity was zero at every cycle. In fact, atomization occurred faster than the 8.5ms cycle time of the valve and, thus, there was no instance where the liquid exited the capillary under charge where it was not spraying in EHD mode. At the given mass flow rates, spray operated in cone-jet mode for every test. At higher mass flows, however, the test produced varicose instabilities that did not produce favorable patterns for pan oiling. This, however, was not due to the valve operation, but rather the amount of energy (joules) introduced to the fluid.

What is the relationship between mass flow rate and the energy required to electro-hydrodynamically atomize good grade vegetable oil? Can flow rates greater than 15 g/min successfully EHD atomize?

EHD performance could be attributed largely to the energy density of the fluid when sprayed. Because voltage, amperage, and spray time were constant with each test, energy density became a function of mass flow and material's properties. When comparing mass flow (g/s) to energy density (J/m3), a relationship (exponential function outlined in equations 28 & 29) between the two became apparent and using this relationship to predict EHD success became possible (see Figure 243). As every test was performed at two distinct voltage levels (25kV producing 2.5 Joules and 50kV producing 5 Joules), each test fell on the plotline of one of either equation 28 or 29 respectively ($E_d = 6\dot{m}^{(-1.004)}\cdot 10^2$ and $E_d=6\dot{m}^{(-1.004)}\cdot 10^4$). It was observed that an increase in energy density generated smaller droplets in greater numbers (the desirable condition for coating applications).

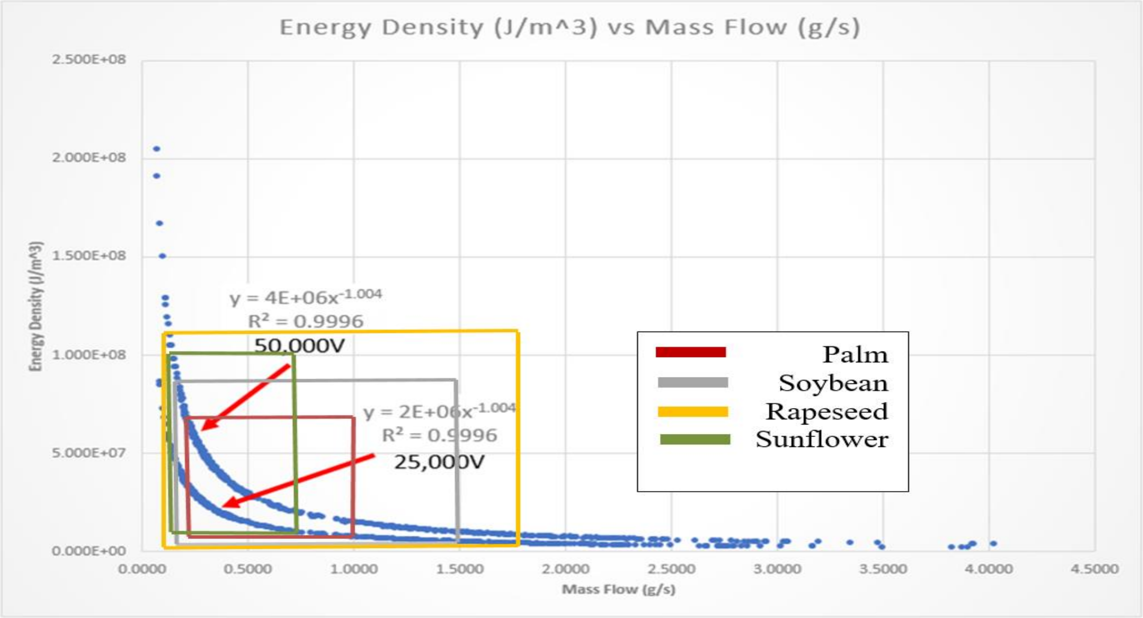

Figure 268: Energy Density Bounds by Oil Type

Figure 268 illustrates the Energy Density vs Mass Flow relationship for successful EHD spraying with respect to pan coating applications. Values within the boxed areas were shown experimentally to produce good coating results that met the given criteria. The performance bounds illustrated in the chart cordially reflect the scores annotated in Table 29. For example, Rapeseed had the largest performance band with a mass flow of up to 1.7g/s and as low as 0.11g/s with an energy density of up to 1.29E+08 J/m3. Any test that fell along either curve within the bounded area produced acceptable results. While this is particular to this specific oil, the premise held true for all of the oils tested. It is therefore reasonable to assume that, with some experimental testing, other vegetable oils could be made to take an electrical charge.

Hypothesis one (1) proved somewhat true. EHD atomization is a function of surface tension and energy density at a given flow rate. Higher concentrations of surfactant did produce greater quantities of droplets per square inch. Higher energy densities also produced more droplets per square inch. Hypothesis two (2) also proved untrue. While EHD atomization can be influenced by the temperature (impact to viscosity and thus mas flow), raising the temperature does not allow for atomization at higher mass flows. In fact, raising temperature contributes to higher mass flow rates and thus lowers energy density. Hypothesis three (3) is untrue. Increased capillary sizes allows for greater mass flow which reduces energy density.

Can emulsifiers other than Lecithin be used as a surfactant in lowering surface tension of the base oil?

Five different emulsifiers (Soy Lecithin, Sunflower Lecithin, Polysorbate 20, Polysorbate 80, and Propylene Glycol) in three different groups (Lecithins, Polysorbates, and Propylene Glycol) were tested. Soy Lecithin was tested with Soybean oil and Palm oil. Soy lecithin was chosen to test with soybean oil because it is derived from Soybeans. It was chosen to test with Palm oil because palm oil is a semi solid at room temperature and it was believed that, of the chosen vegetable oils, that Palm oil would prove the most difficult to atomize. Soy lecithin had already been proved to assist in EHD atomization with soybean oil (Aykas & Barringer, 2004) and, thus, more likely to work with other oils. Sunflower lecithin was chosen to test with Sunflower oil and Rapeseed oil. Sunflower lecithin was chosen to test with Sunflower oil because it is derived from Sunflowers. It was chosen to test with Rapeseed oil because certain countries, like the United Kingdom, do not cultivate soybeans because they are considered GMO’s. Polysorbate 20 was chosen to test with Soybean oil and Rapeseed oil arbitrarily. Polysorbate 80 was chosen to test with Palm and Sunflower oil arbitrarily. Propylene Glycol was tested with all four vegetable oils.

All five emulsifiers were successful in lowering the surface tension of each of the four oils. Soy Lecithin was favored prior to the experiment due to prior research using it for its surfactant properties, and overall, it outperformed all of the other emulsifiers by a slim margin. However, at low mass flow (22ga capillary test), Propylene Glycol performed the best of all of the emulsifiers.

Hypothesis one (1) was unproven. All emulsifiers other than Propylene Glycol had an HBL level greater than 6. However, every emulsifier tested returned positive results. Propylene Glycol, which does not have a recognized HBL number, performed best in the 22ga tests. Thus, any substance that lowers the surface active energy will work. Hypothesis two (2) was proven false by virtue of the fact that both polysorbates and Propylene Glycol were tested successfully.

What is the relationship between the different input variables (concentration of emulsifier in solution, voltage, temperature, and pressure) and the outputs (droplet count, droplet size, area coverage percentage, and sample weight)?

A full factor ANOVA structure DOE was performed using statistical ordinary least squares regression and the results of y-bar and y-hat were graphed for each test group (Interactions plot, Main Effects plot, Surface Plot, and Splatter plots). From this, a performance analysis was conducted for each test group outlining the interactions between the inputs of voltage, pressure, temperature and concentration on the outputs of droplet count, droplet size, coverage area, and sample weight (see sections 6.3 through 6.6). While the specific performance characteristics are dependent on the input conditions and specific to each oil and emulsifier blend, a few generalities can be drawn:

- Increases in Temperature and Pressure (mass flow) generally push down droplet count but elevate droplet size and sample weight.
- Increases in Voltage generally pushes up droplet count and lowers droplet size and coverage area. It generally has little bearing on sample weight.

- Increases in Concentration generally increases up droplet count and lowers droplet size. It tends to elevate sample weight slightly and tends to improve coverage area.

All tests indicate that each of the four outputs were dramatically impacted by the energy density of the individual test at test conditions. Moreover, it was determined that energy density relative to mass flow is inversely exponential in nature and that the regression for this curve is dictated by the energy (Joules) applied to the experiment (see figure 268).

6.6.2. Summary

The experiment successfully expanded on the work of Abu-Ali (2004), Abu-Ali and Barringer (2004 & 2008), and Aykas and Barringer (2012). In scholarly work leading up to this experiment, it was proven that EHD atomization and the subsequent Coulombic attraction of charged particles could successfully mitigate the overspray problem associated with conventional spraying methods. Abu-Ali and Barringer (2004) also proved that soybean oil could be made to carry a charge by the addition of lecithin (a surfactant). However, in order for this previous research to be universally applicable as a method of coating in the baking industry, it must be expanded to include the top four vegetable oil types. The top four vegetable oils make up over 87% of world production (US Foreign Agricultural Service, 2018). Moreover, because soy lecithin is not a commercially viable emulsifier in some regions of the world, therefore, it must be determined if other surfactants can produce similar results. The interaction between the different solutions and the input variables such as voltage, temperature, pressure, and solution concentration must be identified and understood. Finally, because bread and rolls are deposited in discrete cavities, any technology for spray coating needs to be made capable of spot-spraying those discrete cavities.

Based on experimental data, EHD spot-spraying of vegetable oils is viable as a potential technology for pan coating. Given the performance of the twenty-four test groups, it is reasonable to assume that other oils and emulsifiers/surfactants blends would also be capable of carrying a charge and perform in a similar fashion. As this project had a very broad breath (865 separate tests), additional experimentation may be needed with each test group to achieve higher statistical stability. Overall, however, the experiment resulted in the development of new technology (EHD Spot-Spray), a fundamental understanding of the interaction of the inputs relative to the outputs of the experiment, and an understanding of the relationship between energy density and mass flow in achieving the cone-jet mode and subsequent production of kink instabilities.

REFERENCES

Dow Chemical Company. (2003). *A Guide to Glycols* [Brochure]. Author.

Abu-Ali, J., & Barringer, S. (2005). Method for electrostatic atomization of emulsions in an EHD system. *Journal of Electrostatics, 63*(5), 361-369. doi:10.1016/j.elstat.2004.11.004

Abu-Ali, J., & Barringer, S. (2008). Optimization of liquid electrostatic coating. *Journal of Electrostatics, 66*(3-4), 184-189. doi:10.1016/j.elstat.2007.12.003

Abu-Ali, J. (2004). *Food Coating Applications in: Electrostatic Atomization, Nonelectrostatic Coating and Electrostatic Powder Coating.* (Doctoral dissertation, Ohio State University, 2004). ProQuest Dissertations Publishing.

Adam, N. (1941). *The physics and chemistry of surfaces. 3rd. ed*. Oxford, UK: Oxford University Press.

Adamczewski, I. (1969). *Ionization, conductivity, and breakdown in dielectric liquids; translated from Polish*. Taylor & Francis.

Atchley, C. (2014, October 1). Extending the Life of a Pan. Retrieved February 01, 2018, from http://www.bakingbusiness.com/Features/Operations/2014/10/Extending-the-life-of-a-pan.aspx

Atchley, C. (2004). Extending the life of a pan. Retrieved January 27, 2018, from http://www.bakingbusiness.com/Features/Operations/2014/10/Extending-the-life-of-a-pan.aspx

Atlas Steel (Ed.). (2016). Look No Further For the World's Best Source for Aluminized Steel. Retrieved February 01, 2018, from http://www.atlassteel.com/Products/aluminizedSteel.aspx?p=1

Aykas, D. P., & Barringer, S. (2012). The Effect of Temperature, Lecithin Content and Voltage on Droplets/cm2during Electrostatic Spraying of Oil. *Journal of Food Processing and Preservation, 38*(1), 484-492. doi:10.1111/j.1745-4549.2012.00798.x

Bailey, A. G., & Balachandran, W. (1981). The disruption of electrically charged jets of viscous liquid. *Journal of Electrostatics, 10,* 99-105. doi:10.1016/0304-3886(81)90028-0

Bailey, A. G. (1974). Electrostatic Atomization of Liquids. *Science Progress, 61*(244), 555-581.

Bailey, A. G. (1988). *Electrostatic spraying of liquids*. Taunton, Somerset, England: Research Studies Press.

Bailey, A. E. (2005). *E Bailey's industrial oil & fat products* (6th ed.). Hoboken, NJ: John Wiley & Sons.

Barringer, S. A., & Sumonsiri, N. (2015). Electrostatic Coating Technologies for Food Processing. *Annual Review of Food Science and Technology, 6*(1), 157-169. doi:10.1146/annurev-food-022814-015526

Bratton, J. (2013, March 19). Was it ok to eat paste as a child? Retrieved February 01, 2018, from http://www.gpb.org/blogs/the-daily-jog/2013/03/19/was-it-ok-to-eat-paste-as-a-child

Castellanos, A. (1998). Conservation Laws for Electrohydrodynamics Two-Phase Flow. *Electrohydrodynamics,* 280-296. doi:10.1007/978-3-7091-2522-9_19

Cloupeau, M., & Prunet-Foch, B. (1990). Electrostatic spraying of liquids: Main functioning modes. *Journal of Electrostatics, 25*(2), 165-184. doi:10.1016/0304-3886(90)90025-q

Cloupeau, M., & Prunet-Foch, B. (1994). Electrohydrodynamic spraying functioning modes: a critical review. *Journal of Aerosol Science, 25*(6), 1021-1036. doi:10.1016/0021-8502(94)90199-6

Cook, P. M., Rasmussen, G. E., & Skinner, G. W. (1925). *U.S. Patent No. US 1522867 A*. Washington, DC: U.S. Patent and Trademark Office.

Cutnell, J. D., & Johnson, K. W. (1995). *Physics* (3rd ed.). Wylie & Sons, Inc.

Dahlquist, C. A. (1956). An Investigation into the Nature of Tack. *Adhesive Age, 2*(10), 25-29.

Darwin, D. C. (2003). Bakery Release Agents. *Cereal Foods World, 48*(5), 247-249.

DuPont Corporation. (n.d.). *Delrin Design Guide—Module III* [Brochure]. Author.

Dobraszczyk, B. J. (1997). The Rheological Basis Of Dough Stickiness. *Journal of Texture Studies, 28*(2), 139-162. doi:10.1111/j.1745-4603.1997.tb00108.x

Downer, R., Hall, F., Escallon, E., & Chapple, A. (1993). The Effect of Diluent Oils on the Electrostatic Atomization of Some Insecticides. *Pesticide Formulations and Application Systems: 13th Volume, 13*(1183), 203-214. doi:10.1520/stp25134s

Encyclopædia Britannica (Ed.). (2017, August 30). Polytetrafluoroethylene. Retrieved February 01, 2018, from https://www.britannica.com/science/polytetrafluoroethylene

Esteban, B., Riba, J., Baquero, G., Rius, A., & Puig, R. (2012). Temperature dependence of density and viscosity of vegetable oils. *Biomass and Bioenergy, 42*, 164-171. doi:10.1016/j.biombioe.2012.03.007

FALKOVICH, G. (2018). *FLUID MECHANICS: a short course for physicists*. Cambridge, UK: CAMBRIDGE UNIV PRESS.

Farn, R. J. (Ed.). (2007). *Chemistry and technology of surfactants*. Oxford: Blackwell.

Feikert-Ahalt, C. (2014, March 01). Restrictions on Genetically Modified Organisms: England and Wales. Retrieved January 27, 2018, from https://www.loc.gov/law/help/restrictions-on-gmos/england-wales.php

Ferreira, T., & Rasband, W. (2012). *ImageJ User Guide: IJ 1.46r*. National Institute of Health (NIH).

Gaonkar, A. G., VAsisht, N., Khare, A., & Sobel, R. (2014). *Microencapsulation in the food industry: a practical implementation guide*. Elsevier Academic Press.

Garti, N., Yaghmur, A., Leser, M. E., Clement, V., & Watzke, H. J. (2001). Improved Oil Solubilization in Oil/Water Food Grade Microemulsions in the Presence of Polyols and Ethanol. *Journal of Agricultural and Food Chemistry, 49*(5), 2552-2562. doi:10.1021/jf001390b

Gaultney, L. D., Almekinders, H., Escallon, E. C., & Wilkerson, J. B. (1987). *Laboratory studies of electrostatic pesticide applicators* (Tech. No. 87-1065). American Society of Agricultural Engineers (ASAE).

Gelski, J. (2016, June 14). Reasons to increase the supply of sunflower oil. Retrieved January 31, 2018, from http://www.foodbusinessnews.net/articles/news_home/purchasing_news/2016/06/reasons_to_increase_the_supply.aspx?ID=%7BA6481CF8-6CB9-4C6B-BCD4-393F5367E1C9%7D

Gorton, L. (2014, March 13). Big gains reported for high-stability canola oil. Retrieved from www.bakingbusiness.com/articles/news_home/Health-and-Wellness/2014/03/Big_gains_reported_for_high-st.aspx?ID=%7BCB9517BD-D10C-4928-8B5A-D8C28AE12F74%7D

Gorton, L. (2011, April 1). Fats and Oils: The Next Generation. Retrieved from http://www.bakingbusiness.com/News/News-Home/Features/2011/4/Fats-and-Oils.aspx

Gu, W. (2009). *Flow-Limited Field-Injection Electrostatic Spraying (FFESS): Modeling and Application*. Sarbrucken, Germany: VDM Verlag Dr. Muller Aktiengesellschaft and Co.

Matheson Tri-Gas, Inc. (2014). *Guide to Regulators* [Brochure]. Author.

Gunstone, F. (2011). *Vegetable Oils in Food Technology: Composition, Properties and Uses, 2nd Ed*. Portland, OR: Ringgold Inc.

Harkins, W. D. (1926). The Drop-weight Method for the Determination of Surface Tension and the Weight of the Ideal Drop. *Nature, 117*(2950), 690-691. doi:10.1038/117690a0

Harper, C. A. (2003). *Electronic materials handbook*. McGraw-Hill.

Hartman, R., Brunner, D., Camelot, D., Marijnissen, J., & Scarlett, B. (1999). Electrohydrodynamic Atomization In The Cone–Jet Mode Physical Modeling Of The Liquid Cone And Jet. *Journal of Aerosol Science*, *30*(7), 823-849. doi:10.1016/s0021-8502(99)00033-6

Hartman, R., Brunner, D., Camelot, D., Marijnissen, J., & Scarlett, B. (2000). Jet Break-Up In Electrohydrodynamic Atomization In The Cone-Jet Mode. *Journal of Aerosol Science*, *31*(1), 65-95. doi:10.1016/s0021-8502(99)00034-8

Hasenhuettl, G. L., & Hartel, R. W. (2009). *Food emulsifiers and their applications*. New York: Springer.

Huang, M. (2015, July 6). Ask a Toxicologist: Is It Safe to Use Teflon Pans?". Retrieved February 01, 2018, from http://tibbs.unc.edu/ask-a-toxicologist-is-it-safe-to-use-teflon-pans/

Jaworek, A., & Krupa, A. (1999). Jet and drops formation in electrohydrodynamic spraying of liquids. A systematic approach. *Experiments in Fluids, 27*(1), 43-52. doi:10.1007/s003480050327

Jaworek, A. (2007). Micro- and nanoparticle production by electrospraying. *Powder Technology*, *176*(1), 18-35. doi:10.1016/j.powtec.2007.01.035

Jaworek, A., & Krupa, A. (1998). *Main Modes of Electrohydrodynamic Spraying of Liquids* (437th ed., Tech.). Gdansk, Poland: Polish Academy of Sciences.

Jayasinghe, S. N., & Edirisinghe, M. J. (2002). Obtaining fine droplet relics by electrostatic atomization of viscous liquids. *Journal of Materials Science Letters, 21*, 371-372.

Jayjock, M. A. (2012). Engineering Case Report: Estimating Overspray Exposure Potential from Aerosol Sprayed Products onto Surfaces. *Journal of Occupational and Environmental Hygiene*, *9*(9). doi:10.1080/15459624.2012.700191

Jayjock, M. A. (2012). Engineering Case Report: Estimating Overspray Exposure Potential from Aerosol Sprayed Products onto Surfaces. *Journal of Occupational and Environmental Hygiene*, *9*(9). doi:10.1080/15459624.2012.700191

John Wiley and Sons (Ed.). (2008). *Ullmann's Encyclopedia of Industrial Chemistry* (6th ed., Vol. 40). Retrieved from http://onlinelibrary.wiley.com/book/10.1002/14356007

Kinloch, A. J. (2010). *Adhesion and adhesives: science and technology*. London: Chapman and Hall.

Koushki, M., Nahidi, M., & Cheraghali, F. (2015, Summer). Physico-chemical properties, fatty acid profile and nutrition in palm oil. *Journal of Paramedical Sciences, 6*(3), 117-134.

Kralova, I., & Sjoblom, J. (2009). Surfactants Used in Food Industry: A Review. *Journal of dispersion Science and Technology, 30*, 1363-1383.

Kumar, D., Singh, A., & Tarsikka, P. S. (2011). Interrelationship between viscosity and electrical properties for edible oils. *Journal of Food Science and Technology, 50*(3), 549-554. doi:10.1007/s13197-011-0346-8

Lallemand (Ed.). (2000). Oils Used as Lubricating or Release Agents. *Lallemand Baking Update, 2*(18).

Lee, S., Hung, N. X., & Ko, H. S. (2011). Study on Droplet Formation With Surface Tension for Electrohydrodynamic Inkjet Nozzle. *ASME-JSME-KSME 2011 Joint Fluids Engineering Conference: Volume 1, Symposia – Parts A, B, C, and D.* doi:10.1115/ajk2011-09025

Lohman, S. (2012, December 18). A Brief History of Bread. Retrieved February 01, 2018, from http://www.history.com/news/hungry-history/a-brief-history-of-bread

Martin, D., Saha, T., & Mcpherson, L. (2017). Condition monitoring of vegetable oil insulation in in-service power transformers: some data spanning 10 years. *IEEE Electrical Insulation Magazine, 33*(2), 44-51. doi:10.1109/mei.2017.7866678

McLean, D. (1977). *Mechanical Properties of Metals*. R.E. Krieger Pub. Co.

Mora, J. F., & Loscertales, I. G. (1994). The current emitted by highly conducting Taylor cones. *Journal of Fluid Mechanics, 260*(-1), 155. doi:10.1017/s0022112094003472

Musa, J. (2010). Evaluation of the Lubricating Properties of Palm Oil. *Leonardo Electronic Journal of Practices and Technologies, 9*(17), 79-84.

Nieuwenhuyzen, W. V. (1976). Lecithin production and properties. *Journal of the American Oil Chemists Society, 53*(6Part2), 425-427. doi:10.1007/bf02605737

Obahiagbon, F. I. (2012). A Review: Aspects of the African Oil Palm (Elaeis guineesis jacq.) and the Implications of its Bioactives in Human Health. *American Journal of Biochemistry and Molecular Biology, 2*(3), 106-119. doi:10.3923/ajbmb.2012.106.119

Ogata, S., Hatae, T., Schguchi, K., & Shinhara, H. (1977). The Dimensionless Correlation of Mean Particle Diameter in Electrostatic Atomization. *International Chemical Engineering, 3*(2), 132-132.

UDSA, Foreign Agricultural Service. (2018). *Oilseeds: World Market and Trade* (p. 9). USDA.

Orion Ind. (Ed.). (2014, April 3). Non-Stick Baking Advances. Retrieved February 01, 2018, from http://www.orioncoat.com/blog/release-coatings/

Palaniappan, S., & Sastry, S. K. (1991, October). Electrical Conductivity of Selected Juices: Influences of Temperature, Solids Content, Applied Voltage, and Particle Size. *Journal of Food Process Engineering, 14*(4), 247-260.

Palmer, S. J. (1976). The effect of temperature on surface tension. *Physics Education, 11*(2), 119-120. doi:10.1088/0031-9120/11/2/009

Goldsun Electronics Co., LTD. (n.d.). *Push-Pull Solenoids* [Brochure]. Taipei City, Taiwan: Author. Technical Data Sheet for part number SH-T2551L-24V

Rosen, M. J., & Kunjappu, J. T. (2012). *Surfactants and Interfacial Phenomenon* (4th ed.). Hoboken, NJ: John Wiley & Sons.

Rupp, J., Guffey, E., & Jacobsen, G. (1999). Electrostatic spray processes. *Metal Finishing, 97*(5), 208-224. doi:10.1016/s0026-0576(99)80781-8

Sajid, M., & Ilyas, M. (2017). PTFE-coated non-stick cookware and toxicity concerns: a perspective. *Environmental Science and Pollution Research, 24*(30), 23436-23440. doi:10.1007/s11356-017-0095-y

Schneider, C. A., Rasband, W. S., & Eliceri, K. W. (2012, July). NIH Image to ImageJ: 25 years of image analysis. *Nature Methods, 9*(7), 671-675.

DuPont Corporation. (n.d.). *Teflon PTFE Materials Handbook* [Brochure]. Author.

Tomita, Y., Ishibashi, Y., & Yokoyama, T. (1986). Fundamental Studies on An Electrostatic Ink Jet Printer : 1st Report, Electrostatic Drop Formation. *Bulletin of JSME, 29*(257), 3737-3743. doi:10.1299/jsme1958.29.3737

USDA. (2017). Recent Trends in GE Adoption. Retrieved January 27, 2018, from https://www.ers.usda.gov/data-products/adoption-of-genetically-engineered-crops-in-the-us/recent-trends-in-ge-adoption.aspx

Vantzos, O., & Betelu, S. (2006). *<i>Mathematical modeling of charged liquid droplets: numerical simulation and stability analysis</i>* (Unpublished doctoral dissertation). University of North Texas.

Wall, S. (2010). The history of electrokinetic phenomena. *Current Opinion in Colloid & Interface Science, 15*(3), 119-124. doi:10.1016/j.cocis.2009.12.005

Wang, Z., Mitrašinović, A., & Wen, J. (2012). Investigation on Electrostatical Breakup of Bio-Oil Droplets. *Energies, 5*(12), 4323-4339. doi:10.3390/en5114323

Ward, M. R. (1971). *Electrical engineering science*. McGraw-Hill.

Whitaker, S. (2011, July 1). Baking Pans: A Pan of Action. Retrieved February 01, 2018, from http://www.bakingbusiness.com/News/News-Home/Features/2011/7/A-Pan-of-Action.aspx

Widom, B. (2004). Capillarity and Wetting Phenomena: Drops, Bubbles, Pearls, Waves Capillarity and Wetting Phenomena: Drops, Bubbles, Pearls, Waves . *Physics Today, 57*(12), 66-67. doi:10.1063/1.1878340

Wilkerson, J. B., & Gaultney, L. D. (1989). *Electrostatic atomization of vegetable oil for pesticide spraying* (Tech. No. 891524). American Society of Agricultural Engineers (ASAE).

Wissensforum Backwaren (Ed.). (2009). *Release Agents* (Rep.). Berlin: Wissensforum Backwaren.

Xu, Q., Nakajima, M., Liu, Z., & Shii, T. (2011). Soybean-based Surfactants and Their Applications. *Soybean - Applications and Technology*. doi:10.5772/15261

APPENDICES

Appendix A – Patent for Electro-hydrodynamic Oiler

Appendix B – DOE Interaction Charts

Appendix C – DOE Interaction Charts – Soybean Oil

Appendix D – DOE Interaction Charts – Rapeseed Oil

Appendix E – DOE Interaction Charts – Sunflower Oil

Appendix F – Data Table – Palm Oil

Appendix G – Data Table – Soybean Oil

Appendix H – Data Table – Rapeseed Oil

Appendix I – Data Table – Sunflower Oil

Appendix A – Patent for Electro-hydrodynamic Oiler

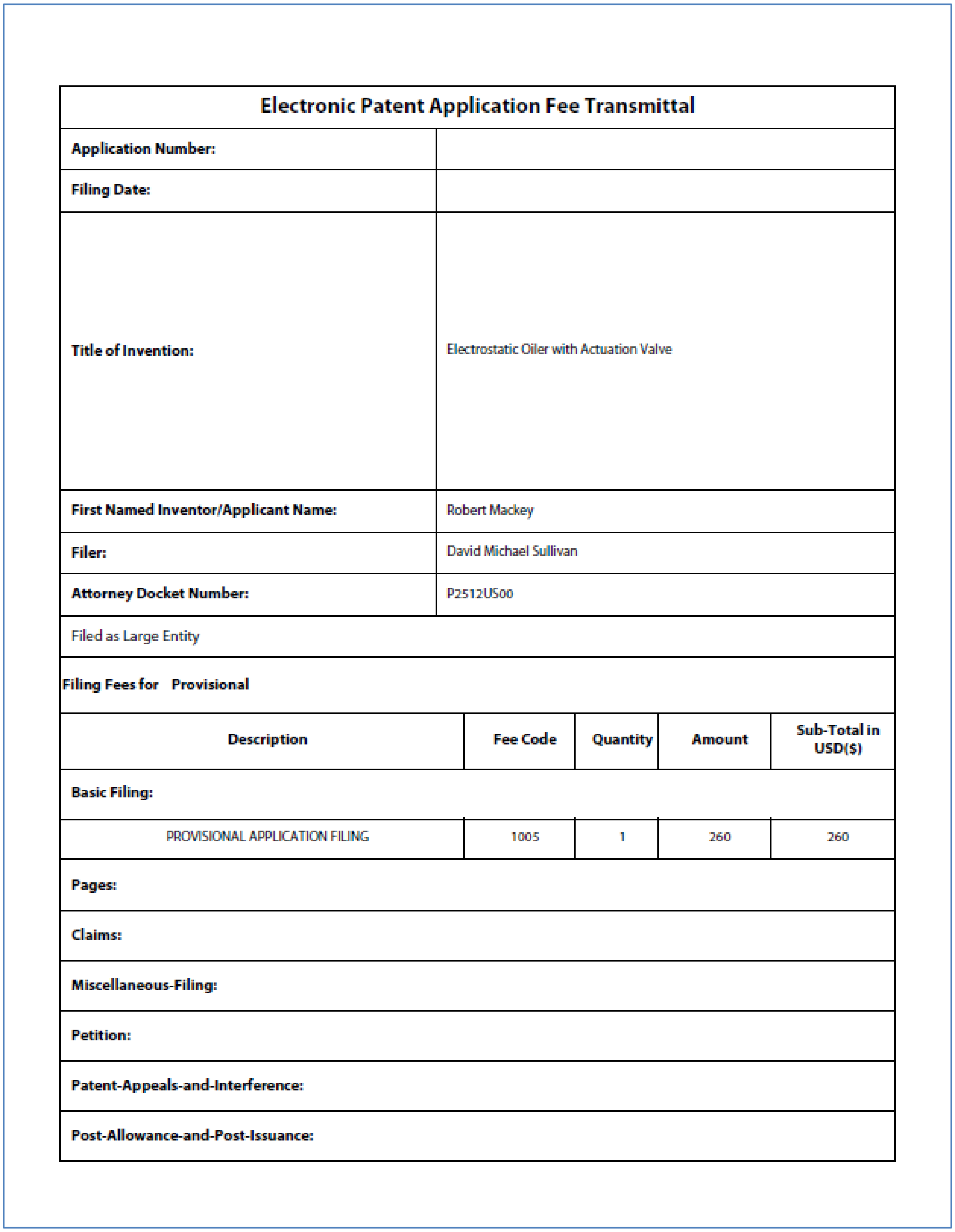

Electronic Patent Application Fee Transmittal

Application Number:	
Filing Date:	
Title of Invention:	Electrostatic Oiler with Actuation Valve
First Named Inventor/Applicant Name:	Robert Mackey
Filer:	David Michael Sullivan
Attorney Docket Number:	P2512US00

Filed as Large Entity

Filing Fees for Provisional

Description	Fee Code	Quantity	Amount	Sub-Total in USD($)
Basic Filing:				
PROVISIONAL APPLICATION FILING	1005	1	260	260
Pages:				
Claims:				
Miscellaneous-Filing:				
Petition:				
Patent-Appeals-and-Interference:				
Post-Allowance-and-Post-Issuance:				

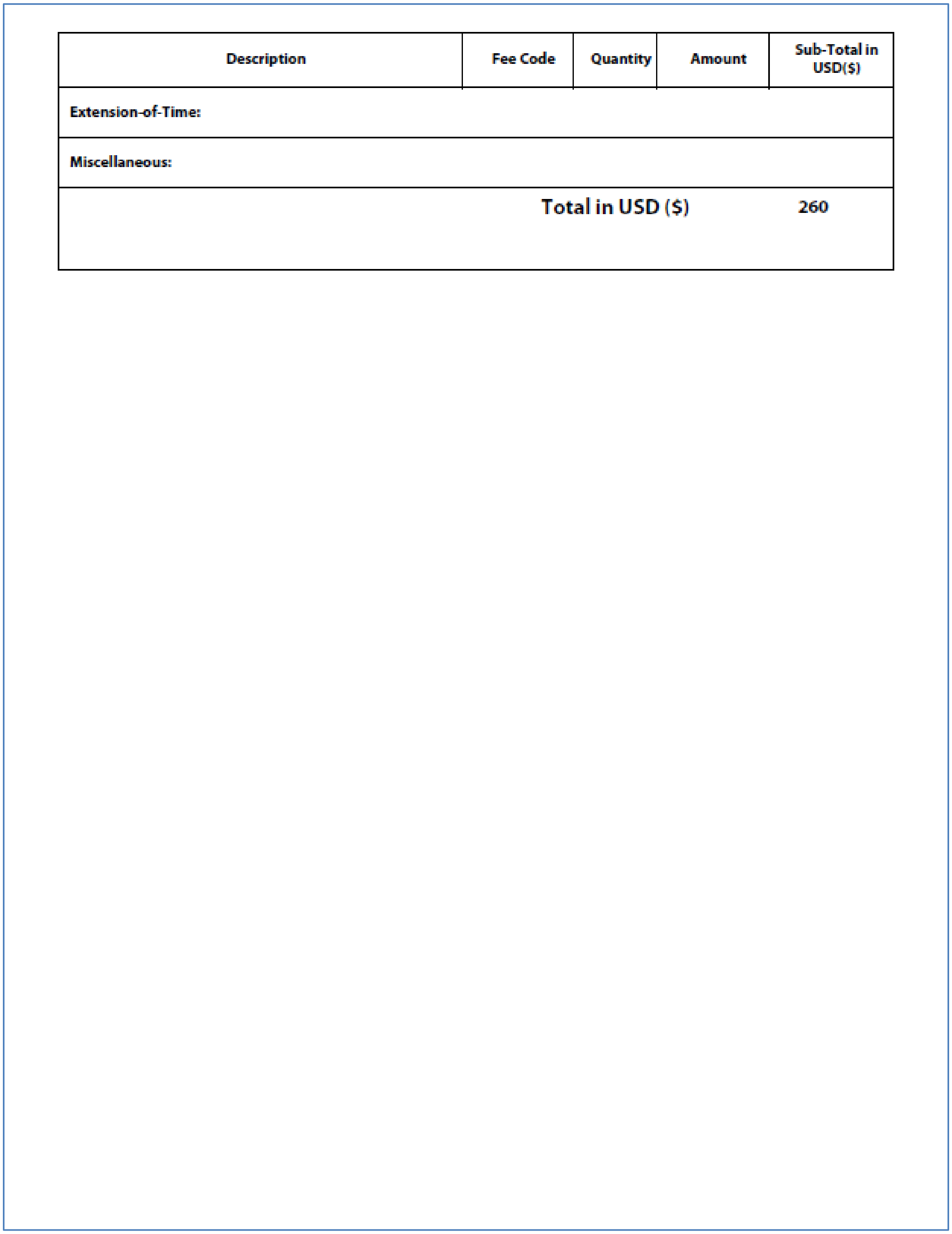

Description	Fee Code	Quantity	Amount	Sub-Total in USD($)
Extension-of-Time:				
Miscellaneous:				
		Total in USD ($)		**260**

Appendix A – Patent for Electro-hydrodynamic Oiler

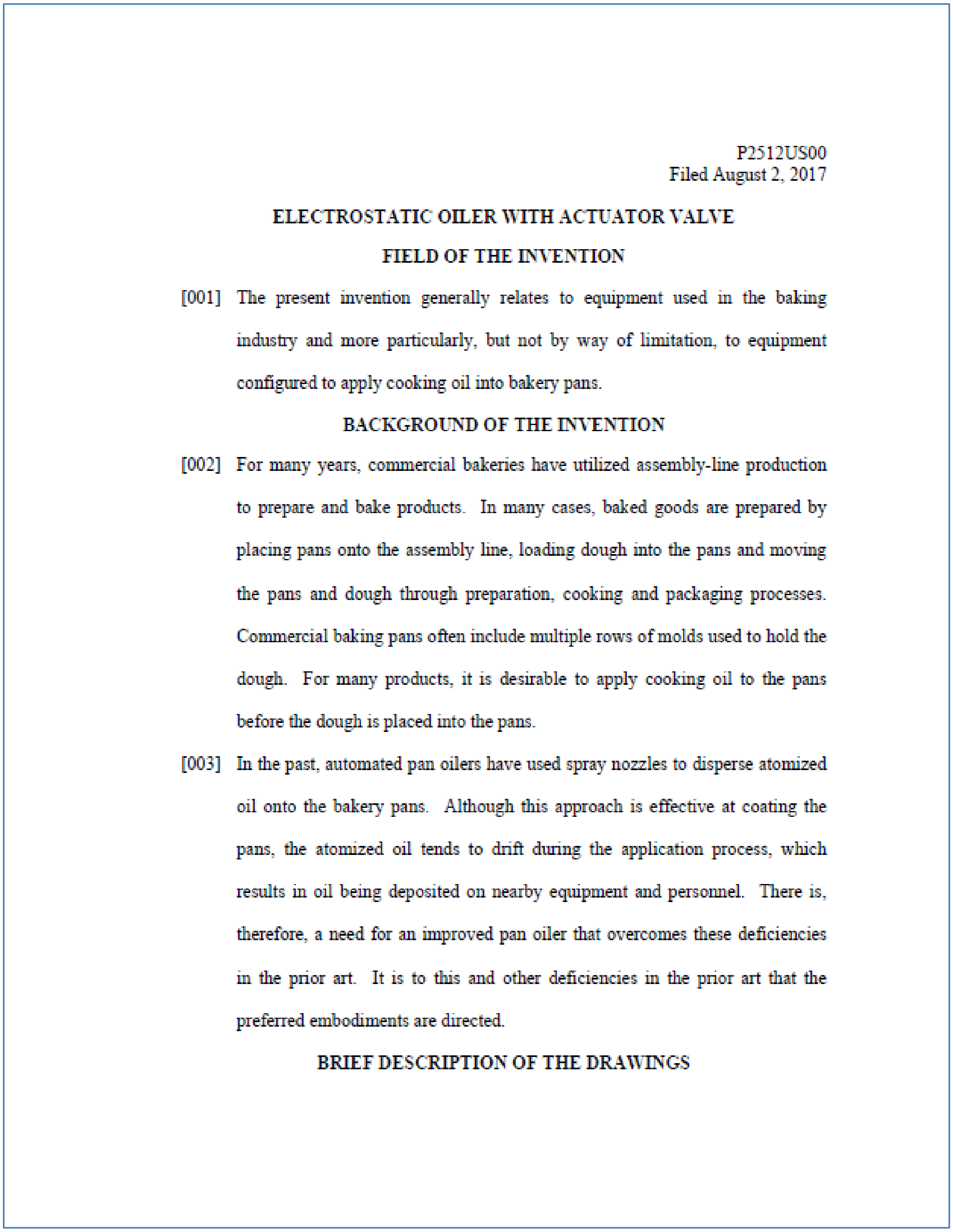

P2512US00
Filed August 2, 2017

ELECTROSTATIC OILER WITH ACTUATOR VALVE

FIELD OF THE INVENTION

[001] The present invention generally relates to equipment used in the baking industry and more particularly, but not by way of limitation, to equipment configured to apply cooking oil into bakery pans.

BACKGROUND OF THE INVENTION

[002] For many years, commercial bakeries have utilized assembly-line production to prepare and bake products. In many cases, baked goods are prepared by placing pans onto the assembly line, loading dough into the pans and moving the pans and dough through preparation, cooking and packaging processes. Commercial baking pans often include multiple rows of molds used to hold the dough. For many products, it is desirable to apply cooking oil to the pans before the dough is placed into the pans.

[003] In the past, automated pan oilers have used spray nozzles to disperse atomized oil onto the bakery pans. Although this approach is effective at coating the pans, the atomized oil tends to drift during the application process, which results in oil being deposited on nearby equipment and personnel. There is, therefore, a need for an improved pan oiler that overcomes these deficiencies in the prior art. It is to this and other deficiencies in the prior art that the preferred embodiments are directed.

BRIEF DESCRIPTION OF THE DRAWINGS

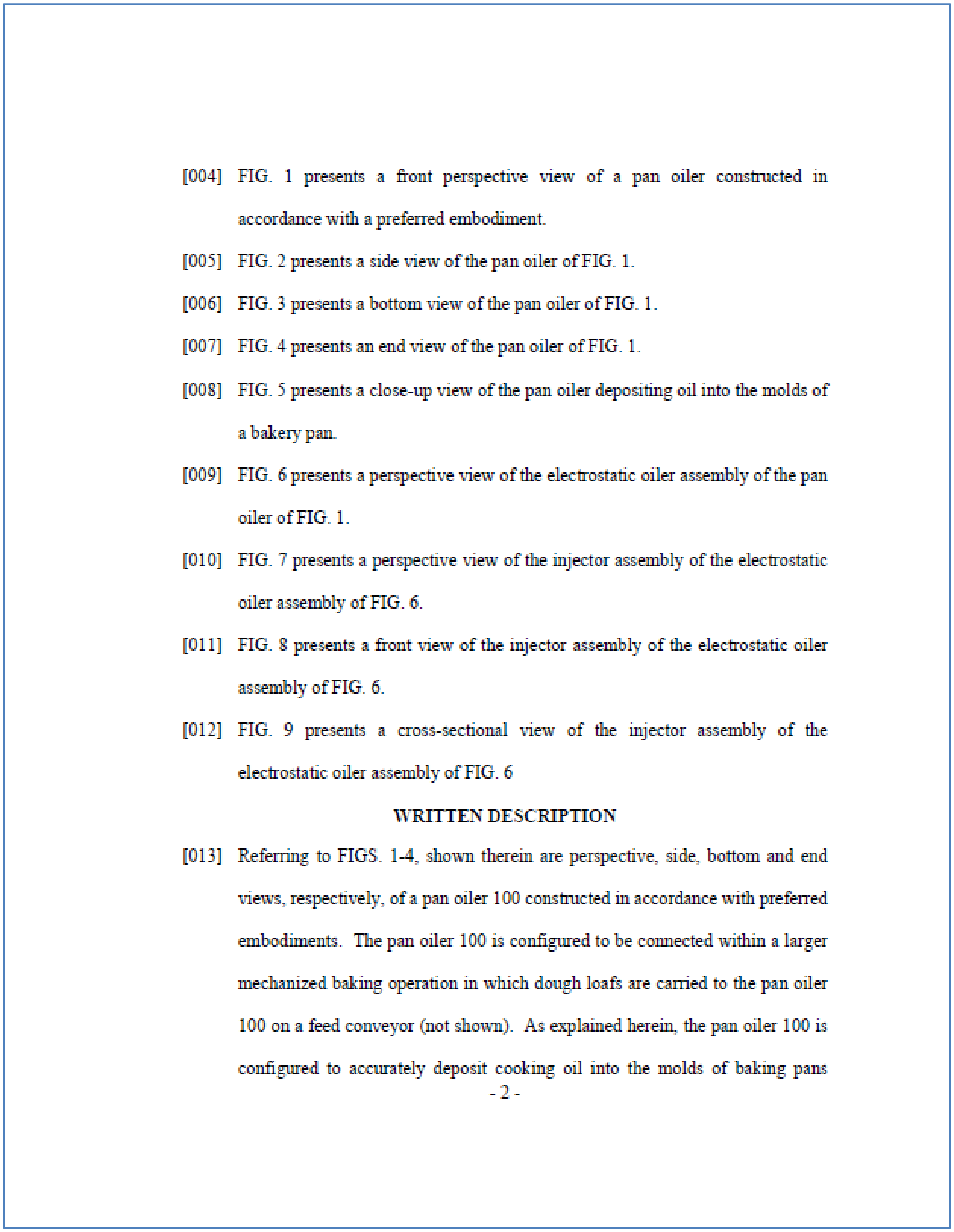

[004] FIG. 1 presents a front perspective view of a pan oiler constructed in accordance with a preferred embodiment.

[005] FIG. 2 presents a side view of the pan oiler of FIG. 1.

[006] FIG. 3 presents a bottom view of the pan oiler of FIG. 1.

[007] FIG. 4 presents an end view of the pan oiler of FIG. 1.

[008] FIG. 5 presents a close-up view of the pan oiler depositing oil into the molds of a bakery pan.

[009] FIG. 6 presents a perspective view of the electrostatic oiler assembly of the pan oiler of FIG. 1.

[010] FIG. 7 presents a perspective view of the injector assembly of the electrostatic oiler assembly of FIG. 6.

[011] FIG. 8 presents a front view of the injector assembly of the electrostatic oiler assembly of FIG. 6.

[012] FIG. 9 presents a cross-sectional view of the injector assembly of the electrostatic oiler assembly of FIG. 6

WRITTEN DESCRIPTION

[013] Referring to FIGS. 1-4, shown therein are perspective, side, bottom and end views, respectively, of a pan oiler 100 constructed in accordance with preferred embodiments. The pan oiler 100 is configured to be connected within a larger mechanized baking operation in which dough loafs are carried to the pan oiler 100 on a feed conveyor (not shown). As explained herein, the pan oiler 100 is configured to accurately deposit cooking oil into the molds of baking pans

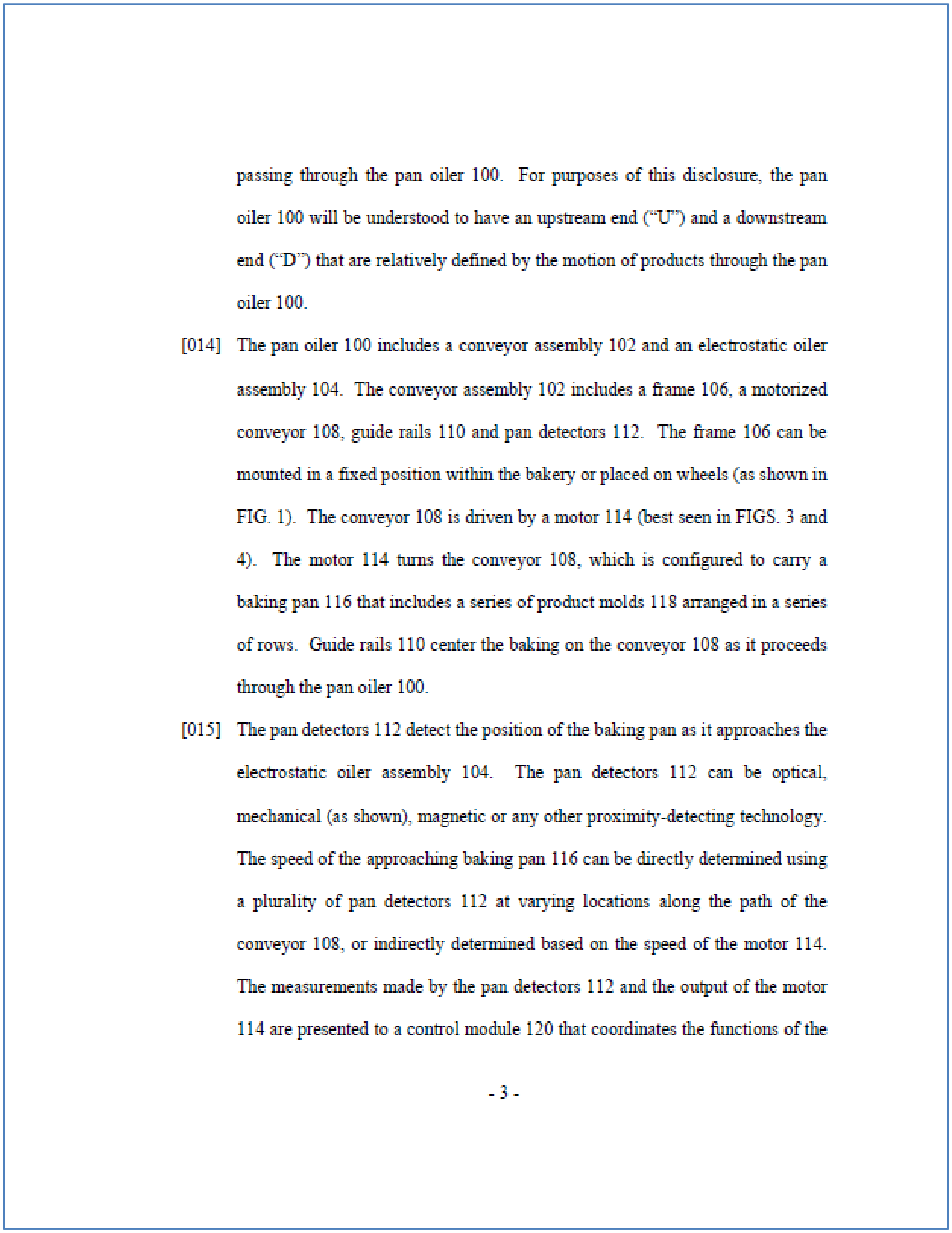

passing through the pan oiler 100. For purposes of this disclosure, the pan oiler 100 will be understood to have an upstream end ("U") and a downstream end ("D") that are relatively defined by the motion of products through the pan oiler 100.

[014] The pan oiler 100 includes a conveyor assembly 102 and an electrostatic oiler assembly 104. The conveyor assembly 102 includes a frame 106, a motorized conveyor 108, guide rails 110 and pan detectors 112. The frame 106 can be mounted in a fixed position within the bakery or placed on wheels (as shown in FIG. 1). The conveyor 108 is driven by a motor 114 (best seen in FIGS. 3 and 4). The motor 114 turns the conveyor 108, which is configured to carry a baking pan 116 that includes a series of product molds 118 arranged in a series of rows. Guide rails 110 center the baking on the conveyor 108 as it proceeds through the pan oiler 100.

[015] The pan detectors 112 detect the position of the baking pan as it approaches the electrostatic oiler assembly 104. The pan detectors 112 can be optical, mechanical (as shown), magnetic or any other proximity-detecting technology. The speed of the approaching baking pan 116 can be directly determined using a plurality of pan detectors 112 at varying locations along the path of the conveyor 108, or indirectly determined based on the speed of the motor 114. The measurements made by the pan detectors 112 and the output of the motor 114 are presented to a control module 120 that coordinates the functions of the

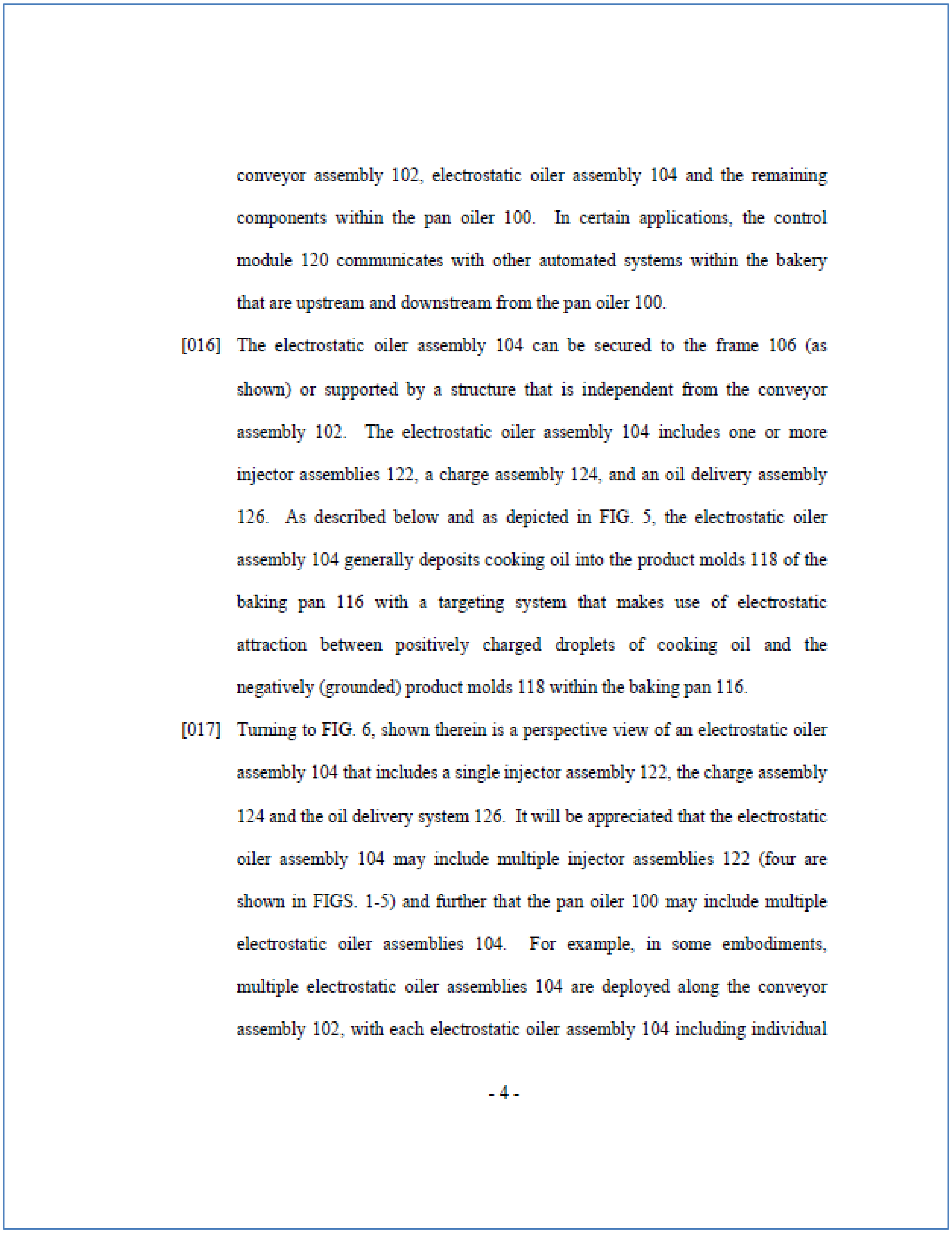

conveyor assembly 102, electrostatic oiler assembly 104 and the remaining components within the pan oiler 100. In certain applications, the control module 120 communicates with other automated systems within the bakery that are upstream and downstream from the pan oiler 100.

[016] The electrostatic oiler assembly 104 can be secured to the frame 106 (as shown) or supported by a structure that is independent from the conveyor assembly 102. The electrostatic oiler assembly 104 includes one or more injector assemblies 122, a charge assembly 124, and an oil delivery assembly 126. As described below and as depicted in FIG. 5, the electrostatic oiler assembly 104 generally deposits cooking oil into the product molds 118 of the baking pan 116 with a targeting system that makes use of electrostatic attraction between positively charged droplets of cooking oil and the negatively (grounded) product molds 118 within the baking pan 116.

[017] Turning to FIG. 6, shown therein is a perspective view of an electrostatic oiler assembly 104 that includes a single injector assembly 122, the charge assembly 124 and the oil delivery system 126. It will be appreciated that the electrostatic oiler assembly 104 may include multiple injector assemblies 122 (four are shown in FIGS. 1-5) and further that the pan oiler 100 may include multiple electrostatic oiler assemblies 104. For example, in some embodiments, multiple electrostatic oiler assemblies 104 are deployed along the conveyor assembly 102, with each electrostatic oiler assembly 104 including individual

injector assemblies 122 that correspond to the number of product molds 118 in each row of the baking pan 116.

[018] The charge assembly 124 includes an amplified power source 128, a positive lead 130 connected between the power source 128 and the injector assembly 122 and a negative lead 132 connected between the power source 128 and a ground contact 134. In some embodiments, the power source 128 is configured to produce about 50,000 volts of electricity. As best seen in FIG. 3, the ground contact 134 is retained below the conveyor 108 in electrical contact with the bottom of the baking pan 116. It will be noted that the baking pan 116 is constructed from a material that conducts electricity, such as steel, copper or conductive metal alloys. In some embodiments the baking pan 116 includes insulating partitions that electrically isolate some product molds 118 from other product molds 118.

[019] The oil delivery system 126 includes a cooking oil tank 136, a pump 138 and tubing 140 that extends from the pump 138 to the injector assembly 122. The pump 138 pressurizes the cooking oil and delivers the oil to the injector assembly 122. In exemplary embodiments, the cooking oil is an emulsified edible cooking oil that exhibits favorable dispersion and coating characteristics. Suitable cooking oils include blends of mineral oil, soy oil and lecithin. The pump 138 is configured to maintain a delivery pressure on the cooking oil of between about 0.5 psi and about 30 psi. In exemplary

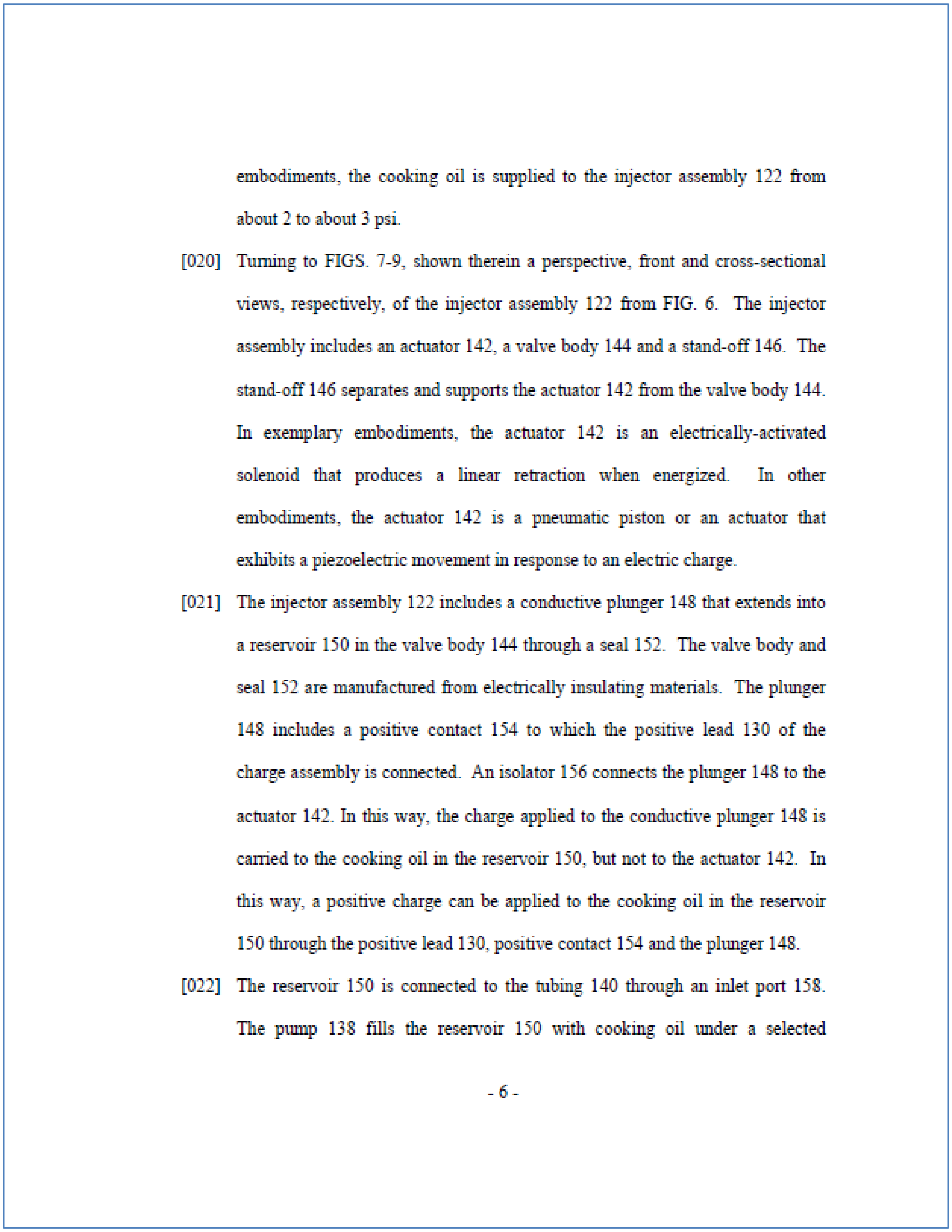

embodiments, the cooking oil is supplied to the injector assembly 122 from about 2 to about 3 psi.

[020] Turning to FIGS. 7-9, shown therein a perspective, front and cross-sectional views, respectively, of the injector assembly 122 from FIG. 6. The injector assembly includes an actuator 142, a valve body 144 and a stand-off 146. The stand-off 146 separates and supports the actuator 142 from the valve body 144. In exemplary embodiments, the actuator 142 is an electrically-activated solenoid that produces a linear retraction when energized. In other embodiments, the actuator 142 is a pneumatic piston or an actuator that exhibits a piezoelectric movement in response to an electric charge.

[021] The injector assembly 122 includes a conductive plunger 148 that extends into a reservoir 150 in the valve body 144 through a seal 152. The valve body and seal 152 are manufactured from electrically insulating materials. The plunger 148 includes a positive contact 154 to which the positive lead 130 of the charge assembly is connected. An isolator 156 connects the plunger 148 to the actuator 142. In this way, the charge applied to the conductive plunger 148 is carried to the cooking oil in the reservoir 150, but not to the actuator 142. In this way, a positive charge can be applied to the cooking oil in the reservoir 150 through the positive lead 130, positive contact 154 and the plunger 148.

[022] The reservoir 150 is connected to the tubing 140 through an inlet port 158. The pump 138 fills the reservoir 150 with cooking oil under a selected

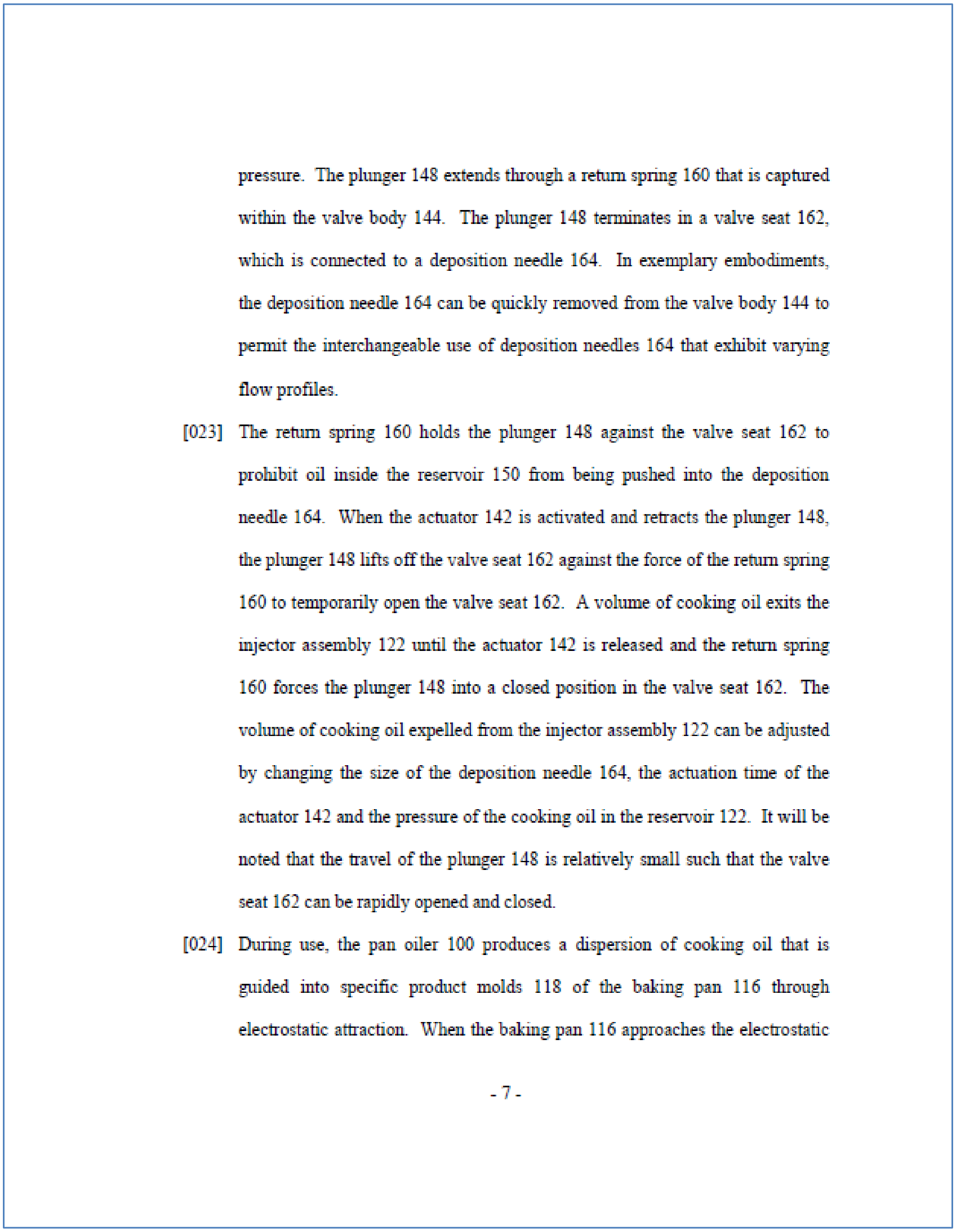

pressure. The plunger 148 extends through a return spring 160 that is captured within the valve body 144. The plunger 148 terminates in a valve seat 162, which is connected to a deposition needle 164. In exemplary embodiments, the deposition needle 164 can be quickly removed from the valve body 144 to permit the interchangeable use of deposition needles 164 that exhibit varying flow profiles.

[023] The return spring 160 holds the plunger 148 against the valve seat 162 to prohibit oil inside the reservoir 150 from being pushed into the deposition needle 164. When the actuator 142 is activated and retracts the plunger 148, the plunger 148 lifts off the valve seat 162 against the force of the return spring 160 to temporarily open the valve seat 162. A volume of cooking oil exits the injector assembly 122 until the actuator 142 is released and the return spring 160 forces the plunger 148 into a closed position in the valve seat 162. The volume of cooking oil expelled from the injector assembly 122 can be adjusted by changing the size of the deposition needle 164, the actuation time of the actuator 142 and the pressure of the cooking oil in the reservoir 122. It will be noted that the travel of the plunger 148 is relatively small such that the valve seat 162 can be rapidly opened and closed.

[024] During use, the pan oiler 100 produces a dispersion of cooking oil that is guided into specific product molds 118 of the baking pan 116 through electrostatic attraction. When the baking pan 116 approaches the electrostatic

oiler assembly 104, the charge assembly 124 supplies a positive charge to cooking oil contained within the reservoirs 150 of one or more injector assemblies 122. In some embodiments, the charge assembly 124 maintains a constant charge, while in other embodiments the cooking oil in the reservoir is only temporarily charged before it is expelled from the injector assembly.

[025] As the baking pan 116 continues to move along the conveyor 108, the actuator 142 is activated and retracts the plunger 148 from the valve seat 162. The pressurized, positively-charged cooking oil is forced from the valve body 144 through the deposition needle 164. Once ejected from the valve body 144, the cooking oil rapidly disperses into small positively-charged droplets. As the droplets fall, the baking pan 116 contacts the ground contact 134 and the positively charged droplets are drawn by electrostatic attraction into the product molds 118.

[026] The coordinated operation of the conveyor assembly 102 and electrostatic oiler assembly 104 provide an enhanced pan oiling system that overcomes many of the deficiencies in the prior art. In particular, the pan oiler 100 provides a more accurate oil coating to the baking pan 116, with less overspray and under lower fluid pressures. The injector assemblies 122 are configured to rapidly cycle to provide targeted oiling to discrete rows of product molds 118 within the baking pan 116. This level of accuracy and precision has not been achieved by prior art spraying systems.

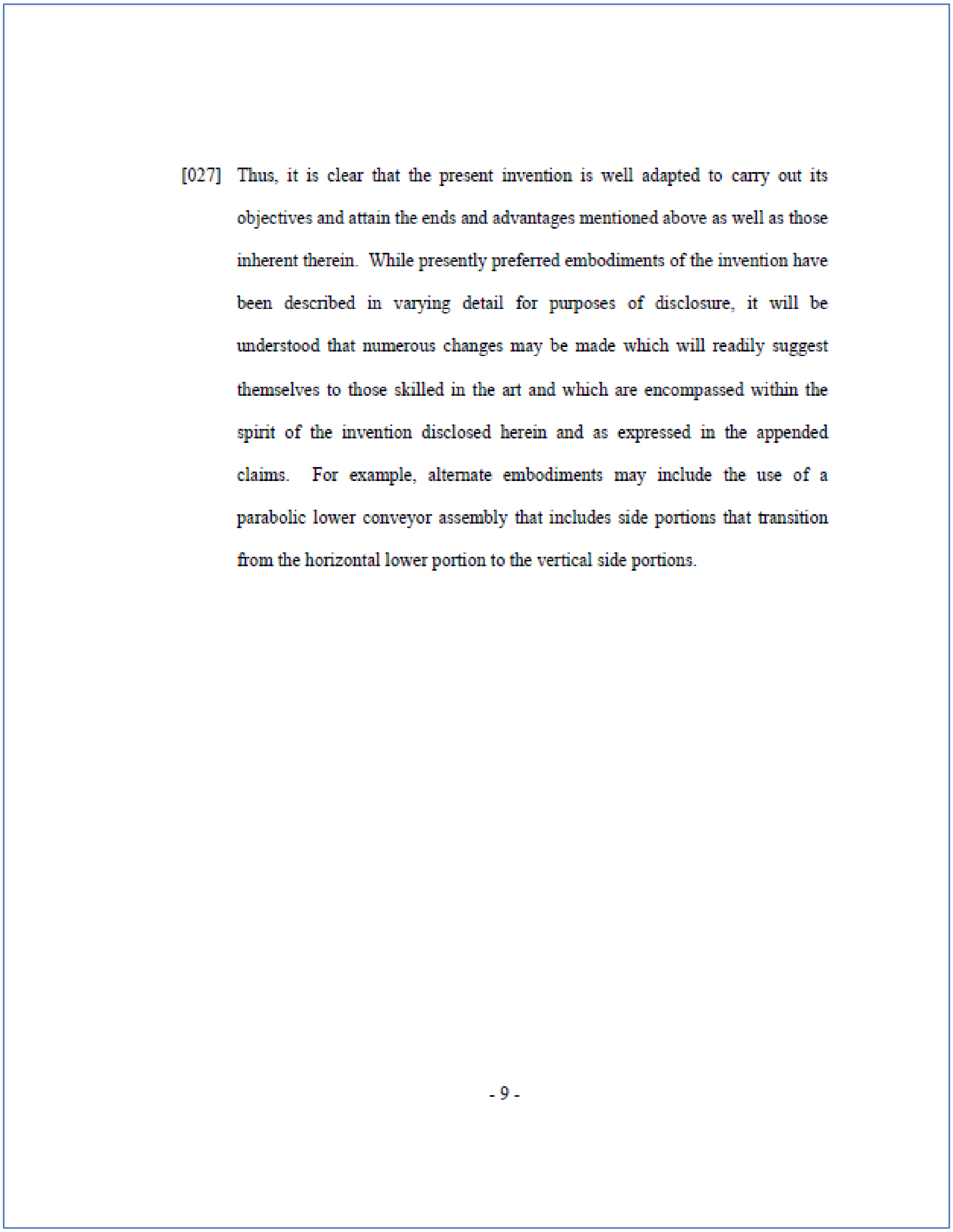

[027] Thus, it is clear that the present invention is well adapted to carry out its objectives and attain the ends and advantages mentioned above as well as those inherent therein. While presently preferred embodiments of the invention have been described in varying detail for purposes of disclosure, it will be understood that numerous changes may be made which will readily suggest themselves to those skilled in the art and which are encompassed within the spirit of the invention disclosed herein and as expressed in the appended claims. For example, alternate embodiments may include the use of a parabolic lower conveyor assembly that includes side portions that transition from the horizontal lower portion to the vertical side portions.

Appendix A – Patent for Electro-hydrodynamic Oiler

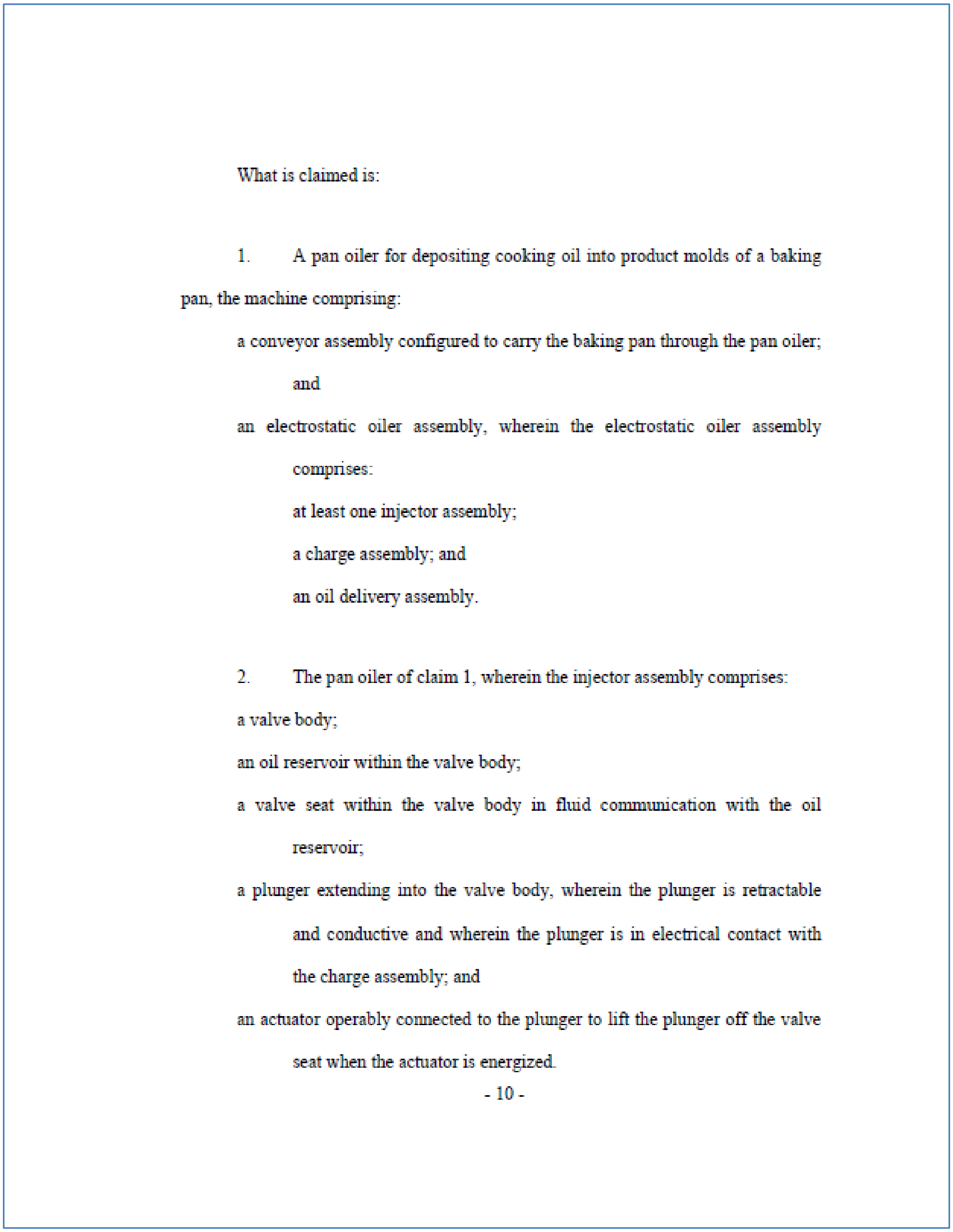

What is claimed is:

1. A pan oiler for depositing cooking oil into product molds of a baking pan, the machine comprising:

a conveyor assembly configured to carry the baking pan through the pan oiler; and

an electrostatic oiler assembly, wherein the electrostatic oiler assembly comprises:

at least one injector assembly;

a charge assembly; and

an oil delivery assembly.

2. The pan oiler of claim 1, wherein the injector assembly comprises:

a valve body;

an oil reservoir within the valve body;

a valve seat within the valve body in fluid communication with the oil reservoir;

a plunger extending into the valve body, wherein the plunger is retractable and conductive and wherein the plunger is in electrical contact with the charge assembly; and

an actuator operably connected to the plunger to lift the plunger off the valve seat when the actuator is energized.

Appendix A – Patent for Electro-hydrodynamic Oiler

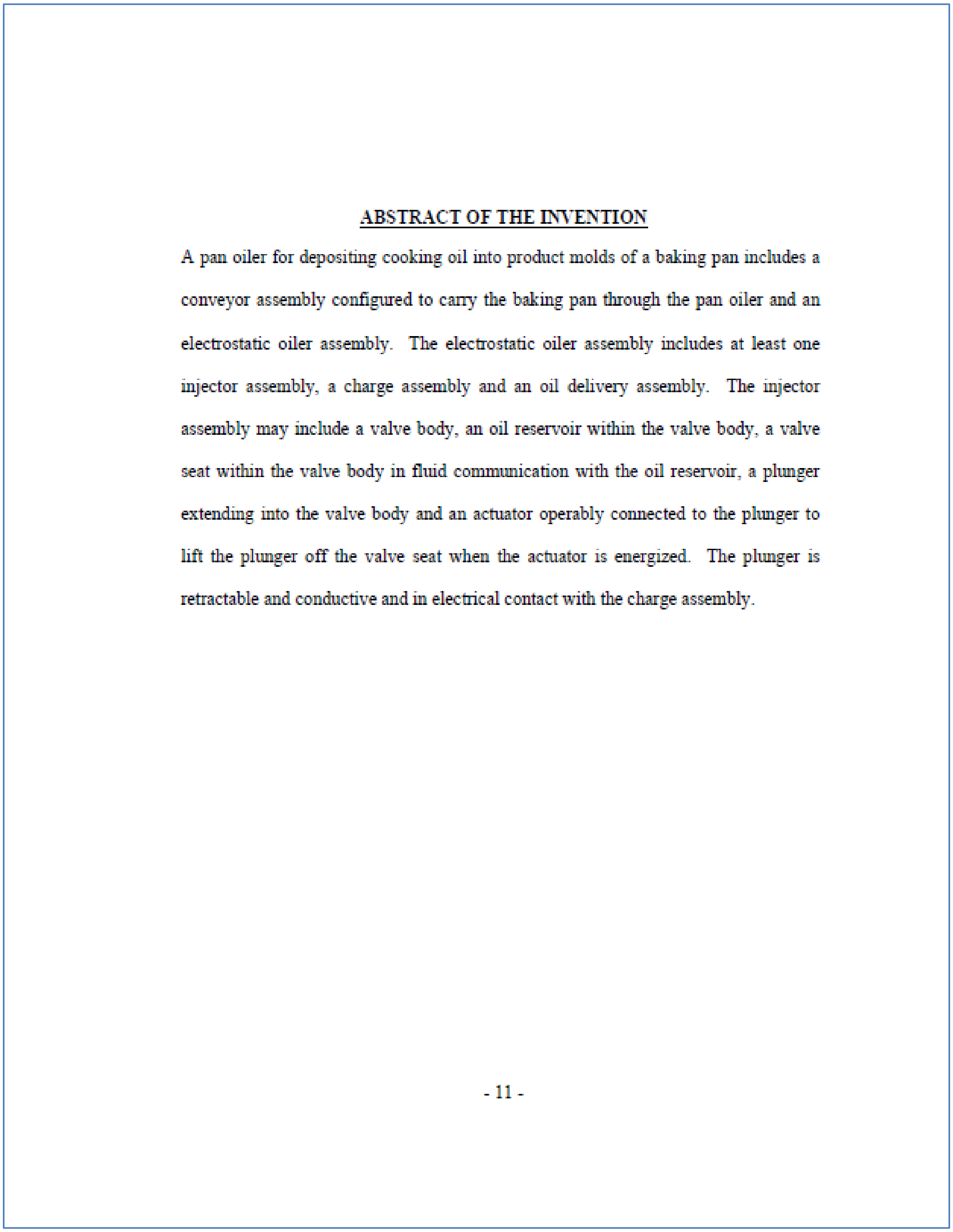

ABSTRACT OF THE INVENTION

A pan oiler for depositing cooking oil into product molds of a baking pan includes a conveyor assembly configured to carry the baking pan through the pan oiler and an electrostatic oiler assembly. The electrostatic oiler assembly includes at least one injector assembly, a charge assembly and an oil delivery assembly. The injector assembly may include a valve body, an oil reservoir within the valve body, a valve seat within the valve body in fluid communication with the oil reservoir, a plunger extending into the valve body and an actuator operably connected to the plunger to lift the plunger off the valve seat when the actuator is energized. The plunger is retractable and conductive and in electrical contact with the charge assembly.

Appendix A – Patent for Electro-hydrodynamic Oiler

1/6

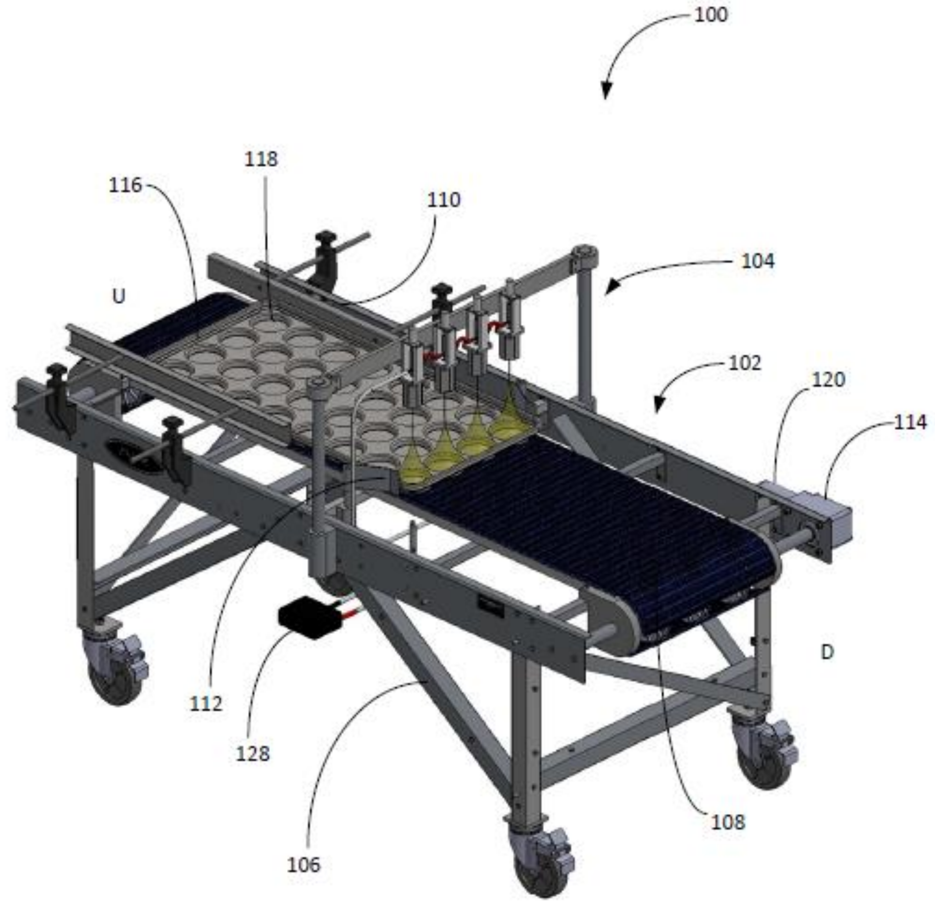

FIG. 1

Appendix A – Patent for Electro-hydrodynamic Oiler

2/6

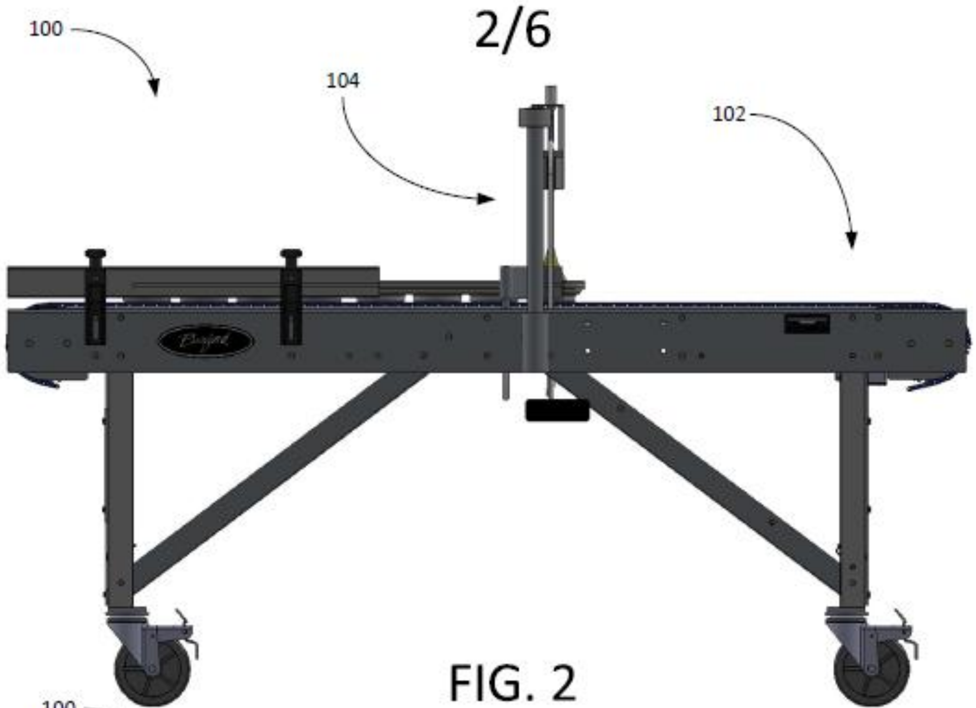

FIG. 2

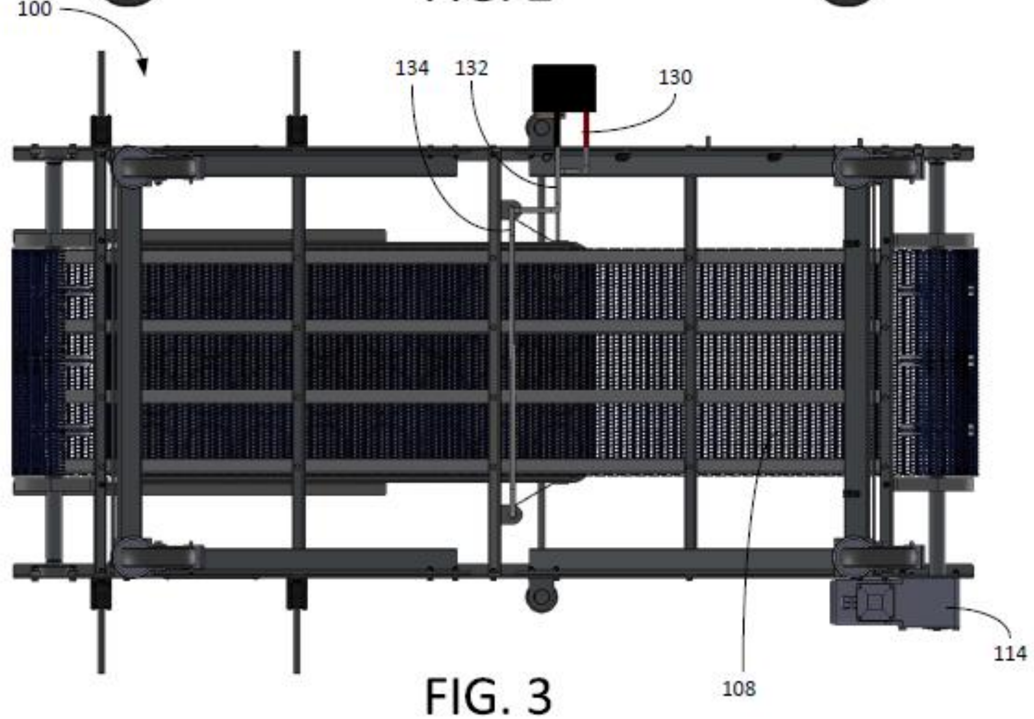

FIG. 3

3/6

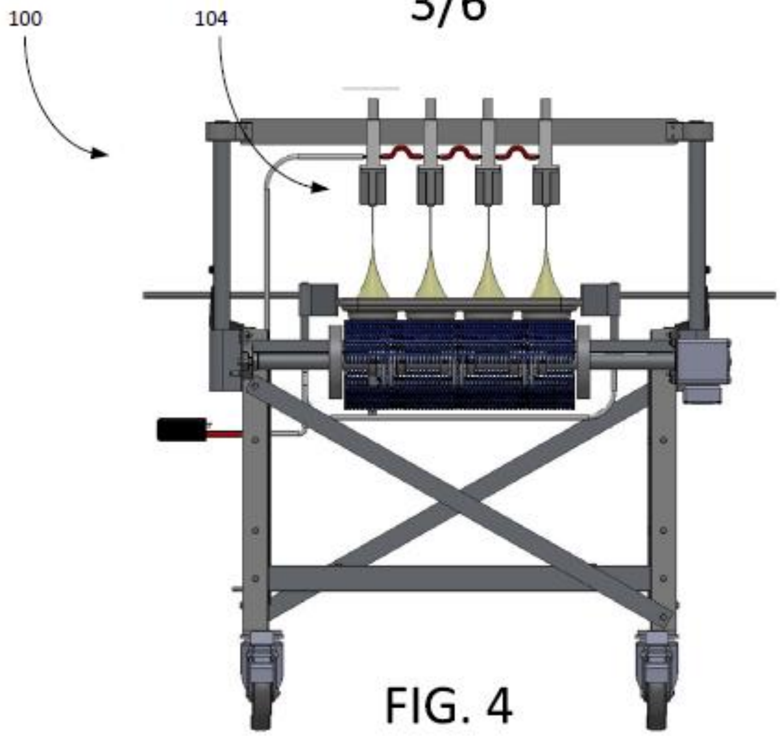

FIG. 4

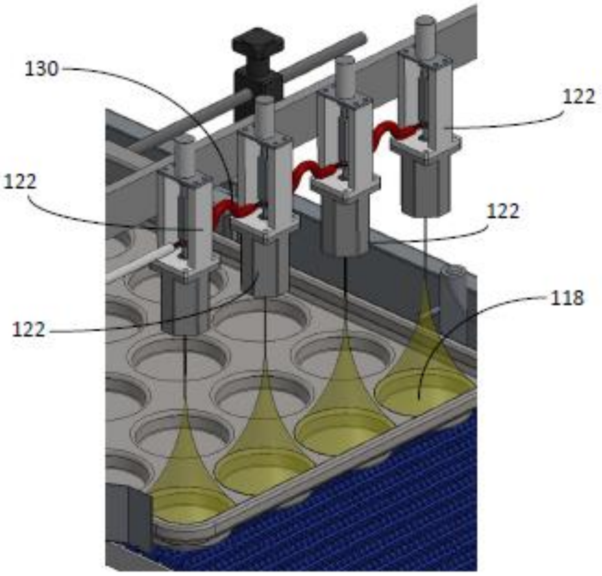

FIG. 5

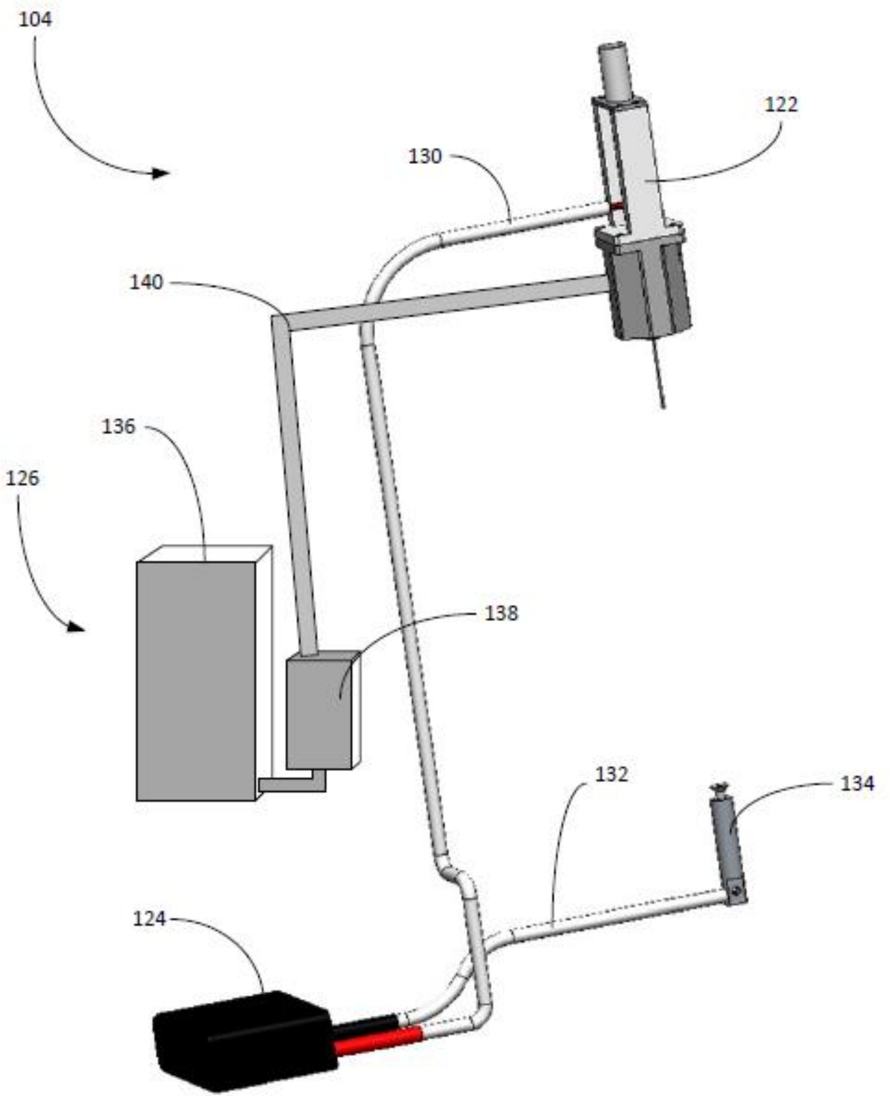

FIG. 6

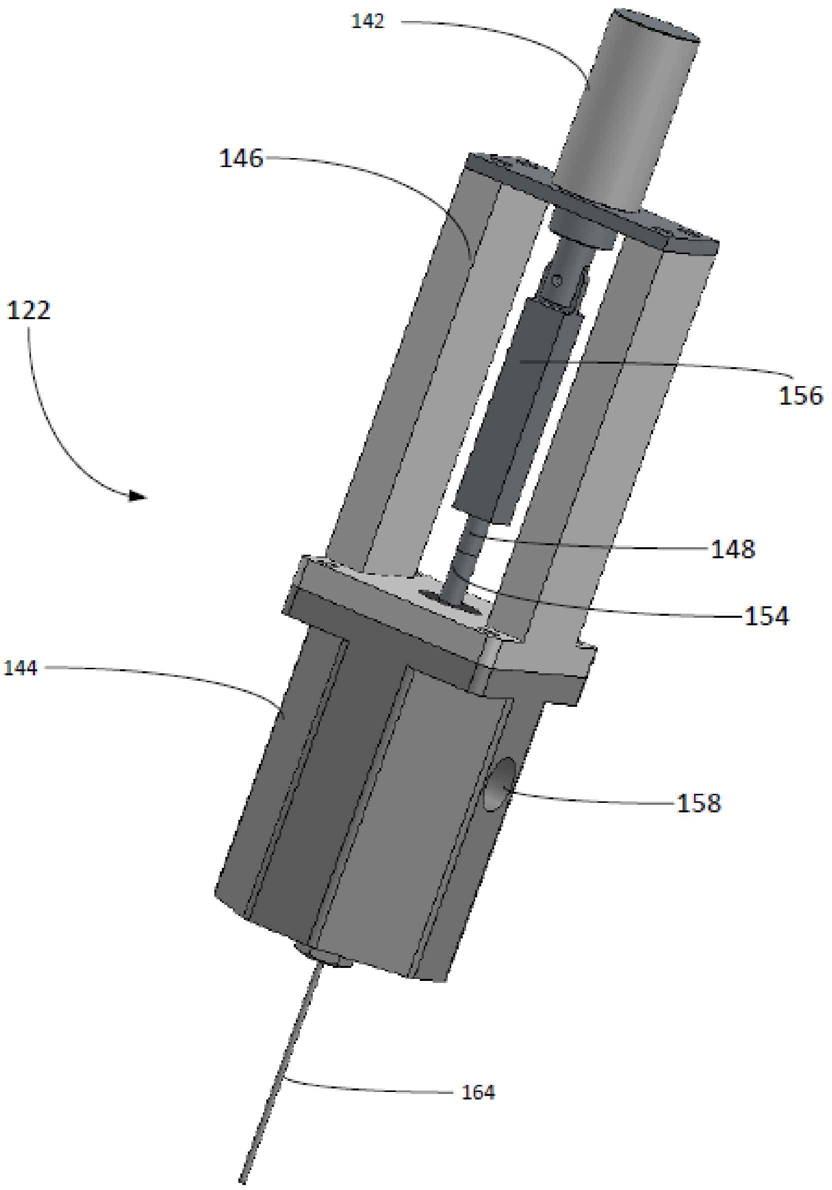

FIG. 7

6/6

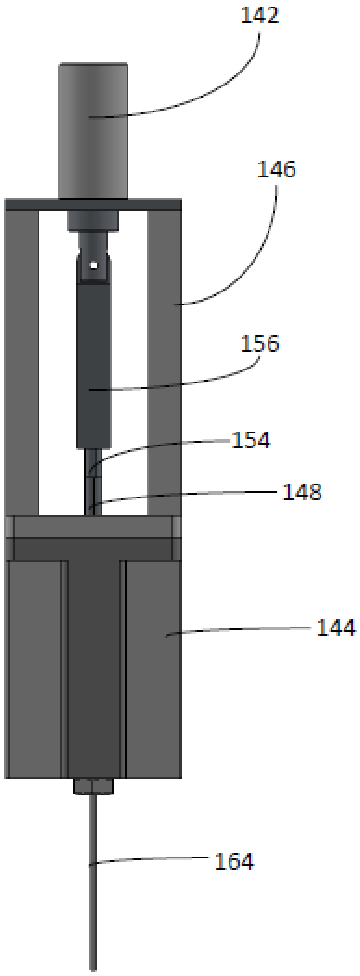
142
146
156
154
148
144
164

FIG. 8

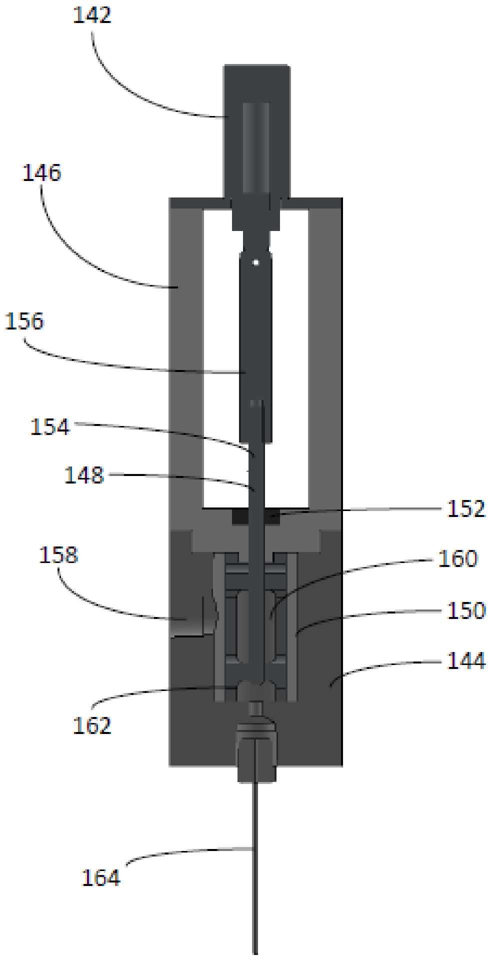
142
146
156
154
148
152
158
160
150
144
162
164

FIG. 9

Appendix B – DOE Interaction Charts – Palm Oil

Table 30: Palm Oil & Soy Lecithin @ 19Ga Interaction chart on Droplet Count Y-bar

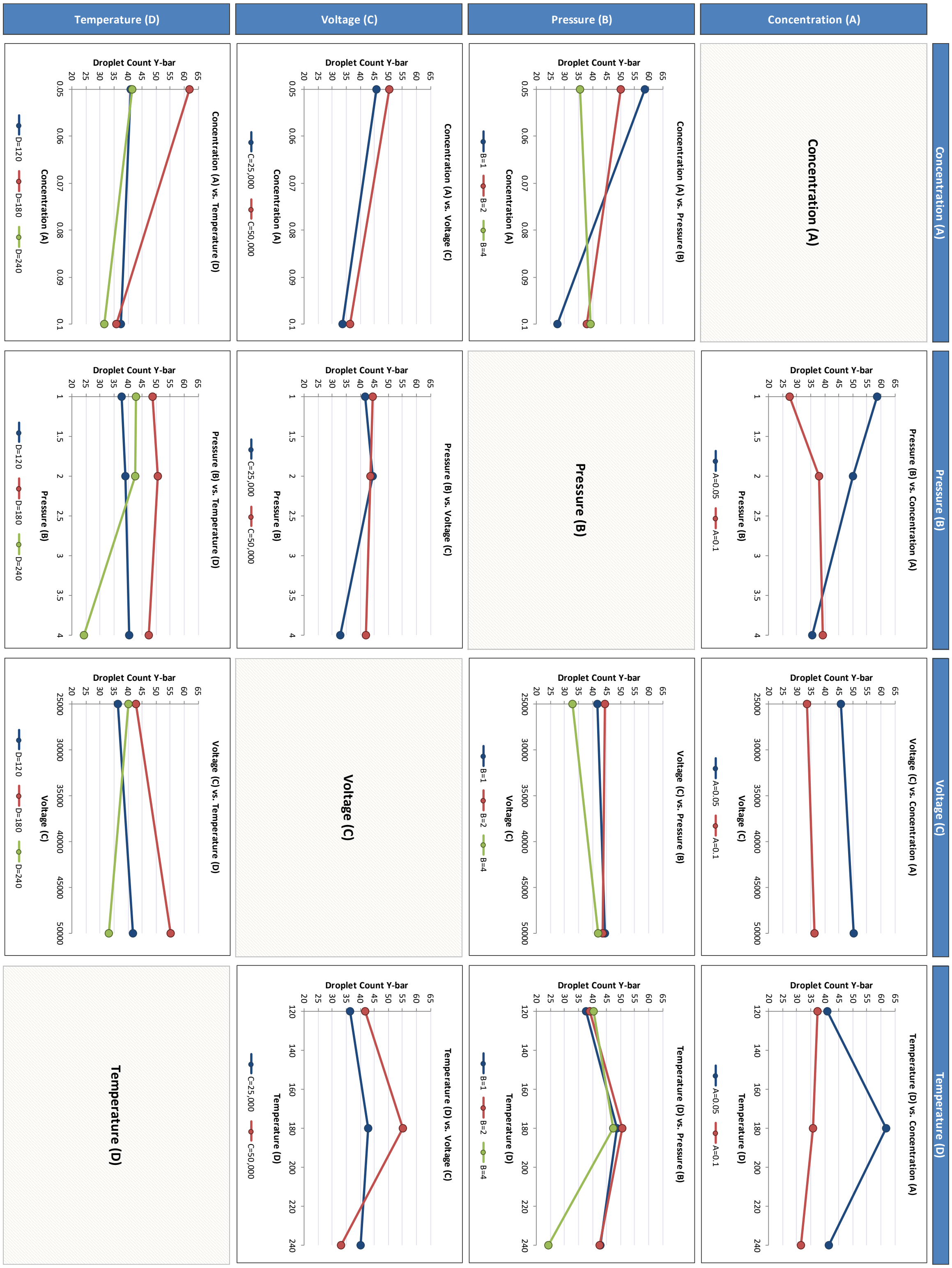

Appendix B – DOE Interaction Charts – Palm Oil

Table 31: Palm Oil & Soy Lecithin @ 19Ga Interaction chart on Droplet Size Y-bar

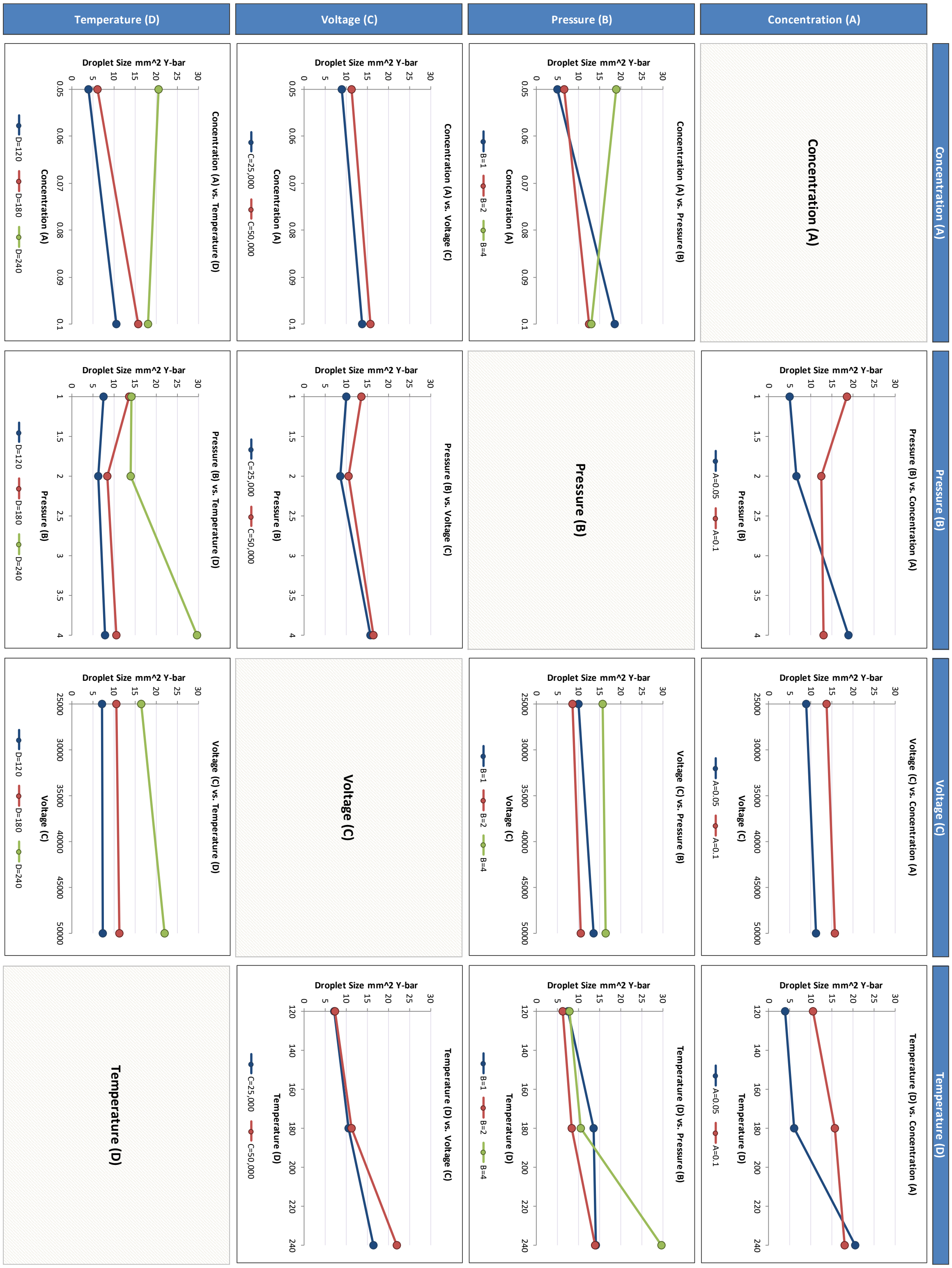

Appendix B – DOE Interaction Charts – Palm Oil

Table 32: Palm Oil & Soy Lecithin @ 19Ga Interaction chart on Coverage Area Y-bar

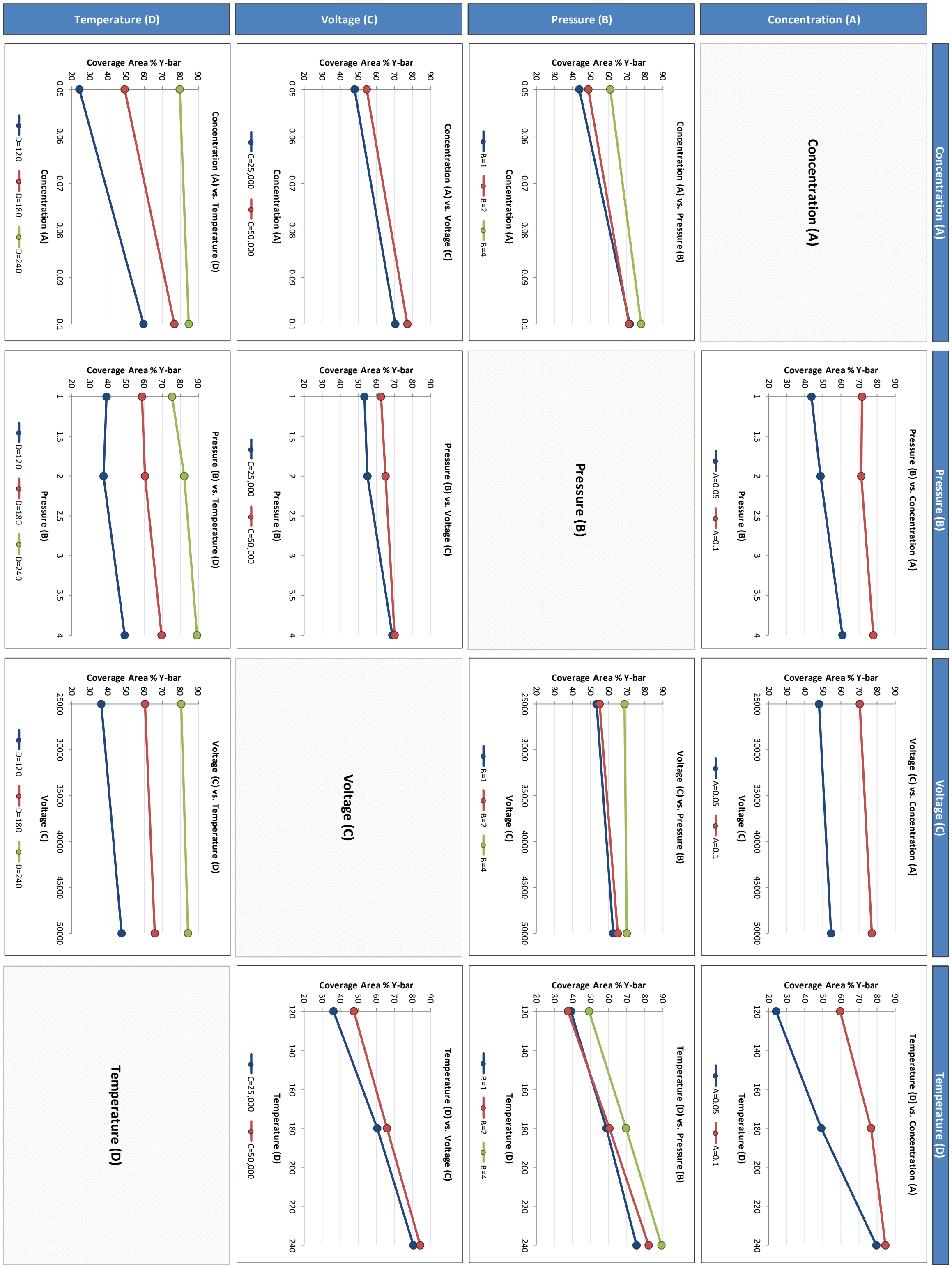

Appendix B – DOE Interaction Charts – Palm Oil

Table 33: Palm Oil & Soy Lecithin @ 19Ga Interaction chart on Sample Weight Y-bar

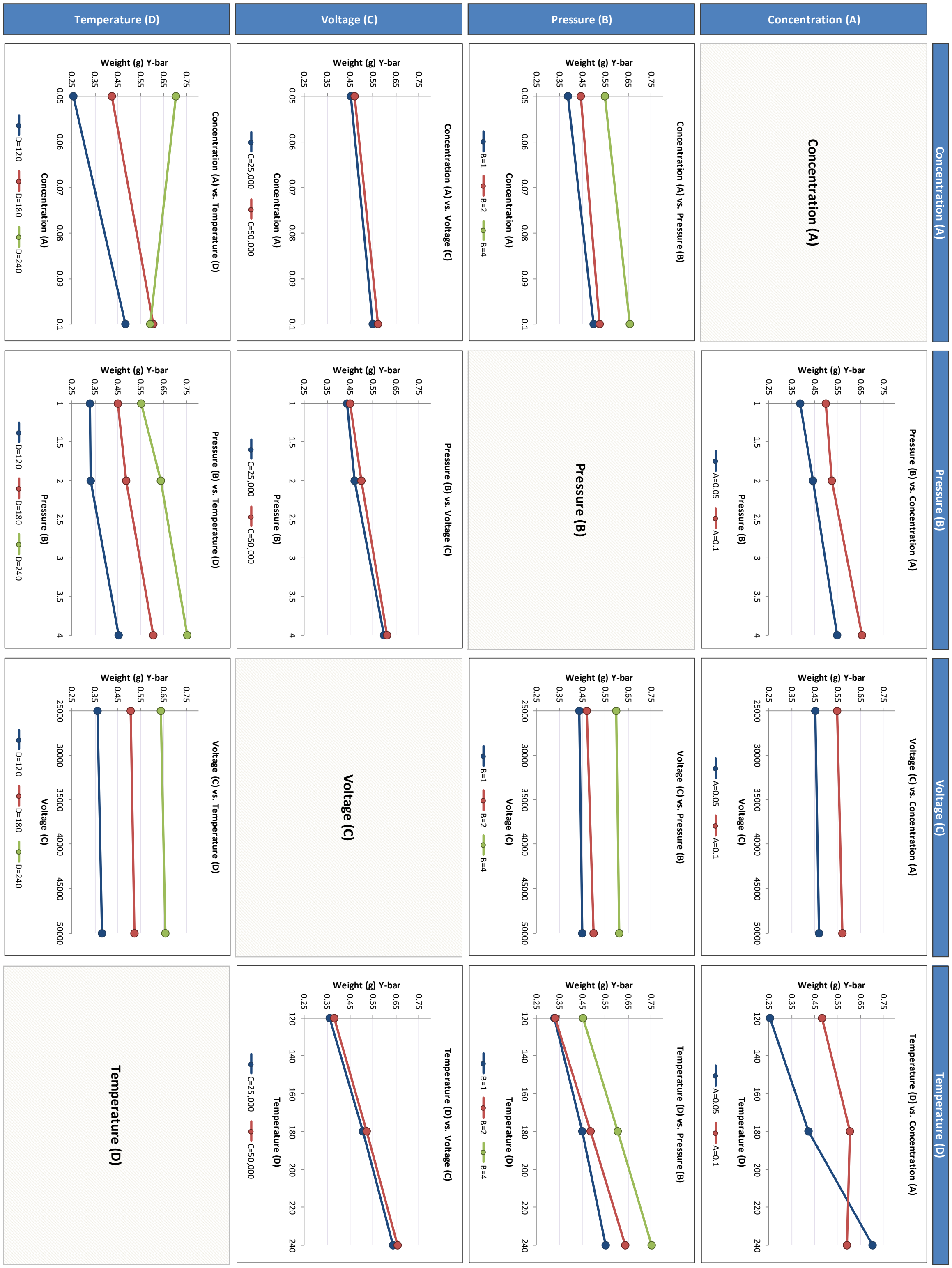

Appendix B – DOE Interaction Charts – Palm Oil

Table 34: Palm Oil & Polysorbate 80 @ 19Ga Interaction chart on Droplet Count Y-bar

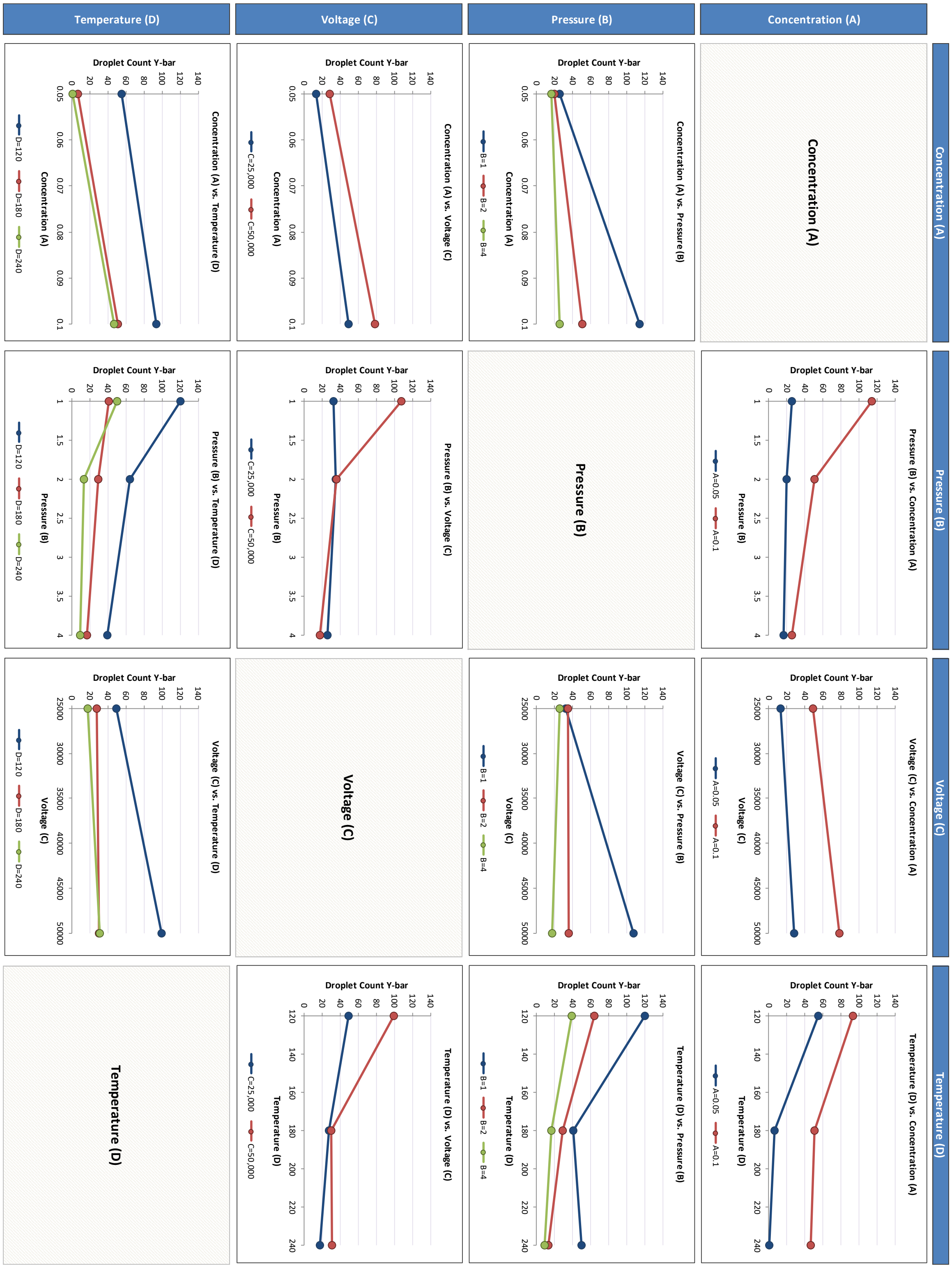

Appendix B – DOE Interaction Charts – Palm Oil

Table 35: Palm Oil & Polysorbate 80 @ 19Ga Interaction chart on Droplet Size Y-bar

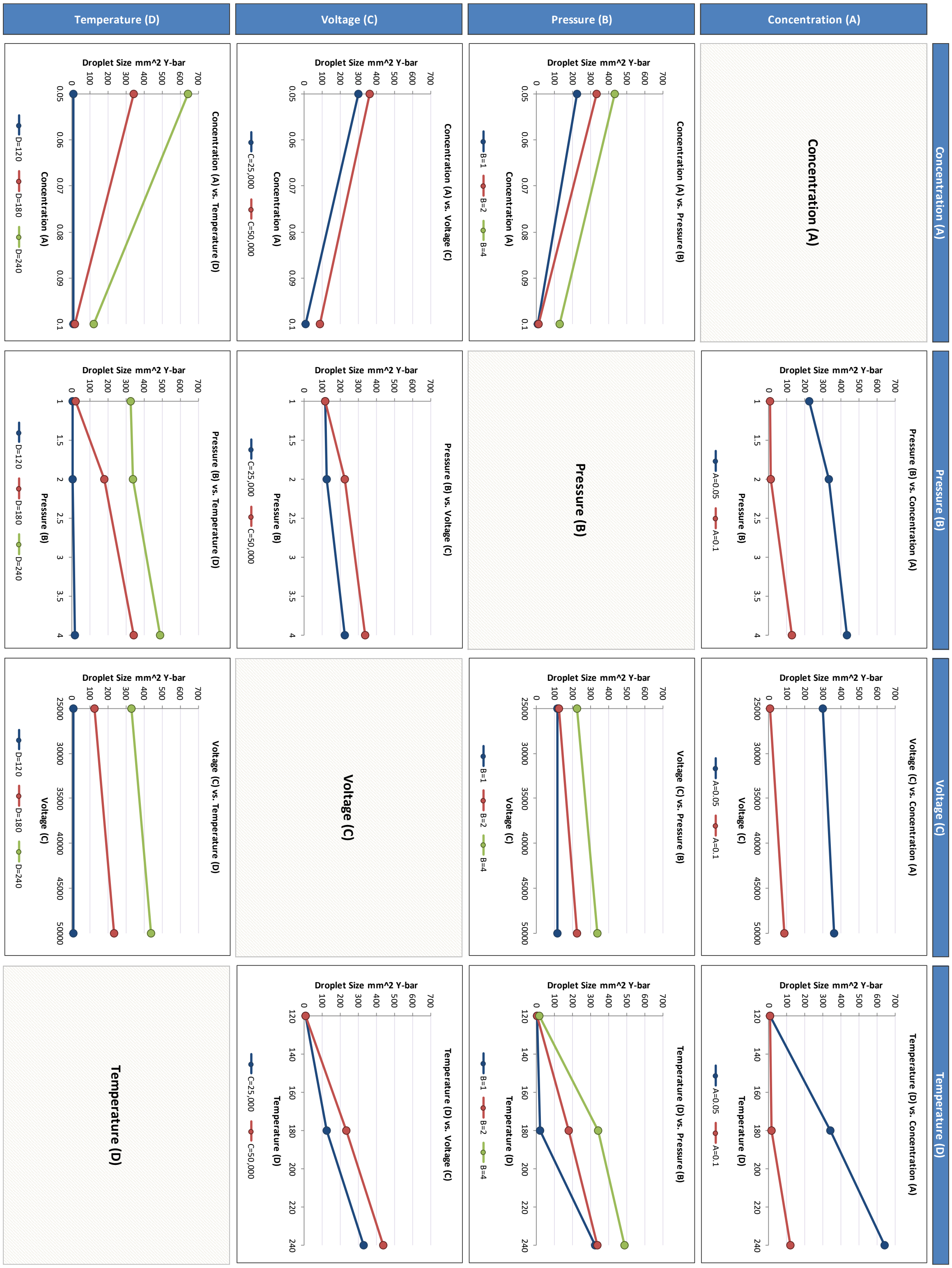

Appendix B – DOE Interaction Charts – Palm Oil

Table 36: Palm Oil & Polysorbate 80 @ 19Ga Interaction chart on Coverage Area Y-bar

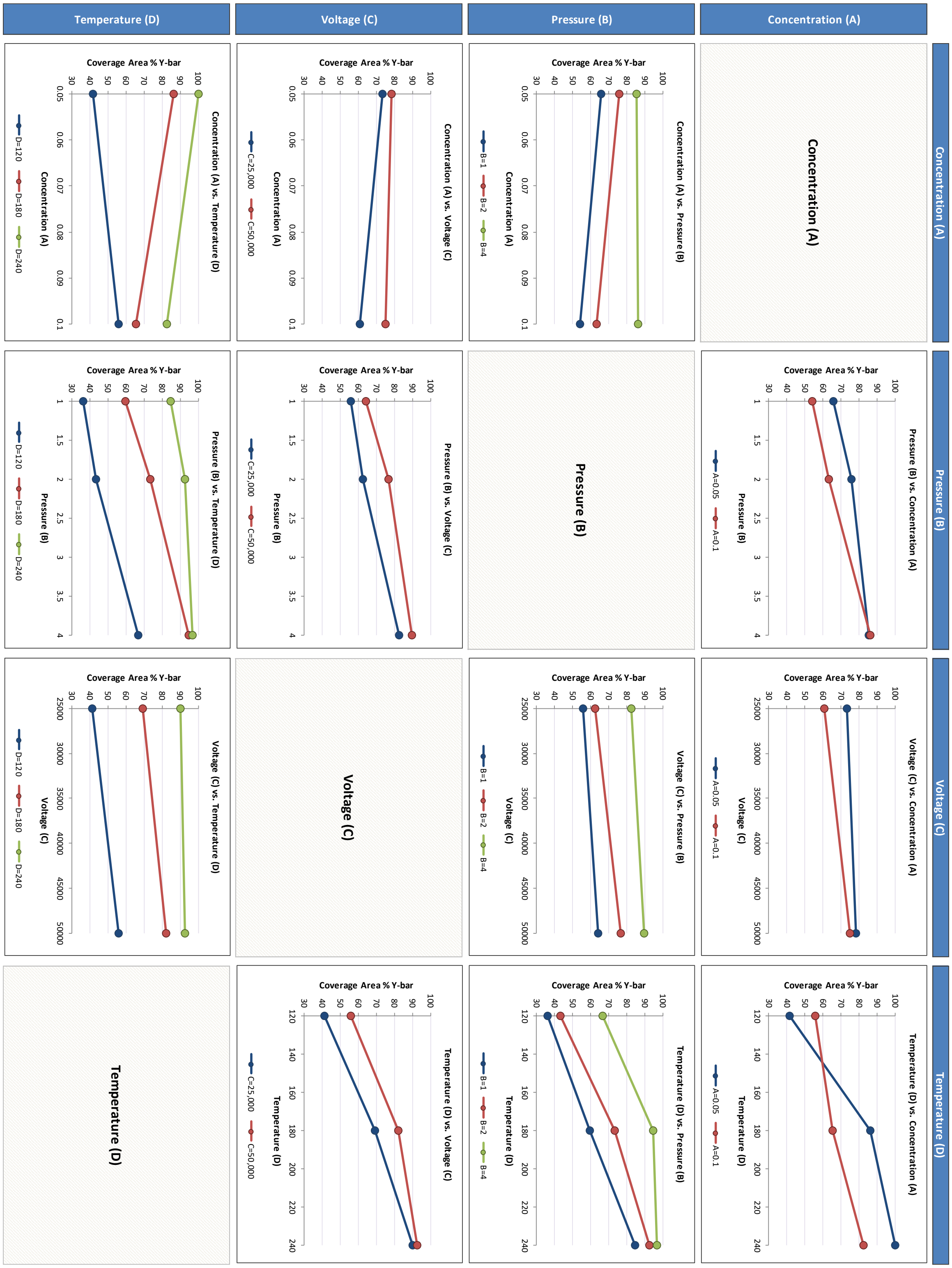

Appendix B – DOE Interaction Charts – Palm Oil

Table 37: Palm Oil & Polysorbate 80 @ 19Ga Interaction chart on Sample Weight Y-bar

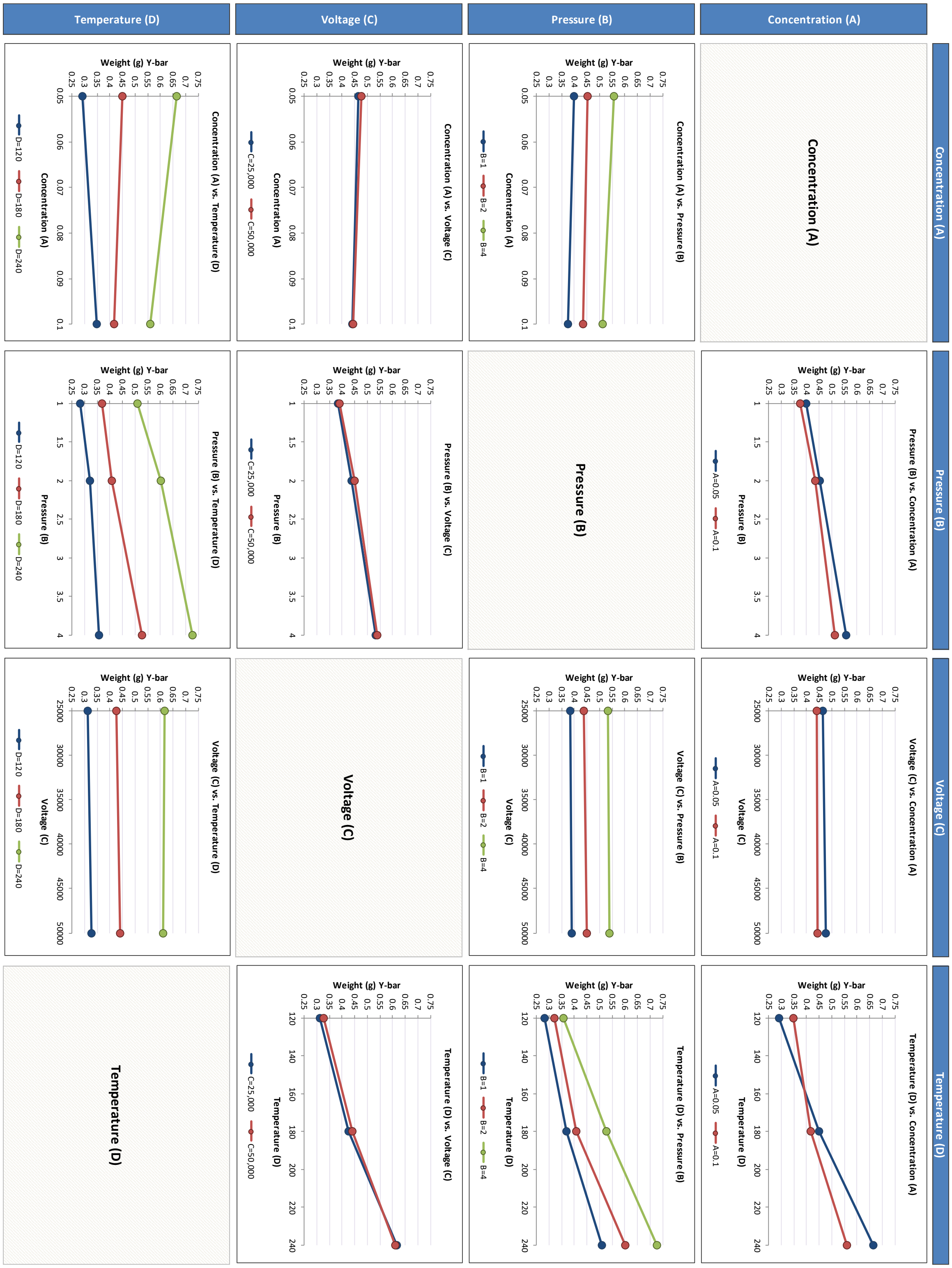

Appendix B – DOE Interaction Charts – Palm Oil

Table 38: Palm Oil & Propylene Glycol @ 19Ga Interaction chart on Droplet Count Y-bar

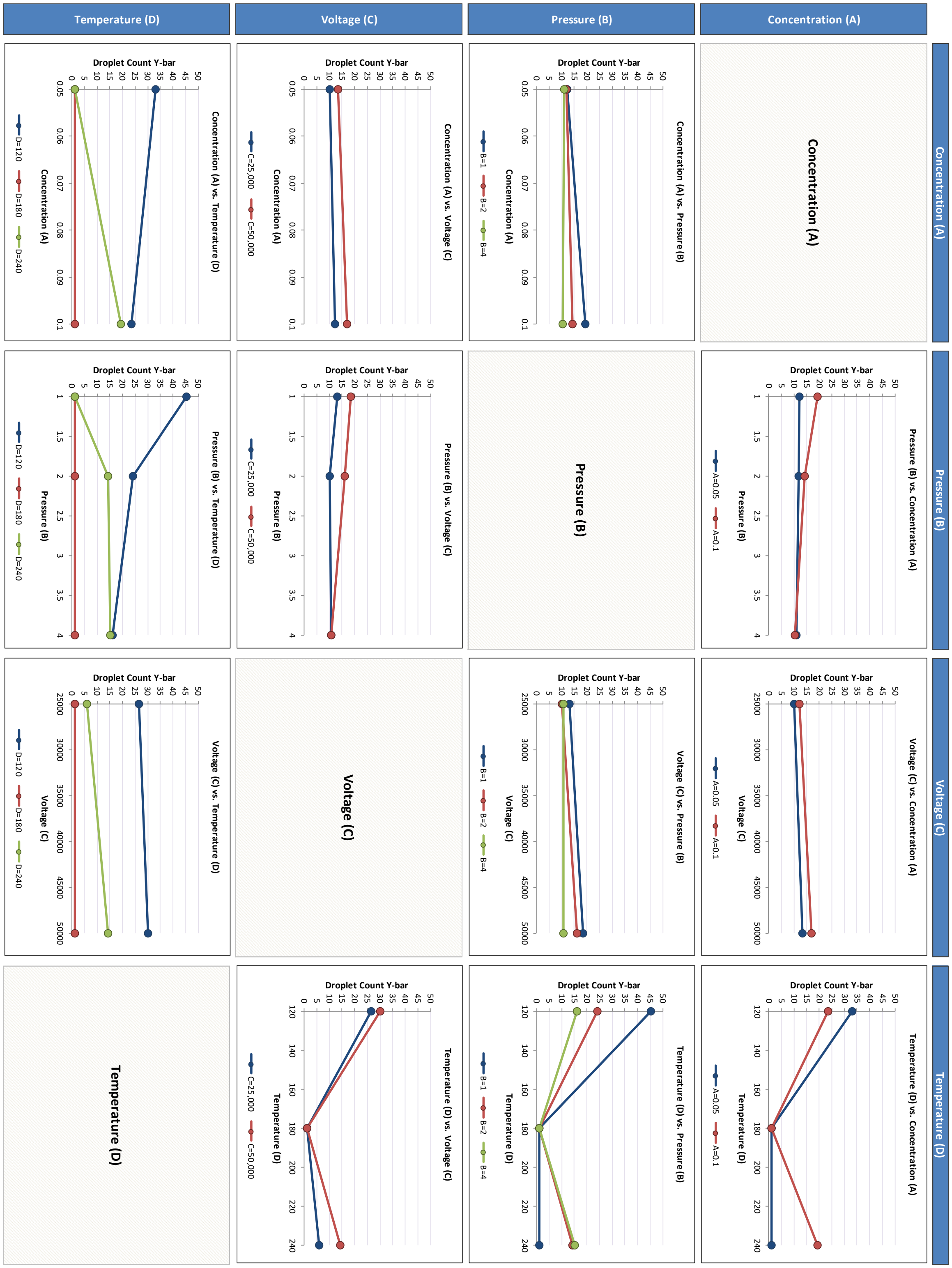

Appendix B – DOE Interaction Charts – Palm Oil

Table 39: Palm Oil & Propylene Glycol @ 19Ga Interaction chart on Droplet Size Y-bar

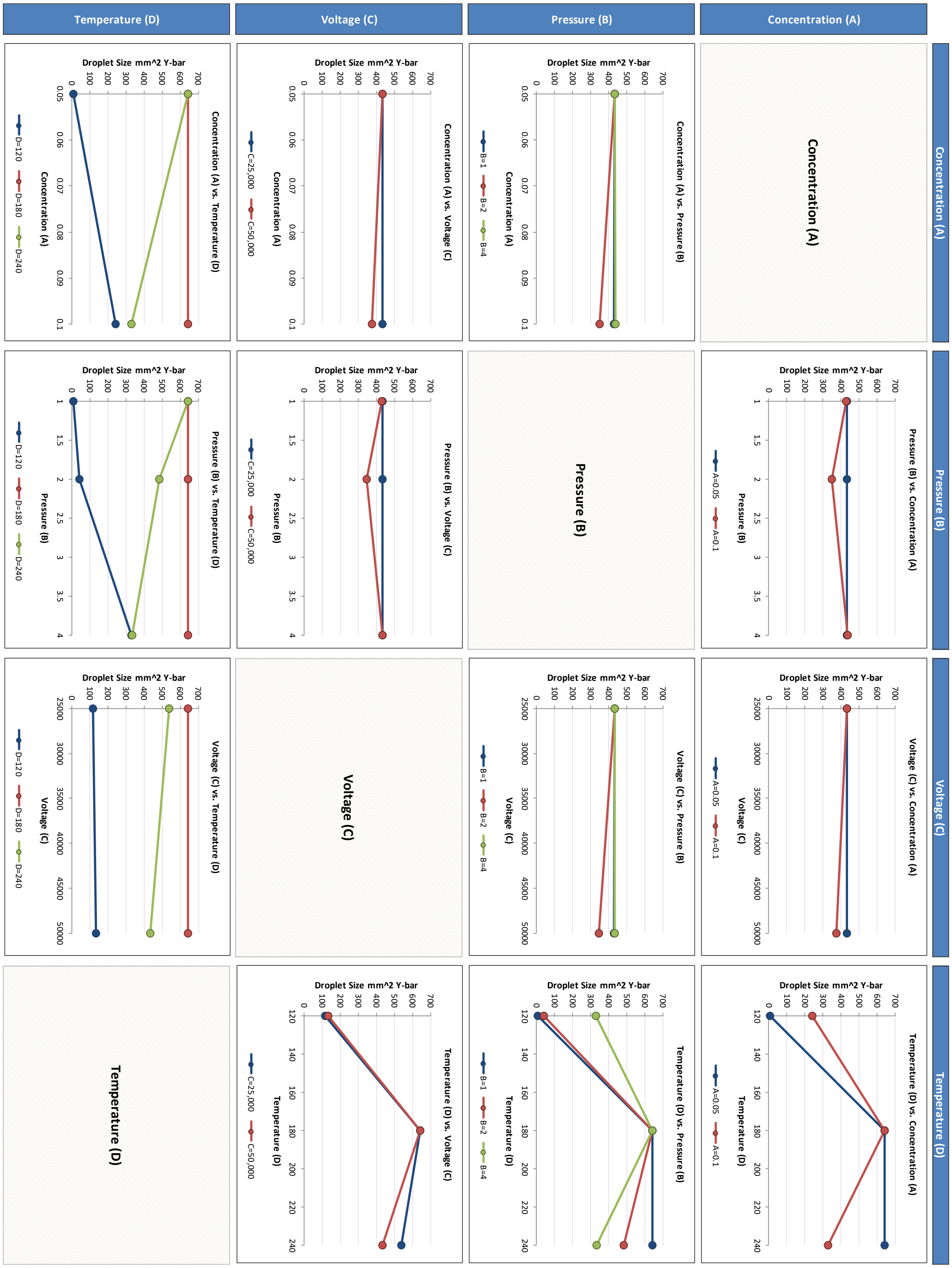

Appendix B – DOE Interaction Charts – Palm Oil

Table 40: Palm Oil & Propylene Glycol @ 19Ga Interaction chart on Coverage Area Y-bar

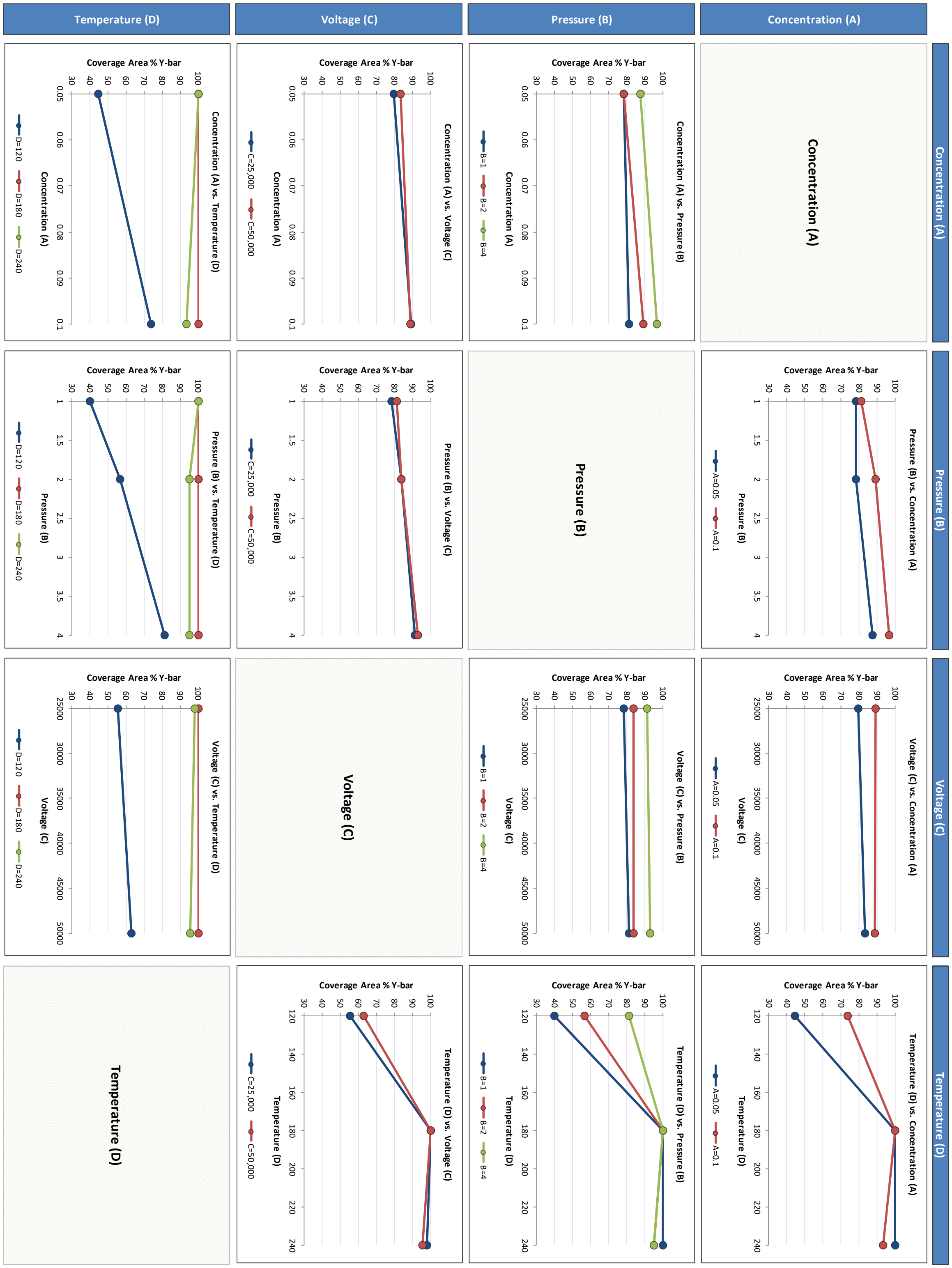

Appendix B – DOE Interaction Charts – Palm Oil

Table 41: Palm Oil & Propylene Glycol @ 19Ga Interaction chart on Sample Weight Y-bar

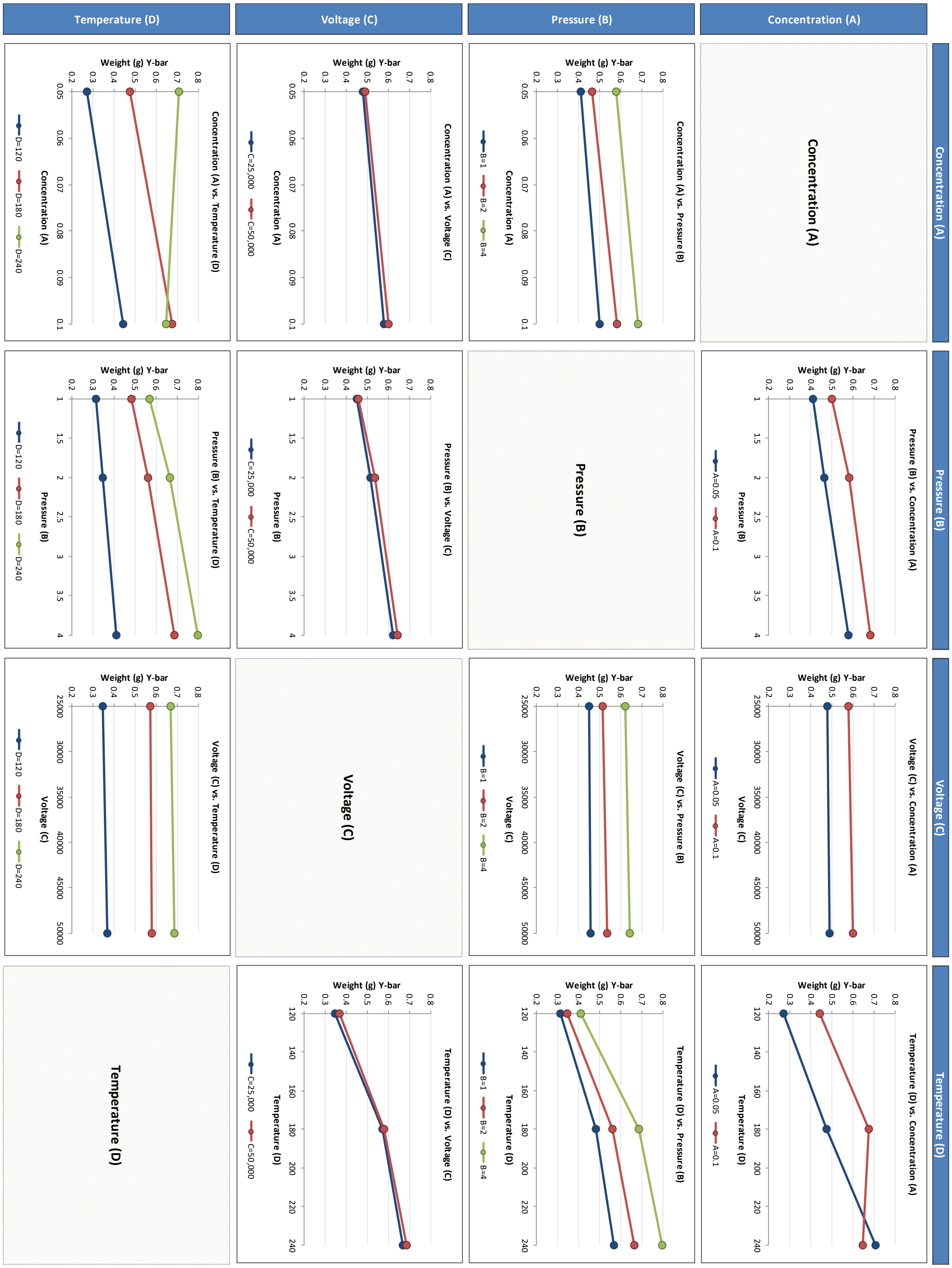

Appendix B – DOE Interaction Charts – Palm Oil

Table 42: Palm Oil & Soy Lecithin @ 22Ga Interaction chart on Droplet Count Y-bar

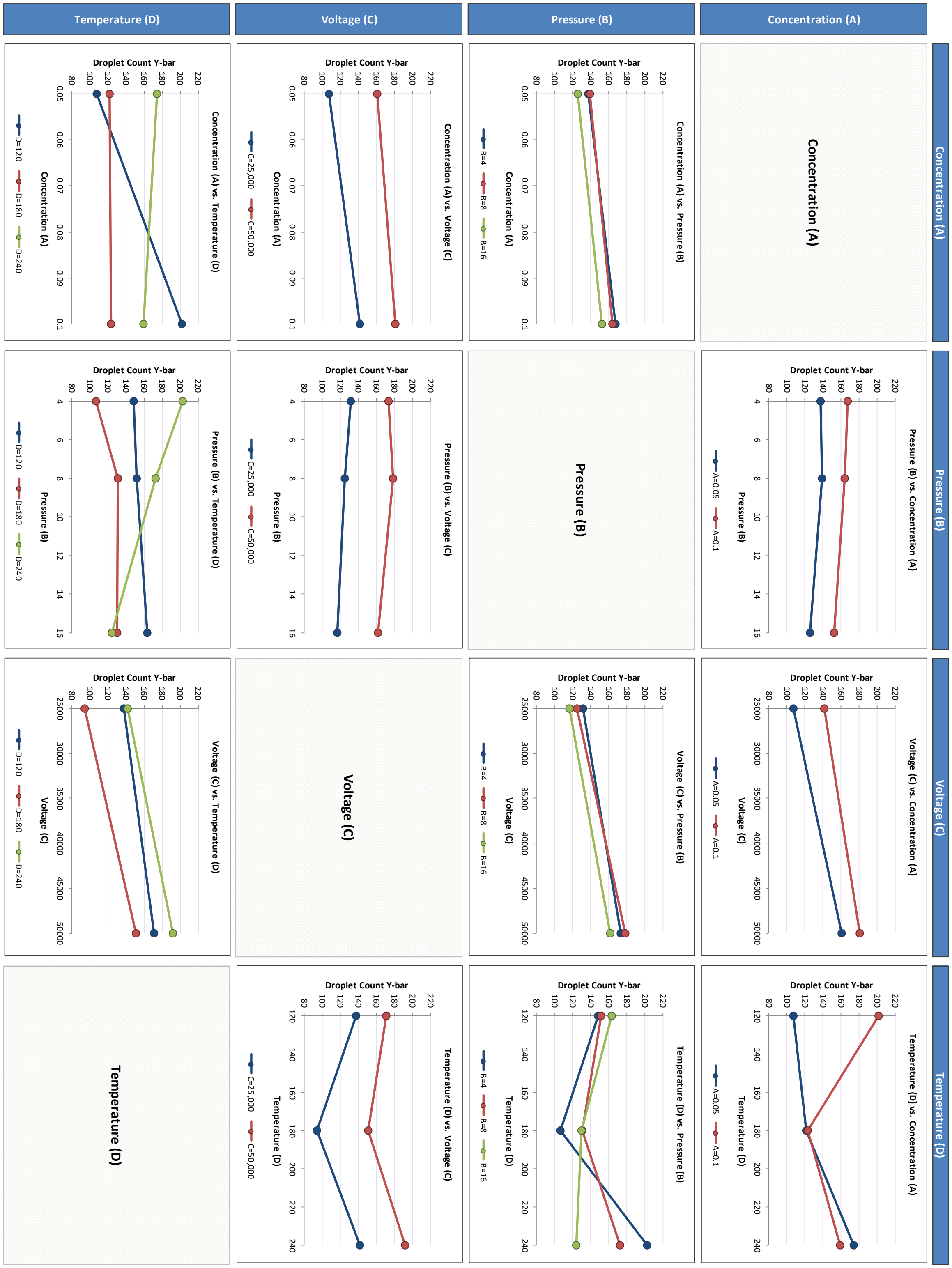

Appendix B – DOE Interaction Charts – Palm Oil

Table 43: Palm Oil & Soy Lecithin @ 22Ga Interaction chart on Droplet Size Y-bar

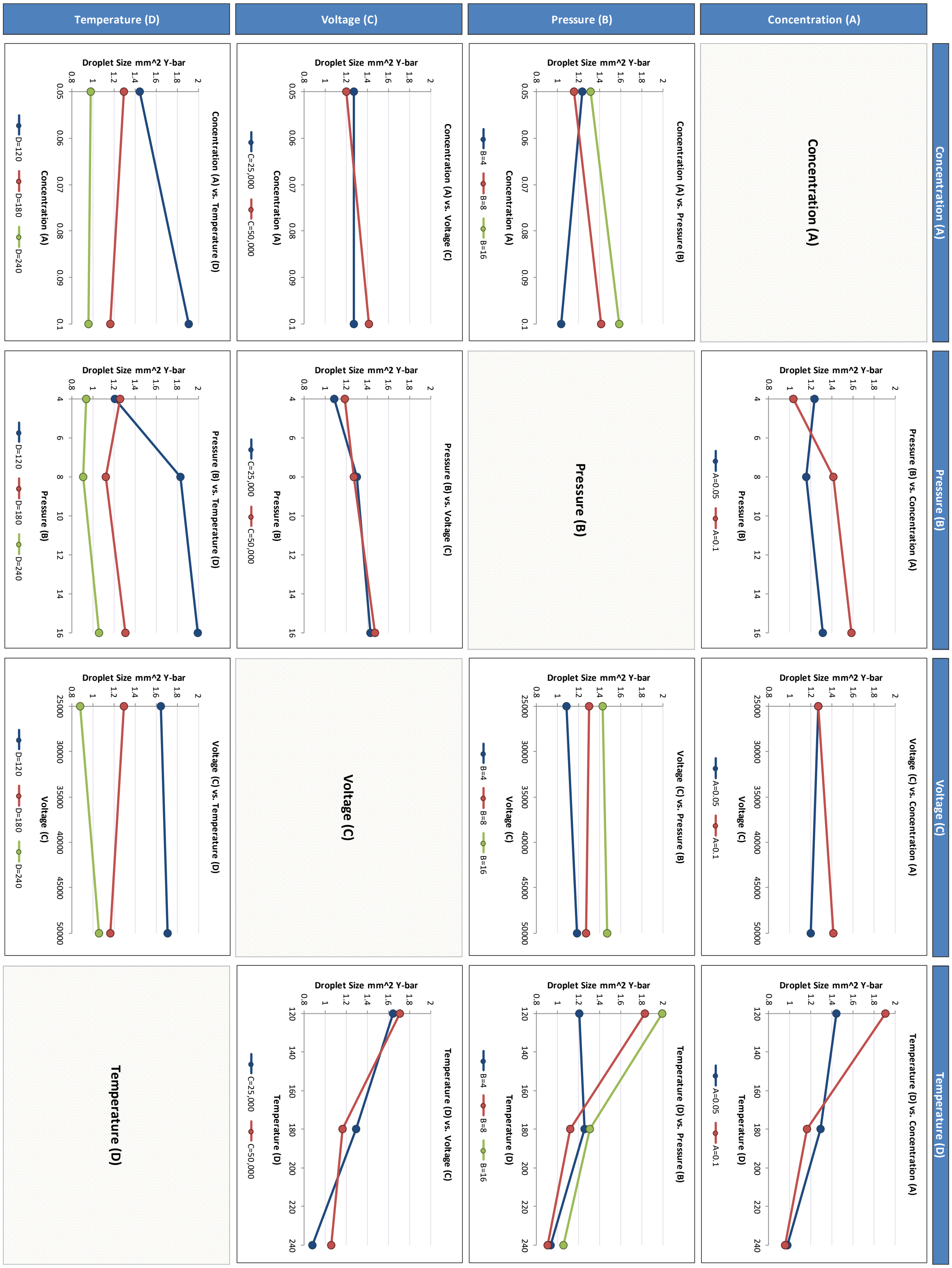

Appendix B – DOE Interaction Charts – Palm Oil

Table 44: Palm Oil & Soy Lecithin @ 22Ga Interaction chart on Coverage Area Y-bar

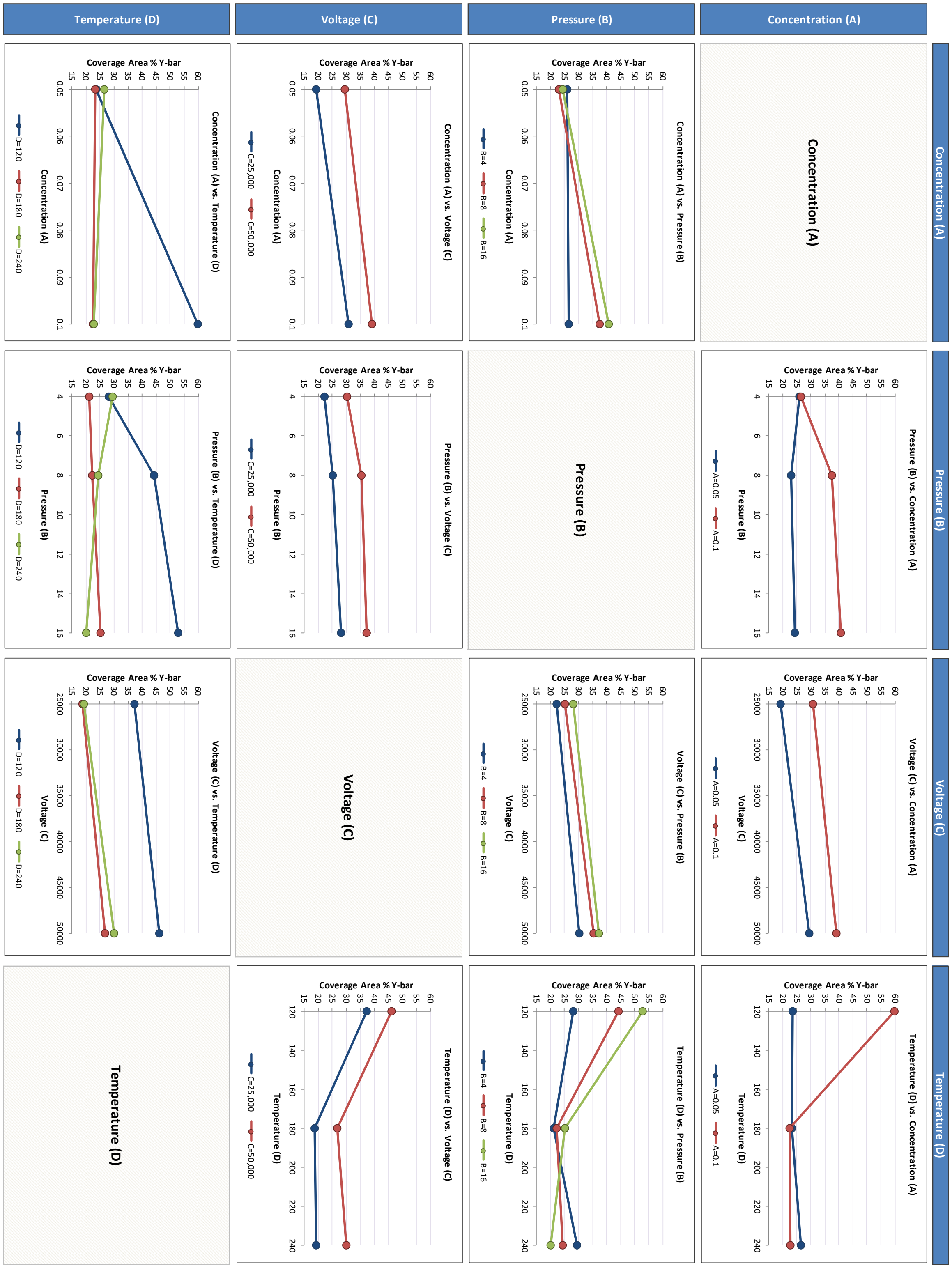

Appendix B – DOE Interaction Charts – Palm Oil

Table 45: Palm Oil & Soy Lecithin @ 22Ga Interaction chart on Sample Weight Y-bar

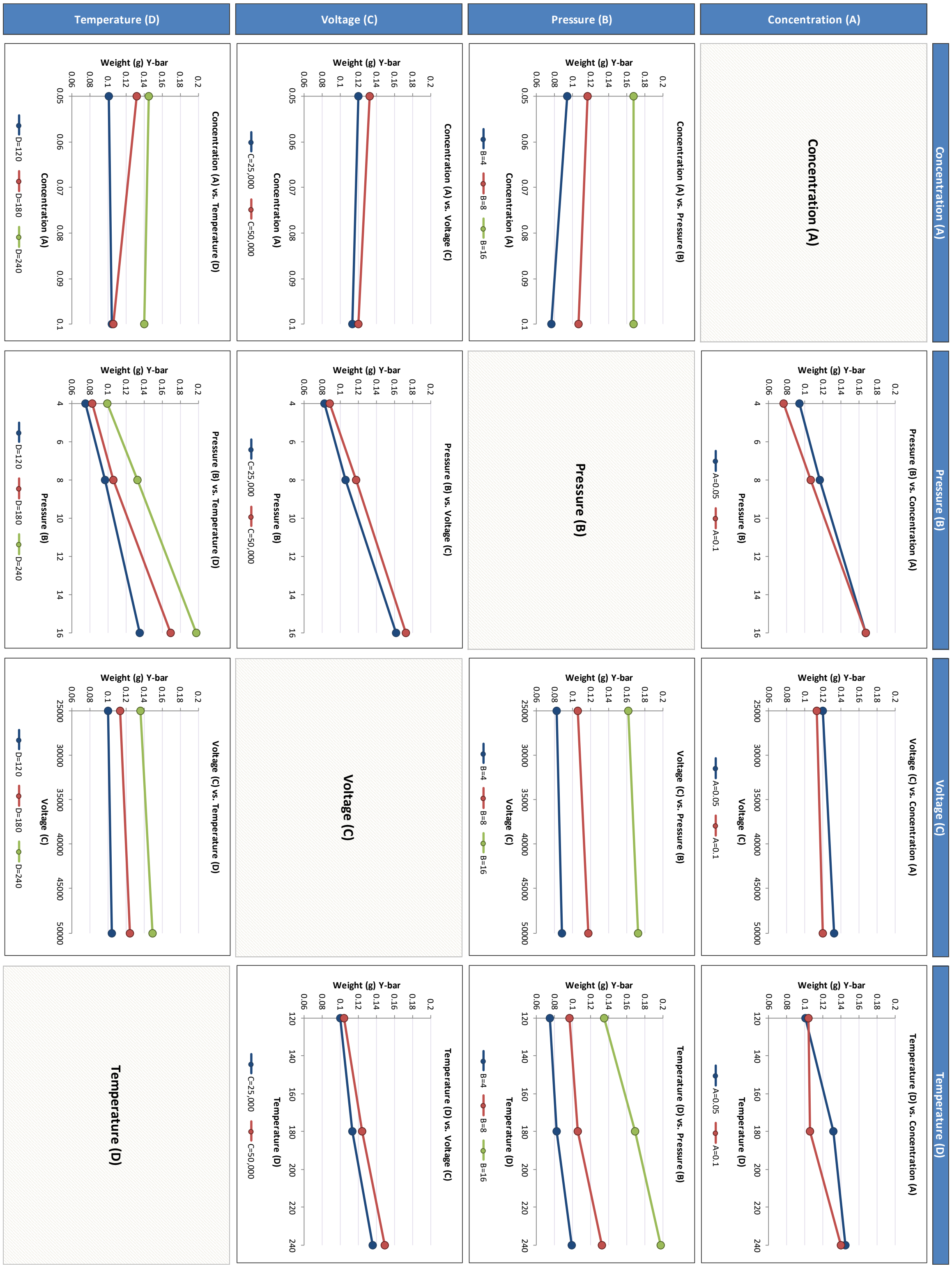

Appendix B – DOE Interaction Charts – Palm Oil

Table 46: Palm Oil & Polysorbate 80 @ 22Ga Interaction chart on Droplet Count Y-bar

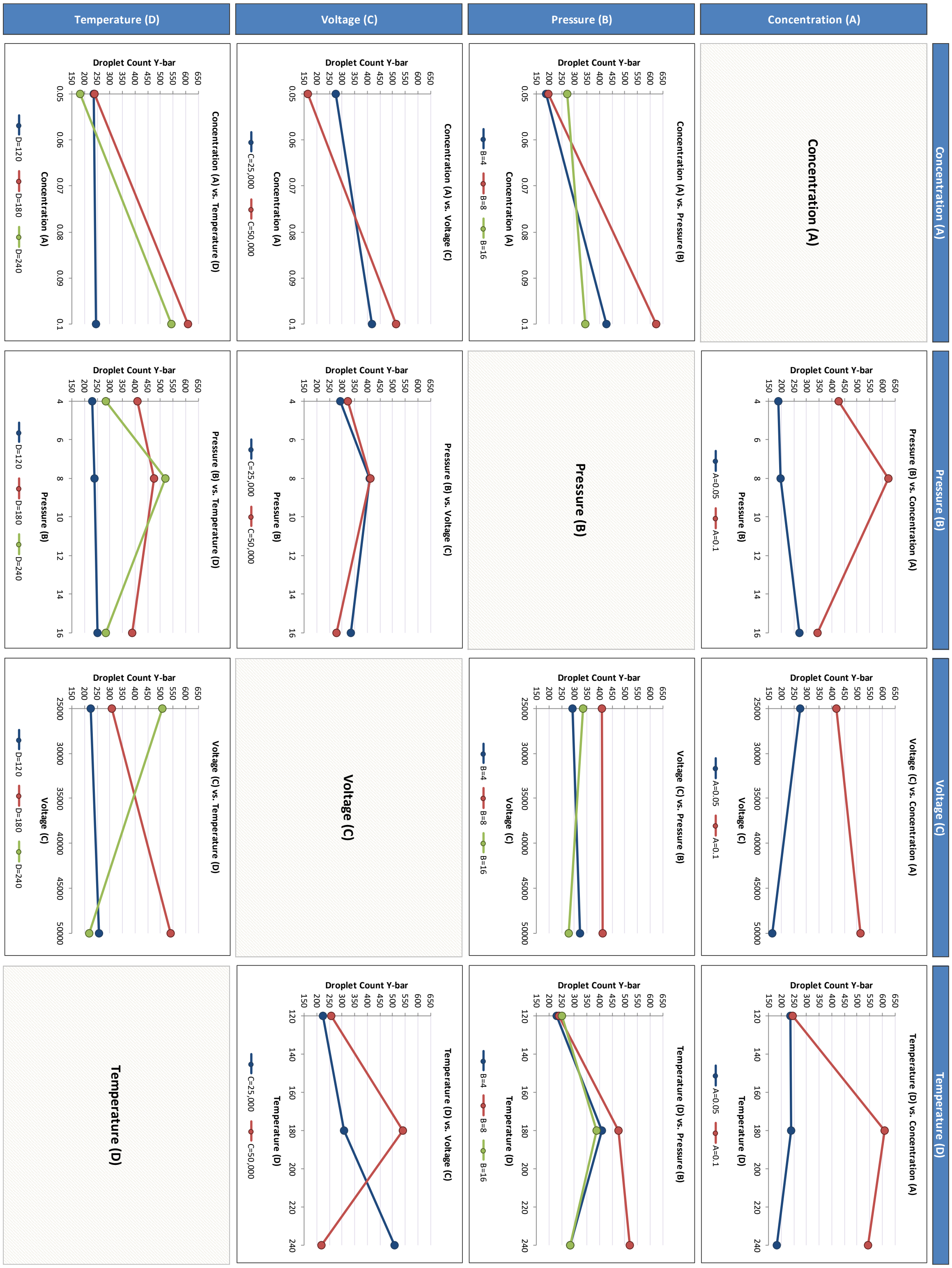

Appendix B – DOE Interaction Charts – Palm Oil

Table 47: Palm Oil & Polysorbate 80 @ 22Ga Interaction chart on Droplet Size Y-bar

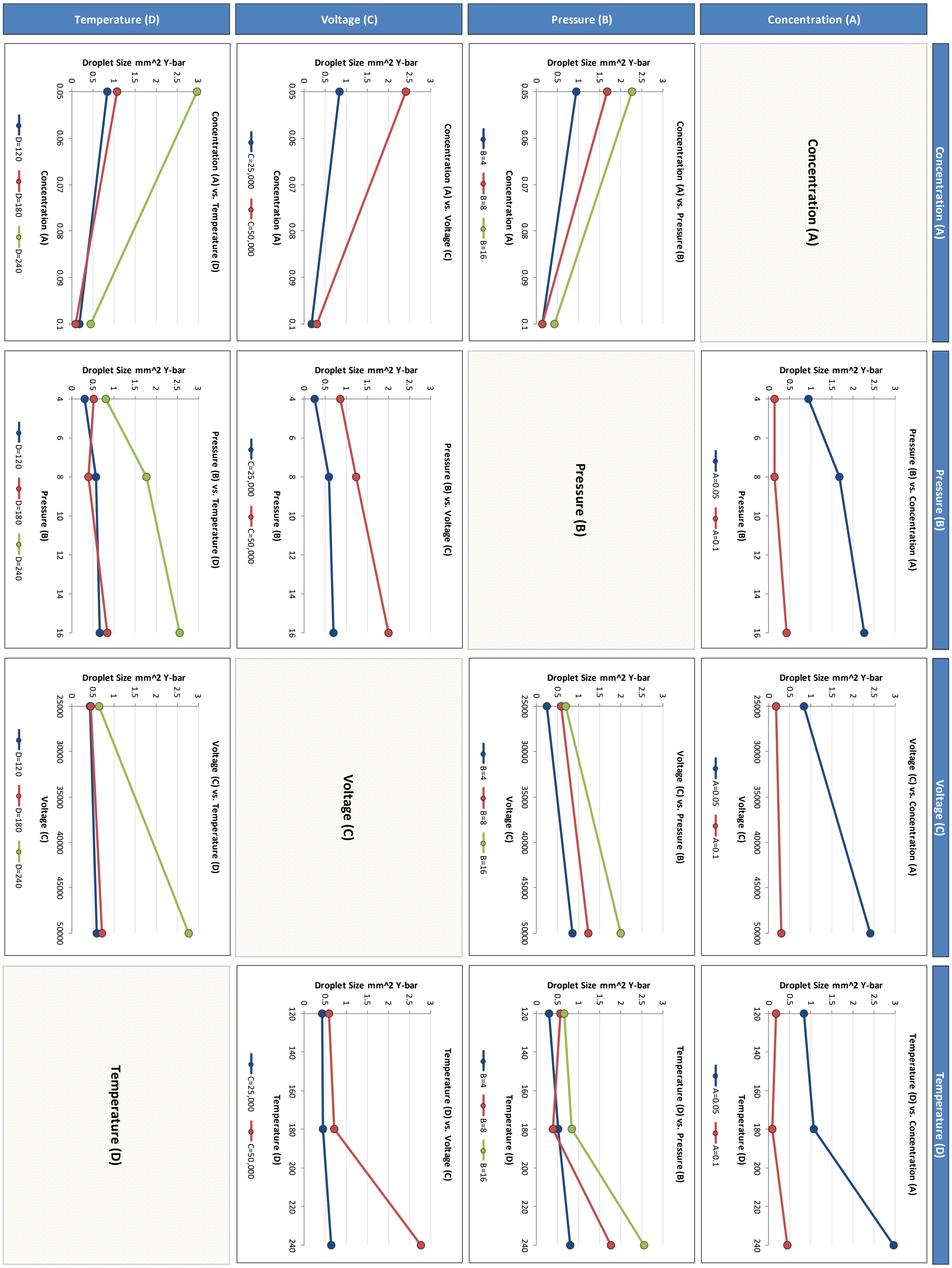

Appendix B – DOE Interaction Charts – Palm Oil

Table 48: Palm Oil & Polysorbate 80 @ 22Ga Interaction chart on Coverage Area Y-bar

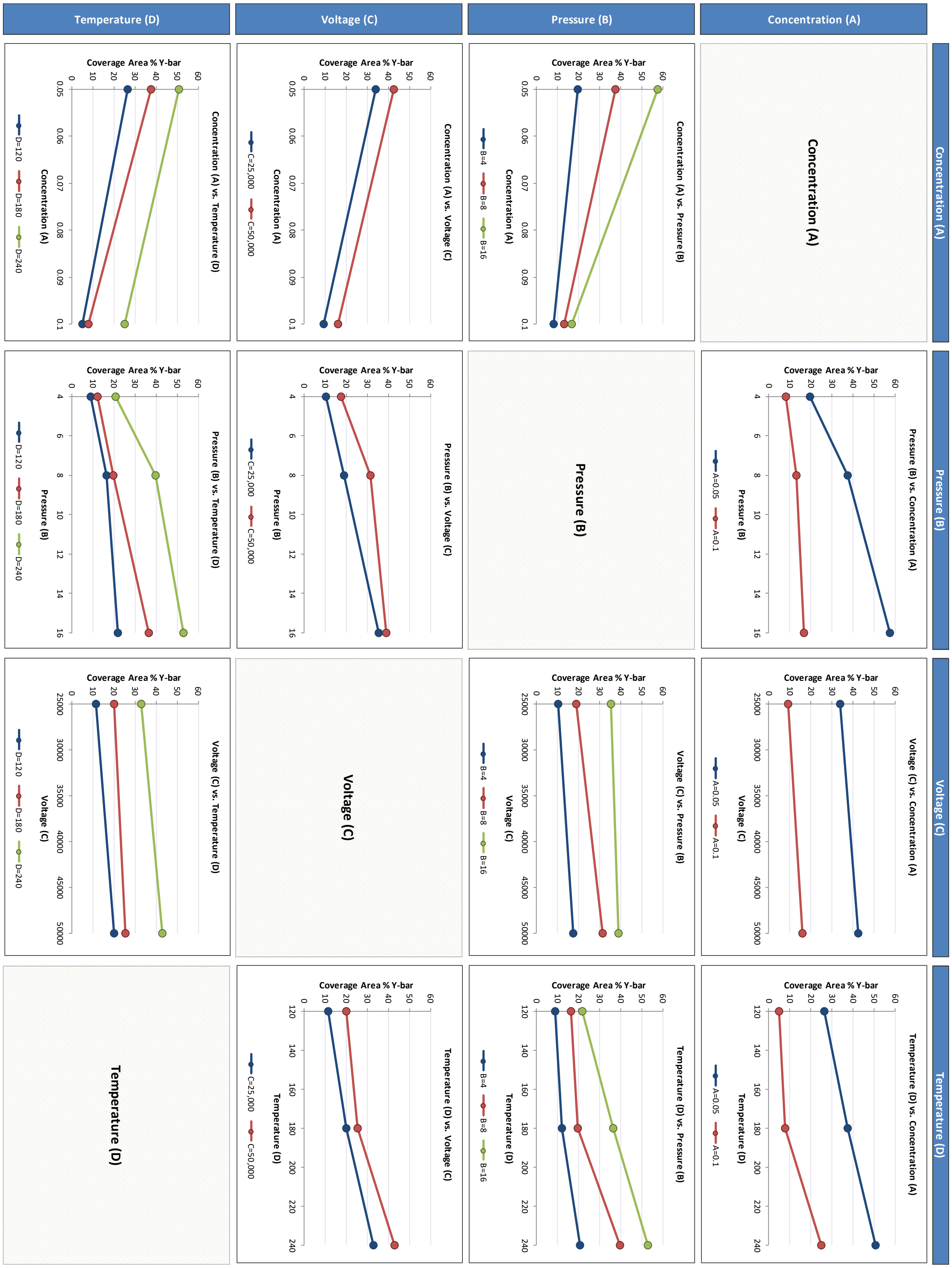

Appendix B – DOE Interaction Charts – Palm Oil

Table 49: Palm Oil & Polysorbate 80 @ 22Ga Interaction chart on Sample Weight Y-bar

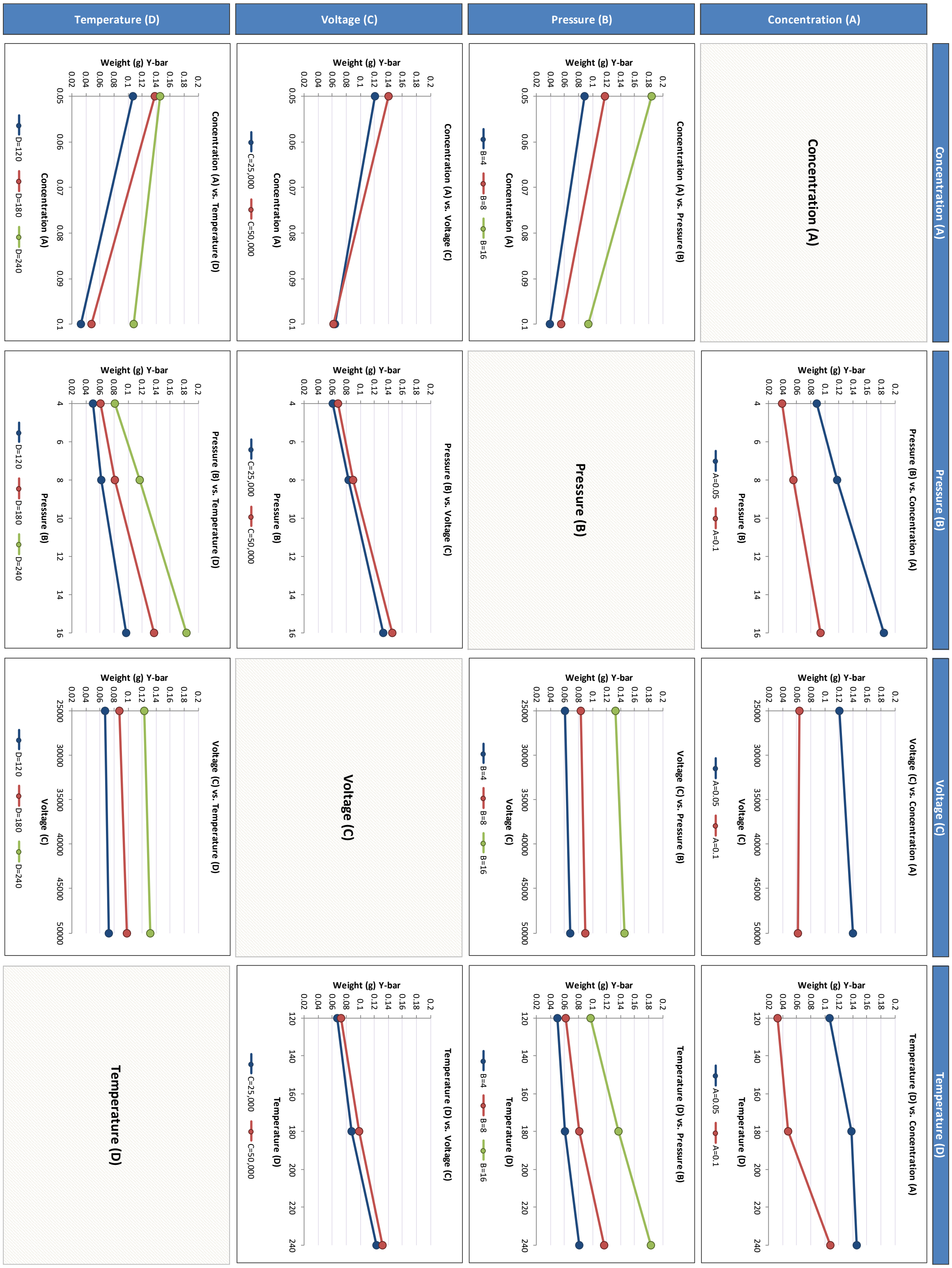

Appendix B – DOE Interaction Charts – Palm Oil

Table 50: Palm Oil & Propylene Glycol @ 22Ga Interaction chart (Concentration & Voltage) on Droplet Count Y-bar

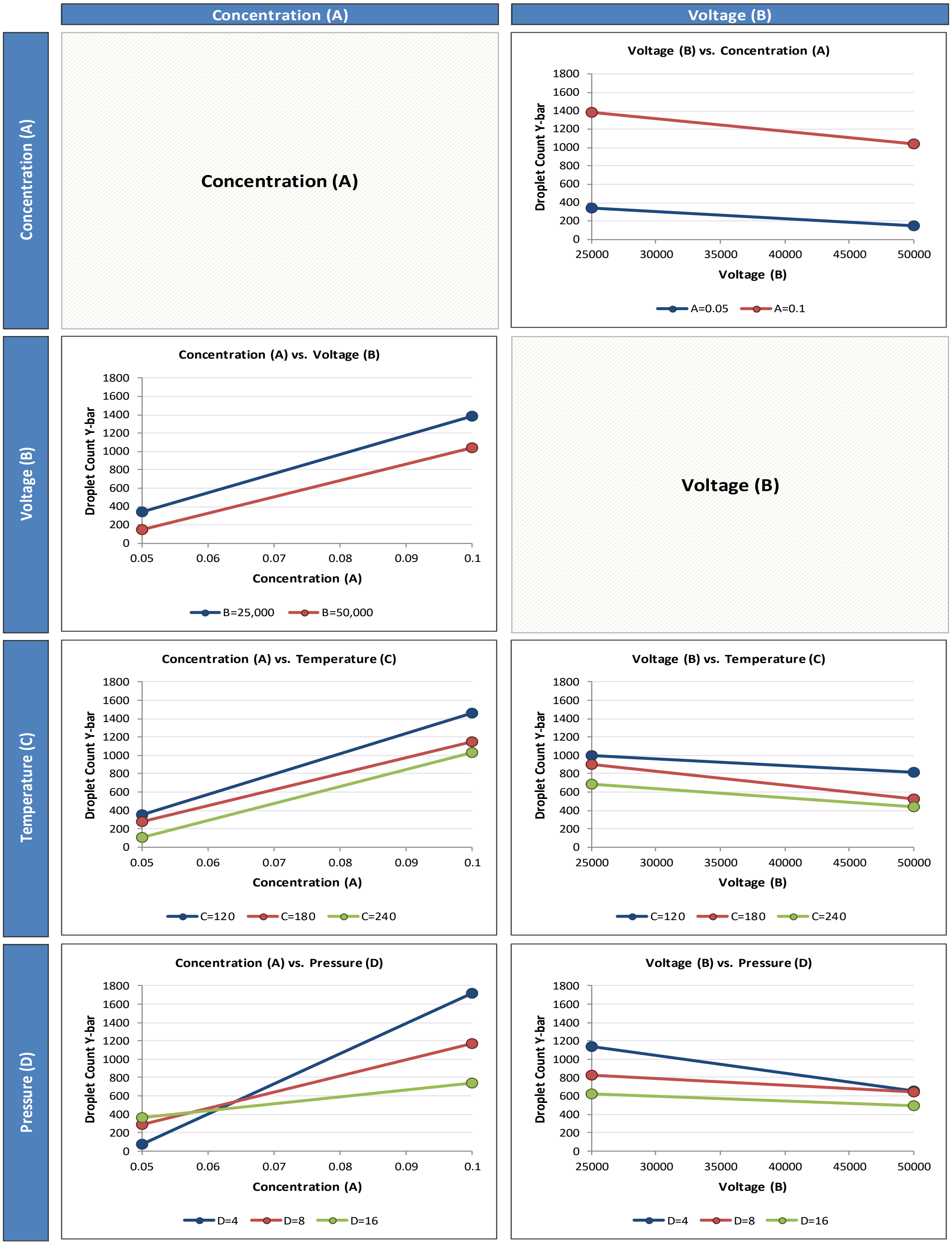

Appendix B – DOE Interaction Charts – Palm Oil

Table 51: Palm Oil & Propylene Glycol @ 22Ga Interaction chart (Temperature & Pressure) on Droplet Count Y-bar

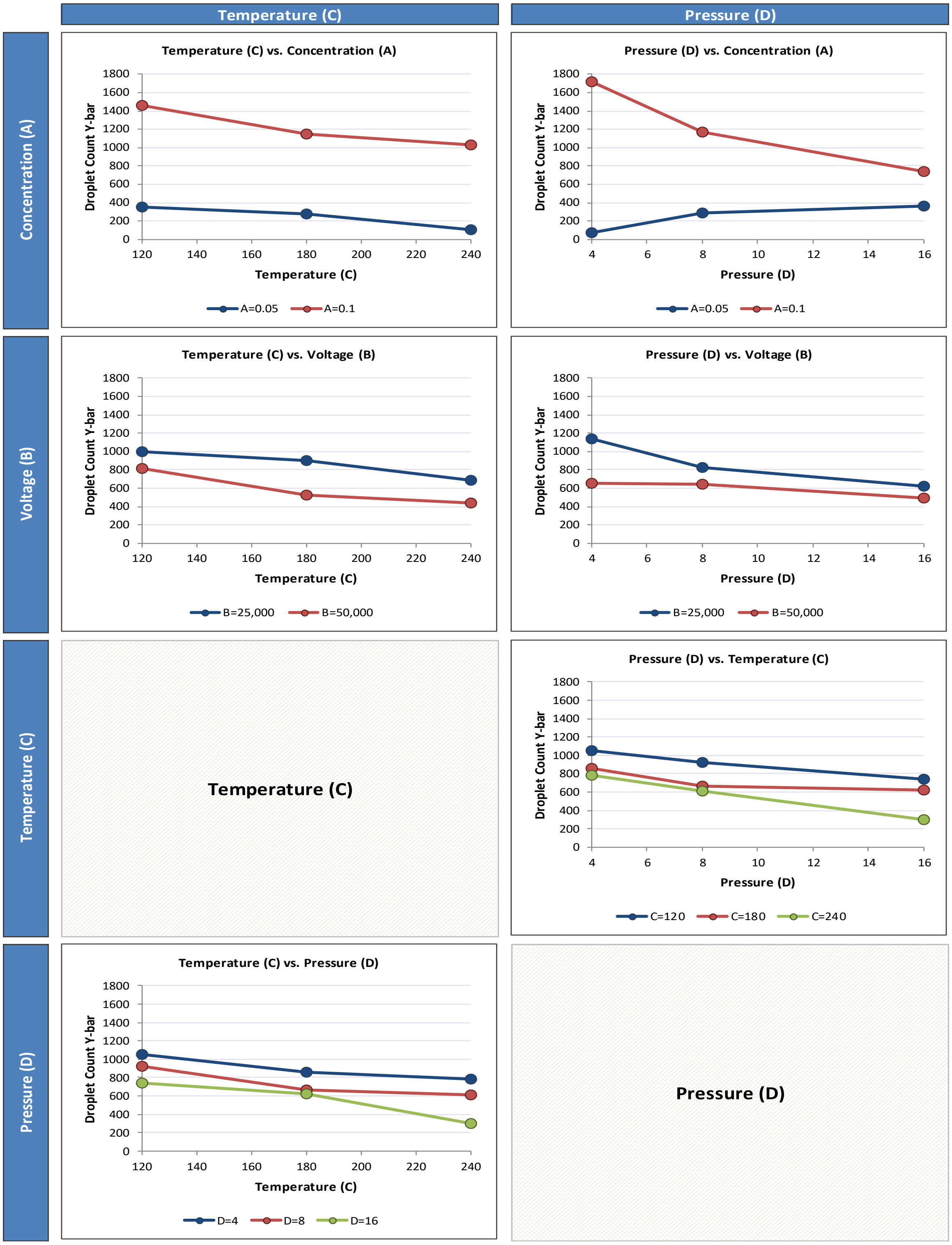

Appendix B – DOE Interaction Charts – Palm Oil

Table 52: Palm Oil & Propylene Glycol @ 22Ga Interaction chart (Concentration & Voltage) on Droplet Size Y-bar

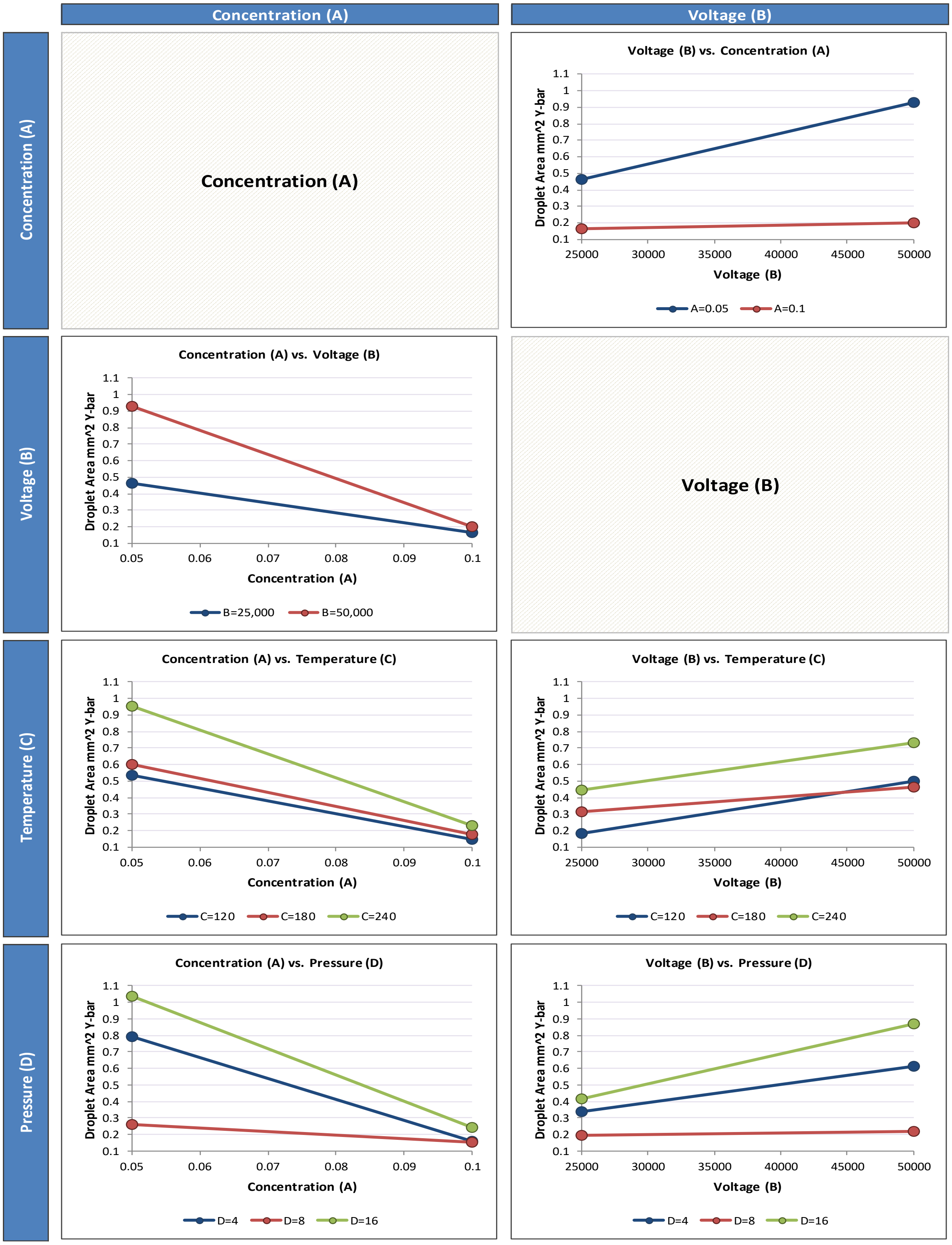

Appendix B – DOE Interaction Charts – Palm Oil

Table 53: Palm Oil & Propylene Glycol @ 22Ga Interaction chart (Temperature & Pressure) on Droplet Size Y-bar

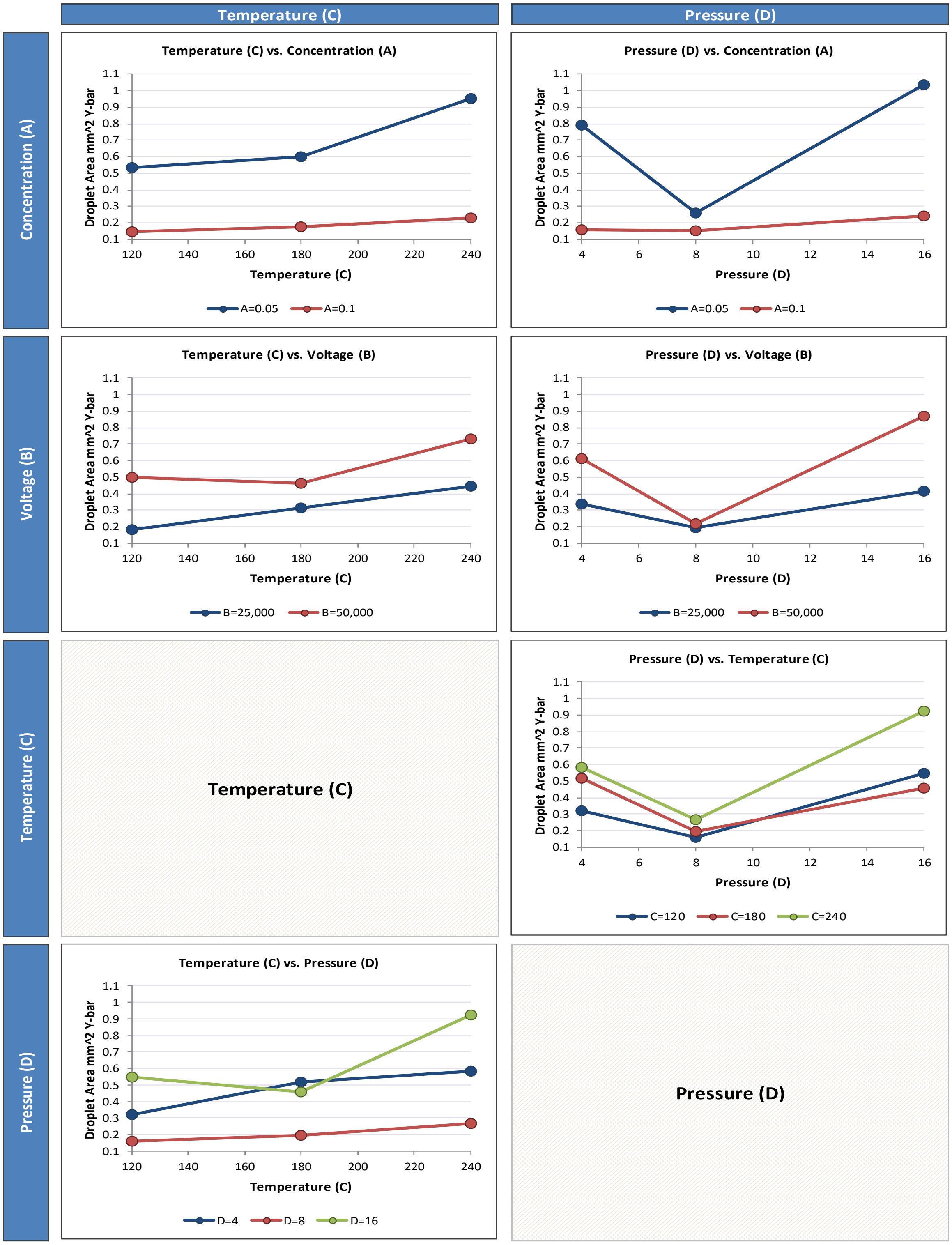

Appendix B – DOE Interaction Charts – Palm Oil

Table 54: Palm Oil & Propylene Glycol @ 22Ga Interaction chart (Concentration & Voltage) on Coverage Area Y-bar

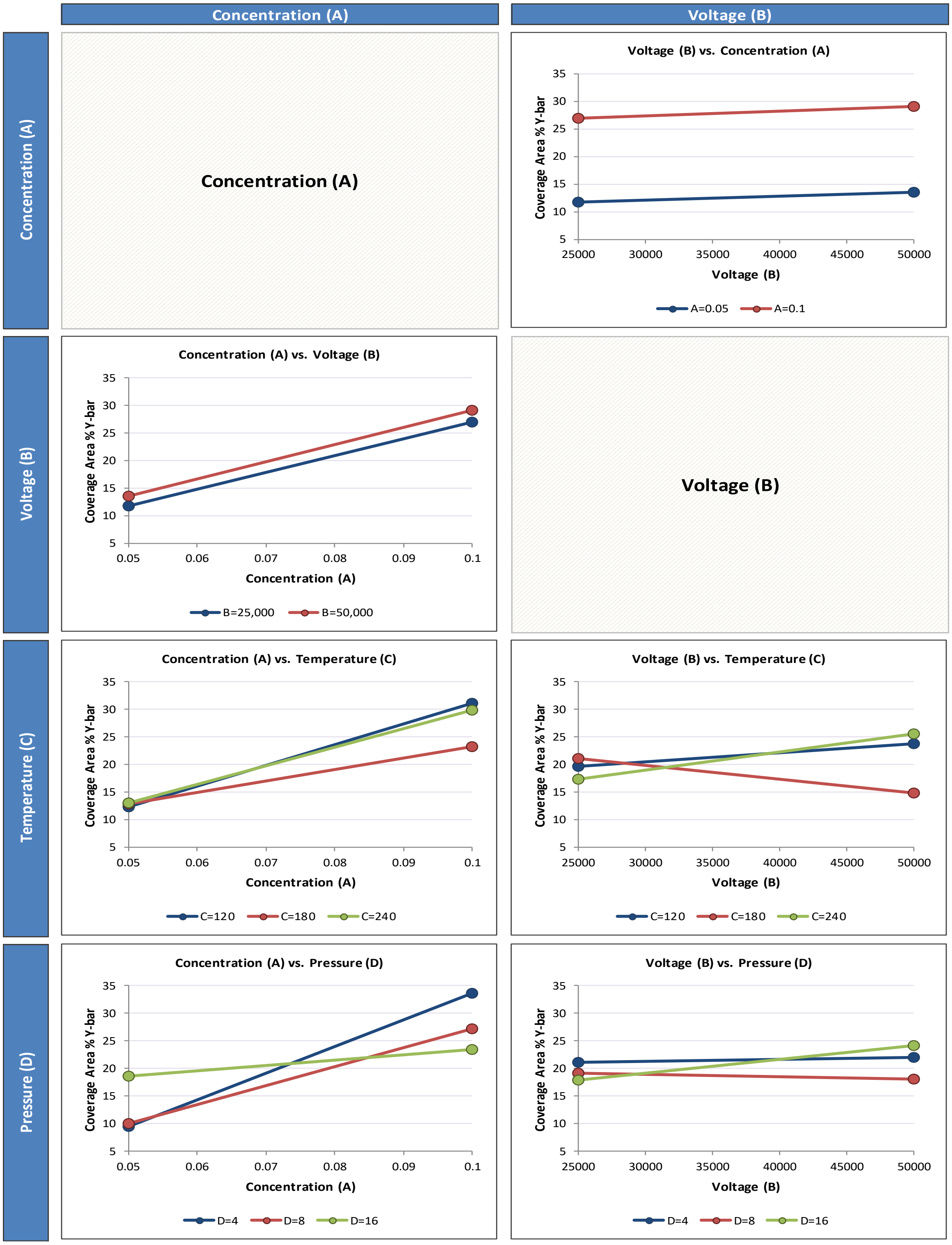

Appendix B – DOE Interaction Charts – Palm Oil

Table 55: Palm Oil & Propylene Glycol @ 22Ga Interaction chart (Temperature & Pressure) on Coverage Area Y-bar

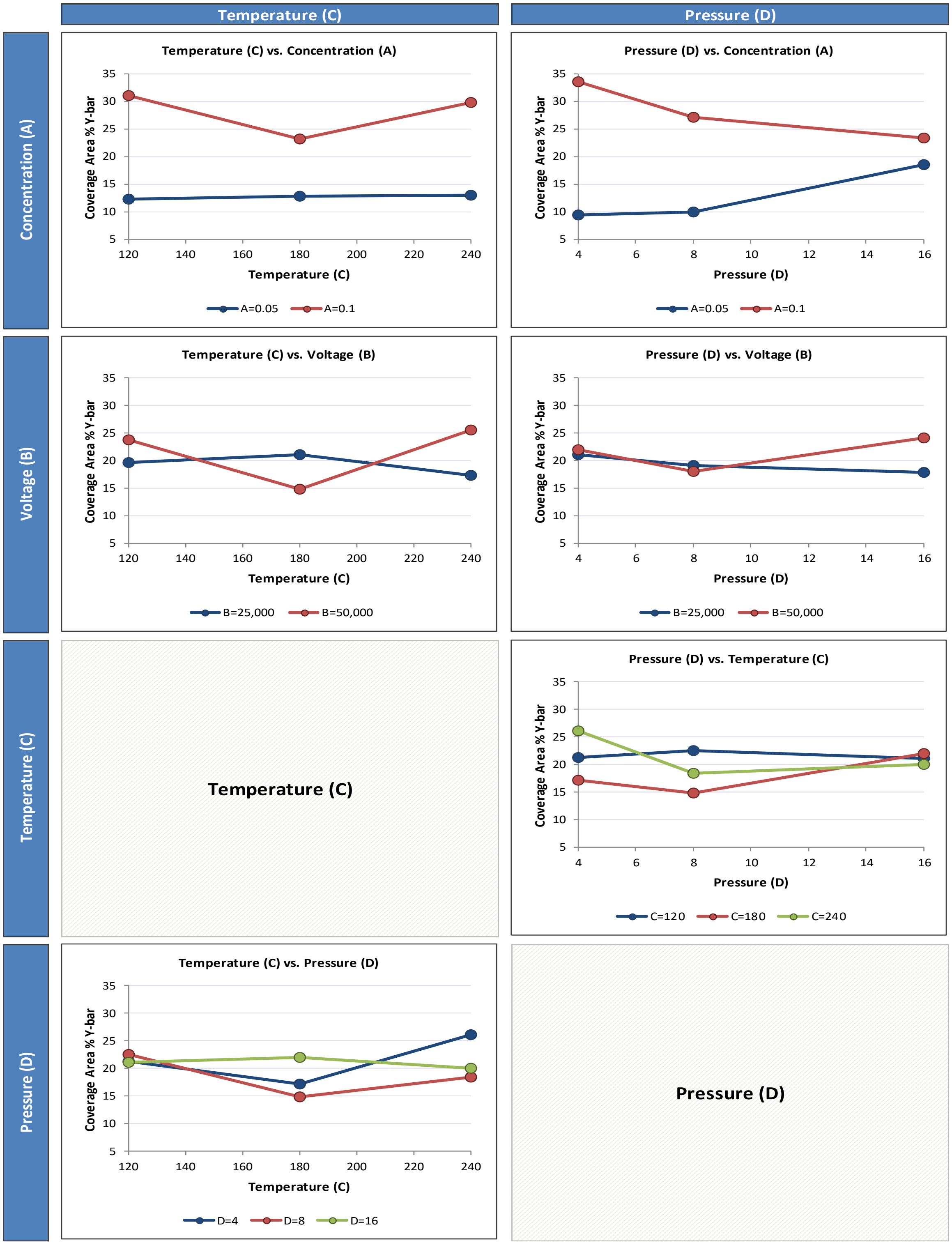

Appendix B – DOE Interaction Charts – Palm Oil

Table 56: Palm Oil & Propylene Glycol @ 22Ga Interaction chart (Concentration & Voltage) on Sample Weight Y-bar

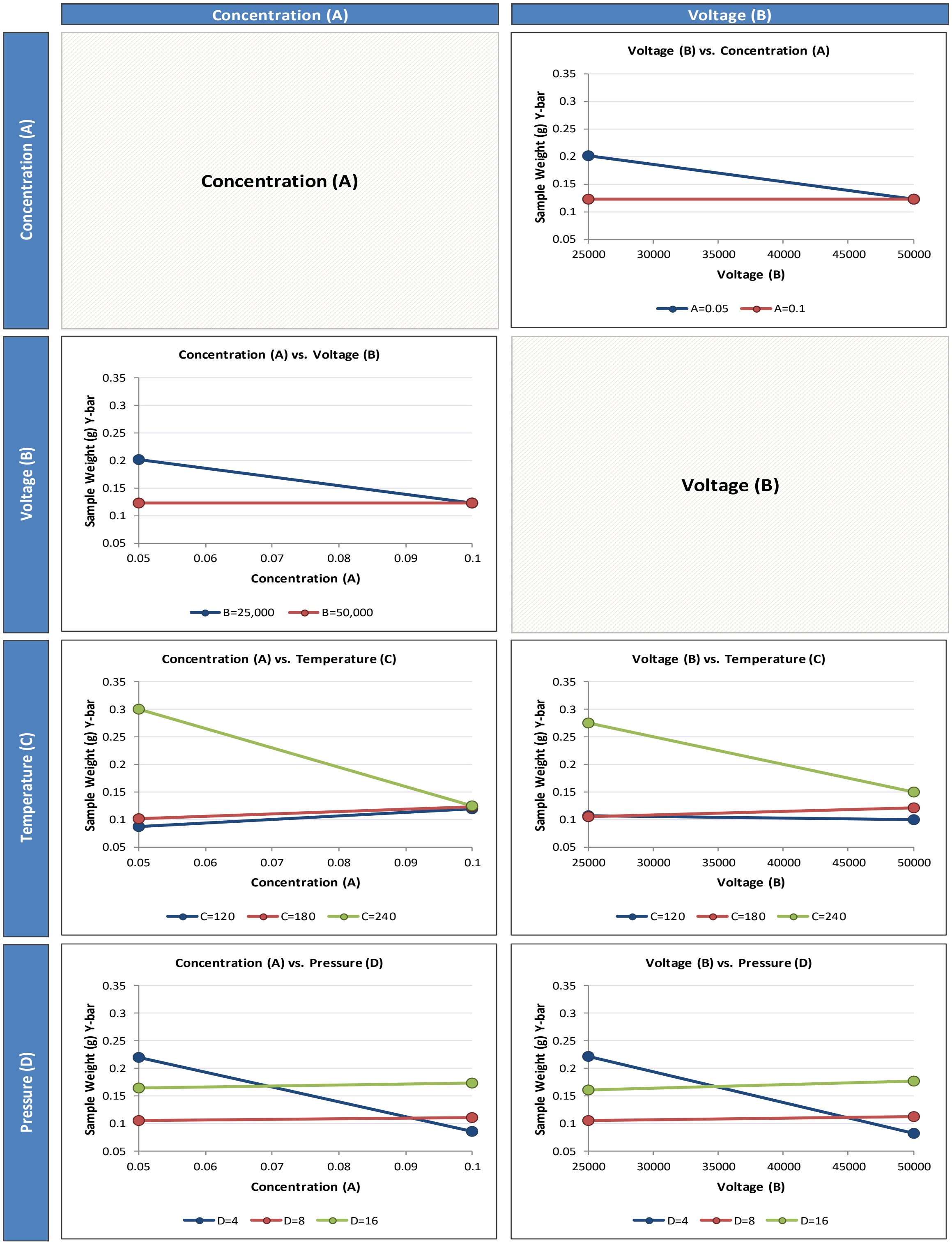

Appendix B – DOE Interaction Charts – Palm Oil

Table 57: Palm Oil & Propylene Glycol @ 22Ga Interaction chart (Temperature & Pressure) on Sample Weight Y-bar

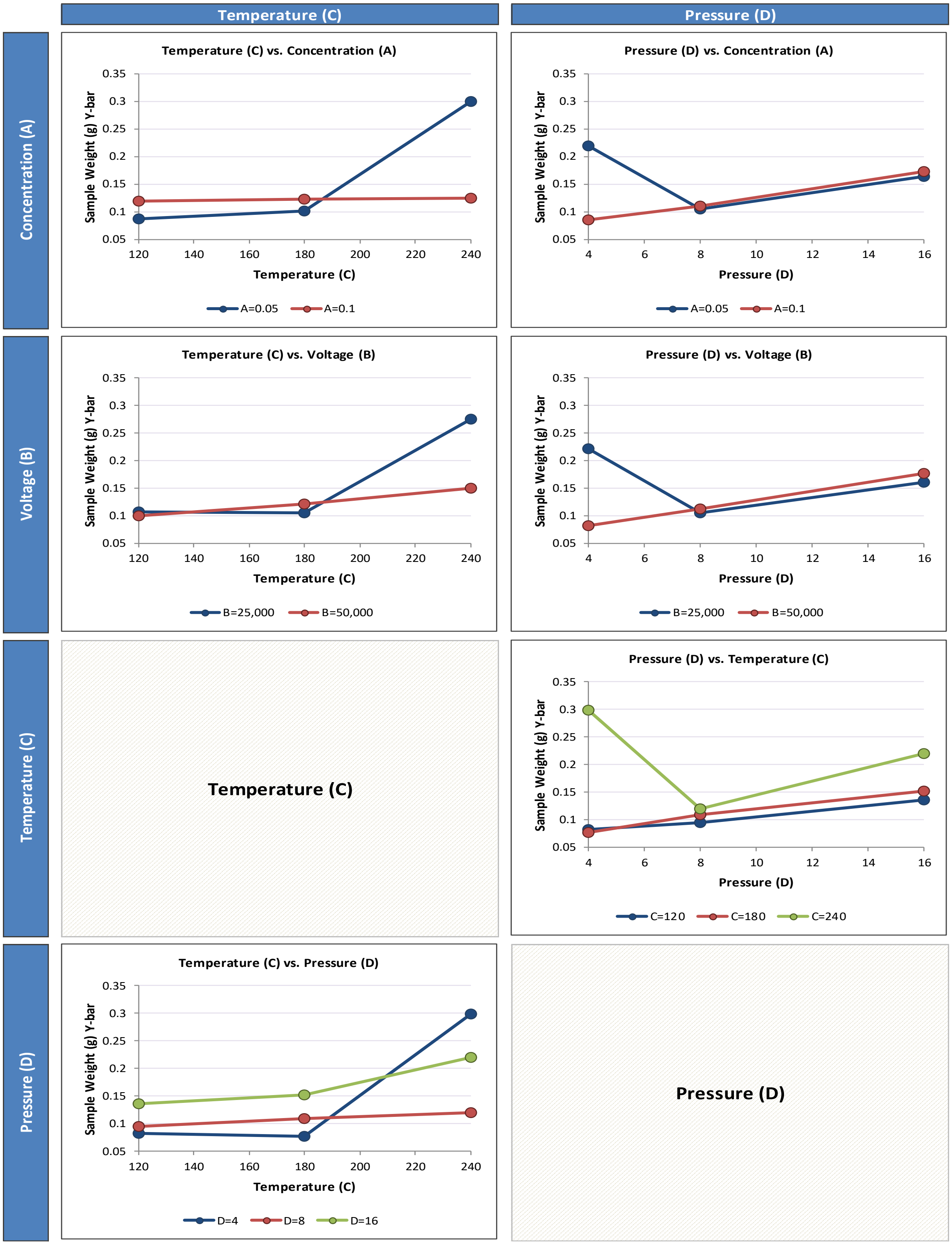

Appendix C – DOE Interaction Charts – Soybean Oil

Table 58: Soybean Oil & Soy Lecithin @ 19Ga Interaction chart on Droplet Count Y-bar

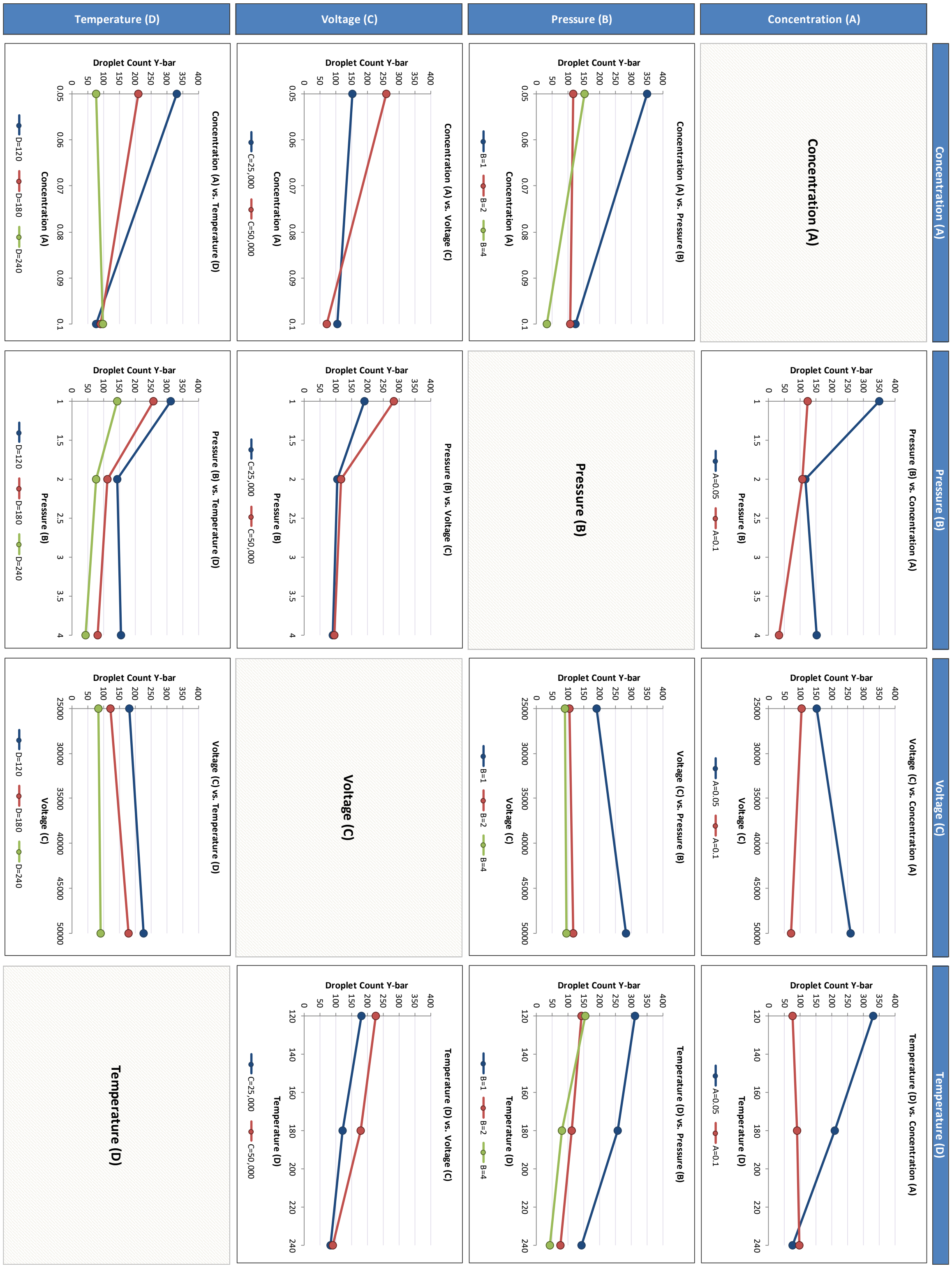

Appendix C – DOE Interaction Charts – Soybean Oil

Table 59: Soybean Oil & Soy Lecithin @ 19Ga Interaction chart on Droplet Size Y-bar

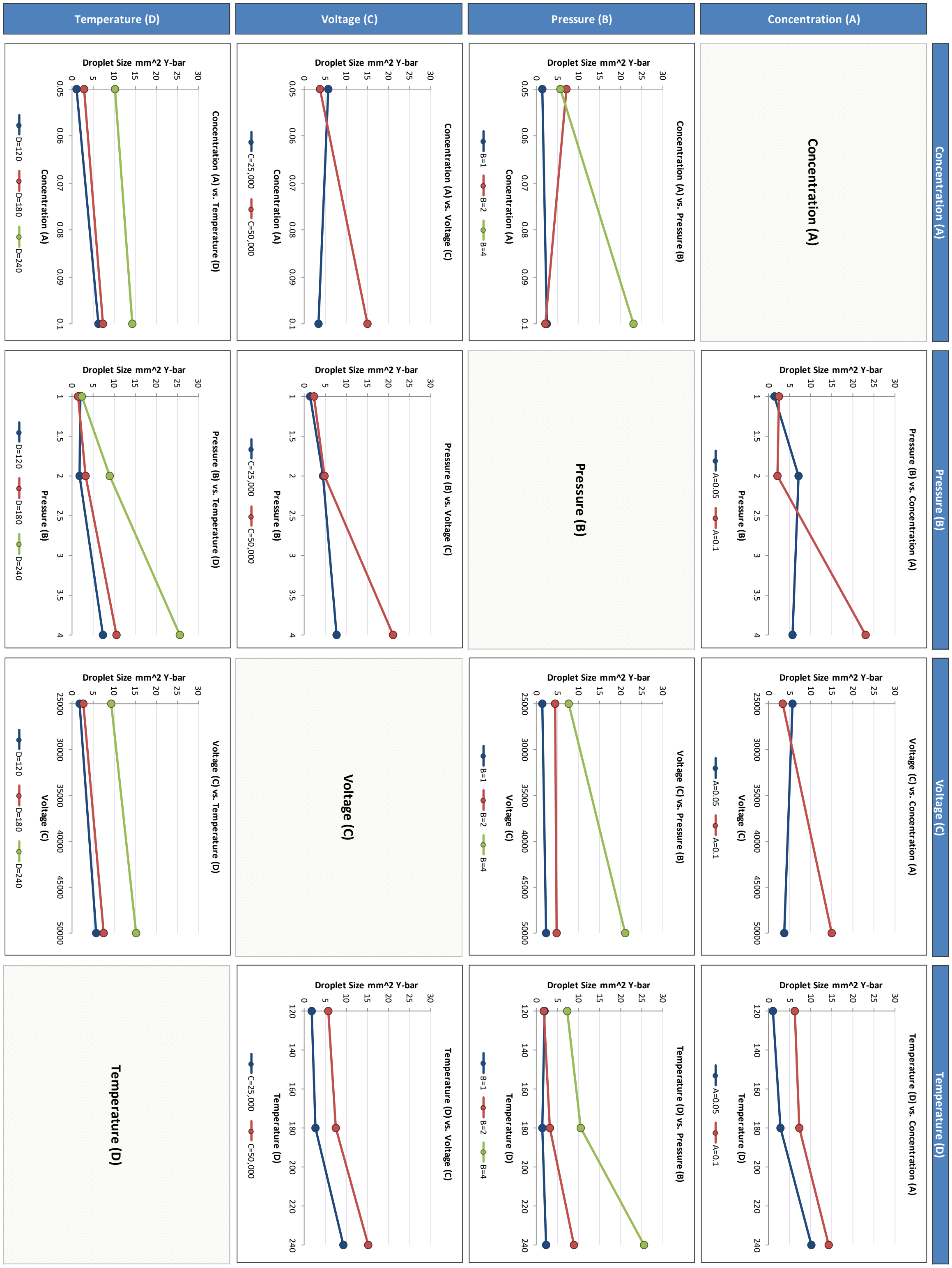

Appendix C – DOE Interaction Charts – Soybean Oil

Table 60: Soybean Oil & Soy Lecithin @ 19Ga Interaction chart (Concentration & Voltage) on Coverage Area Y-bar

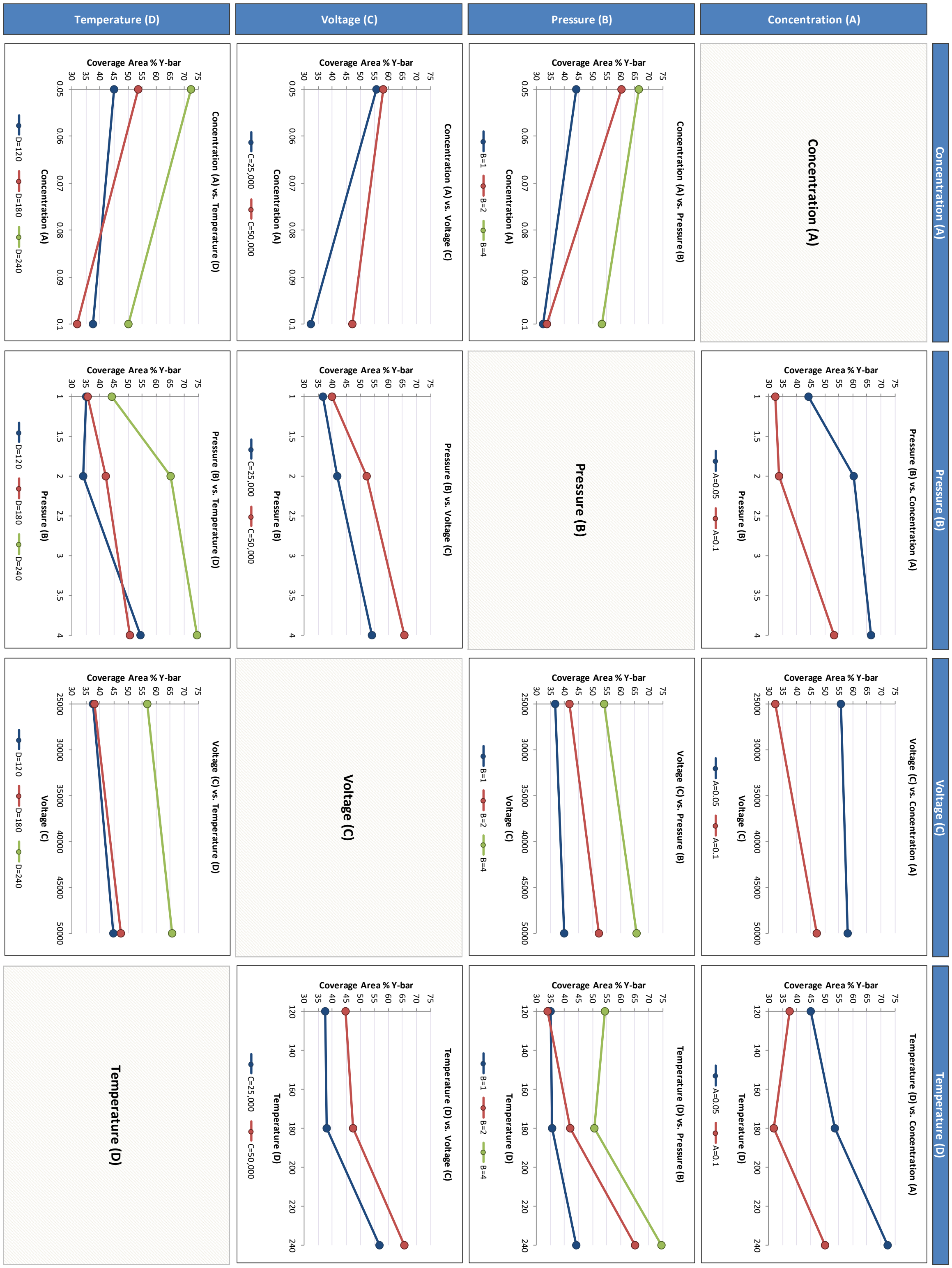

Appendix C – DOE Interaction Charts – Soybean Oil

Table 61: Soybean Oil & Soy Lecithin @ 19Ga Interaction chart on Sample Weight (g) Y-bar

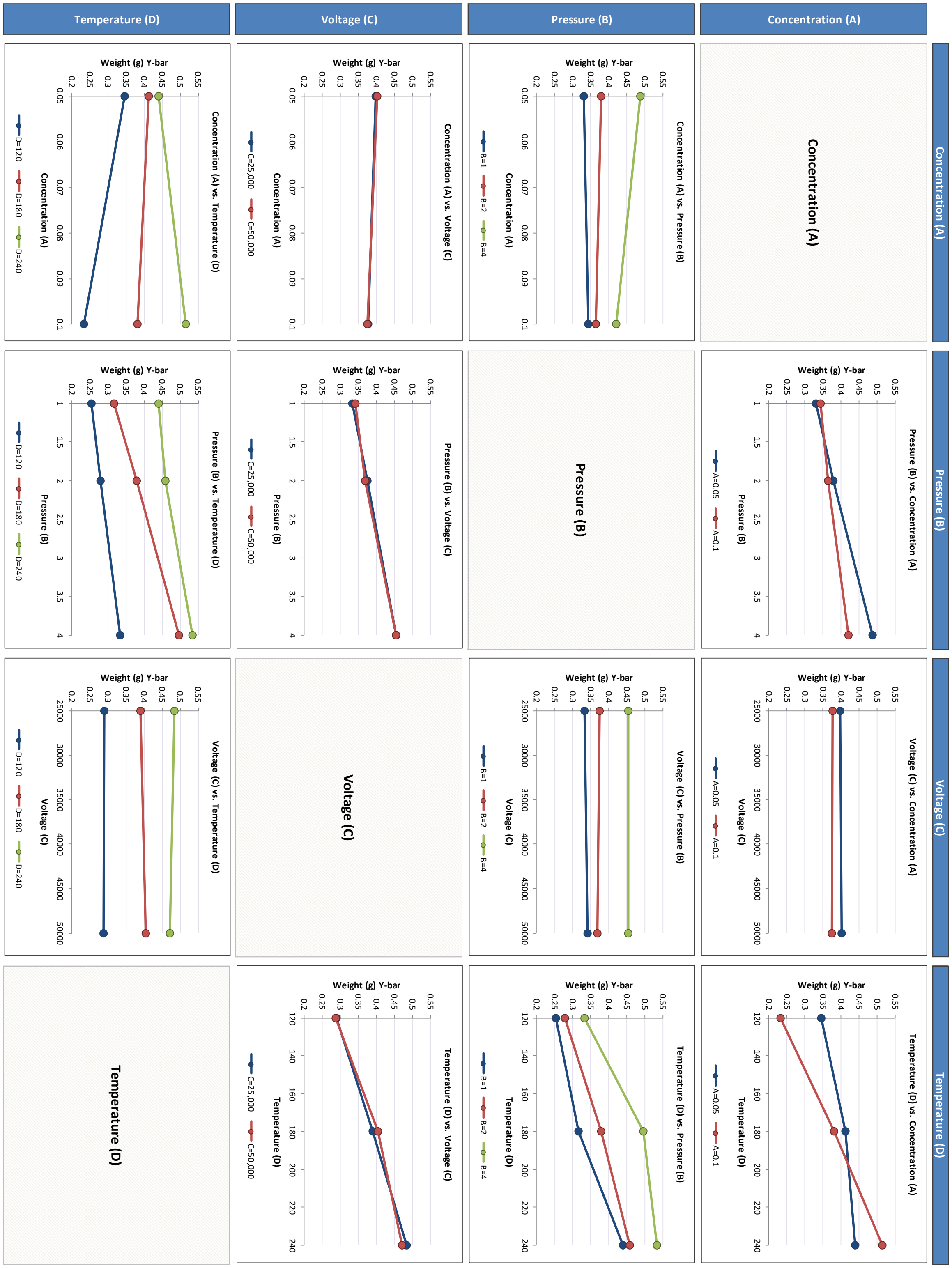

Appendix C – DOE Interaction Charts – Soybean Oil

Table 62: Soybean Oil & Polysorbate 20 @ 19Ga Interaction chart on Droplet Count Y-bar

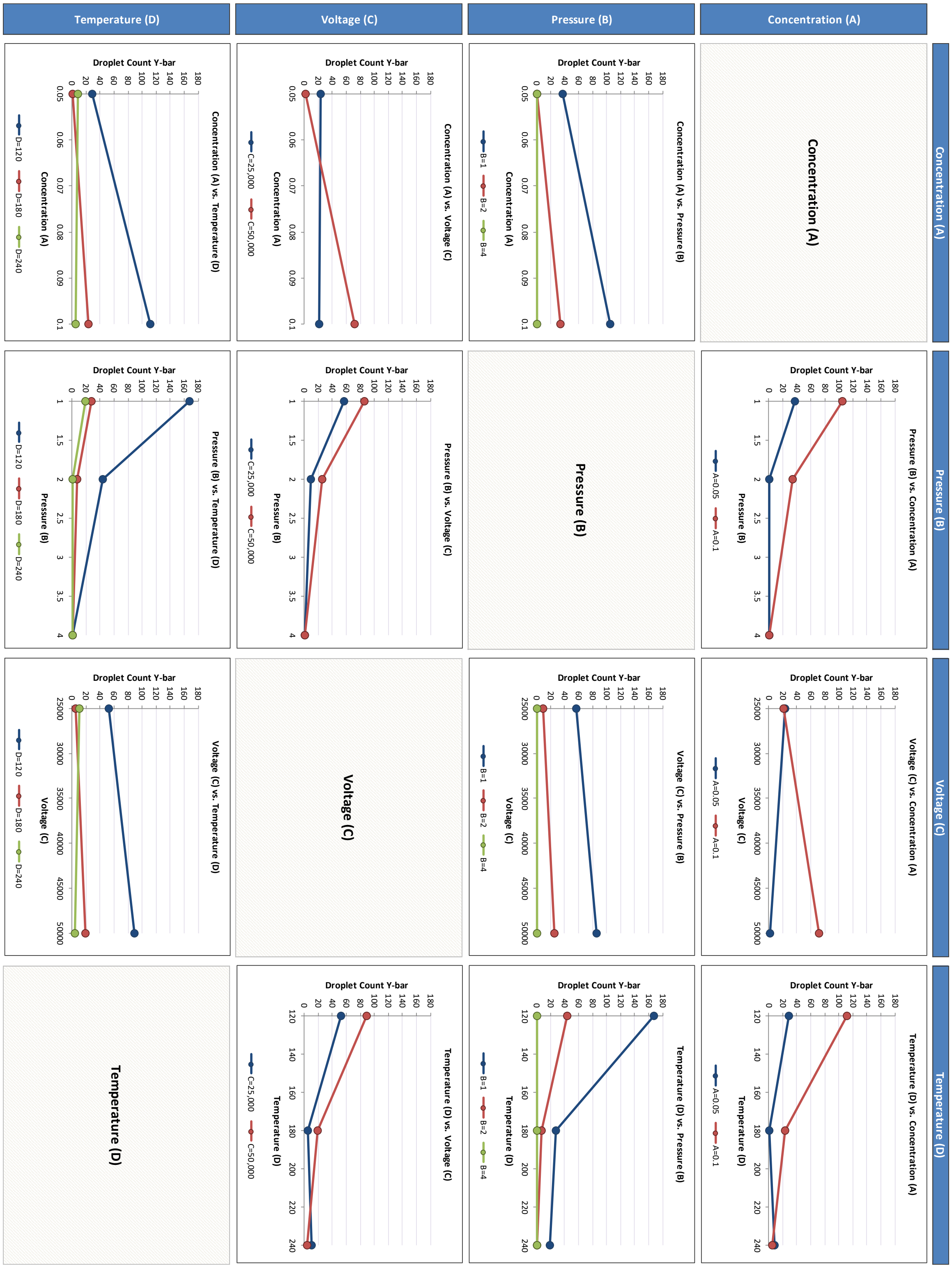

Appendix C – DOE Interaction Charts – Soybean Oil

Table 63: Soybean Oil & Polysorbate 20 @ 19Ga Interaction chart on Droplet Size Y-bar

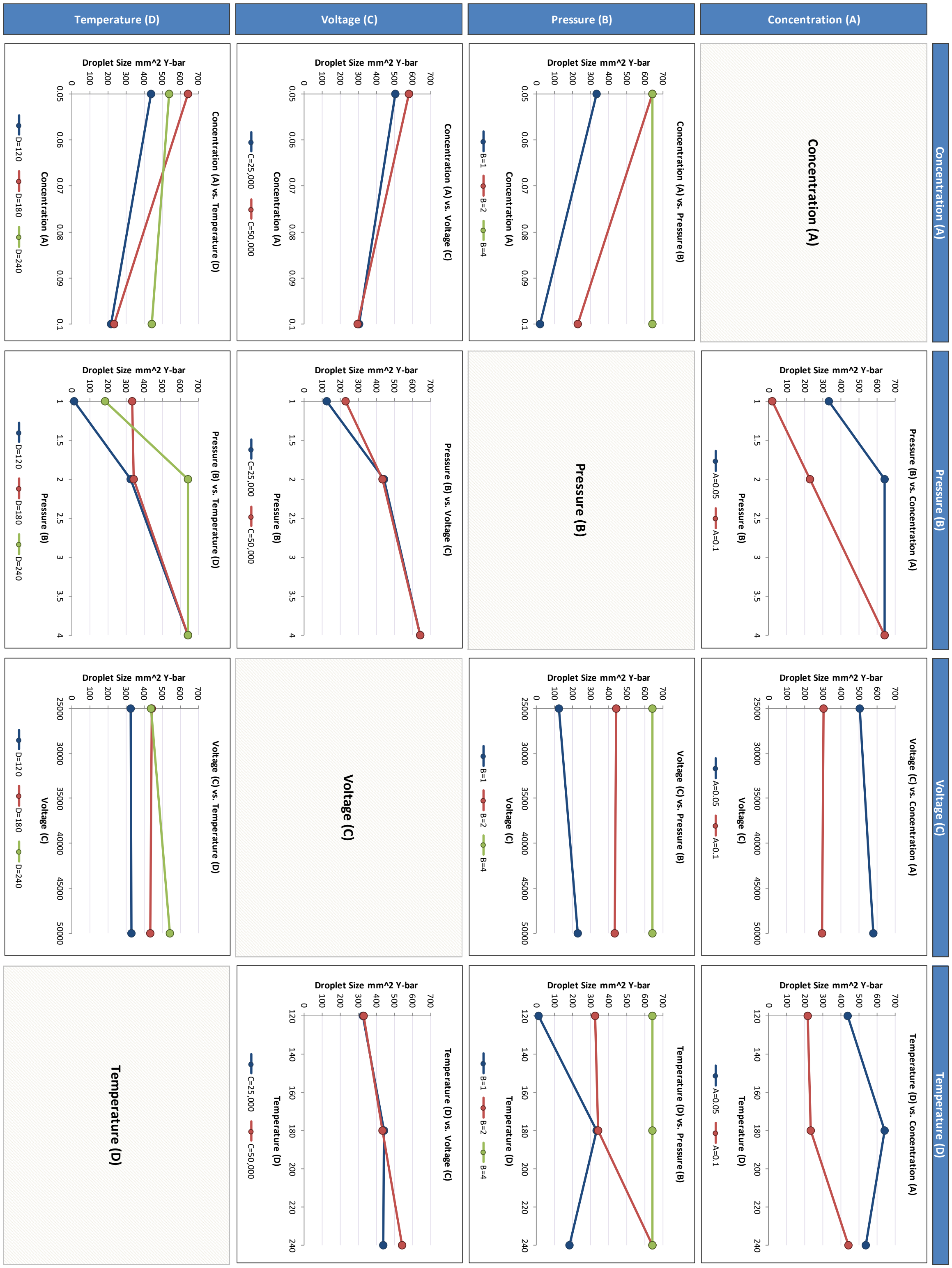

Appendix C – DOE Interaction Charts – Soybean Oil

Table 64: Soybean Oil & Polysorbate 20 @ 19Ga Interaction chart on Coverage Area Y-bar

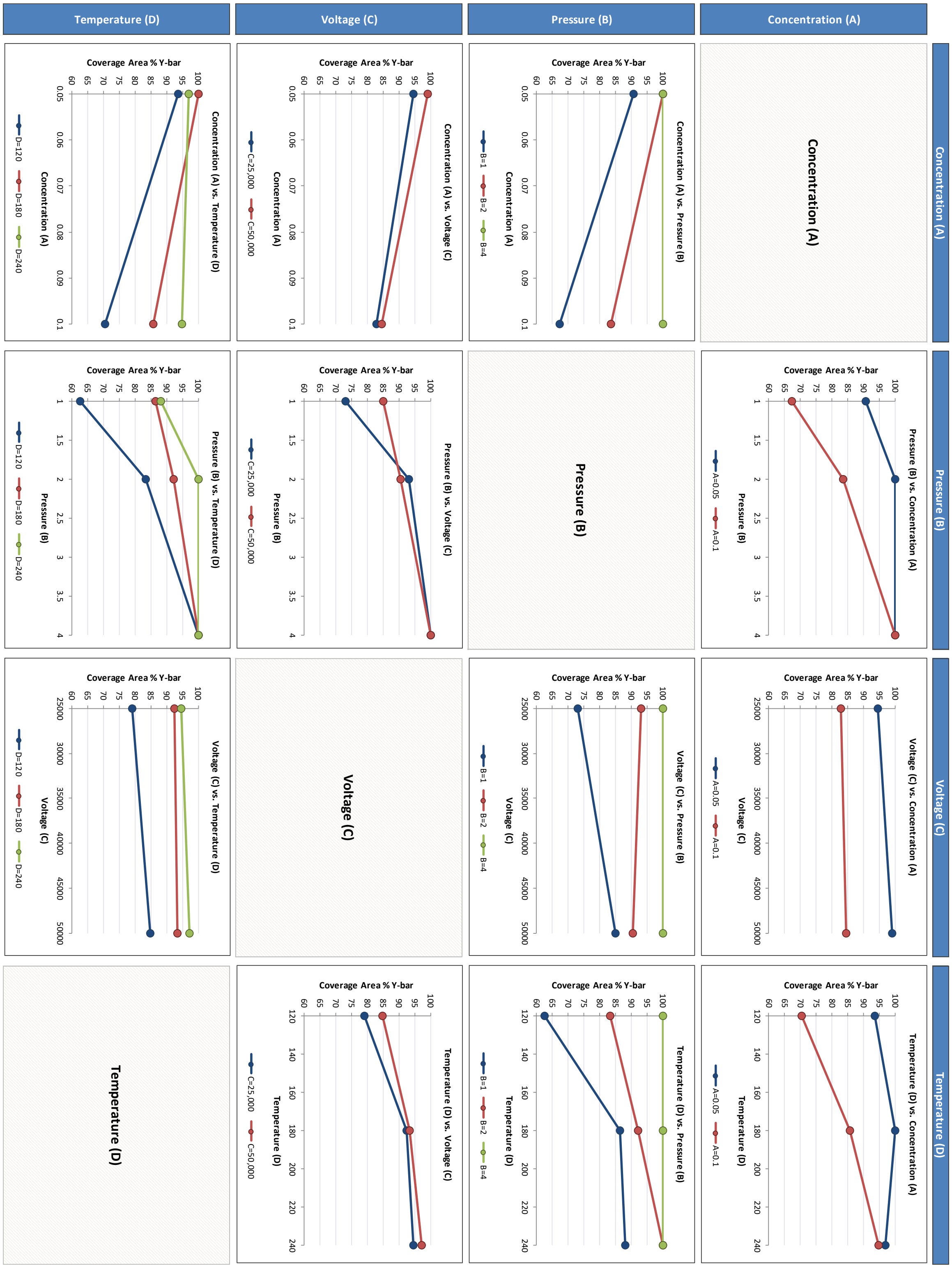

Appendix C – DOE Interaction Charts – Soybean Oil

Table 65: Soybean Oil & Polysorbate 20 @ 19Ga Interaction chart on Sample Weight (G) Y-bar

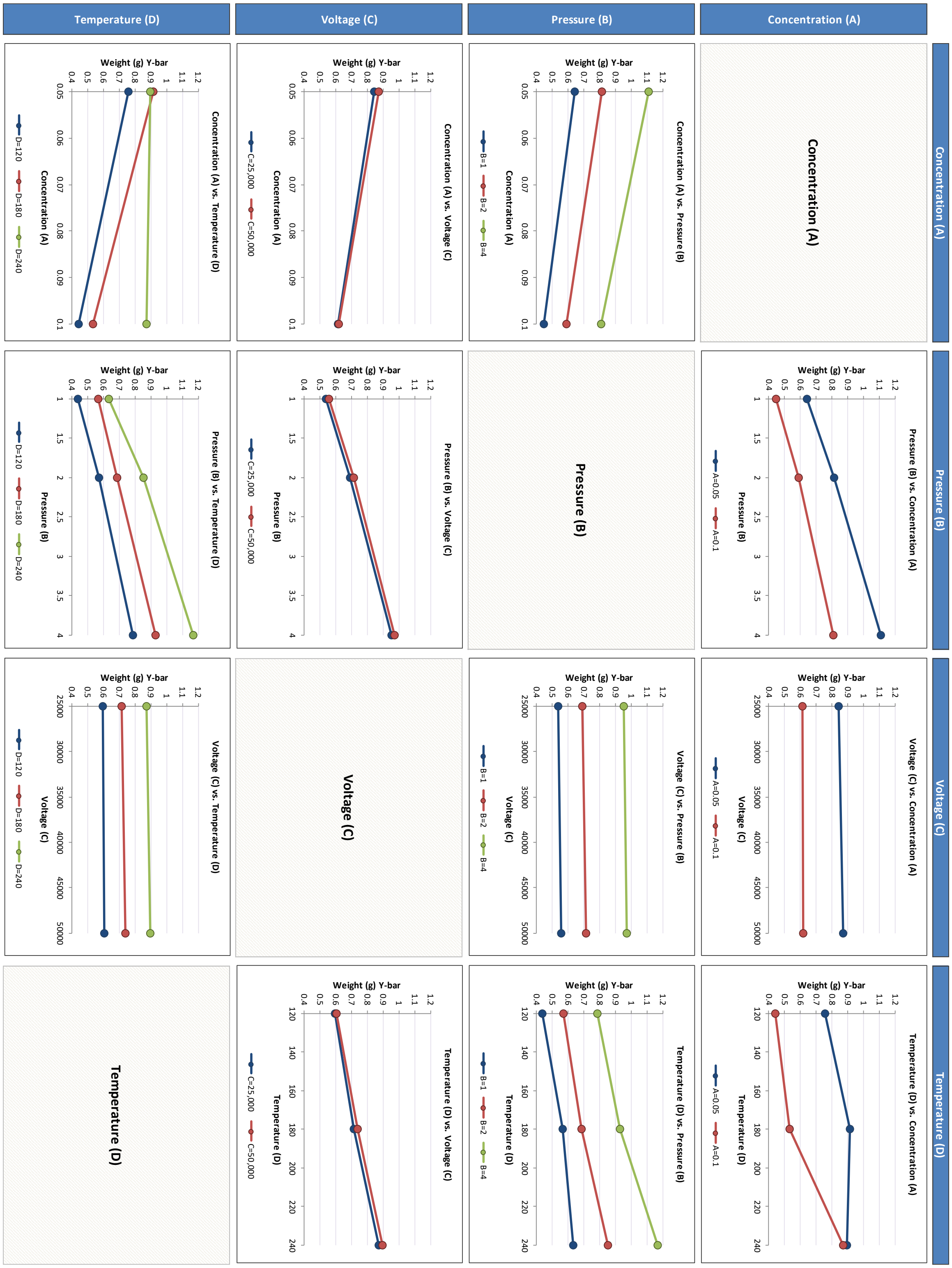

Appendix C – DOE Interaction Charts – Soybean Oil

Table 66: Soybean Oil & Propylene Glycol @ 19Ga Interaction chart on Droplet Count Y-bar

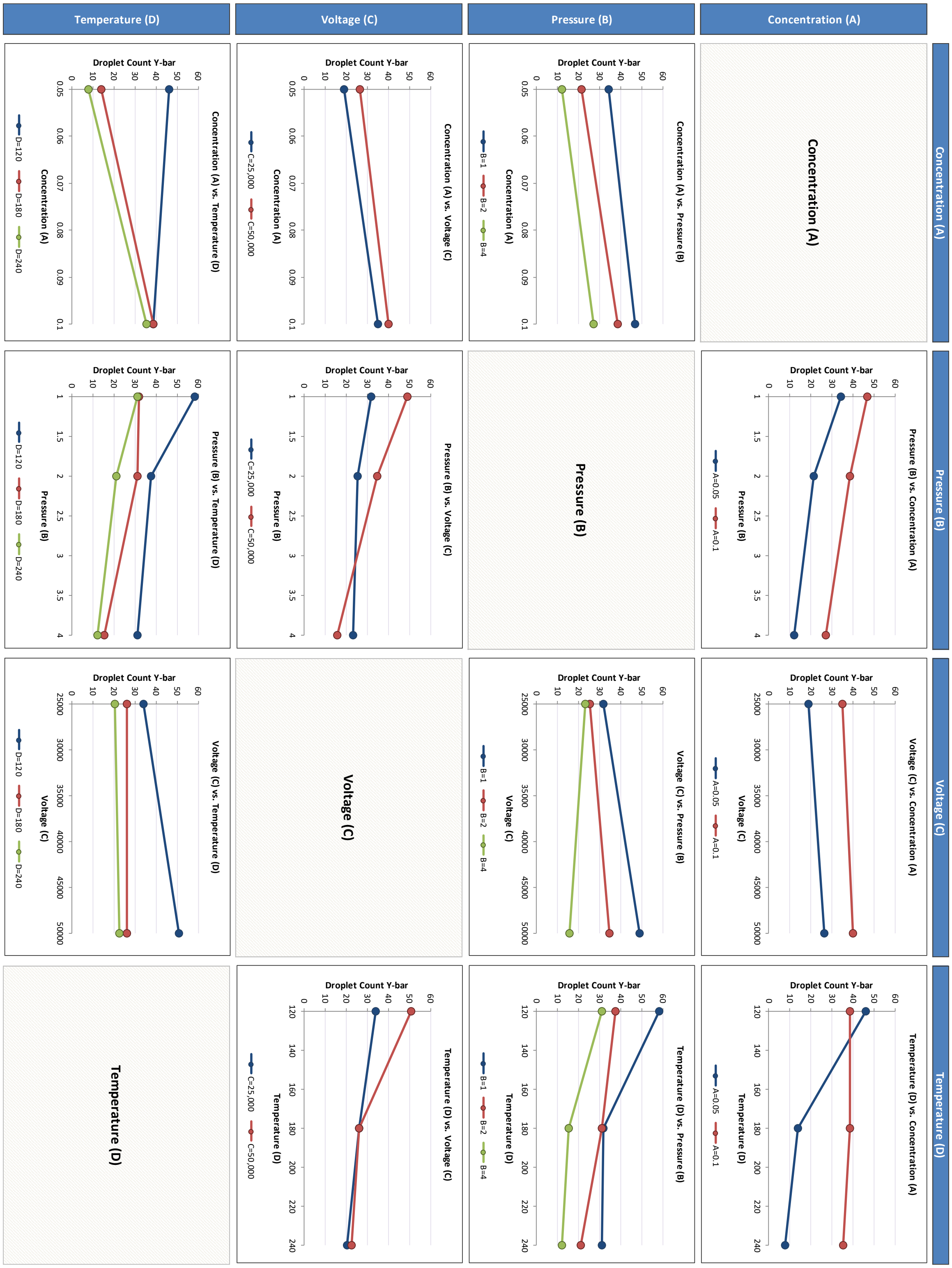

Appendix C – DOE Interaction Charts – Soybean Oil

Table 67: Soybean Oil & Propylene Glycol @ 19Ga Interaction chart on Droplet Size Y-bar

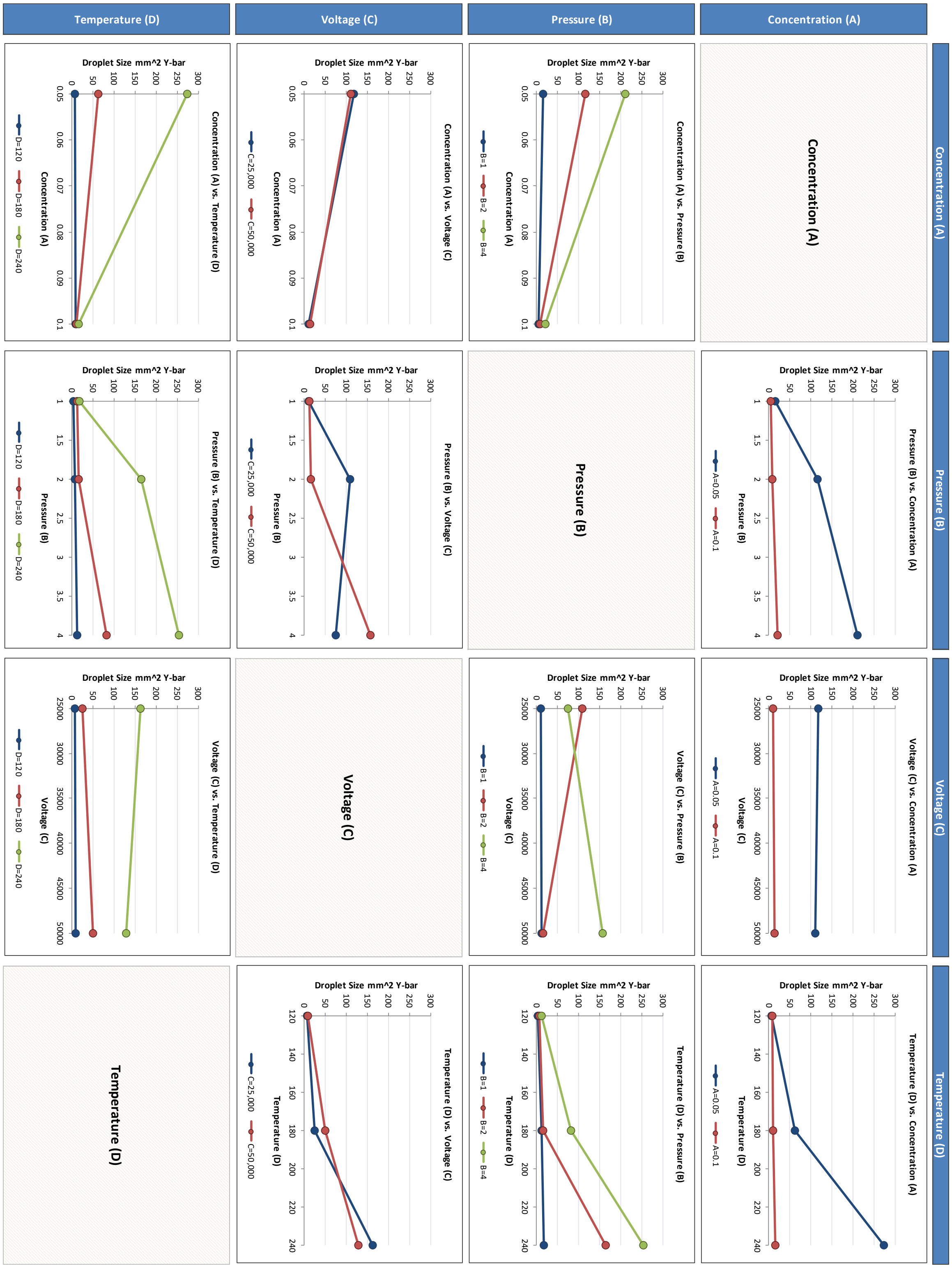

Appendix C – DOE Interaction Charts – Soybean Oil

Table 68: Soybean Oil & Propylene Glycol @ 19Ga Interaction chart on Coverage Area Y-bar

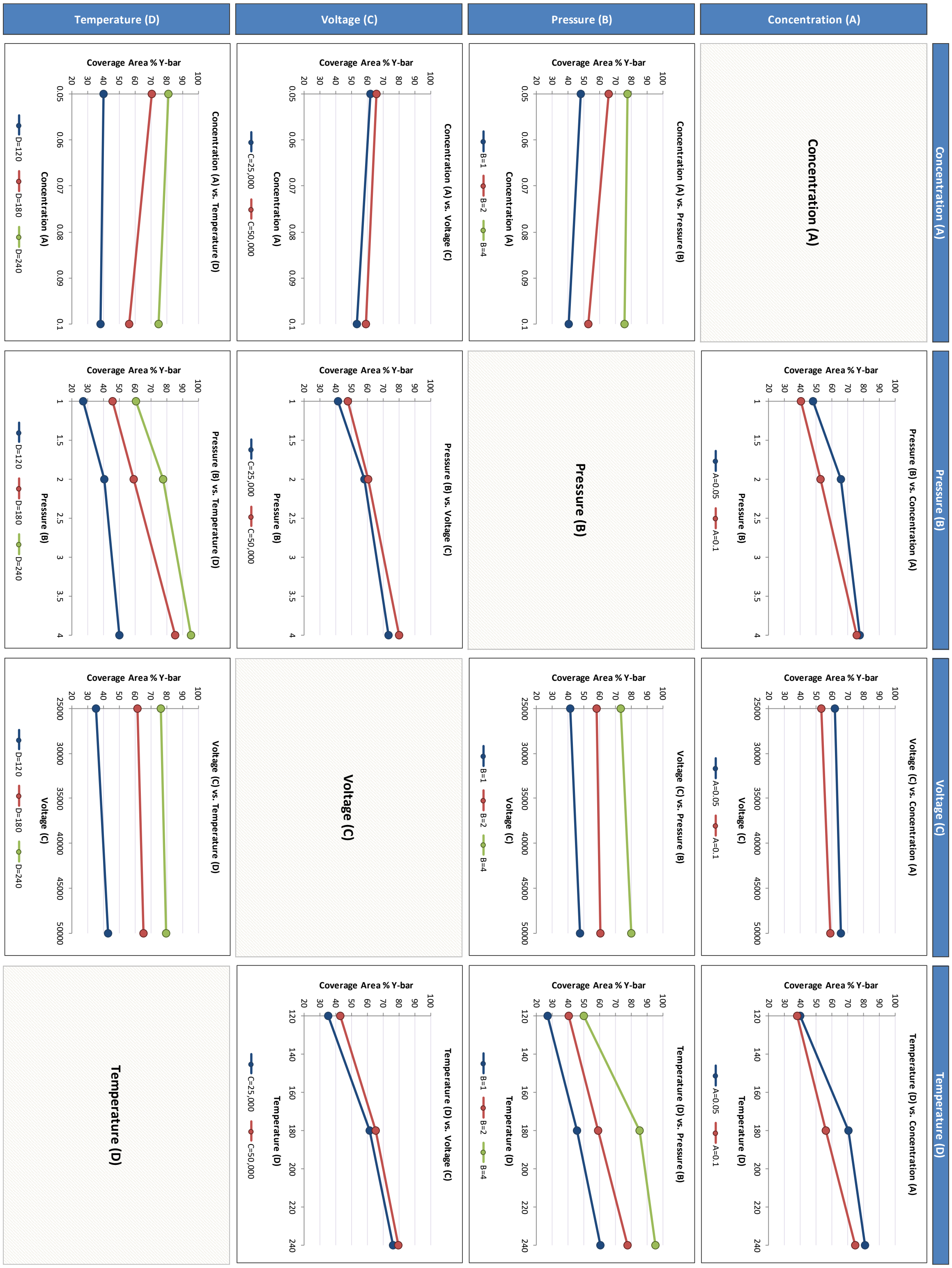

Appendix C – DOE Interaction Charts – Soybean Oil

Table 69: Soybean Oil & Propylene Glycol @ 19Ga Interaction chart on Sample Weight (g) Y-bar

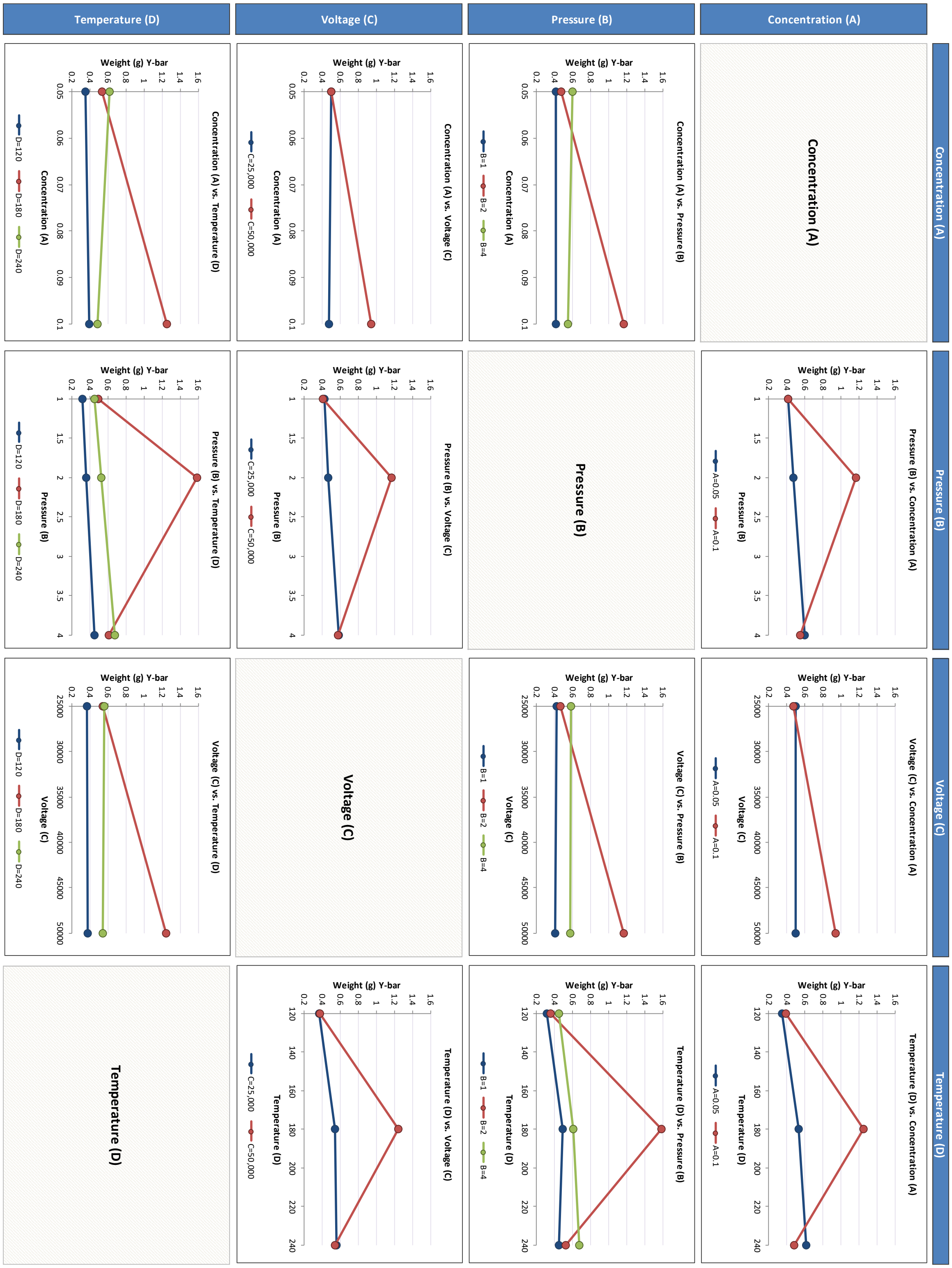

Appendix C – DOE Interaction Charts – Soybean Oil

Table 70: Soybean Oil & Soy Lecithin @ 22Ga Interaction chart on Droplet Count Y-bar

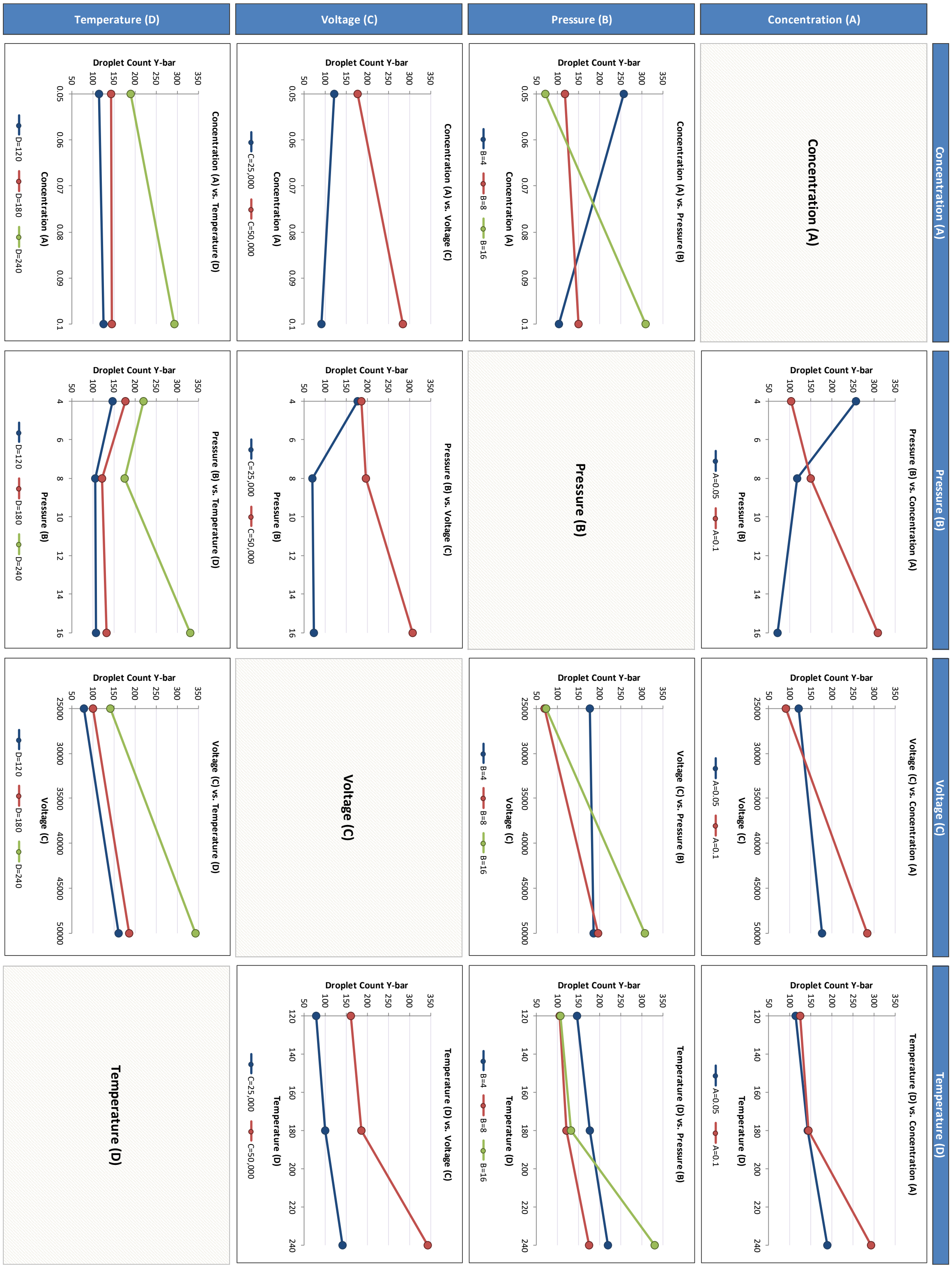

Appendix C – DOE Interaction Charts – Soybean Oil

Table 71: Soybean Oil & Soy Lecithin @ 22Ga Interaction chart on Droplet Size Y-bar

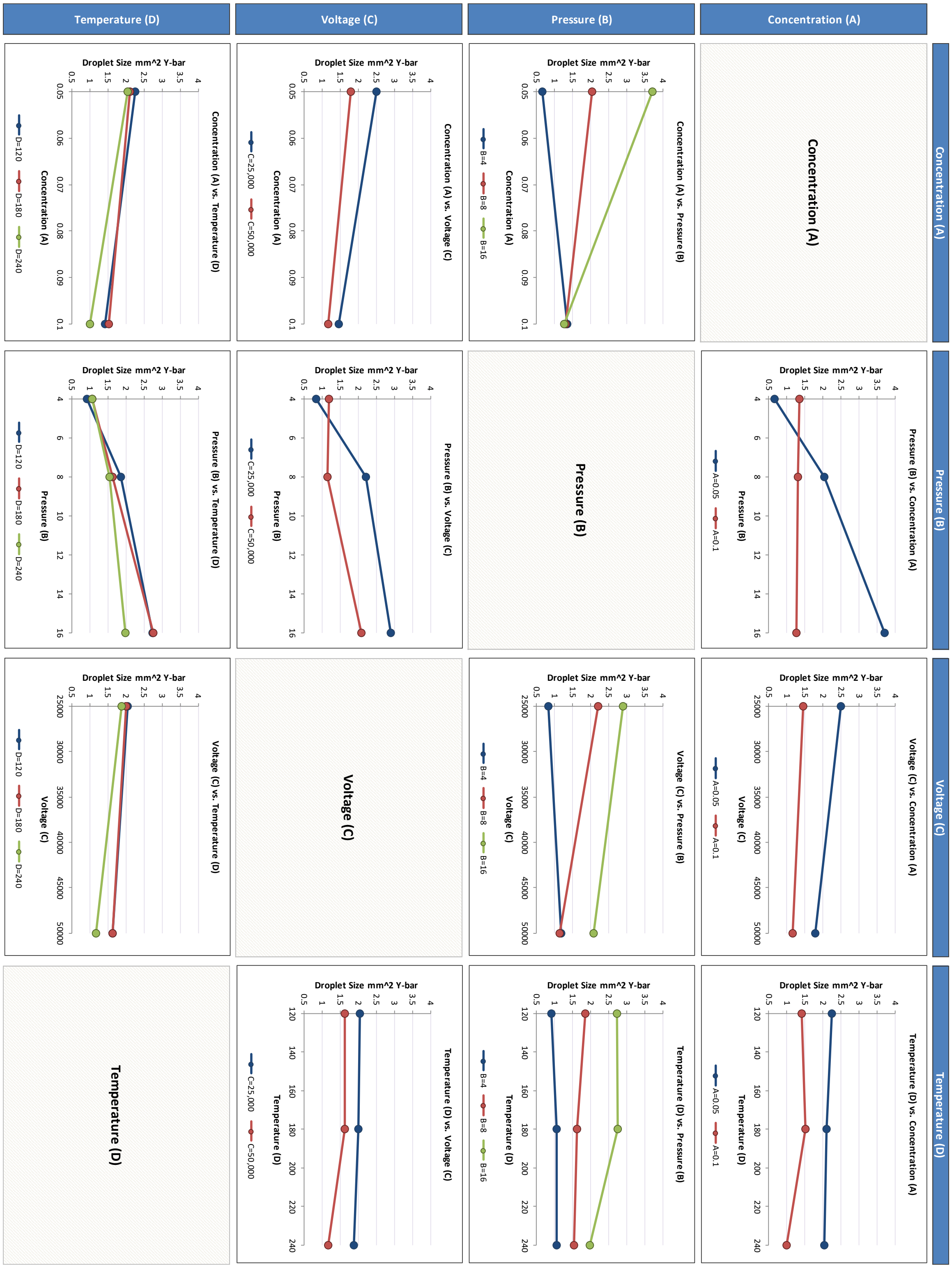

Appendix C – DOE Interaction Charts – Soybean Oil

Table 72: Soybean Oil & Soy Lecithin @ 22Ga Interaction chart on Coverage Area % Y-bar

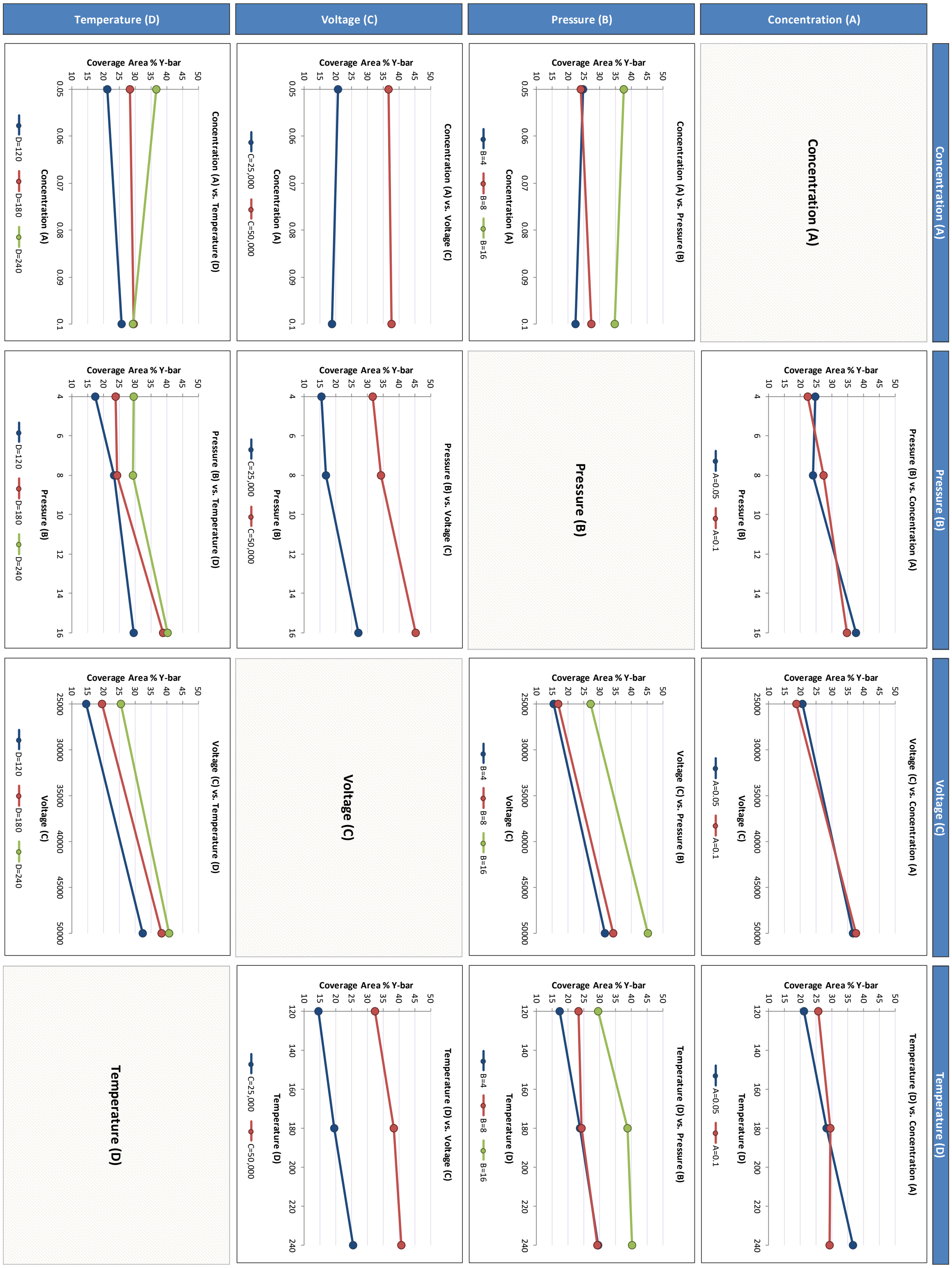

Appendix C – DOE Interaction Charts – Soybean Oil

Table 73: Soybean Oil & Soy Lecithin @ 22Ga Interaction chart on Sample Weight (g) Y-bar

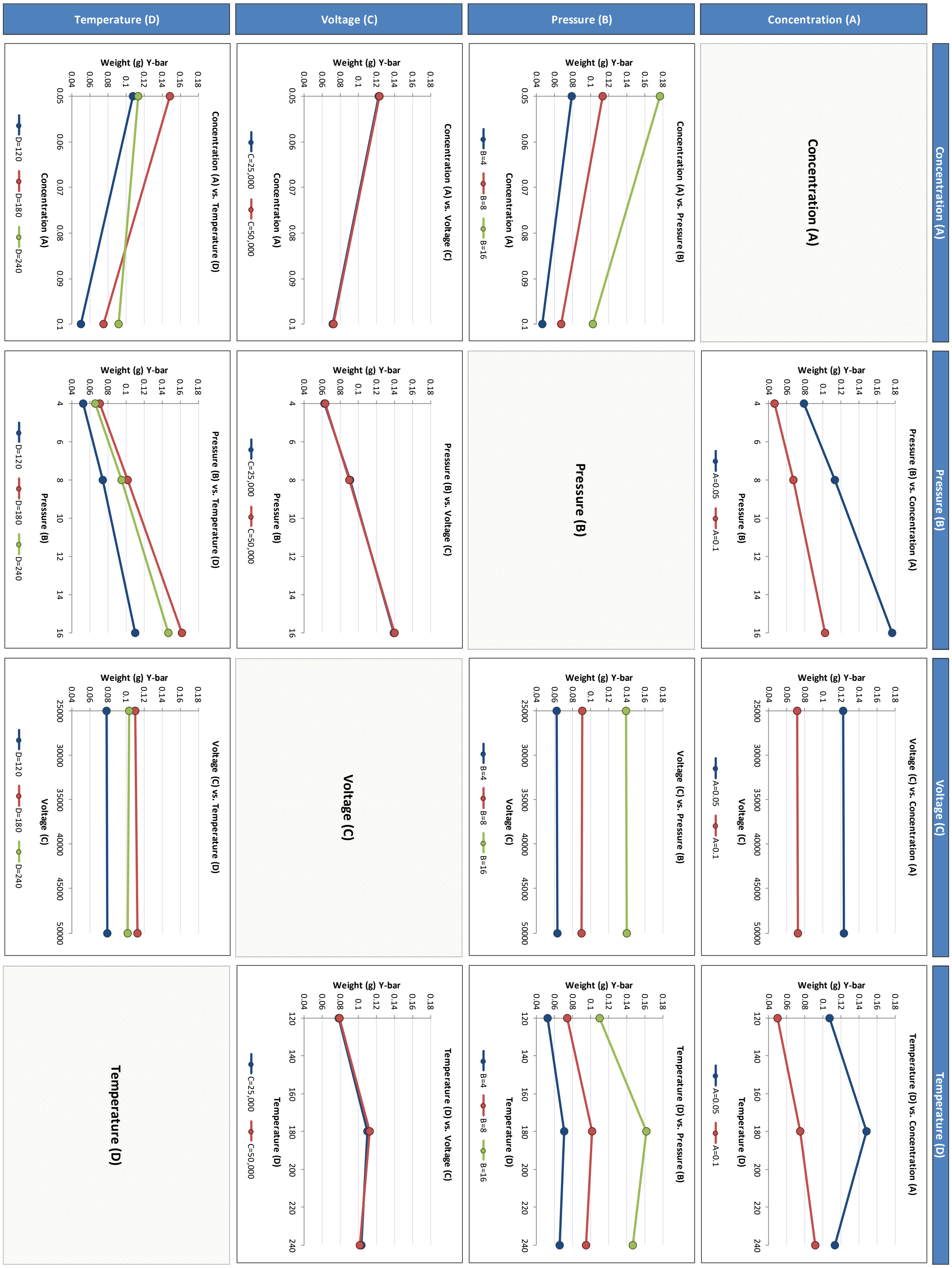

Appendix C – DOE Interaction Charts – Soybean Oil

Table 74: Soybean Oil & Polysorbate 20 @ 22Ga Interaction chart on Droplet Count Y-bar

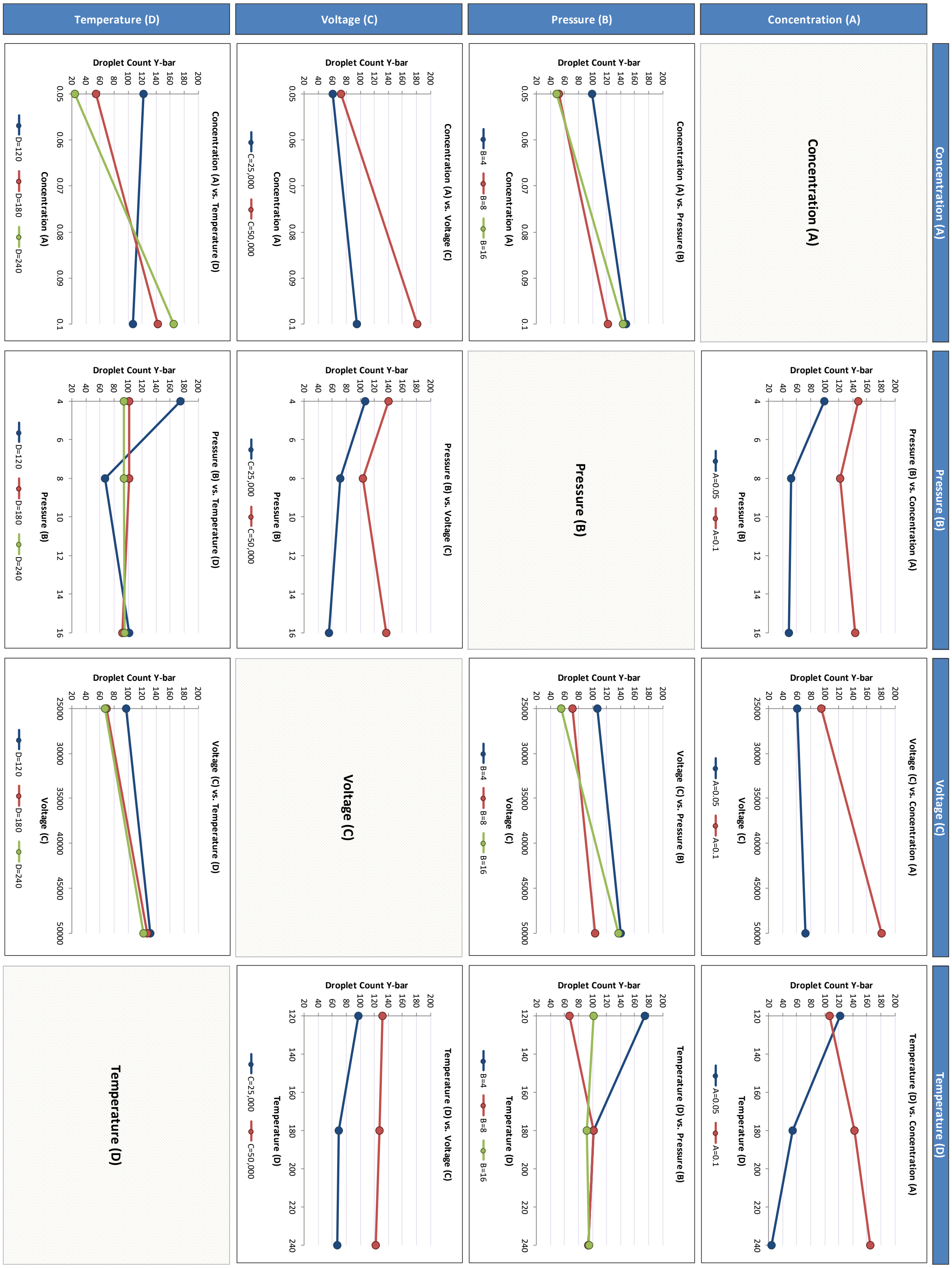

Appendix C – DOE Interaction Charts – Soybean Oil

Table 75: Soybean Oil & Polysorbate 20 @ 22Ga Interaction chart on Droplet Size Y-bar

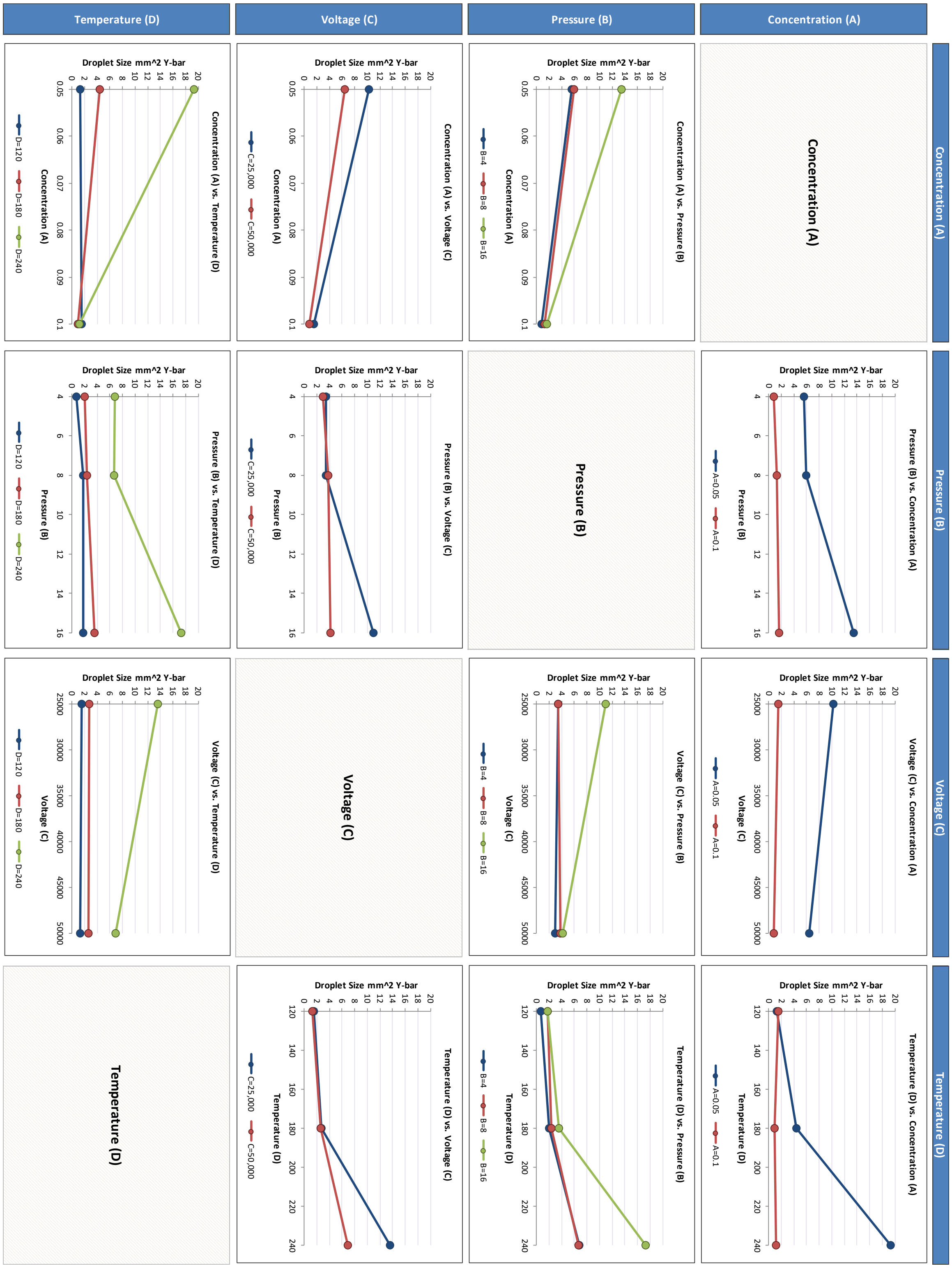

Appendix C – DOE Interaction Charts – Soybean Oil

Table 76: Soybean Oil & Polysorbate 20 @ 22Ga Interaction chart on Coverage Area Y-bar

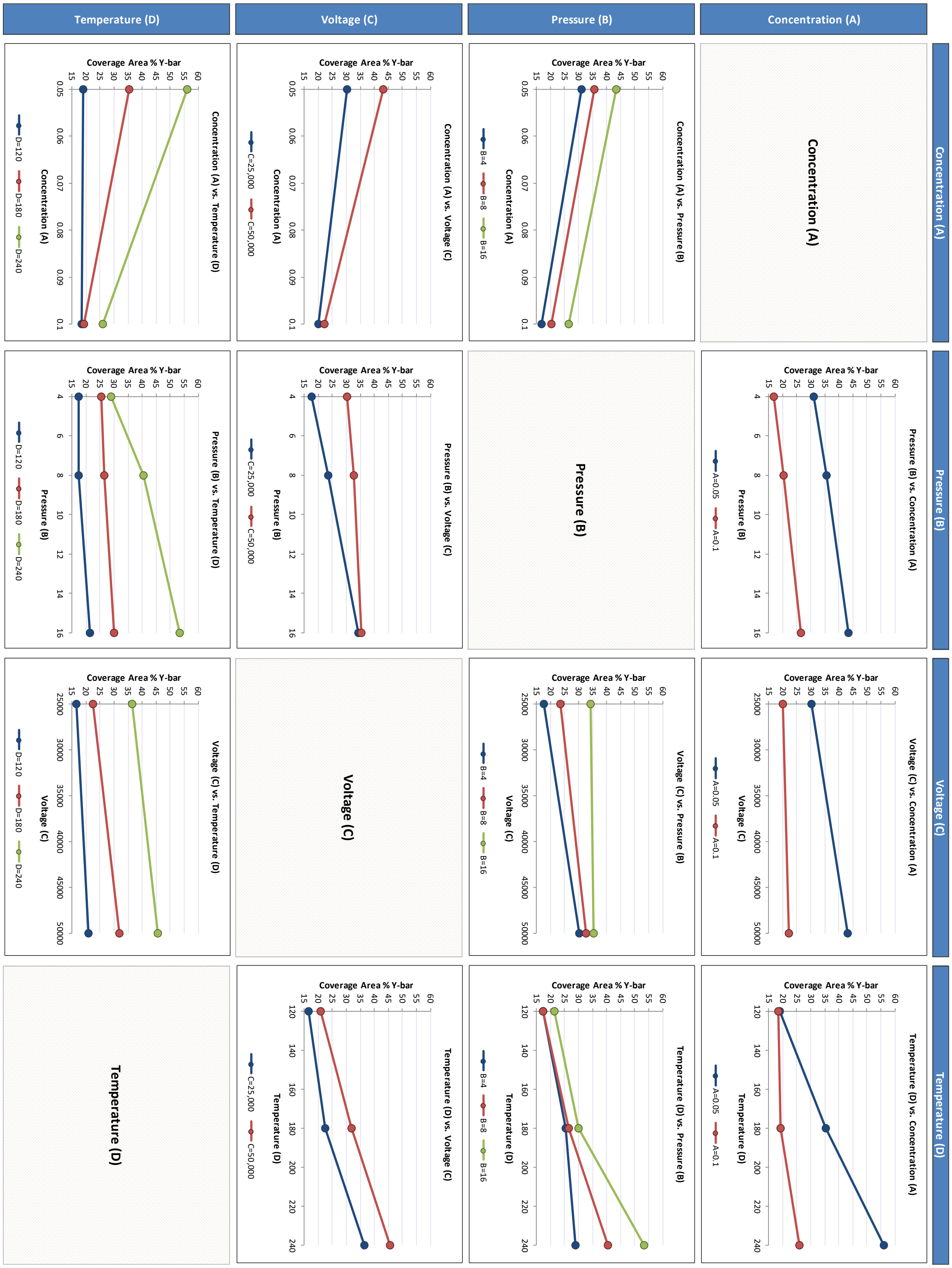

Appendix C – DOE Interaction Charts – Soybean Oil

Table 77: Soybean Oil & Polysorbate 20 @ 22Ga Interaction chart on Sample Weight (g) Y-bar

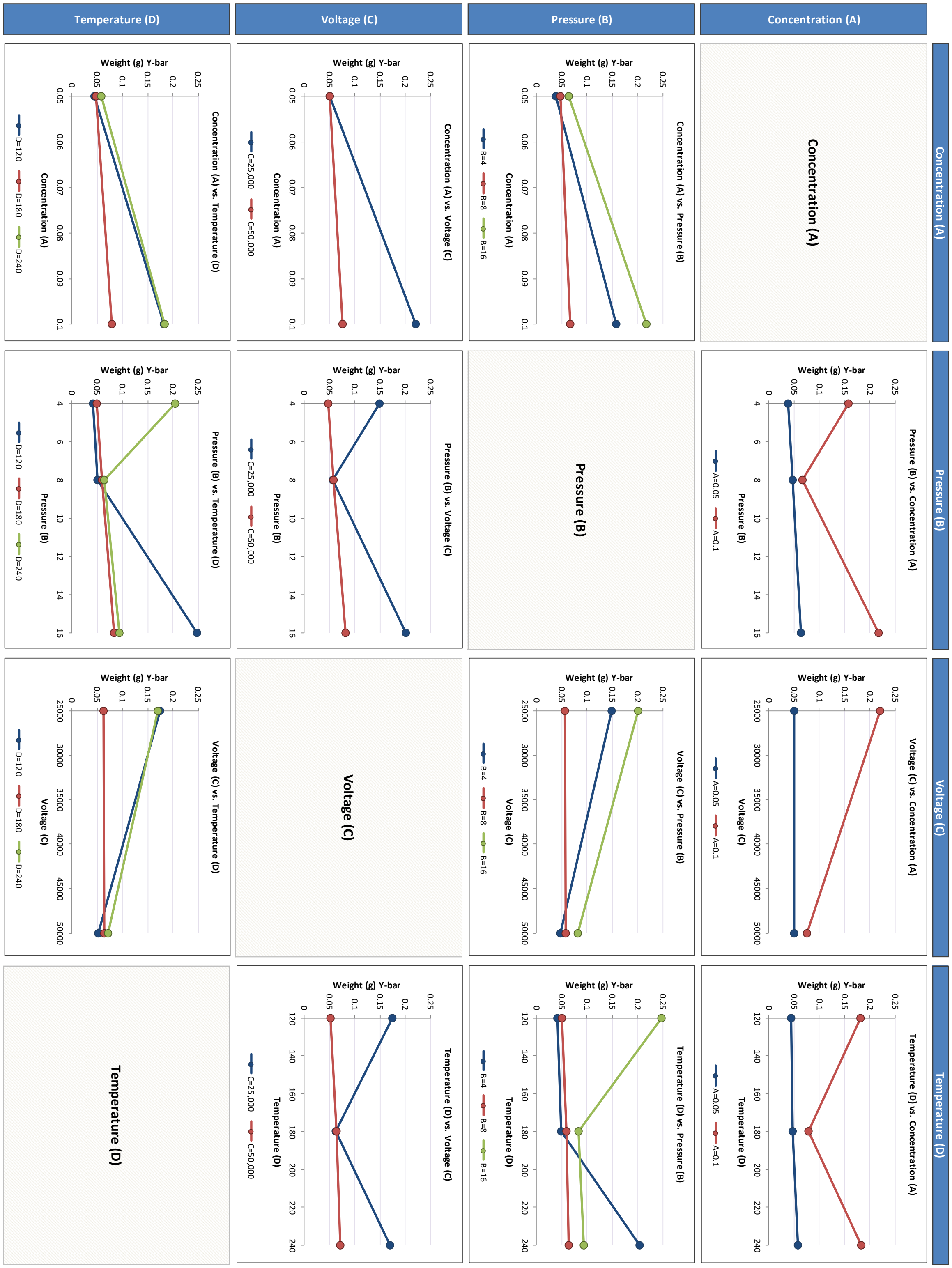

Appendix C – DOE Interaction Charts – Soybean Oil

Table 78: Soybean Oil & Propylene Glycol @ 22Ga Interaction chart on Droplet Count Y-bar

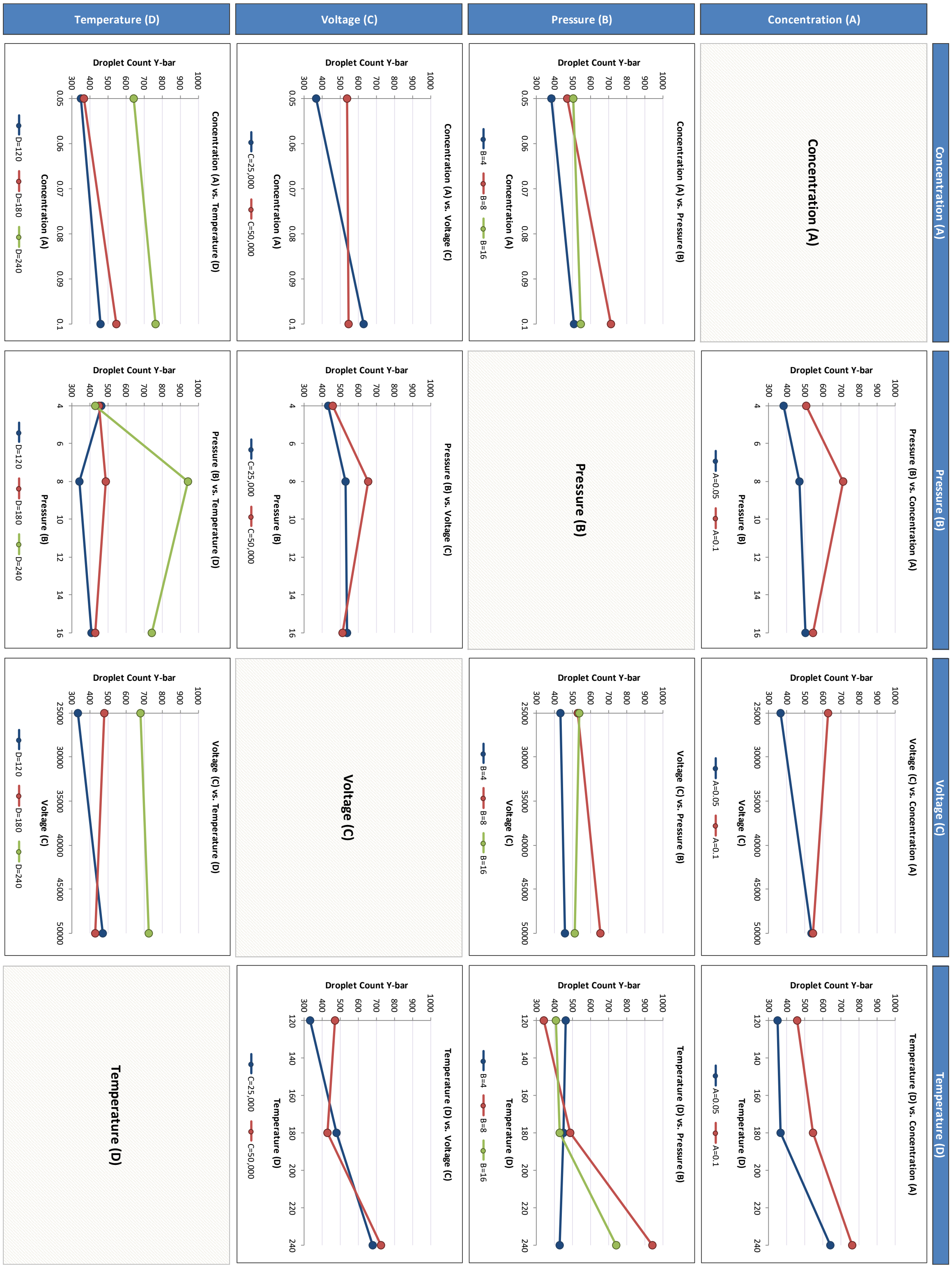

Appendix C – DOE Interaction Charts – Soybean Oil

Table 79: Soybean Oil & Propylene Glycol @ 22Ga Interaction chart on Droplet Size Y-bar

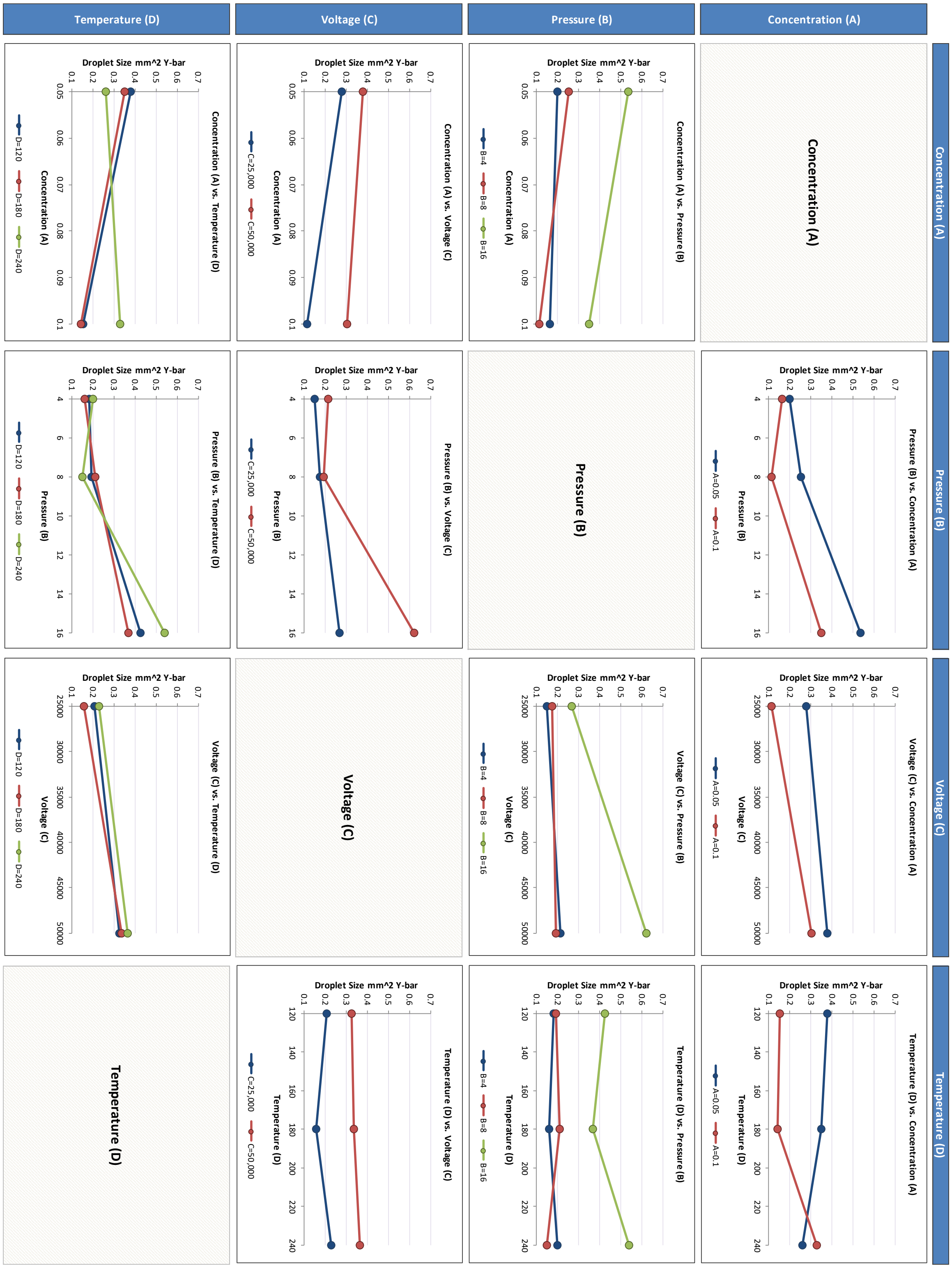

Appendix C – DOE Interaction Charts – Soybean Oil

Table 80: Soybean Oil & Propylene Glycol @ 22Ga Interaction chart on Coverage Area Y-bar

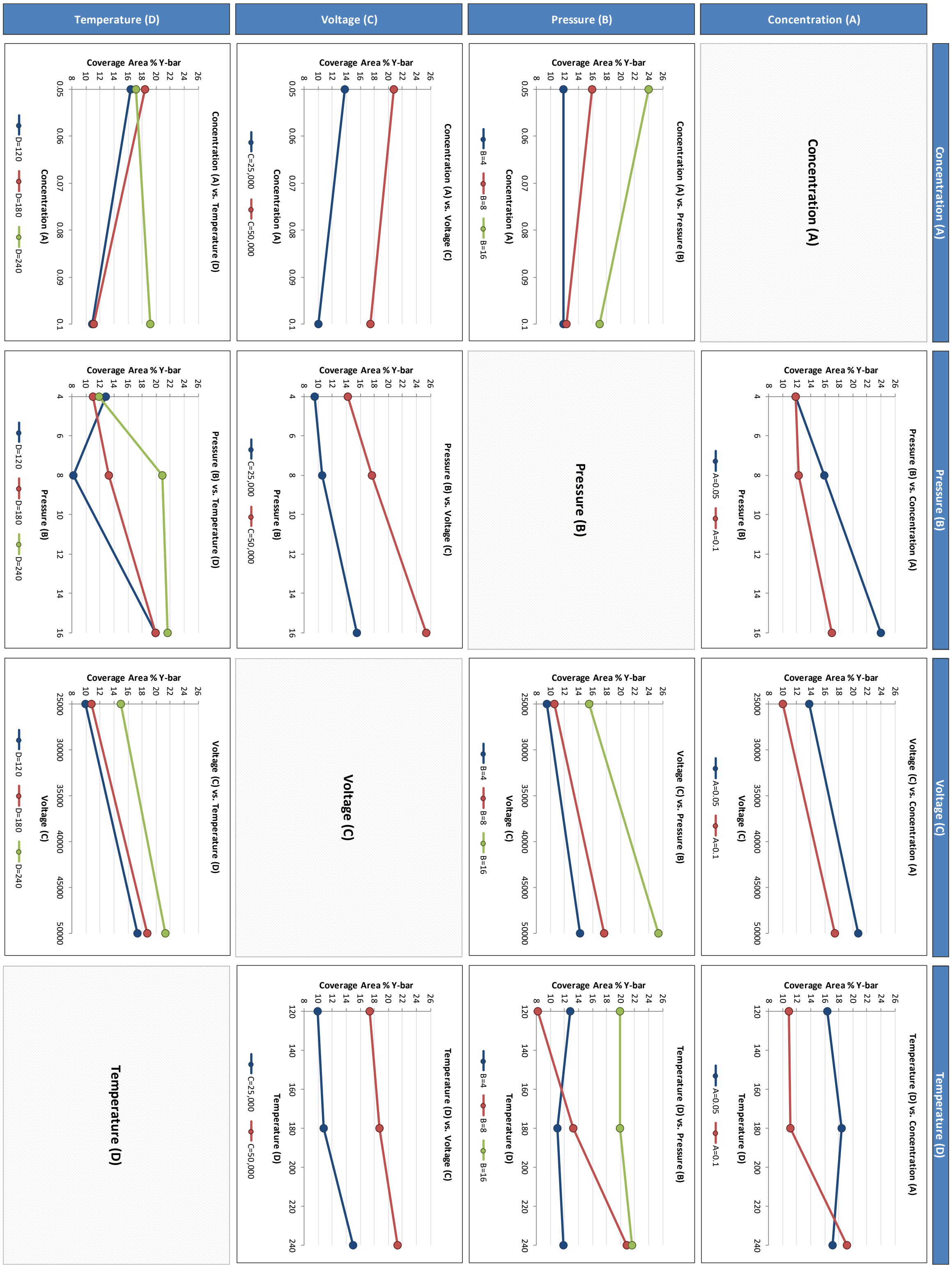

Appendix C – DOE Interaction Charts – Soybean Oil

Table 81: Soybean Oil & Prop Glycol @ 22Ga Interaction chart on Sample Weight Y-bar

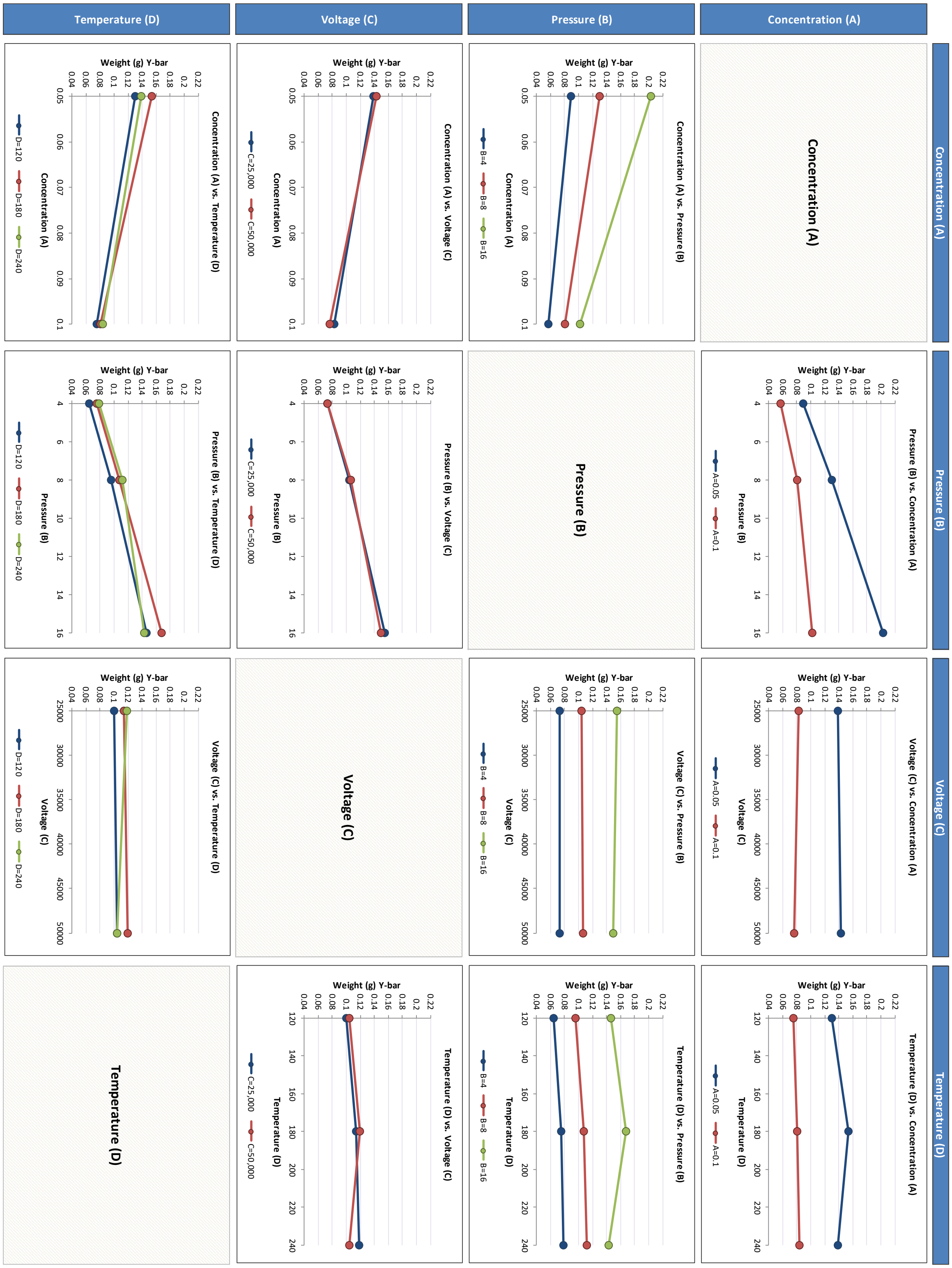

Appendix D – DOE Interaction Charts – Rapeseed Oil

Table 82: Rapeseed Oil & Sunflower Lecithin @ 19Ga Interaction chart on Droplet Count Y-bar

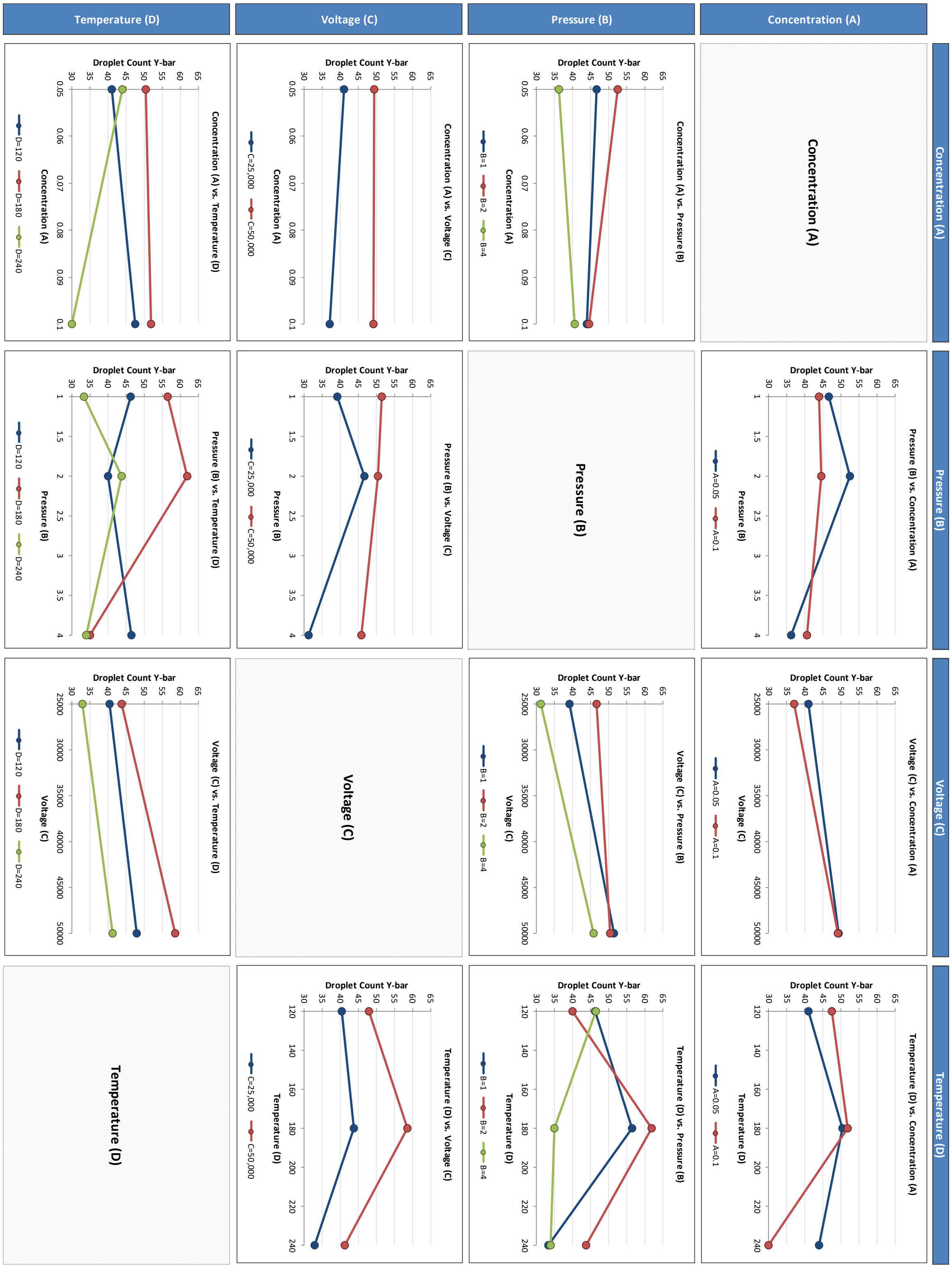

Appendix D – DOE Interaction Charts – Rapeseed Oil

Table 83: Rapeseed Oil & Sunflower Lecithin @ 19Ga Interaction chart on Droplet Size Y-bar

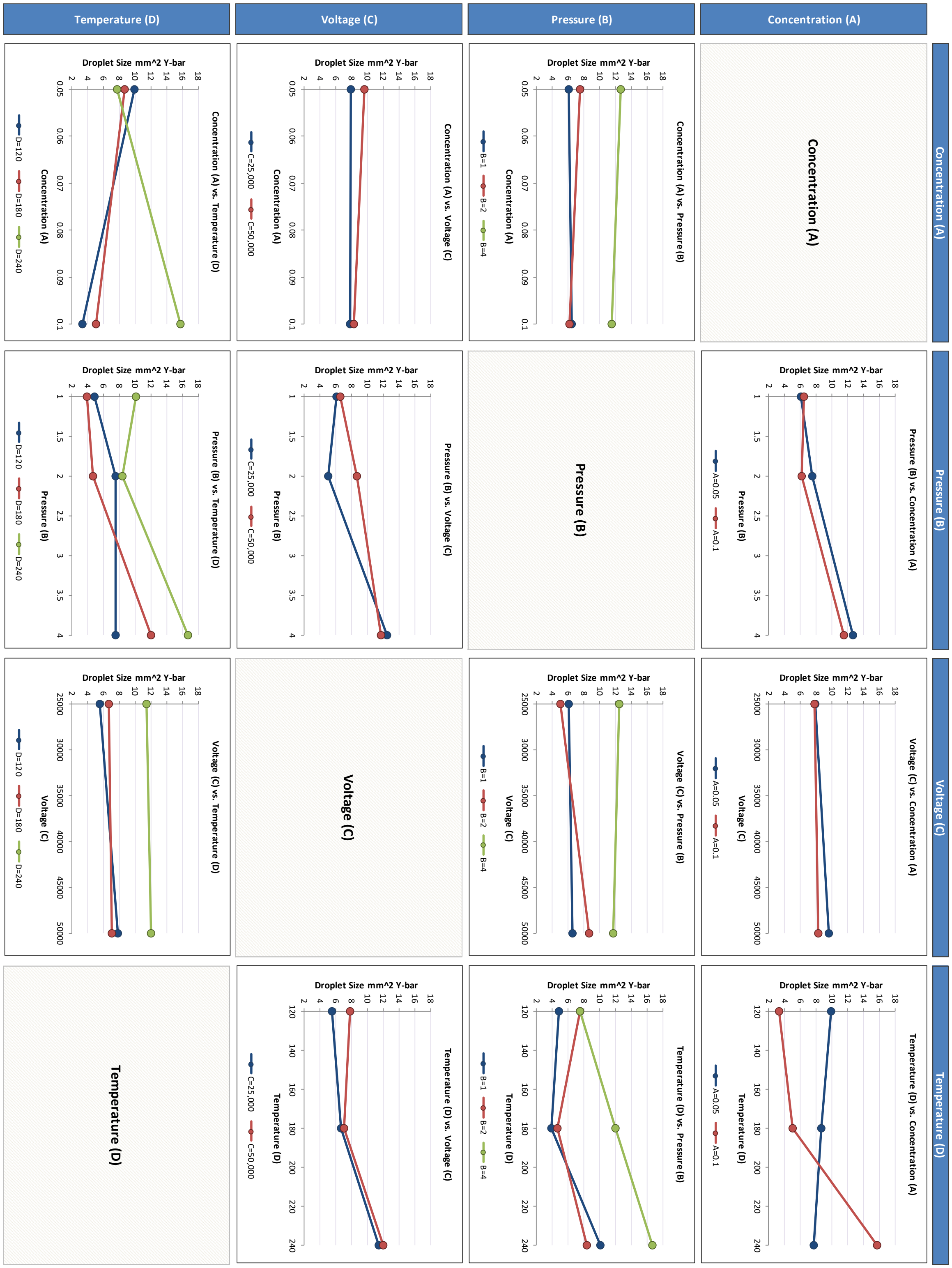

Appendix D – DOE Interaction Charts – Rapeseed Oil

Table 84: Rapeseed Oil & Sunflower Lecithin @ 19Ga Interaction chart on Coverage Area Y-bar

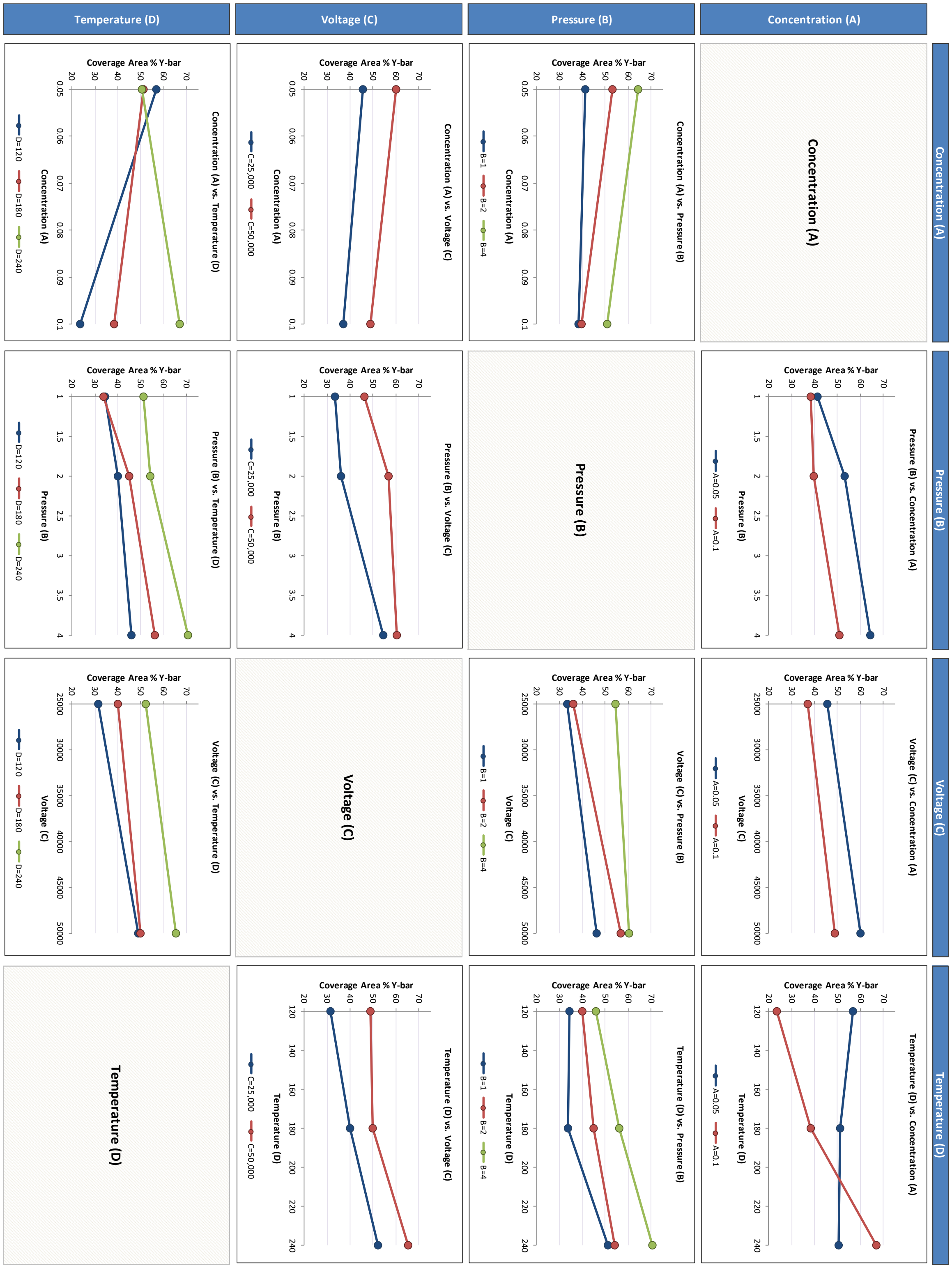

Appendix D – DOE Interaction Charts – Rapeseed Oil

Table 85: Rapeseed Oil & Sunflower Lecithin @ 19Ga Interaction chart on Sample Weight Y-bar

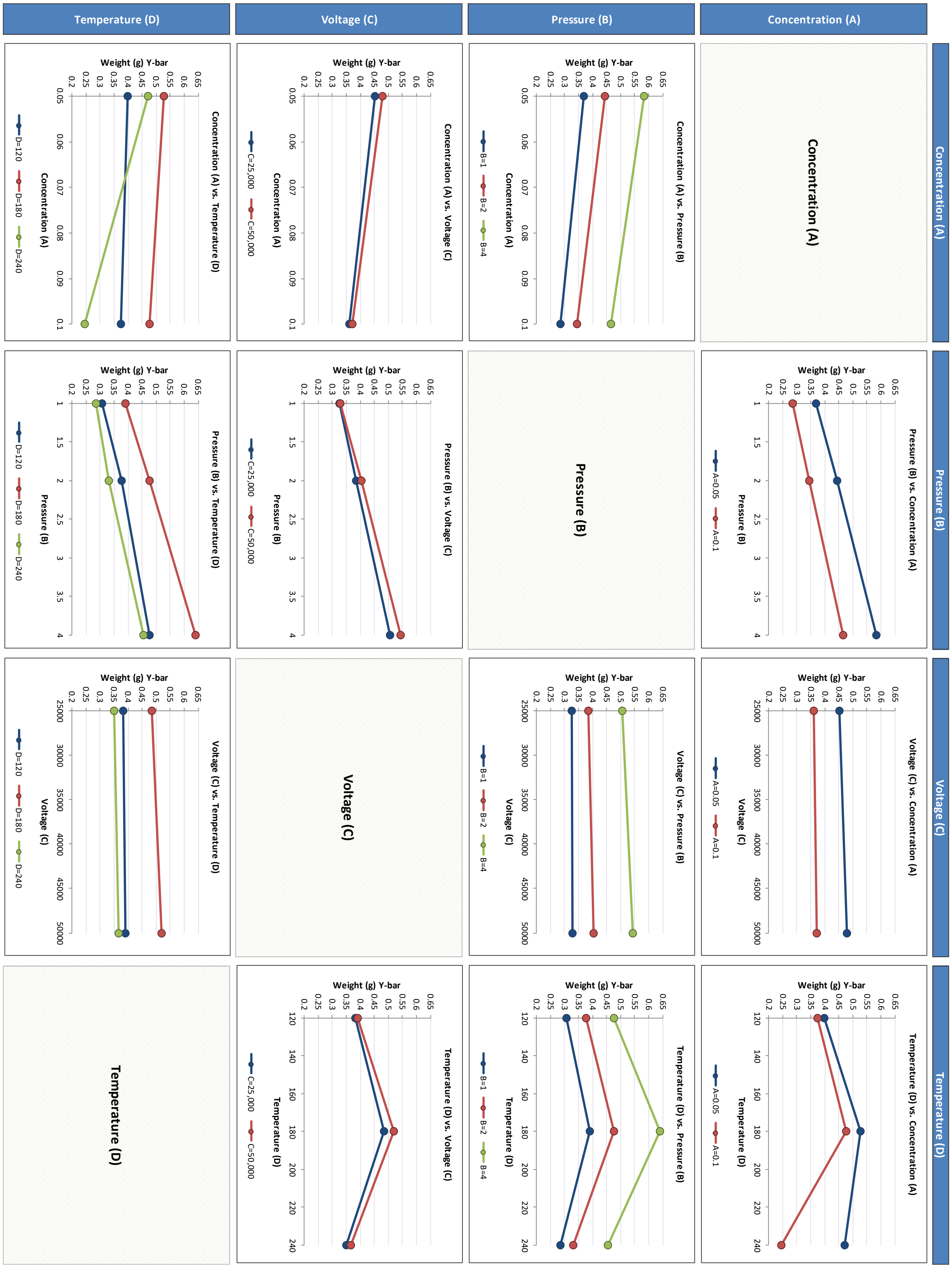

Table 86: Rapeseed Oil & Polysorbate 20 @ 19Ga Interaction chart on Droplet Count Y-bar

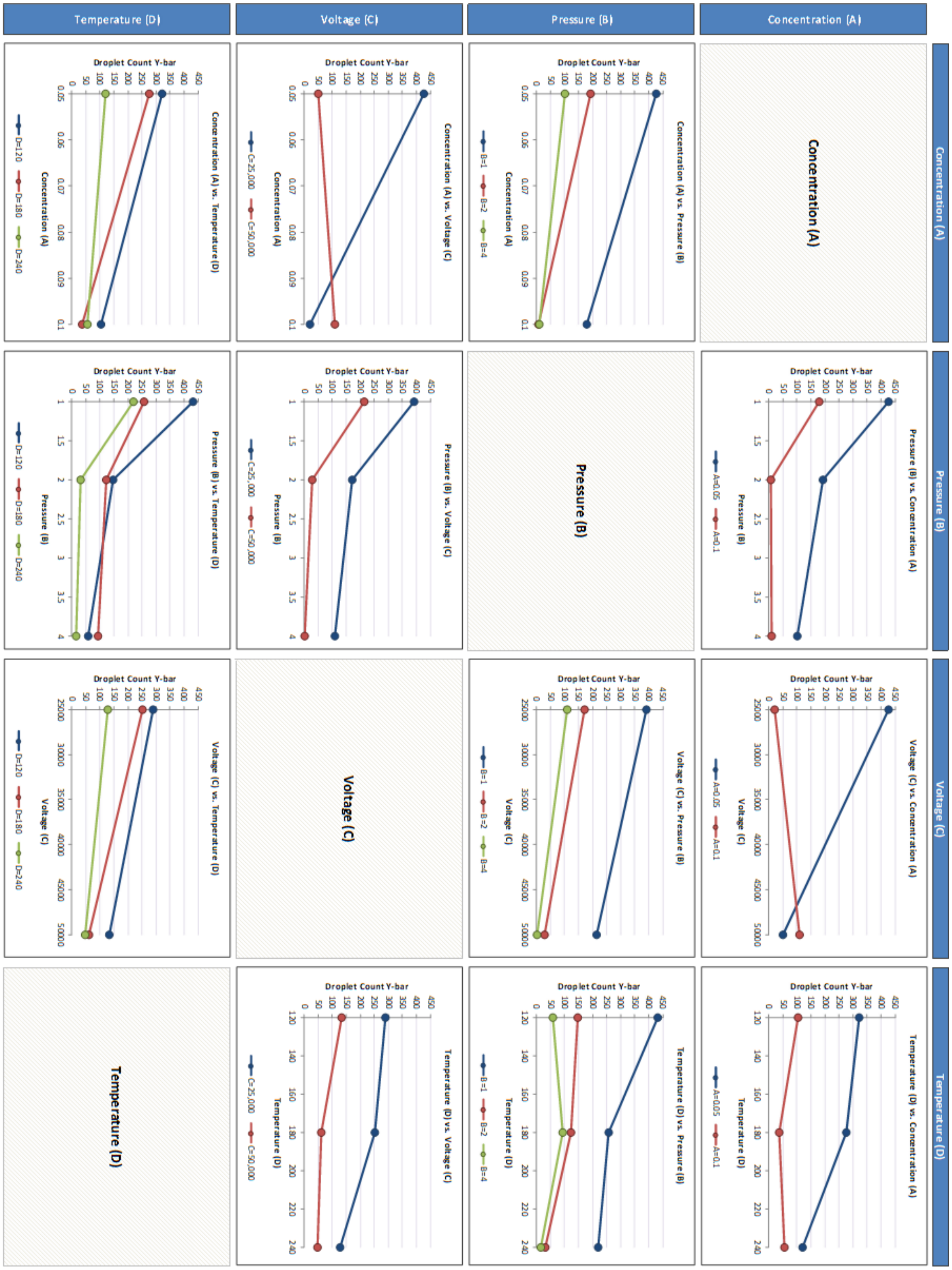

Appendix D – DOE Interaction Charts – Rapeseed Oil

Table 87: Rapeseed Oil & Polysorbate 20 @ 19Ga Interaction chart on Droplet Size Y-bar

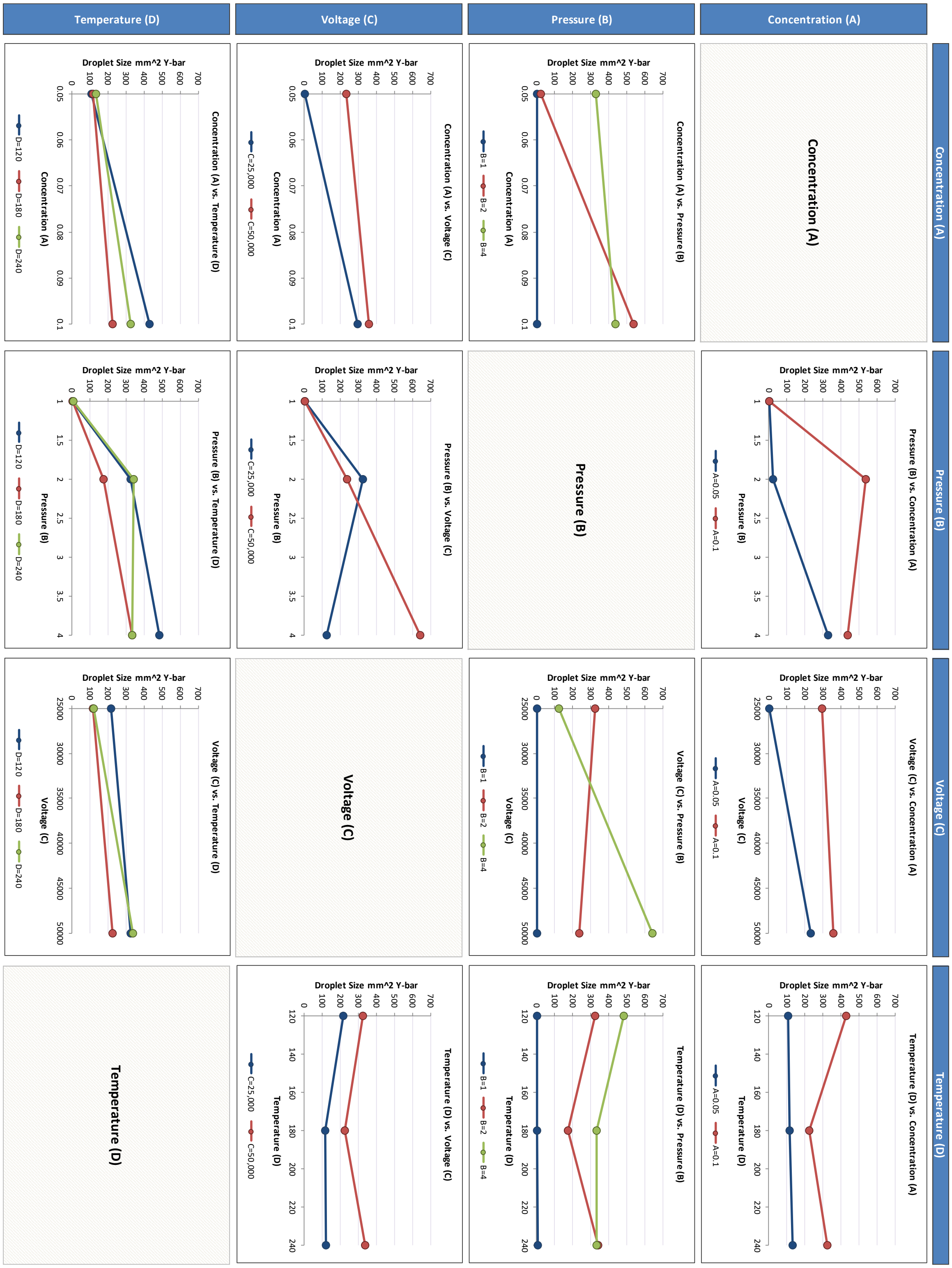

Appendix D – DOE Interaction Charts – Rapeseed Oil

Table 88: Rapeseed Oil & Polysorbate 20 @ 19Ga Interaction chart on Coverage Area Y-bar

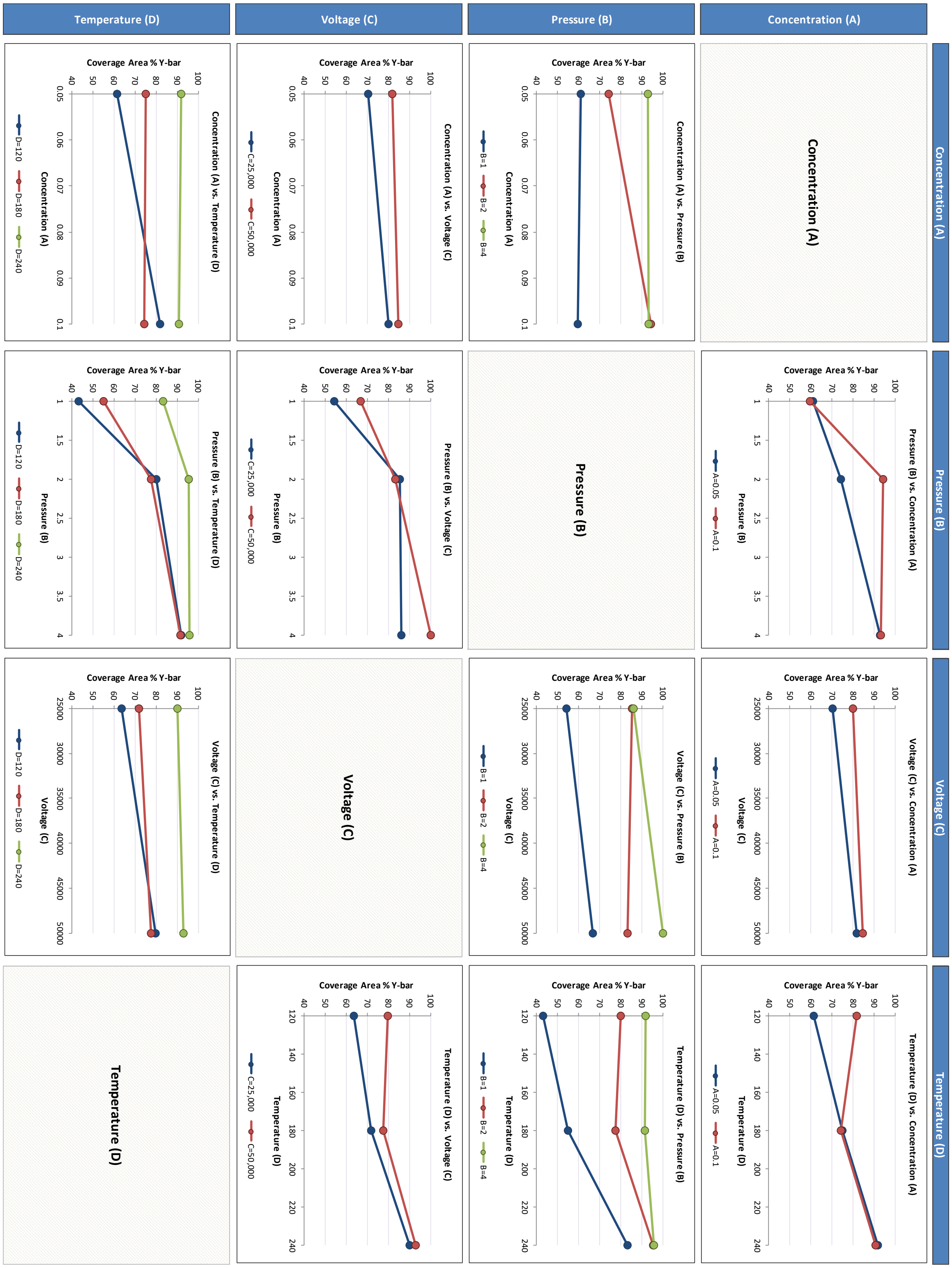

Appendix D – DOE Interaction Charts – Rapeseed Oil

Table 89: Rapeseed Oil & Polysorbate 20 @ 19Ga Interaction chart on Sample Weight Y-bar

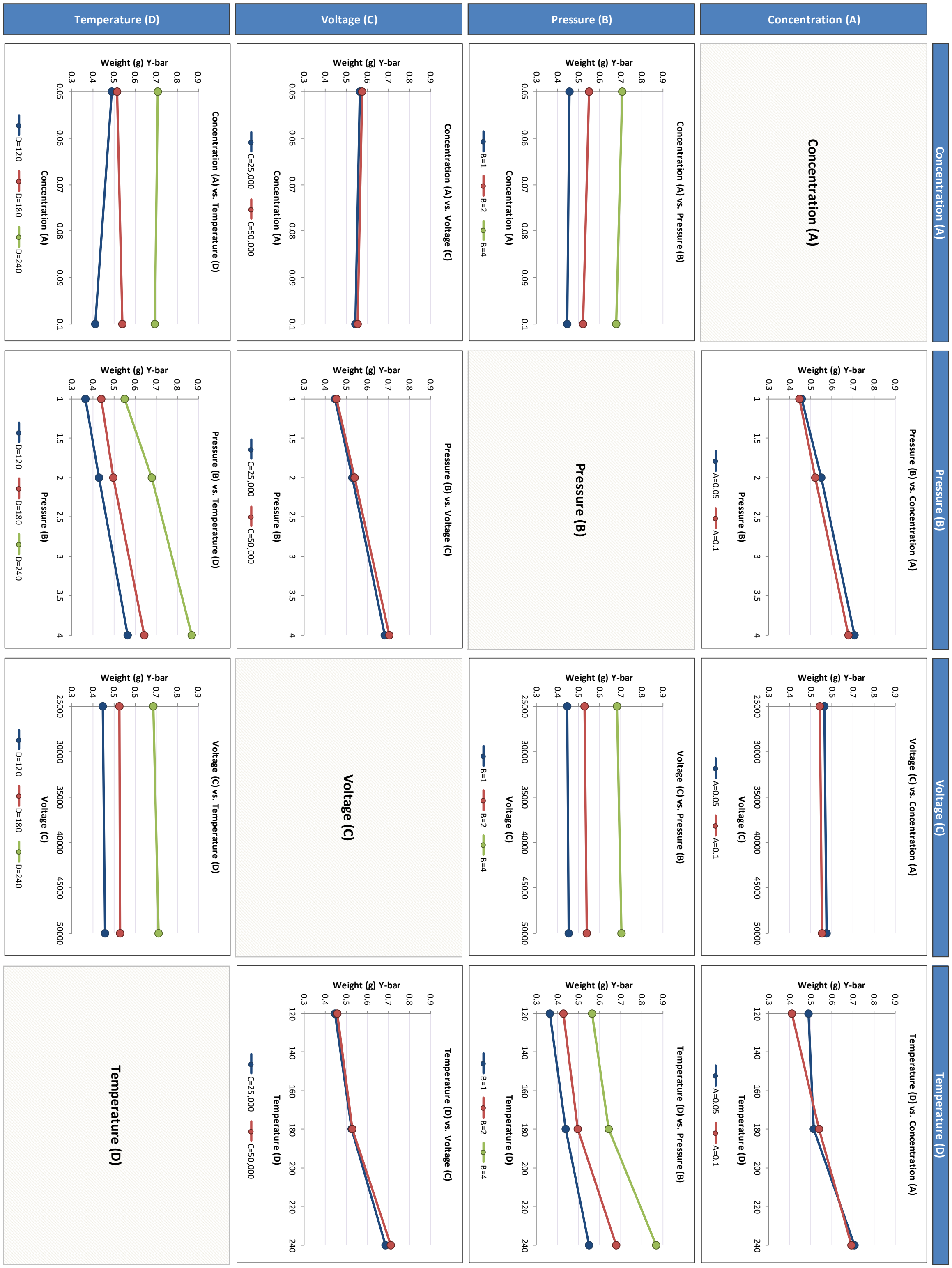

Appendix D – DOE Interaction Charts – Rapeseed Oil

Table 90: Rapeseed Oil & Propylene Glycol @ 19Ga Interaction chart on Droplet Count Y-bar

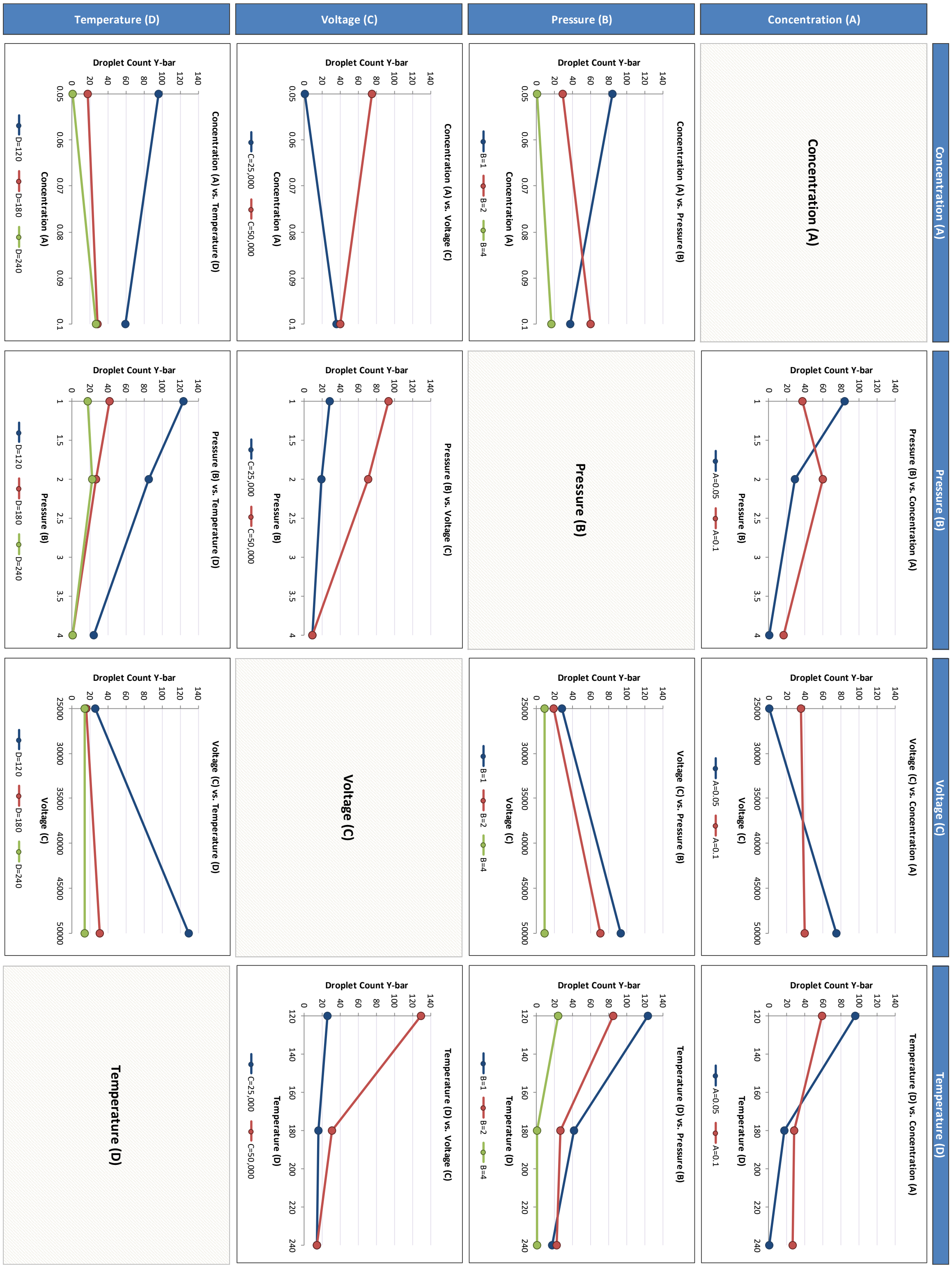

Appendix D – DOE Interaction Charts – Rapeseed Oil

Table 91: Rapeseed Oil & Propylene Glycol @ 19Ga Interaction chart on Droplet Size Y-bar

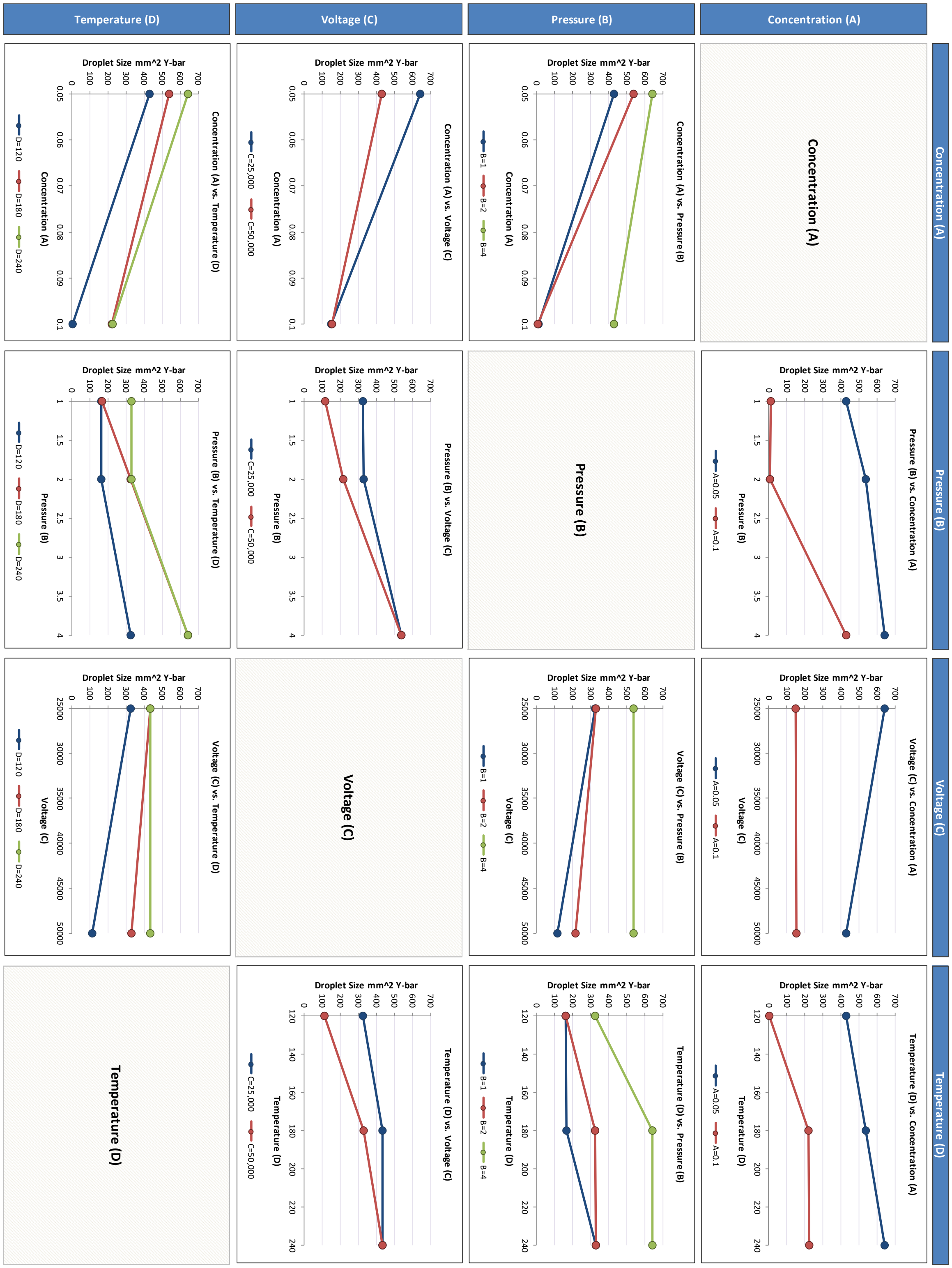

Appendix D – DOE Interaction Charts – Rapeseed Oil

Table 92: Rapeseed Oil & Propylene Glycol @ 19Ga Interaction chart on Coverage Area Y-bar

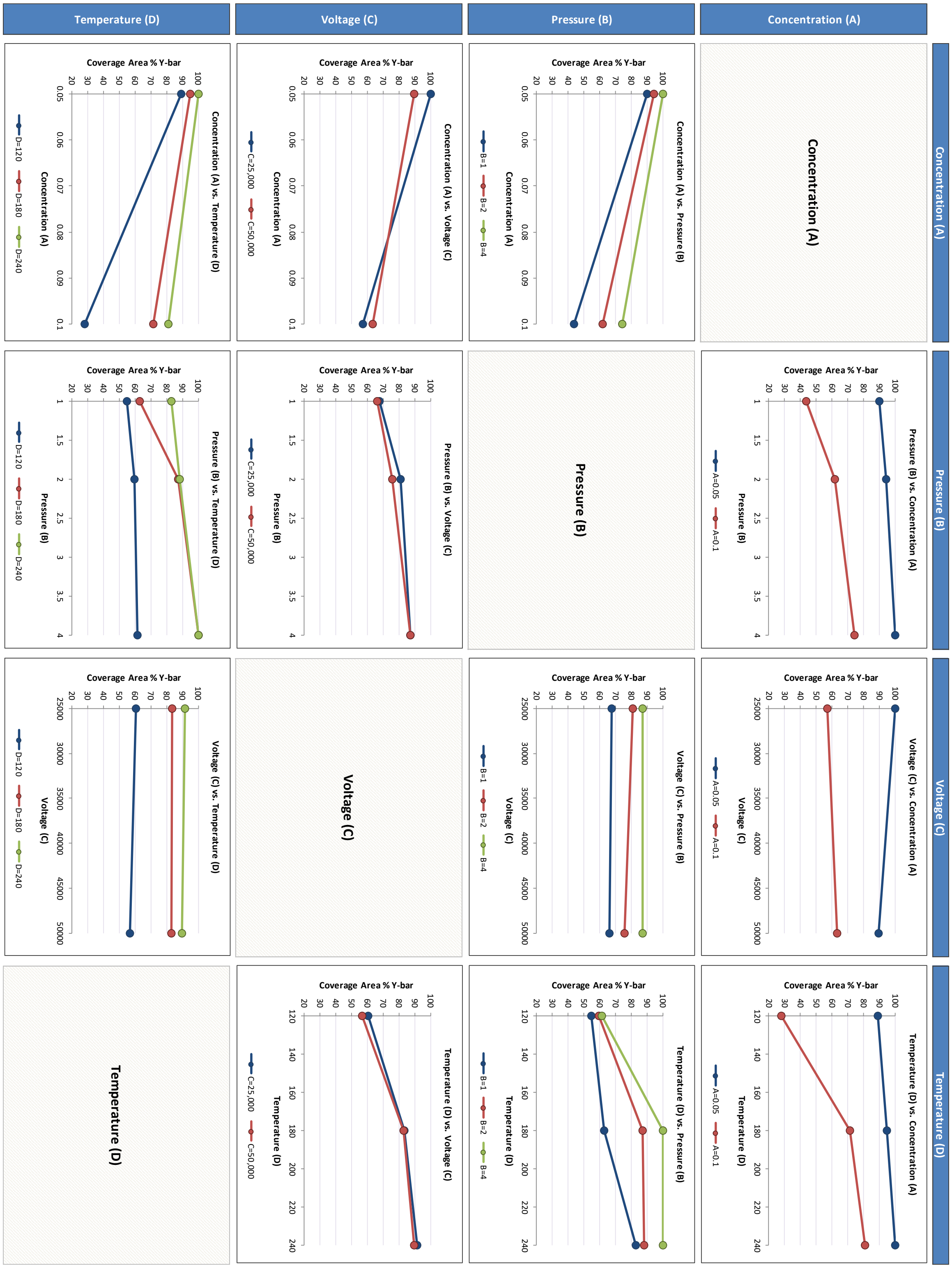

Appendix D – DOE Interaction Charts – Rapeseed Oil

Table 93: Rapeseed Oil & Propylene Glycol @ 19Ga Interaction chart on Sample Weight Y-bar

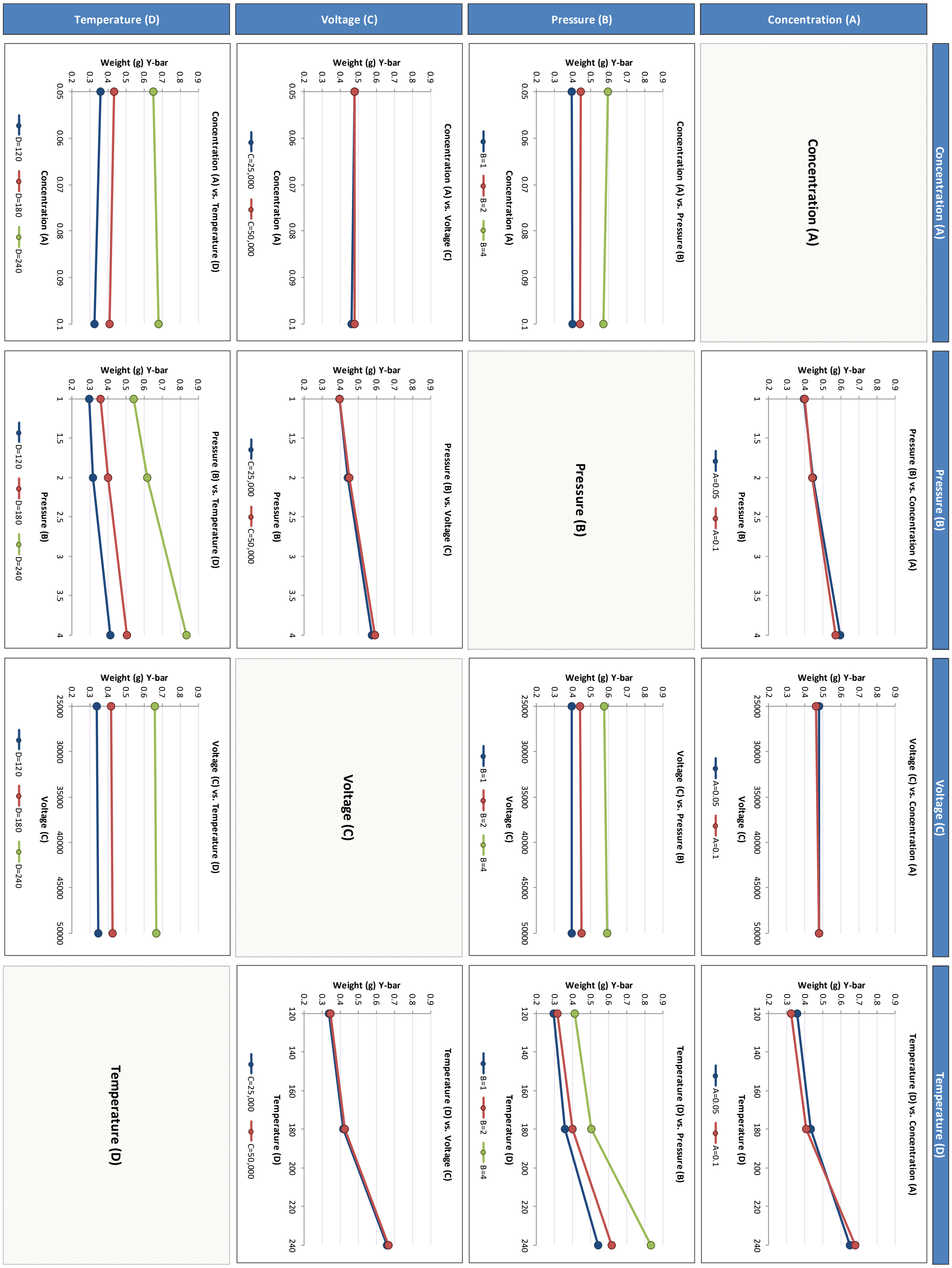

Appendix D – DOE Interaction Charts – Rapeseed Oil

Table 94: Rapeseed Oil & Sunflower Lecithin @ 22Ga Interaction chart on Droplet Count Y-bar

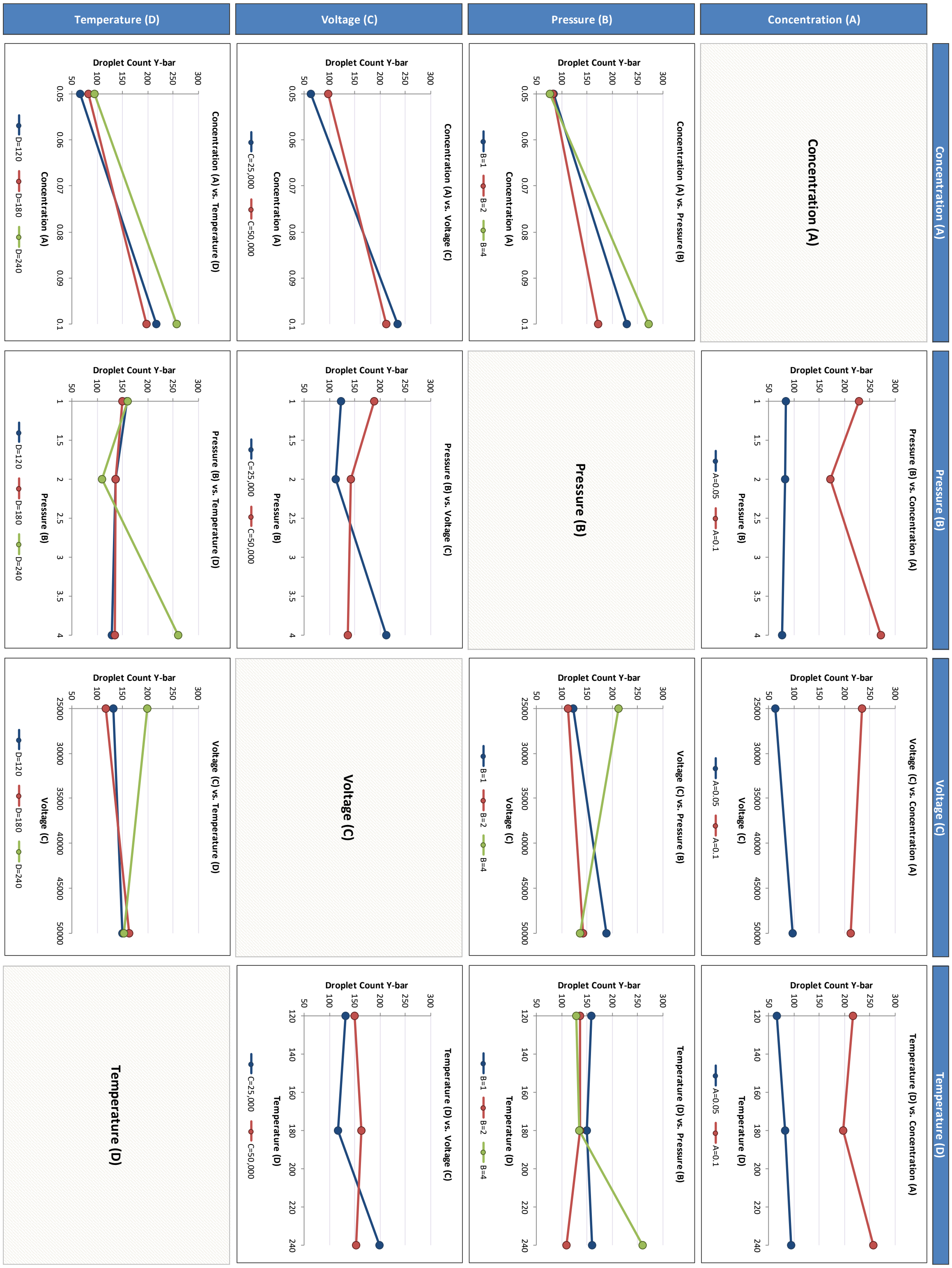

Appendix D – DOE Interaction Charts – Rapeseed Oil

Table 95: Rapeseed Oil & Sunflower Lecithin @ 22Ga Interaction chart on Droplet Size Y-bar

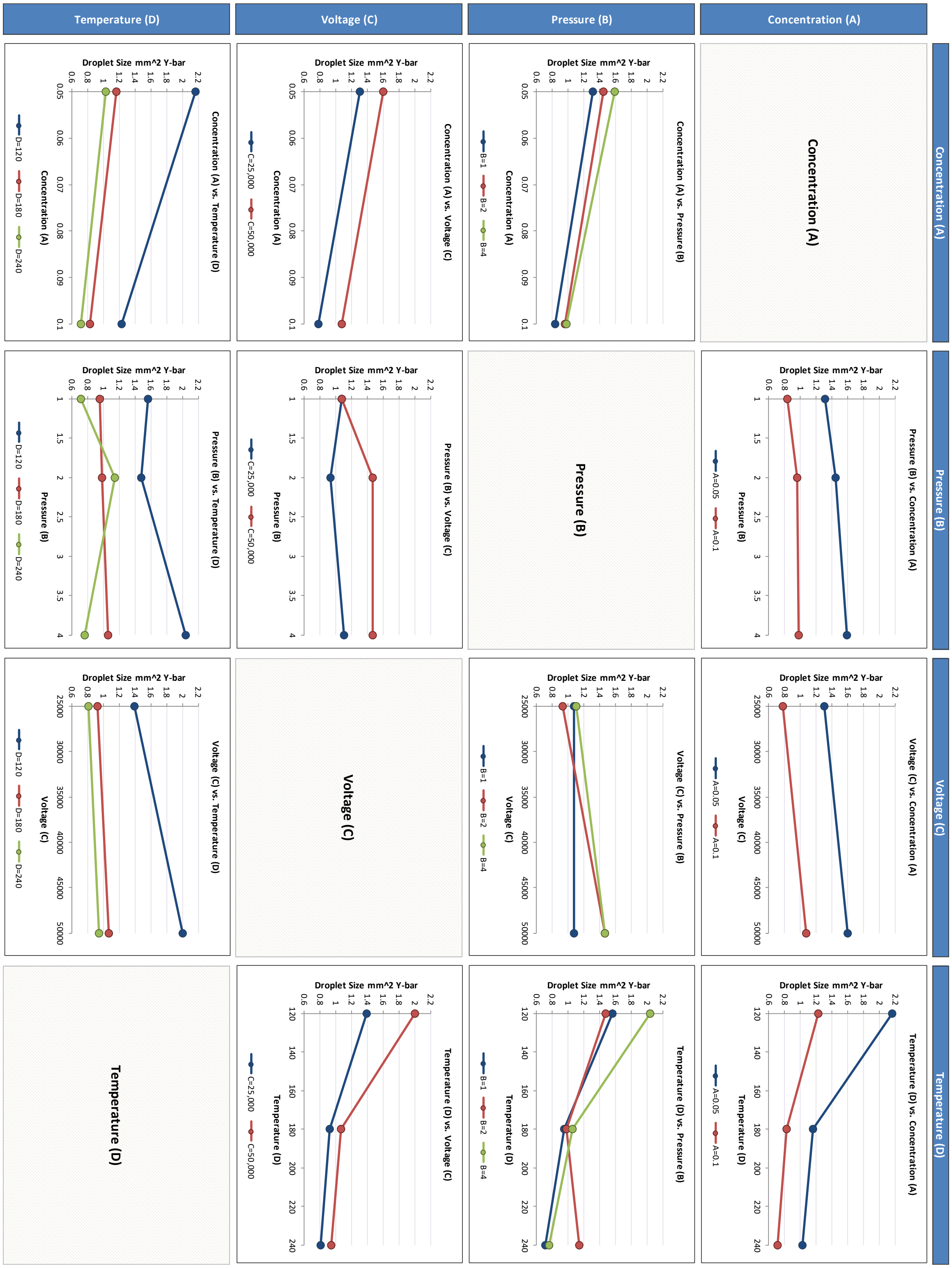

Appendix D – DOE Interaction Charts – Rapeseed Oil

Table 96: Rapeseed Oil & Sunflower Lecithin @ 22Ga Interaction chart on Coverage Area Y-bar

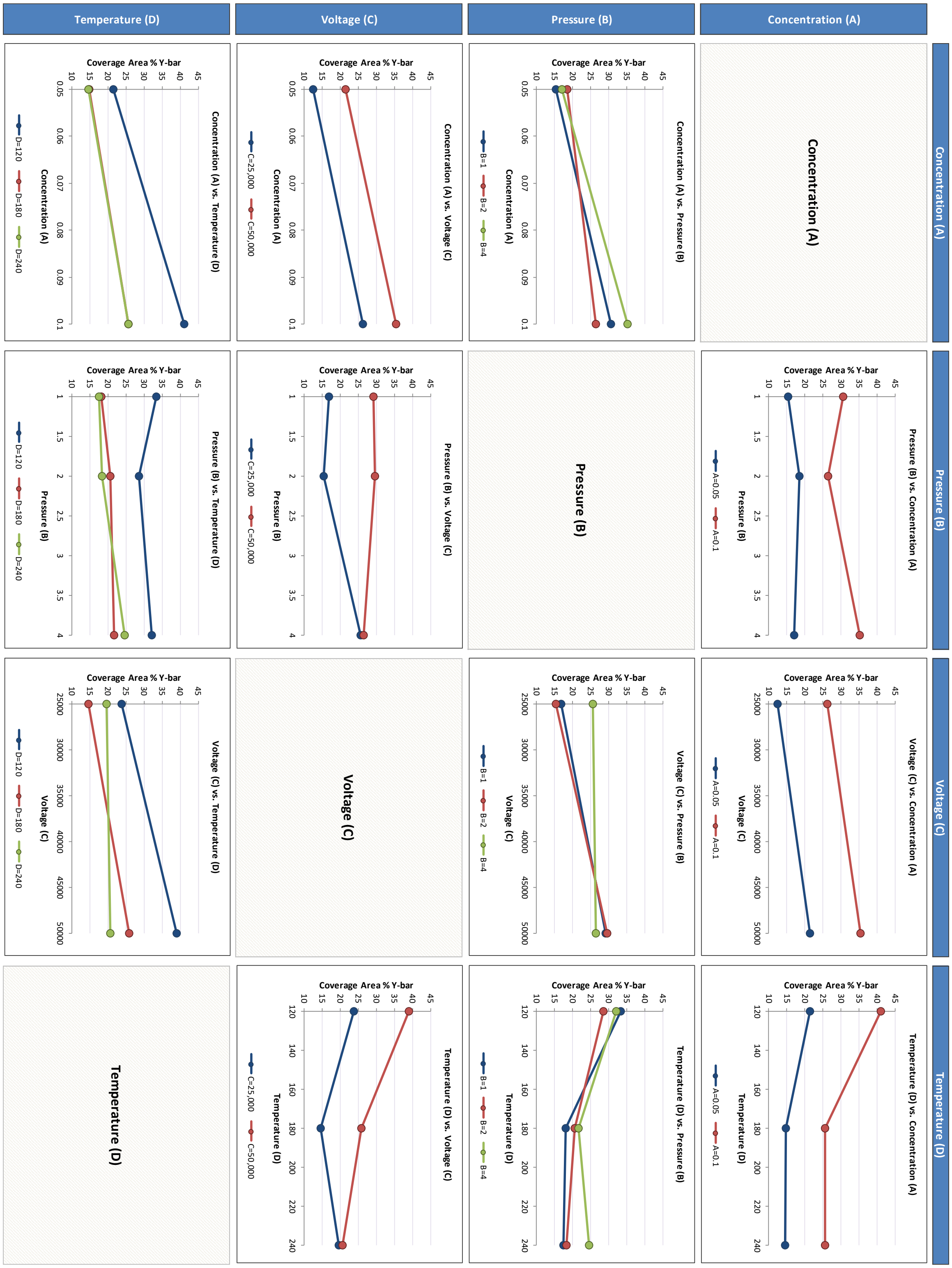

Appendix D – DOE Interaction Charts – Rapeseed Oil

Table 97: Rapeseed Oil & Sunflower Lecithin @ 22Ga Interaction chart on Sample Weight Y-bar

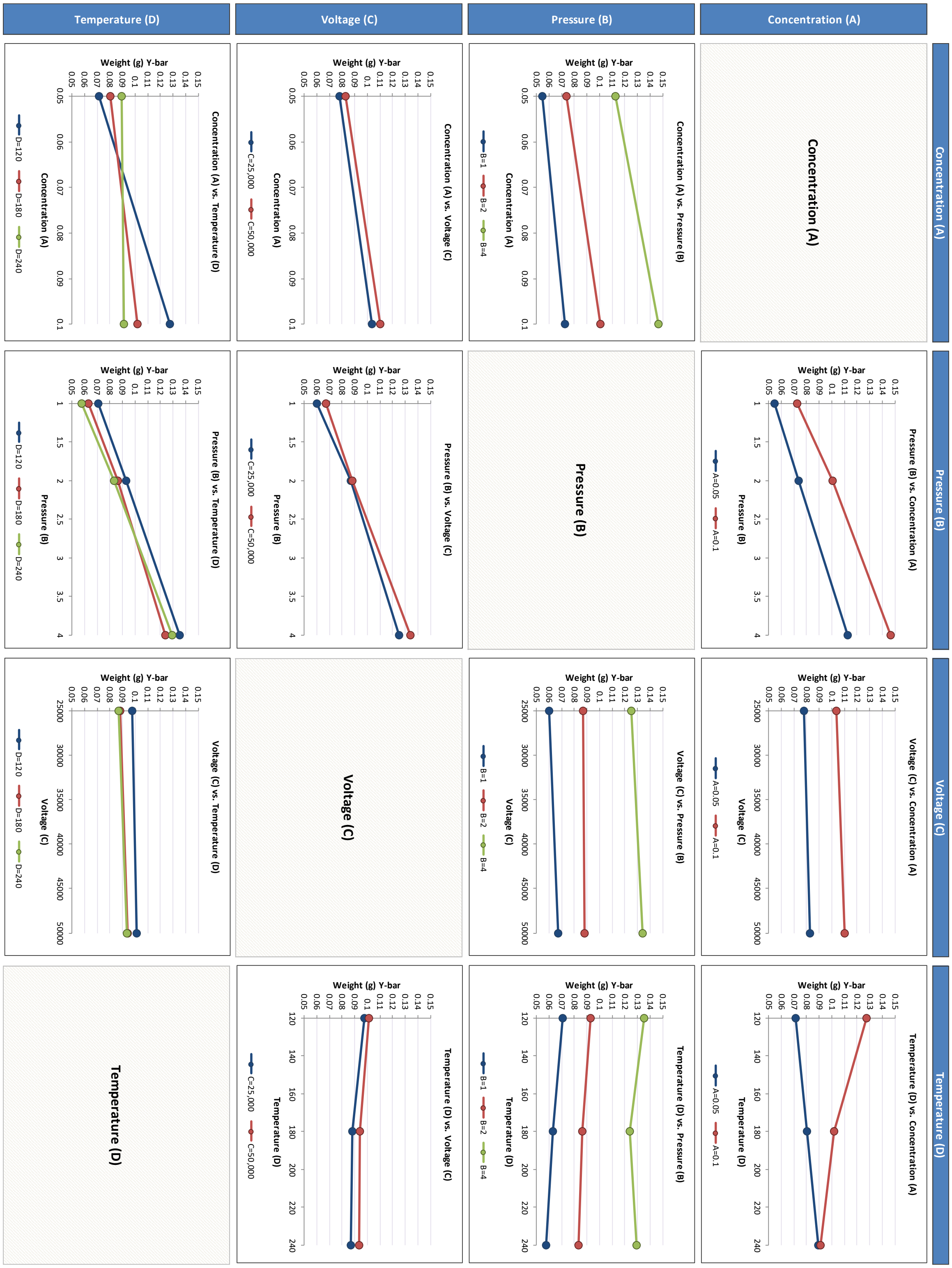

Appendix D – DOE Interaction Charts – Rapeseed Oil

Table 98: Rapeseed Oil & Polysorbate 20 @ 22Ga Interaction chart on Droplet Count Y-bar

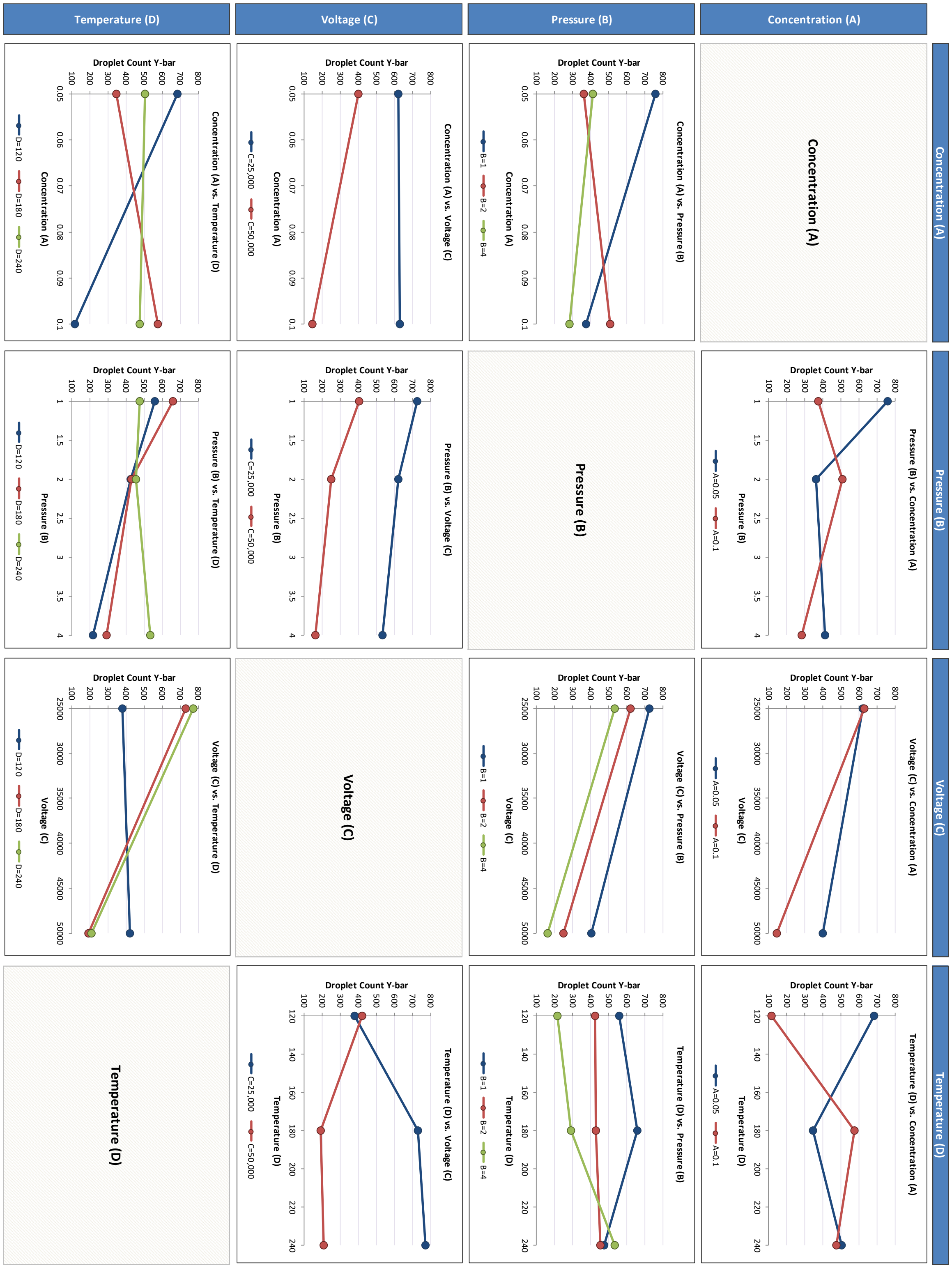

Appendix D – DOE Interaction Charts – Rapeseed Oil

Table 99: Rapeseed Oil & Polysorbate 20 @ 22Ga Interaction chart on Droplet Size Y-bar

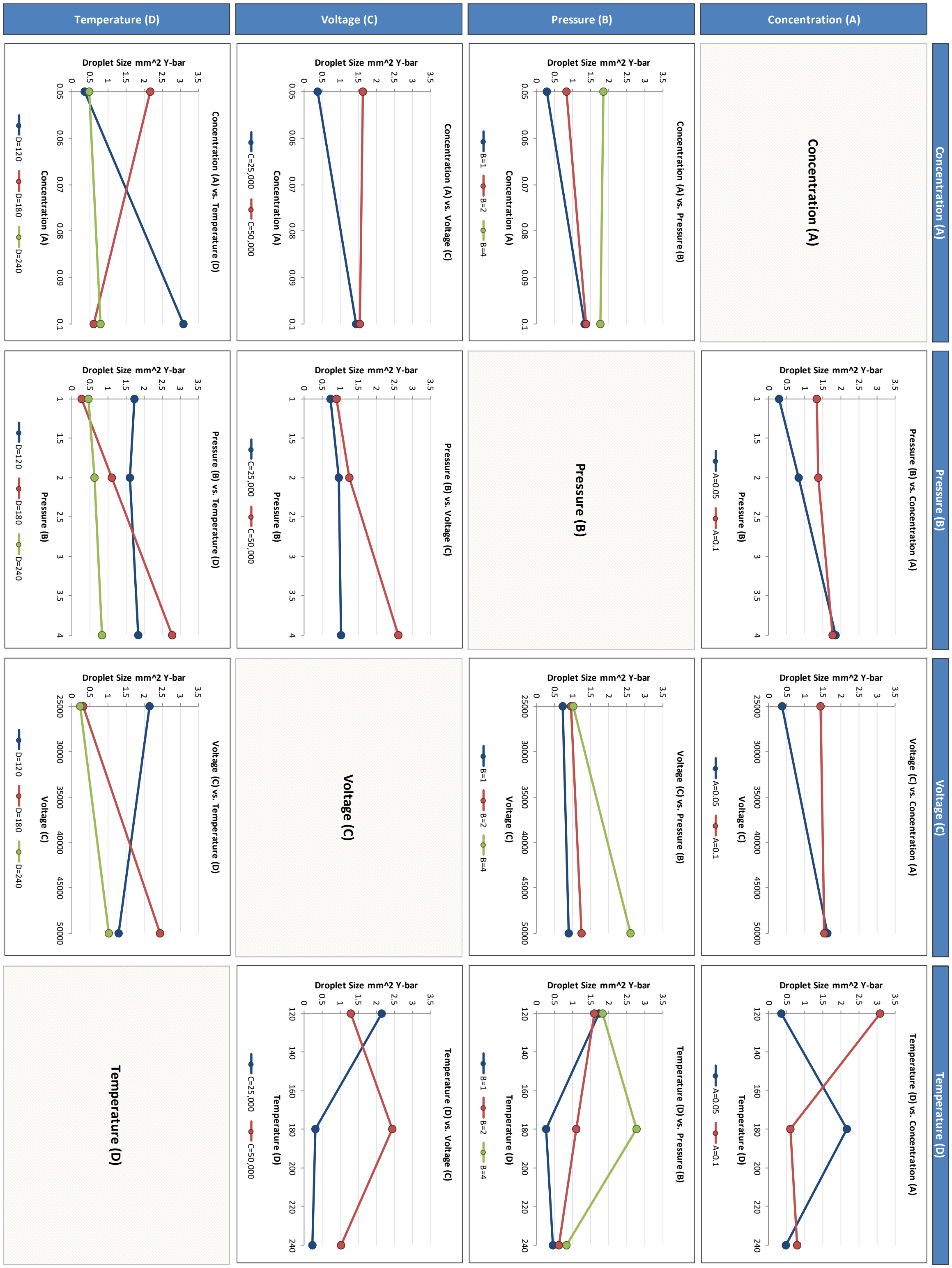

Appendix D – DOE Interaction Charts – Rapeseed Oil

Table 100: Rapeseed Oil & Polysorbate 20 @ 22Ga Interaction chart on Coverage Area Y-bar

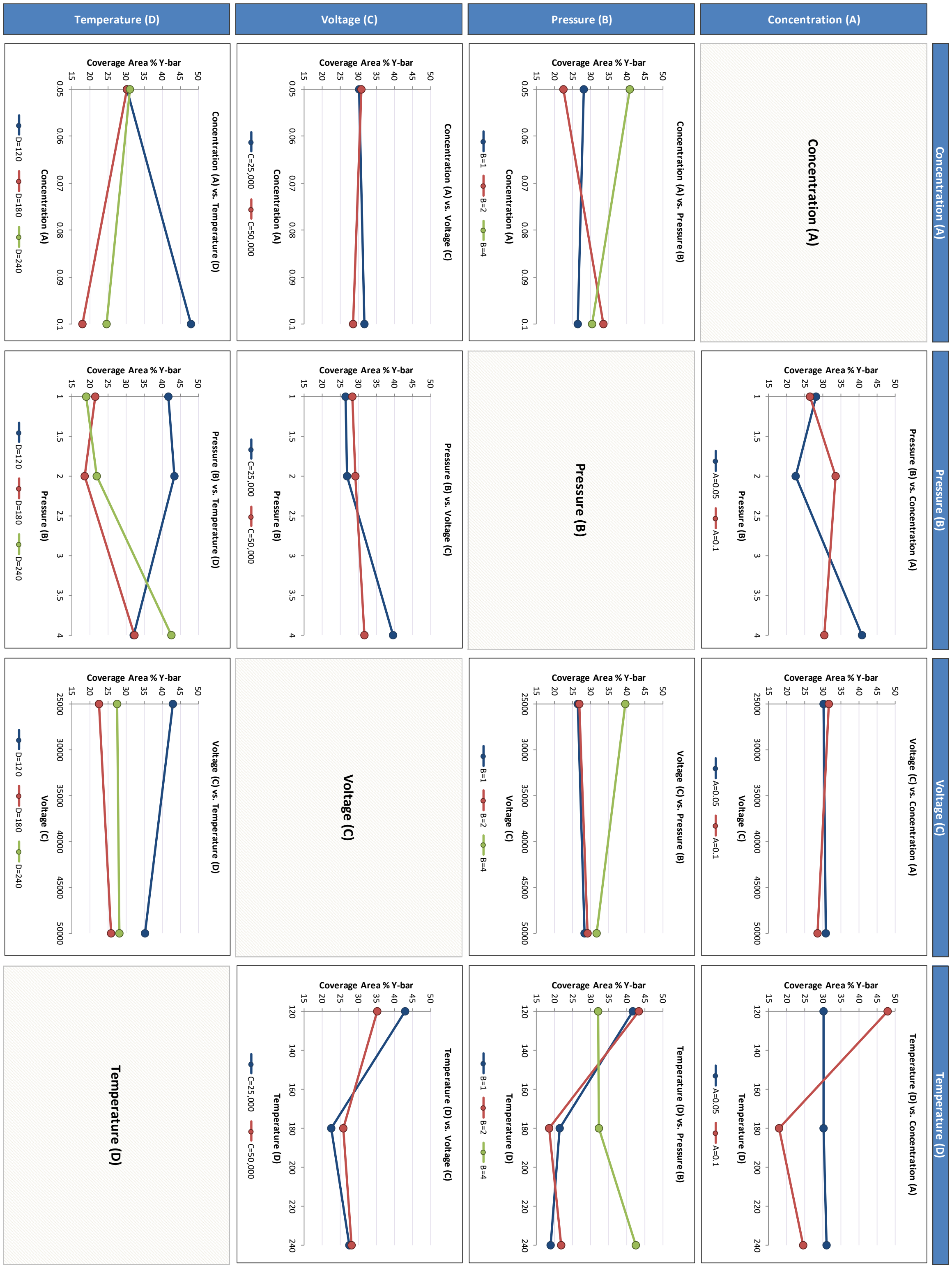

Appendix D – DOE Interaction Charts – Rapeseed Oil

Table 101: Rapeseed Oil & Polysorbate 20 @ 22Ga Interaction chart on Sample Weight Y-bar

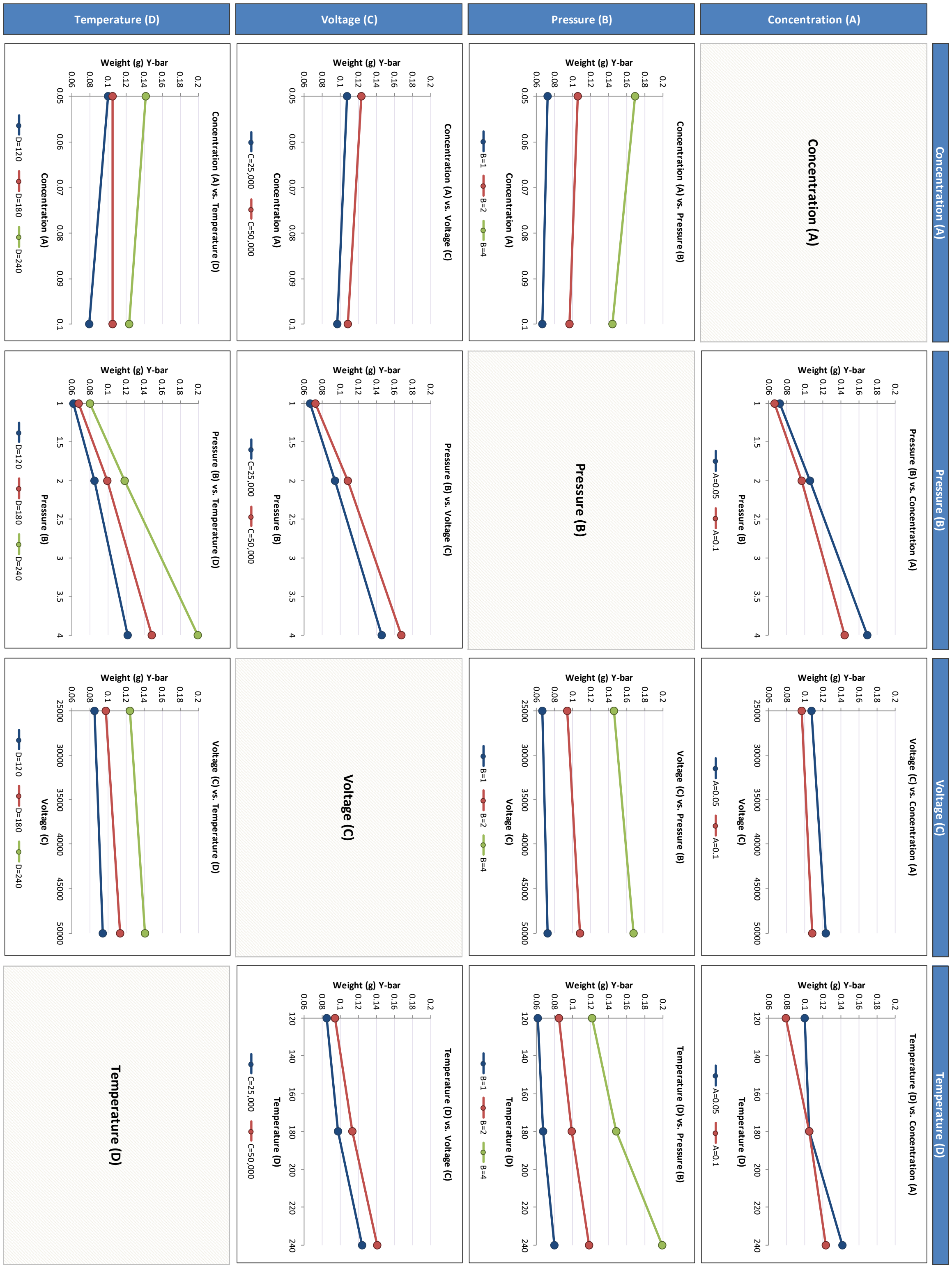

Appendix D – DOE Interaction Charts – Rapeseed Oil

Table 102: Rapeseed Oil & Propylene Glycol @ 22Ga Interaction chart on Droplet Count Y-bar

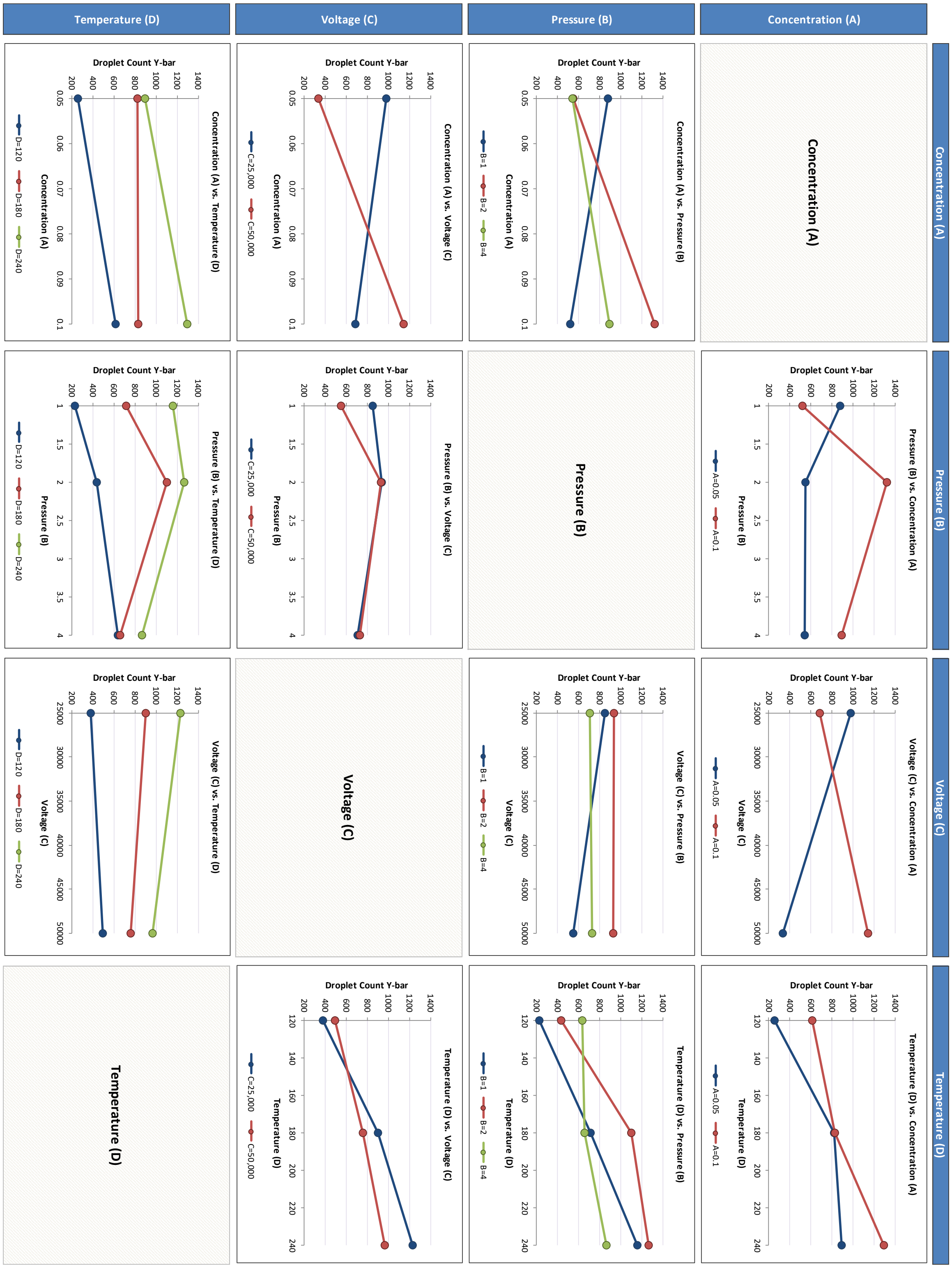

Appendix D – DOE Interaction Charts – Rapeseed Oil

Table 103: Rapeseed Oil & Propylene Glycol @ 22Ga Interaction chart on Droplet Size Y-bar

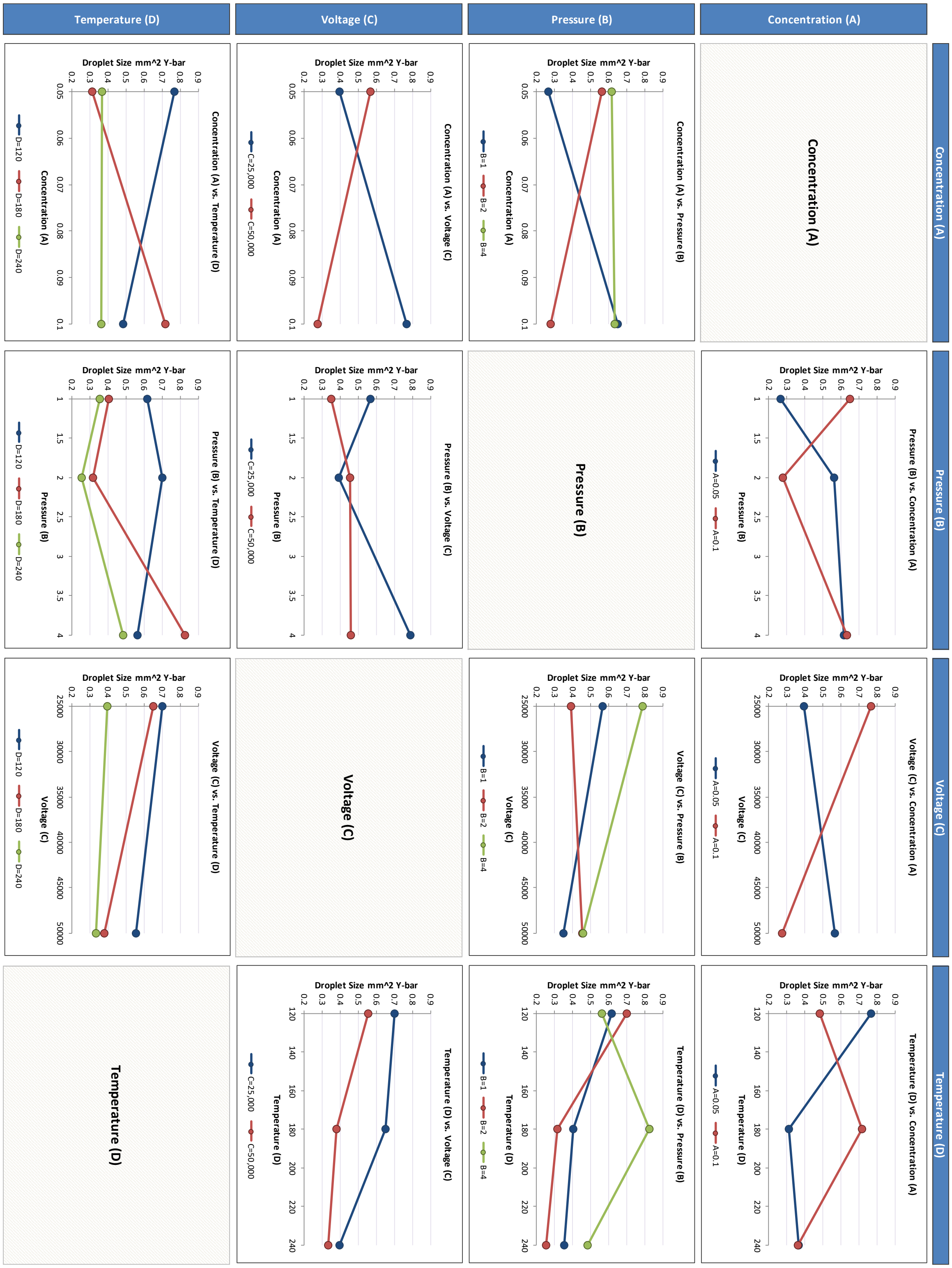

Appendix D – DOE Interaction Charts – Rapeseed Oil

Table 104: Rapeseed Oil & Propylene Glycol @ 22Ga Interaction chart on Coverage Area Y-bar

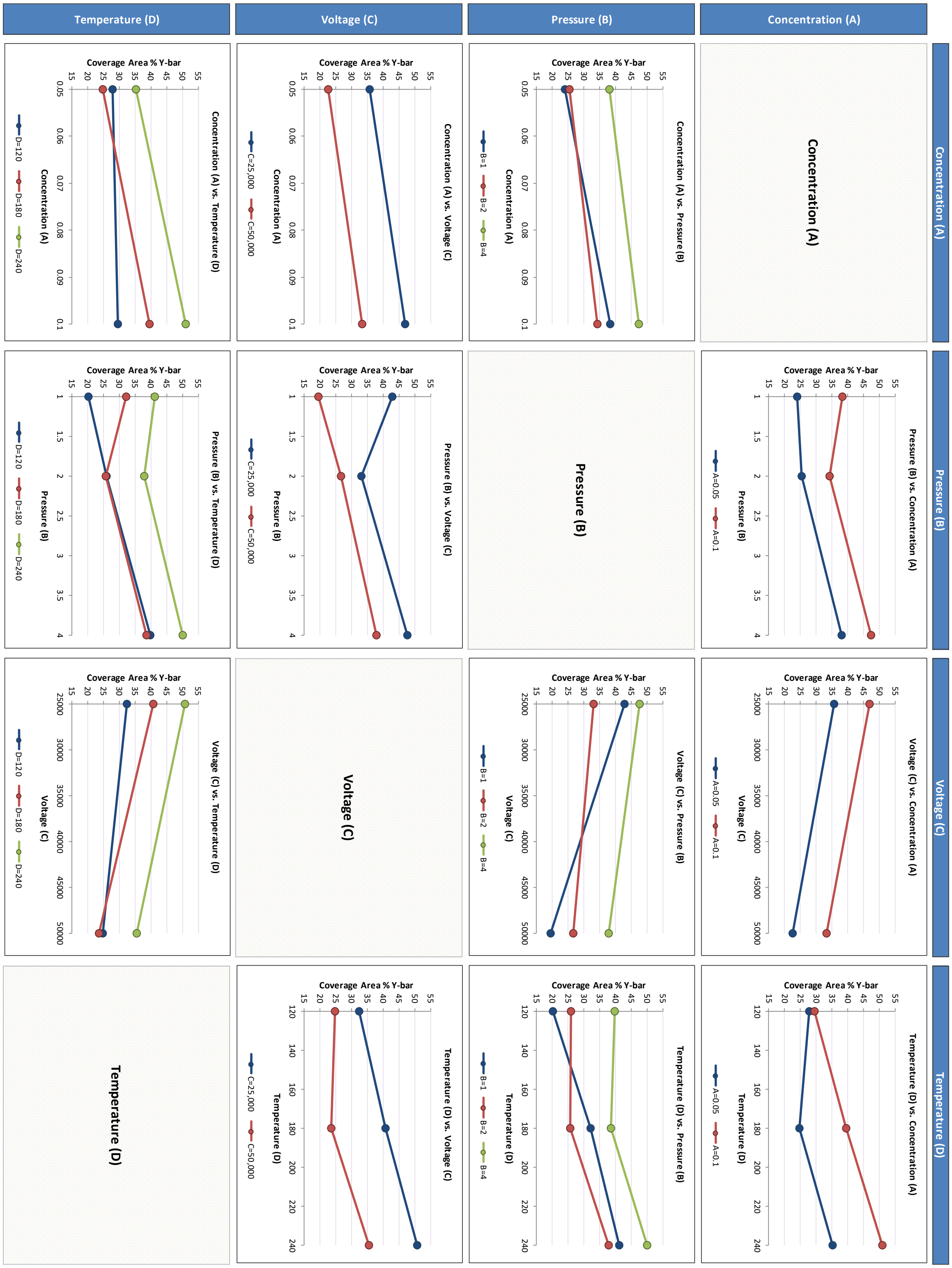

Appendix D – DOE Interaction Charts – Rapeseed Oil

Table 105: Rapeseed Oil & Propylene Glycol @ 19Ga Interaction chart on Sample Weight Y-bar

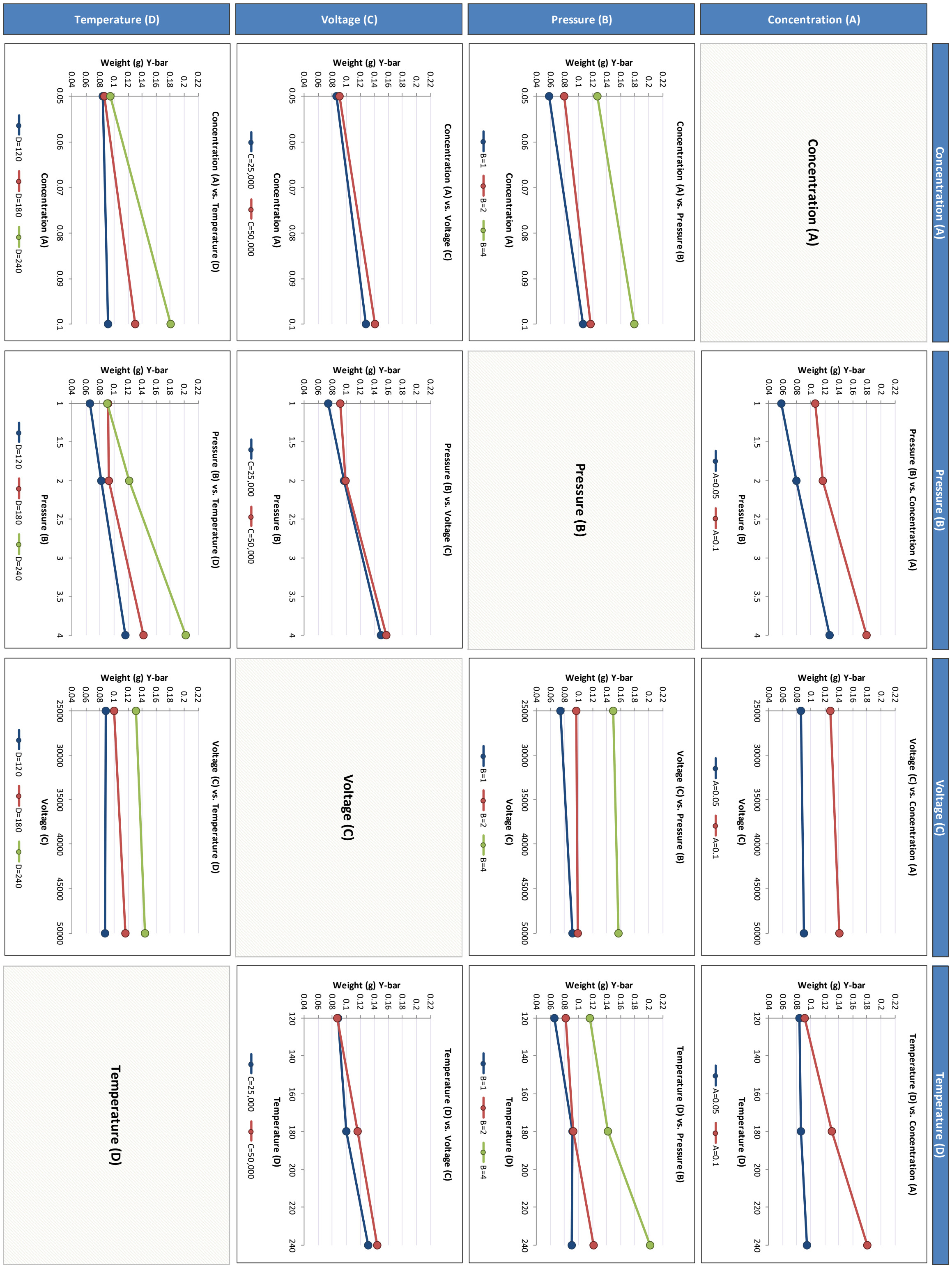

Appendix E – DOE Interaction Charts – Sunflower Oil

Table 106: Sunflower Oil & Sunflower Lecithin @ 19Ga Interaction chart on Droplet Count Y-bar

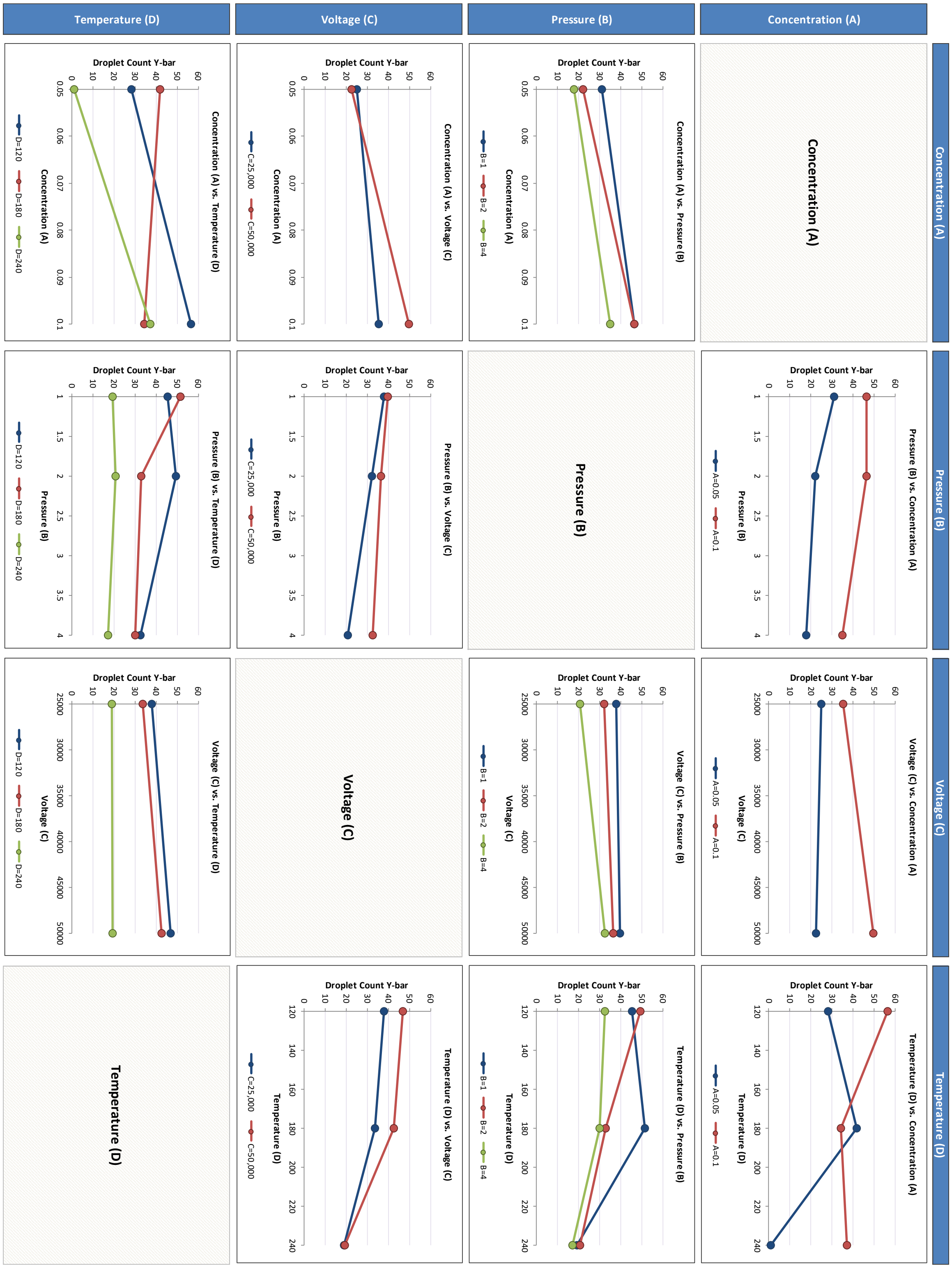

Table 107: Sunflower Oil & Sunflower Lecithin @ 19Ga Interaction chart on Droplet Size Y-bar

Appendix E – DOE Interaction Charts – Sunflower Oil

Table 108: Sunflower Oil & Sunflower Lecithin @ 19Ga Interaction chart on Coverage Area Y-bar

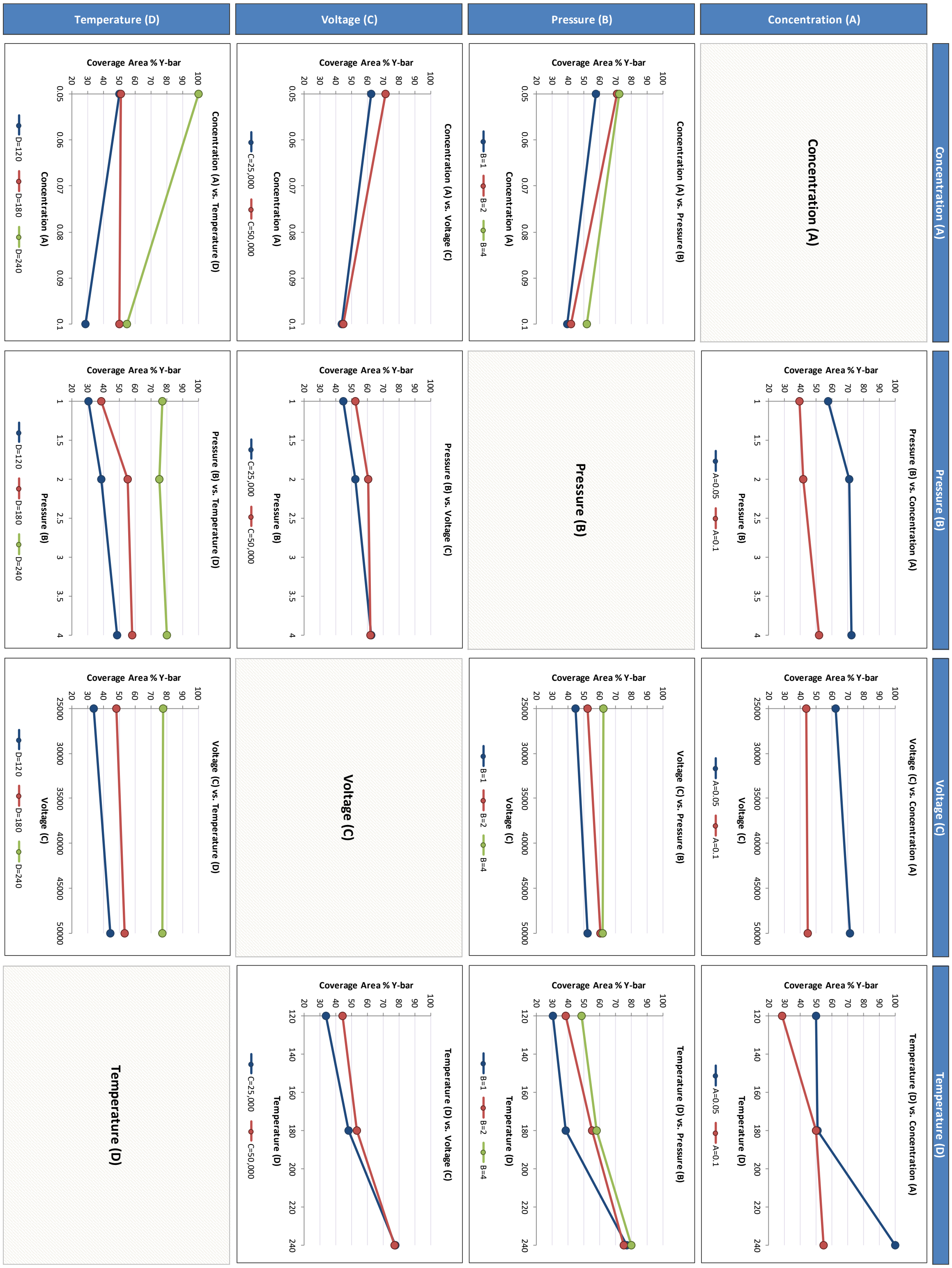

Appendix E – DOE Interaction Charts – Sunflower Oil

Table 109: Sunflower Oil & Sunflower Lecithin @ 22Ga Interaction chart on Sample Weight Y-bar

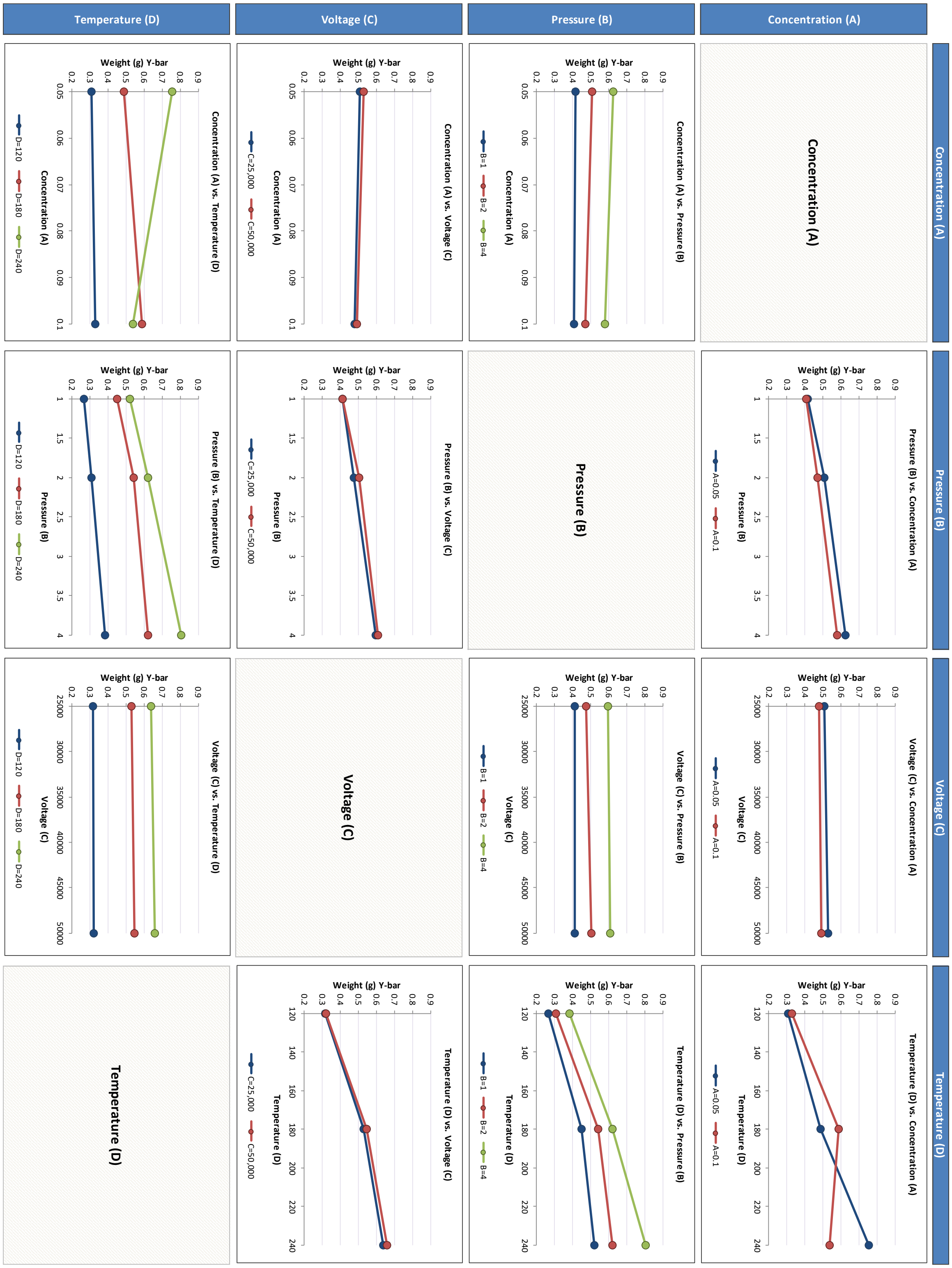

Appendix E – DOE Interaction Charts – Sunflower Oil

Table 110: Sunflower Oil & Polysorbate 80 @ 19Ga Interaction chart on Droplet Count Y-bar

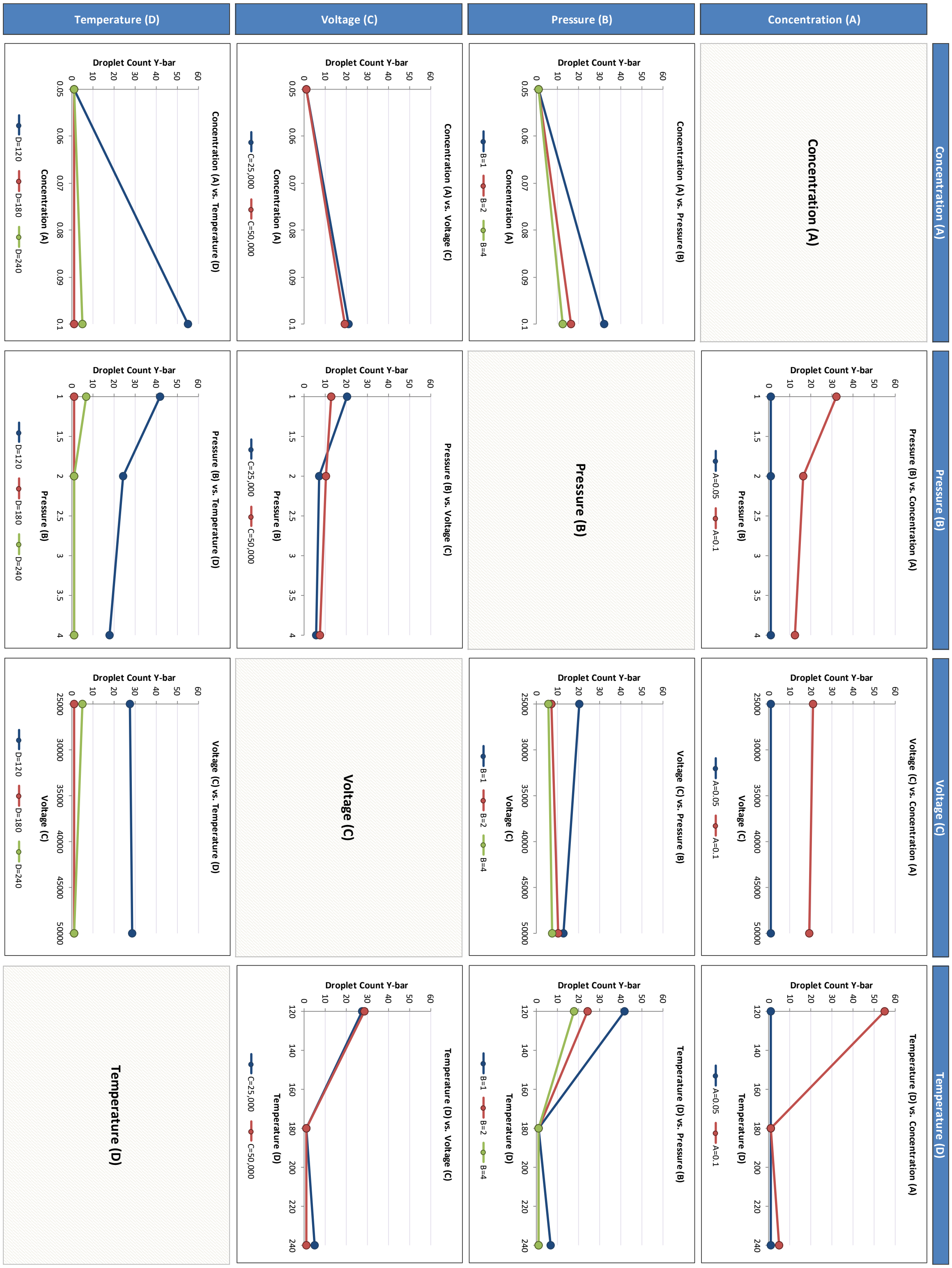

Appendix E – DOE Interaction Charts – Sunflower Oil

Table 111: Sunflower Oil & Polysorbate 80 @ 19Ga Interaction chart on Droplet Size Y-bar

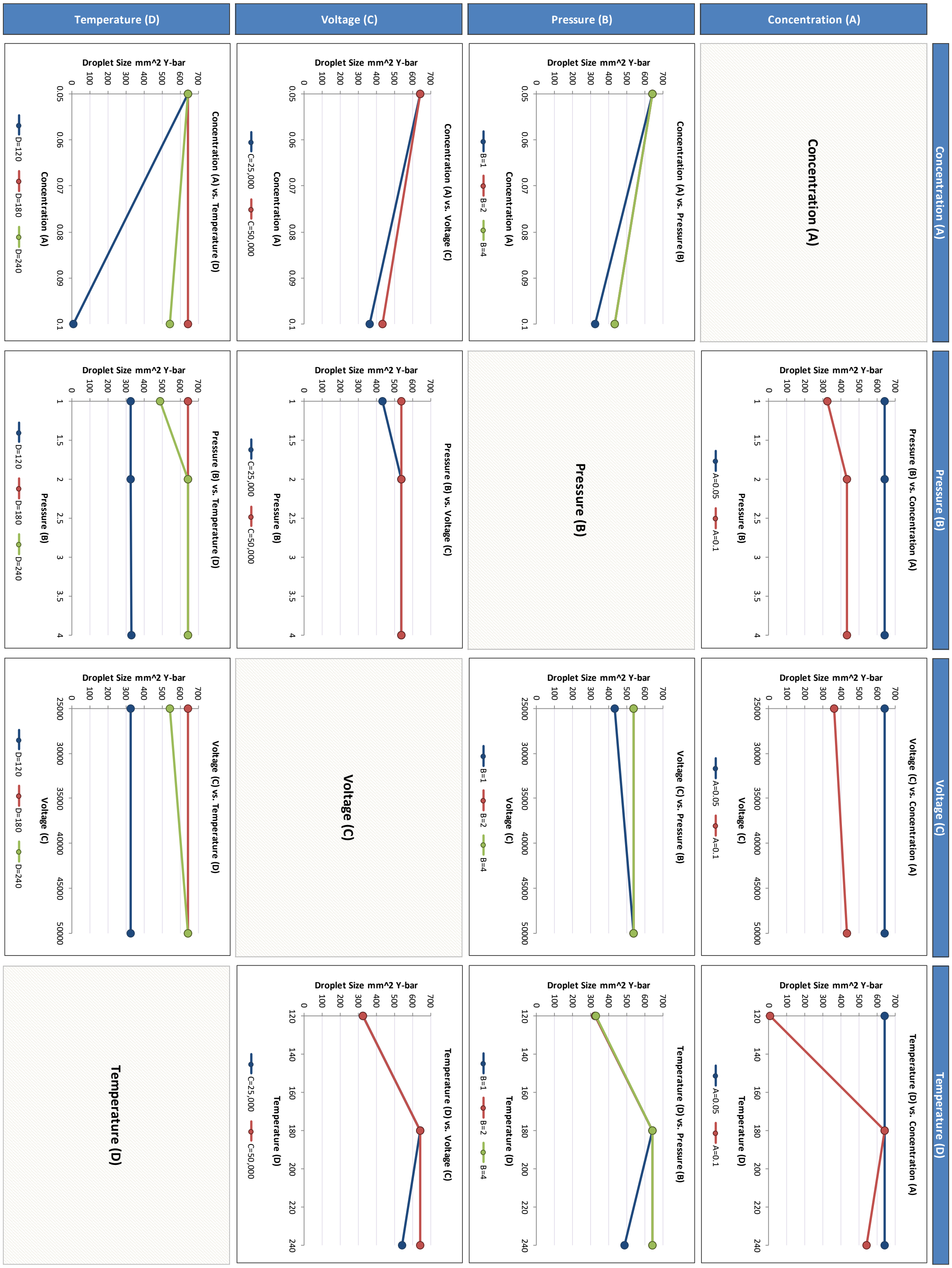

Appendix E – DOE Interaction Charts – Sunflower Oil

Table 112: Sunflower Oil & Polysorbate 80 @ 19Ga Interaction chart on Coverage Area Y-bar

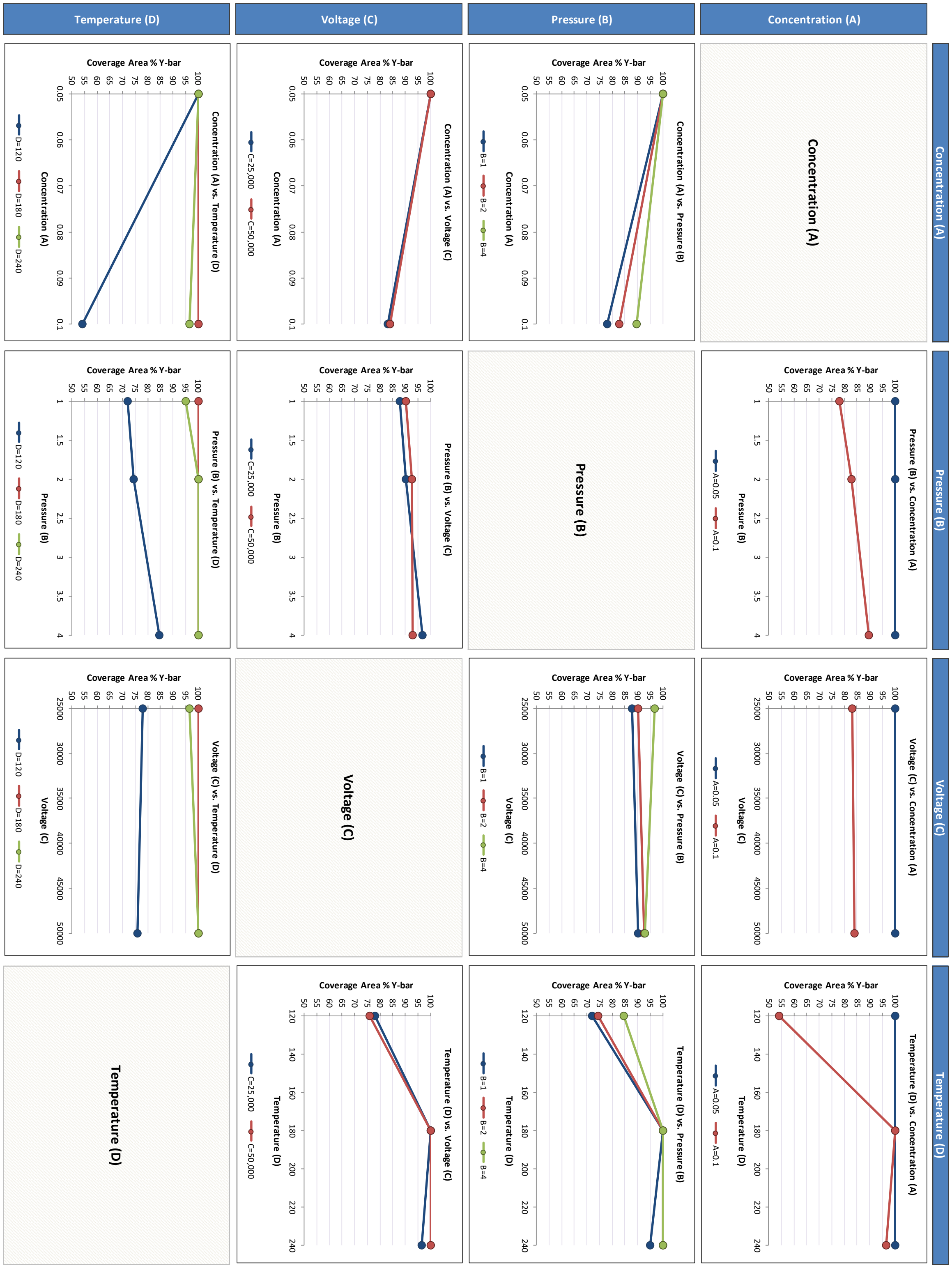

Appendix E – DOE Interaction Charts – Sunflower Oil

Table 113: Sunflower Oil & Polysorbate 80 @ 19Ga Interaction chart on Sample Weight Y-bar

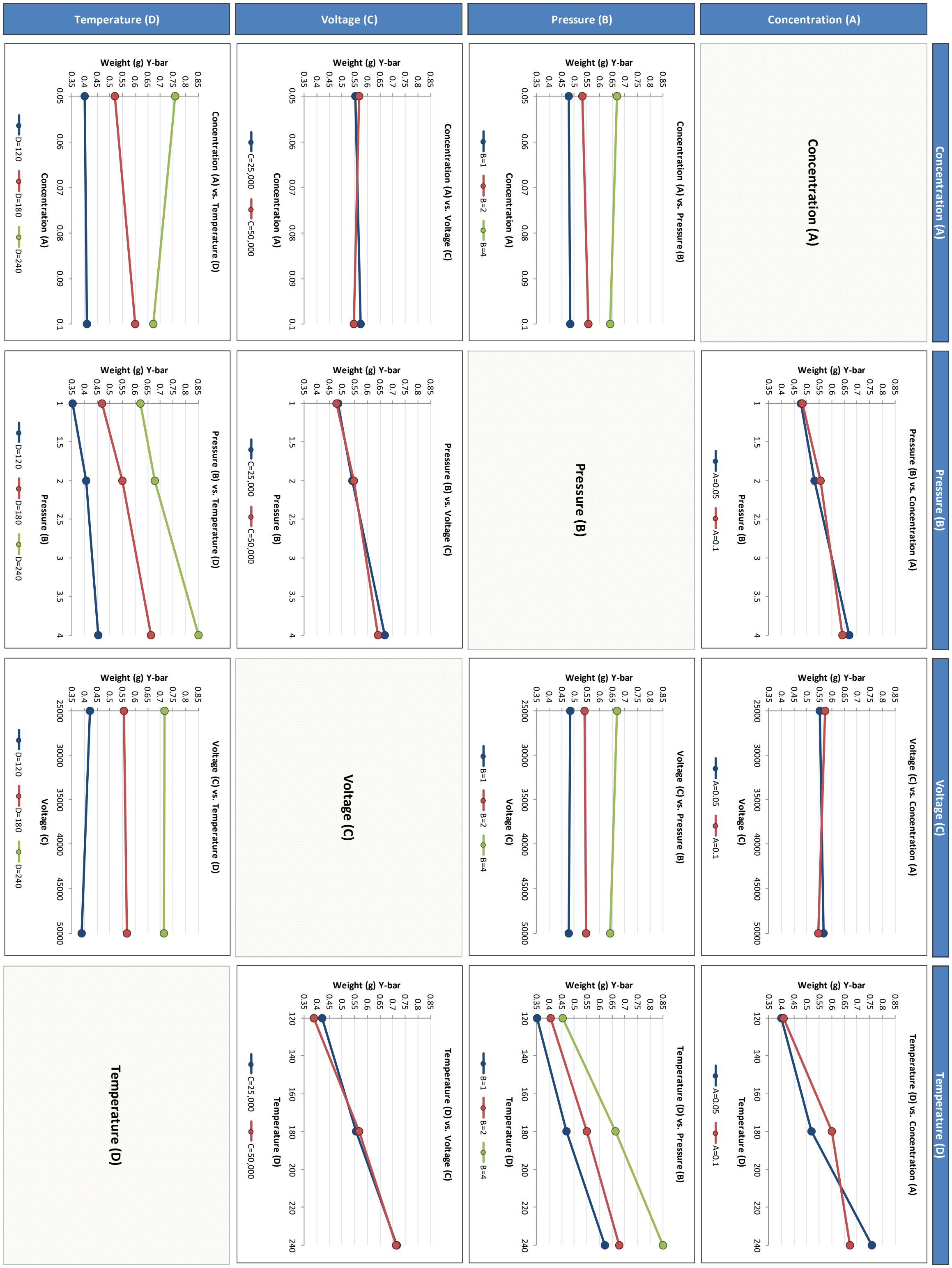

Appendix E – DOE Interaction Charts – Sunflower Oil

Table 114: Sunflower Oil & Propylene Glycol @ 19Ga Interaction chart on Droplet Count Y-bar

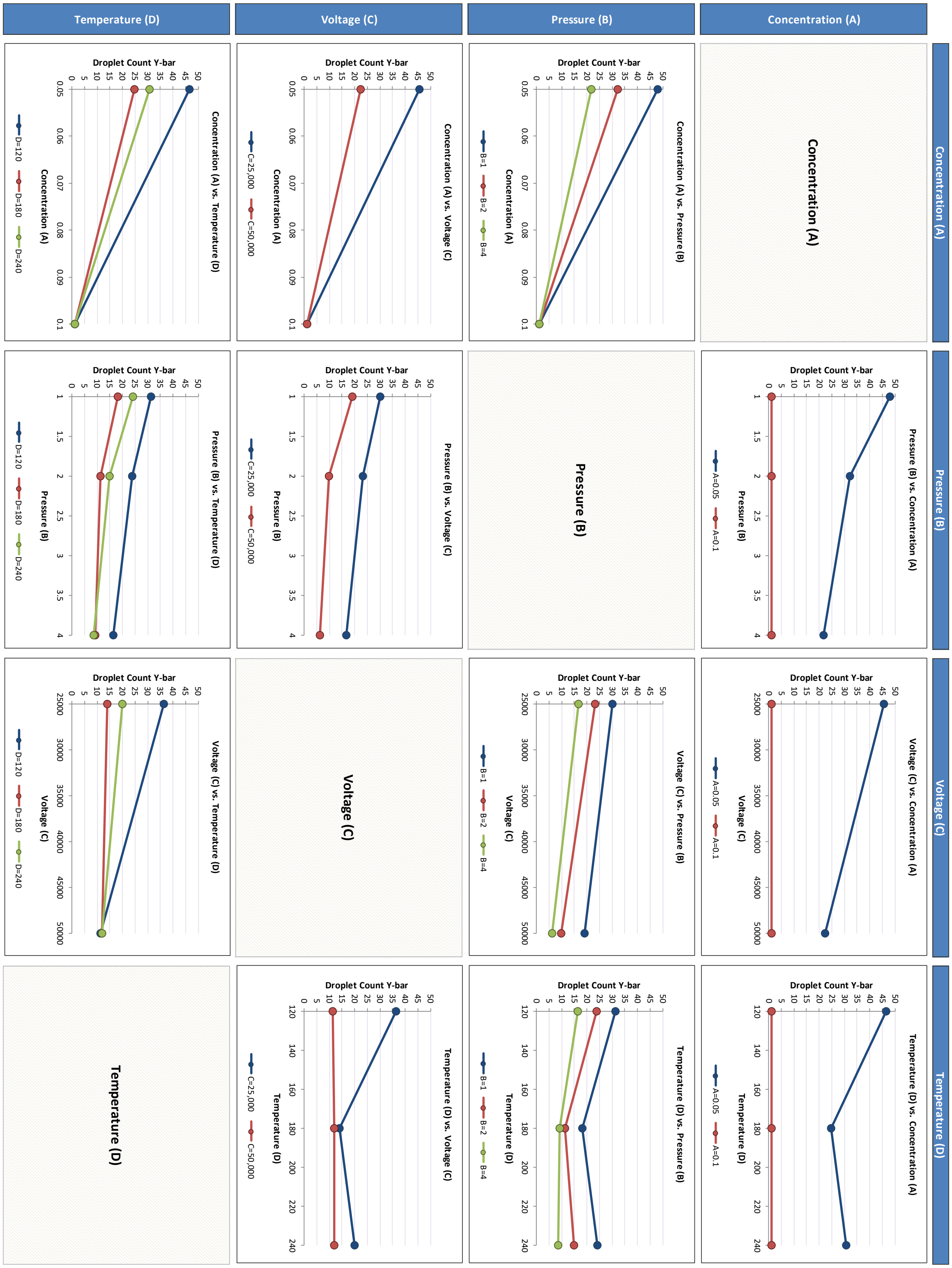

Appendix E – DOE Interaction Charts – Sunflower Oil

Table 115: Sunflower Oil & Propylene Glycol @ 19Ga Interaction chart on Droplet Size Y-bar

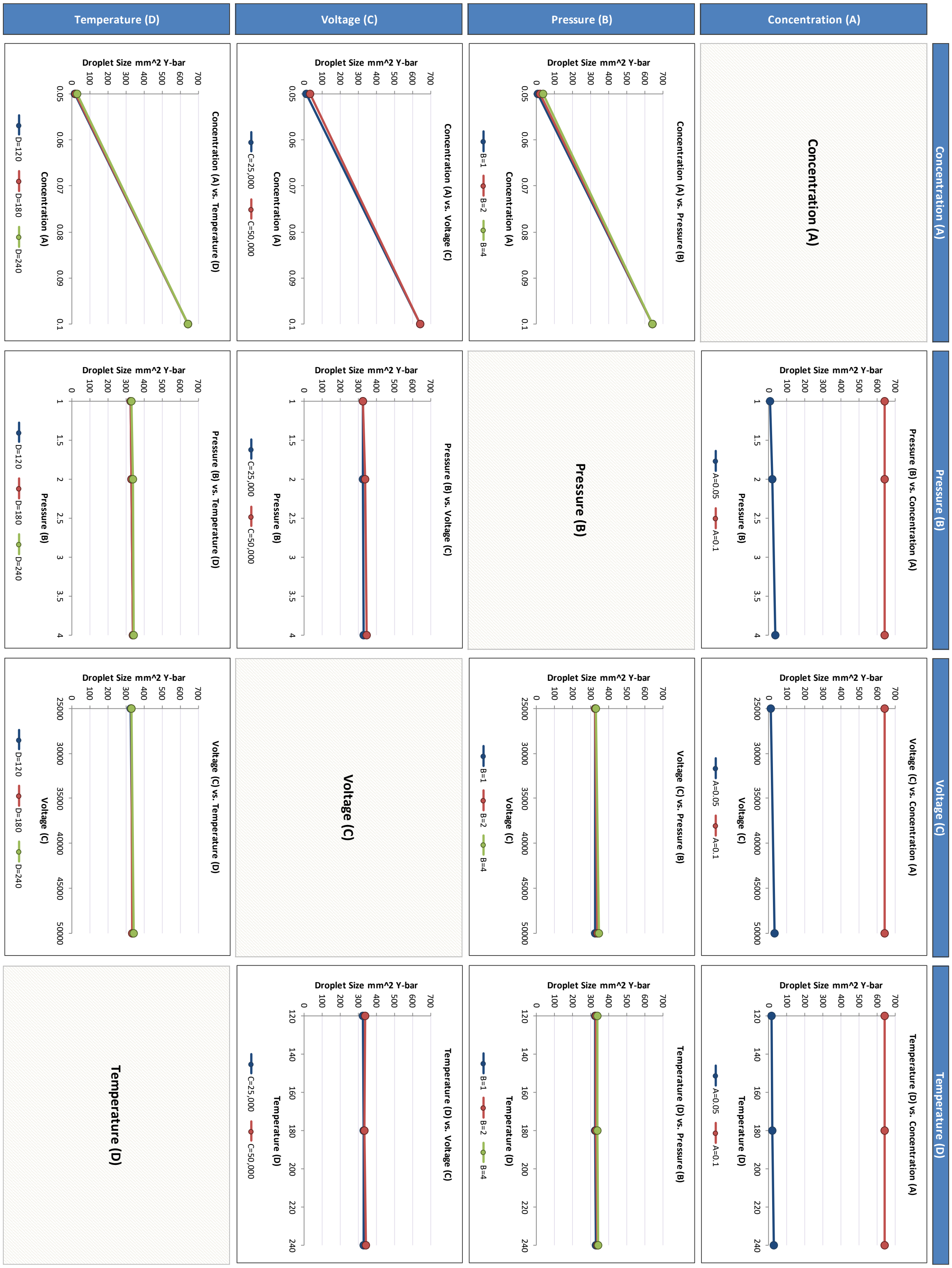

Appendix E – DOE Interaction Charts – Sunflower Oil

Table 116: Sunflower Oil & Propylene Glycol @ 19Ga Interaction chart on Coverage Area Y-bar

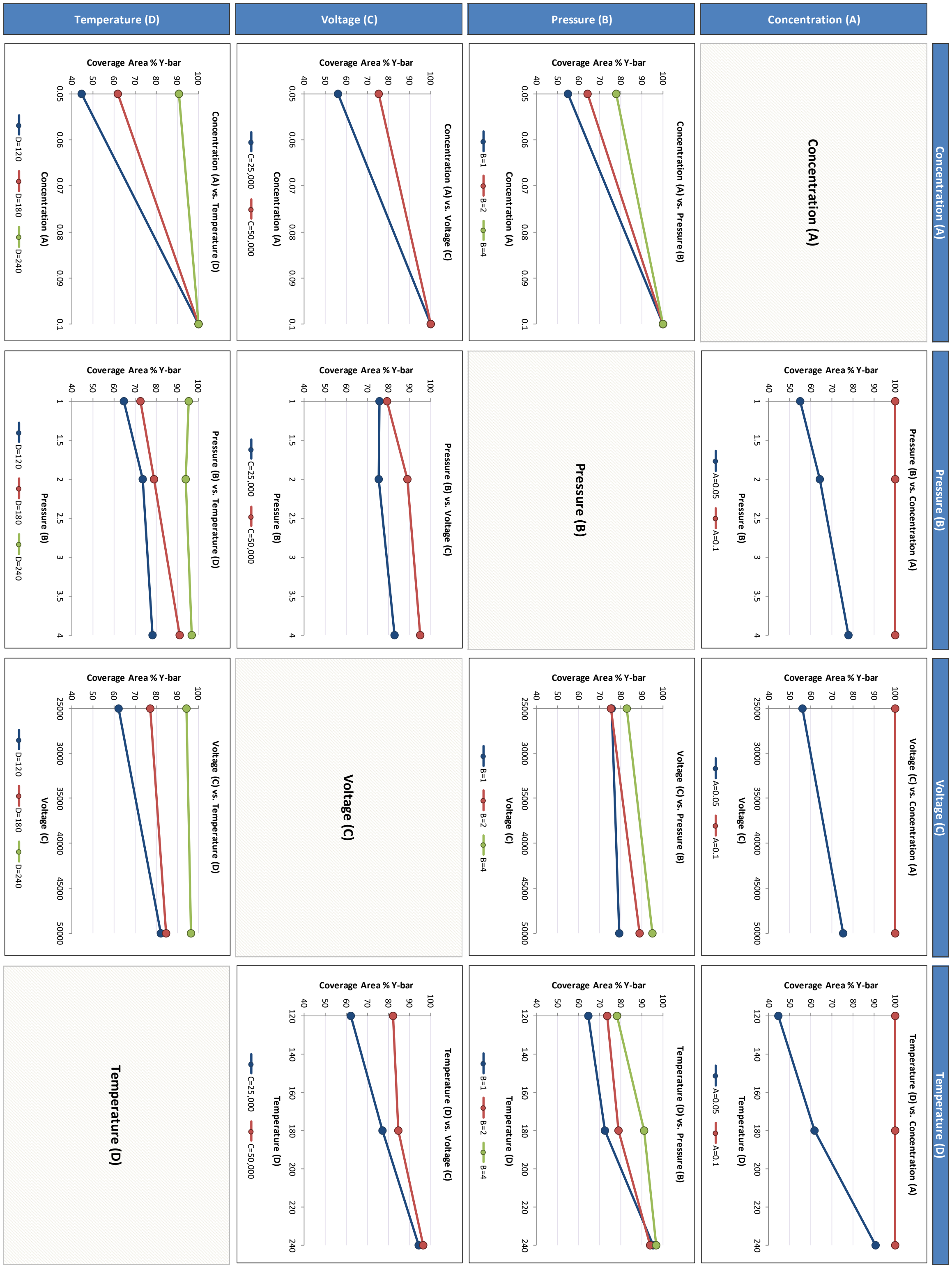

Appendix E – DOE Interaction Charts – Sunflower Oil

Table 117: Sunflower Oil & Propylene Glycol @ 19Ga Interaction chart on Sample Weight Y-bar

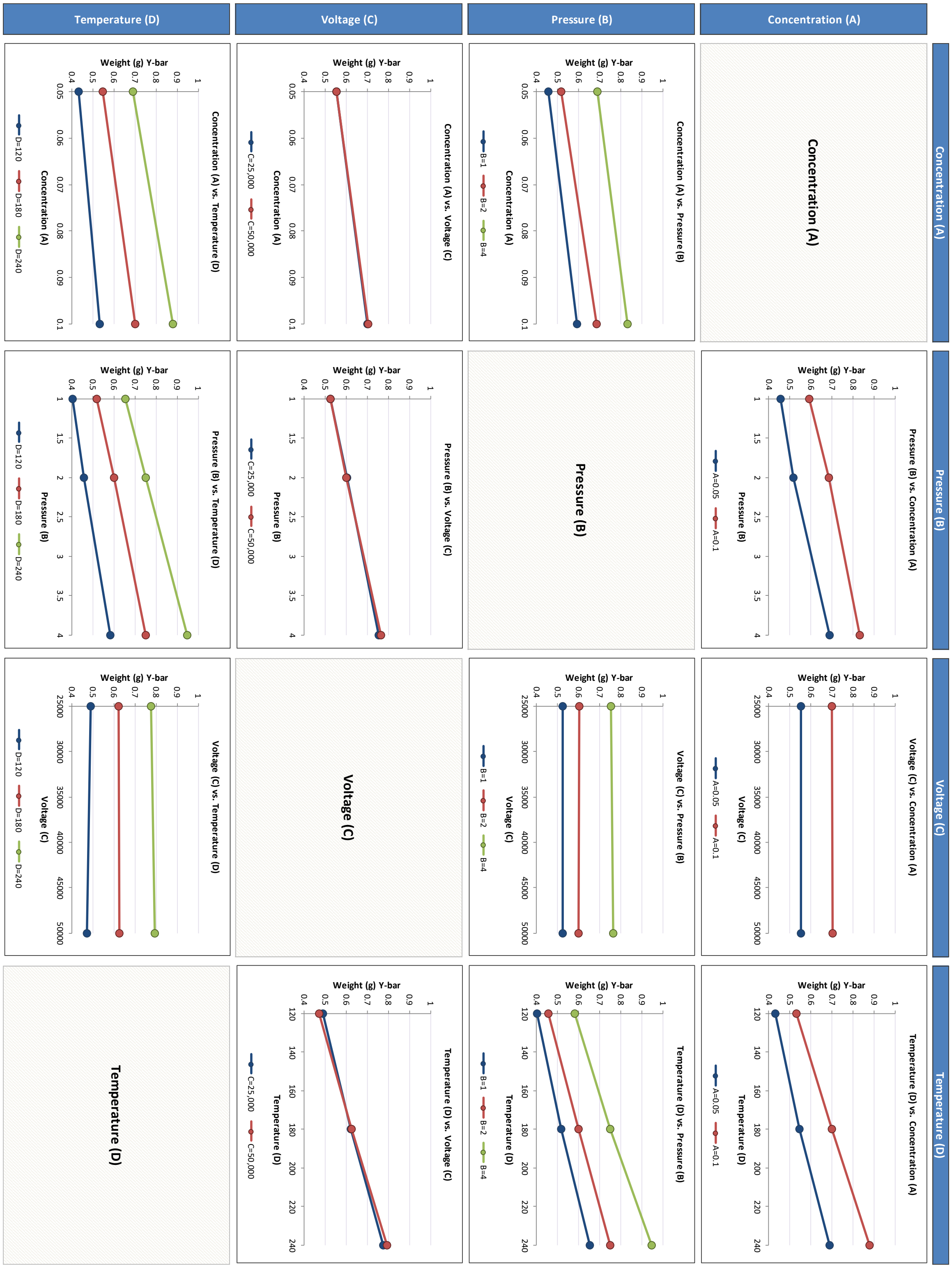

Appendix E – DOE Interaction Charts – Sunflower Oil

Table 118: Sunflower Oil & Propylene Glycol @ 22Ga Interaction chart on Droplet Count Y-bar

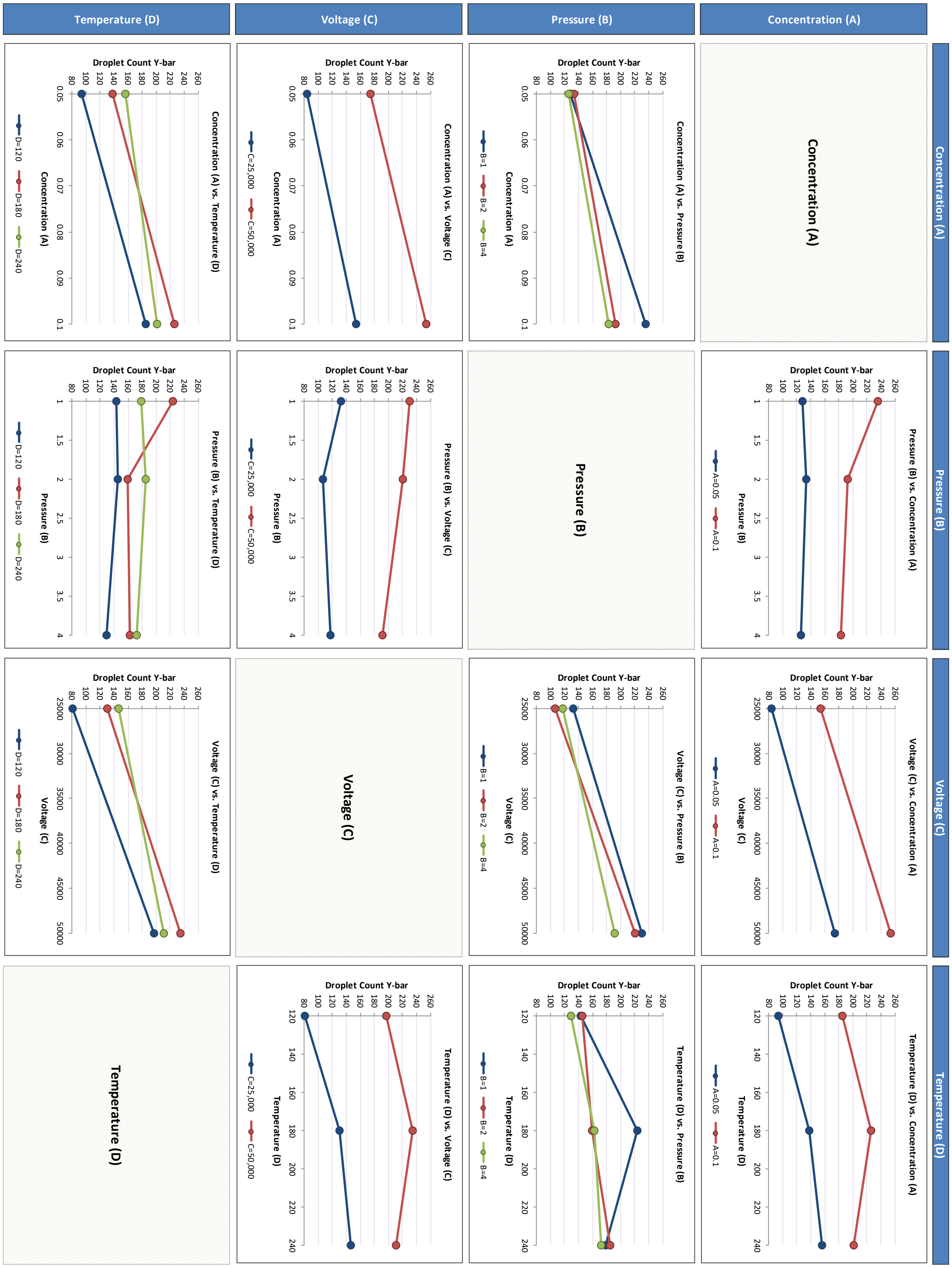

Appendix E – DOE Interaction Charts – Sunflower Oil

Table 119: Sunflower Oil & Propylene Glycol @ 22Ga Interaction chart on Droplet Size Y-bar

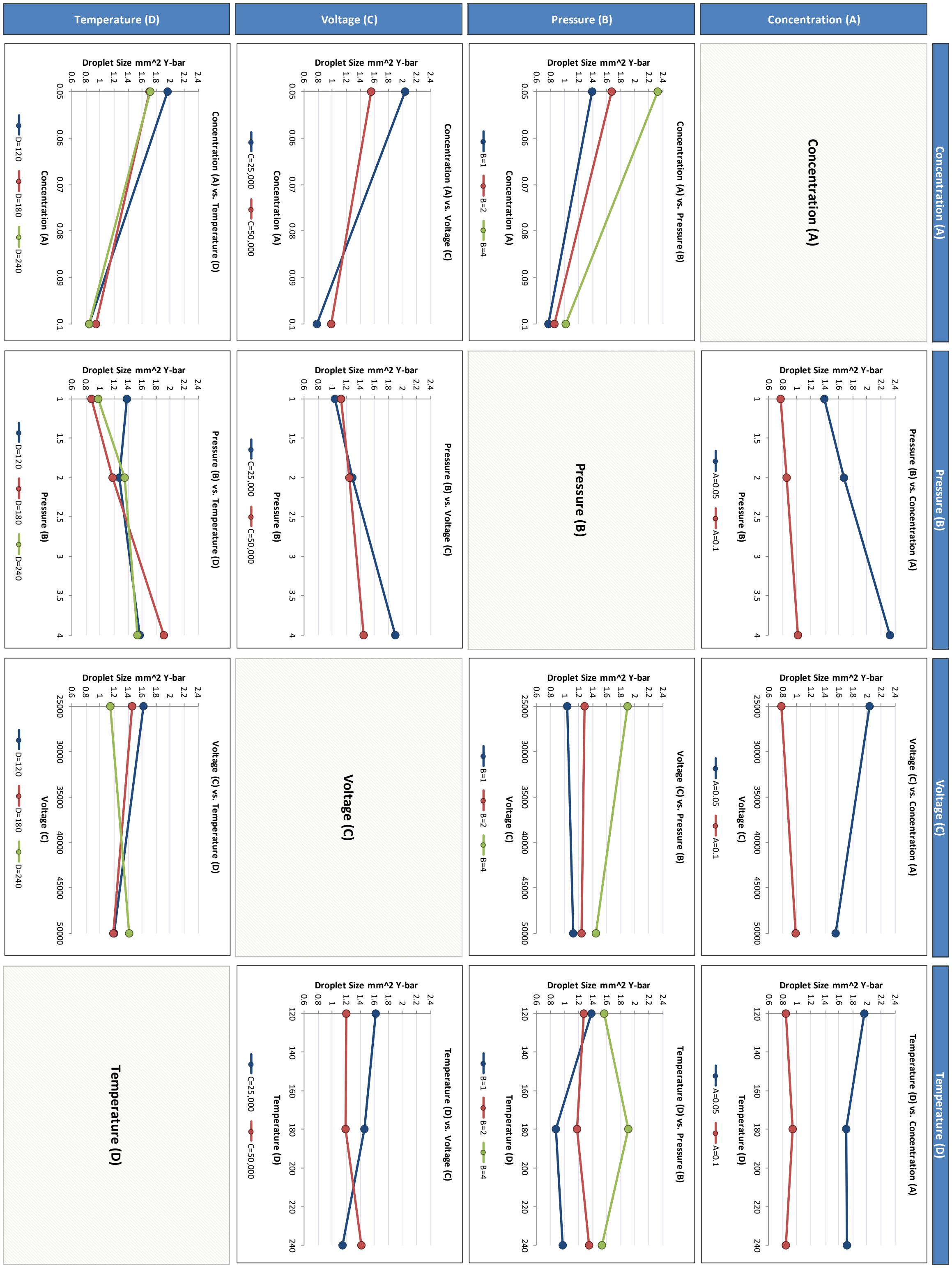

Appendix E – DOE Interaction Charts – Sunflower Oil

Table 120: Sunflower Oil & Propylene Glycol @ 22Ga Interaction chart on Coverage Area Y-bar

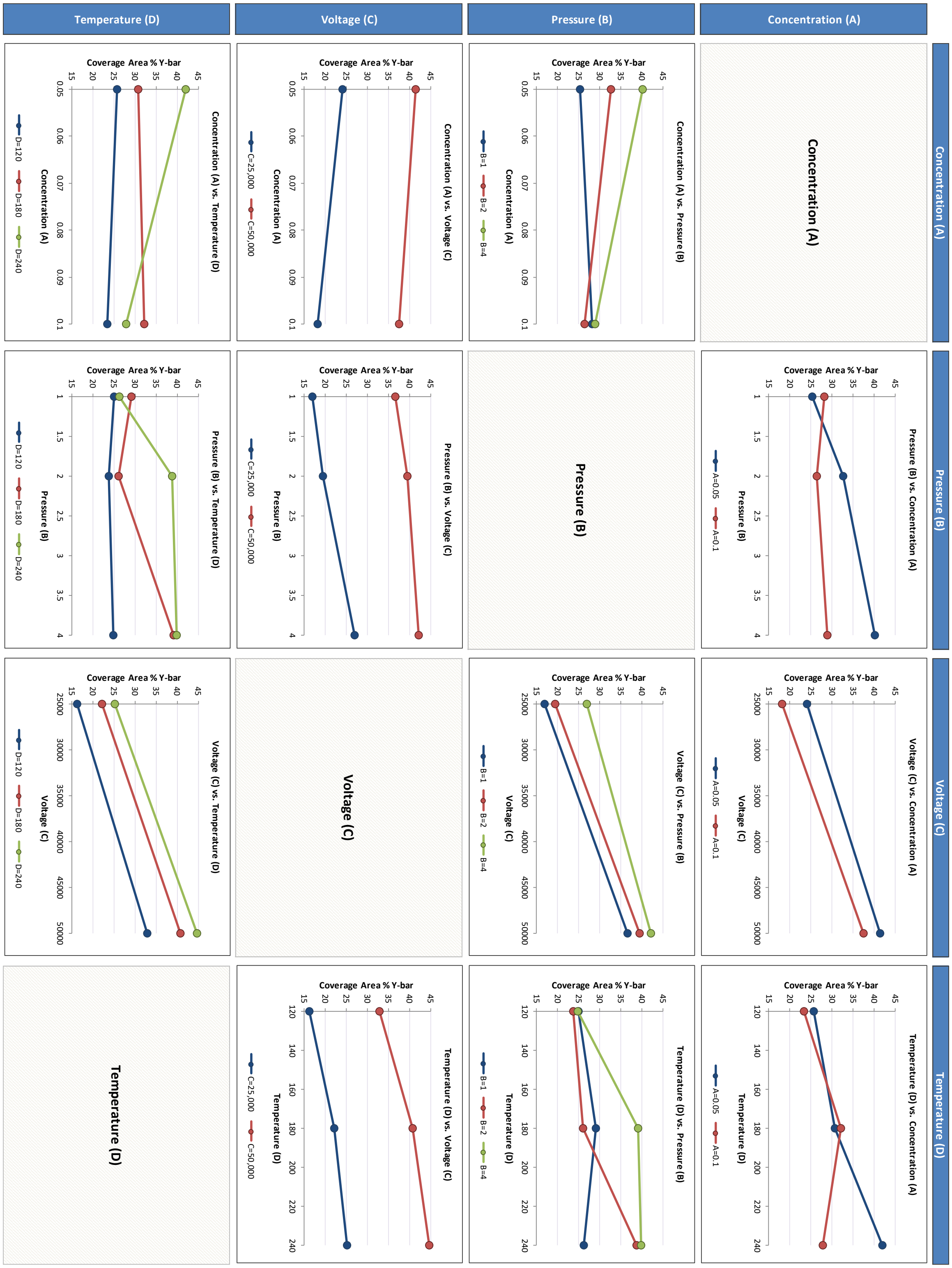

Appendix E – DOE Interaction Charts – Sunflower Oil

Table 121: Sunflower Oil & Propylene Glycol @ 22Ga Interaction chart on Sample Weight Y-bar

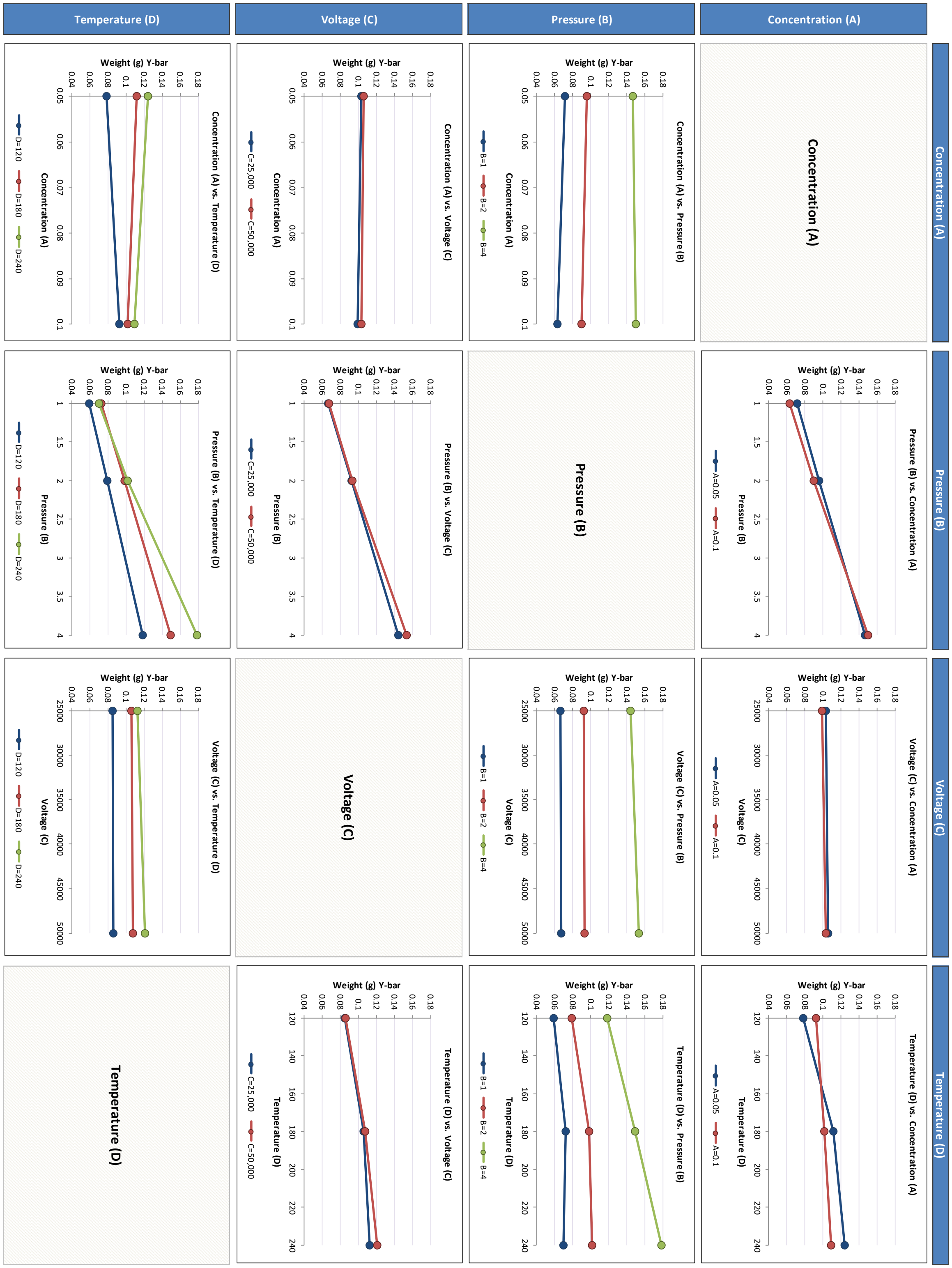

Appendix E – DOE Interaction Charts – Sunflower Oil

Table 122: Sunflower Oil & Polysorbate 80 @ 22Ga Interaction chart on Droplet Count Y-bar

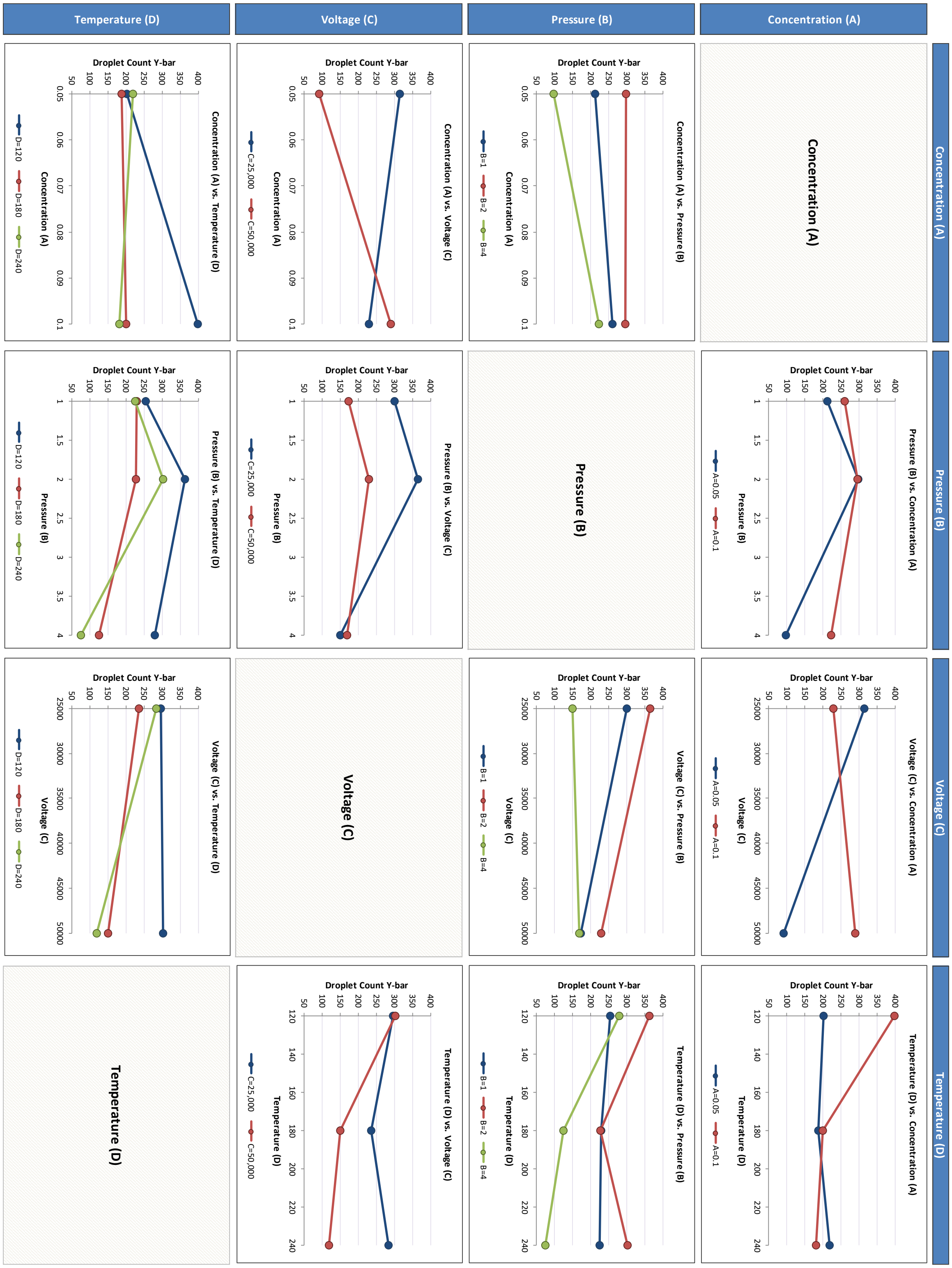

Appendix E – DOE Interaction Charts – Sunflower Oil

Table 123: Sunflower Oil & Polysorbate 80 @ 22Ga Interaction chart on Droplet Size Y-bar

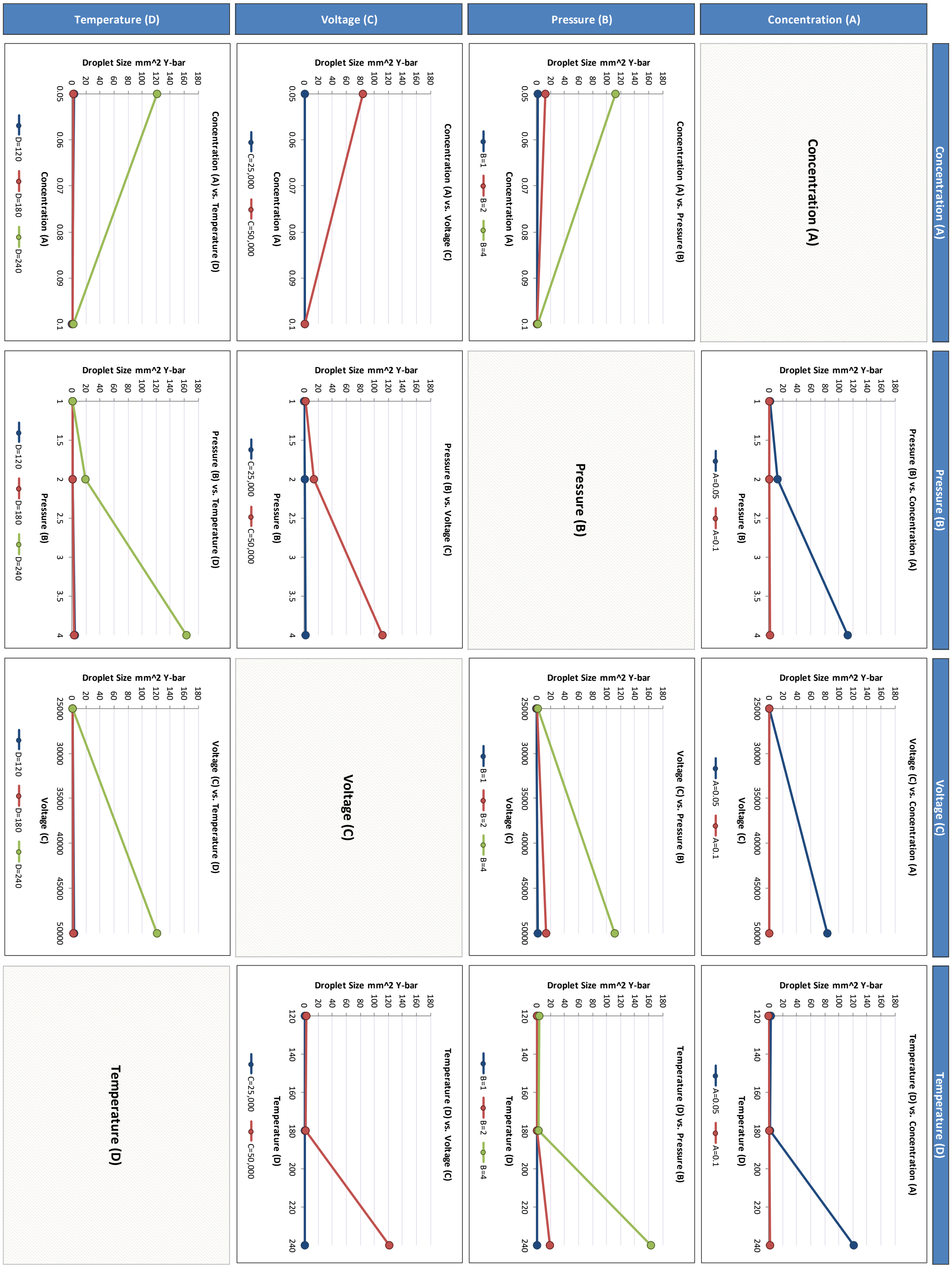

Appendix E – DOE Interaction Charts – Sunflower Oil

Table 124: Sunflower Oil & Polysorbate 80 @ 22Ga Interaction chart on Coverage Area Y-bar

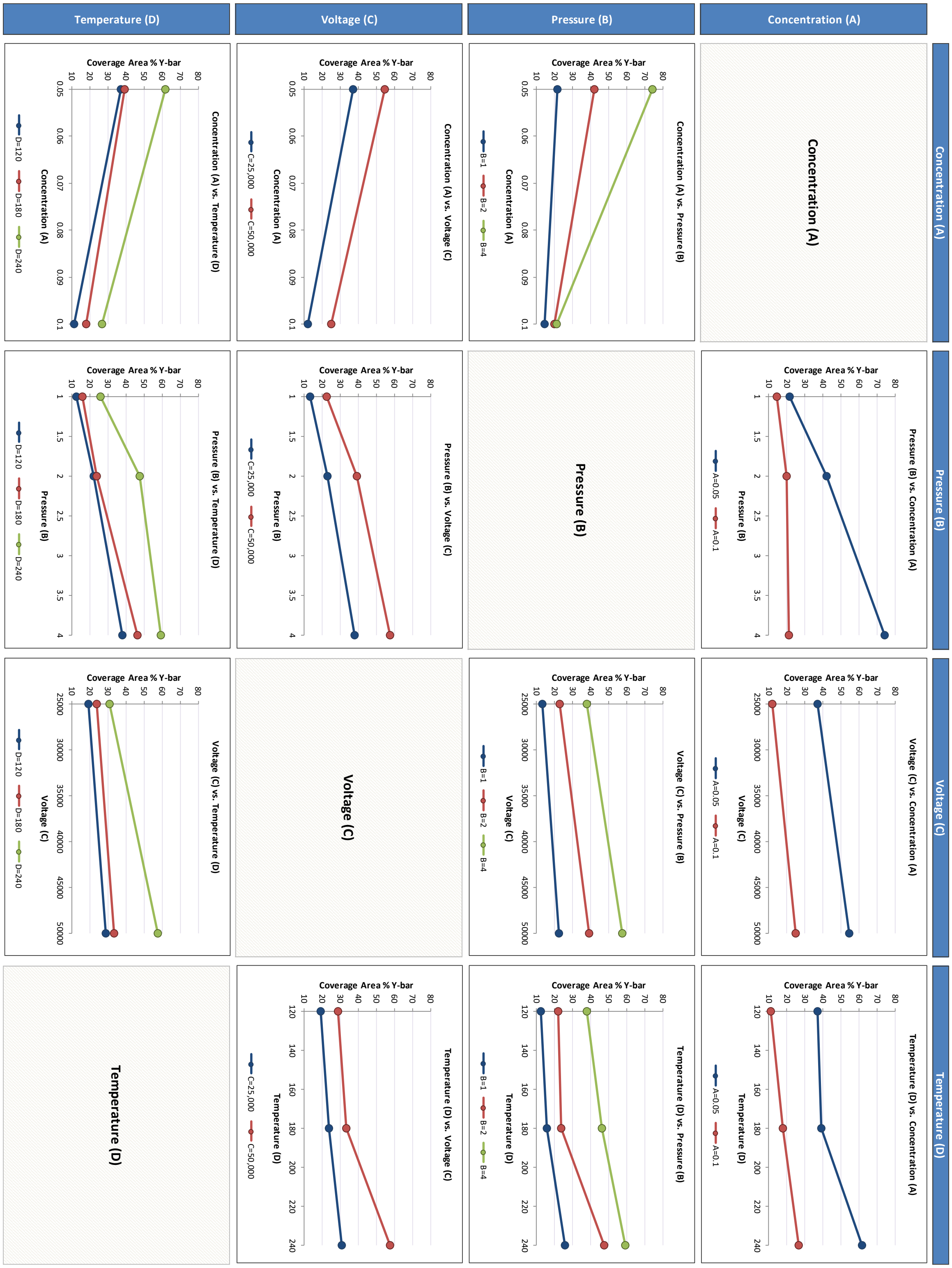

Appendix E – DOE Interaction Charts – Sunflower Oil

Table 125: Sunflower Oil & Polysorbate 80 @ 22Ga Interaction chart on Sample Weight Y-bar

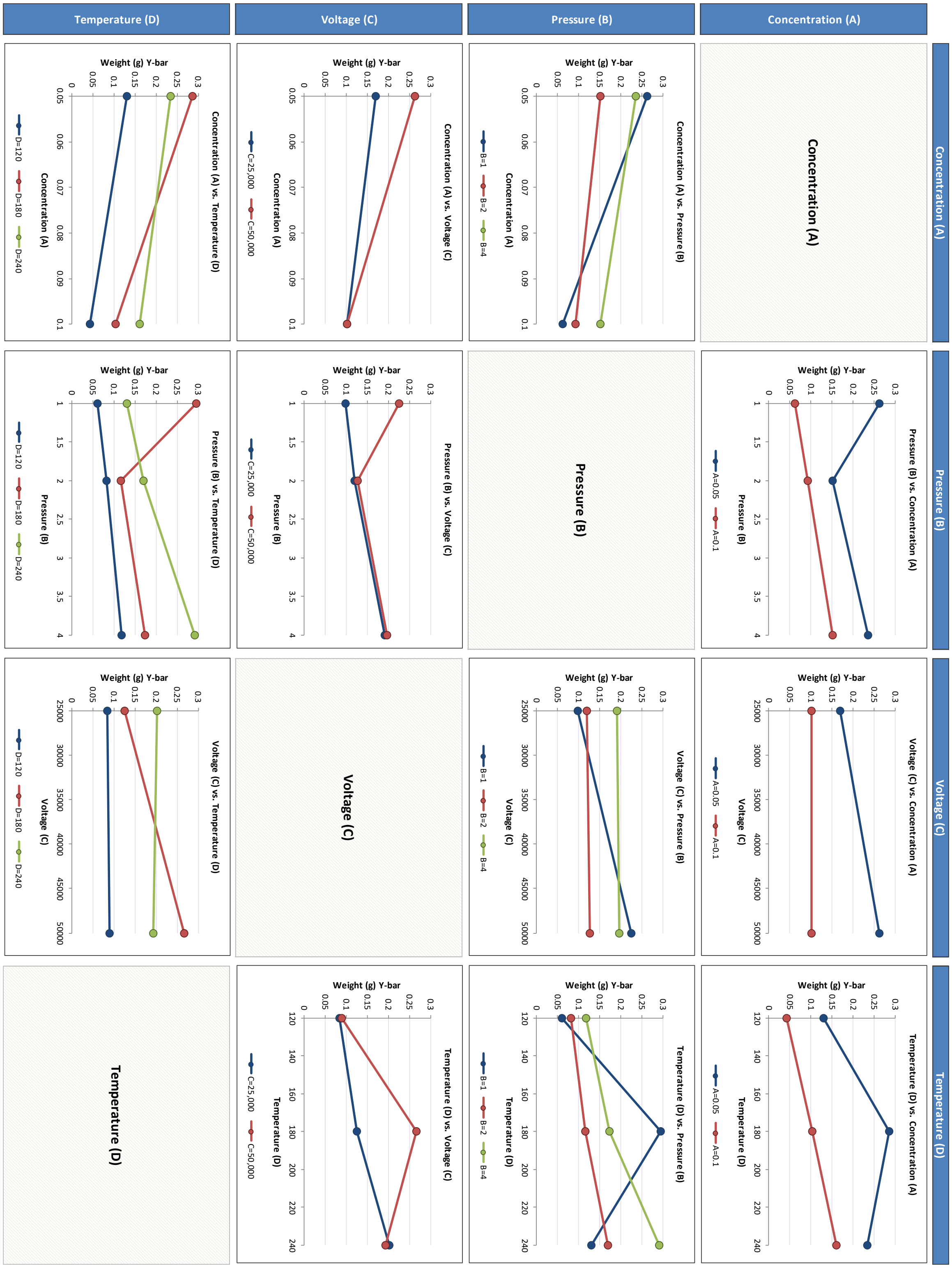

Appendix E – DOE Interaction Charts – Sunflower Oil

Table 126: Sunflower Oil & Propylene Glycol @ 22Ga Interaction chart on Droplet Count Y-bar

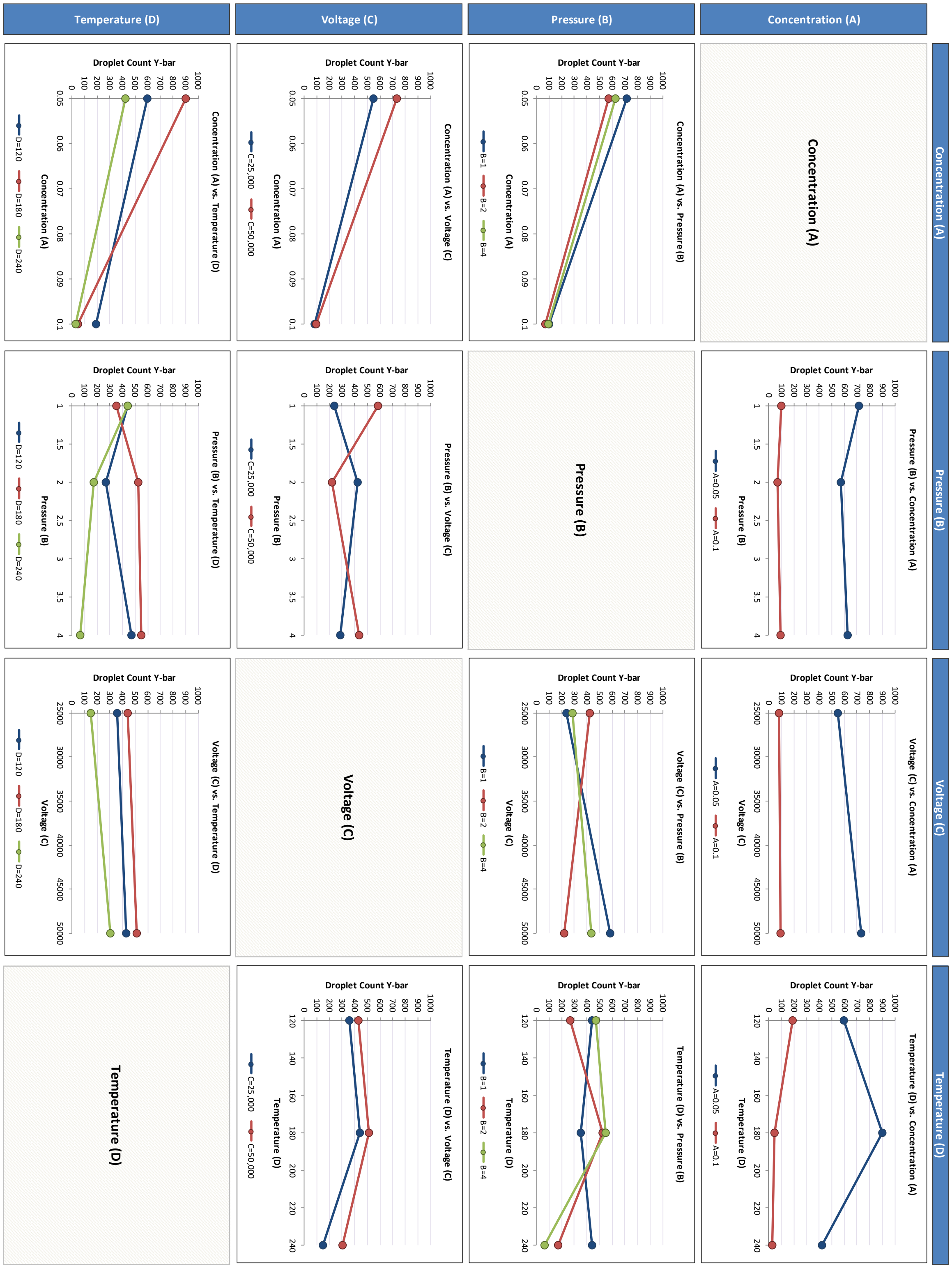

Appendix E – DOE Interaction Charts – Sunflower Oil

Table 127: Sunflower Oil & Propylene Glycol @ 22Ga Interaction chart on Droplet Size Y-bar

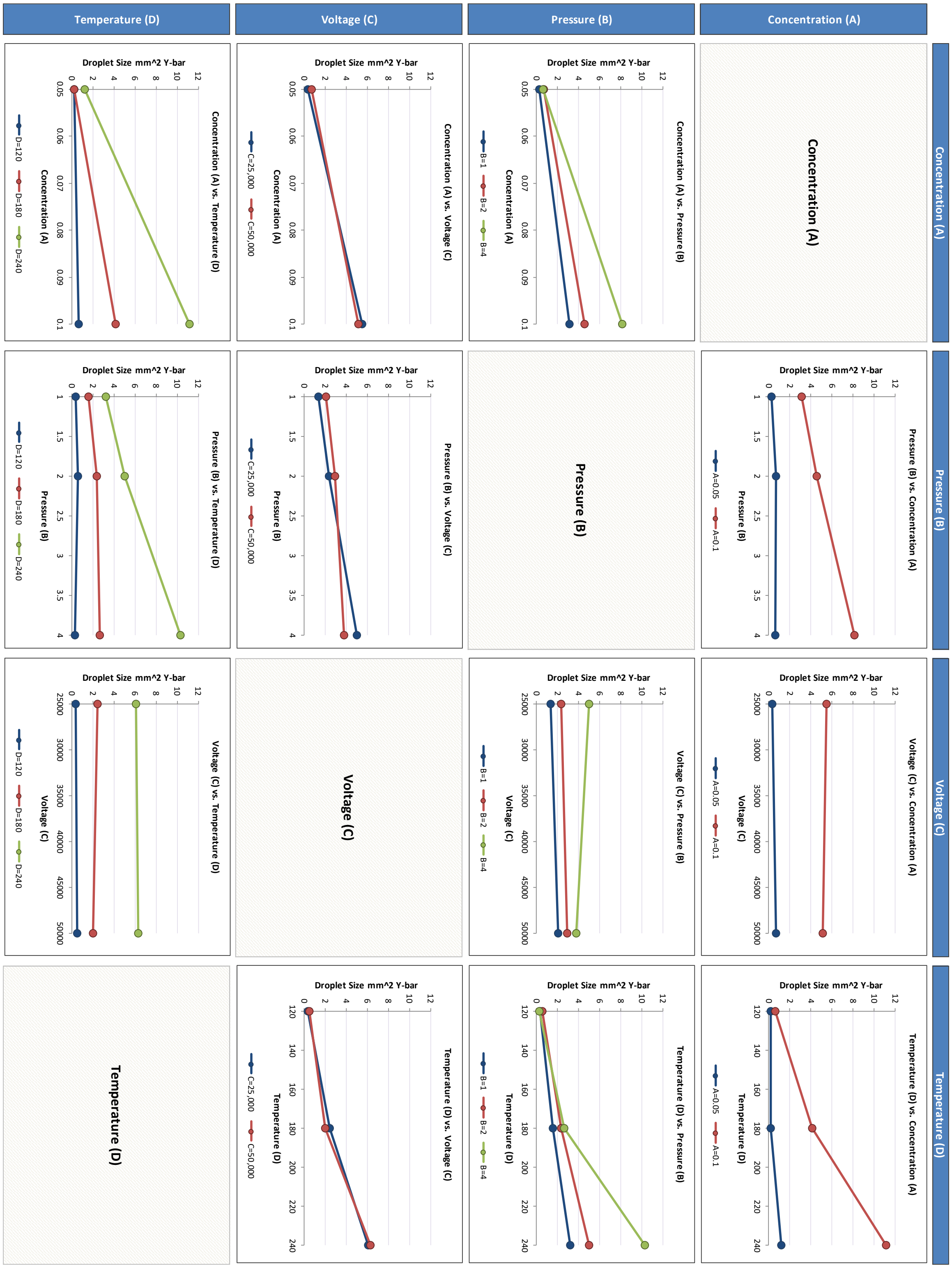

Appendix E – DOE Interaction Charts – Sunflower Oil

Table 128: Sunflower Oil & Propylene Glycol @ 22Ga Interaction chart on Coverage Area Y-bar

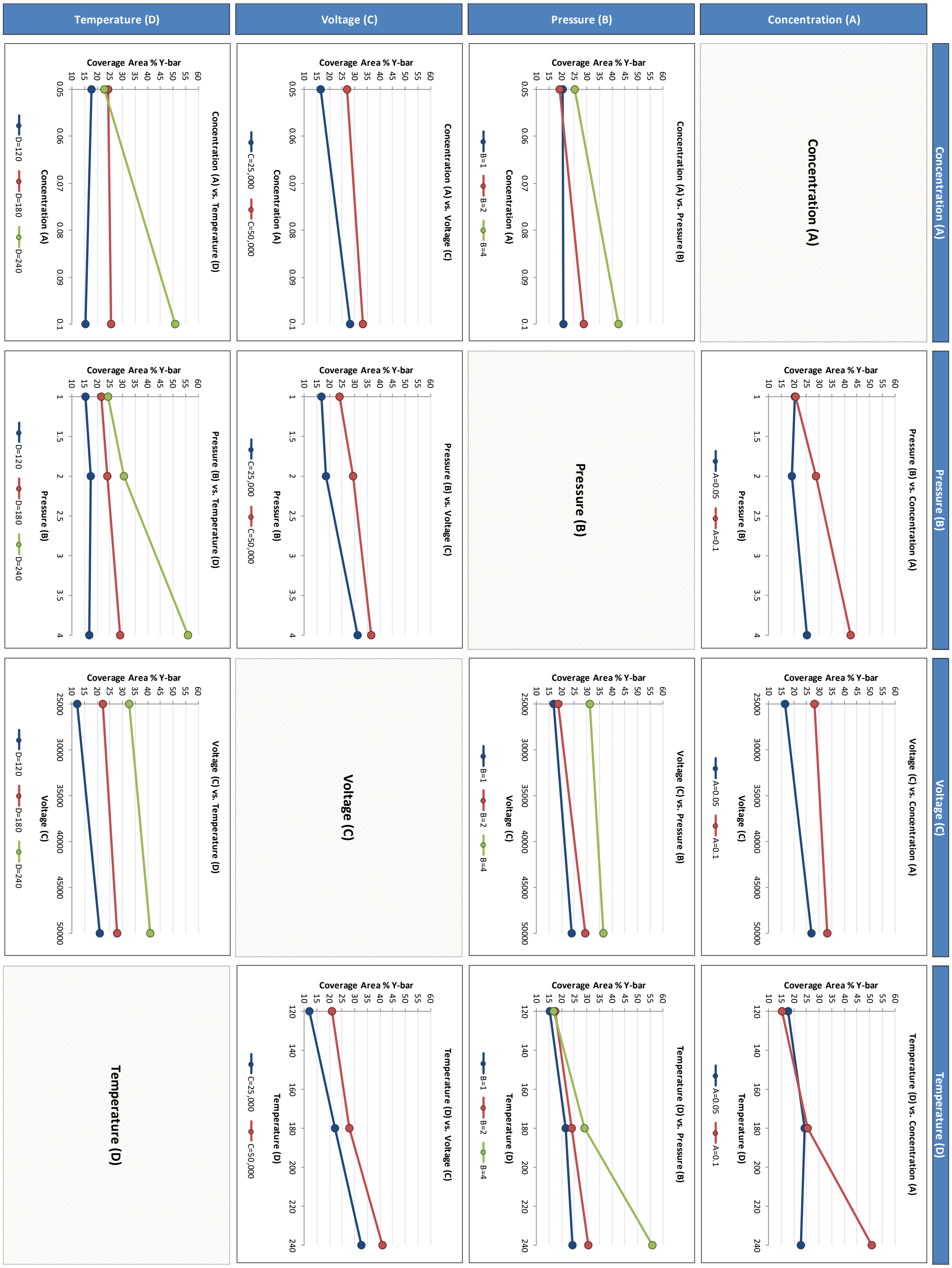

Appendix E – DOE Interaction Charts – Sunflower Oil

Table 129: Sunflower Oil & Propylene Glycol @ 22Ga Interaction chart on Sample Weight Y-bar

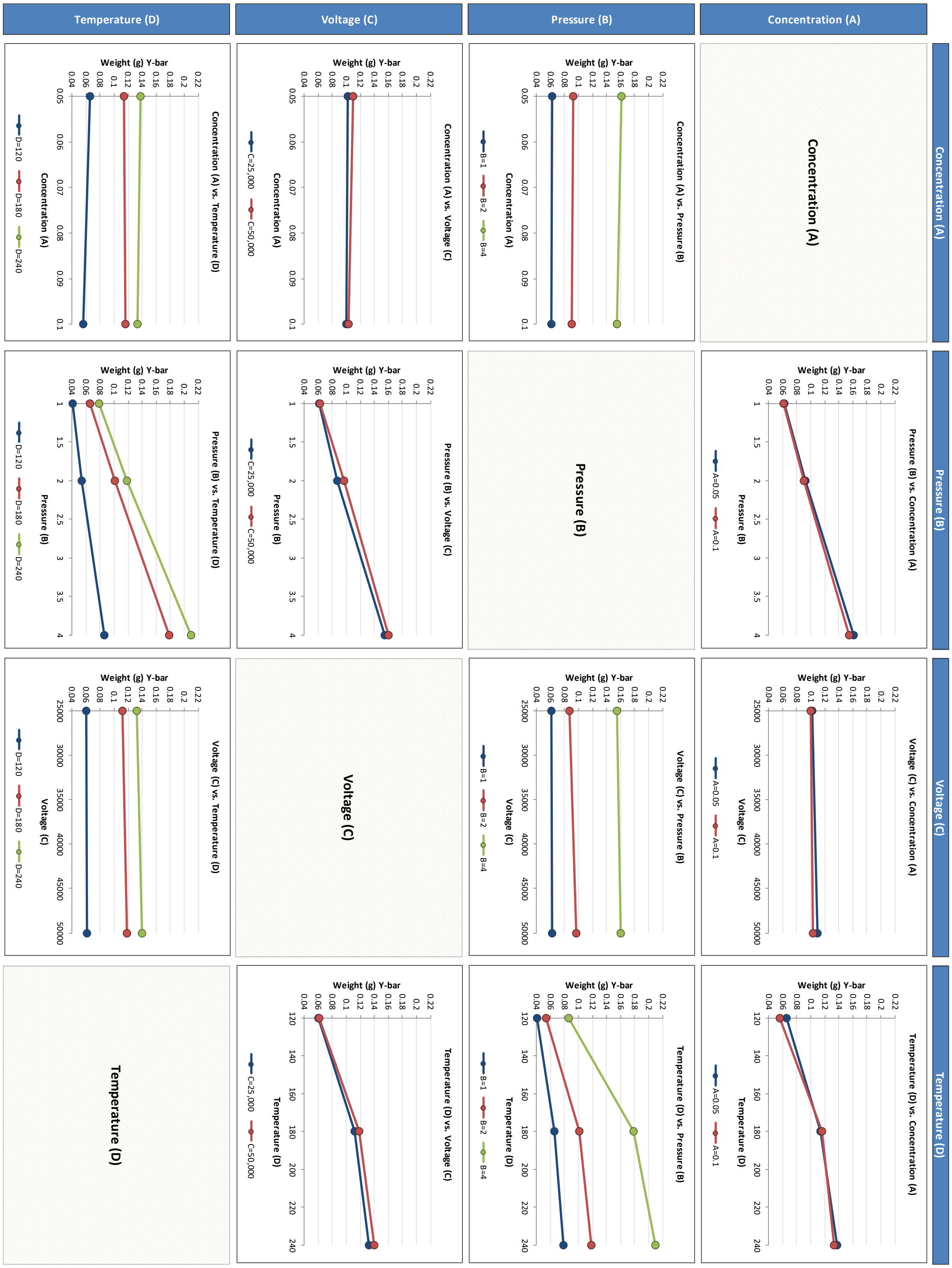

Appendix F – Data Table – Palm Oil

Table 130: Data Table - Palm & Soy Lecithin @ 19ga

Base Oil	Emulsifier	Needle Gauge	Voltage (kV)	Temp (F)	Pressure (psi)	Time (ms)	Concentration	Weight (g)	Density (g/cm^3)	Mass Flow (g/s)	Droplet Count	Total Area (mm^2)	Average Size (mm^2)	% Area Coverage
Palm Oil	Soybean Lecithin	19	25	120	1	317	5%	0.2200	0.8999	0.7333	48	111.745	2.328	17.312
Palm Oil	Soybean Lecithin	19	25	180	1	317	5%	0.3600	0.8786	1.2000	64	241.484	3.773	37.412
Palm Oil	Soybean Lecithin	19	25	240	1	317	5%	0.5810	0.8565	1.9367	58	462.534	7.975	71.658
Palm Oil	Soybean Lecithin	19	50	120	1	317	5%	0.2180	0.8999	0.7267	37	187.408	5.065	29.034
Palm Oil	Soybean Lecithin	19	50	180	1	317	5%	0.3650	0.8786	1.2167	85	261.179	3.073	40.463
Palm Oil	Soybean Lecithin	19	50	240	1	317	5%	0.5870	0.8565	1.9567	60	428.618	7.144	66.403
Palm Oil	Soybean Lecithin	19	25	120	2	317	5%	0.2400	0.8999	0.8000	39	112.174	2.876	17.378
Palm Oil	Soybean Lecithin	19	25	180	2	317	5%	0.3770	0.8786	1.2567	52	247.378	4.757	38.325
Palm Oil	Soybean Lecithin	19	25	240	2	317	5%	0.6560	0.8565	2.1867	67	455.959	6.805	70.639
Palm Oil	Soybean Lecithin	19	50	120	2	317	5%	0.2500	0.8999	0.8333	40	178.204	4.455	27.608
Palm Oil	Soybean Lecithin	19	50	180	2	317	5%	0.4020	0.8786	1.3400	68	359.022	5.28	55.621
Palm Oil	Soybean Lecithin	19	50	240	2	317	5%	0.7390	0.8565	2.4633	35	533.441	15.241	82.643
Palm Oil	Soybean Lecithin	19	25	120	4	317	5%	0.3180	0.8999	1.0600	36	123.624	3.434	19.152
Palm Oil	Soybean Lecithin	19	25	180	4	317	5%	0.5070	0.8786	1.6900	31	429.822	13.865	66.59
Palm Oil	Soybean Lecithin	19	25	240	4	317	5%	0.8180	0.8565	2.7267	17	593.595	34.917	91.962
Palm Oil	Soybean Lecithin	19	50	120	4	317	5%	0.2990	0.8999	0.9967	45	226.671	5.037	35.117
Palm Oil	Soybean Lecithin	19	50	180	4	317	5%	0.5220	0.8786	1.7400	72	372.692	5.176	57.739
Palm Oil	Soybean Lecithin	19	50	240	4	317	5%	0.8360	0.8565	2.7867	12	616.993	51.416	95.587
Palm Oil	Soybean Lecithin	19	25	120	1	317	10%	0.4150	0.8999	1.3833	22	300.448	13.657	46.547
Palm Oil	Soybean Lecithin	19	25	180	1	317	10%	0.5280	0.8786	1.7600	28	463.959	16.57	71.878
Palm Oil	Soybean Lecithin	19	25	240	1	317	10%	0.5180	0.8565	1.7267	31	484.834	15.64	75.112
Palm Oil	Soybean Lecithin	19	50	120	1	317	10%	0.4620	0.8999	1.5400	44	408.102	9.275	63.225
Palm Oil	Soybean Lecithin	19	50	180	1	317	10%	0.5450	0.8786	1.8167	18	556.726	30.929	86.25
Palm Oil	Soybean Lecithin	19	50	240	1	317	10%	0.5170	0.8565	1.7233	22	573.759	26.08	88.889
Palm Oil	Soybean Lecithin	19	25	120	2	317	10%	0.3840	0.8999	1.2800	36	288.867	8.024	44.752
Palm Oil	Soybean Lecithin	19	25	180	2	317	10%	0.5850	0.8786	1.9500	35	462.824	13.224	71.703
Palm Oil	Soybean Lecithin	19	25	240	2	317	10%	0.5770	0.8565	1.9233	37	566.929	15.322	87.831
Palm Oil	Soybean Lecithin	19	50	120	2	317	10%	0.4470	0.8999	1.4900	41	388.599	9.478	60.203
Palm Oil	Soybean Lecithin	19	50	180	2	317	10%	0.5760	0.8786	1.9200	47	493.764	10.506	76.496
Palm Oil	Soybean Lecithin	19	50	240	2	317	10%	0.5830	0.8565	1.9433	31	564.208	18.2	87.409
Palm Oil	Soybean Lecithin	19	25	120	4	317	10%	0.5890	0.8999	1.9633	37	469.167	12.68	72.685
Palm Oil	Soybean Lecithin	19	25	180	4	317	10%	0.6680	0.8786	2.2267	46	493.909	10.737	76.518
Palm Oil	Soybean Lecithin	19	25	240	4	317	10%	0.6770	0.8565	2.2567	30	554.428	18.481	85.894
Palm Oil	Soybean Lecithin	19	50	120	4	317	10%	0.6070	0.8999	2.0233	44	455.706	10.357	70.6
Palm Oil	Soybean Lecithin	19	50	180	4	317	10%	0.7250	0.8786	2.4167	41	504.93	12.315	78.226
Palm Oil	Soybean Lecithin	19	50	240	4	317	10%	0.6840	0.8565	2.2800	38	541.255	14.244	83.853

Appendix F – Data Table – Palm Oil

Table 131: Data Table - Palm & Soy Lecithin @ 22ga

Base Oil	Emulsifier	Needle Gauge	Voltage (kV)	Temp (F)	Pressure (psi)	Time (ms)	Concentration	Weight (g)	Density (g/cm^3)	Mass Flow (g/s)	Droplet Count	Total Area (mm^2)	Average Size (mm^2)	% Area Coverage
Palm Oil	Soybean Lecithin	22	25	120	4	317	5%	0.0710	0.8999	0.2367	70	79.77	1.14	12.358
Palm Oil	Soybean Lecithin	22	25	180	4	317	5%	0.0860	0.8786	0.2867	94	125.887	1.339	19.503
Palm Oil	Soybean Lecithin	22	25	240	4	317	5%	0.1110	0.8565	0.3700	213	210.432	0.988	32.601
Palm Oil	Soybean Lecithin	22	50	120	4	317	5%	0.0800	0.8999	0.2667	139	159.751	1.149	24.749
Palm Oil	Soybean Lecithin	22	50	180	4	317	5%	0.1010	0.8786	0.3367	134	193.991	1.448	30.054
Palm Oil	Soybean Lecithin	22	50	240	4	317	5%	0.1160	0.8565	0.3867	177	235.996	1.333	36.561
Palm Oil	Soybean Lecithin	22	25	120	8	317	5%	0.0930	0.8999	0.3100	60	105.675	1.761	16.372
Palm Oil	Soybean Lecithin	22	25	180	8	317	5%	0.1070	0.8786	0.3567	94	124.235	1.322	19.247
Palm Oil	Soybean Lecithin	22	25	240	8	317	5%	0.1300	0.8565	0.4333	172	138.636	0.806	21.478
Palm Oil	Soybean Lecithin	22	50	120	8	317	5%	0.1010	0.8999	0.3367	158	161.592	1.023	25.034
Palm Oil	Soybean Lecithin	22	50	180	8	317	5%	0.1230	0.8786	0.4100	163	165.216	1.014	25.596
Palm Oil	Soybean Lecithin	22	50	240	8	317	5%	0.1460	0.8565	0.4867	190	194.672	1.025	30.159
Palm Oil	Soybean Lecithin	22	25	120	16	317	5%	0.1290	0.8999	0.4300	71	107.73	1.517	16.69
Palm Oil	Soybean Lecithin	22	25	180	16	317	5%	0.1810	0.8786	0.6033	71	113.745	1.602	17.622
Palm Oil	Soybean Lecithin	22	25	240	16	317	5%	0.1700	0.8565	0.5667	123	116.489	0.947	18.047
Palm Oil	Soybean Lecithin	22	50	120	16	317	5%	0.1290	0.8999	0.4300	146	302.12	2.069	46.806
Palm Oil	Soybean Lecithin	22	50	180	16	317	5%	0.1950	0.8786	0.6500	173	175.877	1.017	27.248
Palm Oil	Soybean Lecithin	22	50	240	16	317	5%	0.2000	0.8565	0.6667	172	129.531	0.753	20.068
Palm Oil	Soybean Lecithin	22	25	120	4	317	10%	0.0750	0.8999	0.2500	184	260.713	1.417	40.391
Palm Oil	Soybean Lecithin	22	25	180	4	317	10%	0.0700	0.8786	0.2333	87	86.845	0.998	13.454
Palm Oil	Soybean Lecithin	22	25	240	4	317	10%	0.0790	0.8565	0.2633	144	91.335	0.634	14.15
Palm Oil	Soybean Lecithin	22	50	120	4	317	10%	0.0750	0.8999	0.2500	200	224.342	1.122	34.756
Palm Oil	Soybean Lecithin	22	50	180	4	317	10%	0.0710	0.8786	0.2367	112	139.826	1.248	21.662
Palm Oil	Soybean Lecithin	22	50	240	4	317	10%	0.0890	0.8565	0.2967	278	221.804	0.798	34.363
Palm Oil	Soybean Lecithin	22	25	120	8	317	10%	0.0920	0.8999	0.3067	207	394.605	1.906	61.134
Palm Oil	Soybean Lecithin	22	25	180	8	317	10%	0.0950	0.8786	0.3167	92	100.12	1.088	15.511
Palm Oil	Soybean Lecithin	22	25	240	8	317	10%	0.1170	0.8565	0.3900	124	113.241	0.913	17.544
Palm Oil	Soybean Lecithin	22	50	120	8	317	10%	0.1000	0.8999	0.3333	182	479.693	2.636	74.316
Palm Oil	Soybean Lecithin	22	50	180	8	317	10%	0.0980	0.8786	0.3267	173	182.248	1.053	28.235
Palm Oil	Soybean Lecithin	22	50	240	8	317	10%	0.1360	0.8565	0.4533	206	184.251	0.894	28.545
Palm Oil	Soybean Lecithin	22	25	120	16	317	10%	0.1410	0.8999	0.4700	235	496.444	2.113	76.911
Palm Oil	Soybean Lecithin	22	25	180	16	317	10%	0.1420	0.8786	0.4733	127	178.896	1.409	27.715
Palm Oil	Soybean Lecithin	22	25	240	16	317	10%	0.2090	0.8565	0.6967	75	72.929	0.972	11.298
Palm Oil	Soybean Lecithin	22	50	120	16	317	10%	0.1420	0.8999	0.4733	202	458.678	2.271	71.06
Palm Oil	Soybean Lecithin	22	50	180	16	317	10%	0.1590	0.8786	0.5300	149	178.23	1.196	27.612
Palm Oil	Soybean Lecithin	22	50	240	16	317	10%	0.2110	0.8565	0.7033	128	198.116	1.548	30.693

Appendix F – Data Table – Palm Oil

Table 132: Data Table - Palm & Polysorbate 80 @ 19ga

Base Oil	Emulsifier	Needle Gauge	Voltage (kV)	Temp (F)	Pressure (psi)	Time (ms)	Concentration	Weight (g)	Density (g/cm^3)	Mass Flow (g/s)	Droplet Count	Total Area (mm^2)	Average Size (mm^2)	% Area Coverage
Palm Oil	Polysorbate 80	19	25	120	1	317	5%	0.2480	0.8999	0.8267	39	169.229	4.339	zz63
Palm Oil	Polysorbate 80	19	25	180	1	317	5%	0.3840	0.8786	1.2800	13	391.219	30.094	60.609
Palm Oil	Polysorbate 80	19	25	240	1	317	5%	0.5520	0.8565	1.8400	1	645.16	645.16	100
Palm Oil	Polysorbate 80	19	50	120	1	317	5%	0.2520	0.8999	0.8400	87	234.863	2.7	36.386
Palm Oil	Polysorbate 80	19	50	180	1	317	5%	0.3950	0.8786	1.3167	14	471.238	33.66	73.006
Palm Oil	Polysorbate 80	19	50	240	1	317	5%	0.5540	0.8565	1.8467	1	645.16	645.16	100
Palm Oil	Polysorbate 80	19	25	120	2	317	5%	0.2830	0.8999	0.9433	28	183.303	6.547	28.398
Palm Oil	Polysorbate 80	19	25	180	2	317	5%	0.4060	0.8786	1.3533	9	538.635	59.848	83.447
Palm Oil	Polysorbate 80	19	25	240	2	317	5%	0.6360	0.8565	2.1200	1	645.16	645.16	100
Palm Oil	Polysorbate 80	19	50	120	2	317	5%	0.3090	0.8999	1.0300	81	287.811	3.553	44.589
Palm Oil	Polysorbate 80	19	50	180	2	317	5%	0.4300	0.8786	1.4333	1	645.16	645.16	100
Palm Oil	Polysorbate 80	19	50	240	2	317	5%	0.6490	0.8565	2.1633	1	645.16	645.16	100
Palm Oil	Polysorbate 80	19	25	120	4	317	5%	0.3320	0.8999	1.1067	26	396.492	15.25	61.426
Palm Oil	Polysorbate 80	19	25	180	4	317	5%	0.5370	0.8786	1.7900	1	645.16	645.16	100
Palm Oil	Polysorbate 80	19	25	240	4	317	5%	0.7900	0.8565	2.6333	1	645.16	645.16	100
Palm Oil	Polysorbate 80	19	50	120	4	317	5%	0.3260	0.8999	1.0867	71	339.19	4.777	52.549
Palm Oil	Polysorbate 80	19	50	180	4	317	5%	0.5530	0.8786	1.8433	1	645.16	645.16	100
Palm Oil	Polysorbate 80	19	50	240	4	317	5%	0.8130	0.8565	2.7100	1	645.16	645.16	100
Palm Oil	Polysorbate 80	19	25	120	1	317	10%	0.3200	0.8999	1.0667	72	198.593	2.758	30.767
Palm Oil	Polysorbate 80	19	25	180	1	317	10%	0.3420	0.8786	1.1400	41	280.383	6.839	43.438
Palm Oil	Polysorbate 80	19	25	240	1	317	10%	0.4550	0.8565	1.5167	30	485.483	16.183	75.213
Palm Oil	Polysorbate 80	19	50	120	1	317	10%	0.3050	0.8999	1.0167	284	326.935	1.151	50.65
Palm Oil	Polysorbate 80	19	50	180	1	317	10%	0.3550	0.8786	1.1833	94	392.487	4.175	60.806
Palm Oil	Polysorbate 80	19	50	240	1	317	10%	0.4780	0.8565	1.5933	167	414.529	2.482	64.221
Palm Oil	Polysorbate 80	19	25	120	2	317	10%	0.3370	0.8999	1.1233	90	241.308	2.681	37.384
Palm Oil	Polysorbate 80	19	25	180	2	317	10%	0.3970	0.8786	1.3233	47	300.327	6.39	46.528
Palm Oil	Polysorbate 80	19	25	240	2	317	10%	0.5710	0.8565	1.9033	35	512.294	14.637	79.367
Palm Oil	Polysorbate 80	19	50	120	2	317	10%	0.3520	0.8999	1.1733	57	403.936	7.087	62.579
Palm Oil	Polysorbate 80	19	50	180	2	317	10%	0.3940	0.8786	1.3133	60	407.143	6.786	63.076
Palm Oil	Polysorbate 80	19	50	240	2	317	10%	0.5550	0.8565	1.8500	15	585.916	39.061	90.772
Palm Oil	Polysorbate 80	19	25	120	4	317	10%	0.3490	0.8999	1.1633	41	410.341	10.008	63.572
Palm Oil	Polysorbate 80	19	25	180	4	317	10%	0.4950	0.8786	1.6500	53	533.175	10.06	82.602
Palm Oil	Polysorbate 80	19	25	240	4	317	10%	0.6900	0.8565	2.3000	34	562.534	16.545	87.15
Palm Oil	Polysorbate 80	19	50	120	4	317	10%	0.4170	0.8999	1.3900	18	575.63	31.979	89.179
Palm Oil	Polysorbate 80	19	50	180	4	317	10%	0.5180	0.8786	1.7267	10	620.133	62.013	96.073
Palm Oil	Polysorbate 80	19	50	240	4	317	10%	0.6130	0.8565	2.0433	1	645.16	645.16	100

Appendix F – Data Table – Palm Oil

Table 133: Data Table - Palm & Polysorbate 80 @ 22ga

Base Oil	Emulsifier	Needle Gauge	Voltage (kV)	Temp (F)	Pressure (psi)	Time (ms)	Concentration	Weight (g)	Density (g/cm^3)	Mass Flow (g/s)	Droplet Count	Total Area (mm^2)	Average Size (mm^2)	% Area Coverage
Palm Oil	Polysorbate 80	22	25	120	4	317	5%	0.0610	0.8999	0.2033	241	80.746	0.335	12.51
Palm Oil	Polysorbate 80	22	25	180	4	317	5%	0.0840	0.8786	0.2800	263	111.699	0.425	17.305
Palm Oil	Polysorbate 80	22	25	240	4	317	5%	0.0950	0.8565	0.3167	293	141.116	0.482	21.862
Palm Oil	Polysorbate 80	22	50	120	4	317	5%	0.0890	0.8999	0.2967	156	122.278	0.784	18.944
Palm Oil	Polysorbate 80	22	50	180	4	317	5%	0.1110	0.8786	0.3700	85	131.486	1.547	20.37
Palm Oil	Polysorbate 80	22	50	240	4	317	5%	0.0890	0.8565	0.2967	84	175.23	2.086	27.147
Palm Oil	Polysorbate 80	22	25	120	8	317	5%	0.0960	0.8999	0.3200	78	88.016	1.128	13.636
Palm Oil	Polysorbate 80	22	25	180	8	317	5%	0.1160	0.8786	0.3867	279	162.708	0.583	25.207
Palm Oil	Polysorbate 80	22	25	240	8	317	5%	0.1200	0.8565	0.4000	186	281.053	1.511	43.542
Palm Oil	Polysorbate 80	22	50	120	8	317	5%	0.0930	0.8999	0.3100	294	261.788	0.89	40.557
Palm Oil	Polysorbate 80	22	50	180	8	317	5%	0.1340	0.8786	0.4467	271	227.57	0.84	35.256
Palm Oil	Polysorbate 80	22	50	240	8	317	5%	0.1500	0.8565	0.5000	84	428.314	5.099	66.356
Palm Oil	Polysorbate 80	22	25	120	16	317	5%	0.1410	0.8999	0.4700	462	192.477	0.417	29.819
Palm Oil	Polysorbate 80	22	25	180	16	317	5%	0.1810	0.8786	0.6033	290	411.664	1.42	63.777
Palm Oil	Polysorbate 80	22	25	240	16	317	5%	0.1920	0.8565	0.6400	386	499.895	1.295	77.446
Palm Oil	Polysorbate 80	22	50	120	16	317	5%	0.1640	0.8999	0.5467	185	274.854	1.486	42.582
Palm Oil	Polysorbate 80	22	50	180	16	317	5%	0.2030	0.8786	0.6767	247	411.715	1.667	63.785
Palm Oil	Polysorbate 80	22	50	240	16	317	5%	0.2260	0.8565	0.7533	60	444.218	7.404	68.82
Palm Oil	Polysorbate 80	22	25	120	4	317	10%	0.0260	0.8999	0.0867	205	9.011	0.044	1.396
Palm Oil	Polysorbate 80	22	25	180	4	317	10%	0.0260	0.8786	0.0867	302	13.725	0.045	2.126
Palm Oil	Polysorbate 80	22	25	240	4	317	10%	0.0690	0.8565	0.2300	456	46.67	0.102	7.23
Palm Oil	Polysorbate 80	22	50	120	4	317	10%	0.0220	0.8999	0.0733	317	16.848	0.053	2.61
Palm Oil	Polysorbate 80	22	50	180	4	317	10%	0.0230	0.8786	0.0767	988	57.753	0.058	8.947
Palm Oil	Polysorbate 80	22	50	240	4	317	10%	0.0720	0.8565	0.2400	304	172.044	0.566	26.654
Palm Oil	Polysorbate 80	22	25	120	8	317	10%	0.0330	0.8999	0.1100	268	31.042	0.116	4.809
Palm Oil	Polysorbate 80	22	25	180	8	317	10%	0.0390	0.8786	0.1300	394	33.853	0.086	5.245
Palm Oil	Polysorbate 80	22	25	240	8	317	10%	0.0960	0.8565	0.3200	1257	135.699	0.108	21.023
Palm Oil	Polysorbate 80	22	50	120	8	317	10%	0.0270	0.8999	0.0900	320	42.355	0.132	6.562
Palm Oil	Polysorbate 80	22	50	180	8	317	10%	0.0350	0.8786	0.1167	955	78.777	0.082	12.205
Palm Oil	Polysorbate 80	22	50	240	8	317	10%	0.1010	0.8565	0.3367	552	183.723	0.333	28.463
Palm Oil	Polysorbate 80	22	25	120	16	317	10%	0.0430	0.8999	0.1433	87	46.287	0.532	7.171
Palm Oil	Polysorbate 80	22	25	180	16	317	10%	0.0770	0.8786	0.2567	322	43.33	0.135	6.713
Palm Oil	Polysorbate 80	22	25	240	16	317	10%	0.1630	0.8565	0.5433	467	172.001	0.368	26.647
Palm Oil	Polysorbate 80	22	50	120	16	317	10%	0.0430	0.8999	0.1433	269	52.396	0.195	8.117
Palm Oil	Polysorbate 80	22	50	180	16	317	10%	0.0860	0.8786	0.2867	693	79.129	0.114	12.259
Palm Oil	Polysorbate 80	22	50	240	16	317	10%	0.1500	0.8565	0.5000	219	254.855	1.164	39.483

Appendix F – Data Table – Palm Oil

Table 134: Data Table - Palm & Propylene Glycol @ 19ga

Base Oil	Emulsifier	Needle Gauge	Voltage (kV)	Temp (F)	Pressure (psi)	Time (ms)	Concentration	Weight (g)	Density (g/cm^3)	Mass Flow (g/s)	Droplet Count	Total Area (mm^2)	Average Size (mm^2)	% Area Coverage
Palm Oil	Propylene Glycol	19	25	120	1	317	5%	0.2200	0.8999	0.7333	24	186.182	7.758	28.844
Palm Oil	Propylene Glycol	19	25	180	1	317	5%	0.4120	0.8786	1.3733	1	645.16	645.16	100
Palm Oil	Propylene Glycol	19	25	240	1	317	5%	0.5990	0.8565	1.9967	1	645.16	645.16	100
Palm Oil	Propylene Glycol	19	50	120	1	317	5%	0.2400	0.8999	0.8000	45	271.194	6.027	42.015
Palm Oil	Propylene Glycol	19	50	180	1	317	5%	0.3790	0.8786	1.2633	1	645.16	645.16	100
Palm Oil	Propylene Glycol	19	50	240	1	317	5%	0.6090	0.8565	2.0300	1	645.16	645.16	100
Palm Oil	Propylene Glycol	19	25	120	2	317	5%	0.2530	0.8999	0.8433	32	192.087	6.003	29.759
Palm Oil	Propylene Glycol	19	25	180	2	317	5%	0.4610	0.8786	1.5367	1	645.16	645.16	100
Palm Oil	Propylene Glycol	19	25	240	2	317	5%	0.6730	0.8565	2.2433	1	645.16	645.16	100
Palm Oil	Propylene Glycol	19	50	120	2	317	5%	0.2490	0.8999	0.8300	36	269.775	7.494	41.795
Palm Oil	Propylene Glycol	19	50	180	2	317	5%	0.4700	0.8786	1.5667	1	645.16	645.16	100
Palm Oil	Propylene Glycol	19	50	240	2	317	5%	0.6880	0.8565	2.2933	1	645.16	645.16	100
Palm Oil	Propylene Glycol	19	25	120	4	317	5%	0.3010	0.8999	1.0033	29	383.184	13.213	59.364
Palm Oil	Propylene Glycol	19	25	180	4	317	5%	0.5580	0.8786	1.8600	1	645.16	645.16	100
Palm Oil	Propylene Glycol	19	25	240	4	317	5%	0.8380	0.8565	2.7933	1	645.16	645.16	100
Palm Oil	Propylene Glycol	19	50	120	4	317	5%	0.3560	0.8999	1.1867	33	424.239	12.856	65.725
Palm Oil	Propylene Glycol	19	50	180	4	317	5%	0.5750	0.8786	1.9167	1	645.16	645.16	100
Palm Oil	Propylene Glycol	19	50	240	4	317	5%	0.8440	0.8565	2.8133	1	645.16	645.16	100
Palm Oil	Propylene Glycol	19	25	120	1	317	10%	0.3890	0.8999	1.2967	50	268.298	5.366	41.566
Palm Oil	Propylene Glycol	19	25	180	1	317	10%	0.5630	0.8786	1.8767	1	645.16	645.16	100
Palm Oil	Propylene Glycol	19	25	240	1	317	10%	0.5280	0.8565	1.7600	1	645.16	645.16	100
Palm Oil	Propylene Glycol	19	50	120	1	317	10%	0.4010	0.8999	1.3367	62	302.279	4.875	46.83
Palm Oil	Propylene Glycol	19	50	180	1	317	10%	0.5750	0.8786	1.9167	1	645.16	645.16	100
Palm Oil	Propylene Glycol	19	50	240	1	317	10%	0.5440	0.8565	1.8133	1	645.16	645.16	100
Palm Oil	Propylene Glycol	19	25	120	2	317	10%	0.4280	0.8999	1.4267	24	479.396	19.975	74.27
Palm Oil	Propylene Glycol	19	25	180	2	317	10%	0.6430	0.8786	2.1433	1	645.16	645.16	100
Palm Oil	Propylene Glycol	19	25	240	2	317	10%	0.6230	0.8565	2.0767	1	645.16	645.16	100
Palm Oil	Propylene Glycol	19	50	120	2	317	10%	0.4560	0.8999	1.5200	4	518.936	129.734	80.396
Palm Oil	Propylene Glycol	19	50	180	2	317	10%	0.6720	0.8786	2.2400	1	645.16	645.16	100
Palm Oil	Propylene Glycol	19	50	240	2	317	10%	0.6770	0.8565	2.2567	54	517.363	9.581	80.152
Palm Oil	Propylene Glycol	19	25	120	4	317	10%	0.4790	0.8999	1.5967	1	645.16	645.16	100
Palm Oil	Propylene Glycol	19	25	180	4	317	10%	0.8000	0.8786	2.6667	1	645.16	645.16	100
Palm Oil	Propylene Glycol	19	25	240	4	317	10%	0.7500	0.8565	2.5000	31	567.577	18.309	87.931
Palm Oil	Propylene Glycol	19	50	120	4	317	10%	0.5120	0.8999	1.7067	1	645.16	645.16	100
Palm Oil	Propylene Glycol	19	50	180	4	317	10%	0.8090	0.8786	2.6967	1	645.16	645.16	100
Palm Oil	Propylene Glycol	19	50	240	4	317	10%	0.7590	0.8565	2.5300	28	598.278	21.367	92.688

Appendix F – Data Table – Palm Oil

Table 135: Data Table - Palm & Propylene Glycol @ 22ga

Base Oil	Emulsifier	Needle Gauge	Voltage (kV)	Temp (F)	Pressure (psi)	Time (ms)	Concentration	Weight (g)	Density (g/cm^3)	Mass Flow (g/s)	Droplet Count	Total Area (mm^2)	Average Size (mm^2)	% Area Coverage
Palm Oil	Propylene Glycol	22	25	120	4	317	5%	0.0580	0.8999	0.1933	69	32.104	0.465	4.974
Palm Oil	Propylene Glycol	22	25	180	4	317	5%	0.0670	0.8786	0.2233	356	60.342	0.169	9.348
Palm Oil	Propylene Glycol	22	25	240	4	317	5%	0.9500	0.8565	3.1667	997	106.7	0.107	16.53
Palm Oil	Propylene Glycol	22	50	120	4	317	5%	0.0610	0.8999	0.2033	106	85.539	0.807	13.252
Palm Oil	Propylene Glycol	22	50	180	4	317	5%	0.0870	0.8786	0.2900	387	90.065	0.233	13.953
Palm Oil	Propylene Glycol	22	50	240	4	317	5%	0.0920	0.8565	0.3067	877	135.403	0.154	20.977
Palm Oil	Propylene Glycol	22	25	120	8	317	5%	0.0810	0.8999	0.2700	65	28.762	0.442	4.456
Palm Oil	Propylene Glycol	22	25	180	8	317	5%	0.0850	0.8786	0.2833	103	34.486	0.335	5.343
Palm Oil	Propylene Glycol	22	25	240	8	317	5%	0.1260	0.8565	0.4200	77	111.049	1.442	17.204
Palm Oil	Propylene Glycol	22	50	120	8	317	5%	0.0780	0.8999	0.2600	96	56.235	0.586	8.712
Palm Oil	Propylene Glycol	22	50	180	8	317	5%	0.1270	0.8786	0.4233	528	78.154	0.148	12.108
Palm Oil	Propylene Glycol	22	50	240	8	317	5%	0.1390	0.8565	0.4633	80	140.071	1.751	21.7
Palm Oil	Propylene Glycol	22	25	120	16	317	5%	0.1250	0.8999	0.4167	48	51.295	1.069	7.947
Palm Oil	Propylene Glycol	22	25	180	16	317	5%	0.1240	0.8786	0.4133	124	36.468	0.294	5.65
Palm Oil	Propylene Glycol	22	25	240	16	317	5%	0.2090	0.8565	0.6967	94	97.018	1.032	15.03
Palm Oil	Propylene Glycol	22	50	120	16	317	5%	0.1230	0.8999	0.4100	83	113.608	1.369	17.601
Palm Oil	Propylene Glycol	22	50	180	16	317	5%	0.1200	0.8786	0.4000	218	84.584	0.388	13.104
Palm Oil	Propylene Glycol	22	50	240	16	317	5%	0.2860	0.8565	0.9533	76	132.995	1.75	20.604
Palm Oil	Propylene Glycol	22	25	120	4	317	10%	0.1180	0.8999	0.3933	1963	256.512	0.131	39.74
Palm Oil	Propylene Glycol	22	25	180	4	317	10%	0.0700	0.8786	0.2333	1558	184.236	0.118	28.543
Palm Oil	Propylene Glycol	22	25	240	4	317	10%	0.0720	0.8565	0.2400	1066	119.11	0.112	18.453
Palm Oil	Propylene Glycol	22	50	120	4	317	10%	0.0880	0.8999	0.2933	2420	215.772	0.089	33.428
Palm Oil	Propylene Glycol	22	50	180	4	317	10%	0.0830	0.8786	0.2767	1311	161.476	0.123	25.016
Palm Oil	Propylene Glycol	22	50	240	4	317	10%	0.0790	0.8565	0.2633	281	130.895	0.466	20.279
Palm Oil	Propylene Glycol	22	25	120	8	317	10%	0.1160	0.8999	0.3867	2233	200.042	0.09	30.991
Palm Oil	Propylene Glycol	22	25	180	8	317	10%	0.1090	0.8786	0.3633	1218	210.576	0.173	32.623
Palm Oil	Propylene Glycol	22	25	240	8	317	10%	0.1110	0.8565	0.3700	429	86.722	0.202	13.435
Palm Oil	Propylene Glycol	22	50	120	8	317	10%	0.1060	0.8999	0.3533	2089	206.377	0.099	31.973
Palm Oil	Propylene Glycol	22	50	180	8	317	10%	0.1160	0.8786	0.3867	1239	256.867	0.207	39.795
Palm Oil	Propylene Glycol	22	50	240	8	317	10%	0.1050	0.8565	0.3500	837	180.639	0.216	27.985
Palm Oil	Propylene Glycol	22	25	120	16	317	10%	0.1480	0.8999	0.4933	839	90.974	0.108	14.094
Palm Oil	Propylene Glycol	22	25	180	16	317	10%	0.1720	0.8786	0.5733	826	96.014	0.116	14.875
Palm Oil	Propylene Glycol	22	25	240	16	317	10%	0.1850	0.8565	0.6167	1222	203.378	0.166	31.508
Palm Oil	Propylene Glycol	22	50	120	16	317	10%	0.1460	0.8999	0.4867	757	331.688	0.438	51.386
Palm Oil	Propylene Glycol	22	50	180	16	317	10%	0.1910	0.8786	0.6367	900	147.008	0.163	22.775
Palm Oil	Propylene Glycol	22	50	240	16	317	10%	0.1990	0.8565	0.6633	615	183.934	0.299	28.496

Appendix G – Data Table – Soybean Oil

Table 136: Data Table – Soybean & Soy Lecithin @ 19ga

Base Oil	Emulsifier	Needle Gauge	Voltage (kV)	Temp (F)	Pressure (psi)	Time (ms)	Concentration	Weight (g)	Density (g/cm^3)	Mass Flow (g/s)	Droplet Count	Total Area (mm^2)	Average Size (mm^2)	% Area Coverage
Soybean Oil	Soybean Lecithin	19	25	120	1	317	5%	0.3150	0.9005	1.05	335	282.862	0.844	43.794
Soybean Oil	Soybean Lecithin	19	25	180	1	317	5%	0.2980	0.8802	0.9933	164	268.759	1.639	41.61
Soybean Oil	Soybean Lecithin	19	25	240	1	317	5%	0.3820	0.8593	1.2733	86	256.122	2.978	39.654
Soybean Oil	Soybean Lecithin	19	50	120	1	317	5%	0.3080	0.9005	1.0267	740	235.75	0.319	36.5
Soybean Oil	Soybean Lecithin	19	50	180	1	317	5%	0.3040	0.8802	1.0133	617	352.616	0.572	54.594
Soybean Oil	Soybean Lecithin	19	50	240	1	317	5%	0.3830	0.8593	1.2767	164	312.434	1.905	48.372
Soybean Oil	Soybean Lecithin	19	25	120	2	317	5%	0.3370	0.9005	1.1233	218	247.253	1.134	38.281
Soybean Oil	Soybean Lecithin	19	25	180	2	317	5%	0.3710	0.8802	1.2367	156	274.115	1.757	42.44
Soybean Oil	Soybean Lecithin	19	25	240	2	317	5%	0.4270	0.8593	1.4233	34	559.991	16.47	86.7
Soybean Oil	Soybean Lecithin	19	50	120	2	317	5%	0.3340	0.9005	1.1133	189	284.442	1.505	44.039
Soybean Oil	Soybean Lecithin	19	50	180	2	317	5%	0.3790	0.8802	1.2633	56	391.317	6.988	60.585
Soybean Oil	Soybean Lecithin	19	50	240	2	317	5%	0.4300	0.8593	1.4333	40	582.588	14.565	90.199
Soybean Oil	Soybean Lecithin	19	25	120	4	317	5%	0.3930	0.9005	1.3100	250	346.954	1.388	53.717
Soybean Oil	Soybean Lecithin	19	25	180	4	317	5%	0.5510	0.8802	1.8367	104	405.795	3.902	62.827
Soybean Oil	Soybean Lecithin	19	25	240	4	317	5%	0.5100	0.8593	1.7000	29	603.334	20.805	93.411
Soybean Oil	Soybean Lecithin	19	50	120	4	317	5%	0.3880	0.9005	1.2933	263	344.888	1.311	53.397
Soybean Oil	Soybean Lecithin	19	50	180	4	317	5%	0.5790	0.8802	1.9300	169	382.802	2.265	59.267
Soybean Oil	Soybean Lecithin	19	50	240	4	317	5%	0.5080	0.8593	1.6933	105	494.182	4.706	76.511
Soybean Oil	Soybean Lecithin	19	25	120	1	317	10%	0.1980	0.9005	0.6600	138	202.75	1.469	31.391
Soybean Oil	Soybean Lecithin	19	25	180	1	317	10%	0.2940	0.8802	0.9800	197	153.365	0.779	23.76
Soybean Oil	Soybean Lecithin	19	25	240	1	317	10%	0.5120	0.8593	1.7067	226	252.708	1.118	39.151
Soybean Oil	Soybean Lecithin	19	50	120	1	317	10%	0.1950	0.9005	0.6500	35	183.675	5.248	28.456
Soybean Oil	Soybean Lecithin	19	50	180	1	317	10%	0.3730	0.8802	1.2433	52	141.399	2.719	21.906
Soybean Oil	Soybean Lecithin	19	50	240	1	317	10%	0.4870	0.8593	1.6233	95	322.146	3.391	49.908
Soybean Oil	Soybean Lecithin	19	25	120	2	317	10%	0.2200	0.9005	0.7333	53	134.688	2.541	20.866
Soybean Oil	Soybean Lecithin	19	25	180	2	317	10%	0.3960	0.8802	1.3200	72	192.751	2.677	29.862
Soybean Oil	Soybean Lecithin	19	25	240	2	317	10%	0.5020	0.8593	1.6733	102	213.881	2.097	33.135
Soybean Oil	Soybean Lecithin	19	50	120	2	317	10%	0.2270	0.9005	0.7567	115	212.461	1.847	32.915
Soybean Oil	Soybean Lecithin	19	50	180	2	317	10%	0.3690	0.8802	1.2300	168	225.224	1.341	34.893
Soybean Oil	Soybean Lecithin	19	50	240	2	317	10%	0.4730	0.8593	1.5767	128	325.095	2.54	50.365
Soybean Oil	Soybean Lecithin	19	25	120	4	317	10%	0.2760	0.9005	0.9200	89	240.09	2.698	37.196
Soybean Oil	Soybean Lecithin	19	25	180	4	317	10%	0.4290	0.8802	1.4300	38	178.736	4.704	27.691
Soybean Oil	Soybean Lecithin	19	25	240	4	317	10%	0.5660	0.8593	1.8867	25	318.862	12.754	49.399
Soybean Oil	Soybean Lecithin	19	50	120	4	317	10%	0.2770	0.9005	0.9233	20	472.793	23.64	73.247
Soybean Oil	Soybean Lecithin	19	50	180	4	317	10%	0.4250	0.8802	1.4167	11	342.955	31.178	53.132
Soybean Oil	Soybean Lecithin	19	50	240	4	317	10%	0.5510	0.8593	1.8367	8	510.976	63.872	79.162

Appendix G – Data Table – Soybean Oil

Table 137: Data Table – Soybean & Soy Lecithin @ 22ga

Base Oil	Emulsifier	Needle Gauge	Voltage (kV)	Temp (F)	Pressure (psi)	Time (ms)	Concentration	Weight (g)	Density (g/cm^3)	Mass Flow (g/s)	Droplet Count	Total Area (mm^2)	Average Size (mm^2)	% Area Coverage
Soybean Oil	Soybean Lecithin	22	25	120	4	317	5%	0.0690	0.9005	0.2300	217	64.465	0.297	9.981
Soybean Oil	Soybean Lecithin	22	25	180	4	317	5%	0.0920	0.8802	0.3067	306	92.5	0.302	14.321
Soybean Oil	Soybean Lecithin	22	25	240	4	317	5%	0.0740	0.8593	0.2467	333	190.389	0.633	29.477
Soybean Oil	Soybean Lecithin	22	50	120	4	317	5%	0.0710	0.9005	0.2367	182	159.011	0.874	24.619
Soybean Oil	Soybean Lecithin	22	50	180	4	317	5%	0.0980	0.8802	0.3267	187	212.45	1.136	32.892
Soybean Oil	Soybean Lecithin	22	50	240	4	317	5%	0.0720	0.8593	0.2400	324	239.124	0.738	37.022
Soybean Oil	Soybean Lecithin	22	25	120	8	317	5%	0.1020	0.9005	0.3400	27	86.755	3.213	13.432
Soybean Oil	Soybean Lecithin	22	25	180	8	317	5%	0.1340	0.8802	0.4467	35	94.315	2.695	14.602
Soybean Oil	Soybean Lecithin	22	25	240	8	317	5%	0.1060	0.8593	0.3533	33	107.886	3.269	16.703
Soybean Oil	Soybean Lecithin	22	50	120	8	317	5%	0.1000	0.9005	0.3333	172	145.951	0.849	22.597
Soybean Oil	Soybean Lecithin	22	50	180	8	317	5%	0.1360	0.8802	0.4533	193	190.671	0.988	29.521
Soybean Oil	Soybean Lecithin	22	50	240	8	317	5%	0.1020	0.8593	0.3400	247	303.162	1.227	46.937
Soybean Oil	Soybean Lecithin	22	25	120	16	317	5%	0.1510	0.9005	0.5033	24	100.443	4.185	15.551
Soybean Oil	Soybean Lecithin	22	25	180	16	317	5%	0.2120	0.8802	0.7067	55	202.394	3.68	31.335
Soybean Oil	Soybean Lecithin	22	25	240	16	317	5%	0.1670	0.8593	0.5567	65	271.081	4.17	41.97
Soybean Oil	Soybean Lecithin	22	50	120	16	317	5%	0.1540	0.9005	0.5133	64	264.825	4.138	41.001
Soybean Oil	Soybean Lecithin	22	50	180	16	317	5%	0.2170	0.8802	0.7233	79	306.414	3.879	47.44
Soybean Oil	Soybean Lecithin	22	50	240	16	317	5%	0.1590	0.8593	0.5300	140	315.185	2.251	48.798
Soybean Oil	Soybean Lecithin	22	25	120	4	317	10%	0.0350	0.9005	0.1167	55	70.022	1.273	10.841
Soybean Oil	Soybean Lecithin	22	25	180	4	317	10%	0.0470	0.8802	0.1567	70	85.132	1.216	13.18
Soybean Oil	Soybean Lecithin	22	25	240	4	317	10%	0.0580	0.8593	0.1933	77	92.451	1.201	14.314
Soybean Oil	Soybean Lecithin	22	50	120	4	317	10%	0.0350	0.9005	0.1167	129	154.071	1.194	23.854
Soybean Oil	Soybean Lecithin	22	50	180	4	317	10%	0.0470	0.8802	0.1567	143	222.603	1.557	34.464
Soybean Oil	Soybean Lecithin	22	50	240	4	317	10%	0.0590	0.8593	0.1967	147	243.599	1.657	37.715
Soybean Oil	Soybean Lecithin	22	25	120	8	317	10%	0.0470	0.9005	0.1567	59	100.315	1.7	15.531
Soybean Oil	Soybean Lecithin	22	25	180	8	317	10%	0.0690	0.8802	0.2300	69	110.244	1.598	17.068
Soybean Oil	Soybean Lecithin	22	25	240	8	317	10%	0.0850	0.8593	0.2833	196	157.453	0.803	24.378
Soybean Oil	Soybean Lecithin	22	50	120	8	317	10%	0.0480	0.9005	0.1600	163	269.671	1.654	41.752
Soybean Oil	Soybean Lecithin	22	50	180	8	317	10%	0.0680	0.8802	0.2267	187	235.376	1.259	36.442
Soybean Oil	Soybean Lecithin	22	50	240	8	317	10%	0.0860	0.8593	0.2867	223	186.908	0.838	28.938
Soybean Oil	Soybean Lecithin	22	25	120	16	317	10%	0.0670	0.9005	0.2233	85	138.52	1.63	21.446
Soybean Oil	Soybean Lecithin	22	25	180	16	317	10%	0.1090	0.8802	0.3633	68	171.081	2.516	26.488
Soybean Oil	Soybean Lecithin	22	25	240	16	317	10%	0.1290	0.8593	0.4300	142	168.062	1.184	26.02
Soybean Oil	Soybean Lecithin	22	50	120	16	317	10%	0.0690	0.9005	0.2300	258	260.971	1.012	40.431
Soybean Oil	Soybean Lecithin	22	50	180	16	317	10%	0.1110	0.8802	0.3700	329	322.029	0.979	49.89
Soybean Oil	Soybean Lecithin	22	50	240	16	317	10%	0.1310	0.8593	0.4367	978	289.195	0.296	44.803

Appendix G – Data Table – Soybean Oil

Table 138: Data Table – Soybean & Polysorbate 20 @ 19ga

Base Oil	Emulsifier	Needle Gauge	Voltage (kV)	Temp (F)	Pressure (psi)	Time (ms)	Concentration	Weight (g)	Density (g/cm^3)	Mass Flow (g/s)	Droplet Count	Total Area (mm^2)	Average Size (mm^2)	% Area Coverage
Soybean Oil	Polysorbate 20	19	25	120	1	317	5%	0.5600	0.9005	1.8667	159	440.158	2.768	68.191
Soybean Oil	Polysorbate 20	19	25	180	1	317	5%	0.6830	0.8802	2.2767	1	645.16	645.16	100
Soybean Oil	Polysorbate 20	19	25	240	1	317	5%	0.6510	0.8593	2.1700	47	532.896	11.338	82.558
Soybean Oil	Polysorbate 20	19	50	120	1	317	5%	0.5810	0.9005	1.9367	13	601.88	46.298	93.246
Soybean Oil	Polysorbate 20	19	50	180	1	317	5%	0.7290	0.8802	2.4300	1	645.16	645.16	100
Soybean Oil	Polysorbate 20	19	50	240	1	317	5%	0.6670	0.8593	2.2233	1	645.16	645.16	100
Soybean Oil	Polysorbate 20	19	25	120	2	317	5%	0.7200	0.9005	2.4000	1	645.16	645.16	100
Soybean Oil	Polysorbate 20	19	25	180	2	317	5%	0.8510	0.8802	2.8367	1	645.16	645.16	100
Soybean Oil	Polysorbate 20	19	25	240	2	317	5%	0.8300	0.8593	2.7667	1	645.16	645.16	100
Soybean Oil	Polysorbate 20	19	50	120	2	317	5%	0.7400	0.9005	2.4667	1	645.16	645.16	100
Soybean Oil	Polysorbate 20	19	50	180	2	317	5%	0.8700	0.8802	2.9000	1	645.16	645.16	100
Soybean Oil	Polysorbate 20	19	50	240	2	317	5%	0.8860	0.8593	2.9533	1	645.16	645.16	100
Soybean Oil	Polysorbate 20	19	25	120	4	317	5%	0.9500	0.9005	3.1667	1	645.16	645.16	100
Soybean Oil	Polysorbate 20	19	25	180	4	317	5%	1.1630	0.8802	3.8767	1	645.16	645.16	100
Soybean Oil	Polysorbate 20	19	25	240	4	317	5%	1.1710	0.8593	3.9033	1	645.16	645.16	100
Soybean Oil	Polysorbate 20	19	50	120	4	317	5%	1.0040	0.9005	3.3467	1	645.16	645.16	100
Soybean Oil	Polysorbate 20	19	50	180	4	317	5%	1.2080	0.8802	4.0267	1	645.16	645.16	100
Soybean Oil	Polysorbate 20	19	50	240	4	317	5%	1.1790	0.8593	3.9300	1	645.16	645.16	100
Soybean Oil	Polysorbate 20	19	25	120	1	317	10%	0.3010	0.9005	1.0033	110	196.912	1.79	30.506
Soybean Oil	Polysorbate 20	19	25	180	1	317	10%	0.4180	0.8802	1.3933	14	465.237	33.231	72.076
Soybean Oil	Polysorbate 20	19	25	240	1	317	10%	0.6140	0.8593	2.0467	11	553.021	50.275	85.676
Soybean Oil	Polysorbate 20	19	50	120	1	317	10%	0.3130	0.9005	1.0433	387	376.524	0.973	58.333
Soybean Oil	Polysorbate 20	19	50	180	1	317	10%	0.4320	0.8802	1.4400	93	476.918	5.128	73.886
Soybean Oil	Polysorbate 20	19	50	240	1	317	10%	0.6090	0.8593	2.0300	17	542.948	31.938	84.116
Soybean Oil	Polysorbate 20	19	25	120	2	317	10%	0.4300	0.9005	1.4333	45	491.74	10.928	76.182
Soybean Oil	Polysorbate 20	19	25	180	2	317	10%	0.5000	0.8802	1.6667	10	530.398	53.04	82.171
Soybean Oil	Polysorbate 20	19	25	240	2	317	10%	0.8260	0.8593	2.7533	1	645.16	645.16	100
Soybean Oil	Polysorbate 20	19	50	120	2	317	10%	0.4030	0.9005	1.3433	129	370.828	2.875	57.45
Soybean Oil	Polysorbate 20	19	50	180	2	317	10%	0.5200	0.8802	1.7333	19	557.546	29.345	86.377
Soybean Oil	Polysorbate 20	19	50	240	2	317	10%	0.8660	0.8593	2.8867	1	645.16	645.16	100
Soybean Oil	Polysorbate 20	19	25	120	4	317	10%	0.6000	0.9005	2.0000	1	645.16	645.16	100
Soybean Oil	Polysorbate 20	19	25	180	4	317	10%	0.6780	0.8802	2.2600	1	645.16	645.16	100
Soybean Oil	Polysorbate 20	19	25	240	4	317	10%	1.1480	0.8593	3.8267	1	645.16	645.16	100
Soybean Oil	Polysorbate 20	19	50	120	4	317	10%	0.5990	0.9005	1.9967	1	645.16	645.16	100
Soybean Oil	Polysorbate 20	19	50	180	4	317	10%	0.6600	0.8802	2.2000	1	645.16	645.16	100
Soybean Oil	Polysorbate 20	19	50	240	4	317	10%	1.1780	0.8593	3.9267	1	645.16	645.16	100

Appendix G – Data Table – Soybean Oil

Table 139: Data Table – Soybean & Polysorbate 20 @ 22ga

Base Oil	Emulsifier	Needle Gauge	Voltage (kV)	Temp (F)	Pressure (psi)	Time (ms)	Concentration	Weight (g)	Density (g/cm^3)	Mass Flow (g/s)	Droplet Count	Total Area (mm^2)	Average Size (mm^2)	% Area Coverage
Soybean Oil	Polysorbate 20	22	25	120	4	317	5%	0.0380	0.9005	0.1267	203	93.564	0.461	14.495
Soybean Oil	Polysorbate 20	22	25	180	4	317	5%	0.0370	0.8802	0.1233	63	110.438	1.753	17.109
Soybean Oil	Polysorbate 20	22	25	240	4	317	5%	0.0430	0.8593	0.1433	12	189.967	15.831	29.43
Soybean Oil	Polysorbate 20	22	50	120	4	317	5%	0.0350	0.9005	0.1167	218	146.697	0.673	22.727
Soybean Oil	Polysorbate 20	22	50	180	4	317	5%	0.0370	0.8802	0.1233	64	287.236	4.488	44.5
Soybean Oil	Polysorbate 20	22	50	240	4	317	5%	0.0410	0.8593	0.1367	36	372.689	10.352	57.739
Soybean Oil	Polysorbate 20	22	25	120	8	317	5%	0.0440	0.9005	0.1467	86	72.475	0.843	11.228
Soybean Oil	Polysorbate 20	22	25	180	8	317	5%	0.0460	0.8802	0.1533	46	156.09	3.393	24.182
Soybean Oil	Polysorbate 20	22	25	240	8	317	5%	0.0550	0.8593	0.1833	28	335.047	11.966	51.907
Soybean Oil	Polysorbate 20	22	50	120	8	317	5%	0.0410	0.9005	0.1367	59	161.406	2.736	25.006
Soybean Oil	Polysorbate 20	22	50	180	8	317	5%	0.0450	0.8802	0.1500	66	288.939	4.378	44.764
Soybean Oil	Polysorbate 20	22	50	240	8	317	5%	0.0560	0.8593	0.1867	30	370.639	12.355	57.421
Soybean Oil	Polysorbate 20	22	25	120	16	317	5%	0.0570	0.9005	0.1900	65	115.503	1.777	17.894
Soybean Oil	Polysorbate 20	22	25	180	16	317	5%	0.0610	0.8802	0.2033	39	290.375	7.446	44.986
Soybean Oil	Polysorbate 20	22	25	240	16	317	5%	0.0740	0.8593	0.2467	8	390.003	48.75	60.421
Soybean Oil	Polysorbate 20	22	50	120	16	317	5%	0.0540	0.9005	0.1800	102	140.331	1.376	21.741
Soybean Oil	Polysorbate 20	22	50	180	16	317	5%	0.0620	0.8802	0.2067	49	234.395	4.784	36.313
Soybean Oil	Polysorbate 20	22	50	240	16	317	5%	0.0790	0.8593	0.2633	31	510.854	16.479	79.144
Soybean Oil	Polysorbate 20	22	25	120	4	317	10%	0.0470	0.9005	0.1567	128	95.733	0.748	14.831
Soybean Oil	Polysorbate 20	22	25	180	4	317	10%	0.0600	0.8802	0.2000	98	107.272	1.095	16.619
Soybean Oil	Polysorbate 20	22	25	240	4	317	10%	0.6700	0.8593	2.2333	138	85.838	0.622	13.298
Soybean Oil	Polysorbate 20	22	50	120	4	317	10%	0.0480	0.9005	0.1600	151	115.407	0.764	17.879
Soybean Oil	Polysorbate 20	22	50	180	4	317	10%	0.0610	0.8802	0.2033	181	149.488	0.826	23.159
Soybean Oil	Polysorbate 20	22	50	240	4	317	10%	0.0650	0.8593	0.2167	191	100.271	0.525	15.534
Soybean Oil	Polysorbate 20	22	25	120	8	317	10%	0.0580	0.9005	0.1933	50	97.683	1.954	15.133
Soybean Oil	Polysorbate 20	22	25	180	8	317	10%	0.0710	0.8802	0.2367	89	97.007	1.09	15.029
Soybean Oil	Polysorbate 20	22	25	240	8	317	10%	0.0650	0.8593	0.2167	130	151.465	1.165	23.466
Soybean Oil	Polysorbate 20	22	50	120	8	317	10%	0.0570	0.9005	0.1900	73	113.748	1.558	17.622
Soybean Oil	Polysorbate 20	22	50	180	8	317	10%	0.0750	0.8802	0.2500	205	139.166	0.679	21.56
Soybean Oil	Polysorbate 20	22	50	240	8	317	10%	0.0780	0.8593	0.2600	187	189.303	1.012	29.328
Soybean Oil	Polysorbate 20	22	25	120	16	317	10%	0.8000	0.9005	2.6667	52	164.904	3.171	25.548
Soybean Oil	Polysorbate 20	22	25	180	16	317	10%	0.1010	0.8802	0.3367	80	109.944	1.374	17.033
Soybean Oil	Polysorbate 20	22	25	240	16	317	10%	0.1110	0.8593	0.3700	87	260.029	2.989	40.285
Soybean Oil	Polysorbate 20	22	50	120	16	317	10%	0.0810	0.9005	0.2700	187	130.971	0.7	20.291
Soybean Oil	Polysorbate 20	22	50	180	16	317	10%	0.1070	0.8802	0.3567	201	138.529	0.689	21.462
Soybean Oil	Polysorbate 20	22	50	240	16	317	10%	0.1100	0.8593	0.3667	254	219.636	0.865	34.027

Appendix G – Data Table – Soybean Oil

Table 140: Data Table – Soybean & Propylene Glycol @ 19ga

Base Oil	Emulsifier	Needle Gauge	Voltage (kV)	Temp (F)	Pressure (psi)	Time (ms)	Concentration	Weight (g)	Density (g/cm^3)	Mass Flow (g/s)	Droplet Count	Total Area (mm^2)	Average Size (mm^2)	% Area Coverage
Soybean Oil	Propylene Glycol	19	25	120	1	317	5%	0.3010	0.9005	1.0033	45	177.943	3.954	27.568
Soybean Oil	Propylene Glycol	19	25	180	1	317	5%	0.4570	0.8802	1.5233	21	328.293	15.633	50.86
Soybean Oil	Propylene Glycol	19	25	240	1	317	5%	0.4940	0.8593	1.6467	15	347.161	23.144	53.784
Soybean Oil	Propylene Glycol	19	50	120	1	317	5%	0.3020	0.9005	1.0067	94	202.439	2.154	31.363
Soybean Oil	Propylene Glycol	19	50	180	1	317	5%	0.4550	0.8802	1.5167	16	365.781	22.861	56.668
Soybean Oil	Propylene Glycol	19	50	240	1	317	5%	0.5020	0.8593	1.6733	14	445.924	31.852	69.084
Soybean Oil	Propylene Glycol	19	25	120	2	317	5%	0.3380	0.9005	1.1267	31	251.354	8.108	38.941
Soybean Oil	Propylene Glycol	19	25	180	2	317	5%	0.5040	0.8802	1.6800	20	479.884	23.994	74.346
Soybean Oil	Propylene Glycol	19	25	240	2	317	5%	0.5830	0.8593	1.9433	1	591.471	591.471	91.633
Soybean Oil	Propylene Glycol	19	50	120	2	317	5%	0.3360	0.9005	1.1200	48	347.124	7.232	53.743
Soybean Oil	Propylene Glycol	19	50	180	2	317	5%	0.4970	0.8802	1.6567	16	392.944	24.559	60.837
Soybean Oil	Propylene Glycol	19	50	240	2	317	5%	0.5740	0.8593	1.9133	13	481.906	37.07	74.611
Soybean Oil	Propylene Glycol	19	25	120	4	317	5%	0.3960	0.9005	1.3200	27	268.279	9.936	41.563
Soybean Oil	Propylene Glycol	19	25	180	4	317	5%	0.6290	0.8802	2.0967	7	523.007	74.715	81.026
Soybean Oil	Propylene Glycol	19	25	240	4	317	5%	0.8010	0.8593	2.6700	2	628.59	314.295	97.384
Soybean Oil	Propylene Glycol	19	50	120	4	317	5%	0.4080	0.9005	1.3600	33	306.536	9.289	47.49
Soybean Oil	Propylene Glycol	19	50	180	4	317	5%	0.6440	0.8802	2.1467	3	644.217	214.739	99.805
Soybean Oil	Propylene Glycol	19	50	240	4	317	5%	0.7460	0.8593	2.4867	1	645.16	645.16	100
Soybean Oil	Propylene Glycol	19	25	120	1	317	10%	0.3280	0.9005	1.0933	26	151.231	5.817	23.429
Soybean Oil	Propylene Glycol	19	25	180	1	317	10%	0.5440	0.8802	1.8133	38	231.233	6.085	35.824
Soybean Oil	Propylene Glycol	19	25	240	1	317	10%	0.4010	0.8593	1.3367	47	367.842	7.826	56.988
Soybean Oil	Propylene Glycol	19	50	120	1	317	10%	0.3200	0.9005	1.0667	69	163.946	2.376	25.399
Soybean Oil	Propylene Glycol	19	50	180	1	317	10%	0.4970	0.8802	1.6567	53	253.485	4.783	39.271
Soybean Oil	Propylene Glycol	19	50	240	1	317	10%	0.3920	0.8593	1.3067	49	404.683	8.259	62.695
Soybean Oil	Propylene Glycol	19	25	120	2	317	10%	0.3750	0.9005	1.2500	29	193.382	6.668	29.959
Soybean Oil	Propylene Glycol	19	25	180	2	317	10%	0.5320	0.8802	1.7733	41	298.771	7.287	46.287
Soybean Oil	Propylene Glycol	19	25	240	2	317	10%	0.4710	0.8593	1.5700	30	437.545	14.585	67.786
Soybean Oil	Propylene Glycol	19	50	120	2	317	10%	0.3660	0.9005	1.2200	42	253.471	6.035	39.269
Soybean Oil	Propylene Glycol	19	50	180	2	317	10%	4.8000	0.8802	16.0000	48	360.556	7.512	55.859
Soybean Oil	Propylene Glycol	19	50	240	2	317	10%	0.4620	0.8593	1.5400	41	500.075	12.197	77.474
Soybean Oil	Propylene Glycol	19	25	120	4	317	10%	0.4770	0.9005	1.5900	46	319.248	6.94	49.459
Soybean Oil	Propylene Glycol	19	25	180	4	317	10%	0.5860	0.8802	1.9533	30	525.974	17.532	81.486
Soybean Oil	Propylene Glycol	19	25	240	4	317	10%	0.5870	0.8593	1.9567	28	587.312	20.975	90.989
Soybean Oil	Propylene Glycol	19	50	120	4	317	10%	0.5000	0.9005	1.6667	19	392.536	20.66	60.813
Soybean Oil	Propylene Glycol	19	50	180	4	317	10%	0.5630	0.8802	1.8767	21	512.046	24.383	79.328
Soybean Oil	Propylene Glycol	19	50	240	4	317	10%	0.5820	0.8593	1.9400	18	604.565	33.587	93.662

Appendix G – Data Table – Soybean Oil

Table 141: Data Table – Soybean & Propylene Glycol @ 22ga

Base Oil	Emulsifier	Needle Gauge	Voltage (kV)	Temp (F)	Pressure (psi)	Time (ms)	Concentration	Weight (g)	Density (g/cm^3)	Mass Flow (g/s)	Droplet Count	Total Area (mm^2)	Average Size (mm^2)	% Area Coverage
Soybean Oil	Propylene Glycol	22	25	120	4	317	5%	0.0780	0.9005	0.2600	503	85.575	0.17	13.258
Soybean Oil	Propylene Glycol	22	25	180	4	317	5%	0.0970	0.8802	0.3233	423	76.917	0.182	11.916
Soybean Oil	Propylene Glycol	22	25	240	4	317	5%	0.0890	0.8593	0.2967	246	41.74	0.17	6.467
Soybean Oil	Propylene Glycol	22	50	120	4	317	5%	0.0810	0.9005	0.2700	356	76.047	0.214	11.781
Soybean Oil	Propylene Glycol	22	50	180	4	317	5%	0.0990	0.8802	0.3300	373	84.254	0.226	13.053
Soybean Oil	Propylene Glycol	22	50	240	4	317	5%	0.0910	0.8593	0.3033	402	94.529	0.235	14.645
Soybean Oil	Propylene Glycol	22	25	120	8	317	5%	0.1220	0.9005	0.4067	134	46.332	0.346	7.178
Soybean Oil	Propylene Glycol	22	25	180	8	317	5%	0.1380	0.8802	0.4600	394	86.043	0.218	13.33
Soybean Oil	Propylene Glycol	22	25	240	8	317	5%	0.1260	0.8593	0.4200	578	91.634	0.159	14.196
Soybean Oil	Propylene Glycol	22	50	120	8	317	5%	0.1210	0.9005	0.4033	469	85.475	0.182	13.242
Soybean Oil	Propylene Glycol	22	50	180	8	317	5%	0.1430	0.8802	0.4767	325	141.515	0.435	21.924
Soybean Oil	Propylene Glycol	22	50	240	8	317	5%	0.1300	0.8593	0.4333	919	166.748	0.181	25.833
Soybean Oil	Propylene Glycol	22	25	120	16	317	5%	0.1830	0.9005	0.6100	416	101.919	0.245	15.79
Soybean Oil	Propylene Glycol	22	25	180	16	317	5%	0.2190	0.8802	0.7300	396	109.223	0.276	16.921
Soybean Oil	Propylene Glycol	22	25	240	16	317	5%	0.1940	0.8593	0.6467	212	158.519	0.748	24.558
Soybean Oil	Propylene Glycol	22	50	120	16	317	5%	0.1930	0.9005	0.6433	214	236.918	1.107	36.704
Soybean Oil	Propylene Glycol	22	50	180	16	317	5%	0.2240	0.8802	0.7467	276	213.408	0.773	33.062
Soybean Oil	Propylene Glycol	22	50	240	16	317	5%	0.2040	0.8593	0.6800	1505	109.546	0.073	16.971
Soybean Oil	Propylene Glycol	22	25	120	4	317	10%	0.0510	0.9005	0.1700	287	51.216	0.178	7.935
Soybean Oil	Propylene Glycol	22	25	180	4	317	10%	0.0540	0.8802	0.1800	407	42.676	0.105	6.612
Soybean Oil	Propylene Glycol	22	25	240	4	317	10%	0.0720	0.8593	0.2400	729	69.882	0.096	10.826
Soybean Oil	Propylene Glycol	22	50	120	4	317	10%	0.0500	0.9005	0.1667	704	118.056	0.168	18.29
Soybean Oil	Propylene Glycol	22	50	180	4	317	10%	0.0530	0.8802	0.1767	590	78.919	0.134	12.226
Soybean Oil	Propylene Glycol	22	50	240	4	317	10%	0.0640	0.8593	0.2133	331	99.644	0.301	15.437
Soybean Oil	Propylene Glycol	22	25	120	8	317	10%	0.0690	0.9005	0.2300	218	34.407	0.158	5.331
Soybean Oil	Propylene Glycol	22	25	180	8	317	10%	0.0730	0.8802	0.2433	624	43.263	0.069	6.702
Soybean Oil	Propylene Glycol	22	25	240	8	317	10%	0.0950	0.8593	0.3167	1215	105.842	0.087	16.397
Soybean Oil	Propylene Glycol	22	50	120	8	317	10%	0.0720	0.9005	0.2400	547	44.928	0.082	6.96
Soybean Oil	Propylene Glycol	22	50	180	8	317	10%	0.0750	0.8802	0.2500	608	72.576	0.119	11.244
Soybean Oil	Propylene Glycol	22	50	240	8	317	10%	0.0970	0.8593	0.3233	1055	174.68	0.166	27.062
Soybean Oil	Propylene Glycol	22	25	120	16	317	10%	0.0990	0.9005	0.3300	449	62.612	0.139	9.7
Soybean Oil	Propylene Glycol	22	25	180	16	317	10%	0.1040	0.8802	0.3467	642	58.593	0.091	9.077
Soybean Oil	Propylene Glycol	22	25	240	16	317	10%	0.1320	0.8593	0.4400	1109	111.545	0.101	17.281
Soybean Oil	Propylene Glycol	22	50	120	16	317	10%	0.1120	0.9005	0.3733	546	111.517	0.204	17.277
Soybean Oil	Propylene Glycol	22	50	180	16	317	10%	0.1220	0.8802	0.4067	395	133.603	0.338	20.698
Soybean Oil	Propylene Glycol	22	50	240	16	317	10%	0.0410	0.8593	0.1367	146	179.805	1.232	27.856

Appendix H – Data Table – Rapeseed Oil

Table 142: Data Table – Rapeseed & Sunflower Lecithin @ 19ga

Base Oil	Emulsifier	Needle Gauge	Voltage (kV)	Temp (F)	Pressure (psi)	Time (ms)	Concentration	Weight (g)	Density (g/cm^3)	Mass Flow (g/s)	Droplet Count	Total Area (mm^2)	Average Size (mm^2)	% Area Coverage
Rapeseed Oil	Sunflower Lecithin	19	25	120	1	317	5%	0.3110	0.8970	1.0367	48	184.544	3.845	28.59
Rapeseed Oil	Sunflower Lecithin	19	25	180	1	317	5%	0.4020	0.8765	1.3400	42	193.088	4.597	29.914
Rapeseed Oil	Sunflower Lecithin	19	25	240	1	317	5%	0.3900	0.8562	1.3000	37	256.878	6.943	39.797
Rapeseed Oil	Sunflower Lecithin	19	50	120	1	317	5%	0.3130	0.8970	1.0433	49	429.701	8.769	66.571
Rapeseed Oil	Sunflower Lecithin	19	50	180	1	317	5%	0.4160	0.8765	1.3867	72	248.159	3.447	38.446
Rapeseed Oil	Sunflower Lecithin	19	50	240	1	317	5%	0.3790	0.8562	1.2633	32	282.264	8.821	43.729
Rapeseed Oil	Sunflower Lecithin	19	25	120	2	317	5%	0.4120	0.8970	1.3733	48	221.648	4.618	34.339
Rapeseed Oil	Sunflower Lecithin	19	25	180	2	317	5%	0.4350	0.8765	1.4500	60	315.129	5.252	48.821
Rapeseed Oil	Sunflower Lecithin	19	25	240	2	317	5%	0.4400	0.8562	1.4667	41	245.035	5.976	37.962
Rapeseed Oil	Sunflower Lecithin	19	50	120	2	317	5%	0.3840	0.8970	1.2800	28	514.581	18.378	79.721
Rapeseed Oil	Sunflower Lecithin	19	50	180	2	317	5%	0.5540	0.8765	1.8467	78	396.483	5.083	61.425
Rapeseed Oil	Sunflower Lecithin	19	50	240	2	317	5%	0.4460	0.8562	1.4867	60	362.39	6.04	56.143
Rapeseed Oil	Sunflower Lecithin	19	25	120	4	317	5%	0.4580	0.8970	1.5267	30	422.592	14.086	65.47
Rapeseed Oil	Sunflower Lecithin	19	25	180	4	317	5%	0.6590	0.8765	2.1967	29	403.986	13.931	62.587
Rapeseed Oil	Sunflower Lecithin	19	25	240	4	317	5%	0.5600	0.8562	1.8667	34	404.145	11.887	62.612
Rapeseed Oil	Sunflower Lecithin	19	50	120	4	317	5%	0.5130	0.8970	1.7100	43	419.834	9.764	65.042
Rapeseed Oil	Sunflower Lecithin	19	50	180	4	317	5%	0.6990	0.8765	2.3300	22	429.627	19.528	66.56
Rapeseed Oil	Sunflower Lecithin	19	50	240	4	317	5%	0.6140	0.8562	2.0467	60	407.437	6.791	63.122
Rapeseed Oil	Sunflower Lecithin	19	25	120	1	317	10%	0.3010	0.8970	1.0033	30	118.886	3.963	18.418
Rapeseed Oil	Sunflower Lecithin	19	25	180	1	317	10%	0.3660	0.8765	1.2200	51	170.189	3.337	26.366
Rapeseed Oil	Sunflower Lecithin	19	25	240	1	317	10%	0.1860	0.8562	0.6200	27	367.566	13.614	56.945
Rapeseed Oil	Sunflower Lecithin	19	50	120	1	317	10%	0.2990	0.8970	0.9967	58	155.688	2.684	24.12
Rapeseed Oil	Sunflower Lecithin	19	50	180	1	317	10%	0.3740	0.8765	1.2467	61	257.524	4.222	39.897
Rapeseed Oil	Sunflower Lecithin	19	50	240	1	317	10%	0.1880	0.8562	0.6267	37	415.088	11.219	64.307
Rapeseed Oil	Sunflower Lecithin	19	25	120	2	317	10%	0.3600	0.8970	1.2000	45	121.549	2.701	18.831
Rapeseed Oil	Sunflower Lecithin	19	25	180	2	317	10%	0.4480	0.8765	1.4933	48	191.253	3.984	29.63
Rapeseed Oil	Sunflower Lecithin	19	25	240	2	317	10%	0.2220	0.8562	0.7400	38	297.02	7.816	46.015
Rapeseed Oil	Sunflower Lecithin	19	50	120	2	317	10%	0.3520	0.8970	1.1733	39	176.137	4.516	27.288
Rapeseed Oil	Sunflower Lecithin	19	50	180	2	317	10%	0.4640	0.8765	1.5467	62	257.511	4.153	39.895
Rapeseed Oil	Sunflower Lecithin	19	50	240	2	317	10%	0.2220	0.8562	0.7400	36	493.983	13.722	76.53
Rapeseed Oil	Sunflower Lecithin	19	25	120	4	317	10%	0.4540	0.8970	1.5133	42	152.288	3.626	23.593
Rapeseed Oil	Sunflower Lecithin	19	25	180	4	317	10%	0.5940	0.8765	1.9800	32	279.958	8.749	43.372
Rapeseed Oil	Sunflower Lecithin	19	25	240	4	317	10%	0.3050	0.8562	1.0167	20	451.603	22.58	69.964
Rapeseed Oil	Sunflower Lecithin	19	50	120	4	317	10%	0.4760	0.8970	1.5867	71	190.348	2.681	29.489
Rapeseed Oil	Sunflower Lecithin	19	50	180	4	317	10%	0.6150	0.8765	2.0500	57	334.626	5.871	51.842
Rapeseed Oil	Sunflower Lecithin	19	50	240	4	317	10%	0.3420	0.8562	1.1400	22	561.243	25.511	86.95

Appendix H – Data Table – Rapeseed Oil

Table 143: Data Table – Rapeseed & Sunflower Lecithin @ 22ga

Base Oil	Emulsifier	Needle Gauge	Voltage (kV)	Temp (F)	Pressure (psi)	Time (ms)	Concentration	Weight (g)	Density (g/cm^3)	Mass Flow (g/s)	Droplet Count	Total Area (mm^2)	Average Size (mm^2)	% Area Coverage
Rapeseed Oil	Sunflower Lecithin	22	25	120	4	317	5%	0.0480	0.8970	0.1600	45	94.217	2.094	14.596
Rapeseed Oil	Sunflower Lecithin	22	25	180	4	317	5%	0.0540	0.8765	0.1800	52	69.156	1.33	10.714
Rapeseed Oil	Sunflower Lecithin	22	25	240	4	317	5%	0.0540	0.8562	0.1800	68	50.768	0.747	7.865
Rapeseed Oil	Sunflower Lecithin	22	50	120	4	317	5%	0.0510	0.8970	0.1700	91	158.098	1.737	24.493
Rapeseed Oil	Sunflower Lecithin	22	50	180	4	317	5%	0.0570	0.8765	0.1900	68	77.667	1.142	12.032
Rapeseed Oil	Sunflower Lecithin	22	50	240	4	317	5%	0.0630	0.8562	0.2100	177	145.836	0.824	22.593
Rapeseed Oil	Sunflower Lecithin	22	25	120	8	317	5%	0.0670	0.8970	0.2233	66	73.329	1.111	11.36
Rapeseed Oil	Sunflower Lecithin	22	25	180	8	317	5%	0.0720	0.8765	0.2400	83	78.606	0.947	12.178
Rapeseed Oil	Sunflower Lecithin	22	25	240	8	317	5%	0.0830	0.8562	0.2767	78	103.535	1.327	16.04
Rapeseed Oil	Sunflower Lecithin	22	50	120	8	317	5%	0.0660	0.8970	0.2200	78	190.858	2.447	29.569
Rapeseed Oil	Sunflower Lecithin	22	50	180	8	317	5%	0.0760	0.8765	0.2533	107	135.529	1.267	20.997
Rapeseed Oil	Sunflower Lecithin	22	50	240	8	317	5%	0.0800	0.8562	0.2667	83	132.935	1.602	20.595
Rapeseed Oil	Sunflower Lecithin	22	25	120	16	317	5%	0.0970	0.8970	0.3233	57	120.601	2.116	18.684
Rapeseed Oil	Sunflower Lecithin	22	25	180	16	317	5%	0.1050	0.8765	0.3500	72	85.576	1.189	13.258
Rapeseed Oil	Sunflower Lecithin	22	25	240	16	317	5%	0.1230	0.8562	0.4100	53	47.985	0.905	7.434
Rapeseed Oil	Sunflower Lecithin	22	50	120	16	317	5%	0.1000	0.8970	0.3333	57	197.932	3.472	30.664
Rapeseed Oil	Sunflower Lecithin	22	50	180	16	317	5%	0.1180	0.8765	0.3933	111	123.195	1.11	19.086
Rapeseed Oil	Sunflower Lecithin	22	50	240	16	317	5%	0.1320	0.8562	0.4400	108	85.004	0.787	13.169
Rapeseed Oil	Sunflower Lecithin	22	25	120	4	317	10%	0.0880	0.8970	0.2933	198	223.855	1.131	34.681
Rapeseed Oil	Sunflower Lecithin	22	25	180	4	317	10%	0.0660	0.8765	0.2200	222	119.2	0.537	18.467
Rapeseed Oil	Sunflower Lecithin	22	25	240	4	317	10%	0.0520	0.8562	0.1733	152	98.059	0.645	15.192
Rapeseed Oil	Sunflower Lecithin	22	50	120	4	317	10%	0.0950	0.8970	0.3167	301	387.955	1.289	60.104
Rapeseed Oil	Sunflower Lecithin	22	50	180	4	317	10%	0.0740	0.8765	0.2467	255	204.267	0.801	31.646
Rapeseed Oil	Sunflower Lecithin	22	50	240	4	317	10%	0.0620	0.8562	0.2067	242	155.842	0.644	24.144
Rapeseed Oil	Sunflower Lecithin	22	25	120	8	317	10%	0.1220	0.8970	0.4067	197	164.494	0.835	25.484
Rapeseed Oil	Sunflower Lecithin	22	25	180	8	317	10%	0.0980	0.8765	0.3267	136	95.496	0.702	14.795
Rapeseed Oil	Sunflower Lecithin	22	25	240	8	317	10%	0.0800	0.8562	0.2667	114	79.513	0.697	12.318
Rapeseed Oil	Sunflower Lecithin	22	50	120	8	317	10%	0.1160	0.8970	0.3867	202	310.01	1.535	48.028
Rapeseed Oil	Sunflower Lecithin	22	50	180	8	317	10%	0.0990	0.8765	0.3300	219	221.413	1.011	34.302
Rapeseed Oil	Sunflower Lecithin	22	1550	240	8	317	10%	0.0900	0.8562	0.3000	161	155.119	0.963	24.032
Rapeseed Oil	Sunflower Lecithin	22	25	120	16	317	10%	0.1640	0.8970	0.5467	227	244.729	1.078	37.914
Rapeseed Oil	Sunflower Lecithin	22	25	180	16	317	10%	0.1330	0.8765	0.4433	137	115.518	0.843	17.896
Rapeseed Oil	Sunflower Lecithin	22	25	240	16	317	10%	0.1280	0.8562	0.4267	732	382.111	0.522	59.198
Rapeseed Oil	Sunflower Lecithin	22	50	120	16	317	10%	0.1810	0.8970	0.6033	174	263.64	1.515	40.844
Rapeseed Oil	Sunflower Lecithin	22	50	180	16	317	10%	0.1400	0.8765	0.4667	217	236.016	1.088	36.564
Rapeseed Oil	Sunflower Lecithin	22	50	240	16	317	10%	0.1350	0.8562	0.4500	147	120.605	0.82	18.685

Appendix H – Data Table – Rapeseed Oil

Table 144: Data Table – Rapeseed & Polysorbate 20 @ 19ga

Base Oil	Emulsifier	Needle Gauge	Voltage (kV)	Temp (F)	Pressure (psi)	Time (ms)	Concentration	Weight (g)	Density (g/cm^3)	Mass Flow (g/s)	Droplet Count	Total Area (mm^2)	Average Size (mm^2)	% Area Coverage
Rapeseed Oil	Polysorbate 20	19	25	120	1	317	5%	0.3770	0.8970	1.2567	1004	223.178	0.222	34.576
Rapeseed Oil	Polysorbate 20	19	25	180	1	317	5%	0.4120	0.8765	1.3733	666	315.826	0.474	48.929
Rapeseed Oil	Polysorbate 20	19	25	240	1	317	5%	0.5570	0.8562	1.8567	553	518.644	0.938	80.35
Rapeseed Oil	Polysorbate 20	19	50	120	1	317	5%	0.3830	0.8970	1.2767	109	300.765	2.759	46.596
Rapeseed Oil	Polysorbate 20	19	50	180	1	317	5%	0.4270	0.8765	1.4233	198	422.349	2.133	65.432
Rapeseed Oil	Polysorbate 20	19	50	240	1	317	5%	0.5760	0.8562	1.9200	30	589.501	19.65	91.328
Rapeseed Oil	Polysorbate 20	19	25	120	2	317	5%	0.4640	0.8970	1.5467	473	324.37	0.686	50.253
Rapeseed Oil	Polysorbate 20	19	25	180	2	317	5%	0.4800	0.8765	1.6000	434	432.691	0.997	67.034
Rapeseed Oil	Polysorbate 20	19	25	240	2	317	5%	0.6890	0.8562	2.2967	121	613.133	5.067	94.989
Rapeseed Oil	Polysorbate 20	19	50	120	2	317	5%	0.4680	0.8970	1.5600	109	452.88	4.155	70.162
Rapeseed Oil	Polysorbate 20	19	50	180	2	317	5%	0.4860	0.8765	1.6200	10	500.675	50.067	77.567
Rapeseed Oil	Polysorbate 20	19	50	240	2	317	5%	0.7040	0.8562	2.3467	7	558.431	79.776	86.514
Rapeseed Oil	Polysorbate 20	19	25	120	4	317	5%	0.6320	0.8970	2.1067	229	436.336	1.905	67.599
Rapeseed Oil	Polysorbate 20	19	25	180	4	317	5%	0.6240	0.8765	2.0800	354	584.994	1.653	90.63
Rapeseed Oil	Polysorbate 20	19	25	240	4	317	5%	0.8400	0.8562	2.8000	18	637.733	35.43	98.8
Rapeseed Oil	Polysorbate 20	19	50	120	4	317	5%	0.6170	0.8970	2.0567	1	645.16	645.16	100
Rapeseed Oil	Polysorbate 20	19	50	180	4	317	5%	0.6550	0.8765	2.1833	1	645.16	645.16	100
Rapeseed Oil	Polysorbate 20	19	50	240	4	317	5%	0.8730	0.8562	2.9100	1	645.16	645.16	100
Rapeseed Oil	Polysorbate 20	19	25	120	1	317	10%	0.3440	0.8970	1.1467	33	193.441	5.862	29.969
Rapeseed Oil	Polysorbate 20	19	25	180	1	317	10%	0.4680	0.8765	1.5600	51	322.927	6.332	50.029
Rapeseed Oil	Polysorbate 20	19	25	240	1	317	10%	0.5300	0.8562	1.7667	41	527.267	12.86	81.686
Rapeseed Oil	Polysorbate 20	19	50	120	1	317	10%	0.3470	0.8970	1.1567	581	394.676	0.679	61.145
Rapeseed Oil	Polysorbate 20	19	50	180	1	317	10%	0.4490	0.8765	1.4967	113	360.925	3.194	55.916
Rapeseed Oil	Polysorbate 20	19	50	240	1	317	10%	0.5420	0.8562	1.8067	253	513.861	2.031	79.609
Rapeseed Oil	Polysorbate 20	19	25	120	2	317	10%	0.3580	0.8970	1.1933	1	645.16	645.16	100
Rapeseed Oil	Polysorbate 20	19	25	180	2	317	10%	0.5350	0.8765	1.7833	1	645.16	645.16	100
Rapeseed Oil	Polysorbate 20	19	25	240	2	317	10%	0.6520	0.8562	2.1733	1	645.16	645.16	100
Rapeseed Oil	Polysorbate 20	19	50	120	2	317	10%	0.4170	0.8970	1.3900	1	645.16	645.16	100
Rapeseed Oil	Polysorbate 20	19	50	180	2	317	10%	0.4850	0.8765	1.6167	47	424.165	9.025	65.713
Rapeseed Oil	Polysorbate 20	19	50	240	2	317	10%	0.6740	0.8562	2.2467	1	645.16	645.16	100
Rapeseed Oil	Polysorbate 20	19	25	120	4	317	10%	0.4970	0.8970	1.6567	1	645.16	645.16	100
Rapeseed Oil	Polysorbate 20	19	25	180	4	317	10%	0.6370	0.8765	2.1233	13	486.781	37.445	75.414
Rapeseed Oil	Polysorbate 20	19	25	240	4	317	10%	0.8590	0.8562	2.8633	38	544.365	14.325	84.335
Rapeseed Oil	Polysorbate 20	19	50	120	4	317	10%	0.5080	0.8970	1.6933	1	645.16	645.16	100
Rapeseed Oil	Polysorbate 20	19	50	180	4	317	10%	0.6630	0.8765	2.2100	1	645.16	645.16	100
Rapeseed Oil	Polysorbate 20	19	50	240	4	317	10%	0.9100	0.8562	3.0333	1	645.16	645.16	100

Appendix H – Data Table – Rapeseed Oil

Table 145: Data Table – Rapeseed & Polysorbate 20 @ 22ga

Base Oil	Emulsifier	Needle Gauge	Voltage (kV)	Temp (F)	Pressure (psi)	Time (ms)	Concentration	Weight (g)	Density (g/cm^3)	Mass Flow (g/s)	Droplet Count	Total Area (mm^2)	Average Size (mm^2)	% Area Coverage
Rapeseed Oil	Polysorbate 20	22	25	120	4	317	5%	0.0610	0.8970	0.2033	858	187.263	0.218	29.011
Rapeseed Oil	Polysorbate 20	22	25	180	4	317	5%	0.0670	0.8765	0.2233	875	164.861	0.188	25.541
Rapeseed Oil	Polysorbate 20	22	25	240	4	317	5%	0.0770	0.8562	0.2567	900	182.837	0.203	28.326
Rapeseed Oil	Polysorbate 20	22	50	120	4	317	5%	0.0710	0.8970	0.2367	1180	243.721	0.207	37.758
Rapeseed Oil	Polysorbate 20	22	50	180	4	317	5%	0.0750	0.8765	0.2500	545	203.981	0.374	31.602
Rapeseed Oil	Polysorbate 20	22	50	240	4	317	5%	0.0850	0.8562	0.2833	190	108.848	0.573	16.863
Rapeseed Oil	Polysorbate 20	22	25	120	8	317	5%	0.0900	0.8970	0.3000	650	229.927	0.354	35.621
Rapeseed Oil	Polysorbate 20	22	25	180	8	317	5%	0.0920	0.8765	0.3067	280	118.843	0.424	18.412
Rapeseed Oil	Polysorbate 20	22	25	240	8	317	5%	0.1190	0.8562	0.3967	316	66.531	0.211	10.307
Rapeseed Oil	Polysorbate 20	22	50	120	8	317	5%	0.0970	0.8970	0.3233	697	166.162	0.238	25.743
Rapeseed Oil	Polysorbate 20	22	50	180	8	317	5%	0.1100	0.8765	0.3667	44	133.506	3.034	20.683
Rapeseed Oil	Polysorbate 20	22	50	240	8	317	5%	0.1260	0.8562	0.4200	198	152.744	0.771	23.664
Rapeseed Oil	Polysorbate 20	22	25	120	16	317	5%	0.1320	0.8970	0.4400	486	167.393	0.344	25.933
Rapeseed Oil	Polysorbate 20	22	25	180	16	317	5%	0.1340	0.8765	0.4467	304	286.275	0.942	44.351
Rapeseed Oil	Polysorbate 20	22	25	240	16	317	5%	0.1990	0.8562	0.6633	934	347.359	0.372	53.814
Rapeseed Oil	Polysorbate 20	22	50	120	16	317	5%	0.1490	0.8970	0.4967	233	174.006	0.747	26.958
Rapeseed Oil	Polysorbate 20	22	50	180	16	317	5%	0.1540	0.8765	0.5133	33	264.353	8.011	40.955
Rapeseed Oil	Polysorbate 20	22	50	240	16	317	5%	0.2460	0.8562	0.8200	488	342.689	0.702	53.091
Rapeseed Oil	Polysorbate 20	22	25	120	4	317	10%	0.0520	0.8970	0.1733	97	346.964	3.577	53.753
Rapeseed Oil	Polysorbate 20	22	25	180	4	317	10%	0.0630	0.8765	0.2100	943	74.031	0.079	11.469
Rapeseed Oil	Polysorbate 20	22	25	240	4	317	10%	0.0790	0.8562	0.2633	679	67.497	0.099	10.457
Rapeseed Oil	Polysorbate 20	22	50	120	4	317	10%	0.0610	0.8970	0.2033	104	300.119	2.886	46.496
Rapeseed Oil	Polysorbate 20	22	50	180	4	317	10%	0.0660	0.8765	0.2200	282	109.824	0.389	17.014
Rapeseed Oil	Polysorbate 20	22	50	240	4	317	10%	0.0780	0.8562	0.2600	136	129.573	0.953	20.074
Rapeseed Oil	Polysorbate 20	22	25	120	8	317	10%	0.0730	0.8970	0.2433	79	355.706	4.503	55.107
Rapeseed Oil	Polysorbate 20	22	25	180	8	317	10%	0.0850	0.8765	0.2833	1236	94.3	0.076	14.609
Rapeseed Oil	Polysorbate 20	22	25	240	8	317	10%	0.1040	0.8562	0.3467	1182	173.245	0.147	26.84
Rapeseed Oil	Polysorbate 20	22	50	120	8	317	10%	0.0810	0.8970	0.2700	276	368.828	1.336	57.14
Rapeseed Oil	Polysorbate 20	22	50	180	8	317	10%	0.1090	0.8765	0.3633	156	132.929	0.852	20.594
Rapeseed Oil	Polysorbate 20	22	50	240	8	317	10%	0.1260	0.8562	0.4200	131	173.666	1.326	26.905
Rapeseed Oil	Polysorbate 20	22	25	120	16	317	10%	0.1010	0.8970	0.3367	95	374.734	3.945	58.055
Rapeseed Oil	Polysorbate 20	22	25	180	16	317	10%	0.1420	0.8765	0.4733	754	128.541	0.17	19.914
Rapeseed Oil	Polysorbate 20	22	25	240	16	317	10%	0.1690	0.8562	0.5633	623	228.346	0.367	35.376
Rapeseed Oil	Polysorbate 20	22	50	120	16	317	10%	0.1060	0.8970	0.3533	48	111.745	2.328	17.312
Rapeseed Oil	Polysorbate 20	22	50	180	16	317	10%	0.1650	0.8765	0.5500	77	154.229	2.003	23.894
Rapeseed Oil	Polysorbate 20	22	50	240	16	317	10%	0.1840	0.8562	0.6133	98	181.619	1.853	28.137

Appendix H – Data Table – Rapeseed Oil

Table 146: Data Table – Rapeseed & Propylene Glycol @ 19ga

Base Oil	Emulsifier	Needle Gauge	Voltage (kV)	Temp (F)	Pressure (psi)	Time (ms)	Concentration	Weight (g)	Density (g/cm^3)	Mass Flow (g/s)	Droplet Count	Total Area (mm^2)	Average Size (mm^2)	% Area Coverage
Rapeseed Oil	Propylene Glycol	19	25	120	1	317	5%	0.2930	0.8970	0.9767	1	645.16	645.16	100
Rapeseed Oil	Propylene Glycol	19	25	180	1	317	5%	0.3600	0.8765	1.2000	1	645.16	645.16	100
Rapeseed Oil	Propylene Glycol	19	25	240	1	317	5%	0.5360	0.8562	1.7867	1	645.16	645.16	100
Rapeseed Oil	Propylene Glycol	19	50	120	1	317	5%	0.2990	0.8970	0.9967	400	446.681	1.117	69.202
Rapeseed Oil	Propylene Glycol	19	50	180	1	317	5%	0.3670	0.8765	1.2233	101	459.22	4.547	71.144
Rapeseed Oil	Propylene Glycol	19	50	240	1	317	5%	0.5150	0.8562	1.7167	1	645.16	645.16	100
Rapeseed Oil	Propylene Glycol	19	25	120	2	317	5%	0.3410	0.8970	1.1367	1	645.16	645.16	100
Rapeseed Oil	Propylene Glycol	19	25	180	2	317	5%	0.4000	0.8765	1.3333	1	645.16	645.16	100
Rapeseed Oil	Propylene Glycol	19	25	240	2	317	5%	0.6220	0.8562	2.0733	1	645.16	645.16	100
Rapeseed Oil	Propylene Glycol	19	50	120	2	317	5%	0.3400	0.8970	1.1333	172	432.223	2.513	66.962
Rapeseed Oil	Propylene Glycol	19	50	180	2	317	5%	0.4070	0.8765	1.3567	1	645.16	645.16	100
Rapeseed Oil	Propylene Glycol	19	50	240	2	317	5%	0.5690	0.8562	1.8967	1	645.16	645.16	100
Rapeseed Oil	Propylene Glycol	19	25	120	4	317	5%	0.4360	0.8970	1.4533	1	645.16	645.16	100
Rapeseed Oil	Propylene Glycol	19	25	180	4	317	5%	0.5220	0.8765	1.7400	1	645.16	645.16	100
Rapeseed Oil	Propylene Glycol	19	25	240	4	317	5%	0.7990	0.8562	2.6633	1	645.16	645.16	100
Rapeseed Oil	Propylene Glycol	19	50	120	4	317	5%	0.4320	0.8970	1.4400	1	645.16	645.16	100
Rapeseed Oil	Propylene Glycol	19	50	180	4	317	5%	0.5340	0.8765	1.7800	1	645.16	645.16	100
Rapeseed Oil	Propylene Glycol	19	50	240	4	317	5%	0.8600	0.8562	2.8667	1	645.16	645.16	100
Rapeseed Oil	Propylene Glycol	19	25	120	1	317	10%	0.2950	0.8970	0.9833	65	102.128	1.571	15.822
Rapeseed Oil	Propylene Glycol	19	25	180	1	317	10%	0.3490	0.8765	1.1633	48	206.677	4.306	32.019
Rapeseed Oil	Propylene Glycol	19	25	240	1	317	10%	0.5530	0.8562	1.8433	52	374.15	7.195	57.965
Rapeseed Oil	Propylene Glycol	19	50	120	1	317	10%	0.2880	0.8970	0.9600	27	225.85	8.365	34.99
Rapeseed Oil	Propylene Glycol	19	50	180	1	317	10%	0.3490	0.8765	1.1633	16	317.192	19.825	49.141
Rapeseed Oil	Propylene Glycol	19	50	240	1	317	10%	0.5650	0.8562	1.8833	17	476.866	28.051	73.878
Rapeseed Oil	Propylene Glycol	19	25	120	2	317	10%	0.2580	0.8970	0.8600	41	163.362	3.984	25.309
Rapeseed Oil	Propylene Glycol	19	25	180	2	317	10%	0.3960	0.8765	1.3200	40	449.358	11.234	69.616
Rapeseed Oil	Propylene Glycol	19	25	240	2	317	10%	0.6300	0.8562	2.1000	28	586.764	20.956	90.904
Rapeseed Oil	Propylene Glycol	19	50	120	2	317	10%	0.3180	0.8970	1.0600	128	292.313	2.284	45.286
Rapeseed Oil	Propylene Glycol	19	50	180	2	317	10%	0.4050	0.8765	1.3500	63	508.446	8.071	78.771
Rapeseed Oil	Propylene Glycol	19	50	240	2	317	10%	0.6500	0.8562	2.1667	61	406.845	6.67	63.03
Rapeseed Oil	Propylene Glycol	19	25	120	4	317	10%	0.3990	0.8970	1.3300	48	151.196	3.15	23.424
Rapeseed Oil	Propylene Glycol	19	25	180	4	317	10%	0.4740	0.8765	1.5800	1	645.16	645.16	100
Rapeseed Oil	Propylene Glycol	19	25	240	4	317	10%	0.8250	0.8562	2.7500	1	645.16	645.16	100
Rapeseed Oil	Propylene Glycol	19	50	120	4	317	10%	0.3870	0.8970	1.2900	48	151.196	3.15	23.424
Rapeseed Oil	Propylene Glycol	19	50	180	4	317	10%	0.4800	0.8765	1.6000	1	645.16	645.16	100
Rapeseed Oil	Propylene Glycol	19	50	240	4	317	10%	0.8550	0.8562	2.8500	1	645.16	645.16	100

Appendix H – Data Table – Rapeseed Oil

Table 147: Data Table – Rapeseed & Propylene Glycol @ 22ga

Base Oil	Emulsifier	Needle Gauge	Voltage (kV)	Temp (F)	Pressure (psi)	Time (ms)	Concentration	Weight (g)	Density (g/cm^3)	Mass Flow (g/s)	Droplet Count	Total Area (mm^2)	Average Size (mm^2)	% Area Coverage
Rapeseed Oil	Propylene Glycol	22	25	120	4	317	5%	0.0550	0.8970	0.1833	343	150.001	0.437	23.239
Rapeseed Oil	Propylene Glycol	22	25	180	4	317	5%	0.0570	0.8765	0.1900	1721	218.67	0.127	33.877
Rapeseed Oil	Propylene Glycol	22	25	240	4	317	5%	0.0620	0.8562	0.2067	1825	254.242	0.139	39.388
Rapeseed Oil	Propylene Glycol	22	50	120	4	317	5%	0.0560	0.8970	0.1867	265	101.877	0.384	15.783
Rapeseed Oil	Propylene Glycol	22	50	180	4	317	5%	0.0550	0.8765	0.1833	236	88.497	0.375	13.71
Rapeseed Oil	Propylene Glycol	22	50	240	4	317	5%	0.0650	0.8562	0.2167	897	117.621	0.131	18.222
Rapeseed Oil	Propylene Glycol	22	25	120	8	317	5%	0.0780	0.8970	0.2600	230	184.678	0.803	28.611
Rapeseed Oil	Propylene Glycol	22	25	180	8	317	5%	0.0670	0.8765	0.2233	1098	154.908	0.141	23.999
Rapeseed Oil	Propylene Glycol	22	25	240	8	317	5%	0.0860	0.8562	0.2867	1243	218.407	0.176	33.837
Rapeseed Oil	Propylene Glycol	22	50	120	8	317	5%	0.0780	0.8970	0.2600	108	138.743	1.285	21.495
Rapeseed Oil	Propylene Glycol	22	50	180	8	317	5%	0.0800	0.8765	0.2667	204	108.583	0.532	16.822
Rapeseed Oil	Propylene Glycol	22	50	240	8	317	5%	0.0880	0.8562	0.2933	396	179.036	0.452	27.737
Rapeseed Oil	Propylene Glycol	22	25	120	16	317	5%	0.1190	0.8970	0.3967	284	308.017	1.085	47.719
Rapeseed Oil	Propylene Glycol	22	25	180	16	317	5%	0.1290	0.8765	0.4300	1385	243.623	0.176	37.743
Rapeseed Oil	Propylene Glycol	22	25	240	16	317	5%	0.1220	0.8562	0.4067	714	347.188	0.486	53.788
Rapeseed Oil	Propylene Glycol	22	50	120	16	317	5%	0.1200	0.8970	0.4000	310	193.315	0.624	29.949
Rapeseed Oil	Propylene Glycol	22	50	180	16	317	5%	0.1290	0.8765	0.4300	274	141.525	0.517	21.926
Rapeseed Oil	Propylene Glycol	22	50	240	16	317	5%	0.1450	0.8562	0.4833	304	246.313	0.81	38.16
Rapeseed Oil	Propylene Glycol	22	25	120	4	317	10%	0.0870	0.8970	0.2900	181	188.27	1.04	29.167
Rapeseed Oil	Propylene Glycol	22	25	180	4	317	10%	0.0690	0.8765	0.2300	561	368.975	0.658	57.163
Rapeseed Oil	Propylene Glycol	22	25	240	4	317	10%	0.1140	0.8562	0.3800	485	485.507	1.001	75.217
Rapeseed Oil	Propylene Glycol	22	50	120	4	317	10%	0.0660	0.8970	0.2200	133	80.593	0.606	12.486
Rapeseed Oil	Propylene Glycol	22	50	180	4	317	10%	0.1840	0.8765	0.6133	337	155.062	0.46	24.023
Rapeseed Oil	Propylene Glycol	22	50	240	4	317	10%	0.1200	0.8562	0.4000	1438	208.7	0.145	32.333
Rapeseed Oil	Propylene Glycol	22	25	120	8	317	10%	0.0820	0.8970	0.2733	316	175.461	0.555	27.183
Rapeseed Oil	Propylene Glycol	22	25	180	8	317	10%	0.1150	0.8765	0.3833	475	253.751	0.534	39.312
Rapeseed Oil	Propylene Glycol	22	25	240	8	317	10%	0.1550	0.8562	0.5167	2263	298.306	0.132	46.215
Rapeseed Oil	Propylene Glycol	22	50	120	8	317	10%	0.0870	0.8970	0.2900	1086	173.934	0.16	26.946
Rapeseed Oil	Propylene Glycol	22	50	180	8	317	10%	0.1070	0.8765	0.3567	2644	146.311	0.055	22.667
Rapeseed Oil	Propylene Glycol	22	50	240	8	317	10%	0.1560	0.8562	0.5200	1155	284.961	0.247	44.147
Rapeseed Oil	Propylene Glycol	22	25	120	16	317	10%	0.1110	0.8970	0.3700	897	251.003	0.28	38.886
Rapeseed Oil	Propylene Glycol	22	25	180	16	317	10%	0.1630	0.8765	0.5433	148	337.423	2.28	52.275
Rapeseed Oil	Propylene Glycol	22	25	240	16	317	10%	0.2510	0.8562	0.8367	838	363.558	0.434	56.324
Rapeseed Oil	Propylene Glycol	22	50	120	16	317	10%	0.1160	0.8970	0.3867	1057	273.972	0.259	42.445
Rapeseed Oil	Propylene Glycol	22	50	180	16	317	10%	0.1450	0.8765	0.4833	831	273.106	0.329	42.311
Rapeseed Oil	Propylene Glycol	22	50	240	16	317	10%	0.2890	0.8562	0.9633	1592	336.651	0.211	52.155

Appendix I – Data Table – Sunflower Oil

Table 148: Data Table – Sunflower & Sunflower Lecithin @ 19ga

Base Oil	Emulsifier	Needle Gauge	Voltage (kV)	Temp (F)	Pressure (psi)	Time (ms)	Concentration	Weight (g)	Density (g/cm^3)	Mass Flow (g/s)	Droplet Count	Total Area (mm^2)	Average Size (mm^2)	% Area Coverage
Sunflower Oil	Sunflower Lecithin	19	25	120	1	317	5%	0.2570	0.8999	0.8567	39	169.229	4.339	26.218
Sunflower Oil	Sunflower Lecithin	19	25	180	1	317	5%	0.3680	0.8786	1.2267	71	191.835	2.702	29.72
Sunflower Oil	Sunflower Lecithin	19	25	240	1	317	5%	0.6280	0.8565	2.0933	1	645.16	645.16	100
Sunflower Oil	Sunflower Lecithin	19	50	120	1	317	5%	0.2570	0.8999	0.8567	22	324.448	14.748	50.265
Sunflower Oil	Sunflower Lecithin	19	50	180	1	317	5%	0.3670	0.8786	1.2233	52	252.074	4.848	39.052
Sunflower Oil	Sunflower Lecithin	19	50	240	1	317	5%	0.6270	0.8565	2.0900	1	645.16	645.16	100
Sunflower Oil	Sunflower Lecithin	19	25	120	2	317	5%	0.2890	0.8999	0.9633	45	210.688	4.682	32.641
Sunflower Oil	Sunflower Lecithin	19	25	180	2	317	5%	0.4450	0.8786	1.4833	26	353.804	13.608	54.813
Sunflower Oil	Sunflower Lecithin	19	25	240	2	317	5%	0.7290	0.8565	2.4300	1	645.16	645.16	100
Sunflower Oil	Sunflower Lecithin	19	50	120	2	317	5%	0.2930	0.8999	0.9767	22	439.078	19.958	68.024
Sunflower Oil	Sunflower Lecithin	19	50	180	2	317	5%	0.5670	0.8786	1.8900	37	454.792	12.292	70.458
Sunflower Oil	Sunflower Lecithin	19	50	240	2	317	5%	0.7390	0.8565	2.4633	1	645.16	645.16	100
Sunflower Oil	Sunflower Lecithin	19	25	120	4	317	5%	0.3750	0.8999	1.2500	18	405.166	22.509	62.77
Sunflower Oil	Sunflower Lecithin	19	25	180	4	317	5%	0.5790	0.8786	1.9300	22	360.755	16.398	55.89
Sunflower Oil	Sunflower Lecithin	19	25	240	4	317	5%	0.9050	0.8565	3.0167	1	645.16	645.16	100
Sunflower Oil	Sunflower Lecithin	19	50	120	4	317	5%	0.3750	0.8999	1.2500	23	384.876	16.734	59.627
Sunflower Oil	Sunflower Lecithin	19	50	180	4	317	5%	0.6090	0.8786	2.0300	43	368.02	8.559	57.015
Sunflower Oil	Sunflower Lecithin	19	50	240	4	317	5%	0.9150	0.8565	3.0500	1	645.16	645.16	100
Sunflower Oil	Sunflower Lecithin	19	25	120	1	317	10%	0.2740	0.8999	0.9133	52	139.317	2.679	21.584
Sunflower Oil	Sunflower Lecithin	19	25	180	1	317	10%	0.5420	0.8786	1.8067	30	282.189	9.406	43.718
Sunflower Oil	Sunflower Lecithin	19	25	240	1	317	10%	0.4090	0.8565	1.3633	34	308.193	9.065	47.747
Sunflower Oil	Sunflower Lecithin	19	50	120	1	317	10%	0.2760	0.8999	0.9200	69	147.409	2.136	22.837
Sunflower Oil	Sunflower Lecithin	19	50	180	1	317	10%	0.5300	0.8786	1.7667	53	266.9	5.036	41.349
Sunflower Oil	Sunflower Lecithin	19	50	240	1	317	10%	0.4170	0.8565	1.3900	41	393.055	9.587	60.894
Sunflower Oil	Sunflower Lecithin	19	25	120	2	317	10%	0.3210	0.8999	1.0700	39	162.011	4.154	25.099
Sunflower Oil	Sunflower Lecithin	19	25	180	2	317	10%	0.5880	0.8786	1.9600	33	291.342	8.829	45.136
Sunflower Oil	Sunflower Lecithin	19	25	240	2	317	10%	0.4850	0.8565	1.6167	49	362.691	7.402	56.19
Sunflower Oil	Sunflower Lecithin	19	50	120	2	317	10%	0.3220	0.8999	1.0733	91	189.402	2.081	29.343
Sunflower Oil	Sunflower Lecithin	19	50	180	2	317	10%	0.5740	0.8786	1.9133	35	327.371	9.353	50.718
Sunflower Oil	Sunflower Lecithin	19	50	240	2	317	10%	0.5330	0.8565	1.7767	32	290.06	9.064	44.937
Sunflower Oil	Sunflower Lecithin	19	25	120	4	317	10%	0.3860	0.8999	1.2867	35	228.531	6.529	35.405
Sunflower Oil	Sunflower Lecithin	19	25	180	4	317	10%	0.6550	0.8786	2.1833	20	377.787	18.889	58.528
Sunflower Oil	Sunflower Lecithin	19	25	240	4	317	10%	0.6730	0.8565	2.2433	28	404.164	14.434	62.615
Sunflower Oil	Sunflower Lecithin	19	50	120	4	317	10%	0.3980	0.8999	1.3267	54	234.254	4.338	36.292
Sunflower Oil	Sunflower Lecithin	19	50	180	4	317	10%	0.6370	0.8786	2.1233	35	389.574	11.131	60.354
Sunflower Oil	Sunflower Lecithin	19	50	240	4	317	10%	0.7230	0.8565	2.4100	39	368.753	9.455	57.129

Appendix I – Data Table – Sunflower Oil

Table 149: Data Table – Sunflower & Sunflower Lecithin @ 22ga

Base Oil	Emulsifier	Needle Gauge	Voltage (kV)	Temp (F)	Pressure (psi)	Time (ms)	Concentration	Weight (g)	Density (g/cm^3)	Mass Flow (g/s)	Droplet Count	Total Area (mm^2)	Average Size (mm^2)	% Area Coverage
Sunflower Oil	Sunflower Lecithin	22	25	120	4	317	5%	0.0560	0.8999	0.1867	40	82.85	2.071	12.835
Sunflower Oil	Sunflower Lecithin	22	25	180	4	317	5%	0.0780	0.8786	0.2600	95	105.864	1.114	16.401
Sunflower Oil	Sunflower Lecithin	22	25	240	4	317	5%	0.0800	0.8565	0.2667	114	122.516	1.075	18.981
Sunflower Oil	Sunflower Lecithin	22	50	120	4	317	5%	0.0550	0.8999	0.1833	116	187.68	1.618	29.076
Sunflower Oil	Sunflower Lecithin	22	50	180	4	317	5%	0.0810	0.8786	0.2700	228	224.581	0.985	34.793
Sunflower Oil	Sunflower Lecithin	22	50	240	4	317	5%	0.0790	0.8565	0.2633	174	260.173	1.495	40.307
Sunflower Oil	Sunflower Lecithin	22	25	120	8	317	5%	0.0750	0.8999	0.2500	45	90.821	2.018	14.07
Sunflower Oil	Sunflower Lecithin	22	25	180	8	317	5%	0.1040	0.8786	0.3467	65	118.94	1.83	18.427
Sunflower Oil	Sunflower Lecithin	22	25	240	8	317	5%	0.1100	0.8565	0.3667	176	278.919	1.585	43.211
Sunflower Oil	Sunflower Lecithin	22	50	120	8	317	5%	0.0720	0.8999	0.2400	176	283.298	1.61	43.89
Sunflower Oil	Sunflower Lecithin	22	50	180	8	317	5%	0.1030	0.8786	0.3433	197	241.269	1.225	37.378
Sunflower Oil	Sunflower Lecithin	22	50	240	8	317	5%	0.1130	0.8565	0.3767	143	253.691	1.774	39.303
Sunflower Oil	Sunflower Lecithin	22	25	120	16	317	5%	0.1070	0.8999	0.3567	40	114.42	2.86	17.726
Sunflower Oil	Sunflower Lecithin	22	25	180	16	317	5%	0.1520	0.8786	0.5067	52	176.329	3.391	27.318
Sunflower Oil	Sunflower Lecithin	22	25	240	16	317	5%	0.1690	0.8565	0.5633	127	306.02	2.41	47.41
Sunflower Oil	Sunflower Lecithin	22	50	120	16	317	5%	0.1040	0.8999	0.3467	143	234.058	1.637	36.261
Sunflower Oil	Sunflower Lecithin	22	50	180	16	317	5%	0.1530	0.8786	0.5100	193	321.858	1.668	49.864
Sunflower Oil	Sunflower Lecithin	22	50	240	16	317	5%	0.1970	0.8565	0.6567	204	404.911	1.985	62.73
Sunflower Oil	Sunflower Lecithin	22	25	120	4	317	10%	0.0620	0.8999	0.2067	146	147.423	1.01	22.839
Sunflower Oil	Sunflower Lecithin	22	25	180	4	317	10%	0.0650	0.8786	0.2167	220	134.195	0.61	20.79
Sunflower Oil	Sunflower Lecithin	22	25	240	4	317	10%	0.0600	0.8565	0.2000	182	64.691	0.355	10.022
Sunflower Oil	Sunflower Lecithin	22	50	120	4	317	10%	0.0640	0.8999	0.2133	270	229.804	0.851	35.602
Sunflower Oil	Sunflower Lecithin	22	50	180	4	317	10%	0.0660	0.8786	0.2200	354	287.322	0.812	44.513
Sunflower Oil	Sunflower Lecithin	22	50	240	4	317	10%	0.0620	0.8565	0.2067	243	232.206	0.956	35.974
Sunflower Oil	Sunflower Lecithin	22	25	120	8	317	10%	0.0830	0.8999	0.2767	82	70.782	0.863	10.966
Sunflower Oil	Sunflower Lecithin	22	25	180	8	317	10%	0.0950	0.8786	0.3167	118	93.257	0.79	14.448
Sunflower Oil	Sunflower Lecithin	22	25	240	8	317	10%	0.0900	0.8565	0.3000	153	101.196	0.661	15.678
Sunflower Oil	Sunflower Lecithin	22	50	120	8	317	10%	0.0850	0.8999	0.2833	279	168.012	0.602	26.029
Sunflower Oil	Sunflower Lecithin	22	50	180	8	317	10%	0.0930	0.8786	0.3100	256	219.523	0.858	34.009
Sunflower Oil	Sunflower Lecithin	22	50	240	8	317	10%	0.0940	0.8565	0.3133	270	367.821	1.362	56.984
Sunflower Oil	Sunflower Lecithin	22	25	120	16	317	10%	0.1260	0.8999	0.4200	131	119.755	0.914	18.553
Sunflower Oil	Sunflower Lecithin	22	25	180	16	317	10%	0.1430	0.8786	0.4767	229	228.24	0.997	35.36
Sunflower Oil	Sunflower Lecithin	22	25	240	16	317	10%	0.1670	0.8565	0.5567	124	100.424	0.81	15.558
Sunflower Oil	Sunflower Lecithin	22	50	120	16	317	10%	0.1360	0.8999	0.4533	201	171.537	0.853	26.575
Sunflower Oil	Sunflower Lecithin	22	50	180	16	317	10%	0.1480	0.8786	0.4933	178	284.862	1.6	44.132
Sunflower Oil	Sunflower Lecithin	22	50	240	16	317	10%	0.1820	0.8565	0.6067	234	216.007	0.923	33.465

Appendix I – Data Table – Sunflower Oil

Table 150: Data Table – Sunflower & Polysorbate 80 @ 19ga

Base Oil	Emulsifier	Needle Gauge	Voltage (kV)	Temp (F)	Pressure (psi)	Time (ms)	Concentration	Weight (g)	Density (g/cm^3)	Mass Flow (g/s)	Droplet Count	Total Area (mm^2)	Average Size (mm^2)	% Area Coverage
Sunflower Oil	Polysorbate 80	19	25	120	1	317	5%	0.3270	0.8999	1.0900	1	645.16	645.16	100
Sunflower Oil	Polysorbate 80	19	25	180	1	317	5%	0.4400	0.8786	1.4667	1	645.16	645.16	100
Sunflower Oil	Polysorbate 80	19	25	240	1	317	5%	0.6770	0.8565	2.2567	1	645.16	645.16	100
Sunflower Oil	Polysorbate 80	19	50	120	1	317	5%	0.3220	0.8999	1.0733	1	645.16	645.16	100
Sunflower Oil	Polysorbate 80	19	50	180	1	317	5%	0.4390	0.8786	1.4633	1	645.16	645.16	100
Sunflower Oil	Polysorbate 80	19	50	240	1	317	5%	0.6680	0.8565	2.2267	1	645.16	645.16	100
Sunflower Oil	Polysorbate 80	19	25	120	2	317	5%	0.3860	0.8999	1.2867	1	645.16	645.16	100
Sunflower Oil	Polysorbate 80	19	25	180	2	317	5%	0.4750	0.8786	1.5833	1	645.16	645.16	100
Sunflower Oil	Polysorbate 80	19	25	240	2	317	5%	0.7010	0.8565	2.3367	1	645.16	645.16	100
Sunflower Oil	Polysorbate 80	19	50	120	2	317	5%	0.3880	0.8999	1.2933	1	645.16	645.16	100
Sunflower Oil	Polysorbate 80	19	50	180	2	317	5%	0.5320	0.8786	1.7733	1	645.16	645.16	100
Sunflower Oil	Polysorbate 80	19	50	240	2	317	5%	0.7090	0.8565	2.3633	1	645.16	645.16	100
Sunflower Oil	Polysorbate 80	19	25	120	4	317	5%	0.4920	0.8999	1.6400	1	645.16	645.16	100
Sunflower Oil	Polysorbate 80	19	25	180	4	317	5%	0.6070	0.8786	2.0233	1	645.16	645.16	100
Sunflower Oil	Polysorbate 80	19	25	240	4	317	5%	0.8780	0.8565	2.9267	1	645.16	645.16	100
Sunflower Oil	Polysorbate 80	19	50	120	4	317	5%	0.4910	0.8999	1.6367	1	645.16	645.16	100
Sunflower Oil	Polysorbate 80	19	50	180	4	317	5%	0.6300	0.8786	2.1000	1	645.16	645.16	100
Sunflower Oil	Polysorbate 80	19	50	240	4	317	5%	0.9170	0.8565	3.0567	1	645.16	645.16	100
Sunflower Oil	Polysorbate 80	19	25	120	1	317	10%	0.3850	0.8999	1.2833	94	304.546	3.24	47.181
Sunflower Oil	Polysorbate 80	19	25	180	1	317	10%	0.5030	0.8786	1.6767	1	645.16	645.16	100
Sunflower Oil	Polysorbate 80	19	25	240	1	317	10%	0.5690	0.8565	1.8967	24	516.941	21.539	80.087
Sunflower Oil	Polysorbate 80	19	50	120	1	317	10%	0.3800	0.8999	1.2667	72	264.247	3.67	40.938
Sunflower Oil	Polysorbate 80	19	50	180	1	317	10%	0.4990	0.8786	1.6633	1	645.16	645.16	100
Sunflower Oil	Polysorbate 80	19	50	240	1	317	10%	0.5670	0.8565	1.8900	1	645.16	645.16	100
Sunflower Oil	Polysorbate 80	19	25	120	2	317	10%	0.4350	0.8999	1.4500	38	263.803	6.942	40.869
Sunflower Oil	Polysorbate 80	19	25	180	2	317	10%	0.5910	0.8786	1.9700	1	645.16	645.16	100
Sunflower Oil	Polysorbate 80	19	25	240	2	317	10%	0.6520	0.8565	2.1733	1	645.16	645.16	100
Sunflower Oil	Polysorbate 80	19	50	120	2	317	10%	0.4160	0.8999	1.3867	57	365.082	6.405	56.56
Sunflower Oil	Polysorbate 80	19	50	180	2	317	10%	0.5950	0.8786	1.9833	1	645.16	645.16	100
Sunflower Oil	Polysorbate 80	19	50	240	2	317	10%	0.6460	0.8565	2.1533	1	645.16	645.16	100
Sunflower Oil	Polysorbate 80	19	25	120	4	317	10%	0.5050	0.8999	1.6833	30	522.711	17.424	80.98
Sunflower Oil	Polysorbate 80	19	25	180	4	317	10%	0.7120	0.8786	2.3733	1	645.16	645.16	100
Sunflower Oil	Polysorbate 80	19	25	240	4	317	10%	0.8210	0.8565	2.7367	1	645.16	645.16	100
Sunflower Oil	Polysorbate 80	19	50	120	4	317	10%	0.3310	0.8999	1.1033	40	369.899	9.247	57.306
Sunflower Oil	Polysorbate 80	19	50	180	4	317	10%	0.7030	0.8786	2.3433	1	645.16	645.16	100
Sunflower Oil	Polysorbate 80	19	50	240	4	317	10%	0.7840	0.8565	2.6133	1	645.16	645.16	100

Appendix I – Data Table – Sunflower Oil

Table 151: Data Table – Sunflower & Polysorbate 80 @ 22ga

Base Oil	Emulsifier	Needle Gauge	Voltage (kV)	Temp (F)	Pressure (psi)	Time (ms)	Concentration	Weight (g)	Density (g/cm^3)	Mass Flow (g/s)	Droplet Count	Total Area (mm^2)	Average Size (mm^2)	% Area Coverage
Sunflower Oil	Polysorbate 80	22	25	120	4	317	5%	0.0850	0.8999	0.2833	392	101.846	0.26	15.778
Sunflower Oil	Polysorbate 80	22	25	180	4	317	5%	0.0960	0.8786	0.3200	392	91.385	0.233	14.158
Sunflower Oil	Polysorbate 80	22	25	240	4	317	5%	0.2270	0.8565	0.7567	252	108.996	0.433	16.886
Sunflower Oil	Polysorbate 80	22	50	120	4	317	5%	0.0930	0.8999	0.3100	41	122.295	2.983	18.946
Sunflower Oil	Polysorbate 80	22	50	180	4	317	5%	0.9600	0.8786	3.2000	47	138.287	2.942	21.424
Sunflower Oil	Polysorbate 80	22	50	240	4	317	5%	0.1140	0.8565	0.3800	152	269.97	1.776	41.825
Sunflower Oil	Polysorbate 80	22	25	120	8	317	5%	0.1160	0.8999	0.3867	336	171.383	0.51	26.551
Sunflower Oil	Polysorbate 80	22	25	180	8	317	5%	0.1360	0.8786	0.4533	244	164.571	0.674	25.496
Sunflower Oil	Polysorbate 80	22	25	240	8	317	5%	0.1950	0.8565	0.6500	745	317.031	0.426	49.116
Sunflower Oil	Polysorbate 80	22	50	120	8	317	5%	0.1310	0.8999	0.4367	245	212.255	0.866	32.883
Sunflower Oil	Polysorbate 80	22	50	180	8	317	5%	0.1290	0.8786	0.4300	217	154.691	0.713	23.965
Sunflower Oil	Polysorbate 80	22	50	240	8	317	5%	0.2050	0.8565	0.6833	8	604.262	75.533	93.615
Sunflower Oil	Polysorbate 80	22	25	120	16	317	5%	0.1770	0.8999	0.5900	158	332.669	2.105	51.538
Sunflower Oil	Polysorbate 80	22	25	180	16	317	5%	0.1990	0.8786	0.6633	153	425.426	2.781	65.909
Sunflower Oil	Polysorbate 80	22	25	240	16	317	5%	0.3060	0.8565	1.0200	161	442.314	2.747	68.525
Sunflower Oil	Polysorbate 80	22	50	120	16	317	5%	0.1800	0.8999	0.6000	36	496.696	13.797	76.95
Sunflower Oil	Polysorbate 80	22	50	180	16	317	5%	0.1960	0.8786	0.6533	73	537.958	7.369	83.343
Sunflower Oil	Polysorbate 80	22	50	240	16	317	5%	0.3600	0.8565	1.2000	1	645.16	645.16	100
Sunflower Oil	Polysorbate 80	22	25	120	4	317	10%	0.0310	0.8999	0.1033	292	46.42	0.159	7.192
Sunflower Oil	Polysorbate 80	22	25	180	4	317	10%	0.0610	0.8786	0.2033	211	67.954	0.322	10.528
Sunflower Oil	Polysorbate 80	22	25	240	4	317	10%	0.0920	0.8565	0.3067	258	100.875	0.391	15.628
Sunflower Oil	Polysorbate 80	22	50	120	4	317	10%	0.0300	0.8999	0.1000	296	52.541	0.178	8.14
Sunflower Oil	Polysorbate 80	22	50	180	4	317	10%	0.0680	0.8786	0.2267	266	108.282	0.407	16.776
Sunflower Oil	Polysorbate 80	22	50	240	4	317	10%	0.0890	0.8565	0.2967	237	184.246	0.777	28.544
Sunflower Oil	Polysorbate 80	22	25	120	8	317	10%	0.0390	0.8999	0.1300	319	54.444	0.171	8.435
Sunflower Oil	Polysorbate 80	22	25	180	8	317	10%	0.0960	0.8786	0.3200	309	82.748	0.268	12.82
Sunflower Oil	Polysorbate 80	22	25	240	8	317	10%	0.1330	0.8565	0.4433	240	88.086	0.367	13.647
Sunflower Oil	Polysorbate 80	22	50	120	8	317	10%	0.0430	0.8999	0.1433	554	126.149	0.228	19.544
Sunflower Oil	Polysorbate 80	22	50	180	8	317	10%	0.1050	0.8786	0.3500	137	206.496	1.507	31.991
Sunflower Oil	Polysorbate 80	22	50	240	8	317	10%	0.1460	0.8565	0.4867	218	216.955	0.995	33.612
Sunflower Oil	Polysorbate 80	22	25	120	16	317	10%	0.0530	0.8999	0.1767	279	40.715	0.146	6.308
Sunflower Oil	Polysorbate 80	22	25	180	16	317	10%	0.1580	0.8786	0.5267	108	89.272	0.827	13.83
Sunflower Oil	Polysorbate 80	22	25	240	16	317	10%	0.2610	0.8565	0.8700	44	136.19	3.095	21.099
Sunflower Oil	Polysorbate 80	22	50	120	16	317	10%	0.0610	0.8999	0.2033	647	105.491	0.163	16.343
Sunflower Oil	Polysorbate 80	22	50	180	16	317	10%	0.1380	0.8786	0.4600	165	140.051	0.849	21.697
Sunflower Oil	Polysorbate 80	22	50	240	16	317	10%	0.2420	0.8565	0.8067	91	311.088	3.419	48.195

Appendix I – Data Table – Sunflower Oil

Table 152: Data Table – Sunflower & Propylene Glycol @ 19ga

Base Oil	Emulsifier	Needle Gauge	Voltage (kV)	Temp (F)	Pressure (psi)	Time (ms)	Concentration	Weight (g)	Density (g/cm^3)	Mass Flow (g/s)	Droplet Count	Total Area (mm^2)	Average Size (mm^2)	% Area Coverage
Sunflower Oil	Propylene Glycol	19	25	120	1	317	5%	0.3540	0.8999	1.1800	92	133.64	1.453	20.704
Sunflower Oil	Propylene Glycol	19	25	180	1	317	5%	0.4350	0.8786	1.4500	37	287.543	7.771	44.547
Sunflower Oil	Propylene Glycol	19	25	240	1	317	5%	0.5770	0.8565	1.9233	49	578.952	11.815	89.694
Sunflower Oil	Propylene Glycol	19	50	120	1	317	5%	0.3570	0.8999	1.1900	31	245.62	7.923	38.052
Sunflower Oil	Propylene Glycol	19	50	180	1	317	5%	0.4420	0.8786	1.4733	34	294.102	8.65	45.563
Sunflower Oil	Propylene Glycol	19	50	240	1	317	5%	0.5730	0.8565	1.9100	46	591.667	12.862	91.663
Sunflower Oil	Propylene Glycol	19	25	120	2	317	5%	0.4370	0.8999	1.4567	69	155.745	2.257	24.129
Sunflower Oil	Propylene Glycol	19	25	180	2	317	5%	0.5120	0.8786	1.7067	21	268.925	12.806	41.663
Sunflower Oil	Propylene Glycol	19	25	240	2	317	5%	0.6410	0.8565	2.1367	47	555.159	11.812	86.008
Sunflower Oil	Propylene Glycol	19	50	120	2	317	5%	0.3600	0.8999	1.2000	24	452.289	18.845	70.07
Sunflower Oil	Propylene Glycol	19	50	180	2	317	5%	0.5240	0.8786	1.7467	22	477.998	21.727	74.053
Sunflower Oil	Propylene Glycol	19	50	240	2	317	5%	0.6390	0.8565	2.1300	10	578.436	57.844	89.614
Sunflower Oil	Propylene Glycol	19	25	120	4	317	5%	0.5470	0.8999	1.8233	54	184.09	3.409	28.52
Sunflower Oil	Propylene Glycol	19	25	180	4	317	5%	0.6730	0.8786	2.2433	23	500.217	21.749	77.496
Sunflower Oil	Propylene Glycol	19	25	240	4	317	5%	0.8170	0.8565	2.7233	20	586.146	29.307	90.808
Sunflower Oil	Propylene Glycol	19	50	120	4	317	5%	0.5240	0.8999	1.7467	10	549.237	54.924	85.09
Sunflower Oil	Propylene Glycol	19	50	180	4	317	5%	0.6930	0.8786	2.3100	12	567.97	47.331	87.992
Sunflower Oil	Propylene Glycol	19	50	240	4	317	5%	0.8840	0.8565	2.9467	12	626.995	52.25	97.137
Sunflower Oil	Propylene Glycol	19	25	120	1	317	10%	0.4510	0.8999	1.5033	1	645.16	645.16	100
Sunflower Oil	Propylene Glycol	19	25	180	1	317	10%	0.6010	0.8786	2.0033	1	645.16	645.16	100
Sunflower Oil	Propylene Glycol	19	25	240	1	317	10%	0.7350	0.8565	2.4500	1	645.16	645.16	100
Sunflower Oil	Propylene Glycol	19	50	120	1	317	10%	0.4470	0.8999	1.4900	1	645.16	645.16	100
Sunflower Oil	Propylene Glycol	19	50	180	1	317	10%	0.5990	0.8786	1.9967	1	645.16	645.16	100
Sunflower Oil	Propylene Glycol	19	50	240	1	317	10%	0.7280	0.8565	2.4267	1	645.16	645.16	100
Sunflower Oil	Propylene Glycol	19	25	120	2	317	10%	0.5160	0.8999	1.7200	1	645.16	645.16	100
Sunflower Oil	Propylene Glycol	19	25	180	2	317	10%	0.6810	0.8786	2.2700	1	645.16	645.16	100
Sunflower Oil	Propylene Glycol	19	25	240	2	317	10%	0.8320	0.8565	2.7733	1	645.16	645.16	100
Sunflower Oil	Propylene Glycol	19	50	120	2	317	10%	0.5140	0.8999	1.7133	1	645.16	645.16	100
Sunflower Oil	Propylene Glycol	19	50	180	2	317	10%	0.6830	0.8786	2.2767	1	645.16	645.16	100
Sunflower Oil	Propylene Glycol	19	50	240	2	317	10%	0.8860	0.8565	2.9533	1	645.16	645.16	100
Sunflower Oil	Propylene Glycol	19	25	120	4	317	10%	0.6290	0.8999	2.0967	1	645.16	645.16	100
Sunflower Oil	Propylene Glycol	19	25	180	4	317	10%	0.8170	0.8786	2.7233	1	645.16	645.16	100
Sunflower Oil	Propylene Glycol	19	25	240	4	317	10%	1.0490	0.8565	3.4967	1	645.16	645.16	100
Sunflower Oil	Propylene Glycol	19	50	120	4	317	10%	0.6300	0.8999	2.1000	1	645.16	645.16	100
Sunflower Oil	Propylene Glycol	19	50	180	4	317	10%	0.8200	0.8786	2.7333	1	645.16	645.16	100
Sunflower Oil	Propylene Glycol	19	50	240	4	317	10%	1.0440	0.8565	3.4800	1	645.16	645.16	100

Appendix I – Data Table – Sunflower Oil

Table 153: Data Table – Sunflower & Propylene Glycol @ 22ga

Base Oil	Emulsifier	Needle Gauge	Voltage (kV)	Temp (F)	Pressure (psi)	Time (ms)	Concentration	Weight (g)	Density (g/cm^3)	Mass Flow (g/s)	Droplet Count	Total Area (mm^2)	Average Size (mm^2)	% Area Coverage
Sunflower Oil	Propylene Glycol	22	25	120	4	317	5%	0.0380	0.8999	0.1267	531	68.805	0.13	10.66
Sunflower Oil	Propylene Glycol	22	25	180	4	317	5%	0.0600	0.8786	0.2000	329	112.984	0.343	17.504
Sunflower Oil	Propylene Glycol	22	25	240	4	317	5%	0.0860	0.8565	0.2867	138	82.96	0.601	12.852
Sunflower Oil	Propylene Glycol	22	50	120	4	317	5%	0.0460	0.8999	0.1533	780	135.525	0.174	20.996
Sunflower Oil	Propylene Glycol	22	50	180	4	317	5%	0.0620	0.8786	0.2067	976	210.043	0.215	32.541
Sunflower Oil	Propylene Glycol	22	50	240	4	317	5%	0.0830	0.8565	0.2767	1553	180.1	0.116	27.902
Sunflower Oil	Propylene Glycol	22	25	120	8	317	5%	0.0510	0.8999	0.1700	565	91.25	0.162	14.137
Sunflower Oil	Propylene Glycol	22	25	180	8	317	5%	0.0790	0.8786	0.2633	1269	129.173	0.102	20.012
Sunflower Oil	Propylene Glycol	22	25	240	8	317	5%	0.1250	0.8565	0.4167	575	105.229	0.183	16.302
Sunflower Oil	Propylene Glycol	22	50	120	8	317	5%	0.0580	0.8999	0.1933	218	105.471	0.484	16.34
Sunflower Oil	Propylene Glycol	22	50	180	8	317	5%	0.1190	0.8786	0.3967	759	145.678	0.192	22.569
Sunflower Oil	Propylene Glycol	22	50	240	8	317	5%	0.1260	0.8565	0.4200	58	171.868	2.963	26.627
Sunflower Oil	Propylene Glycol	22	25	120	16	317	5%	0.1000	0.8999	0.3333	528	109.993	0.208	17.041
Sunflower Oil	Propylene Glycol	22	25	180	16	317	5%	0.1800	0.8786	0.6000	907	134.969	0.149	20.91
Sunflower Oil	Propylene Glycol	22	25	240	16	317	5%	0.1980	0.8565	0.6600	90	119.135	1.324	18.457
Sunflower Oil	Propylene Glycol	22	50	120	16	317	5%	0.0990	0.8999	0.3300	949	180.236	0.19	27.923
Sunflower Oil	Propylene Glycol	22	50	180	16	317	5%	0.1820	0.8786	0.6067	1167	209.881	0.18	32.516
Sunflower Oil	Propylene Glycol	22	50	240	16	317	5%	0.2090	0.8565	0.6967	118	223.828	1.897	34.676
Sunflower Oil	Propylene Glycol	22	25	120	4	317	10%	0.0420	0.8999	0.1400	326	69.947	0.215	10.837
Sunflower Oil	Propylene Glycol	22	25	180	4	317	10%	0.0700	0.8786	0.2333	63	105.047	1.667	16.274
Sunflower Oil	Propylene Glycol	22	25	240	4	317	10%	0.0730	0.8565	0.2433	41	214.598	5.234	33.246
Sunflower Oil	Propylene Glycol	22	50	120	4	317	10%	0.0390	0.8999	0.1300	134	124.329	0.928	19.262
Sunflower Oil	Propylene Glycol	22	50	180	4	317	10%	0.0700	0.8786	0.2333	32	133.126	4.16	20.624
Sunflower Oil	Propylene Glycol	22	50	240	4	317	10%	0.0740	0.8565	0.2467	22	149.665	6.803	23.187
Sunflower Oil	Propylene Glycol	22	25	120	8	317	10%	0.0560	0.8999	0.1867	83	62.058	0.748	9.614
Sunflower Oil	Propylene Glycol	22	25	180	8	317	10%	0.1030	0.8786	0.3433	32	122.507	3.828	18.979
Sunflower Oil	Propylene Glycol	22	25	240	8	317	10%	0.1060	0.8565	0.3533	23	213.208	9.27	33.031
Sunflower Oil	Propylene Glycol	22	50	120	8	317	10%	0.0520	0.8999	0.1733	209	194.201	0.929	30.086
Sunflower Oil	Propylene Glycol	22	50	180	8	317	10%	0.1050	0.8786	0.3500	43	223.489	5.197	34.624
Sunflower Oil	Propylene Glycol	22	50	240	8	317	10%	0.1180	0.8565	0.3933	39	298.996	7.667	46.322
Sunflower Oil	Propylene Glycol	22	25	120	16	317	10%	0.0720	0.8999	0.2400	128	63.617	0.497	9.856
Sunflower Oil	Propylene Glycol	22	25	180	16	317	10%	0.1760	0.8786	0.5867	30	249.755	8.325	38.693
Sunflower Oil	Propylene Glycol	22	25	240	16	317	10%	0.2060	0.8565	0.6867	27	530.649	19.654	82.21
Sunflower Oil	Propylene Glycol	22	50	120	16	317	10%	0.0740	0.8999	0.2467	272	77.1	0.283	11.945
Sunflower Oil	Propylene Glycol	22	50	180	16	317	10%	0.1740	0.8786	0.5800	83	153.986	1.855	23.856
Sunflower Oil	Propylene Glycol	22	50	240	16	317	10%	0.2260	0.8565	0.7533	31	568.295	18.332	88.043

VITA

Robert Joseph Mackey

Candidate for the Degree of: **Doctor of Philosophy**

Thesis: ELECTRO-HYDRODYNAMIC SPOT-SPRAY APPLICATION OF FOOD-GRADE OIL & EMULSIFIER BLENDS AS A RELEASE AGENT IN BAKING

Major Field: BioSystems and Agricultural Engineering

Biographical:45-year-old non-traditional student (mechanical engineer) born and raised in Oklahoma. Married for 27 years to Angela Mackey (a social worker and high school sweetheart). 6 children (2 adopted) aged 26 (Tyler), 24 (Kaleb), 22 (Kaity), (Jacob) 21, (Hannah) 20, and (Dakota) 17. Passionate about OSU football and playing the guitar

Education: Master of Science in Engineering and Technology Management
Oklahoma State University, Stillwater, OK in 2013

Bachelor of Science in Mechanical Engineering
Oklahoma State University, Stillwater, OK in 2016

Experience: Vice President for an OEM equipment manufacturer. Over 22 years of experience in Industrial Management. Seventeen years of experience in cellular and continuous manufacturing as a Maintenance Supervisor, Plant Engineer, Corporate Engineer, Plant Manager, Engineering Director and Vice President. Four years Military experience in Industrial Electricity and Process Automation from entry level Technician to Maintenance Supervisor. Diversely traveled, highly decorated, versatile manager geared towards problem solving. Able to balance high stress situations with day-to-day operations to produce timely and tangible results.

Extensive experience with progressive management systems such as Deming, Six Sigma, and Lean Manufacturing. Strong technical background to include broad experience with industrial controls, three phase electricity, advanced PLC/HMI Programming, fluid dynamics, thermal processing, structural design and analysis, and two stage anhydrous ammonia refrigeration. Project Engineer managing multimillion dollar capital projects ranging from line upgrades to green field design builds.

Professional Memberships:
Pi Tau Sigma Honor Society – Member
ASBAE (OSU Chapter) – Treasurer
SW Oklahoma Technology Center- Board Member